Lecture Notes in Nanoscale Science and Technology 29

Kailash Chandra Khulbe
Takeshi Matsuura

Nanotechnology in Membrane Processes

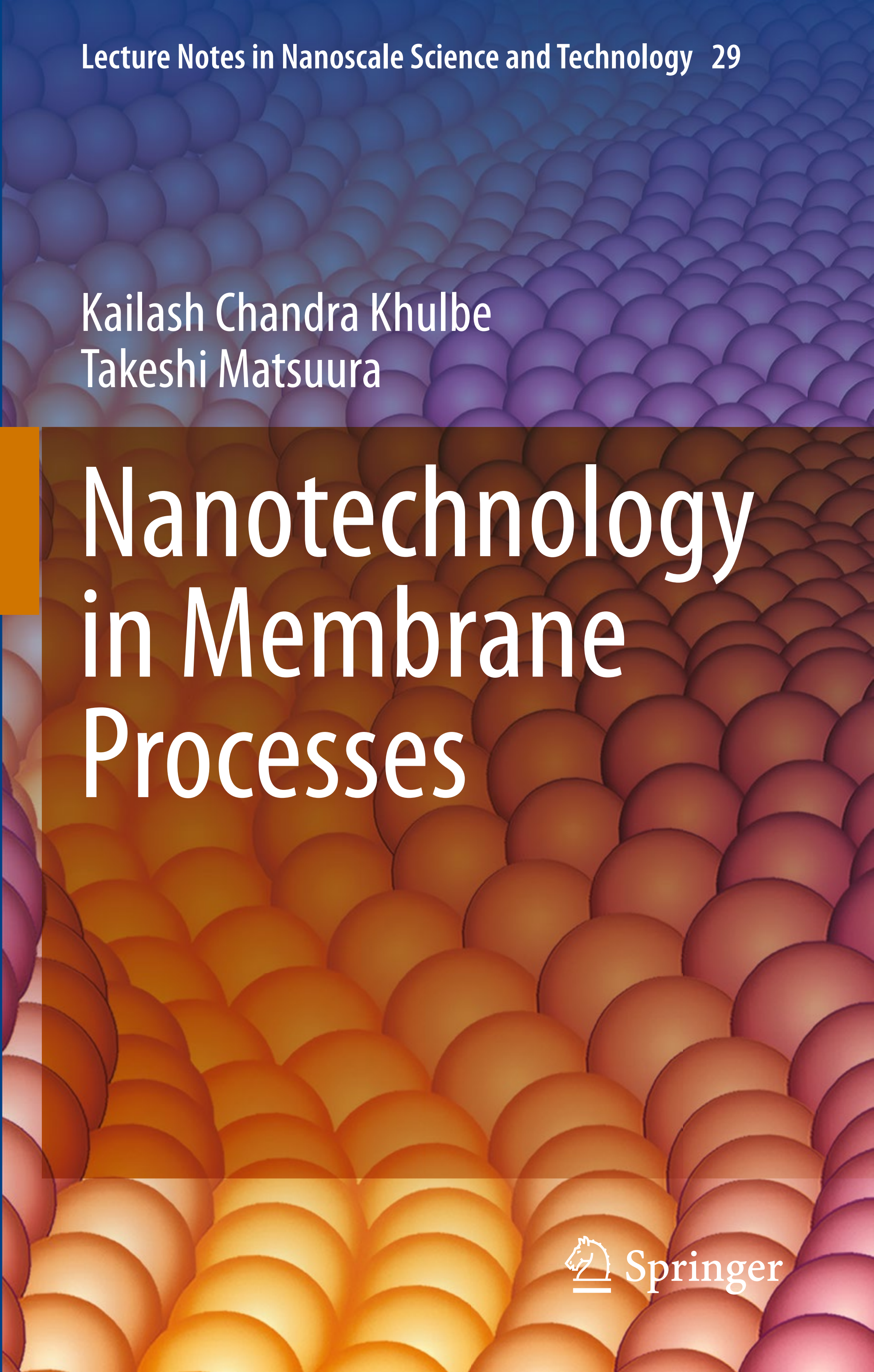

Springer

Lecture Notes in Nanoscale Science and Technology

Volume 29

Lecture Notes in Nanoscale Science and Technology (LNNST) aims to report latest developments in nanoscale science and technology research and teaching – quickly, informally and at a high level. Through publication, LNNST commits to serve the open communication of scientific and technological advances in the creation and use of objects at the nanometer scale, crossing the boundaries of physics, materials science, biology, chemistry, and engineering. Certainly, while historically the mysteries in each of the sciences have been very different, they have all required a relentless step-by-step pursuit to uncover the answer to a challenging scientific question, but recently many of the answers have brought questions that lie at the boundaries between the life sciences and the physical sciences and between what is fundamental and what is application. This is no accident since recent research in the physical and life sciences have each independently cut a path to the edge of their disciplines. As both paths intersect one may ask if transport of material in a cell is biology or is it physics? This intersection of curiosity makes us realize that nanoscience and technology crosses many if not all disciplines. It is this market that the proposed series of lecture notes targets.

More information about this series at http://www.springer.com/series/7544

Kailash Chandra Khulbe • Takeshi Matsuura

Nanotechnology in Membrane Processes

Springer

Kailash Chandra Khulbe
Department of Chemical and Bioloical
Engineering
The University of Ottawa
Ottawa, ON, Canada

Takeshi Matsuura
Department of Chemical and Bioloical
Engineering
The University of Ottawa
Ottawa, ON, Canada

ISSN 2195-2159 ISSN 2195-2167 (electronic)
Lecture Notes in Nanoscale Science and Technology
ISBN 978-3-030-64182-5 ISBN 978-3-030-64183-2 (eBook)
https://doi.org/10.1007/978-3-030-64183-2

© Springer Nature Switzerland AG 2021
This work is subject to copyright. All rights are reserved by the Publisher, whether the whole or part of the material is concerned, specifically the rights of translation, reprinting, reuse of illustrations, recitation, broadcasting, reproduction on microfilms or in any other physical way, and transmission or information storage and retrieval, electronic adaptation, computer software, or by similar or dissimilar methodology now known or hereafter developed.
The use of general descriptive names, registered names, trademarks, service marks, etc. in this publication does not imply, even in the absence of a specific statement, that such names are exempt from the relevant protective laws and regulations and therefore free for general use.
The publisher, the authors, and the editors are safe to assume that the advice and information in this book are believed to be true and accurate at the date of publication. Neither the publisher nor the authors or the editors give a warranty, expressed or implied, with respect to the material contained herein or for any errors or omissions that may have been made. The publisher remains neutral with regard to jurisdictional claims in published maps and institutional affiliations.

This Springer imprint is published by the registered company Springer Nature Switzerland AG
The registered company address is: Gewerbestrasse 11, 6330 Cham, Switzerland

Preface

Nanoscience deals with the fundamental principles and properties of matter at the nanometer (10^{-9} m) scale. Nanotechnology is the application of these structures into useful nanoscale processes or devices. Thus, nanoscience and nanotechnology are defined as the research and development of materials, devices, and systems exhibiting physical, chemical, and biological properties that are different from those found on a larger scale (matter smaller than scale of things like molecules and viruses). In other words, nanotechnology refers broadly to a field of applied science and technology whose unifying theme is the control of matter on the molecular level in scales smaller than 1 μm, normally 1–100 nm, and the fabrication of devices within that size range. Nanotechnology is being used to enhance conventional ceramic and polymeric water treatment membrane materials through various avenues.

Membrane technology is widely recognized as effective tools in many industrial sectors since it allows separation and purification processes to be carried out with less energy consumption. Desalination and water production industries, gas industries, petroleum and petrochemical industries, food industries and medical industries are some of those examples. An avenue is also widely open to the use of membrane technology for the production of renewable energies by pressure retarded osmosis and fuel cells. Thus, membrane technology has the potential to contribute to the sustainable growth of human activities.

Related closely to nanoscience and technology, there is no doubt that membrane science and technology can benefit enormously by the progress of nanoscience and technology. Indeed, some membranes and membrane processes are called nanofibrous membranes, nanocomposite membranes, and nanofiltration. As well, membranes for reverse osmosis, forward osmosis, pressure retarded osmosis, ultrafiltration, and some gas separation membranes are known to possess sub-nano or nano-sized pores, even though those processes do not bear the" name "nano-" explicitly. Mixed matrix membranes are fabricated by incorporating nanoparticles into the host polymeric membranes to enhance their permeation and separation performance.

Acknowledging that membrane research and development are deeply influenced by nanoscience and technology, the authors have decided to write a book in which involvement of nanoscience and technology in membrane technology, either implicitly or explicitly, is comprehensively summarized.

The book consists of the following six chapters.

Chapter 1 briefly gives an overview of nanoscience and technology and membrane science and technology and their relationship.

Chapter 2 outlines methods for the preparation of membranes with nanoscale pores and/or nanocomposite membranes to enhance membrane performance. In particular, the structure and properties of a variety of nanoparticles are described in detail.

Chapter 3 is for the characterization of membranes. In this chapter, a number of advanced characterization methods are depicted. The use of these modern characterization instruments is essential nowadays for membrane research, especially for the development of nanocomposite membranes.

Not only membrane preparation but also the pre- and post-modification of membranes are important to enhance membrane performance, where a variety of techniques developed for nanotechnologies can be applied. Chapter 4 gives an overview of such modification methods.

It is important to predict the performance of nanocomposite membranes where nanoparticles are incorporated. Even though such prediction methods are still early in development, a number of model equations have been proposed for both gas and liquid separation. Chapter 5 summarizes such model predictions.

And finally in Chap. 6, examples are given for the applications of membrane technologies where nanotechnology is heavily involved, encompassing many gas and liquid separation and purification processes, separation of liquid mixtures, and sensors.

The authors believe that this book will be useful not only for researchers directly involved in membranes and membrane separation processes, but also provides a valuable guide to graduate students, industrialists involved in R & D, and researchers in the public sector.

Ottawa, ON, Canada

Kailash Chandra Khulbe
Takeshi Matsuura

Abbreviation

AFM	Atomic force microscope
AGMD	Air gap membrane distillation
AlOOH	Boehmite
APTMOS	Aminopropyl-trimethoxysilane
AQPs	Aquaporins
BET	Brunauer–Emmett–Teller
BPEI	Branched polyethylenimine
BTCA	Butanetetracarboxylic acid
CCS	CO_2 Capture and separation
CM-NPs	Cell membrane-coated nanoparticles
CMS	Carbon molecular sieve
CNC	Cellulose manocrystals
CNFs	Carbon nanofibers
CNM	Carbon nanomaterial
CNTs	Carbon nanotubes
CS	Chitosan
CSs	Carbon spheres
DCMD	Direct contact membrane distillation
EC	Ethylcellulose
ED	Electrodialysis
ENFs	Electrospun nanofibers
EPDM	Ethylene–propylene diene rubber
Fh	Ferrihydrite
FO	Forward osmosis
FTIR	Fourier transform infrared
GCM	Graphene-containing membrane
GCMs	Graphene-containing membranes
GNM	Glycosylated nanofibrous membrane
GO	Graphene oxide
GS	Gas separation
HA	Humic acid

HF	Hollow fiber
HFM	Hollow fiber membrane
HNTs	Halloysite nanotubes
IEC	Ion exchange capacity
IP	Interfacial polymerization
IPA	*iso*-Propyl alcohol
LEP	Liquid entry pressure
LPI	Linear polyimide
MAS	Magnesium aluminum silicate
MD	Membrane distillation
MMCHF	Mixed matrix composite hollow fiber
MMM	Mixed matrix membrane
MMMC	Mixed matrix membrane contactor
MNPs	Magnetic nanoparticles
MOF	Metal-organic framework
MPD	*m*-Phenylenediamine
MPL	Maximum permissible limits
MTBE	Methyl tert-butyl ether
MWCNTs	Multi-walled carbon nanotubes
MWCO	Molecular weight cut-off
NaAlg	Sodium alginate
NF	Nanofiltration
NFMs	Nanofiber membranes
NIPAM	*N*-Isopropyl acrylamide
NIPS	Non-solvent-induced phase separation
NPTs	Nanoparticles
NTs	Nanotubes
PA	Polyamide
PAA	Polyacrylic acid
PAHM	Poly(acrylonitrile-*co*-hydroxyethyl methacrylate)
PALS	Positron annihilation lifetime spectroscopy
PAN	Polyacrylonitrile
PANI	Polyaniline
PCL	Poly(ε-caprolactone)
PDA	Polydopamine
PDMS	Polydimethylsiloxane
PEBA	Poly(ether block amide)
PEG	polyethylene glycol
PEI	polyetherimide
PEN	poly(arylene) ether nitrile
PES	Polyethersulfone
PI	Polyimide
PIA	Poly(itaconic acid)
PLLA	Poly(l-lactic acid)
PMETAC	Polymer trimethyl ammonium chloride

PMMA	Poly(methyl methacrylate)
PNCMs	Polymer nanocomposite membranes
POEM	Poly(oxyethylenemethacrylate)
PP	Polypropylene
PPO	Poly(phenylene oxide)
PPSU	Polyphenylsulfone
PPX	Poly(p-xylylene)
PRO	Pressure retarded osmosis
PS	Polystyrene
PSA	Pressure swing adsorption
PSf	Polysulfone
PTFE	polytetrafluoroethylene
PTMSP	Poly(1-trimethylsilyl-1-propyne)
PUR	Polyurethane
PV	Pervaporation
PVA	Polyvinyl alcohol
PVAc	Polyvinyl acetate
PVC	Poly(vinyl chloride)
PVDF	Poly(vinylidene fluoride)
PVP	Poly(vinyl pyrrolidone)
PWF	Pure water flux
RC	Regenerated cellulose
RO	Reverse osmosis
ROS	Reactive oxygen species
SA	Sodium alginate
SAGD	Steam-assisted gravity drainage
SDS	Sodium dodecyl sulfate
SGMD	Sweeping gas membrane distillation
SWCNTs	Single-walled carbon nanotubes
TDS	Dissolved matter content
TFC	Thin film composite
TFN	Thin film nanocomposite
TFNC	Thin film nanofibrous composite
TMC	Trimesoyl chloride
TTIP	Titanium tetraisopropoxide
UF	Ultrafiltration
UTDR	Ultrasonic time-domain reflectometry
UV	Ultraviolet
VMD	Vacuum membrane distillation
WCA	Water contact angle

Contents

Chapter 1
Introduction

1.1 History of Nanotechnology

'The vision of nanotechnology introduced in 1959 by the late Nobel Physicist Richard P Faynman who in dinner talk said, "There is plenty of room at the bottom"' [1].

The American physicist Richard Feynman lectured, "There's Plenty of Room at the Bottom," at an American Physical Society meeting at Caltech on December 29, 1959, which is often held to have provided inspiration for the field of nanotechnology. He was the father of Nanotechnology and received the Noble prize in Physics, 1965. The Japanese scientist called Norio Taniguchi of Tokyo University of Science was the first to use the term "nano-technology" in a 1974 conference [2]. The term was not used again until 1981 when Eric Drexler, who was unaware of Taniguchi's prior use of the term, published his first paper on nanotechnology in 1981 [3–5]. Nanotechnology is being used to enhance conventional ceramic and polymeric water treatment membrane materials through various avenues. Among the numerous concepts proposed, the most promising to date include zeolitic and catalytic nanoparticle coated ceramic membranes, hybrid inorganic–organic nanocomposite membranes, and bio-inspired membranes such as hybrid protein–polymer biomimetic membranes, aligned nanotube membranes, and isoporous block copolymer membranes.

Membrane science and nanotechnology is an expanding field and has become a prominent part of many activities. Green nanotechnology has been described as the development of clean technologies, to minimize potential environmental and human health risks associated with the manufacture and use of nanotechnology products, and to encourage replacement of existing products with new nano-products that are more environmentally friendly throughout their lifecycle. Although green nanotechnology poses many advantages over traditional methods, there is still much debate about the concerns brought about by nanotechnology. The development in the field of nanotechnology started in 1958 and the various stages of development have been summarized in Table 1.1.

K. C. Khulbe, T. Matsuura, *Nanotechnology in Membrane Processes*, Lecture Notes in Nanoscale Science and Technology 29,
https://doi.org/10.1007/978-3-030-64183-2_1

Nanotechnology can help improve energy efficiency. Nanotechnology is revolutionizing in many technology and industry sectors: information technology, homeland security, medicine, transportation, energy, food safety, and environmental science, among many others. Nanotechnology offers the ability to control matter at the nanoscale and create materials that have specific properties with a specific function. Surveys from selected European Union (EU) media show relatively high optimism with respect to the chances/risk ratio associated with nanotechnology (Fig. 1.1) [25], where most of them have been attributed to the prospect of improvement in the quality of life and health [26].

Nanomaterials in various shapes/morphologies, such as nanoparticles, tubes, wires, fibres *etc.*, and functions as adsorbents and catalysts and their composites with polymers are used for the detection and removal of gases (SO_2, CO, NO_x, *etc.),* contaminated chemicals (arsenic, iron, manganese, nitrate, heavy metals, *etc.),* organic pollutants (aliphatic and aromatic hydrocarbons) and biological substances, such as viruses, bacteria, parasites and antibiotics [27].

1.2 Nano

The prefix "nano" stems from the ancient Greek for "dwarf". In science it means one billionth (10^{-9}) of something, thus a nanometer (nm) is one billionth of a meter, or 0.000000001 m. A nanometer is about three to five atoms wide, or some 40,000 times smaller than the thickness of human hair. A virus is typically 100 nm in size.

1.3 Nano Scale and Nanostructures

The nano scale is the place where the properties of most common things are determined just above the scale of an atom. Nano scale objects have at least one dimension (height, length, depth) that measures between 1 and 999 nm (1–999 nm) (Fig. 1.2) [16].

1.4 Nano Technology

Nanoscience deals with the fundamental principles and properties of matter at the nanometer (10^{-9} m) scale. Nanotechnology is the application of these structures into useful nano-scale processes or devices. Nanotechnology is defined as the research and development of materials, devices, and systems exhibiting physical, chemical, and biological properties that are different from those found on a larger scale (matter smaller than scale of things like molecules and viruses) [28, 29]. In other words, nanotechnology refers broadly to a field of applied science and technology whose

Table 1.1 Periodical development in nanotechnology

Year	Development in nanotechnology	Reference
Ninth century B.C.	Artisans in Mesopotamia used finely divided materials of this type as early as the ninth century BC, to obtain a glittering effect on the surface of ceramic vessels	[6, 7]
Middle ages	In the Middle Ages and the Renaissance, the production of glittering metallic films led to methods of covering glassy surfaces developed in various Far Eastern or European centres which became famous thanks to these methods that are largely employed even today. During the Renaissance and in later times, the development of visual arts (painting in particular) and printing and engraving methods contributed to the technique of producing fine inorganic and organic dust particles, close to nanoparticles in size, and dispersions that were stable in different solvents and used as dyes or ink	[6, 7]
Four centuries ago	Nanofibers were first produced via electrospinning	[8, 9]
1857	Michael Faraday was the first to provide a scientific description of the optical properties of nanometric metal particles	[10]
1857	Very thin gold or silver films on glassy surfaces heated at 500 °C changed both the properties of the deposited metals and those of the glass, so that white light crossed the metallic film; this caused a marked reduction of reflection	[11]
1867	James Clark Maxwell suggested a series of concepts of differentiation in nanotechnology, but without using the word “nanotechnology” to define thin, monomolecular layers	[12]
1914	First accurate observations and measurements were made by Zsigmondy, who used dark field ultramicroscopy which allowed the visualisation of particles smaller than monochromatic light wavelength. With this method, Zsigmondy was able to see 1/10,00,000-mm particles and he was the first to apply the term “nanoparticles” explicitly to such particles	[13]
1920	Irving Langmuir and Katharine B. Blodgett, dealing with nanoparticle characterisation and related phenomena that define interface in colloid science, introduced the concept of monolayer, a layer of material one molecule thick. Langmuir received the Nobel Prize for his theoretical contributions in chemistry in 1932	[14, 15]
1959	R. Feynman initiated thought process	[16]
1974	The term nanotechnology was used by Taniguchi for the first time	[16]
1981	BM Scanning Tunneling Microscope	[16]
1985	“Bucky Ball”	[16]
1986	Binnig invented the atomic force microscope	[17]
1986	First experimental implementation was made by Binnig, Quate and Gerber	[18]
1986	First book on nanotechnology Engines of Creation was published by K. Eric Drexler, Atomic Force Microscope	[16]
1991	S. Iijima discovered Carbon Nano tube for the first time	[19]
1999	1st nano medicine book by R. Freitas “Nano medicine” was published	[16]
2000	For the first time National Nanotechnology Initiative was launched	[16]

(continued)

Table 1.1 (continued)

Year	Development in nanotechnology	Reference
2001	For developing theory of nanometer-scale electronic devices and for synthesis and characterization of carbon nanotubes and nano wires, Feynman Prize in Nanotechnology was awarded	[16]
2002	Feynman Prize in Nanotechnology was awarded for using DNA to enable the self-assembly of new structures and for advancing our ability to model molecular machine systems	[16]
2003	Feynman Prize in Nanotechnology was awarded for modeling the molecular and electronic structures of new materials and for integrating single molecule biological motors with nano-scale silicon devices	[16]
2003	First time, Khil et al. used Polyurethane (PU) to produce nanofibrous membranes to be applied as skin substitutes	[20]
2004	First policy conference on advanced nanotech was held. First center for nano mechanical systems was established. Feynman Prize in Nanotechnology was awarded for designing stable protein structures and for constructing a novel enzyme with an altered function	[16]
2005–2010	3D Nano systems like robotics, 3D networking and active nano products that change their state during use were prepared	[16]
2008	Polyvinylidene fluoride nanofiber membrane could be used in membrane distillation (MD) to produce drinking water	[21]
2008	The first book was written on Synthetic Membranes, "Characterization by Atomic Force Microscopy"	[22]
2011	Era of molecular nanotechnology started	[16]
2014	Heavy metals removal from aqueous solution in a batch adsorption mode was done by using platinum nanoparticles/Zeolite-4AS	[23]

unifying theme is the control of matter on the molecular level in scales smaller than 1 μm, normally 1–100 nm, and the fabrication of devices within that size range. Nanotechnology is being used to enhance conventional ceramic and polymeric water treatment membrane materials through various avenues. Among the numerous concepts proposed, the most promising to date include zeolitic and catalytic nanoparticle coated ceramic membranes, hybrid inorganic–organic nanocomposite membranes, and bio-inspired membranes such as hybrid protein–polymer biomimetic membranes, aligned nanotube membranes, and isoporous block copolymer membranes [30].

The top ten nanotechnology applications are:

1. Energy storage, production, and conversion.
2. Agricultural productivity enhancement.
3. Water treatment and remediation.
4. Disease diagnosis and screening.
5. Drug delivery systems.
6. Food processing and storage.
7. Air pollution and remediation.
8. Construction.
9. Health monitoring.

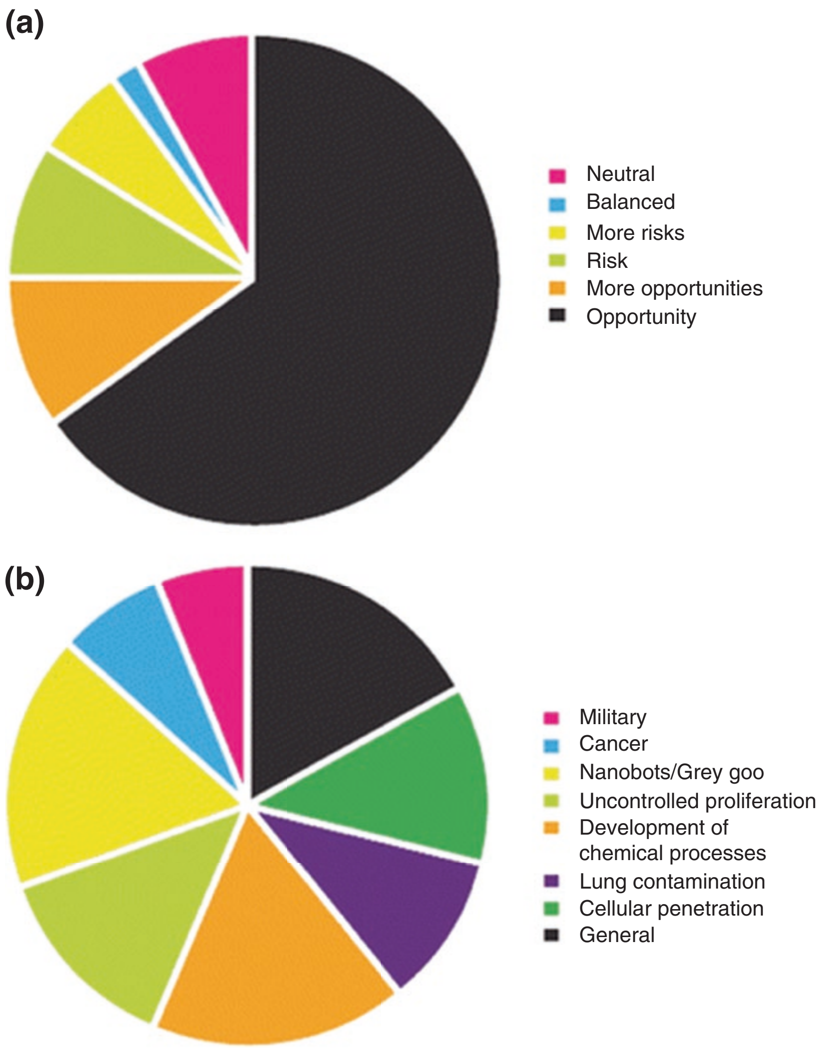

Fig. 1.1 European Union (EU) result of people survey: (**a**) balance between perceptual opportunities and risks of nanotechnology and (**b**) hypothetical risks of nanotechnology development [24]

10. Vector and pest detection and control.

1.5 Nanofibers

"With the ability to mass-produce nanofibers, electrospinning may well be one of the most significant nanotechnologies of this century" [31].

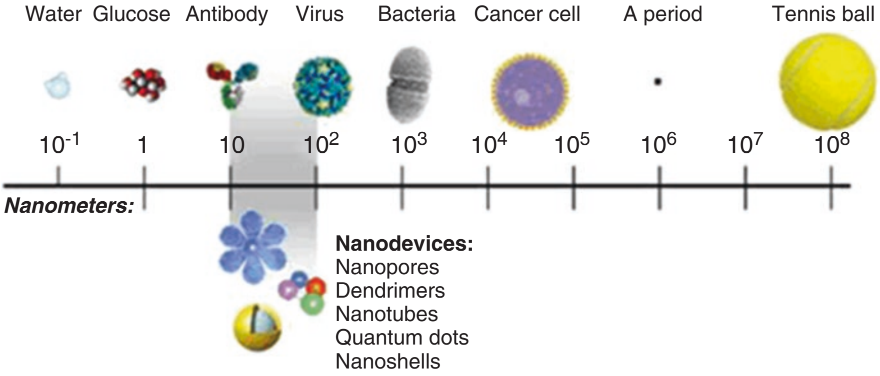

Fig. 1.2 Nanoscale and nanostructures [16]

Nanofibers were first produced via electrospinning more than four centuries ago [8, 9]. Beginning with the development of the electrospinning method, Gilbert first documented the electrostatic attraction between liquids by preparing an experiment in which he observed a spherical water drop on a dry surface warp changed into a cone shape when it was held below an electrically charged amber [32]. This deformation later came to be known as the Taylor cone [33]. Afterward, Religh analyzed the unstable states of liquid droplets that were electrically charged, and noted that the liquid was ejected in tiny jets when equilibrium was established between the surface tension and electrostatic force [34]. In 1887, Boys published a manuscript about nanofiber development and production [35]. In 1899, Cooley filed the first modern electrospinning patent [36].

The nanofibres/nanowires are classically defined as one-dimensional nanomaterials which typically have a diameter in the range 1–100 nm and length of the order of 1000 nm and above. Nanofibers have attracted a great deal of attention due to their remarkable properties. Compared to conventional fibrous structures, nanofibers are lightweight with small diameters, controllable pore structures and high surface-to-volume ratio, making them ideal for use in applications as varied as filtration, sensors, protective clothing, tissue engineering, functional materials and energy storage. Nanofibres are a relatively new class of materials that have promising potential for use in many medical and health care applications. Nanofibers can be generated from different polymers/inorganic materials and hence have different physical properties and application potentials. Nanofibers have many possible technological and commercial applications. They are used in tissue engineering, drug delivery, cancer diagnosis, lithium-air battery, optical sensors, and air filtration. The diameters of nanofibers depend on the type of polymer/inorganic material used and the method of production. All polymer nanofibers are unique for their large surface area-to-volume ratio, high porosity, appreciable mechanical strength, and flexibility in functionalization. The preparation and applications of electrospun fibers is briefly shown in Fig. 1.3 [37].

1.6 Nanoparticles (NPTs)

Nanoparticles are always present in the atmosphere of the planet. It originates from volcanic eruptions or fine desert dust lifted by air currents, and interstellar dust as such or resulting from meteorite disintegration. Nanoparticles are also produced from the various human activities, from the industrial exhaust gas, thermal power or cement plant stacks, engine jets or fireworks. Many properties of the nanoparticles are directly connected to their small size. The small size leads to many distinct properties, which influence the lattice symmetry and cell parameters.

Nanoparticle research is currently an area of intense scientific research, due to a wide variety of potential applications in biomedical, optical, and electronic fields. Nanoparticles are considered a discovery of the twentieth century, but a brief overview of the field reveals that artisans in Mesopotamia used finely divided materials of this type as early as the ninth century BC, to obtain a glittering effect on the surface of ceramic vessels [7]. Nanoparticles may contain a single material or may consist of a combination of several materials, and often have unexpected visible properties because they are small enough to confine their electrons and produce quantum effects. Nanoparticles have an extremely high surface area to volume ratio. This provides a tremendous driving force for diffusion, especially at elevated temperatures. The large surface area to volume ratio also reduces the incipient melting temperature of nanoparticles. Nanoparticles can exist as suspensions, colloids, or dispersed aerosols depending on their chemical and electromagnetic properties. The properties of nanoparticles are dependent on their size [38]. For instance, copper nanoparticles smaller than 50 nm are super hard materials and do not exhibit the properties of malleability or ductility of bulk copper. Nanoparticles are of great scientific interest as they are, in effect, a bridge between bulk materials and atomic or molecular structures. A bulk material should have constant physical properties regardless of its size, but at the nano-scale size-dependent properties are often observed. Thus, the properties of materials change as their size approaches the nanoscale and as the percentage of the surface in relation to the percentage of the volume of a material becomes significant. For bulk materials larger than 1 μm (or micron), the percentage of the surface is insignificant in relation to the volume. The interesting and sometimes unexpected properties of nanoparticles are therefore largely due to the large surface area of the material, which dominates the contributions made by the small bulk of the material [39]. Other changes that are dependent on the size of nanoparticles are super paramagnetism exhibited by magnetic materials, quantum confinement by semiconductor Q-particles, and surface plasmon resonance in some metal particles [40].

Nanoparticles are particles between 1 and 100 nanometres (nm) in size with a surrounding interfacial layer. The interfacial layer is an integral part of nanoscale matter, fundamentally affecting all of its properties. The interfacial layer typically consists of ions, inorganic and organic molecules [41]. The term is sometimes used for larger particles, up to 500 nm, or fibers and tubes that are less than 100 nm in only two directions. At the lowest range, metal particles smaller than 1 nm are usually

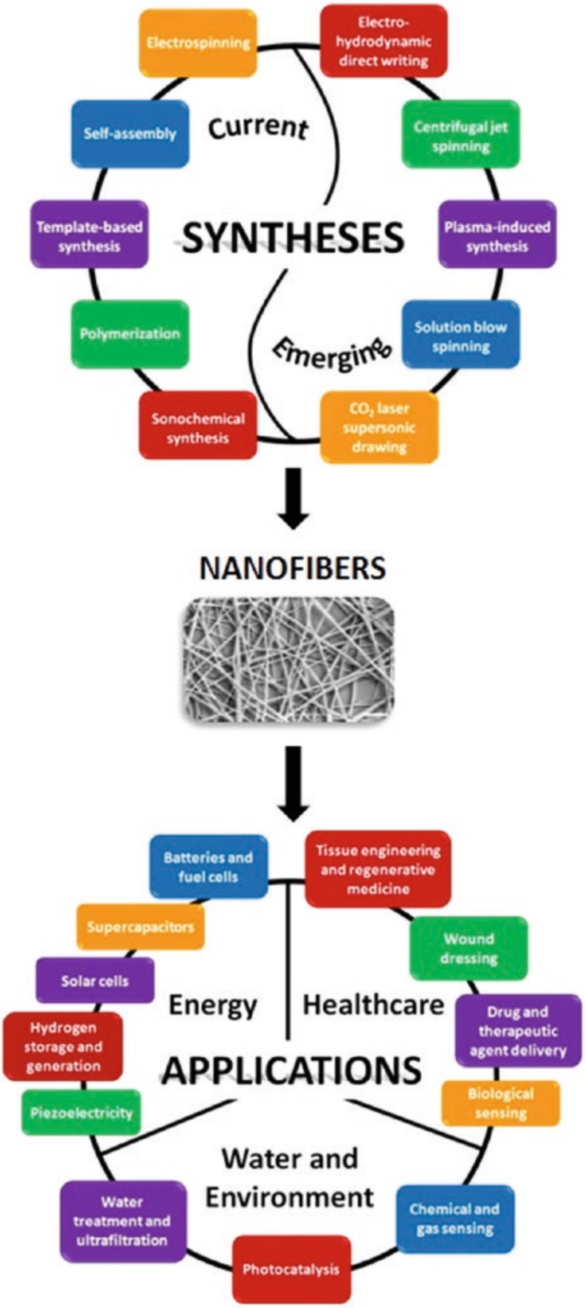

Fig. 1.3 Syntheses and applications of nanofiber technology. Different strategies have been developed for the synthesis of nanofibers, ranging from current methods (e.g., electrospinning, self-assembly, and polymerization and template-based synthesis) to emerging strategies (e.g., solution

Table 1.2 EPA terminology for particle sizes

EPA description	Particle sizes
Super coarse	$d_{pa} > 10\ \mu m$
Coarse	$2.5\ \mu m < d_{pa} \leq 10\ \mu m$
Fine	$0.1\ \mu m < d_{pa} \leq 2.5\ \mu m$
Ultrafine	$d_{pa} \leq 0.1\ \mu m$

called atom clusters instead. Organic molecules coating inorganic nanoparticles are known as stabilizers**,** capping and surface ligands**,** or passivating agents [42]. In nanotechnology, a particle is defined as a small object that behaves as a whole unit with respect to its transport and properties. Particles are further classified according to diameter [43]. The EPA (U.S. Environmental Protection Agency) has defined four terms for categorizing particles of different sizes. Table 1.2 displays the EPA terminology along with the corresponding particle sizes [44].

Figure 1.4 provides a visual comparison and surface area of the size of a fine particle (1.0 μm), coarse particle (10 μm), and a supercoarse particle (100 μm). There is a substantial difference in size between these particles [45]. The diagram assumes that all particles in each category are perfect spheres, have the same density, and are present in an equal amount of mass. The mass, particle number, and surface area of coarse particles are all arbitrarily designated as 1.

The shortest definition of nanoparticles, which is probably the most intuitive one, takes into consideration only their size, which is limited conventionally to about 100 nm in any direction. This definition cannot be exhaustive, as it does not give net values. But without a classification, no matter how general, it is difficult to differentiate between the molecular and atomic field on the one hand and the nanoparticle field on the other.

The presence of dispersed inorganic nanoparticles in the polymeric matrix has been useful for the improvement of membrane performance for processes, ranging from gas separation and pervaporation, to nanofiltration and ultrafiltration. Each of these inorganic nanofillers can be incorporated in most of the polymeric materials available to produce membranes with specific characteristics, as a result of the synergism in properties between the polymeric materials and nanoparticles. Polymeric membranes modified by adding nanoparticles possess properties of both organic and inorganic membranes such as good hydrophilicity, selectivity, permeability, mechanical strength, and thermal and chemical stability.

Nanoparticles are being developed to clean industrial water pollutants in ground water through chemical reactions that render the pollutants harmless. This process would cost less than the methods that require pumping the water out of the ground for treatment [7].

Fig. 1.3 (continued) blow spinning, centrifugal jet spinning, and electrohydrodynamic writing). Simultaneously, nanofiber technology has increasingly found applications in a wide range of areas, such as energy storage and generation, water treatment and environmental remediation, and healthcare and biomedical engineering [37]

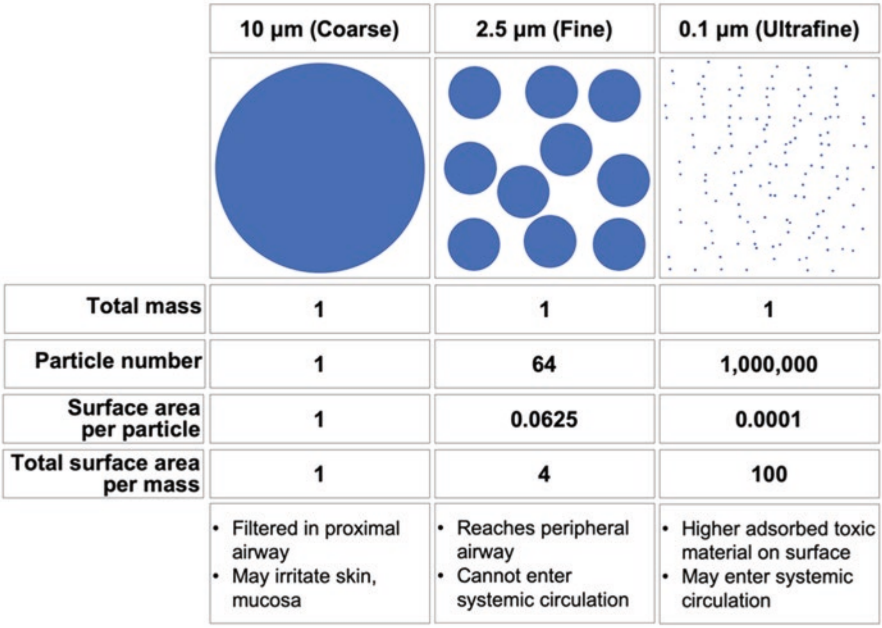

	10 µm (Coarse)	2.5 µm (Fine)	0.1 µm (Ultrafine)
Total mass	1	1	1
Particle number	1	64	1,000,000
Surface area per particle	1	0.0625	0.0001
Total surface area per mass	1	4	100
	• Filtered in proximal airway • May irritate skin, mucosa	• Reaches peripheral airway • Cannot enter systemic circulation	• Higher adsorbed toxic material on surface • May enter systemic circulation

Fig. 1.4 Comparison of the surface area of particles with different diameters [45]

Origin

1. Natural
2. Inthropogenic

Size

1. 1–10 nm
2. 10–100 nm
3. Over 100 nm

Chemical Composition

1. Inorganic substances.
2. Organic substances.
3. Elements of the living kingdom.

Since the range of particle sizes of concern for air emission evaluation is quite broad it is beneficial to divide this range into smaller categories. Defining different size categories is useful since particles of different sizes behave differently in the atmosphere and the respiratory system.

The importance of nanomaterial was realized when it was found that size can influence the physiochemical properties of a substance e.g. the optical properties. A 20-nm gold (Au), platinum (Pt), silver (Ag), and palladium (Pd) NPs have characteristic wine red color, yellowish gray, black and dark black colors, respectively.

Figure 1.5 shows an example of this illustration, in which Au NPs were synthesized with different sizes.

Nanoparticles affect the permeability, selectivity, hydrophilicity, conductivity, mechanical strength, thermal stability, and the antiviral and antibacterial properties of the polymeric membranes [48]. However, it is necessary to choose appropriate nanoparticles to be incorporated into polymeric membranes, as nanoparticles might change or even deteriorate the performances of the membranes. The potential for nanoparticles (NPs) is infinite, with novel new applications constantly being explored. The possible toxic health effects of these NPs associated with human exposure are unknown. Many fine particles generally considered "nuisance dusts" are likely to acquire unique surface properties when engineered to nanosize and

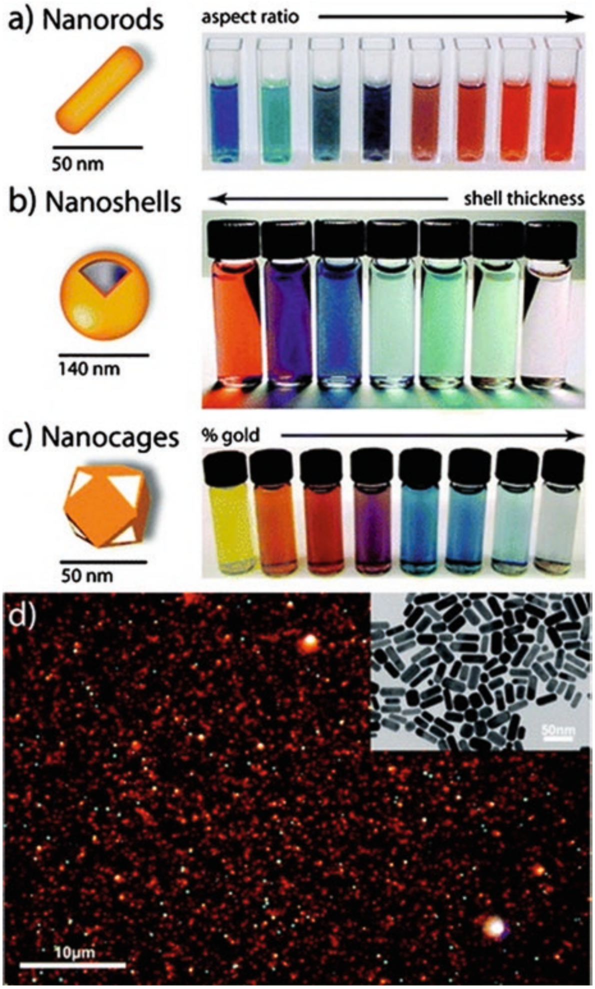

Fig. 1.5 Color dependence of Au NPs on size and shape [46, 47]

may exhibit toxic biological effects. So far, we do not have enough knowledge about the health effects associated with NPT exposure.

1.7 Membrane

Membrane separation technology is a new type of high-efficiency separation technology developed rapidly in recent decades. Membrane separations are powerful tools for various applications, including wastewater treatment and the removal of contaminants from drinking water. Membrane separation processes operate without heating and therefore use less energy than conventional thermal separation processes such as distillation, sublimation, or crystallization. The separation process is purely physical and both fractions (permeate and retentate) can be used. Membranes can be homogenous, heterogeneous, having positive and negative charges, can even be bipolar, symmetrical, and asymmetrical. The choice of material (polymer, chemical) used depends on the necessities imposed and kind off goal.

1.7.1 Membrane Definition

A membrane is a permselective barrier that allows particular species to pass through it while posing a partition for non-selective species. The membrane technologies are fast-developing and cutting-edge separation technologies that could be extensively employed in environmental remediation, green energy, food, chemical and pharmaceutical sectors.

In general, six major membrane processes, including microfiltration (MF), ultrafiltration (UF), reverse osmosis (RO), electro dialysis (ED), gas separation (GS) and pervaporation (PV) have found use in such applications. The key membrane performance variables are selectivity, permeability, and durability.

The commercial success of membrane technologies is grounded in the continuous innovation in the areas of membrane materials and processes. Recent developments in the materials science of membranes have been fueled in large part by advances in nanotechnology. Membranes with improved permeability, selectivity, and resistance to fouling have been developed using newly available nanomaterials.

In membrane separation process the following terminologies are used:

1. Volume flux: The volume of the solvent collected on the permeate side per unit area of the membrane per unit time (kg m^{-2} h^{-1}).
2. Mass flux of solute: The mass of the permeated solute collected on the permeate side per unit area of the membrane per unit time (kg m^{-2} h^{-1}).
3. Solvent flux: Flux is calculated based only on solvent permeation.

4. Concentration polarization (CP): CP occurs when solutes on the membrane surface build up thereby reducing flux and is considered a major hindrance in the sustainable use of membrane.
5. Fouling: Process resulting in loss of performance of a membrane due to the deposition of suspended or dissolved substances on its external surfaces, at its pore openings, or within its pores.
6. Permeability: Specific flux of clean, deionized water through a new membrane.
7. Specific flux: Flux divided by transmembrane pressure.
8. Permeate: Water and permeable components that pass through a membrane.

Membrane can be divided into three groups:

1. Biological Membranes.
2. Artificial membranes.
3. Theoretical membranes.

Further Membranes can be divided as

Biological Membranes

1. Cell membrane and intercellular membranes
2. Mucous membranes
3. S-layer
4. Serous membranes and mesothelial surrounded organs, including:
    (a) The peritoneum that lines the abdominal cavity
    (b) The pericardium that surrounds heart
    (c) The pleura that surrounds the lungs
    (d) The periosteum that surrounds bone
    (e) The meanings that surround the brain (the dura mater, the arachnoid, and the pia matter)

Artificial membranes are used in:

1. Reverse osmosis
2. Filtration (microfiltration, ultrafiltration)
3. Pervaporation
4. Dialysis
5. Emulsion liquid membranes
6. Membrane based solvent extraction
7. Membrane reactors
8. Gas permeation
9. Supported liquid membranes

1.7.1.1 Composite Membranes

Composite membranes are made of a porous layer as a support coated with a selective thin layer. Sometimes composite membrane is used for mixed matrix membrane (MMM). Figure 1.6 shows the schematic of thin film composite membrane.

1.7.1.2 Nanocomposite Membranes

Nanocomposites are a composite in which at least one dimension of the dispersed phase (i.e. the filler) is in the nanometer range. In the other words, a nanocomposite is like a multiphase solid material in which one of the phases has one, two, or three dimensions of less than 100 nm, or structures with nanoscale repeat distances between the different phases that make up the material. Adding nanoparticulates appropriately to a polymer matrix can enhance its performance, often to a dramatic degree, simply by capitalizing on the nature and properties of the nanoscale filler [50]. This strategy is particularly effective in yielding high performance composites, when good dispersion of the filler is achieved and the properties of the nanoscale filler are substantially different from or better than those of the matrix: e.g. reinforcing a polymer matrix by much stiffer nanoparticles of ceramics, clays, or carbon nanotubes [51].

Nanocomposite materials are two-phase systems that consist of a matrix and dispersed particles of nanometer scale. Generally, nanocomposite filtration membranes present a polymer matrix and inorganic dispersed particles, which can be particles (e.g., calcium carbonate), fibers (e.g., glass fibers), or plate-shaped particles (e.g., mica). Nanoporous membrane for water purification can generally be divided into three types based on their material composition [52]:

1. Inorganic, organic.

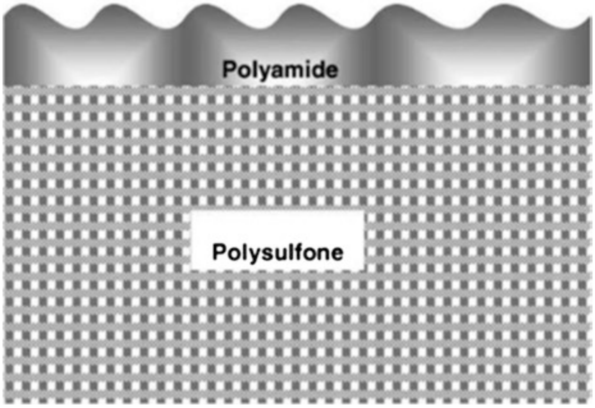

Fig. 1.6 Schematic of thin film composite membrane [49]

2. Inorganic-organic hybrid membranes.
3. Inorganic membranes are mainly made of ceramics (Al_2O_3, TiO_2, ZrO_2, SiO_2, TiO_2-SiO_2, TiO_2-ZrO_2, Al_2O_3-SiC), graphene, and carbon nanotubes (CNTs).

Organic membranes are mainly made of polymeric materials such as polyvinyl alcohol (PVA), polyimide (PI), polypropylene (PP), polyethersulfone (PES), cellulose acetate (CA), cellulose nitrates, polysulfone (PSf), polyvinylidene fluoride (PVDF), polyacrylonitrile (PAN), polytetrafluoroethylene (PTFE), and biomacromolecules. Inorganic-organic hybrid membranes are usually made by introducing inorganic materials (metals, metal oxide, or carbon-based materials) into a polymeric matrix system.

Nanocomposite membranes consist of nanoparticles embedded in a thin-film composite membrane (Fig. 1.7). Zeolite nanoparticles are dispersed onto polyamide films to produce relatively smooth and hydrophilic, negatively charged surfaces that could be optimized to produce more effective.

1.7.1.3 Mixed Matrix Membranes (MMMs)

Mixed matrix membranes (MMMs) are considered as a new-generation membrane and have become a focus for research and development in both academic and industrial interests due to their unique properties combining inherent characteristics of polymer and inorganic fillers. MMMs are heterogeneous membranes consisting of inorganic fillers dispersed in a polymer matrix. By adding filler particles to a polymer matrix to make MMMs, it is possible to move beyond the performance limitations of conventional polymer films. The use of filler particles can result in increasing the polymer's free volume, thus increasing the membrane permeability. Figure 1.8 shows MMM schematically.

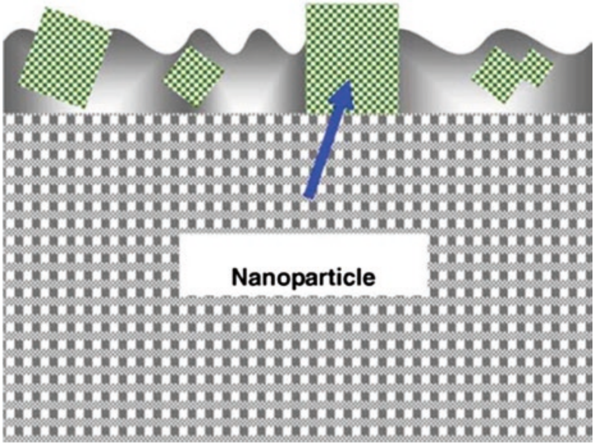

Fig. 1.7 Thin-film nanocomposite membrane [49]

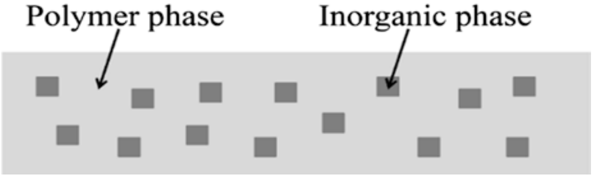

Fig. 1.8 Schematic diagram of MMM

Mixed matrix membranes generally contain porous materials as fillers playing a sieving role with sorption capacity. Gas transport mechanism through MMMs is solution-diffusion and the dispersed phase (porous nanoparticles) shows the same mechanism, solution-diffusion. Therefore, addition of porous nanoparticles ideally improves sorption or diffusion coefficient, or both. Hybrid membranes composed of porous inorganic materials with molecular sieving effect (such as MOFs and Zeolites) are called mixed matrix membranes. On the other hand, there are another type of MMMs that contain nano particles which are not permeable or have no sieving effect. Polymer containing TiO_2 is one of such examples. The presence of nanoparticles in polymer matrix makes the diffusion path longer for undesired gas to pass through membrane. They provide better affinity with the specific component and can also improve the solubility of a gas molecule.

For water purification applications, polymeric membranes have been widely used. However, the trade-off issue between the selectivity and permeability has limited its use in various applications [53]. To overcome this limitation and to enhance the properties and performance of polymeric membrane, MMMs with incorporation of fillers such as silica and zeolites are a proper choice. Metal-organic frameworks (MOFs) are a new class of hybrid inorganic-organic materials that are introduced as novel fillers for incorporation in polymeric matrix to form composite membranes for different applications especially for desalination. Major advantage of MOFs over other inorganic fillers is the possibility of preparing different structures with different pore sizes and functionalities, which are designed especially for a targeted application.

1.7.1.4 Liquid Membranes

Solids are not the only materials that have been used as membranes and it is possible to use a liquid as a membrane. Liquid membranes are present in various forms in daily life; an oil layer on a water surface is a typical organic liquid membrane of an immiscible liquid phase, beer froth, foam on soap, detergent or surfactant solutions, oil films coated on a metal surface—popularly used in rust protection and lubrication are familiar liquid films separating two phases.

A liquid membrane (LM) is literally a membrane made of liquid. It consists of a liquid phase (e.g. a thin oil film) existing either in supported or unsupported form that serves as a membrane barrier between two phases of aqueous solutions or gas mixtures. In other words, liquid membrane system involves a liquid which is an immiscible with the source (feed) and receiving (product) phases and serves as a semipermeable barrier between these two liquid and gas phases. Following three types of liquid membranes are usually considered.

1. Bulk (BLM),
2. Supported or immobilized (SLM or ILM).
3. Émulsion (ELM) liquid membrane.

Some authors add to these definitions: polymeric inclusion membranes, gel membranes, dual module hollow-fiber membranes [54]. These three configurations are shown schematically in Fig. 1.9.

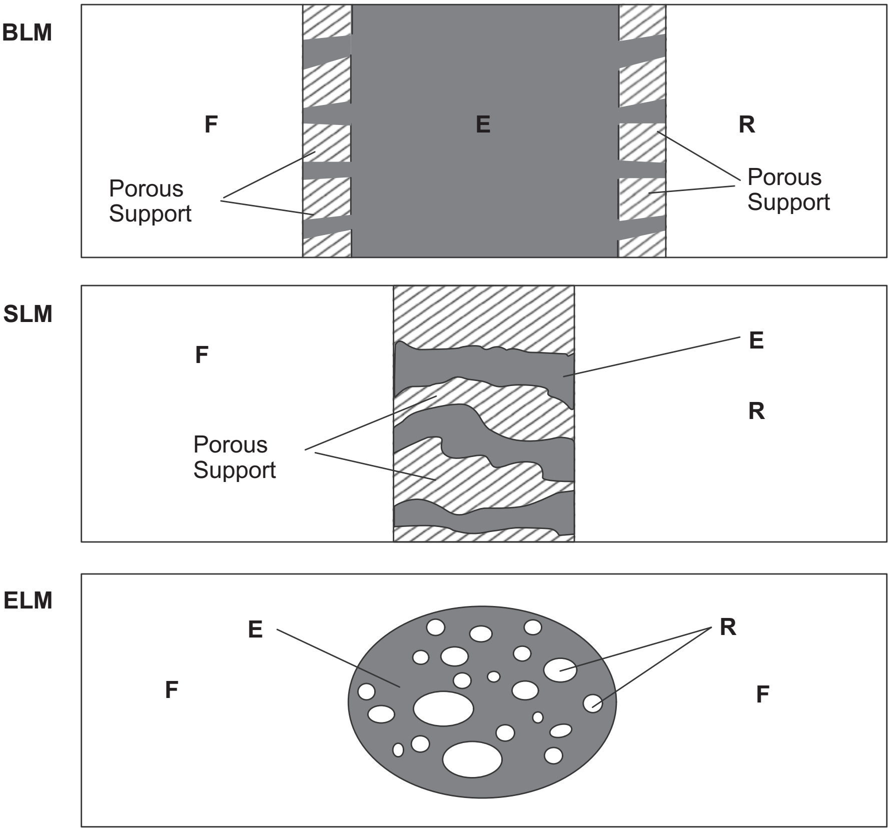

Fig. 1.9 Three configurations of liquid membrane systems: bulk (BLM), supported (immobilized) (SLM or ILM), and emulsion (ELM). F is the source or feed phase, E is the liquid membrane, and R is the receiving phase [54]

1.7.1.5 Ion-Exchange Membranes

An ion-exchange membrane is a semi-permeable membrane that transports certain dissolved ions, while blocking other ions or neutral molecules [55]. These membranes have the function of desalination and concentration of saline water. Further the membranes separate ionic species dissolved in a solution. Based on the fundamental studies, application of ion-exchange membranes is extending widely in many fields. The largest application is the demineralization of salt solutions. The other applications are desalination and reuse of sewage or industrial waste, refining of amino acid solutions, desalination of milk and sugar liquor, recovery of the useful components from industrial waste, production of inorganic chemicals, and so forth. Electro dialysis is a technology based on the ion-exchange membrane.

Ion exchange membranes (IEMs) have attracted much interest from the academic and industrial fields, due to their potential applications in electro membrane processes which include [56].

1. water purification, e.g., desalination by electro dialysis (ED), desalination by membrane capacitive deionization (MCDI), and diffusion dialysis.
2. energy production, e.g., as fuel cells, and reverse electro dialysis.
3. energy storage e.g., flow batteries.
4. chlor-alkali process.

IEMs contain charged groups, affixed to the polymer backbone of the membrane material, which partially or totally prevent ions with the same charge from passing through the membrane. Membranes with fixed positively charged groups, termed anion exchange membranes (AEMs), preclude the passage of cations but permit the passage of anions. Membranes with fixed negatively charged groups, termed cation exchange membranes (CEMs), prevent the passage of anions but allow cations to pass through. Based on this mode of operation, electro membrane desalination was developed, as evidenced by electro dialysis (ED) desalination—which is the first large-scale industrial process to utilize IEMs. To date, ED has been the most widely researched and commercially adopted electro membrane desalination process.

Ion-exchange membranes are traditionally used in electro dialysis or diffusion dialysis by means of an electrical potential or concentration gradient, respectively, to selectively transport cationic and anionic species. When applied in an electro dialysis desalination process, anion- and cation-exchange membranes are typically arranged in an alternating pattern between two electrodes (an anode and a cathode) within the electro dialysis stack. A galvanic potential is supplied as a voltage generated at the electrodes [57]. Incorporation of nanomaterials (NMs) into IEMs has also been investigated as a means of improving their properties [58, 59].

Most of the cases where nanomaterials (NMs) were incorporated in IEMs are in the fuel cells research area, with fewer reports related to ED desalination. The properties of IEMs primarily depend on:

1. Membrane material, which chiefly determines the mechanical, chemical, and thermal stability of IEMs.

2. Type, concentration, and distribution of the ion exchange groups which determine the electrochemical properties of the IEMs and happen to considerably influence the other IEMs properties.

The electrochemical properties are the most significant properties in ED.

1.7.1.6 Ceramic Membranes

The use of ceramics (compared to polymers) offers a narrow pore size distribution exactly matching the components to be separated, resistance against aggressive chemicals, high temperatures, a high and constant flux, and a long service life. Ceramic carriers are an ideal base for membranes and micro-filtration applications in the chemical, pharmaceutical and food industry as well as in water and wastewater processing.

1.7.1.7 Cell Membranes

A membrane either on the surface or interior of a cell is composed of protein and lipid especially in sheets of a thickness of only a few molecules, limiting the diffusion and transport of materials. The cell membrane is one of the most fundamental constituents in biological systems, creating the physical boundaries of cells. The major components of cell membranes include amphiphilic lipids, cholesterols, and membrane proteins. Artificial membranes are traditionally reconstructed either by painting a lipid solution or by folding two monolayers [60, 61]. The lipid conventionally used to create biomimetic membranes is lecithin, isolated from egg yolk**.** Cell membrane (also known as the plasma membrane (PM) or cytoplasmic membrane, and historically referred to as the plasmalemma) is a biological membrane that consists of a lipid bilayer with embedded proteins and separates the interior of all cells from the outside environment (the extracellular space) to protect the cell from its environment. Cell membranes contain a variety of biological molecules, notably lipids and proteins. The cell membrane controls the movement of substances in and out of cells and organelles. In this way, it is selectively permeable to ions and organic molecules [59].

The permeability of a membrane is the rate of passive diffusion of molecules through the membrane. These molecules are known as permeant molecules. Permeability depends mainly on the electric charge and polarity of the molecule and to a lesser extent the molar mass of the molecule. Due to the cell membrane's hydrophobic nature, small electrically neutral molecules pass through the membrane more easily than charged, large ones. The inability of charged molecules to pass through the cell membrane results in pH partition of substances throughout the fluid compartments of the body.

1.7.1.8 Biometric Membranes

Biological membranes rely on their intricate structures and a host of different mechanisms to implement efficient separations. Biological membranes play an essential role in the cellular protection as well as in the control and the transport of nutrients and display an overly complex composition in terms of lipids and protein. Biomimetic membranes incorporate biological elements or borrow concepts, ideas or inspiration from biological systems [62].

Biomimetic membranes technology is based on a combination of biologically derived membranes' proteins (e.g. aquaporin) and bioinspired synthetic polymers. Biometric-hybrid membranes are basically biomimetic membranes that are based on natural/biological membrane proteins. Such membranes are composed of artificial lipid bilayers, BCP bilayers, or solid-state nanopores, which are formed by reordering natural membrane proteins.

Aquaporins, also known as the water channels in living cell membranes, have been found to be the functional unit of nature's water purification systems. A promising approach to this concept is based on the use of aquaporin molecules, a naturally-existing protein that serves the important function of maintaining osmoregulation in living organisms by facilitating water transport through cell walls. Thus biomimetic membrane is an innovation in water filtration technology that aims to replicate a natural process occurring at the cell level—specifically, the highly-selective and efficient transport of water molecules across a cell membrane [63]. The application of biomimetic membranes for the separation of liquid and gas gives it an edge over other membranes in the long run as in this way they can be termed as more versatile as their benefits are widespread in nature. The key advantage of the aquaporin molecule is the ability to restrict the passage of contaminants including bacteria, viruses, minerals, proteins, DNA, dissolved gases, salts, detergents, and even protons without encumbering the passage of water. A breakthrough in biomimetic membrane technology using aquaporins (AQPs) can potentially reduce industrial water treatment costs by 30%, say researchers at the National University of Singapore (NUS) Environmental Research Institute [64]. AQPs are membrane proteins that selectively conduct water molecules in and out of cells, preventing the passage of ions and other solutes. These channels are present in all living things from bacteria to mangrove plants and human kidneys and are examples of membrane structures that allow high volume of water molecules to pass through a small surface area at very low pressures, leaving behind impurities such as salt.

1.8 Pores in Membrane

Membrane pore is defined as a minute opening by which matter passes through a membrane. Figure 1.10 shows the range of nominal membrane pore sizes of different membranes.

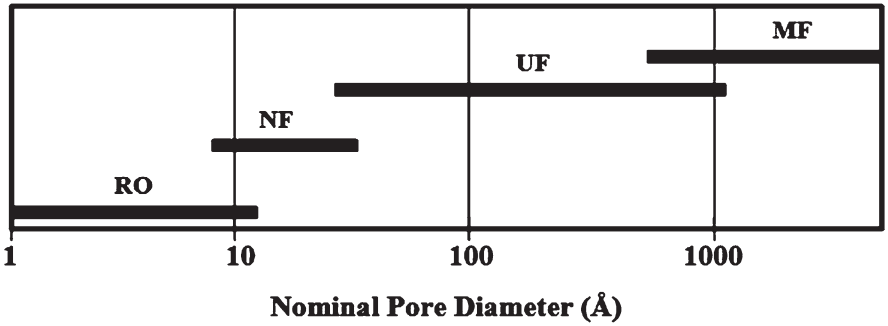

Fig. 1.10 Range of nominal membrane pore sizes

Membrane permeation properties are largely governed by the pore sizes and pore size distribution. However, thermal, chemical, mechanical, and biological stability of the membrane cannot be ignored.

Nanopore is a pore of nanometer size. It may, for example, be created by a pore-forming protein or as a hole in synthetic materials such as silicon or graphene.

Biological Nanopores: It may be formed by pore-forming proteins, typically a hollow core passing through a mushroom-shaped protein molecule. Examples of pore-forming proteins are alpha haemolysins and MspA porin. In typical laboratory nanopore experiments, a single protein nanopore is inserted into a lipid bilayer membrane and single-channel electrophysiology measurements are taken [65].

Solid-state nanopores: Solid-state nanopores are generally made in silicon compound membranes, one of the most common being silicon nitride. Solid-state nanopores can be manufactured with several techniques including ion-beam sculpting [66, 67].

1.9 Filtration

Filtration is a process of removing particulate matters from water by forcing the water through a porous media. This porous media can be natural, in the case of sand, gravel and clay, or it can be membrane made of various materials. Sometimes, large particles are settled before filtration; this is called sedimentation. The size of materials that can be removed during filtration depends upon the size of the pores of the filter. The chart below summarizes the various separation processes relative to common materials that would be filtered out through each process (Fig. 1.11). Particle filtration refers to conventional media filtration, while the other types are membrane filtrations.

Figure 1.12 demonstrates a comparative length scales of filtration and particle sizes. Shaded area denotes nanotechnology realm. IX = ion exchange; RO = reverse osmosis; NF = nanofiltration; MF = microfiltration [69]. The appellation 'nano' is

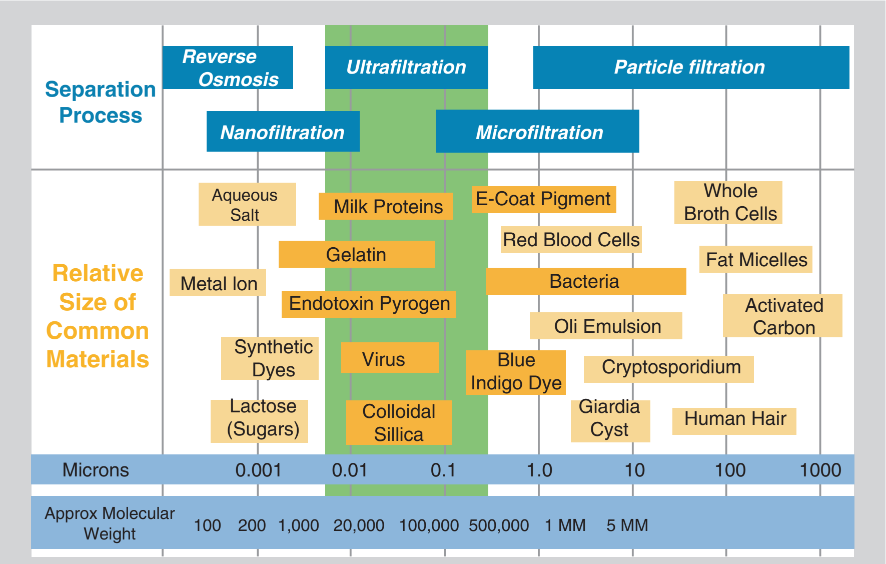

Note: 1 micron (micrometer) = 4 × 10-5 inches = 1 × 104 Angstrom units ©2004 - Koch Membrane Systems

Fig. 1.11 Size of materials that are removed by various separation processes [68]

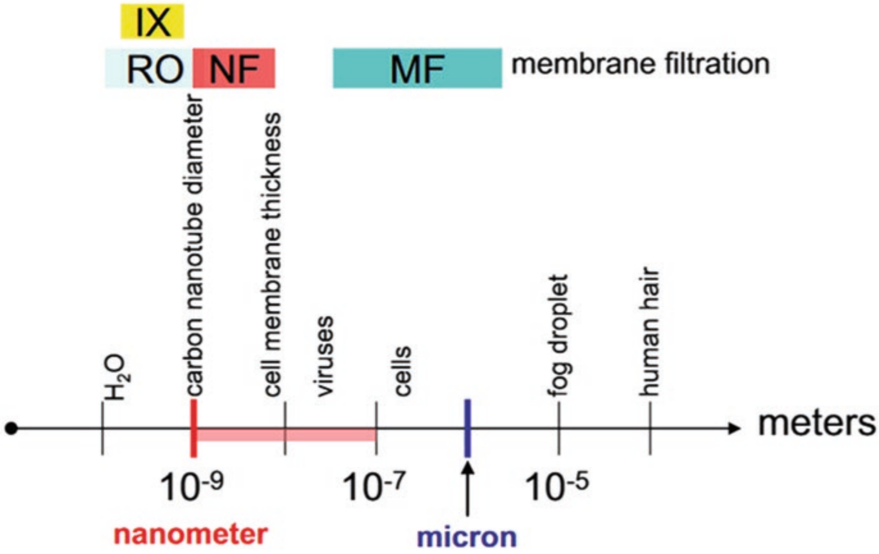

Fig. 1.12 Comparative length scales of filtration and particle sizes. Shaded area denotes nanotechnology realm. *IX* ion exchange, *RO* reverse osmosis, *NF* nanofiltration, *MF* microfiltration [69]

commonly applied to structures and processes having at least one dimension in the 1–100 nm range (Fig. 1.12). Three to five atoms could potentially be lined up in a nanometer.

The chart below (Fig. 1.13) summarizes the types of particles that are removed from the water with each type of membrane filter. The green arrow indicates that the particle is small enough to pass through the filter, whereas the deflected orange arrow indicates that the filter blocks the particle from passing through the filter.

1.9.1 Ultrafiltration (UF)

Ultrafiltration is a variety of membrane filtration in which forces like pressure or concentration gradients lead to a separation through a semipermeable membrane. Suspended solids and solutes of high molecular weight are retained in the so-called retentate, while water and low molecular weight solutes pass through the membrane in the permeate (filtrate). This separation process is used in industry and research for purifying and concentrating macromolecular (10^3–10^6 Da) solutions, especially protein solutions. Ultrafiltration is not fundamentally different from microfiltration. Both separate matters based on size exclusion or particle capture. It is fundamentally different from membrane gas separation, which separates gases based on different amounts of absorption and different rates of diffusion. Ultrafiltration

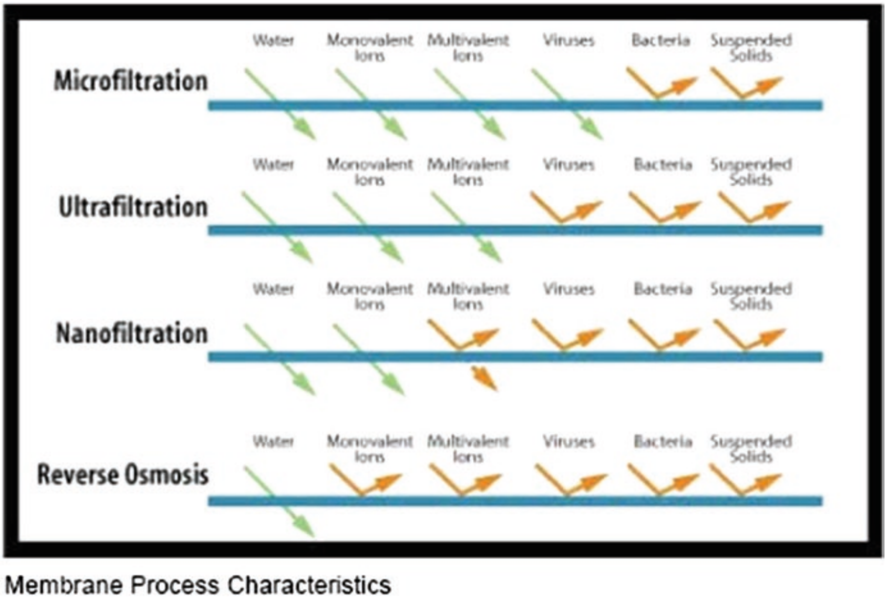

Fig. 1.13 Substances removed from water by membrane filtration processes [68]

membranes are defined by the molecular weight cut-off (MWCO) of the membrane used. Ultrafiltration is applied in crossflow or dead-end mode.

1.9.2 Nanofiltration (NF)

NF is a pressure-driven membrane separation technique. Nanofiltration membranes are defined as having a pore size in the order of nanometers (nm) (1×10^{-9} m). In other words, nano-filtration membranes possess pores with a size of approximately 1 nm. As a comparison, the atomic radius of a hydrated sodium ion and a chlorine ion is about 0.97 nm (0.97×10^{-9} m) and 1.8 nm (1.8×10^{-9} m), respectively [70].

This demonstrates that nanofiltration membranes are near the range to remove rather small ions. Most nanofiltration membranes are hydrophilic, thus they are used to remove charged molecules or uncharged (mostly organic) compounds from aqueous solution.

Nanofiltration is a relatively recent membrane filtration process used most often with low total dissolved solids water such as surface water and fresh groundwater, for the purpose of softening (polyvalent cation removal) and removal of disinfection by-product precursors such as natural organic matter and synthetic organic matter. Nanofiltration is also becoming more widely used in food processing applications such as in dairy industry, for simultaneous concentration and partial (monovalent ion) demineralisation [68, 71]. Different types of nanofiltration membranes are used for different separation processes.

Nano-filtration membranes possess pores with a size of approximately 1 nm. Nano-filtration membranes are characterised based on their retention [69, 70] of charged and uncharged particles. The retention of a nano-filtration membrane can be determined via experimental filtration tests with pre-selected molecules. A simple salt solution (NaCl or Na_2SO_4) is selected for charged particles. Polysaccharides (dextrins) or polyethylene glycols (PEG) with various molecular weights are selected for uncharged particles. The salt retention of a typical nanofiltration membrane is considerably lower than, for example, reverse osmosis, while salt retention is almost zero for ultra-filtration.

A nano-filtration membrane is also ion-selective. This is the ability to distinguish various ions from one another. Because a nanofiltration membrane collects solid charged groups in its membrane structure, electrostatic repulsion/attraction forces may occur between the components in the liquid and the (nanofiltration) membrane surface, which results in a certain degree of ion selectivity. Based on the sieve effect (pore size 1 nm) and the ionic size of chlorides (0.12 nm in size) and sulphates (0.23 nm in size), these ions are expected to diffuse through the membrane. Despite this, the retention for chlorides is maximum 90% and that of sulphates is minimum 90%.

NF membrane meanwhile exhibits pore size that falls between those of UF and RO membranes. In addition to its nano-scale pore structure, the NF membrane usually possesses negative surface charge that allows it to reject effectively multivalent ions [72]. In other words, the separation process in NF is governed by steric exclusion coupled with charge repulsion mechanisms.

A nanofiltration membrane can be tubular, spiral, or flat in shape. A schematic diagram of an SWM (spiral-wound modules) is shown in Fig. 1.14 [73] The major components of an SWM module are the membrane, the feed and permeate spacers which keep the membrane leaves apart, the collection tube, and the envelope. A collection tube that was placed on the module winder was stuck to the permeate spacer and wound up two or three turns.

1.9.2.1 Specific Advantages and Disadvantages

Here are a few specific advantages and disadvantages of NF:

Advantages

1. Lower discharge volumes, lower retentate concentrations than RO for low value salts.
2. Reduction salt content and dissolved matter content (TDS) in brackish water.
3. Reduction in heavy metals.
4. Reduction in nitrates and sulphates.
5. Reduction in colour, tannins and turbidity.
6. Softens hard water when specific softening membranes are used.
7. “chemical-free”, e.g. needs no salt or chemicals during operation.
8. pH of water after nanofiltration is normally non-aggressive.
9. Disinfection.

Disadvantages

1. Higher energy consumption than UF and MF (0.3–1 kWh m^{-3}).
2. Pre-treatment is needed for some heavily polluted waters (pre-filtration 0.1–20 microns). This is always the case with spiral-wound membranes.
3. Limited retention for salts and univalent ions.
4. Nanofiltration membranes are a little more expensive than reverse osmosis membranes.
5. Membranes are sensitive to free chlorine (lifespan of 1000 ppm h). An active carbon filter or a bi-sulphite treatment is recommended for high chlorine concentrations.

Effectiveness

Micro-pollutants like herbicides and insecticides, as well as low-molecular weight components like colorants and sugars can be very successfully blocked using a nanofiltration membrane.

NF can be implemented for removing the following particles or solutes (removal yield indicated in brackets):

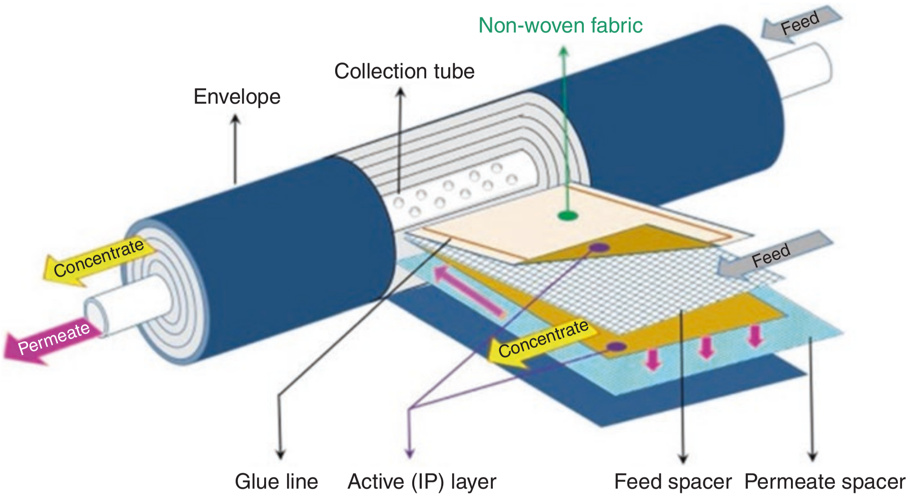

Fig. 1.14 Configuration of the SWM module and its working principle [73]

1. Dissolved matter (>75%).
2. Harmful micro-organisms, e.g. bacteria, protozoa, algae, fungi (>90%).
3. Persistent organic matter (50–75%).
4. Organic compounds (50–90%).
5. Nutrients (incl. phosphates).
6. Metals (50–90%).
7. Inorganic salts (e.g. sulphates).

1.9.3 Microfiltration (MF)

Microfiltration is a type of physical filtration process where a contaminated fluid is passed through a special pore-sized membrane to separate microorganisms and suspended particles from process liquid. It is commonly used in conjunction with various other separation processes such as ultrafiltration and reverse osmosis to provide a product stream which is free of undesired contaminants.

Microfiltration usually serves as a pre-treatment for other separation processes such as ultrafiltration, and a post-treatment for granular media filtration. Microfiltration membranes (MF) can trap particles between 0.1 and 1 microns. The filters used in the microfiltration process are specially designed to prevent particles such as, sediment, algae, protozoa or large bacteria from passing through a filter. More microscopic, atomic or ionic materials such as water (H_2O), monovalent species such as Sodium (Na^+) or Chloride (Cl^-) ions, dissolved or natural organic matter, and small colloids and viruses will still be able to pass through the filter [74–76].

1.9.4 Reverse Osmosis (RO)

Reverse osmosis is a water purification technology that uses a semipermeable membrane to remove ions, molecules, and larger particles from drinking water. In reverse osmosis, an applied pressure is used to overcome osmotic pressure, a colligative property, that is driven by chemical potential differences of the solvent, a thermodynamic parameter. Reverse osmosis can remove many types of dissolved and suspended species from water, including bacteria, and is used in both industrial processes and the production of potable water. The result is that the solute is retained on the pressurized side of the membrane and the pure solvent can pass to the other side. To be “selective”, this membrane should not allow large molecules or ions to pass through the pores (holes) but should allow smaller components of the solution (such as solvent molecules) to pass freely [77].

Reverse osmosis (RO) is a well-established membrane technology for the treatment of water in a variety of applications. Today, only polymeric RO/NF membranes are commercially available. Major problems associated with polymeric RO/NF membranes are:

1. excessive fouling due to poor feed flow hydrodynamics.
2. low resistance to chlorine and other oxidants.
3. extensive pre-treatment/chemical usage and associated waste generation.
4. lack of desirable surface charge to reduce fouling potential.

1.9.5 Forward Osmosis (FO)

Forward osmosis is an osmotic process that, like reverse osmosis (RO), uses a semi-permeable membrane to effect separation of water from dissolved solutes. The driving force for this separation is an osmotic pressure gradient, such that a "draw" solution of high concentration (relative to that of the feed solution), is used to induce a net flow of water through the membrane into the draw solution, thus effectively separating the feed water from its solutes. In contrast, the reverse osmosis process uses hydraulic pressure as the driving force for separation, which serves to counteract the osmotic pressure gradient that would otherwise favor water flux from the permeate to the feed. Hence significantly more energy is required for reverse osmosis compared to forward osmosis.

1.9.6 Pressure Retarded Osmosis (PRO)

In PRO a semipermeable membrane allows the solvent to pass to the concentrated solution side, which is under pressure, by osmosis. The technique can be used to generate power from the salinity gradient energy resulting from the difference in the salt concentration between sea and river water. In PRO, the water potential between fresh water and sea water corresponds to a pressure of 26 bars. This pressure is equivalent to a column of water (hydraulic head) 270 m high. However, the optimal working pressure is only half of this, 11–15 bar. This method of generating power was invented by Prof. Sidney Loeb in 1973 at the Ben-Gurion University of the Negev, Beersheba, Israel [78]. Figure 1.15 shows that the water potential between fresh water (right) and sea water (left) corresponds to a hydraulic head of 270 m [79, 80].

1.10 Summary

Nanotechnology is the science that deals with the manipulation of matter on an atomic, molecular, and supramolecular scale—in other words, much smaller than what the naked eye can see. The introductory chapter gives relevant historical

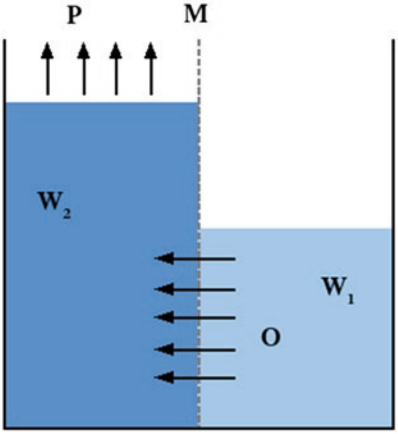

Fig. 1.15 The water potential between fresh water (right) and sea water (left) corresponds to a hydraulic head of 270 m [79, 80]

information about nanoparticles, nanotechnology, and different types of membranes. Although, nanoparticles are considered as a discovery of the twentieth century, it is true that artisans in Mesopotamia used finely divided materials of this type as early as in the ninth century BC, to obtain a glittering effect on the surface of ceramic vessels. The shortest definition of nanoparticles, which is probably the most intuitive one, takes into consideration only their size, which is limited conventionally to about 100 nm in any direction. Nanotechnology may be able to create many new materials and devices with a vast range of applications including a new avenue for the membrane process. There are many processes to use nanotechnology in different membrane processes in different ways, but mixing nanoparticles in membrane formation material is the main. The presence of nanoparticles in polymer matrix makes the diffusion path longer for undesired gas to pass through membrane. But the use of nanoparticles is controversial with respect to environment (health hazard). Although green nanotechnology poses many advantages over traditional methods, there is still much debate about the concerns brought about by nanotechnology.

References

1. Feynman RP (1960) There's plenty of room at the bottom. Eng Sci 23:22–36
2. Taniguchi N (1974) On the basic concept of nanotechnology. Proceedings of the international conference on production engineering, Tokyo, 1974, Part II. Japan Society of Precision Engineering
3. Bassett DR, Taniguchi N (2010) In: Guston DH (ed) Encyclopedia of nanoscience and society. SAGE, London, p 747. isbn: 9781452266176. Accessed 3 Aug 2014
4. Koodali RT, Klabunde KJ (2012) Nanotechnology: fundamental principles and applications. In: Kent JA (ed) Handbook of industrial chemistry and biotechnology, vol 1, 12th edn. Springer, New York, p 250. isbn: 9781461442592

5. Maynard AD (2010) Tracing and disputing the story of nanotechnology. In: Hodge GA, Bowman DM, Maynard AD (eds) International handbook on regulating nanotechnologies. Edward Elger, Cheltenham. isbn: 9781848446731
6. Radu M, Repanovici A (2004) O istorie a tiparului şi a tipăriturilor, Braşov Ed. Univ. Transilvania
7. Strambeanu N, Demetrovici L, Dragos D, Lungu M (2015) Chapter 1. Nanoparticles: definition, classification, general physical properties. In: 'Nanoparticles' promises and risks: characterization, manipulation, and potential hazards to humanity and the environment. Springer, Cham, pp 3–5. https://doi.org/10.1007/978-3-319-11728-7
8. Nascimento ML, Araújo ES, Cordeiro ER, de Oliveira AH, de Oliveira HP (2015) A literature investigation about electrospinning and nanofibers: historical trends, current status and future challenges. Recent Pat Nanotechnol 9(2):76–85
9. Tucker N, Stanger J, Staiger M, Hussam R, Hofman K (2012) The history of the science and technology of electrospinning from 1600 to 1995. J Eng Fibers Fabr 7:63–73
10. Faraday M (1857) Experimental relations of gold (and other metals) to light. Phil Trans R Soc Lond 147:145–181
11. Turner T (1908) Transparent silver and other metallic films. Proc R Soc Lond A 81:301–310
12. Joshi DR (2010) Engineering physics. Tata McGraw-Hill Education, New York
13. Zsigmondy RA (1966) Properties of colloids, nobel lectures. Chemistry 1922–1941. Elsevier Publishing Co, Amsterdam
14. Langmuir I (1917) The constitution and fundamental properties of solids and liquids. J Am Chem Soc 39:1848–1906
15. Blodgett KB (1935) Films built by depositing successive monomolecular layers on a solid surface. J Am Chem Soc 57:1007–1022
16. Nikalje AP (2015) Nanotechnology and its applications in medicine. Med Chem 5:5081–5089
17. Bennig GK (1988) Atomic force microscope and method for imaging surfaces with atomic resolution. US4724318A
18. Binnig G, Quate CF, Gerber C (1986) Atomic force microscope. Phy Rev Lett 56(9):930–933
19. Iijima S (1991) Helical microtubules of graphitic carbon. Nature 354:56–58
20. Khil MS, Kim HY, Email A, Kim IS, Bhattarai N (2003) Electrospun nanofibrous polyurethane membrane as wound dressing. J Biomed Mater Res Part B Appl Biomater 67(2):675–679
21. Feng YC, Khulbe KC, Matsuura T, Gopal R, Kaur S, Ramakrishna S, Khayet M (2008) Production of drinking water from saline water by air-gap membrane distillation using polyvinylidene fluoride nanofiber membrane. J Membr Sci 311(1–2):1–6
22. Khulbe KC, Feng YC, Matsuura T (2008) Synthetic membranes, characterization by atomic force microscopy. Springer, Berlin
23. Mehdizadeh S, Sadjadi S, Ahmadi SJ, Outokesh M (2014) Removal of heavy metals from aqueous solution using platinum nanopartcles/zeolite-4A. J Environ Health Sci Eng 12:7
24. European commission, communicating nanotechnology (2010) Why, to whom, saying what and how? http://cordis.europa.eu/nanotechnology
25. Yunus IS, Harwin, Kurniawan A, Adityawarman D, Indarto A (2012) Nanotechnologies in water and air pollution treatment. Environ Technol Rev 1(1):136–148
26. Abdulhady AM, El-Shazly MM, Kased RF (2018) Evaluation of antibacterial activity and toxic metal removal of chemically synthesized magnetic iron oxide titanium coated nanoparticles and application in bacterial treatment. J Environ Sci Health Part A 53(3):205–212
27. Khin MM, Nair AS, Babu VJ, Murugan R, Ramakrishna S (2012) A review on nanomaterials for environmental remediation. Energy Environ Sci 8:8075–8109
28. Freitas RAJ (1999) Basic capabilities, vol 1. Landes Bioscience, Texas. Nanomedicine. https://www.nanomedicine.com. Last accessed on 26 Sept 2000
29. Patil M, Mehta DS, Guvva S (2008) Future impact of nanotechnology on medicine and dentistry. J Indian Soc Periodontol 12(2):34–40
30. Theresa M, Pendergast M, Hoek EMV (2011) A review of water treatment membrane nanotechnologies. Energy Environ Sci 4:1946–1971

31. Ramakrishna S, Fujihara K, Teo WE, Yong T, Ma Z, Ramaseshan R (2006) Electrospun nanofibers: solving global issues. Mater Today 9(3):4050
32. Gilbert W (1600) De magnete, magneticisque corporibus, et de magno magnete tellure
33. Taylor G (1964) Disintegration of water drops in an electric field. Proc R Soc Lond A 280(1382):383–397
34. Rayleigh L (1882) On the equilibrium of liquid conducting masses charged with electricity London Edinburgh and Dublin. Philos Mag 14(87):184–186
35. Boys VM, Doi Y, Hellwich KH, Hess M, Hodge P, Kubisa P, Rinaudo M, Schué F (2012) On the production, properties, and some suggested uses of the finest threads. Pure Appl Chem 84(2):377–410
36. Cooley J (1899) Electrical method of dispersing fluid. US745276A
37. Kenry, Lim CT (2017) Nanofiber technology: current status and emerging developments. Prog Polym Sci 70:1–17
38. Njuguna J, Ansari F, Sachse S, Zhu H, Rodriguez VM (2014) Nanomaterials, nanofillers, and nanocomposites: types and properties. Health Environ Safety Nanomater 2014:3–27
39. Niemann B, Rauscher F, Adityawarnan D, Voist A, Sundmacher K (2006) The synthesis of silver nanoparticles using the water-in-oil biomicroemulsion method. Chem Eng Process 45(10):917–935
40. Mandal A (2018) Properties of nanoparticles. News Medical Life Sciences
41. Vert M, Doi Y, Hellwich KH, Hess M, Hodge P, Kubisa P, Rinaudo M, Schué F (2012) Terminology for biorelated polymers and applications (IUPAC recommendations). Pure Appl Chem 84(2):377–410
42. Batista CAS, Larson RG, Kotov NA (2015) Nonadditivity of nanoparticle interactions. Science 350(6257):1242477
43. De Lorey GT (2010) Nanoparticles: properties, classification, characterization, and fabrication. Nova Science Publishers, Technology & Engineering, 353 pages
44. U.S. Environmental Protection Agency, Module 3: characteristics of particles particle size categories
45. Kwon H, Ryu MH, Carlsten C (2020) Ultrafine particles: unique physicochemical properties relevant to health and disease. Exp Mol Med 52:318–328
46. Dreaden EC, Alkilany AM, Huang X, Murphy CJ, El-Sayed AM (2012) The golden age: gold nanoparticles for biomedicine. Chem Soc Rev 41:2740–2779
47. Khan I, Saeed K, Khan I (2019) Review nanoparticles: properties, applications and toxicities. Arab J Chem 12(2):908–931
48. Ng LY, Mohammad, Leo CP, Hilal N (2013) Polymeric membranes incorporated with metal/metal oxide nanoparticles: a comprehensive review. Desalin 308:15–33
49. Jeong BH, Hoek EMV, Yan Y, Subramani A, Huang X, Hurwitz G, Ghosh AK, Jawor A (2007) Interfacial polymerization of thin film nanocomposites: a new concept for reverse osmosis membranes. J Membr Sci 294:1–7
50. Manias E (2007) Nanocomposites: stiffer by design. Nat Mater 6:9–11
51. Pinnavaia TJ, Beall GW (2001) Polymer-clay nanocomposites. Wiley & Sons Ltd, Chichester; 2000. 0-471-6300-9. pp xi + 345
52. Wang Z, Wu A, Ciacchi LC, Wei G (2018) Recent advances in nanoporous membranes for water purification. Nanomaterials 8:65
53. Elrasheedy A, Nady N, Bassyouni M, El-Shazly A (2019) Metal organic framework based polymer mixed matrix membranes: review on applications in water purification. Membranes (Basel) 9(7):88
54. Kislik VS (2010) Liquid membranes: principles and applications in chemical separations and wastewater treatment. Elsevier, pp 1–15
55. Tanaka Y (2015) Ion exchange membranes: fundamentals and applications, vol 12, 2nd edn. Elsevier, Japan, p 47. isbn: 978-0-444-63319-4
56. Alabi A, AlHajaj A, Levente C, Szekely G, Peter B, Zou L (2018) Review of nanomaterials-assisted ion exchange membranes for electromembrane desalination. npj Clean Water 1(1):10

57. Davis TS (1990) Electrodialysis. In: Handbook of industrial membrane technology, 1st edn. Noyes Publication, New Jersey, pp 40–102. isbn: 9780815512059
58. Kim DJ, Jo MJ, Nam SY (2015) A review of polymer–nanocomposite electrolyte membranes for fuel cell application. J Ind Eng Chem 21:36–52
59. Mishra AK, Bose S, Kuila T, Kim NH, Lee JH (2012) Silicate-based polymer-nanocomposite membranes for polymer electrolyte membrane fuel cells. Polym Sci 37:842–869
60. Montal M, Mueller P (1972) Formation of bimolecular membranes from lipid monolayers and a study of their electrical properties. Proc Natl Acad Sci U S A 69:3561–3566
61. Mueller P, Rudin DO, Tien HT, Wescott WC (1962) Reconstitution of cell membrane structure in vitro and its transformation into an excitable system. Nature 194:979–980
62. Purkait MK, Sinha MK, Mondel P, Singh R (2018) Biologically responsive membranes. Interface Sci Technol 25:145–117
63. Gunderso J (2014) Biomimetic Membranes: Nature Inspires Next Generation of Water Filtration Technology. Water Technology Jun 19th, 2014
64. National University of Singapore (2015) Highly efficient nature-inspired membrane that can potentially lower cost of water purification by 30 per cent. Science. https://www.asianscientist.com/2015/12/tech/nature-inspired-membrane-slash-cost-water-purification/
65. Bayley H (2009) Membrane-protein structure: piercing insights. Nature 459(7247):651–652
66. Li J, Stein D, McMullan C, Branton D, Aziz MJ, Golovchenko JA (2001) Ion-beam sculpting at nanometre length scales. Nature 412(6843):166–169
67. Storm AJ, Chen JH, Ling XS, Zandbergen HW, Dekker C (2003) Fabrication of solid-state nanopores with single-nanometre precision. Nat Mater 2(8):537–540
68. Ultrafiltration, Nanofiltration and Reverse Osmosis, Safe Drinking Water Foundation (2016). https://www.safewater.org/fact-sheets-1/2017/1/23/ultrafiltrationnanoandro
69. Mayer PT, Brady RC (2011) A report for the joint water reuse & desalination task force. SAND2010-8355 Unlimited Release, Printed January 2011
70. Roth CD, Poh SC, Vuong DX (2009) Treatment, and reuse. In: Nanotechnology applications for clean water. 2nd edn. Elsevier, pp 107–114
71. Roy Y, Warsinger DM, Lienhard JH (2017) Effect of temperature on ion transport in nanofiltration membranes: diffusion, convection and electromigration. Desalin 420:241–257
72. Chai YK, Lam HC, Koo CH, Lau WJ, Lai SO, Ismail AF (2019) Performance evaluation of polyamide nanofiltration membranes for phosphorus removal process and their stability against strong acid/alkali solution. Chinese J Chem Eng 27(8):789–1797
73. Chen BZ, Ju X, Liu N, Chu CH, Lu JP, Wang C, Sun SP (2020) Pilot-scale fabrication of nanofiltration membranes and spiral-wound modules. Chem Eng Res Design 160:395–404
74. Baker R (2012) Microfiltration technology and applications, 3rd edn. Wiley, California, p 303
75. Microfiltration/Ultrafiltration (2008) Hyflux membranes. Accessed 27 Sept 2013. <“Archived copy”. Archived from the original on 2013-10-15. Retrieved 2013-10-15. rel=“nofollow>”
76. Crittenden J, Trussell R, Hand D, Howe K, Tchobanoglous G (2012) Principles of water treatment, 2nd edn. Wiley, New Jersey, 8.1
77. Warsinger DM, Tow EW, Nayar KG, Maswadeh LA, Lienhard V, John H (2016) Energy efficiency of batch and semi-batch (CCRO) reverse osmosis desalination. Water Res 106:272–282
78. Sidney L (1975) Method and apparatus for generating power utilizing pressure-retarded-osmosis. US3906250A
79. Helfer F, Lemckert C, Yuri GA, Yuri GA (2014) Osmotic power with pressure retarded osmosis: theory, performance and trends—a review. J Membr Sci 453:337–358
80. Arimasen N (2013) Blue energy cell mechanism. File: Blue energy mechanism.png, https://commons.wikimedia.org/wiki/File:Blue_energy_mechanism.pngdoi:10.1016/j.memsci.2013.10.053

Chapter 2
Membrane Preparation

2.1 Material

2.1.1 Materials of Nanoporous Membranes

A porous medium or a porous material is a material containing pores (voids). The skeletal portion of the material is often called the “matrix” or “frame”. The pores are typically filled with a fluid (liquid or gas). According to Wikipedia, nanoporous materials consist of a regular organic or inorganic framework supporting a regular, porous structure. The size of the pores is generally up to 1000 nm more or less. Most nanoporous materials can be classified as bulk materials or membranes. Activated carbon and zeolites are two examples of bulk nanoporous materials, while cell membranes can be thought of as nanoporous membranes [1]. Nanoporous materials can be subdivided into three categories:

1. Microporous materials: 0.2–2 nm
2. Mesoporous materials: 2–50 nm
3. Macroporous materials: 50–1000 nm

There are many natural nanoporous materials, but artificial materials can also be manufactured. One method of doing so is to combine polymers with different melting points, so that upon heating one polymer degrades. A nanoporous material with consistently sized pores has the property of letting only certain substances pass through, while blocking others.

According to Kargari and Shirazi [2] the world population will be around nine billion by 2050 and approximately 75% will face freshwater shortages by 2075. Membrane filtration process is the main process for purification of water. The conventional water processes such as flocculation, sedimentation, coagulation, and activated carbon are unable to remove organic pollutants to meet the necessary specifications [3, 4]. For the progress and improvements in filtration, electrospun

K. C. Khulbe, T. Matsuura, *Nanotechnology in Membrane Processes*, Lecture
Notes in Nanoscale Science and Technology 29,
https://doi.org/10.1007/978-3-030-64183-2_2

nanofibrous membranes (ENMs)/electrospun nanofiber membranes opened a new avenue for the treatment of water/wastewater.

For preparation of nanofibers, in general, there are three fundamentally different categories of membrane materials: Organic (polymeric), inorganic (ceramic) materials and biological materials. Almost any soluble polymer with sufficiently high molecular weight can be electrospun. However, nanofibers made of natural polymers, polymer blends, nanoparticle- or drug-impregnated polymers, and ceramic precursors have been successfully demonstrated. Different fiber morphologies have also been shown, such as beaded, ribbon, porous, and core-shell fibers (Fig. 2.1). Dense homogeneous polymer membranes are usually prepared (1) from solution by solvent evaporation only or (2) by extrusion of the melted polymer.

Piezoelectric materials are materials that generate electrical current when a mechanical stress is applied to it. The properties of nanofibers prepared from piezoelectric materials may be tailored or enhanced by controlling the organization of the fibers. Electrospinning has been shown to increase the piezoelectricity of certain materials especially polymers. For electrospinning of inorganic piezoelectric material, electrospinning is usually carried out using its precursor material in solution form followed by annealing process. Chen et al. [6] constructed vanadium doped ZnO piezoelectric nanofiber by electrospinning. Precursors in the form of zinc acetate and vanadyl acetylacetonate was used in combination with poly(vinylpyrrolidone) (PVP) as the base solution for electrospinning. Polymer such as poly(l-lactic acid) (PLLA) has been shown to exhibit piezoelectric properties after electrospinning to form fibers due to electric dipole component along the main carbon chain of PLLA polymer nanofibers that can be polarized along the direction of alignment during electrospinning process [7].

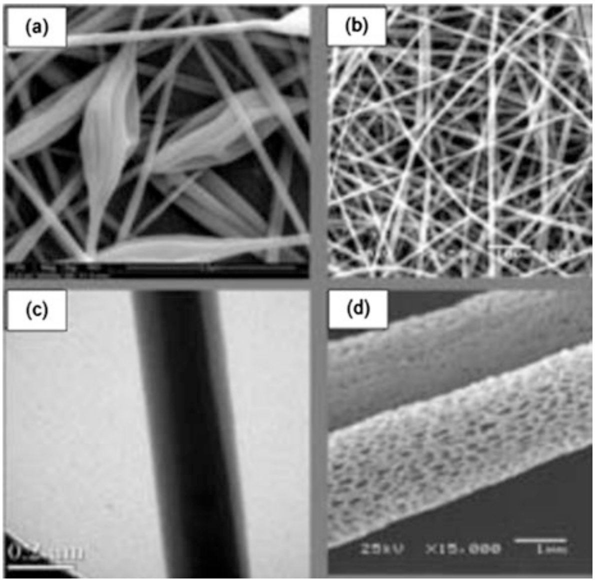

Fig. 2.1 Different fiber morphologies: (**a**) beaded; (**b**) smooth; (**c**) core-shell; and (**d**) porous fibers [5]

2.1.1.1 Materials of Nanoparticles for MMM

In the development of nanotechnology, many novel functional nanomaterials are being explored to enhance the performance of membranes. The chemical features of nanomaterials in the scale between 1 and 100 nm are completely different compared to the materials in micro- and macroscale. Its surface area increases as the size of a material decreases, which is crucial for the binding processes. More binding sites exist on the nanomaterial surface. Incorporation of nanoparticles in polymeric membranes affect the permeability, selectivity, hydrophilicity, conductivity, mechanical strength, thermal stability, and the antiviral and antibacterial properties of the membrane. Nanocomposites offer added stability, which is important for sustaining antimicrobial activity and reducing the likelihood of migration of metal ions into stored foods. Organic–inorganic hybrid nanocomposite membranes have significantly higher water flux, mechanical strength, selectivity, stability, hydrophilicity etc. compared with conventional polymeric membranes. Polymers are largely engineered to form nanocomposites with metal/metal oxide nanomaterials for food application. However, it is not clear yet how far nanoparticles are harmful to the environment and human health. A significant number of studies on membrane nanotechnology have focused on creating synergism or multifunction by adding nanomaterials into polymeric or inorganic membranes.

The hydrophobic membrane can be changed to hydrophilic by incorporating nanoparticles such as SiO_2, TiO_2, Al_2O_3 etc. with polymer to form hydrophilic membrane [8]. Wu et al. [9] developed polysulfone (PSf)-based hybrid membranes via doping with SiO_2–graphene oxide (GO) nanohybrid. The hybrid membranes exhibited improved water permeability with the rejection to egg albumin (>98%). Compared with SiO_2/PSf and GO/PSf hybrid membranes, SiO_2–GO/PSf hybrid membrane had improved properties, such as water permeation rate, protein rejection, and antifouling ability.

Metallic/bi-metallic catalyst nanoparticles such as nano zero-valent iron (nZVI) and noble metals supported on nZVI have been incorporated into polymeric membranes for reductive degradation of contaminants, particularly chlorinated compounds [10]. nZVI serves as the electron donor and the noble metals catalyze the reaction. Table 2.1 summarizes nanomaterials mostly used for MMM membranes for filtrations etc.

On adding hydrophilic metal oxide nanoparticles, fouling is reduced by increasing the hydrophilicity of the membrane and the mechanical and thermal stability of polymeric membranes are enhanced. It also reduces the negative impact of compaction and heat on membrane permeability. Nanoparticles incorporated membranes are also used for water treatment.

Antimicrobial nanomaterials such as nano-Ag and CNTs can reduce membrane biofouling. Nano-Ag has been doped or surface grafted on polymeric membranes to inhibit bacterial attachment and biofilm formation on the membrane surface as well as inactivate viruses. However, its long-term efficacy against membrane biofouling has not been reported. Appropriate replenishment of nano-Ag needs to be addressed for practical application of this technology. CNTs inactivate bacteria upon direct

Table 2.1 Nanomaterials mostly used for MMM membranes [11]

Nanomaterial shape	Diagram	Nanomaterials
Tubular		CNTs, HNTs
Ball		Ag, TiO_2, SiO_2
Flake		GO, zeolite
Massive		Boehmite, $CaCO_3$
Linear		CNFs

contact. High bacterial inactivation (>90%) has been achieved using polyvinyl-N-carbazole-SWNT nanocomposite at 3 wt.% of SWNT. As CNTs are insoluble in water and not consumed, there is no need for replenishment. However, as direct contact is required for inactivation, long term filtration experiments are needed to determine the impact of fouling on the antimicrobial activity of CNTs. Addition of oxidized MWNT at low weight percentage (up to 1.5 wt.%) also increases the hydrophilicity and permeability of polysulfone membranes [12, 13].

2.1.2 Nanomaterials/Nanoparticles

2.1.2.1 Carbon Nanomaterials

Carbon nanomaterials (CNMs) have received tremendous attention in the field of novel membrane science and technology. Application of CNM could improve the membrane separation process. However, homogeneous bulk fabrications of CNM based membranes are still at the premature stage and require further improvements. Major challenges for the CNMs reinforced membrane are poor dispersion and distribution, and weak interfacial interaction between the dissimilar surface of CNM and matrix. Further, some form of CNM based membranes are fragile, which causes significant challenges for handling and uses. Considering these challenges, however, it is very hard to predict how CNM based membranes will shape the future membrane processes [14].

The advantages of CNM based membranes are:

1. Its ability to remove organics from feed water that could foul the RO.
2. More reliable in treating all the feed water than a chemical feed system.

The disadvantage of using carbon filters is that they are notorious for breeding bacteria which can result in biological fouling of the RO.

2.1.2.2 Carbon Nanotubes (CNTs)

Due to great properties in adsorption, ability to attach a functional group to enhance the adsorption, large surface area, and the diversity in pollutants- CNT interactions, CNTs have attracted much attention to its application in membrane technology. CNTs also exhibit remarkable mechanical and electrical properties. The definition of CNTs membrane is that it is an open tip single hollow structure or polymer composite arranged perpendicularly with impermeable filler matrices [15]. CNTs are allotropes of carbon with a cylindrical nanostructure. Depending on their manufacturing process, CNTs are categorized as single-walled nanotubes and multi-walled nanotubes, respectively. Figure 2.2 shows schematic representation of single-walled carbon nanotube (SWCNT) and multi-walled carbon nanotube (MWCNT).

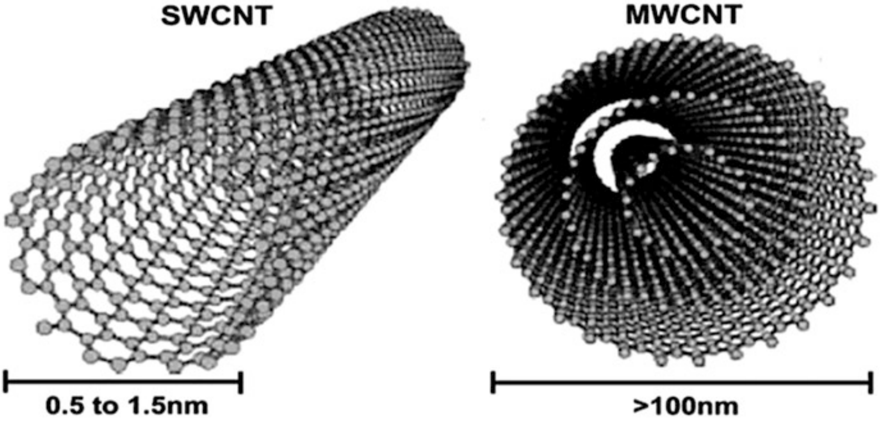

Fig. 2.2 Schematic representation of single walled carbon nanotube (SWCNT) and multi walled carbon nanotube (MWCNT) [16]

CNTs are composed of graphite lamellae rolled into columns. Due to their unique characteristics, such as high aspect ratios, molecularly smooth surfaces, nanoscale diameters and inner hollow cavities, CNTs are ideal candidates in various fields, particularly separation technology. CNTs (unaligned) also found their application in thin film nanocomposite (TFN) membranes due to their antimicrobial activities. Carbon nanotubes (CNTs) are unique nano systems with extraordinary mechanical and electronic properties, which derive from their unusual molecular structure. An ideal carbon nanotube can be thought of as a single graphite layer (graphene sheet), rolled up to make a seamless hollow cylinder. These cylinders can be tens of microns long, with diameters as small as 0.7 nm and are closed at both ends by fullerene-like caps. CNTs having wall thickness of one carbon sheet are named single-wall carbon nanotubes (SWCNTs). In consequence of the Van der Waals interactions between nanotubes, they often aggregate in large ropes: ordered arrays of SWCNTs arranged on a triangular lattice. SWCNTs can be considered as the building blocks of multi-wall carbon nanotubes (MWCNTs), which consist of a coaxial array of SWCNTs with increasing diameter. MWCNTs are also usually as long as many microns, with the external diameter that ranges from two to several tens of nanometers, providing very high aspect ratio structures, as shown in Fig. 2.3 [17].

CNTs possess a high specific surface area including highly accessible adsorption sites and an adjustable surface chemistry. CNTs are incredibly useful as a nano-adsorbents to remove heavy metals like arsenic and polar organic compounds in the water. In contrast, the production of CNTs has the high cost. With regard to production cost, nanometals and zeolites have low price and ability to use as the disinfectant. Although CNTs and nanometals are available in the markets, commercial entry of polymeric nanoadsorbents is ongoing. In terms of application, polymeric nano-adsorbents can be used for removal of both heavy metals and organic pollutants. The only limitation of this new nanoadsorbent is its high price to produce it.

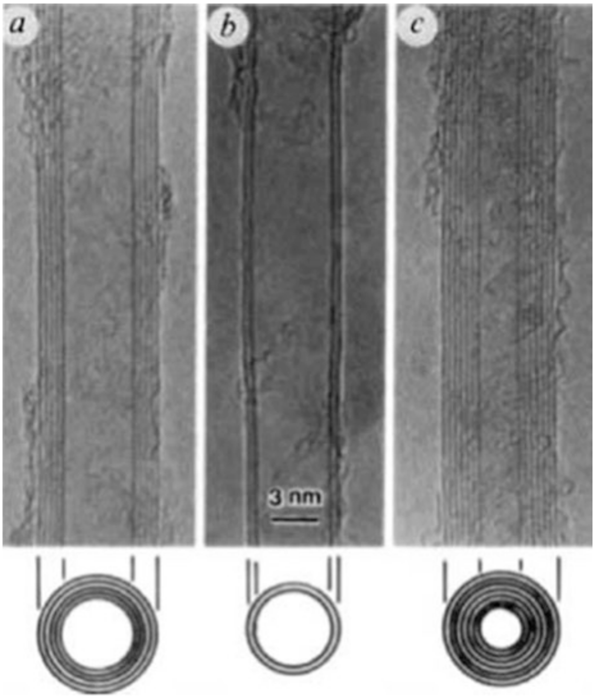

Fig. 2.3 Electron micrographs of microtubules of graphitic carbon [17]

Tiraferri et al. [18] covalently bonded SWNTs to a TFC (Thin Film Composite) membrane surface. This approach is advantageous as it uses relatively small amount of the nanomaterial and minimizes perturbation of the active layer. The resulting TFN membrane exhibited moderate anti-bacterial properties (60% inactivation of bacteria attached on the membrane surface in 1 h contact time), potentially reducing or delaying membrane biofouling. Due to their hydrophobic surface, CNTs have to be stabilized in aqueous suspension in order to avoid aggregation that reduces the active surface. They can be used for adsorption of persistent contaminants as well as to preconcentrate and detect contaminants. Metal ions are absorbable by CNTs through electrostatic attraction and chemical bonding. Furthermore, CNTs exhibit antimicrobial properties by causing oxidative stress in bacteria and destroying the cell membranes.

Well-aligned CNT can serve as robust pores in membranes for water purification. The hollow CNT structure meanwhile provides frictionless transport of water molecules for enhanced water permeability. By designing appropriate pore diameters, it can constitute energy barriers at the channel entries, rejecting salt ions and permitting water through the hollow nanotubes [19]. The salt rejection ability of CNT membranes often gets similar performance of commercial NF membrane [20]. Holt et al. [21] have synthesized CNT membrane with pore diameter less than 2 nm, which enhanced ion selectivity and superior to conventional polycarbonate membranes in water permeability.

The potentiality of CNT membranes in sea and brackish water desalinations is illustrated in great details by Das et al. [15]. Although RO, NF, MF, UF and other membranes have been used to mitigate freshwater crisis, CNT-based membranes have remarkable accomplishments in terms of water permeability, desalination capacity, solute selectivity, robustness, antifouling, energy savings and scalability. CNT-membranes could be used at all levels from the point of generation (POG) to the point of use (POU) treatments. CNTs rupture bacterial cell through the production of reactive oxygen species (ROS), causing disruption of their metabolic pathway and oxidative stress. This has brought a new revolution in membrane technology with self-cleaning power.

Carbon nanotubes can play a variety of roles in future space systems, including wiring, high-strength lightweight composite materials, thermal protection and cooling systems and electronics/sensors. Successful development of these technologies is highly dependent on a reliable method to produce controlled carbon nanotubes [22].

2.1.2.3 Nano Metal Oxides

Nanoscale metal oxides have a high surface area which can be a good alternative to activated carbon to remove pollutants, heavy metals, and even radionuclides. Due to superparamagnetic properties, some metal oxide is applied to facilitate separation and recovery for filters and slurry reactors. Nano-metal and nano-metal oxide are mostly compressed into porous pellets for industrial usage.

2.1.2.4 Nanosilver/Ag Nanoparticles

Silver nanoparticles are nanoparticles of silver of between 1 and 100 nm in size. While frequently described as being ‘silver’ some are composed of a large percentage of silver oxide due to their large ratio of surface to bulk silver atoms. Numerous shapes of nanoparticles can be constructed depending on the application at hand. Commonly used silver nanoparticles are spherical, but diamond, octagonal, and thin sheets are also common [23]. Ag nanoparticles have the most comprehensive antibacterial spectrum; they are effective against various aquatic microorganisms, such as bacteria, fungi, and algae. Ag nanoparticles are one of the most promising nanomaterials today as they have high antibacterial activity. The toxicity of Ag depends on size of nanoparticles: small nanoparticles (1–10 nm) are able to pass through bacterial cell wall, while larger nanoparticles not. By attaching to bacterial cell wall Ag nanoparticles change the permeability of membrane and inhibit cell respiration. At the same time, these nanoparticles are non-toxic at low concentrations for human cells [24, 25]. Silver nanoparticles are also incorporated into the membranes to facilitate the separation of olefins [26]. The membranes containing AgBr nanocomposites were also tested for the separation of olefin/paraffin mixtures. The incorporation of AgBr nanocomposites in the membranes resulted in an increment of mixed gas total permeance and mixed gas selectivity [27].

Due to antimicrobial property of nanosilver, it is used in drinking water filters, and it has an application for water disinfection systems also [26]. It has been noted that the introduction of silver nano particles has shown to have synergistic activity with common antibiotics already used today, such as; penicillin G, ampicillin, erythromycin, clindamycin, and vancomycin against E. coli and S. aureus [28].

2.1.2.5 Iron Oxides

Iron oxide nanoparticles are iron oxide particles with diameters between about 1 and 100 nm. The two main forms are magnetite (Fe_3O_4) and its oxidized form maghemite (γ-Fe_2O_3). Iron oxide nanoparticles are classified based on the size of the iron oxide [29].

1. standard size of superparamagnetic iron oxide is 60–150 nm.
2. ultrasmall size of superparamagnetic iron oxide is 5–40 nm
3. subset size of monocrystalline iron oxide is 10–30 nm.

Iron oxide nanoparticles, with their superparamagnetic properties, are used in a rapidly expanding number of applications, such as for cell labeling, separation, and tracking; for therapeutic agents in cancer therapy; and for diagnostic agents. These applications require the tailored properties of nanoparticles, such as specific sizes, shapes, surface characteristics, and magnetism. Usually, iron oxide nanoparticles are synthesized by coprecipitating ferrous (Fe^{2+}) and ferric (Fe^{3+}) ions in an aqueous solution, which is probably the simplest and most efficient chemical pathway to obtain large quantities of magnetite nanoparticles [30].

2.1.2.6 Nano-zero Valent Iron

The iron nanoparticle technology has received considerable attention for its potential applications in groundwater treatment. Chlorinated hydrocarbon fluids and perchlorates in groundwater are removed by nano-zero valent iron particles. The benefits of nano-zero valent iron are that it has high reactivity, low lifetime, and a high surface area compared with conventional granular iron. Nano zero-valent iron particles with the diameter in the range of 10–100 nm can be synthesized from Fe(II) and Fe(III) precursor. They have a typical core-shell structure. The core contains zero-valent iron that decreases its reactions with environmental pollutants. The shell consists of iron oxides or hydroxide to provide sites for chemical complex formation. It has been found that nano-zero valent iron particles can remove organic and inorganic contaminants like nitrate, perchlorate, selenite, arsenite, and chromate [31].

2.1.2.7 Graphene

Graphene is an allotrope of carbon in the form of a single layer of atoms in a two-dimensional hexagonal lattice in which one atom forms each vertex. It is the basic structural element of other allotropes, including graphite, charcoal, carbon nanotubes and fullerenes. It can also be considered as an indefinitely large aromatic molecule, the ultimate case of the family of flat polycyclic aromatic hydrocarbons.

Graphene is being touted as a ‘wonder material’ with all kinds of potentially ground-breaking applications. Since the first report on graphene in 2004 by Geim and Novoselov [32], graphene and its derivatives have been widely studied and applied to prepare high-performance materials or functional materials. Graphene is an allotrope (form) of carbon consisting of a single layer of carbon atoms arranged in a hexagonal lattice. In other words, graphene is a form of carbon consisting of sheets that have the thickness of one atom. The atoms are arranged in a honeycomb pattern. A pattern of shapes with six sides (Fig. 2.4) [33].

Graphene oxide (GO) is a carbon nanomaterial having two-dimensional structure produced by the oxidation of graphite layer via chemical method. Inducing hydrophilic functional groups in GO required special oxidation process [34]. The presence of these hydroxyl and carboxyl groups as functional groups in GO increases the adsorption of heavy metals [35].

Graphene-based membranes have been extensively studied, represented by two distinct research directions:

1. creating pores in graphene basal plane.
2. engineering nanochannels in graphene layers.

Graphene-based membranes have the potentials to become the preferred candidates to next-generation membranes coupling high permeability to high selectivity. However, it is not expected that the uptake of graphene-based membranes may

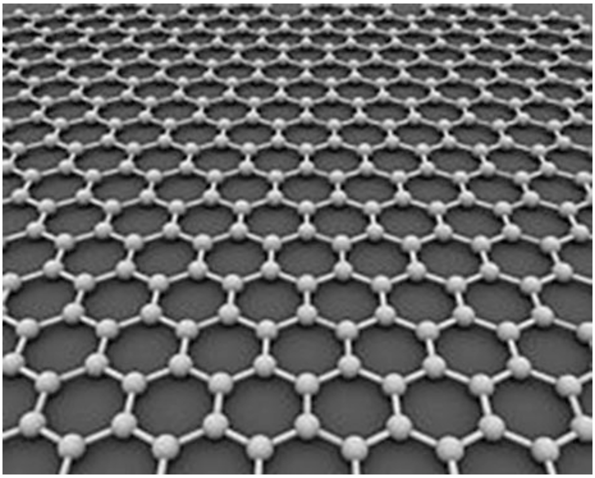

Fig. 2.4 Graphene is an atomic-scale hexagonal lattice made of carbon atoms [32]

occur in the short term, as industrial membranes employed within current desalination processes must satisfy many additional criteria, and the novel desalination processes need to take full advantages of the novel membranes are still to be designed [36]. Graphene is of interest as advanced material for various membrane-based separations, because of its exceptional physical and thermal properties and atomic scale thickness. Its atomic scale pores generated by chemical or thermal treatment can play as robust channel for water transport or ion, gas, and nanoparticle separations. Pristine graphene is not promising for hybrid membranes, because it does not form homogeneous composites with polymer matrix. Furthermore, graphite and graphene are generally hydrophobic in nature which limits their application in water filtration [18]. Yang et al. [37] reported that the adsorption of phenanthrene, a model aromatic pollutant, onto the graphene nanosheets loaded on silica particles increased up to 100-fold compared with pristine graphene at the same level.

Graphene-based nanomaterials are also versatile functional materials with extraordinary properties, and it has been widely investigated in layered membranes with two-dimensional nanochannels, showing very intriguing separation properties. Graphene oxide membranes can form a perfect barrier when dealing with liquids and gasses. They can effectively separate organic solvent from water and remove water from a gas mixture to an exceptional level. Graphene-based materials have excellent advantages in the desalination process due to their intriguing features, including single atomic layer structure, large specific surface area, hydrophobic property, rich modification approaches etc. [38]. Graphene-containing membranes (GCMs) are advanced separation devices constructed from or modified by graphene and its derivatives; these membranes not only present attractive functions and performance but also generate less residual nanomaterials afterwards, thus lowering impacts to the environment compared to those caused by directly using graphene-based nanomaterials [39].

GCMs are divided into monolayer porous graphene membranes (SGMs), multilayer pristine graphene-containing membranes (MGMs), multilayer composite graphene-containing membranes (CGMs), and conventional membranes modified with graphene-based materials (PGMs). Zhu et al. [39] discussed the applications of GCMs in isotope separation, gas separation, desalination, ion separation, nanofiltration, ultrafiltration, and pervaporation. Graphene oxide (GO), the oxidation state of graphene nanosheets, could be an attractive candidate as a carbon filler because it contains epoxide, hydroxyl, and carboxylic acid groups at the edges and basal plane of the nanosheets, which can provide good compatibility with polymers. When appropriately embedded into the polymer matrix, GO can significantly improve mechanical properties of the polymer host, even at low filling amounts [40, 41] materials for oil–water separation.

When oriented horizontally in the polymer matrix, GO nanosheets may act as barrier, because they hinder diffusion pathway of permeating molecules across the membranes. Since hydroxyl (OH) groups are bonded to the surface of the GO nanosheets, these nanosheets can form aqueous solutions and further enhance the hydrophilicity of polymeric membrane [18, 42]. Inspired by the two-dimensional structure and hydrophobic property, some researchers began to use graphene or graphene-related materials to fabricate superhydrophobic materials for oil–water separation in recent years [43–45]. The researchers have successfully synthesised a graphene membrane with pores whose size, shape and density can be tuned with atomic precision at the nanoscale [46]. Engineering pores at the nanoscale in graphene can change its fundamental properties. It becomes permeable or sieve-like, and this change alone, combined with graphene's intrinsic strength and nano-slimness, points to its future use as the most resilient, energy-efficient and selective filter for extremely small substances including greenhouse gases, salts and biomolecules.

2.1.2.8 Silica

Silica as an inorganic additive to prepare hybrid nanocomposite membranes has a wide range of applications due to its mild reactivity, thermal resistance, convenient operation, mechanical strength, small size, nontoxic nature, strong surface energy, good suspendability in aqueous solution and environmental friendliness.

2.1.2.9 Halloysite Nanotubes (HNTs)

Halloysite is an aluminosilicate clay mineral with the empirical formula $Al_2Si_2O_5(OH)_4$. Its main constituents are aluminium (20.90%), silicon (21.76%) and hydrogen (1.56%). Halloysite typically forms by hydrothermal alteration of alumino-silicate minerals [47]. Halloysite nanotubes are formed by 10–15 revolutions of kaolin aluminosilicate sheets and have diameters of 50–60 nm, lumens in the range of 12–15 nm, and lengths within the range of 500–900 nm. Halloysite may be considered as an efficient, divalent, nano-adsorbent both for cations and anions. Adsorption of metal ions on the halloysite was used for synthesis of Fe, Co, Ni, Pd and Ag nanoparticles on the tube surface [48].

Halloysite nanotubes (HNTs) are natural occurring mineral clay nanotubes that have excellent application potential in different field. It is eco friendly nanotubes with low cost than carbon nanotubes. In recent years there has been growing concern about the effect of carbon nanotubes on human health and on environment because of their potential toxic nature. HNTs have been used extensively for enhancing properties of polymers. Halloysite nanotubes find numerous commercial applications such as, additives in polymers and plastic, electronic components, drug delivery vehicles, cosmetics and in home and personal care products. Two types of halloysite nanotubes models are developed for effective studies in field of nanotechnology [49].

1. Single walled halloysite nanotube.
2. Multi walled halloysite nanotube.

Chemically, the outer surface of the halloysite nanotubes has properties similar to SiO_2 while the inner cylinder core is related to Al_2O_3. By means of suitable modifications, such as supramolecular functionalization or covalent modifications, it is possible to obtain novel nanomaterials with tunable properties for several applications. Halloysite nanotubes find numerous commercial applications such as, additives in polymers and plastic, electronic components, drug delivery vehicles, cosmetics and in home and personal care products.

For the development of membrane separation techniques in water treatment and other fields, the requirements of membrane function, such as permeability, selectivity, anti-pollution, chemical and thermal stability are necessary. Joo et al. [50] modified the functional groups of halloysite nanotubes (HNT) from hydroxyl groups (HNT-OH) to carboxylic acids (HNT-COOH).

The incorporation of HNT into the silicone rubbers enhanced the crosslink density of the nanocomposites. The functionalized HNTs are used to enhance the chemical interactions as natural rubber (NR) filler [51]. There are few examples of MMM membrane containing HNTs. Ge et al. [52] modified the raw HNTs by either alkali etching or (3-aminopropyl) triethoxysilane grafting to improve the filler dispersion and filler-matrix interface affinity. On surface etching, the defect holes were formed on the surfaces of etched-HNTs, resulting in the rougher HNT walls and significant increment of surface area and CO_2 adsorption capacity. It was concluded that surface etching of halloysite is more effective than grafting to enhance the membrane performance. Compared to the pure polymer membrane and MMMs with untreated HNTs, MMMs containing 10 wt.% etched HNTs filler exhibited both increased CO_2 permeability (807.7 Barrer) and higher CO_2 selectivity (CO_2/CH_4 selectivity of 27.8) on the well-known limit of Robeson upper bound. Murali et al. [53] synthesized PANi (polyaniline)–HNTs loaded polysulfone mixed matrix membranes and reported that the prepared membranes showed better gas permeation properties than those of PSf. Mishra and Mukhopadhyay [54] prepared halloysite nanotubes (HNTs) embedded poly(vinyl chloride) ultrafiltration (UF) membranes (PVC/HNTs). It was reported that the membrane showed very high fouling resistance including BSA rejection (>90%). Duan et al. [55] prepared a novel mixed matrix membrane, polyethersulfone (PES) ultrafiltration membrane, containing Cu NPs@HNTs. It was reported by Duan et al. that the pure water flux of the hybrid membrane was greatly enhanced, and the maximum could reach as high as 212 L m^{-2} h^{-1}. Mishra and Mukhopadhyay [56] prepared TiO_2@HNTs by synthesizing TiO_2 nanoparticles *in situ* on the functionalized halloysite nanotubes (HNTs) surface and then prepared photocatalytic PVC membrane TiO_2@HNTs M2 (2 wt.%) and TiO_2@HNTs M3 (3 wt.%). In water treatment, TiO_2@HNTs 2 (2 wt.%) and TiO_2@HNTs 3 (3 wt.%) degraded MB dye up to 83.21% and 87.47% and RB dye up to 96.84% and 96.87%, respectively.

The modified HNTs have obtained a lot of extraordinary achievements in various fields, such as biomedical application, industrial catalyst, nanofillers and tissue engineering scaffolds, but the core challenges are the need for further research, such as surface utilized percentage, transport pathway, and uptake mechanisms in vivo [57].

2.1.2.10 Zeolite

Zeolite is composed of alumino silicates, which provide negatively charged defect sites to neutralize the positive charges of protons and ultimately form Brønsted acid sites. Zeolite was the first nanomaterial to be induced into FO membranes. Before that, zeolite was frequently used as a modifier in polymeric membranes for gas separation or pervaporation due to its uniform pore size distribution, channel structures and abundant negatively charged sites. The unique sub-nanometer pores of zeolites provide shape selectivity, which improves the adsorption efficiency of gas molecules.

Leo and his co worker [58] studied the effects of silane-grafting on the separation performance of MMM for gas permeation. The 3-aminopropyltrimethoxysilane (APMS) was added to modify SAPO-34 zeolite before the impregnation into the asymmetric polysulfone (PSf) MMMs through dry–wet phase inversion method. Highest CO_2/N_2 selectivity of 28, CO_2/CH_4 selectivity of 31 and a satisfactory CO_2 permeance of 706 GPU were achieved from PSf/SAPO-34E modified MMMs.

2.1.2.11 Boehmite

Boehmite nanoparticles, which have the chemical composition AlOOH, contain abundant hydroxyl groups on their surfaces. Studies have revealed that due to their porous and hydrophilic structure, incorporating boehmite nanoparticles can enhance the performance of membranes, such as their water flux, structural parameter and separation performance.

2.1.2.12 Nano-$CaCO_3$

$CaCO_3$ nanoparticles are among the most widespread, industrialized and inexpensive nanomaterials. The mature production technology of $CaCO_3$ nanoparticles is due to their surface polarity and their readily tunable particle size in production processes.

2.1.2.13 TiO_2 Nanoparticles

TiO_2 nanoparticles are one of the most promising metal oxide nanoparticles due to their high hydrophilicity and excellent photocatalytic properties with perfect mechanisms. As an acknowledged photo-catalytic material, TiO_2 has been extensively used in disinfection and decomposition applications; these characteristics also make TiO_2 a promising anti-fouling modifier. Titanium dioxide (TiO_2) has been the focus of numerous investigations in recent years, particularly because of its photocatalytic effects that decompose organic chemicals and kill bacteria. TiO_2 photocatalysis is known to generate various active oxygen species, such as hydroxyl radical, hydrogen peroxide, etc., by reductive reactions or oxidative reactions under light. These active oxygen species further destroy the outer membrane of the bacterium cells and decompose the endotoxin from them. Moreover, due to the chemical stability, controllable morphology, surface properties, photocatalytic function and antifouling performance of TiO_2 nanoparticles, they are useful in membrane processes.

According to nanometals, nano TiO_2 has the low price, high availability and ability to remove organic pollutants and micro-organisms, and it is known as an ideal nanomaterial for water treatment in both large-scale and small-scale. Nano-TiO_2 has high chemical stability, low toxicity properties, and low cost.

2.1.2.14 Metal/Metal-oxide Nanoparticles

For decades, metal nanoparticles and metal oxide nanoparticles have been widely used to address various environmental issues, especially in water desalination and regeneration. Metal nanoparticles and metal oxide nanoparticles are known to be environmentally friendly, stable to UV irradiation, antibacterial and highly hydrophilic. Due to the higher affinity of metal oxides to water, membranes incorporating metal and metal oxide nanoparticles are more hydrophilic than pure polymeric membranes.

The antibacterial properties of metal oxide nanoparticles are affected by morphological and physicochemical properties of nanomaterials such as crystal structure, shape, size, concentration, and pH. The modified membrane using a metal oxide nanoparticle has better antifouling properties and also improved other properties such as mechanical strength, water flux, hydrophilicity, permeability, porosity, and rejection tendency [59].

Metal oxides represent an important class of materials used for developing mixed matrix membranes with enhanced properties in comparison with the purely polymeric membranes. The results of using metal oxides additives in polymeric membranes are shown in Table 2.2 [12].

2.1.2.15 Polymeric Nanoparticles

Polymer-based nanoparticles can improve the efficacy, solubility, toxicity, bioavailability and pharmacokinetic profile of a drug molecule. Numerous applications are being developed. However, there are a number of challenges specially to introduce nanoparticles in medical field.

Challenges with conventional production:

1. The formulation process has significant batch-to-batch variability.
2. Maintaining precise control over the particle size is difficult.
3. Loading the nanoparticles is inefficient.
4. Production is time consuming and labor-intensive.
5. The manufacturing process is difficult to scale-up.

Table 2.2 Antibacterial mechanism of several metal oxide nanoparticles

Nanoparticles	Mechanism	Characteristic	Influence factor
Ag_2O	DNA loses its replication ability and the cell cycle halts at the G2/M phase owing to the DNA damage	High antimicrobial activity against both bacteria and drug-resistant bacteria, antifungal activity on spore-producing fungal plant pathogens, high stability, nontoxicity	Particle size and shape of particles
ZnO	ROS generation on the surface of the particles; zinc ion release, membrane dysfunction; and nanoparticles internalization into cell	Photocatalytic activity; high stability; bactericidal effects on both Gram-positive and Gram-negative bacteria; antibacterial activity against spores which are resistant to high temperature and high pressure	Particle size and concentration
TiO_2	Oxidative stress via the generation of ROS; lipid peroxidation that causes to enhance membrane fluidity and disrupt the cell integrity	Suitable photocatalytic properties; high stability; effective antifungal for fluconazole resistant strains	Crystal structure, shape and size
CuO	Crossing of nanoparticles from the bacteria cell membrane and then damaging the vital enzymes of bacteria	Effective against Gram-positive and Gram-negative bacteria; high stability; antifungal activity	Particle size and concentration
MgO and CaO	Damaging the cell membrane and then causing the leakage of intracellular contents and death of the bacterial cells	Effective against both Gram-positive and Gram-negative bacteria; high stability; low cost; availability	Particle size, pH and concentration

However, these can be solved by the improvement in:

1. Reproducible polymer nanoparticle manufacturing process.
2. Control of particle size through instrument parameters.
3. High drug loading efficiency in a one-step formulation process.
4. Rapid, effortless polymer nanoparticle production and optimization.
5. A seamless path to scaling up production.

2.1.3 Fibrous Materials

Fibrous materials including cotton fibers, cellulose acetate nanofibers, fibrous polymer have shown enhanced oil sorption capacities for the oil water separation. Some of these sorbents can be produced by electrospinning, which is a simple top-down method to fabricate fibrous polymer films with chemical inertness, high porosity, uniform pass through size and interconnected open pore structure. However, almost all of these sorbents are made of either organic polymers or biological fibers, which may be swollen or even dissolved in the oil absorption process when being recycled by rinsing with organic solvent. Some work has been done to overcome these problems [19].

Nanofibers are fibers with diameters in the nanometer range. Nanofibers can be generated from different polymers and hence have different physical properties and application potentials. Examples of natural polymers include collagen, cellulose, silk fibroin, keratin, gelatin and polysaccharides such as chitosan and alginate. Examples of synthetic polymers include poly(lactic acid) (PLA), polycaprolactone (PCL), polyurethane (PU), poly(lactic-co-glycolic acid) (PLGA), poly(3-hydroxybutyrate-co-3-hydroxyvalerate) (PHBV), and poly(ethylene-co-vinylacetate) (PEVA). These polymers are for tissue engineering.

Synthetic polymers have been used to produce electrospun nanofibers membranes. This type of polymers can be tailored to exhibit excellent mechanical properties, thermal stability and an appropriated degradation profile. Synthetic polymer-based electrospun nano/microfibers have emerged as potent materials in crucial biomedical applications such as tissue engineering, drug delivery and diagnostics. Appropriate functionalization with dedicated biomolecules (i.e. cell adhesive peptides, therapeutic molecules, bio-probes) is a critical requirement for the performances of such materials in their related application [60]. Owing to flexibility and robustness of electrospinning process as well as advances in conjugation and polymer/material engineering, high degree of control over biofunctionalization can now be achieved, to fit as best as possible the requirements of the targeted application. In 2003, for the first time, Khil et al. used polyurethane (PU) to produce nanofibrous membranes to be applied as skin substitutes [61]. Kumbar et al. produced polylactide-polyglycolide (PLGA) nanofibers that were then seeded on the surface with human skin fibroblasts [62]. Tallawi et al. [63] discussed the hydrophobic character of the synthetic polymers used (e.g. polycaprolactone (PCL) and poly(glycolic acid) (PGA)), and the absence of peptide sequences on the materials' surface impaired cell adhesion and/or proliferation.

2.1.4 Nanoparticle Synthesis

Two basic strategies are used to produce nanoparticles: 'top-down' and 'bottom-up'. The term 'top-down' refers here to the mechanical crushing of source material using a milling process. In the 'bottom-up' strategy, structures are built up by chemical processes. As well, in the top-down approach a dispersion of preformed polymers produces polymeric nanoparticles, whereas in the bottom-up approach polymerization of monomers leads to the formation of nanoparticles. Different methods for producing polymeric nanoparticles are illustrated in Fig. 2.5.

Two basic strategies are used to produce nanoparticles: 'top-down' and 'bottom-up'. The term 'top-down' refers here to the mechanical crushing of source material

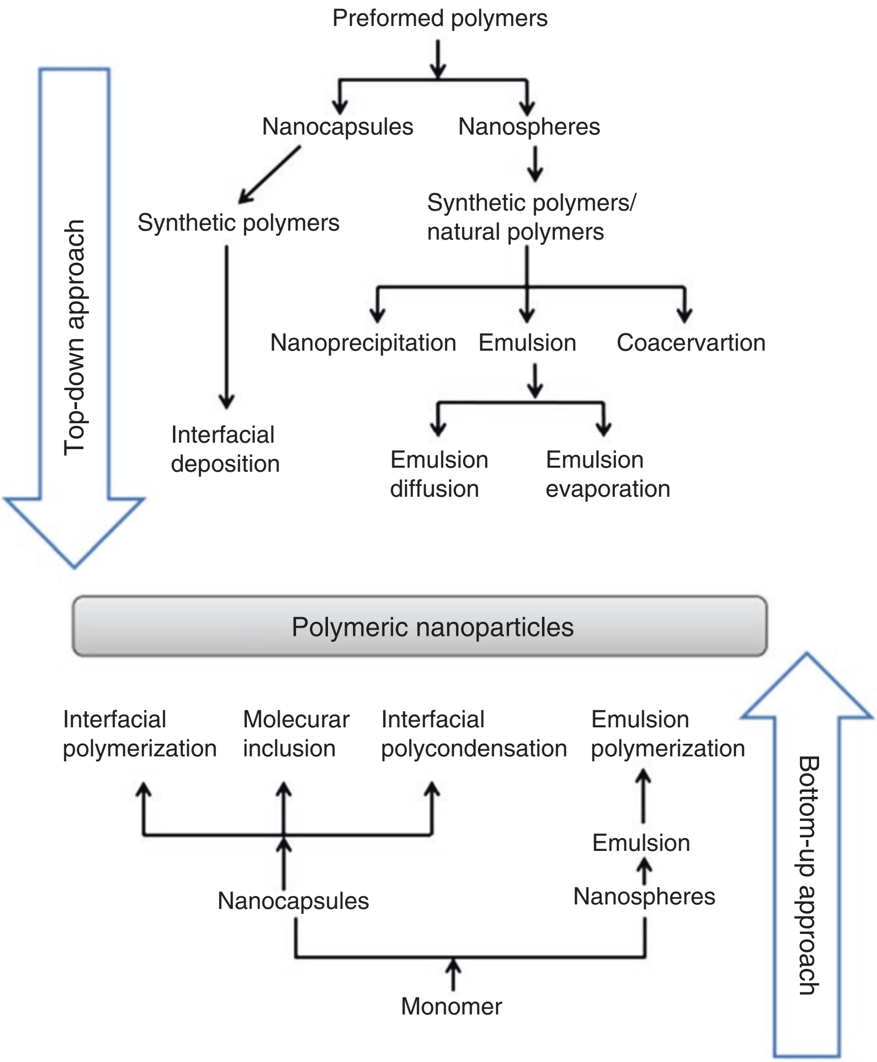

Fig. 2.5 Top-down and bottom-up approaches for synthesizing polymeric nanoparticles [64]

using a milling process. In the ‘bottom-up’ strategy, structures are built up by chemical processes (Fig. 2.6). The selection of the respective process depends on the chemical composition and the desired features specified for the nanoparticles.

Top-down refers to mechanical-physical particle production processes based on principles of microsystem technology. The traditional mechanical-physical crushing methods for producing nanoparticles involve various milling techniques. The nanoparticles are generally classified into the organic, inorganic and carbon-based particles in nanometric scale that has improved properties compared to larger sizes

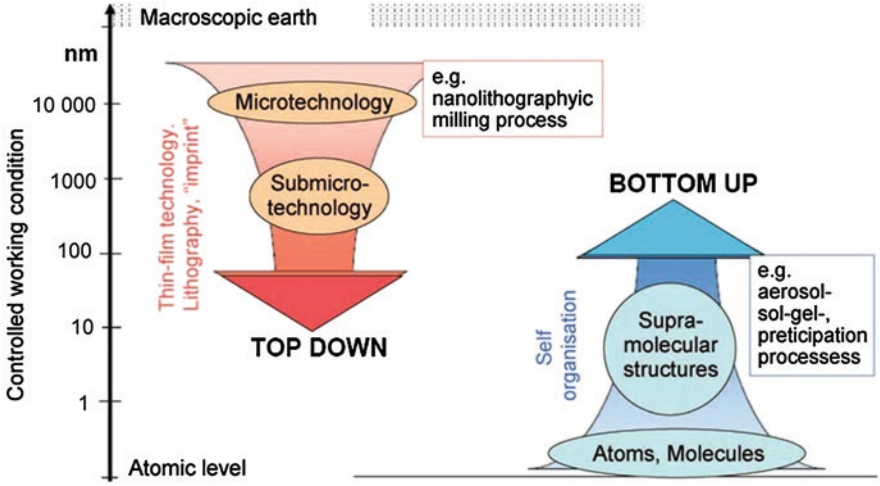

Fig. 2.6 Methods of nanoparticle production: top-down and bottom-up [65]

of respective materials. The nanoparticles show enhanced properties such as high reactivity, strength, surface area, sensitivity, stability, etc. because of their small size. The nanoparticles are synthesised by various methods for research and commercial uses that are classified into three main processes.

1. Physical.
2. Chemical.
3. Mechanical.

These processes have seen a vast improvement over time. A number of synthesis approaches to a great variety of nanoparticles are available. Nanoparticles can be derived from larger molecules or synthesized by 'bottom-up' methods that, for example, nucleate and grow particles from fine molecular distributions in liquid or vapour phase. Synthesis can also include functionalization by conjugation to bioactive molecules.

The selection of appropriate method for the preparation of polymer nanoparticles depends on the physicochemical character of the polymer [66].

1. Emulsification-Solvent Evaporation Method: Emulsification-solvent evaporation involves two steps. The first step requires emulsification of the polymer solution into an aqueous phase. During the second step solvent is evaporated, inducing polymer precipitation as nanospheres. The nanoparticles are collected by ultracentrifugation and washed with distilled water to remove stabilizer residue.
2. Salting Out Method: Salting-out is based on the separation of a water miscible solvent from aqueous solution via a salting-out effect. Polymer and salting-out agent are initially dissolved in a solvent which is subsequently emulsified into an aqueous gel containing the salting-out agent (electrolytes, such as magnesium

chloride and calcium chloride, or non-electrolytes such as sucrose) and a colloidal stabilizer such as polyvinylpyrrolidone or hydroxyethyl cellulose. This oil/water emulsion is diluted with a sufficient volume of water or aqueous solution to enhance the diffusion of solvent into the aqueous phase, thus inducing the formation of nanospheres.

3. Emulsions-Diffusion Method: The encapsulating polymer is dissolved in a partially water-miscible solvent (such as propylene carbonate, benzyl alcohol), and saturated with water to ensure the initial thermodynamic equilibrium of both liquids. Subsequently, the polymer-water saturated solvent phase is emulsified in an aqueous solution containing stabilizer, leading to solvent diffusion to the external phase and the formation of nanospheres or nano capsules, according to the oil-to-polymer ratio. Finally, the solvent is eliminated by evaporation or filtration, according to its boiling point.
4. Solvent Displacement/Precipitation method: Solvent displacement involves the precipitation of a preformed polymer from an organic solution and the diffusion of the organic solvent in the aqueous medium in the presence or absence of surfactant. Polymers are dissolved in a semi polar water miscible solvent such as acetone or ethanol. The solution is then poured or injected into an aqueous solution containing stabilizer under magnetic stirring. Nano particles are formed instantaneously by the rapid solvent diffusion. The solvent is then removed from the suspensions under reduced pressure.
5. Inert Gas Condensation: Inert-gas condensation is frequently used to produce metallic nanoparticles. The metal is evaporated in a vacuum chamber containing a reduced atmosphere of an inert gas [67]. Buhrman Condensation of the supersaturated metal vapor results in creation of nanometer-size particles, which can be entrained in the inert gas stream and deposited on a substrate or studied in situ.
6. Radiolysis Method: Nanoparticles can be formed using radiation chemistry. Radiolysis from gamma rays can create strongly active free radicals in solution. It is a simple technique, and a minimum number of chemicals are needed. It needs water, a soluble metallic salt, a radical scavenger (often a secondary alcohol), and a surfactant (organic capping agent). In this process, reducing radicals will drop metallic ions down to the zero-valence state. A scavenger chemical will preferentially interact with oxidizing radicals to prevent the re-oxidation of the metal. Once in the zero-valence state, metal atoms begin to coalesce into particles. A chemical surfactant surrounds the particle during formation and regulates its growth. In sufficient concentrations, the surfactant molecules stay attached to the particle. This prevents it from dissociating or forming clusters with other particles. Formation of nanoparticles using the radiolysis method allows for tailoring of particle size and shape by adjusting precursor concentrations and gamma doses.
7. Gas Phase Processes (Aerosol Processes): Gas phase processes are among the most common industrial-scale technologies for producing nanomaterials in powder or film form.

8. Milling Processes: The mechanical production approach uses milling to crush microparticles. This approach is applied in producing metallic and ceramic nanomaterials. For metallic nanoparticles, for example, traditional source materials (such as metal oxides) are pulverized using high-energy ball mills. Such mills are equipped with grinding media composed of wolfram carbide or steel. Milling involves thermal stress and is energy intensive. Lengthier processing can potentially abrade the grinding media, contaminating the particles. Purely mechanical milling can be accompanied by reactive milling: here, a chemical or chemo-physical reaction accompanies the milling process.

Particles can also be produced from droplets using centrifugal forces, compressed air, sonic waves, ultrasound, vibrations, electrostatics, and other methods. The droplets are transformed into a powder either through direct pyrolysis (thermal cleavage of chemical compounds) or via direct reactions with another gas. In spray pyrolysis, droplets of the source material are transported through a high-temperature field (flame, oven), which rapidly vaporizes the readily volatile components or leads to decomposition reactions. The formed particles are collected on filters [68]. Depending on the process, further particle growth involves condensation (transition from gaseous into liquid aggregate state), chemical reaction(s) on the particle surface and/or coagulation processes (adhesion of two or more particles), as well as coalescence processes (particle fusion). Examples include processes in flame-, plasma-, laser- and hot wall reactors, yielding products such as fullerenes and carbon nanotubes.

Numerous techniques for the production of nZVI particles have been successfully implemented in recent years. These techniques can be divided into bottom-up approaches (generation of iron nanoparticles from ions or smaller particles via deposition, nucleation, precipitation, agglomeration, etc.) and top-to-bottom approaches (size reduction of larger particles, e.g., via milling, ablation, etc.) [69]. The typical range of primary nZVI particles, obtained through the different methods, is 10–100 nm, with a corresponding specific surface area on the order of 10–50 $m^2\ g^{-1}$ [70]. The choice of synthesis method influences both the size and shape of the nanoparticles produced. Yuvakkumar et al. [71] synthesized zero valent iron (nZVI) (50–100 nm) by the method of ferric iron reduction using sodium borohydride as a reducing agent under atmospheric conditions. Table 2.3 shows the summary of nZVI synthesis methods [72].

2.2 Method (Preparation of Membranes)

The membranes are prepared in various shapes such as flat sheet, tubular, hallow fiber, and spiral wound, which have different separation efficiencies. The most common techniques for fabricating of nanoporous membranes are.

1. Phase inversion.
2. Interfacial polymerization.

Table 2.3 Summary of nZVI synthesis methods

Chemical synthesis Methods	Liquid-phase reduction or borohydride reduction of ferrous salts
	Gas-phase reduction
	Microemulsion
	Controlled chemical co-precipitation
	Chemical vapor condensation
	Pulse electrodeposition
	Liquid flame spray
	Thermal reduction of ferrous iron
	Electrolysis
Physical synthesis Methods	Polyphenolic plant extract
	Inert gas condensation
	Ultrasound shot peening
	Severe plastic deformation
	High-energy ball milling

3. Track-etching.
4. Electrospinning.

2.2.1 Flat Sheet

2.2.1.1 Phase Inversion Technique

Membranes can be prepared by phase inversion techniques. Phase inversion is a stratification process that converts homogeneous solution into a solid state in a controlled manner. It can be categorized into four different techniques:

1. Thermal precipitation (TIPS): It is based on the phenomenon that the solvent quality usually decreases when the temperature is decreased. After demixing is induced, the solvent is removed by extraction, evaporation or freeze drying.
2. Air casting of dope solution: In this process, polymer is dissolved in a mixture of a volatile solvent and less volatile nonsolvent. During the evaporation of the solvent, the solubility of the polymer decreases and then phase separation takes place.
3. Precipitation from the vapor phase: Phase separation of the polymer solution is induced by penetration of nonsolvent vapor in the solution.
4. Immersion precipitation: In this process, homogeneous polymer solution is cast as a thin film on a support or extruded through a die and is subsequently immersed in a nonsolvent bath. Precipitation can occur because of the good solvent in the polymer solution is exchanged with nonsolvent in the coagulation bath.

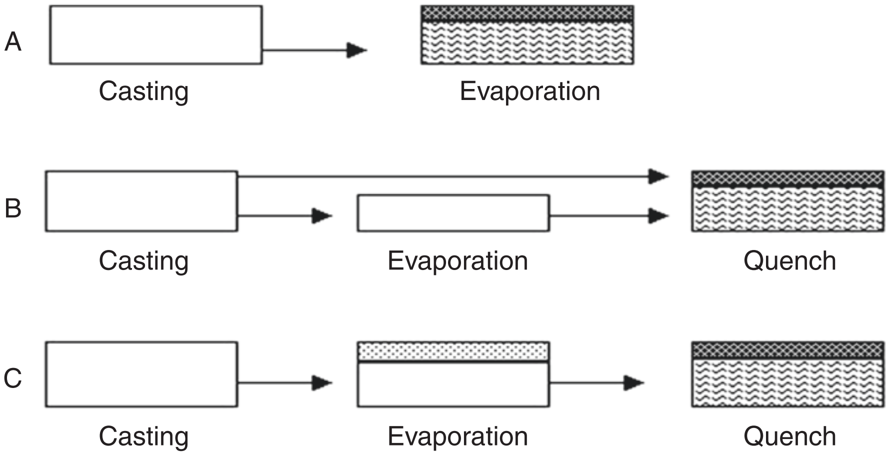

Fig. 2.7 Schematic representations of immersion precipitation phase inversion processes: (**a**) dry, (**b**) wet, (**c**) dry/wet

Among these techniques, immersion precipitation is widely used to produce commercial separation membranes. Immersion precipitation technique can be further divided into three categories namely wet, dry and dry/wet phase inversion technique as shown in Fig. 2.7.

2.2.2 Interfacial Polymerization (IP)

The interfacial polymerization is a self-growth polymerization. IP occurs in a mixed monolayer of the adsorbed monomers. This technique is based on a polycondensation reaction between two monomers (such as polyamines and polyacyl chlorides) dissolved in immiscible solvents, one of which, the aqueous polyamine solution, initially penetrates into the substrate. An ultra-thin film (from 10 nm to several micrometers thick) can be quickly formed when the polyamine filled substrate is brought into contact with organic polyacyl chloride solution at the organic solution-substrate interface and attached to the substrate. The structural morphology of the membranes created by this method can be controlled by concentration of monomers, reaction time, solvent type, and post-treatment conditions. Mostly, in TFC hollow fiber (HF) fabrication, the selective layer is deposited on the lumen side of the fiber. When the interfacial pressure of the adsorbed mixed monolayer exceeds the equilibrium spreading pressure of the polymer, the latter is precipitated from the monolayer, giving rise to a thick film at the interface. Figure 2.8 shows IP between trimesoyl chloride (TMC) and 1,3-phenylenediamine (MPD) [73].

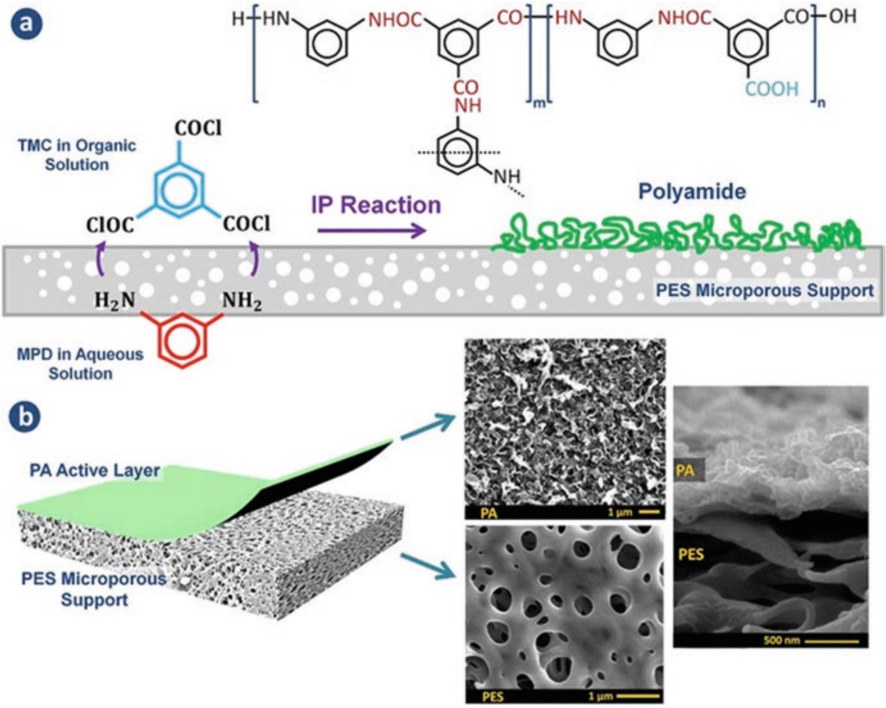

Fig. 2.8 (**a**) Schematic representation of the interfacial polymerization reaction between MPD and TMC at the surface of the microporous PES support and the chemical formula of PA layer. The m and n in polymer structure represent the cross linked and the linear parts, respectively (m + n = 1). (**b**) Structure of the synthesized TFC membranes with the top and cross-sectional morphologies [73]

2.2.3 Track-Etching

Etched ion-track membranes have been widely used as templates for the creation of nanowires and nanotubes. In the track-etching process, non-porous polymer membranes are irradiated with high energy heavy ions, resulting in a linearly damaged track across the irradiated polymer membrane to form nanopores [74]. The advantage of this technique is that it can precisely control the pore size distribution of the membrane, and the pore size. Furthermore, pore size and pore density can be adjusted in the range of a few nanometers to tens of micrometers and 1–10^{10} cm^{-2}, respectively. Two separate processing steps are used to fabricate etched ion-track membranes.

1. Irradiation of the template material with energetic heavy ions and creation of latent tracks.
2. Selective ion-track dissolution and formation of channels by chemical etching.

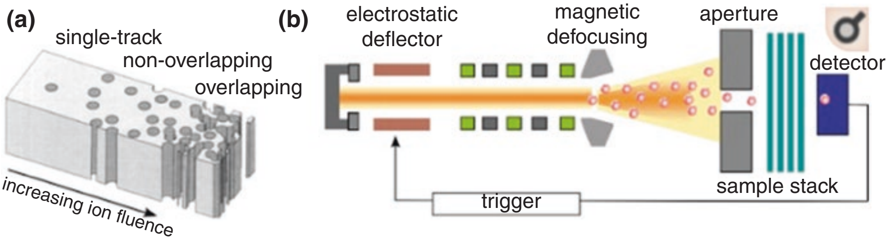

Fig. 2.9 (**a**) Track-etched membrane illustrating the porosity regime available by means of ion-track technology: single channel, non-overlapping channels, and overlapping channels. (**b**) Schematic of single-ion irradiation setup [74]

Control over the irradiation and etching conditions enables the production of various membranes with channels of predefined geometries, sizes and aspect ratios. A schematic representation of the single-ion irradiation system is presented in Fig. 2.9.

The ion beam is strongly defocused and adjusted in such a way that single projectiles pass through the aperture with a frequency of about 1 Hz. The ions are detected by a solid-state particle detector placed behind the sample. As soon as the detector has registered a single ion impact, the entire ion beam is deflected by an electrostatic chopper system. Materials commonly used as multi- and single-pore etched-ion-track membranes include polymers such as polyimide (PI), polyethylene terephthalate (PET) and polycarbonate (PC), and inorganic materials such as mica and glass.

2.2.4 Mixed Matrix Membranes (MMMs)

Mixed matrix membranes are considered a new-generation membrane. MMMs can be defined as incorporation of dispersed nanomaterials such as zeolite, carbon molecular sieve, and carbon nanotubes in a continuous polymer phase. In other words, MMM is the incorporation of a solid phase in a continuous polymer matrix. Figure 2.10 presented a schematic of an ideal MMM structure including the dispersed phase and the polymer matrix. MMM could offer the physicochemical stability of a ceramic material and the membrane forming ease of polymeric materials while promising the desired morphology with higher permeability, selectivity, higher hydrophilicity, higher fouling resistance, higher thermal, mechanical, and chemical strength over a wider temperature and pH range. These types of MMMs are named as inorganic filler-based MMMs, organic filler-based MMMs, biofiller-based MMMs, and hybrid filler-based [75].

Membrane performance is heavily dependent on the structure and properties of the membrane. The application of these membranes is a good way to reach contributory effects between the polymeric matrix and solid particles. By adding filler

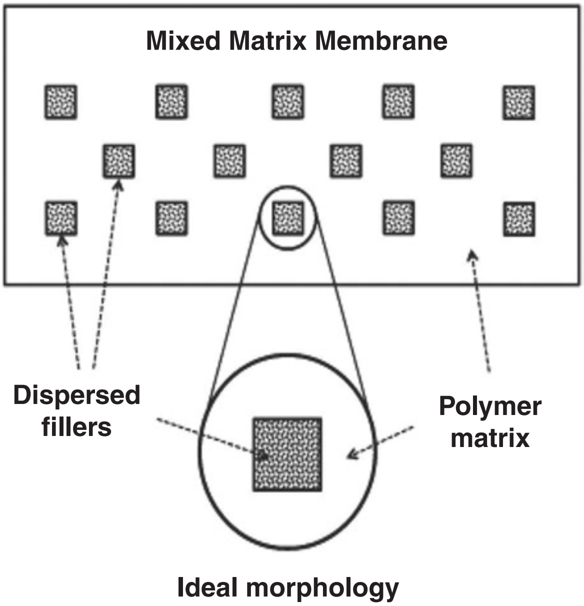

Fig. 2.10 Schematic diagram of an ideal MMM structure [75]

particles to a polymer matrix to make mixed matrix membranes (MMMs), it is possible to move beyond the performance limitations of conventional polymer films. The use of filler particles can result in increasing the polymer's free volume, thus increasing the membrane permeability. Furthermore, by combining gas-selective filler particles with permeability that matches with the polymer matrix, it is possible to simultaneously improve both the permeability and selectivity of the membrane.

In MMMs, solid particles are added to the polymer dope and hollow fiber or the flat sheet membranes are formed by the phase inversion method. The composite mixed matrix PVDF hollow fiber membrane was constructed by Wang et al. [76] via nonsolvent induced phase separation (NIPS) for the membrane distillation (MD).

In making MMMs, to avoid particle agglomerations and improve the particle–matrix interaction, complex multistep fabrication procedures are used. The polymer is gradually added to the filler particle suspension and mixing times can vary from a few hours to days. These initial steps are referred to as "priming" of the filler particle. Finally, when the filler particle and polymer are successfully combined and properly degassed to avoid air bubble defects in the film, the MMM is cast either as a free-standing film or on the surface of a support. In general, this process can be time-consuming and labor-intensive, which, on a large scale, will lead to increased manufacturing cost.

The following steps are typically used to prepare mixed-matrix membranes [77]:

1. Separate preparation of a polymer solution and a suspension of inorganic material.
2. The solution and the solid material are mixed to form a homogeneous mixed-matrix suspension.

3. This suspension is then cast (or spun).
4. The NIPS process is then used to induce phase separation.

Mixed-matrix membranes containing inorganic oxides (e.g., silica) can also be prepared by using the sol—gel method to synthesize nanoparticles in situ within a polymer solution, followed by phase separation.

Hybrid inorganic—organic materials can be constructed with a variety of properties according to the desired application. Some of the techniques used for the incorporation of inorganic building blocks into organic polymers include:

1. Preparation of interpenetrating networks by: (a) sol—gel processes in the presence of preformed polymers; (b) polymerization in sol—gel networks; (c) simultaneous formation of interpenetrating networks; (d) dual network precursors.
2. Incorporation of metals and metal complexes in polymers by coordination interactions.
3. Insertion of polymers in 2D layered materials.

One of the major difficulties experienced in preparation of MMMs is pore blockage of inorganic fillers by the polymer chains resulting in low permeability when they are mixed. Depending on the pore size of inorganic fillers, the polymer chain can fill the pores in various degrees. The inorganic filler could be completely excluded from the transport process as a result of filling by the polymer chains; therefore, no improvement in performance could be obtained. On the other hand, the blockage may narrow a part of the pores. Since blockage of the pores by polymer chains may completely eliminate the function of the inorganic filler, investigations are necessary to suppress this effect.

Development of mixed matrix membranes (MMMs) by incorporating inorganic fillers into the polymer matrix has become a potential alternative to overcome the limitations of polymeric and inorganic membranes in gas separation. Fabrication of defect-free MMMs with improved separation performance and without compromising the mechanical and thermal stability is extremely difficult and challenging. Poor adhesion between inorganic filler and polymer phase has been identified as one of the major problems in MMMs fabrication, especially when utilizing glassy polymer. Excellent adhesion between inorganic particle and polymer phase contributes to proper interfacial contact between them [78, 79]. Filler particles, such as porous carbon, metal oxides, silica, zeolites, or metal organic frameworks (MOFs), are among the many different types of additives used to fabricate MMMs. MOFs are of particular interest for MMMs because their properties are easily tailored to yield a strong interaction at the polymer–particle interface. However, defects such as the no uniform distribution of particles, within the matrix, can reduce the effectiveness of MMMs [79]. A rational choice of both inorganic and polymeric phases toward the preparation of MMMs is necessary.

Figure 2.10 shows the reaction mechanism of silane coupling agent with inorganic materials [79, 80]. Referring to Fig. 2.11, after the silane group reacts with hydroxyl groups attached on the surface of inorganic material, –NH in silane group will bond with polymer chain and consequently promote the adhesion between the

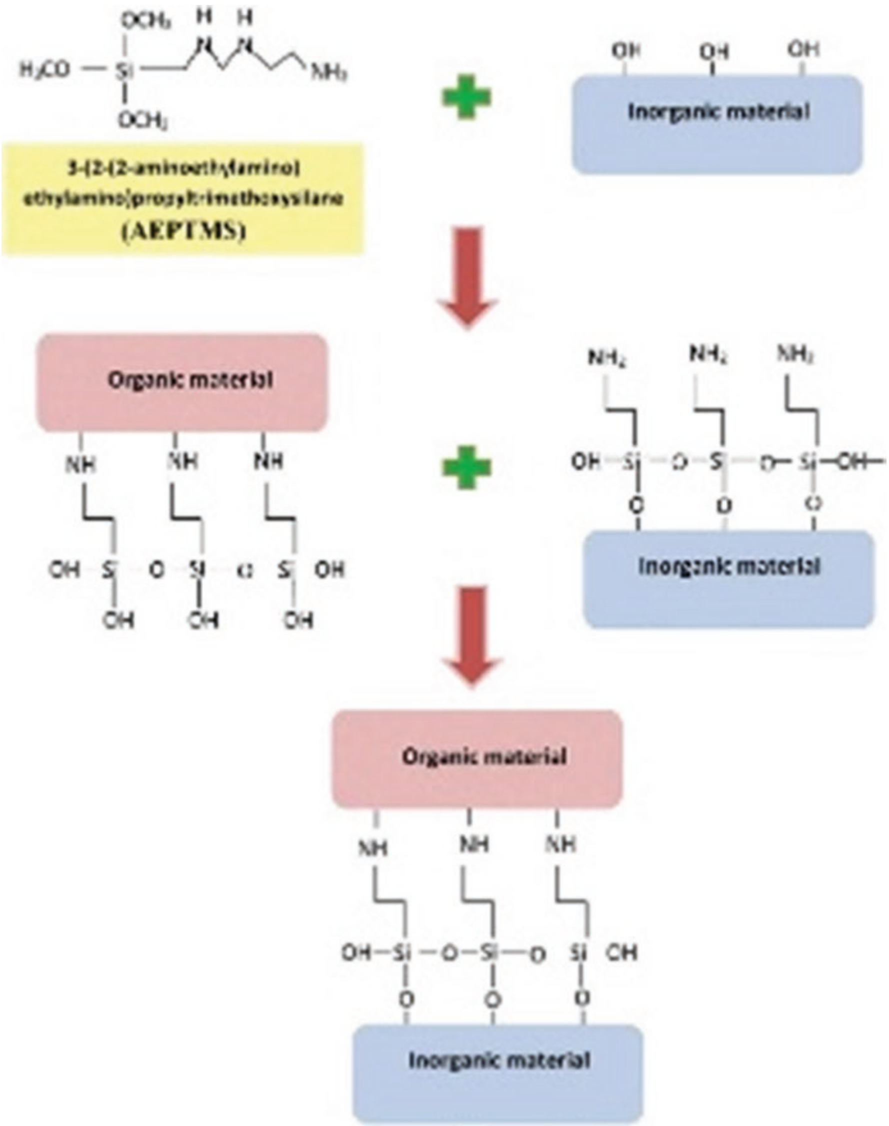

Fig. 2.11 Silane coupling agent reaction mechanism with organic and inorganic materials [79]

inorganic filler and polymer phase [81]. However, the availability of inorganic filler pores after the silanization process is important to ensure that the inorganic filler can fully demonstrate its advantage for the enhancement of separation. Therefore, the formation of undesirable new voids from multilayer deposition of silane must be prevented.

Permeability of a gas through an MMM depends on several factors such as intrinsic properties of the filler and polymer, the filler loading, and the filler–polymer matrix interface [82].

Marti et al. [83] prepared MMMs by growing MOF (UiO-66) in situ within a Matrimid polymer matrix while simultaneously curing the matrix. The gas separation performance for MMMs, prepared using this approach, was evaluated for the CO_2/N_2 separation and compared with MMMs made using the traditional post synthesis mixing. It was found that MMMs prepared using both the in-situ MOF growth strategy and by traditional post synthesis mixing are equivalent in performance. However, using the in-situ MOF growth allows for a simpler, faster, and potentially more economical fabrication alternative for MMMs.

Two types of mixed matrix membranes were developed by UOP in the late 1980s. The first type includes adsorbent polymers, such as silicalite-cellulose acetate (CA), NaX-CA, and AgX-CA. The silicalite-CA has a CO_2/H_2 selectivity of 5.15 ± 2.2. In contrast, the CA membrane has a CO_2/H_2 selectivity of 0.77 ± 0.06. The second type of mixed matrix membrane is PEG-silicone rubber. The PEG-silicone rubber mixed matrix membrane has high selectivity for polar gases, such as SO_2, NH_3, and H_2S [84].

2.2.5 Hollow Fiber Membranes (HFMs)

There are four techniques to fabricate HFMs.

1. Melt spinning: In this process, a melted thermoplastic polymer is extruded through a spinneret into air and is subsequently cooled.
2. Dry spinning: Polymer solution in an appropriate solvent is extruded through a spinneret into air.
3. Dry-jet wet spinning: Polymer solution in an appropriate solvent is extruded through a spinneret into air and a subsequent coagulant (usually water).
4. Wet spinning: Polymer solution in an appropriate solvent is extruded directly into a coagulant (usually water).

A spinneret is used in all the above techniques. The use of a spinneret is common. A spinning dope, prepared by dissolving polymer in a proper solvent or by melting, is forced through a metal nozzle that has fine holes to form a filament. As soon as the dope solution emerges from the nozzle in the form of long fibers, it solidifies by evaporation of solvent, cooling, or coagulation. A schematic diagram for the formation of a hollow fiber is shown in Fig. 2.12. The properties, such as average pore diameter and wall thickness of the HF, depend on the spinning parameters which are as follows.

1. Dimensions of the spinneret.
2. Driving force.
3. Temperature.

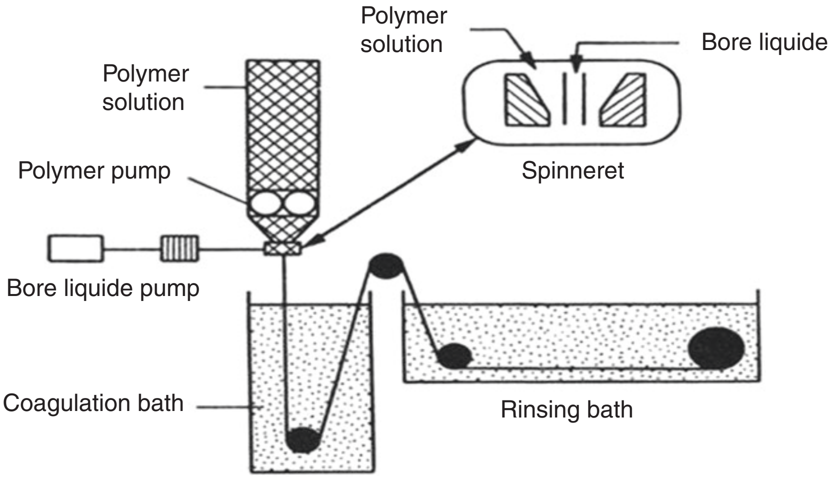

Fig. 2.12 Apparatus for the fabrication of hollow fibers (HFs) [85]

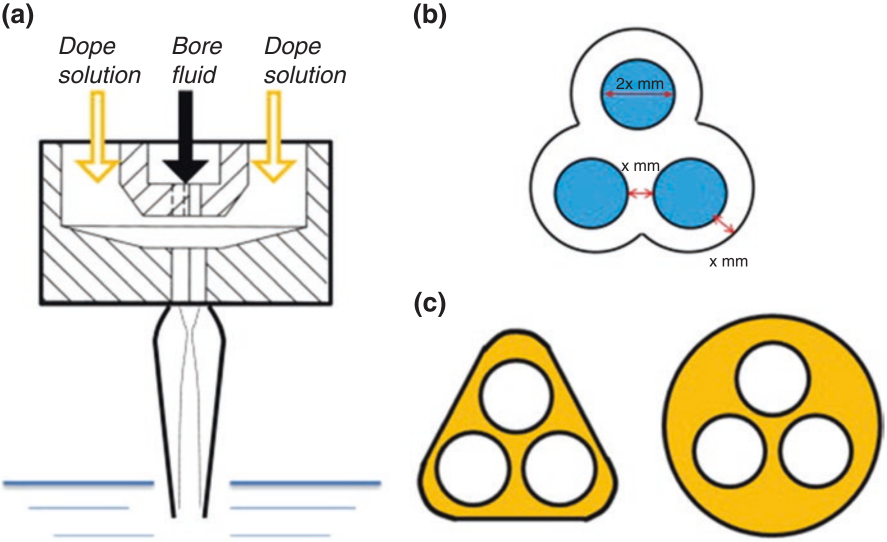

Fig. 2.13 (**a**) Single layer tri-needle spinneret; (**b**) bottom view of the tri-needle spinneret; and (**c**) cross section [86]

4. Length of air gap (for dry-jet wet spinning).
5. Coagulant.
6. Composition of “dope” (polymer) and “bore” (coagulant) solutions; and
7. Speed at which produced fiber is collected by a motorized spool.

Chung's group designed and fabricated a tri-bore blossom spinneret (Fig. 2.13) for making a tri-bore thin-film composite (TFC) hollow fiber (HF) membrane.

2.2.6 TFC Hollow Fiber Fabrication

A thin film composite (TFC) membrane consists of a nano-thin selective dense layer and a porous substrate. By modifying the top selective layer and bottom porous substrate, the overall membrane performance can be maximized. There are many ways or techniques to make thin selective layers on the surface of a support. The most common ones are:

1. Interfacial polymerisation reaction.
2. Dipping method.
3. Plasma treatment.
4. Chemical reaction.

There are also three other methods, but these are not very common:

1. Chemical vapour deposition (CVD).
2. Sputtering.
3. Spray pyrolysis.

The spray pyrolysis method has been successfully applied to produce fine metals or metal oxide particles. Li et al. [87] obtained a Pd-Ag alloy membrane on the surface of a porous alumina hollow fiber by spray pyrolysis of $Pd(NO_3)_2$ and $AgNO_3$ solutions on a H_2-O_2 flame.

2.2.6.1 Dip Coating

Making the TFC membrane by interfacial polymerization (IP) is described before. In industries, coated fabrics are often manufactured by dip coating. This technique is also common in academic research where thin film coating is needed. Thin film composite hollow fiber membranes are fabricated in the same way. There are five stages in the dip coating process [88]:

1. Immersion: With a constant speed, the substrate is immersed in the solution of the coating material (preferably jitter-free).
2. Start-up: The substrate has remained inside the solution for a while and is starting to be pulled up.
3. Deposition: The thin layer deposits itself on the substrate while it is pulled up. To avoid jitters, the withdrawing should be at a constant speed. The thickness of the coating depends on the withdrawal speed (faster withdrawal gives a thicker coating material).
4. Drainage: Excess liquid will drain from the surface.

5. Evaporation: A thin layer is formed on the surface by evaporation of the solvent. For volatile solvents, such as alcohols, evaporation starts during the deposition and drainage steps.

To fabricate thin films by self-assembly via the sol-gel technique, the dip coating method is generally used. Self-assembly can give a film thicknesses of exactly one monolayer. The sol-gel technique creates films of an increased, precisely controlled thickness that are mainly determined by the deposition speed and solution viscosity. Functional coatings are applied to change the surface properties of the substrate, such as adhesiveness and wettability.

2.2.6.2 Chemical Vapor Deposition (CVD)

Chemical vapor deposition (CVD) is a coating process in which materials in a vapor state are condensed through the processes of condensation, chemical reaction or conversion to form a solid layer over a substrate. This process is used to produce high quality, high-performance, solid materials, typically under vacuum. The process is often used to produce thin films, including modification of membrane surfaces. CVD is classified by operating conditions:

1. *Atmospheric pressure CVD* (APCVD)—CVD at atmospheric pressure.
2. *Low-pressure CVD* (LPCVD)—CVD at sub-atmospheric pressures. Reduced pressures tend to reduce unwanted gas-phase reactions and improve film uniformity across the wafer.
3. *Ultrahigh vacuum CVD* (UHVCVD)—CVD at very low pressure, typically below 10^{-6} Pa ($\approx 10^{-8}$ torr). Note that in other fields, a lower division between high and ultra-high vacuum is common, often 10^{-7} torr.

CVD system contains a system of metering the mixture of reactive and carrier gases, a heated reaction chamber, and a system for the treatment and disposal of exhaust gases. The gas mixture (which typically consists of hydrogen, nitrogen or argon, and reactive gases such as metal halides and hydrocarbons) is carried into a reaction chamber that is heated to the desired temperature. Different types of CVD methods have been developed over the last few decades. These include moderate-temperature CVD, plasma-assisted CVD and laser CVD. The deposition of coatings by CVD can be achieved in a number of ways such as thermal decomposition, oxidation and hydrolysis. From CVD an uniformly coated layer with thickness 2–100 μm can be obtained [89].

2.2.7 Nanofiber Preparation

There are many techniques for NFs preparation. Most common method is electrospinning.

2.2.7.1 Electrospinning

Nanofibers were first produced via electrospinning more than four centuries ago [90, 91] Beginning with the development of the electrospinning method, English physicist William Gilbert (1544–1603) first documented the electrostatic attraction between liquids by conducting an experiment in which he observed a spherical water drop on a dry surface warped into a cone shape when it was held below an electrically charged amber [92]. This deformation later came to be known as the Taylor cone [3]. In 1882, English physicist Lord Rayleigh (1842–1919) analyzed the unstable states of liquid droplets that were electrically charged, and noted that the liquid was ejected in tiny jets when equilibrium was established between the surface tension and electrostatic force [93]. In 1887, British physicist Charles Vernon Boys (1855–1944) published a manuscript about nanofiber development and production [94]. In 1900, American inventor John Francis Cooley (1861–1903) filed the first modern electrospinning patent [95].

Electrospinning term in science web was first introduced by Doshi and Reneker in 1993, and they also highlighted the unique features of electrospinning as a fabrication technique and the distinct morphology of electrospun nanofibers [96, 97]. Electrospinning was first patented in the US in 1902 [98]. It is a simple, flexible, and affordable technology based on electrostatic forces which is used for producing nanofibers with a high surface-to-volume ratio. The nanofibers produced by electrospinning have such advantages as high encapsulation efficiency, controlled release of the encapsulated component, and high thermal, light, and storage stability with increased protection of bioactive compounds. Electrospinning is used as a favored

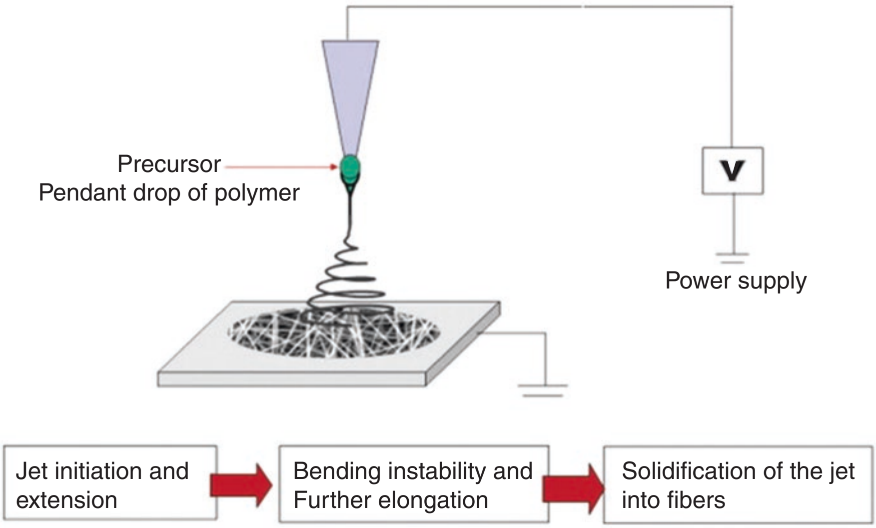

Fig. 2.14 Basic principle of electrospinning

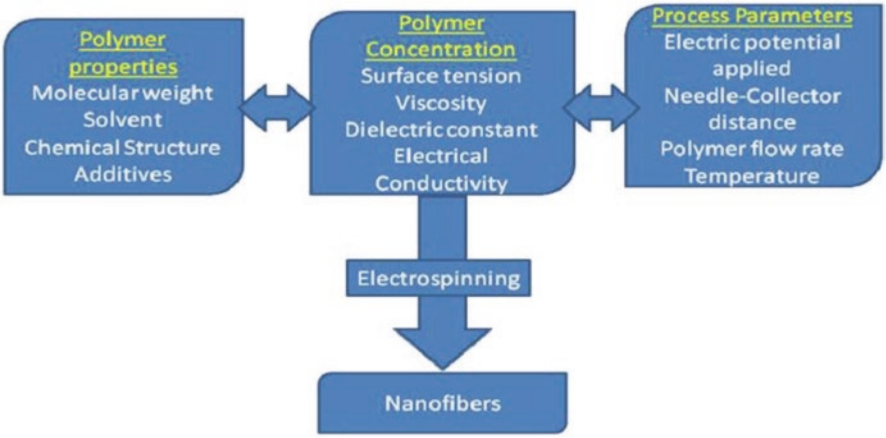

Fig. 2.15 Major parameters governing electrospinning technology [99]

tool to spin many synthetic and natural polymers into nanofibers. A typical electrospinning apparatus is schematically illustrated in Fig. 2.14.

The major parameters governing electrospinning technology are given in Fig. 2.15. Electrospun nanofibers possess high density of pores, high surface area to volume ratio, high permeability, low basis weight and small fiber diameter [99].

Electrospinning has an advantage with its comparative low cost and relatively high production rate. Micron size yarns consisting of nanofibers can be produced at a rate of 70 m/min, and different assemblies can be formed. Electrospinning is a simple, efficient and inexpensive way to make ultra fine fibers using various materials (e.g., polymers, ceramics, or even metals). The resulting nanofibers have high specific surface area and porosity and form nanofiber mats with complex pore structure.

Electrospinning process can be classified into two groups:

1. Solution electrospinning.
2. Melt electrospinning.

Solution electrospinning is limited mainly by its low productivity, extra solvent extraction process, and requirement of toxic solvent. Several setups including multijets from single needle, multijets from multineedle, and needleless systems have been proposed for solution electrospinning to increase its productivity [100]. For single needle electrospinning (SNE) process, a single jet is initiated from the Taylor cone formed by the application of electric field. Li et al. prepared poly(lactic acid) (PLA)/chitosan core-shell structure nanofibers from a homogeneous solution using SNE and found that this method was simpler and more effective in producing core-shell structures from homogeneous solutions than other methods [101].

To increase the productivity, multineedle electrospinning (MNE) system is used which is a simple way to improve the productivity and a simple technique to fabricate composite fibers from the polymers that cannot be easily dissolved in common solvents. However, the needle configuration, number of needles, and needle gauge need to be optimized for the MNE design. For example, needles can be arranged in one- or two-dimensional configuration. However, charged jets could interfere with each other and restrain jets injected from the spinneret, leading to low production efficiency [102, 103].

Multijets from multineedle electrospinning (MNE) system usually needs a big space and optimization of the relative distance between needles to avert strong charge repulsions between the jets. Therefore, needleless electrospinning has been developed and widely used due to its notable ability to increase the production of nanofibers. For the needleless electrospinning, an electric field is applied on a large area, producing numerous polymeric jets from free liquid surface [100]. Sasithorn and Martinová prepared silk nanofibers by both needle electrospinning and needleless electrospinning and found that the mass production rate of needleless electrospinning was much higher than that of needle electrospinning. In addition, the production rate of needleless electrospinning could be increased significantly with the increase of solution concentration and applied voltage. However, nanofibers produced by needle electrospinning were much smaller and had a narrow diameter distribution [104].

It is known that the increases in the molecular weight and viscosity of polymers lead to higher surface tension of their Taylor cone, which makes the fabrication of nanofibers by the conventional electrospinning methods impossible. Therefore, higher electrostatic force is required for the electrospinning to fabricate desired nanofibers [105]. Due to low productivity and uncontrollability of the needle spinning process and with other drawbacks researchers tried to develop other technology such as *Bubble Electrospinning* [105, 106].

Bubble electrospinning has attracted considerable attention due to its high throughput. Unlike conventional electrospinning, bubble electrospinning uses electrostatic force rather than Taylor cone to overcome the surface tension of a polymer bubble [107, 108]. The electrospinning ability of bubble electrospinning depends geometrically on the sizes of the obtained bubbles, which avoids using high voltages and thus makes it the best candidate in the green production. Figure 2.16 shows a typical bubble electrospinning setup.

In a typical bubble electrospinning process, bubbles are formed on the surface of a polymer solution by a controllable syringe pump as the gas pump slowly turned on. The number of the bubbles is reduced with the decrease of the tube diameter. Multiple jets are then ejected from the bubbles to the grounded collector when the applied voltage surpasses a critical value. The fluid jets are usually solidified into fibers in less than 0.001 s.

Figure 2.17 shows an experimental setup of blown bubble spinning.

Blown bubble spinning produces nanofibers using blowing air and has been used commercially as a one- step process to convert polymer resin directly into a nonwoven mat of fibers. Blown bubble spinning process is very similar to bubble electrospinning except that it uses blowing air instead of electronic force to produce fine fibers. However, a weak electronic field can significantly improve the performance of the blown bubble spinning, which actually turns into an electrostatic-field-assisted

Fig. 2.16 Bubble electrospinning setup for tunable bubble size [100, 109]

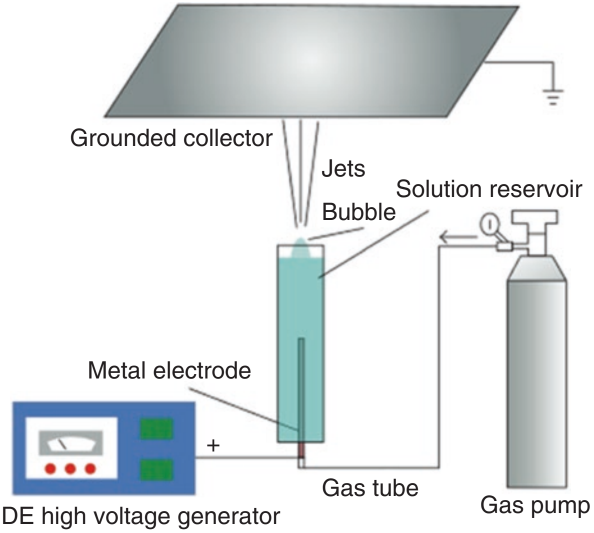

Fig. 2.17 Blown bubble spinning (the only acting force is blowing air) [100, 109]

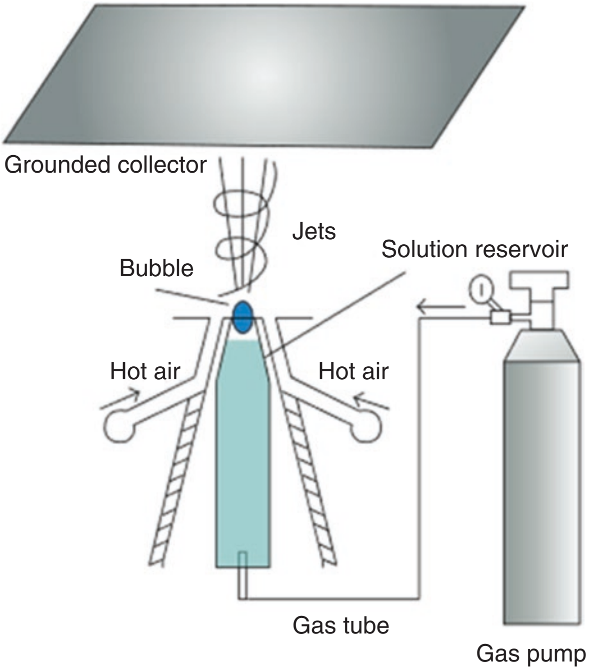

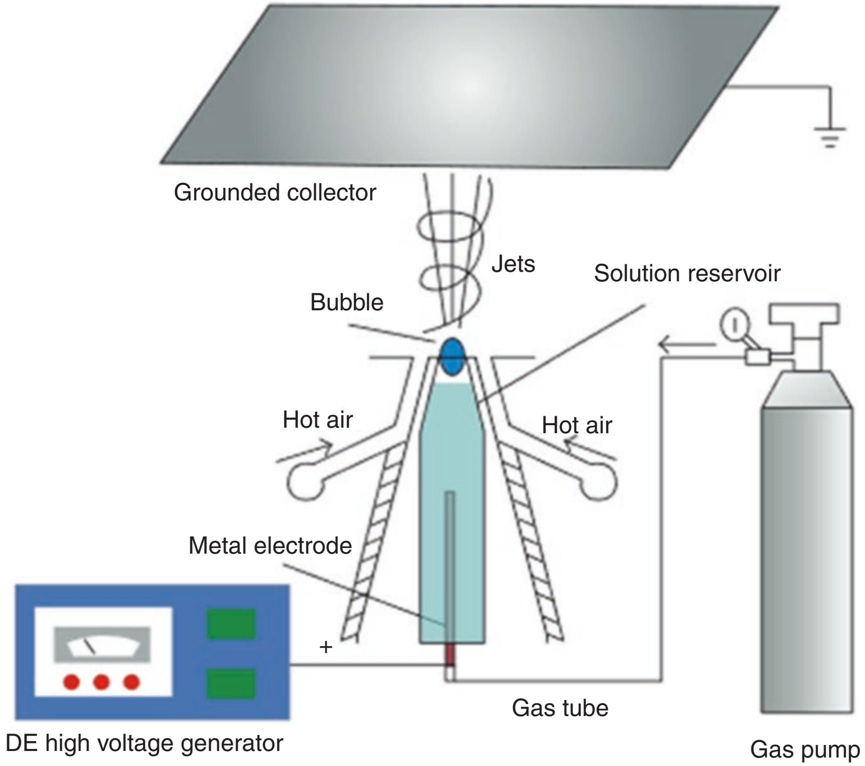

Fig. 2.18 Air-jet assisted bubble electrospinning or electrostatic field-assisted blown bubble spinning [100]

blown bubble spinning (Fig. 2.18). It can also be called as air-jet assisted bubble electrospinning, depending on which one is the major functional force.

2.2.7.2 Centrifugal Spinning

Centrifugal spinning, also called rotary spinning or rotational jet spinning, has been well developed. Since no high voltage is required by the centrifugal spinning, the system can alleviate safety-related concerns. In addition, centrifugal spinning can remarkably improve the production efficiency by increasing the rotational speed, allowing the fast and large-scale fabrication of nanofibers.

During a typical spinning process, a polymer solution is introduced into a highly rotating spinneret and then ejected as jets at a high rotating speed which is used to overcome the surface tension. The jets are then deposited on the collectors to form dried nanofibers as the solvent evaporates during the stretching process. Figure 2.19 shows a typical setup for centrifugal spinning [109].

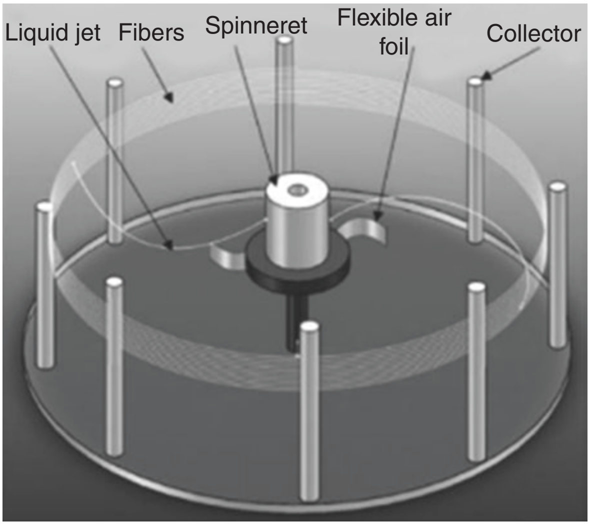

Fig. 2.19 Setup of centrifugal spinning [100, 110]

Erickson et al. fabricated highly aligned chitosan/polycaprolactone (PCL) nanofibers via centrifugal electrospinning system. Compared with those produced by the conventional electrospinning, the nanofibers produced by centrifugal electrospinning showed more uniform diameters and were aligned vertically. The diameter distribution of the nanofibers produced by centrifugal electrospinning was from 100 to 275 nm, which was much narrower than that of the nanofibers produced by the conventional electrospinning (25–450 nm) [111].

2.2.7.3 Melt Electrospinning

Melt Electrospinning is a new and revolutionary technique that bridges the gap between current additive manufacturing, such as 3D printing and solution electrospinning. Melt electrospinning is a form of electrospinning where a polymer melt is used to form fibrous material. Melt electrospinning typically produces microfibers in the range of 5–40 μm, although this technology has been shown to produce submicron diameter fibers. Within the field of regenerative medicine this is highly advantageous as melt electrospinning can produce fibres with higher resolution compared to 3D printing. Controlled deposition of 3D scaffolds is possible with programmable porosity and alignment requirements. It also overcomes the negative requirements of solution electrospinning; toxic solvents are not required within the process.

The electrified molten jet is not subject to the ‘whipping motion’ observed in solution electrospinning, leading to a greater control over the deposition of the fiber [112]. Additionally, during deposition the fibers do not repel each other. These advantages are attributed to the elimination of solvent in this process. With no solvent needed for this process it also has implications for the overall application, as residual solvent does not need to be removed before using the desired scaffold on cells or *in vivo*. Melt electrospun fibers have been directly deposited onto cells showing no issues with cell viability [113–115]. The Spraybase® Melt Electrospinning instrument is designed so that user's own proprietary polymer, medical grade or laboratory grade polymers can be used as received.

2.2.8 Formation of a Superhydrophilic Membranes

Membranes formed by superhydrophobic materials are limited to the separation of oil-rich oil/water mixtures and not suitable for water-rich oil/water mixtures or oil-in-water emulsions. Underwater superoleophobic surfaces have been proposed by Xu et al. [116] to separate oils from water. Zhang et al. [117] fabricated superhydrophilic and under water superoleophobic PAA-g-PVDF membranes for effective separation of oil-in-water emulsions.

Figure 2.20a shows the schematic of the process for membrane formation. A PAA-g-PVDF concentrated N-methylpyrrolidone (NMP) solution on the substrate is immersed into salty water, and the solvent exchange between water and NMP occurs immediately at the interface of the two liquids. As a result of the instant increase in salt concentration at the interface, NaCl is squeezed out from the water and tends to crystallize into small crystal seeds at the interface [117].

This structure is similar to those of most of traditional polymeric membranes formed by a phase-inversion process. On the top of the membrane, there is a thin skin layer or a so-called separation layer. The enlarged top-view SEM image of the membrane surface shows that it is composed of numerous spherical micro-particles of a sub-micrometer scale. Such a structure is different from the traditional membranes. The micro-particles are disorderly arranged but closely connected, thus giving rise to a rather rough surface. On the surfaces of these micro-particles there are much finer protrusion structures of the nanometer scale. The bottom surface of the membrane is completely different from the top surface. It gives a typical porous structure and no micro-spheres are observed. These results indicate that the existence of NaCl in water affect only the microstructure of the top surface of the membrane. In other words, NaCl seeds are only produced at the interface of two liquids during the phase-inversion process.

Electrospun ceramic nanofibers are micro-nano porous in nature, therefore, are most suitable for removal of particulate molecules and small particles from both air and aqueous solutions compared to normal filter. These properties of electrospun nanofiber membranes make them suitable as filters in environment science. The other properties of nanofibers such as high aspect ratio, high porosity, and large surface area make them useful in a variety of applications including fabrication of electric and optical devices, optical waveguides, optoelectronic components, fluidic devices, gas storage units, tissue engineering scaffolds, bioreactors etc.

The production of nanofibers by the electrospinning process is influenced both by the electrostatic forces and the viscoelastic behavior of the polymer. Process

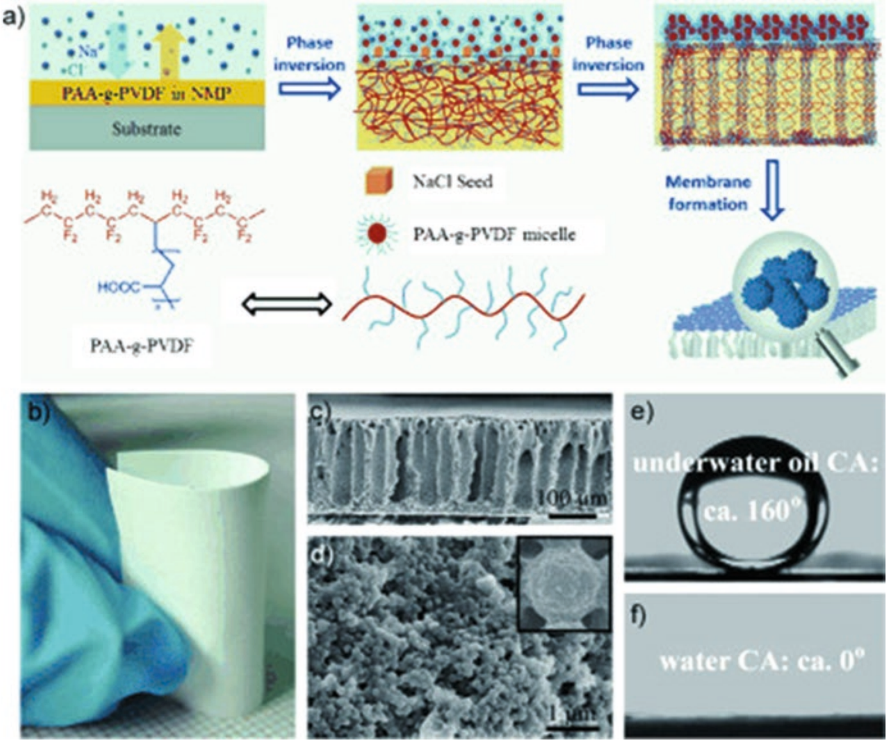

Fig. 2.20 (**a**) Formation of a superhydrophilic underwater superoleophobic PAA-g-PVDF membrane by a salt-induced phase-inversion process, (**b**) photograph of an as-prepared PAA-g-PVDF membrane, (**c**) cross-section, (**d**) top-view SEM images of the membrane, (**e**) photographs of an underwater oil droplet, (**f**) a water droplet on the membrane. (The PAA-g-PVDF membrane was prepared by using PAA-g-PVDF with a graft ratio of 2.5 wt.% in the case of a salt concentration of 35%.) [117]

parameters, like solution feed rate, applied voltage, nozzle-collector distance, spinning environment, and material properties, like solution concentration, viscosity, surface tension, conductivity, and solvent vapor pressure, influence the structure and properties of electrospun nanofibers.

2.2.9 Freeze-Drying

Freeze-drying (FD) can fabricate porous structures with controllable sizes directly from polymers, such as chitin, without structure-directing additives or pre-treatments needed, which cannot be achieved by other techniques, such as self-assembly and electrospinning [118]. In addition, no high temperature and further leaching step are required for the freeze-drying process [119]. Therefore, it has drawn increasing attention in the fabrication of nanofibers. Starting with solution, emulsion, or dispersion, freezing causes the solute or solids to be excluded by ice front in the interstitial spaces between ice crystals. Then porous structures are created by the following sublimation.

2.2.10 Cell Membrane

The cell membrane, also known as the plasma membrane, is a double layer of lipids and proteins that surrounds a cell and separates the cytoplasm (the contents of the cell) from its surrounding environment. It is selectively permeable, which means that it only lets certain molecules enter and exit. It can also control the amount of some substances that go into or out of the cell. All cells have a cell membrane. Many types of membranes have been used to construct biomimetic core-shell nanoparticles for cancer therapy (Table 2.4) [120].

The preparation of cell-membrane coated nanoparticles involves three steps:

1. Membrane extraction from cells or bio-vesicles.
2. Core nanoparticle preparation.
3. Fusion of the two into core-shell nanoparticles.

Figure 2.21 presents schematic illustration of the preparation of cell-membrane coated nanoparticles.

Table 2.4 Currently explored source cells for membrane coated nanoparticles

Source cells	Key features
RBCs	Suppressing immune attack by the abundant “self-markers” on their surface Prolonged blood circulation time (about 120 days) Biocompatible and biodegradable
Platelets	Selective adherence to the vasculatures of the disease sites Specific aggregation surrounding circulating tumor cells through P-selection and CD44 receptors Good immune-compatibility
Bacteria	Immunogenicity Tumor tropism Secret outer membrane vesicles
Immune cells	Homing to the diseased sites Ability to penetrate the vasculature Targeting metastatic cancer cells through VCAM-1-α4 integrins interaction Ability of avoiding the immune clearance
Cancer cells	Achieve vaccine applications by promoting a tumor-specific immune response Allow a unique tumor sites targeting by an inherent homotypic binding
Stem cells	Natural active target effect to solid tumors at diverse development
Cancer cells	Achieve vaccine applications by promoting a tumor-specific immune response Allow a unique tumor sites targeting by an inherent homotypic binding

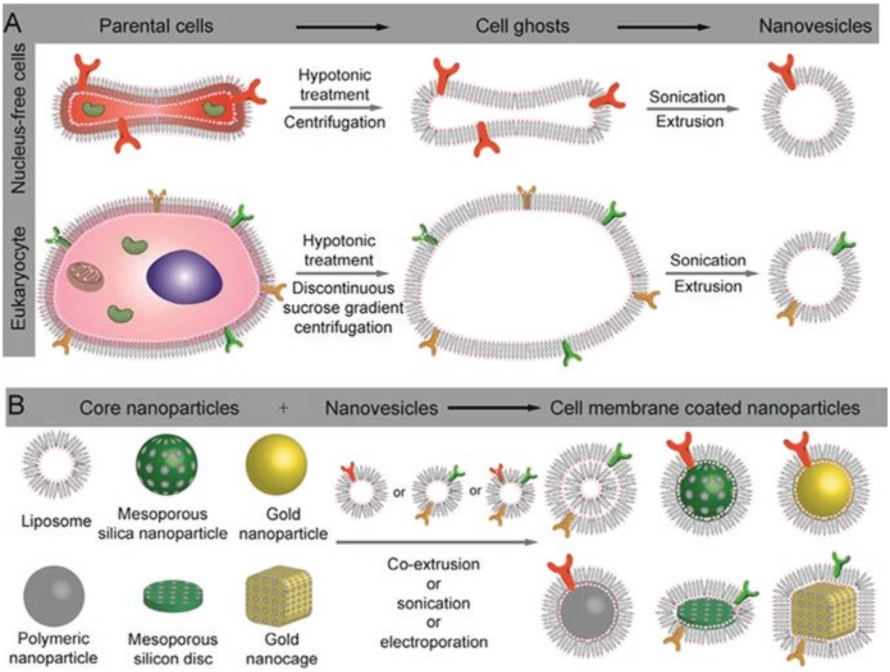

Fig. 2.21 Schematic illustration of the preparation of cell-membrane coated nanoparticles. (**a**) Extract of intact cell ghost from parent cells and further processing into nanovesicles. (**b**) Different types of nanoparticles that have been used as inner cores, and their fusion with nanovesicles to construct cell membrane coated nanoparticles [120]

2.2.11 Ion-Exchange Membrane (IEM)

Among the separation membranes, ion exchange membranes are one of the advanced separation membranes. Ion-exchange membranes are traditionally used in; electrodialysis or diffusion dialysis by means of an electrical potential or concentration gradient, respectively, to selectively transport cationic and anionic species. Exemplary applications of ion-exchange membranes utilized in electrodialysis and EDR (electrodialysis reversal) include seawater desalination, industrial wastewater treatment of highly scaling waters, food and beverage production, and other industrial wastewaters etc. [121].

The properties of IEMs primarily depend on:

1. Membrane material, which chiefly determines the mechanical, chemical, and thermal stability of IEMs.
2. The type, concentration, and distribution of the ion exchange groups which determine the electrochemical properties of the IEMs and also happen to considerably influence the other IEMs properties. The electrochemical properties are the most significant properties in ED (electrodialysis).

An ion-exchange membrane is a semi-permeable membrane that transports certain dissolved ions, while blocking other ions or neutral molecules. Ion-exchange membranes are therefore electrically conductive. They are often used in desalination and chemical recovery applications, moving ions from one solution to another with little passage of water. There are different methods of classifying ion-exchange membranes based on their function, materials constituting the membranes, etc. Classification based on function is clear; ion-exchange membranes have an electrical charge, which is positive or negative. The function of ion-exchange membranes is determined from the species of the charge of the ion-exchange groups fixed in the membranes and their distribution [122]. Cation exchange membranes, in which cation exchange groups (negatively charged) exist and cations selectively permeate through the membranes.

1. Anion exchange membranes, in which anion exchange groups (positively charged) exist and anions selectively permeate through the membranes.
2. Amphoteric ion exchange membranes, in which both cation and anion exchange groups exist at random throughout the membranes.
3. Bipolar ion-exchange membranes which have a cation exchange membrane layer and anion exchange membrane layer (bilayer membranes).
4. Mosaic ion exchange membranes, in which domains having cation exchange groups exist over cross-sections of the membranes and domains of anion exchange groups also exist. An insulator may exist around the respective domains.

Incorporation of nanomaterials (NMs) into IEMs has been investigated as a means of improving their properties. Many approaches have been attempted to synthesize robust IEMs suitable for different applications. Some of the methods adopted to create IEMs with enhanced properties include variation of functional groups, combination of polymers, adjustment of cross-link density, inclusion of additives, and surface modification [123].

There are several methods of incorporating nanomaterials into ion exchange membranes [123].

1. Blending: The polymer is dissolved in a solvent, followed by addition of the NMs. Hereafter, the solution is thoroughly mixed (usually via sonication or stirring) to ensure a uniform dispersion of the NM in the polymer. Afterwards, the solvent is removed (by phase inversion) and the NMs are rearranged and embedded in the polymer to form mixed matrix membranes. Solution blending is the most frequently used technique in fabricating polymeric nanocomposites and is thus commonly used in synthesizing NMs-assisted IEMs. The method of solution blending is based on the solubility of the polymer and a suitable solvent. A schematic description of the general procedure of the solution blending method is illustrated in Fig. 2.22.
2. In situ polymerization: Polymerization involves the use of monomers rather than pre-formed polymers. Basically, NMs or their precursors are dispersed in a liquid monomer or monomer solution, followed by polymerization. The

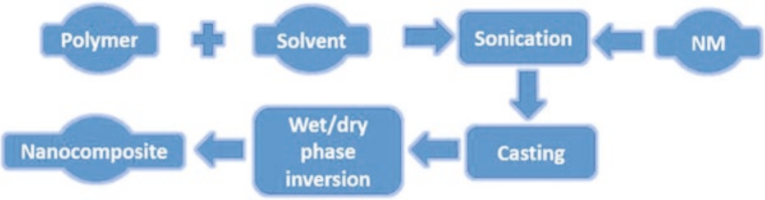

Fig. 2.22 General schematic representation of solution blending method of NM incorporation in IEMs. The polymer is dissolved in a solvent, followed by addition of the NMs. Hereafter, the solution is thoroughly mixed (usually via sonication or stirring) to ensure a uniform dispersion of the NM in the polymer. Afterwards, the solvent is removed (by phase inversion) and the NMs are rearranged and embedded in the polymer to form mixed matrix membranes [123]

polymerization is usually induced by the diffusion of an appropriate initiator or by applying heat or UV irradiation.

3. Melt mixing: Melt mixing involves the dispersion of NMs in a molten polymer matrix. Techniques such as extrusion and injection molding are used to mix a thermoplastic polymer with NMs at elevated temperatures.
4. In situ sol-gel: In situ sol-gel technique involves mixing a polymer with a NM precursor—such as tetraethoxysilane (TEOS) for silica—followed by hydrolysis and polycondensation of the precursor. The in-situ sol-gel technique is used for incorporating only NMs which have precursors e.g., silica and TiO_2, as such its applicability is limited to a few NMs.

Solution blending is by far the most frequently used technique in fabricating polymeric nanocomposites and is thus commonly used in synthesizing NMs-assisted IEMs.

2.2.12 Other Methods for the Preparation of Membranes

There are other methods for the preparation of membranes [124].

2.2.12.1 Spraying

Figure 2.23 shows a general schematic diagram for fabrication of sprayed membranes. It comprises a spray gun a template (stainless steel), a heater, a temperature controller, and a nitrogen gas line.

Polymer powder is injected in heat source (flame or plasma) and transported to a preheated substrate. The thickness of coating is governed by the number of repeated passes of the spray gun across the substrate. A large particle size or molecular weight distribution may facilitate the formation of numerous heterogeneous microstructures of the coated surface such as creating voids, trapped gases, unmelted particles, splits and pyrolyzed material.

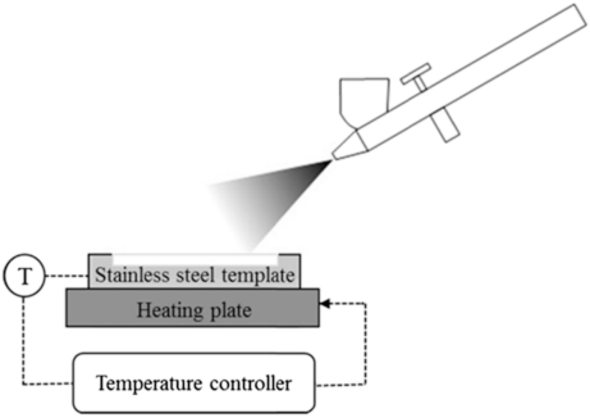

Fig. 2.23 Schematic diagram for fabrication of sprayed membranes [125]

Xing et al. [126] successfully used a solution-spray process to fabricate Nafion/polytetrafluoroethylene composite membrane. Prapainainar et al. [127] successfully fabricated homogeneous composite membranes by spraying Nafion/functionalized MOR (mordenite) powder in methanol, ethanol and DMF mixture. The spray gun was connected to a nitrogen gas line to create pressure.

2.2.12.2 Foaming

Current membrane fabrication methods usually involve multi-step processes and the use of organic solvents or additives. Dixon et al. [128] have introduced a process in which a liquid solution of polymer is sprayed into compressed CO_2. Techniques based on the use of highly compressed gases or supercritical fluids have been developed to form polymeric materials such as micro-spheres, porous fibers and porous foams. A rapid expansion of supercritical solutions (RESS) and a microcellular foaming process are well-known processes. In the RESS process, supercritical solution is expanded through a nozzle to form microspheres or microfibers. In the microcellular foaming process, a pellet of polymer is saturated with CO_2 at high pressure in the supercritical region and nucleation is induced by super saturation caused by a sudden pressure drop. In the precipitation with a compressed fluid antisolvent (PCA) precipitation, a polymer solution is sprayed through a capillary into a vessel containing a compressed gas. The CO_2 is miscible with the diluents but is an antisolvent (nonsolvent) for the polymer. Porous microspheres and fibers are produced by this technique. Ge et al. [129] described the process to prepare thermoplastic polyurethane (TPU) perforated membrane by using a physical foaming technique with CO_2 as the blowing agent. Various processing parameters, which included the saturation pressure, the foaming temperature, and the membrane thickness, were applied to adjust the TPU membrane's perforated morphology. Figure 2.24 shows

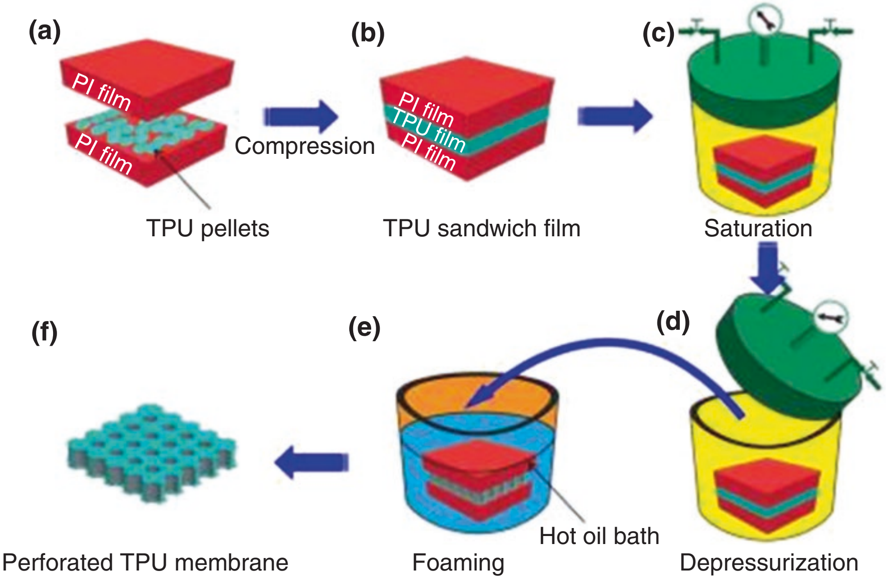

Fig. 2.24 Schematic for preparation of TPU perforated membrane [129]

the preparation process. The base material, meaning the TPU pellets, was dispersed between two PI films and compressed under 15 MPa and 190 °C to achieve a thickness of about 20 μm TPU film (Fig. 2.24a,b). This was close to the cell size of the foamed materials obtained through the traditional technique. The sandwich film was saturated in a high-pressure chamber at 25 °C for 12 h (Fig. 2.24c), allowing sufficient CO_2 dissolution in the TPU's matrix. The saturated TPU was removed from the chamber (Fig. 2.24d) and placed into a high-temperature oil bath to foam via the temperature-induced foaming method (Fig. 2.24e). The presence of large amounts of interface area between the TPU and the PI films could act as the heterogeneous nucleation sites. These tended to enhance cell nucleation on the TPU's surface, which resulted from the lower energy barrier required for heterogeneous nucleation. Consequently, a perforated membrane could be easily prepared (Fig. 2.24f) during the foaming.

2.2.12.3 Particle Leaching

Particle (particulate, salt, porogen) leaching is applied in combination with various different techniques such as solvent casting, compression molding or foaming. In particle leaching, particles, e.g., salt, sugar, or specially prepared spheres, are incorporated in a polymer sample. After processing the polymer sample in the final form, the particles are dissolved and washed out creating (additional) porosity in the scaffold. This method ensures that membranes with highly controlled porosity and pore sizes are produced [130]. However, this technique may not be applicable to all materials (e.g., soluble protein scaffolds). Also, the washing out post-process is time-consuming and there is a risk of residues remaining from the method of processing (i.e., organic solvents). Thus, this method is preferred for polymers that are not soluble in common organic solvents. Porous membranes produced via this method include polyethylene membranes using tapioca starch as the leachable component and 2,3-dialdehydecellulose membranes with sodium chloride (NaCl) used as the leachable component [131]. To improve the performance of an ionic polymer metal composite (IPMC), Jung et al. [132] suggested a porous Nafion membrane fabricated with the particulate leaching method with zinc oxide and proposed an ionic polymer metal composite (IPMC) actuator that uses the porous Nafion membrane. To fabricate this membrane, the proper ratio of Nafion and zinc oxide powder is dispersed in a solvent. The mixture is cast into a membrane and the embedded zinc oxide particles are dissolved by an acid solution, leaving the spaces of the zinc oxide particles as pores. Further followed via electroless plating and ion exchange procedures, an IPMC actuator with the porous Nafion membrane is fabricated.

2.2.12.4 Precipitation from the Vapor Phase

Once a solvent-polymer mixture is cast on the film, it is placed in a vapor atmosphere that contains a nonsolvent saturated with the same solvent. Due to the high concentration of solvent in the vapor atmosphere, the solvent from the cast film stays instead of being evaporated into the atmosphere. Membrane forms by diffusion of nonsolvent into the cast film. This process results in a porous membrane.

2.2.12.5 Sintering

Sintering or frittage is the process of compacting and forming a solid mass of material by heat or pressure without melting it to the point of liquefaction. In the process of ceramic membrane preparation sintering is necessary. Porous membranes can be obtained from both organic and inorganic material using the sintering technique. This method involves pressing a powder of particles of a given size and then sintering at elevated temperatures. The temperature required for sintering depends on the material used. During the sintering, the interface between the contacting particles disappears. Traditionally, this method is used for ceramic powders; however, other materials (glasses, metals and certain polymers) can also be processed. Production of polymeric membranes with a controlled and graded porosity is possible with this technique. Membranes with desirable properties including higher thermal and mechanical stabilities with a better chemical and microbial resistance can be fabricated with sintering technique. Scaffolds fabricated by sintering are mainly used in hard tissue engineering applications. The membranes prepared with this technique can be used in harsh environments (higher temperature and exposure to various chemicals), especially ceramic membranes, which have relatively long life of use and are typically applied to separation processes due to their permeation characteristics. By monitoring the conditions of the sintering procedure (temperature, pressure, particle size, green density, and the addition of sintering additives), the pore sizes, porosity and pore tortuosity can be controlled [133]. For medical purposes, sintering can be conducted to form 3D porous scaffolds by sintering polymeric microspheres onto existing molds, which is widely used in bone tissue engineering [134].

As in the process, various shaping techniques such as slip/tape casting, extrusion, and pressing are used to make membrane precursors from particle suspension, slurry, or paste. No matter which process is adopted to prepare the ceramic membrane precursors, sintering (firing step) is necessary to yield the membranes promising mechanical strength and pore structure [135]. Li et al. [136] prepared a porous, sintered, and reaction-bonded Si_3N_4 (SRBSN) planar membrane by phase-inversion tape-casting, nitration, and sintering of silicon slurry. The membrane was comprised of uniform rod-likeβ-Si_3N_4 crystals with a large length/diameter ratio and had high porosity and bending strength. It was reported that sintered membranes have excellent potential for the treatment of oily wastewater.

2.2.12.6 Stretching

Extrusion-stretching technique to prepare porous polymeric membranes from either filled or unfilled semi crystalline polymers comprises two consecutive steps. An oriented film is produced by melt-extrusion process with a rapid haul-off speed. After solidifying, the film is then stretched in either a parallel or perpendicular direction to the original orientation of the polymer crystallites. For unfilled systems, the second stretching deforms the crystalline structure of the film and produces slit-like pores with diameters ranging from ca. 20 to 50 nm. For filled systems, the second stretching results in partial removal of the solid fillers yielding a porous structure. Membranes prepared by this technique have been used as inert separating porous barriers in batteries and in some medical devices [130]. Lu et al. [137] fabricated PVC hollow fiber via a melt spinning method and on-line stretching treatment. The surface pores gradually became narrow and long when the stretching ratio increased, and the changes in the pore size of the outer surface were more obvious. The surface of the membrane became smooth with the increment of stretching ratio, and the roughness of the inner surface was larger than that of the outer surface at the same stretching ratio. The mean pore size, porosity and PWF of the resultant membrane were also controlled by the on-line stretching treatment which made them increase.

Li and Xiao [138] fabricated ultrahigh molecular weight polyethylene (UHMWPE)/SiO_2 hybrid hollow fibre membranes via thermally induced phase separation-stretching (TIPS-S), using mineral oil as diluent and SiO_2 as additive. The area of interfacial microvoid and the pores connectivity increased with increasing draw ratios. The permeability of membrane showed the best performance at the fivefolds draw ratio. The effects of heat-treatment and drawing temperature on pore structure have been mainly produced from the pore's contraction and defect formation. Wang et al. [139] prepared TiO_2/PP composite membranes via melt extruding/annealing/stretching. Compared to the virgin PP membrane, the PP/TiO_2 composite membranes at high TiO_2 loadings showed significant improvements in terms of the water vapor permeability, polarity, and electrolyte uptake capability.

2.3 Summary

The present chapter described the materials used for membranes preparation for the use of nanotechnology in various aspects. For each application, membranes for a desired performance are expected to be designed and manufactured. Even though chemical and physical properties of the membrane, especially those of the membrane surface, are known to govern the membrane performance, they depend on the many parameters involved in membrane fabrication. Because of the complexity arising among those parameters, to make a desirable membrane for a particular aim is still considered to be an art, even several decades after the emergence of industrial membrane processes. The increasing number of researches, in which membrane technology based on nanomaterials was applied for the separation processes, showed that these nanocomposite materials can be efficiently used for the selective separation of target compound/s from environmental samples.

References

1. Holister P, Román C, Vas CR, Harper T (2003) Nanoporous materials. Científica White Papers nr. 5: 11 pages
2. Kargari A, Shirazi MMMA (2014) Water desalination: solar-assisted membrane distillation. In: Capehart BL (ed) Encyclopedia of energy engineering and technology, 2nd edn. CRC Press, Boca Raton, pp 1–15
3. Taylor G (1969) Electrically driven jets. Proc R Soc Lond A 313:453–475
4. Tlili I, Alkanhal TA (2019) Nanotechnology for water purification: electrospun nanofibrous membrane in water and wastewater treatment. J Water Reuse Desalin 9(3):232–248
5. Ramakrishna S, Fujihara K, Teo WE, Yong T, Ma Z, Ramaseshan R (2006) Electrospun nanofibers: solving global. Mater Today 9(3):40–50
6. Chen YQ, Zheng XJ, Feng X (2010) The fabrication of vanadium-doped ZnO piezoelectric nanofiber by electrospinning. Nanotechnology 21:055708
7. Zhu J, Jia L, Huang R (2017) Electrospinning poly(l-lactic acid) piezoelectric ordered porous nanofibers for strain sensing and energy harvesting. J Mater Sci Mater Electron 28:12080–12085
8. Faneer KA, Rohani R, Mohammad AW (2016) Polyethersulfone nanofiltration membrane incorporated with silicon dioxide prepared by phase inversion method for xylitol purification. Polym Polym Composites 24(9):803–808
9. Wu H, Tang B, Wu P (2014) Development of novel SiO_2–GO nanohybrid/polysulfone membrane with enhanced performance. J Membr Sci 451:94-102

10. Wu L, Shamsuzzoha M, Ritchie SMC (2005) Preparation of cellulose acetate supported zero-valent iron nanoparticles for the dechlorination of trichloroethylene in water. J Nanopart Res 7(4–5):469–447
11. Sun W, Shi J, Chen C, Li N, Xu Z, Li J, Lv H, Qian X, Lhao L (2008) A review on organic–inorganic hybrid nanocomposite membranes: a versatile tool to overcome the barriers of forward osmosis. RSC Adv 8:10040–10056
12. Zunita M, Makertihartha IGBN, Saputra FA, Syaifi YS, Wenten IG (2018) Metal oxide based antibacterial membrane. IOP Conf Ser Mater Sci Eng 395:012021
13. Pedro XQ, Alvarez JJ, Li Q (2013) Applications of nanotechnology in water and wastewater treatment. Water Res 47(12):931–3946
14. Mondal S (2017) Carbon nanomaterials based membranes. J Membr Sci Technol 6(4):e122. https://doi.org/10.4172/2155-9589.1000e122
15. Das R, Ali ME, Hamid SBA, Ramakrishna S, Chowdhury ZZ (2014) Carbon nanotube membranes for water purification: a bright future in water desalination. Desalin 336:97–109
16. Ribeiro B, Botelho EC, Costa ML, Bande CF (2017) Carbon nanotube buckypaper reinforced polymer composites: a review. Polímeros 27(3):247–255
17. Iijima S (1991) Helical microtubules of graphitic carbon. Nature 354:56–58
18. Tiraferri A, Vecitis CD, Elimelech M (2011) Covalent binding of single-walled carbon nanotubes to polyamide membranes for antimicrobial surface properties. ACS Appl Mater Inter 3:2869–2877
19. Al-anzi BSS, Siang OC (2017) Recent developments of carbon based nanomaterials and membranes for oily wastewater treatment. RSC Adv 7:20981–20994
20. Ahn CH, Baek Y, Lee C, Kim SO, Kim S, Lee S, Kim H, Bae SS, Park J, Yoon J (2012) Carbon nanotube-based membranes: fabrication and application to desalination. J Ind Eng Chem 18(5):1551–1559
21. Holt K, Park HG, Wang Y, Stadermann M, Artyukhin AB, Grigoropoulos CP, Noy A, Bakajin O (2006) Fast mass transport through sub-2-nanometer carbon nanotubes. Science 312(5776):1034–1037
22. Ames technology capabilities and facilities, https://www.nasa.gov/centers/ames/research/technology-onepagers/carbon_nanotube_growth.html#backtoTop. Accessed 19 Oct 2018
23. Graf C, Vossen DLJ, Imhof A, van Blaaderen A (2003) A general method to coat colloidal particles with silica. Langmuir 19(17):6693–6700
24. Zhao GJ, Stevens SE (1998) Multiple parameters for the comprehensive evaluation of the susceptibility of Escherichia coli to the silver ion. Biometals 11:27–32
25. Vardanyan Z, GevorkyanV AM, Vardapetyan H, Trchounian A (2015) Effects of various heavy metal nanoparticles on Enterococcus hirae and Escherichia coli growth and proton-coupled membrane transport. J Nanobiotechnol 13:69. https://doi.org/10.1186/s12951-015-0131-3
26. Kim M, Kang SW (2019) PEBAX-1657/Ag nanoparticles/7,7,8,8-tetracyanoquinodimethane complex for highly permeable composite membranes with long-term stability. Sci Rep 9:4266. https://doi.org/10.1038/s41598-019-40185-6
27. Ng LY, Mohammad AW, Leo CP, Hilal N (2013) Polymeric membranes incorporated with metal/metal oxide nanoparticles: a comprehensive review. Desalin 308:15–33
28. Tugulea AM, Bérubé D, Giddings M, Lemieux F, Hnatiw J, Priem J, Avramescu ML (2014) Nano-silver in drinking water and drinking water sources: stability and influences on disinfection by-product formation. Environ Sci Pollut Res Int 21(20):11823–11831
29. Galdiero S, Falanga A, Vitiello M, Cantisani M, Marra V, Galdiero M (2011) Silver nanoparticles as potential antiviral agents. Molecules 16(10):8894–8918
30. Heo DN, Min KH, Choi GH, Kwon IK, Park K, Lee SC (2014) Chapter 2. Scale-up production of theranostic nanoparticles. Academic Press, pp 457–470
31. Muthuraman A, Kaur J (2017) Chapter 6—Antimicrobial nanostructures for neurodegenerative infections: present and future perspectives. In: Ficai A, Grumezescu AM (eds) Nanostructures for antimicrobial therapy, Elsevier, pp 139–167. isbn: 978-0-323-46152-8
32. Geim AK, Novoselov KS (2007) The rise of graphene. Nat Mater 6:183–191

33. File:Graphen.jpg—Wikipedia
34. Gopalakrishnan A, Krishnan R, Thangavel S, Venugopal G, Kim SJ (2015) Removal of heavy metal ions from pharma-effluents using graphene-oxide nanosorbents and study of their adsorption kinetics. J Ind Eng Chem 30:14–19
35. Lingamdinne LP, Koduru JR, Choi YL, Chang YY, Yang JK (2015) Studies on removal of Pb (II) and Cr (III) using graphene oxide based inverse spinel nickel ferrite nano-composite as sorbent. Hydrometallurgy 165:64–72
36. Boretti A, Al-Zubaidy S, Vaclavikova M, Al-Abri M, Castelletto S, Sergey S (2018) Outlook for graphene-based desalination membranes. npj Clean Water 1:5
37. Yang K, Chen B, Zhu L (2015) Graphene-coated materials using silica particles as a framework for highly efficient removal of aromatic pollutants in water. Sci Rep 5:11641
38. Song N, Gao X, Ma Z, Wang X, Wei Y, Gao C (2018) A review of graphene-based separation membrane: materials, characteristics, preparation and applications. Desalin 437:59–72
39. Zhu X, Yang K, Chen B (2017) Membranes prepared from graphene-based nanomaterials for sustainable applications: a review. Environ Sci Nano 4:2267–2285
40. Ganesh BM, Isloor AM, Ismail AF (2013) Enhanced hydrophilicity and salt rejection study of graphene oxide-polysulfone mixed matrix membrane. Desalin 313:199–207
41. Huiliang D, Jingyuan L, Jing Z, Gang S, Xiaoyi L, Yuliang Z (2011) Separation of hydrogen and nitrogen gases with porous graphene membrane. J Phys Chem C 115(47):23261–23266
42. Yoon HW, Cho YH, Park HB (2016) Graphene-based membranes: status and prospects. Phil Trans R Soc A 374:20150024. https://doi.org/10.1098/rsta.2015.0024
43. Awad FS, Zied KMA, El-Maaty WMA, El-Wakil AM, El-Shall MSY (2020) Effective removal of mercury(II) from aqueous solutions by chemically modified graphene oxide nanosheets. Arab J Chem 13(1):2659–2670
44. Zhang L, Li H, Lai X, Su X, Liang T, Zeng X (2017) Thiolated graphene-based superhydrophobic sponges for oil-water separation. Chem Eng J 316:736–743
45. Ong CS, Al-Anzi BS, Lau WJ (2018) Carbon-based polymer nanocomposites for environmental and energy applications, pp 261–280. isbn: 9780128135747
46. Catalan Institute of Nanoscience and Nanotechnology (ICN2) (2018) https://phys.org/news/2018-04-closer-nanoporous-graphene-smart-filters.html
47. Kerr PF (1952) Formation and occurrence of clay minerals. Clay Clay Miner 1:19–32
48. Vinokurov VA, Stavitskaya AV, Chudakov YA, Ivanov EV, Shrestha LK, Ariga K, Darrat YA, Lvov YM (2017) Formation of metal clusters in halloysite clay nanotubes. Sci Technol Adv Mater 18(1):147–151
49. Kamble R, Ghag M, Gaikawad S, Panda BK (2012) Halloysite nanotubes and applications: a review. J Adv Sci Res 3(2):25–29
50. Joo Y, Jeon Y, Lee SU, Sim JH, Ryu J, Lee S, Lee H, Sohn D (2012) Aggregation and stabilization of carboxylic acid functionalized halloysite nanotubes (HNT-COOH). J Phys Chem C 116(34):18230–18235
51. Berahman R, Raiati M, Mazidi MM, Paran SMR (2016) Preparation and characterization of vulcanized silicone rubber/halloysite nanotube nanocomposites: effect of matrix hardness and HNT content. Mater Des 104:333–345
52. Ge L, Lin R, Wang L, Rufford TE, Villacorta B, Liu S, Liu LX, Zhu Z (2017) Surface-etched halloysite nanotubes in mixed matrix membranes for efficient gas separation. Sep Purif Technol 173:63–71
53. Murali RS, Padaki M, Matsuura T, Abdullah MS, Ismail AF (2014) Polyaniline in situ modified halloysite nanotubes incorporated asymmetric mixed matrix membrane for gas separation. Sep Purif Technol 132:187–119
54. Mishra G, Mukhopadhyay M (2018) Enhanced antifouling performance of halloysite nanotubes (HNTs) blended poly(vinyl chloride) (PVC/HNTs) ultrafiltration membranes: for water treatment. J Indus Eng Chem 63:366–379
55. Duan L, Zhao Q, Liu J, Zhang Y (2015) Antibacterial behavior of halloysite nanotubes decorated with copper nanoparticles in a novel mixed matrix membrane for water purification. Water Res Technol 1(6):874–881

56. Mishra G, Mukhopadhyay M (2019) TiO_2 decorated functionalized halloysite nanotubes (TiO_2@HNTs) and photocatalytic PVC membranes synthesis, characterization and its application in water treatment. Sci Rep 9:4345
57. Yang Y, Chen Y, Leng F, Huang L, Wang Z, Tian W (2017) Recent advances on surface modification of halloysite nanotubes for multifunctional applications. Appl Sci 7(1215):1–9. https://doi.org/10.3390/app7121215
58. Junaidi MUM, Khoo CP, Leo CP, Ahmad A (2014) The effects of solvents on the modification of SAPO-34 zeolite using 3-aminopropyl trimethoxy silane for the preparation of asymmetric polysulfone mixed matrix membrane in the application of CO_2 separation. Micropor Mesopor Mater 192:52–59
59. Subhan MA (2020) Antibacterial property of metal oxide-based nanomaterials. Nanotoxicity 2020:283–300
60. Pertici V, Martrou G, Gigmes D, Trimaille T (2018) Synthetic polymer-based electrospun fibers: biofunctionalization strategies and recent advances in tissue engineering. Drug delivery and diagnostics. Curr Med Chem 25(20):2385–2400
61. Khil MS, Cha DI, Kim HY, Email A, Kim IS, Bhattarai N (2003) Electrospun nanofibrous polyurethane membrane as wound dressing. J Biomed Mater Res Part B Appl Biomater 67(2):675–679
62. Kumbar G, Nukavarapu SP, James R, Nair LS, Laurencin CT (2008) Electrospun poly(lactic acid-co-glycolic acid) scaffolds for skin tissue engineering. Biomaterials 29:4100–4107
63. Tallawi M, Rosellini E, Barbani N, Cascone MG, Rai R, Saint-Pierre G, Boccaccini AR (2015) Strategies for the chemical and biological functionalization of scaffolds for cardiac tissue engineering: a review. J R Soc Interface 12(108):20150254. https://doi.org/10.1098/rsif.2015.0254
64. Krishnaswamy K, Orsat V (2017) Chapter 2: Sustainable delivery systems through green nanotechnology in nano- and microscale drug delivery systems. In: Design and fabrication. Elsevier, pp 17–32
65. Nanoparticle production—How nanoparticles are made. https://www.nanowerk.com/how_nanoparticles_are_made.php. Accessed 14 May 2019
66. Pal SL, Jana U, Manna PK, Mohanta GP, Manavalan R (2011) Nanoparticle: an overview of preparation and characterization. J Appl Pharma Sci 1(6):228–234
67. Granqvist CG, Buhrman RA (1976) Ultrafine metal particles. J Appl Phys 47:2200–2219
68. Nanoparticle production—How nanoparticles are made https://www.nanowerk.com/how_nanoparticles_are_made.php
69. Crane RA, Scott TB (2012) Nanoscale zero-valent iron: future prospects for an emerging water treatment technology. J Hazard Mater 211–212:112–125
70. Sun YP, Li XQ, Cao J, Zhang WX, Wang HP (2006) Characterization of zero valent iron nanoparticles. Adv Colloid Interface Sci 120(1–3):4–56
71. Yuvakumar R, Elango V, Rajendra V, Kannan N (2011) Preparation and characterization of zero valent iron nanoparticles. Digest J Nanomate Biostruct 6(4):1771–1776
72. Chekli L (2015) Development of methods for the characterisation of engineered nanoparticles used for soil and groundwater remediation. Dissertation, School of Civil and Environmental Engineering Faculty of Engineering and Information Technology University of Technology, Sydney (UTS), New South Wales, Australia
73. Khorshidi B, Thundat T, Fleck BA, Sadrzadeh M (2016) A novel approach toward fabrication of high performance thin film composite polyamide membranes. Sci Rep 6:22069
74. Toimil-Molares ME (2012) Characterization and properties of micro- and nanowires of controlled size, composition, and geometry fabricated by electrodeposition and ion-track technology. Beilstein J Nanotechnol 3:860–883
75. Maghami M, Abdelrasoul A (2018) Chapter 7. Zeolite mixed matrix membranes (zeolite-mmms) for sustainable engineering, zeolites and their applications. In: Rashed MN, Palanisamy PN (eds.) IntechOpen, https://doi.org/10.5772/intechopen.73824

76. Wang Y, Foo SW, Chung TS (2009) Mixed matrix PVDF hollow fiber membranes with nanoscale pores for desalination through direct contact membrane distillation. Ind Eng Chem Res 48(9):4474–4483
77. Vital V, Sousa JM (2013) Handbook of membrane reactors: fundamental materials science, design and optimisation. isbn-10: 0857094149
78. Wiryoatmojo AS (2010) Development of mixed membranes for separation of CO_2 from CH_4. MSc thesis. Universiti Teknologi Petronas: Malaysia
79. Jusoh N, Yeong YF, Chew TL, Lau KK, Shariff AM (2016) Current development and challenges of mixed matrix membranes for CO_2/CH_4 separation. Sep Purif Rev 45(4):321–344
80. Miyatake K, Ohama O, Kawara Y, Urano A (2007) Study on analysis method for reaction of silane coupling agent on inorganic materials. SEI Tech Rev 65:21–24
81. Faucheu J, Gauthier C, Chazeau L, Cavaillé JY, Mellon V, Lami EB (2010) Miniemulsion polymerization for synthesis of structured clay/polymer nanocomposites: short review and recent advances. Polymer 51:6–17
82. Zimmerman CM, Singh A, Koros WJ (1997) Tailoring mixed matrix composite membranes for gas separations. J Membr Sci 37:145–154
83. Marti AM, Venna SR, Roth EA, Culp JT, Hopkinson DP (2018) Simple fabrication method for mixed matrix membranes with in situ MOF growth for gas separation materials. ACS Appl Mater Interfaces 10(29):24784–24790
84. Kulprathipanja S (2002) Mixed matrix membrane development. Membr Technol 2002(4):9–12
85. Vinogradov NE, Kagramanov GG (2016) The development of polymer membranes and modules for air separation. J Phys Conf Ser 751:012038
86. Luo L, Wang P, Zhang S, Han G, Chung TS (2014) Novel thin-film composite tri-bore hollow fiber membrane fabrication for forward osmosis. J Membr Sci 461:28–38
87. Li ZY, Maeda H, Kusakabe K, Morooka S, Anzai H, Akiyama S (1993) Preparation of palladium-silver alloy membranes for hydrogen separation by the spray pyrolysis method. J Membr Sci 78(3):247–254
88. Khulbe KC, Matsuura T (2018) Thin film composite and/or thin film nanocomposite hollow fiber membrane for water treatment, pervaporation, and gas/vapor separation. Polymers (Basel) 10(10):1051
89. Ni L, Wang J, Zhang Y, Meng J, Jhang Y (2011) The performance improvement of hollow fiber composite reverse osmosis membranes by post-treatments. Desalin Water Treat 34:32–33
90. Nascimento ML, Araújo ES, Cordeiro ER, de Oliveira AH, de Oliveira HP (2015) A literature investigation about electrospinning and nanofibers: historical trends, current status and future challenges. Recent Pat Nanotechnol 9(2):76–85
91. Tucker N, Stanger JJ, Staiger MP, Razzaq HA, Hofman K (2012) The history of the science and technology of electrospinning from 1600 to 1995. J Eng Fiber Fabr 7(2):63–73
92. Gilbert W (1600) De magnete, magneticisque corporibus, et de magno magnete tellure
93. Strut J (1882) On the equilibrium of liquid conducting masses charged with electricity London, Edinburgh, and Dublin. Philos Mag 14(87):184–186
94. Boys C (1887) On the production, properties, and some suggested uses of the finest threads. Philos Mag 23(145):489–499
95. Cooley J (1988) Improved methods of and apparatus for electrically separating the relatively volatile liquid component from the component of relatively fixed substances of composite flu Espacenet. GB190006385 (A)
96. Doshi J, Reneker DH, (1993) Electrospinning process and applications of electropsun fibers. Proceedings of IEEE industry application society 28th annual meeting, Toronto, Canada, October 2−8
97. Xue J, Xie J, Liu W, Xia Y (2017) Electrospun nanofibers: new concepts, materials, and applications. ACC Chem Res 50:1976–1987
98. Pike RD (1996) Superfine microfiber nonwoven web. US5935883

99. Balamurugan R, Sundarrajan S, Ramakrishna S (2011) Recent trends in nanofibrous membranes and their suitability for air and water filtrations. Membranes (Basel) 1(3):232–248
100. Zhao Y, Qiu Y, Wang H, Chen Y, Jin S, Chen S (2016) Preparation of nanofibers with renewable polymers and their application in wound dressing. Int J Polym Sci 2016:4672839. https://doi.org/10.1155/2016/4672839
101. Li YJ, Chen F, Nie J, Yang DZ (2012) Electrospun poly(lactic acid)/chitosan core-shell structure nanofibers from homogeneous solution. Carbohydr Polym 90(4):1445–1451
102. Kim IG, Lee JH, Unnithan AR, Park CH, Kim CS (2015) A comprehensive electric field analysis of cylinder-type multi-nozzle electrospinning system for mass production of nanofibers. J Ind Eng Chem 31:251–256
103. Nuryantini AY, Munir MM, Ekaputra MP, Suciati T, Khairurrijal K (2014) Electrospinning of poly(vinyl alcohol)/chitosan via multi-nozzle spinneret and drum collector. Adv Mater Res 896:41–44
104. Sasithorn N, Martinová L (2014) Fabrication of silk nanofibres with needle and roller electrospinning methods. J Nanomater 2014:947315
105. Chen RX, Li Y, He JH (2014) Mini-review on bubbfil spinning process for mass-production of nanofibers. Revista Materia 19(4):325–344
106. He JH, Kong H, Yang RR, Dou H, Faraz N (2012) Review on fiber morphology obtained by bubble electrospinning and blown bubble spinning. Therm Sci 16(5):1263–1279
107. Li ZB, Liu HY, Dou H (2014) On air blowing direction in the blown bubble-spinning. Revista Materia 19(4):345–349
108. Heand JH, Liu Y (2012) Control of bubble size and bubble number in bubble electrospinning. Comput Math Appl 64(5):1033–1035
109. Alghoraibi I, Alomari S (2018) Different methods for nanofiber design and fabrication. In: Barhoum A, Bechelany M, Makhlouf A (eds) Handbook of nanofibers. Springer, Cham, pp 1–46
110. Lu Y, Li Y, Zhang S, Fu K, Lee H, Zhang X (2013) Parameter study and characterization for polyacrylonitrile nanofibers fabricated via centrifugal spinning process. Eur Polym J 49(12):3834–3845
111. Erickson AE, Edmondson D, Chang FC, Wood D, Gong A, Levengood SL, Zhang M (2015) High through put and high-yield fabrication of uniaxially-aligned chitosan based nanofibers by centrifugal electrospinning. Carbohydr Polym 134:467–474: Article 10199
112. Melt Electrospinning—Spraybase®. https://www.spraybase.com/meltelectrospin
113. Brown TD, Dalton PD, Hutmacher DW (2011) Direct writing by way of melt electrospinning. Adv Mater 23:5651–5657
114. Dalton PD, Klinkhamme K, Salber J, Klee D, Möllere M (2006) Direct in vitro electrospinning with polymer melts. Biomacromolecules 7(3):686–690
115. Dalton PD, Grafahrend D, Klinkhammer K, Klee D, Möller M (2007) Electrospinning of polymer melts: phenomenological observations. Polymer 48(23):6823–6833
116. Xue Z, Wang S, Lin L, Chen L, Liu M, Feng L, Jiang L (2011) A novel superhydrophilic and underwater superoleophobic hydrogel-coated mesh for oil/water. Adv Mater 23:4270–4273
117. Zhang W, Zhu Y, Liu X, Wang D, Li J, Jiang L, Jin J (2014) Salt-induced fabrication of superhydrophilic and underwater superoleophobic PAA-g-PVDF membranes for effective separation of oil-in-water emulsions. Angew Chem Int Ed 53:856–860
118. Wu J, Meredith JC (2014) Assembly of chitin nanofibers into porous biomimetic structures via freeze drying. ACS Macro Lett 3(2):185–190
119. Salamian N, Irani S, Zandi M, Saeed SM, Atyabi SM (2013) Cell attachment studies on electrospun nanofibrous PLGA and freeze-dried porous PLGA. Nano Bulletin 2(1):130103
120. Zhai Y, Su J, Ran W, Zhang P, Yin Q, Zhang Z, Yu H, Li Y (2017) Preparation and application of cell membrane-camouflaged nanoparticles for cancer therapy. Theranostics 7(10):2575–2592
121. Tanaka Y (2015) Ion exchange membranes: fundamentals and applications. Elsevier, Japan, p 47. isbn: 978-0-444-63319-4

122. Sata T Membrane processes—preparation and characterization of ion-exchange membranes, UNESCO-EOLSS
123. Alabi A, Al Hajaj A, Cseri L, Szekely G, Budd P, Zou L (2018) Review of nanomaterials-assisted ion exchange membranes for electromembrane desalination. npj Clean Water 1:10
124. Khulbe KC, Matsuura T, Feng C (2015) The art of making polymeric membranes. In: Thakur VK, Thakur MK (eds) Hand book for pharmaceutical technologies (processing and applications). Scrivener Publishing, Beverly, pp 33–66, isbn: 978-1-119-04138-2
125. Du Z (2016) Improvement of nafion composite membrane for direct methanol fuel cell: effect of analcime and mordenite addition and fabrication method, Kasetsart University, Bangkok
126. Xing D, He G, Hou Z, Ming P, Song S (2013) Properties and morphology of Nafion/polytetrafluoroethylene composite membrane fabricated by a solution-spray process. Int J Hydrog Energy 38:8400–8408
127. Prapainainar P, Maliwan S, Sarakham K, Du Z, Prapainainar C, Holmes SM, Kongkachuichay P (2018) Homogeneous polymer/filler composite membrane by spraying method for enhanced direct methanol fuel cell performance. Int J Hydrog Energy 43(31):14675–14690
128. Dixon DJ, Johnston KP, Bodmeier R (1993) Polymeric materials formed by precipitation with compressed fluid antisolvent. AIChE J 39(1):127–139
129. Ge C, Zhai W, Park CB (2019) Preparation of thermoplastic polyurethane (tpu) perforated membrane via CO_2 foaming and its particle separation performance. Polymers (Basel) 11(5):847. https://doi.org/10.3390/polym11050847
130. Sanguanruksa J, Rujiravanit R, Supaphol P, Tokura S (2004) Porous polyethylene membranes by template-leaching technique: preparation and characterization. Polym Test 23(1):91–99
131. Roy-Chowdhury P, Kumar V (2006) Fabrication and evaluation of porous 2,3-dialdehydecellulose membranes as a potential biodegradable tissue engineering scaffold. J Biomed Mater Res Part A 76(2):300–309
132. Jung SY, Ko SY, Park JO, Park S (2015) Enhanced ionic polymer metal composite actuator with porous nafion membrane using zinc oxide particulate leaching method, smart materials and structures. J Intellig Mater Syst Struct 28(11):1514–1523
133. Qiu M, Feng J, Fan Y, Xu N (2009) Pore evolution model of ceramic membrane during constrained sintering. J Mater Sci 44(3):689–699
134. Rezwan K, Chen QZ, Blaker JJ, Boccaccini AR (2006) Biodegradable and bioactive porous polymer/inorganic composite scaffolds for bone tissue engineering. Biomaterials 27(18):3413–3431
135. Cui Z (2014) Sintering method for ceramic membrane preparation. In: Drioli E, Giorno L (eds) Encyclopedia of membranes. Springer, Berlin
136. Li L, Gao EZ, Abadikhah H, Wang JW, Hao LY, Xu X, Agathopoulos S (2018) Preparation of a porous, sintered and reaction-bonded Si_3N_4 (srbsn) planar membrane for filtration of an oil-in-water emulsion with high flux performance. Materials 11:990. 15 pages
137. Lu F, Liu H, Xiao C, Wang X, Chen K, Huang H (2019) Effect of on-line stretching treatment on the structure and performance of polyvinyl chloride hollow fiber membranes. RSC Adv 9:6699–6707
138. Li N, Xiao C (2009) Preparation and properties of UHMWPE/SiO2 hybrid hollow fibre membranes via thermally induced phase separation-stretching method. Iranian Polymer J 18(6):479–489
139. Wang S, Ajji A, Guo S, Xiong C (2017) Preparation of microporous polypropylene/titanium dioxide composite membranes with enhanced electrolyte uptake capability via melt extruding and stretching. Polymers (Basel) 9(3):110. https://doi.org/10.3390/polym9030110

Chapter 3
Membrane Characterization

3.1 Introduction

Membrane processes can cover a wide range of separation problems and a specific membrane is required for problem. Membranes may differ significantly in their structure and consequently in their functionality. To know which membrane is used in a particular separation process, different membranes must be characterized in terms of structure and mass transport properties. Because of a variety of membranes, different techniques are required for characterization. Membrane characterization is a very important part of membrane research and development because the design of membrane processes and systems depends on reliable data relating to membrane properties. Characterization results of membrane can predict the performance of the particular membrane.

Many researchers are working on membrane development, either for membrane water treatment or membrane gas separation. Many of them are attempting to find the cause and effect relationship between membrane fabrication-membrane morphology-membrane performances. The ultimate goal of the research is to provide a rational guideline for membrane fabrication conditions to achieve some specific membrane morphology, which enables the desired separation performance. For this reason, membrane morphology characterization is one of the indispensable components of membrane research [1].

A small change in one of the membrane formation parameters can change the structure of the top selective layer and consequently have a drastic effect on membrane performance. Xu et al. [2] discussed in detail the techniques for the characterization of membrane surfaces, in 'Surface Engineering of Polymeric Membranes'. Lee et al. [3] used dynamic hysteresis as a parameter of showing physical surface characteristics of RO membranes.

Different techniques and approaches are routinely used to characterize the physical and chemical properties of membrane surface. Characterization of membranes is

K. C. Khulbe, T. Matsuura, *Nanotechnology in Membrane Processes*, Lecture Notes in Nanoscale Science and Technology 29,
https://doi.org/10.1007/978-3-030-64183-2_3

important since this allows insight into the relationship between membrane chemistry, structure, and transport properties**.** The most widely used characterization method is the measurement of water flux and solute (usually NaCl) rejection; these can be easily measured and thus give a quick indication of the suitability of the membrane for a particular application. However, fluxes provide only limited information about the characteristics and structure of the membrane and the role these play in water and solute transport. As a result, other characterization techniques are beginning to be employed in order to determine parameters such as pore size, barrier layer thickness, and membrane elemental composition.

There are many common methods such as bubble point method, liquid-liquid porosimetry, nitrogen adsorption/desorption, permporometry, scanning electron microscopy, transmission electron microscopy and contact angle measurement to characterize the membranes [4]. Tylkowsk and Tsibranska [5] wrote an article, focused particularly on the main techniques used for membrane characterization with supporting review of the literature and comparative discussion. Characterization techniques can be classified into static and dynamic techniques. The static techniques mainly give information on membrane morphology and structure, chemical and physical properties. The dynamic techniques are of fundamental importance when investigating membrane performance. Tylkowsk and Tsibranska [5] discussed the following methods for membrane characterization in detail.

1. Bubble point test; The bubble point test is a measure of the radius of the largest pore.
2. Liquid-liquid displacement porosimetry: The liquid-liquid porosimetry (LLDP) is a method that can be used to provide information on the pore size distribution of membranes with small pores.
3. Liquid and air permeability; Permeability of a membrane for a certain liquid can be considered as a characteristic parameter; often the so-called hydraulic radius is calculated from the measured fluxes.
4. Nitrogen adsorption/desorption (pore size distribution); In this method the pore size distribution is determined by the adsorption/desorption isotherms of a gas (usually nitrogen) subjected to adsorption and capillary condensation in the pores.
5. Electron microscopy; The aim of this method is to acquire visual information of the membrane structure and porosity through magnification by scanning electron microscope (SEM) or transmission electron microscope (TEM).
6. Stress - strain property; Most materials are subjected to stress and the accompanying deformation during processing and use. The mechanical properties of the membranes characterized by stress-strain tests are needed to confirm the potential suitability of membranes in applications.
7. Contact angle; The hydrophobic/hydrophilic characteristics of solids plays a key role in many processes such as: wetting, flotation, enhanced oil recovery, cleaning technologies, super hydrophobicity, liquid spreading, plants protection, etc.

Khulbe et al. [1] also discussed the following methods in detail;

1. Mercury Intrusion Porosimetry.
2. Adsorption-Desorption Method (Barett-Joyner-Halenda (BJH) Method).
3. Gas Liquid Equilibrium Method (Permporometry).
   Liquid Displacement Permporometry (LDP)
4. Diffusional Permoporometry (DP).
5. Liquid Solid Equilibrium Method (Thermoporometry).
6. Gas Permeability Method.
7. Mass Transportation.

Table 3.1 shows the main characterization method [5].

New techniques such as AFM, ATR-FTIR, X-ray Photoelectron Spectroscopy (XPS), Positron Annihilation Lifetime Spectroscopy (PALS) etc. are available to go deep into the understanding of the structure, mechanism, morphology etc. of the membrane, which can help to make desirable membranes. These new techniques to characterize the membranes are well described by Ismail et al. [6]. It should be noted that most of the characterization methods are routinely used. In more recent years, novel volume electron microscopy techniques have opened the door for nanometer-scale visualization of cells and tissues in three dimensions [7].

Table 3.1 Main characterization method

Method type	Characteristic	Typology
Bubble point method	Maximum pore size	Dynamic non destructive
Gas and liquid-liquid and liquid displacement methods (GLDP-LLDP)	Pore size distribution	Dynamic non destructive
Mercury porosimetry (MP)	Pore size distribution	Static destructive
Scanning Electron Microscopy (SEM), Transmission Electron Microscopy (TEM)	Top layer thickness, Surface porosity, Pore size distribution, Qualitative structure analysis	Static non destructive
Atomic force microscopy (AFM)	Surface porosity	Static non destructive
Flux and retention measurement	Permeability, Selectivity, MWCO	Dynamic non destructive
Gas adsorption/desorption (GAD)	Pore size distribution	Static non destructive
Permporometry	Pore size distribution	Dynamic non destructive
SEM + X-ray microanalysis (EDS)	Chemical analysis Surface studies	Static destructive
X-ray photoelectron spectroscopy	Chemical analysis Surface studies	Static destructive
Infrared Spectroscopy (FT-IR, ATR, Photoacoustic)	Functional group analysis Surface studies	Static destructive
Contact angle measurement	Surface studies	Non destructive
Stress-Strain measurements		Destructive

Many articles are available for the characterization of membrane [1, 5, 6, 8, 9].

3.2 Methods

3.2.1 Pore Size and Pore Size Distribution

There is not a unique definition of “pore diameter” or “pore size”. Every method of pore size determination defines a pore size in terms of a pore model which is best suited to the quantity measured in the particular experiment. In the vast majority of porous media, the pore sizes are distributed over a wide spectrum of values, called “pore size distribution”. In other words, pore size distribution is a probability density function giving the distribution of pore volume by a characteristic pore size. The most popular methods of determining pore size distribution are mercury intrusion porosimetery, sorption isotherm and image analysis. The first of these is used mostly but not exclusively to determine the size of relatively larger pores whereas sorption isotherms are best suited in the case of smaller pores. The use of imaging to analyze section of a sample has some advantages over the other two methods, but the most complete information on pore size distribution may be obtained if all three methods are used jointly.

Whereas pore size is a measure of the diameter of the pore, pore size distribution is a measure of the range of pore sizes. There are some practical techniques for measuring these parameters which are described below.

1. **Gas permeation**
   Permeation, from an engineering aspect, is the penetration of permeate, such as liquid, gas, or even vapor, through a microporous membrane, and is related to polymer’s intrinsic permeability. This method allows measurement of the mean pore size (μm). An inert gas (either dried air or nitrogen) is employed as the standard gas. In this method, the gas permeation flux for the dry membrane is measured at various pressures. One of the limitations of this technique is that the pore size distribution cannot be determined.
2. **Bubble point**
   This method is based on determination of the pressure necessary to blow nitrogen through a liquid filled membrane. However, this method is able to measure only the maximum pore size present in the membrane.
3. **Wet/dry flow method**
   The bubble point together with the gas permeation test, which is known as the wet/dry flow technique, can be employed for measuring the maximum pore size, the mean pore size and the pore size distribution of membranes. In this method, the gas permeation is determined through a dry membrane sample, and a straight line is observed between the gas flux and the applied pressure. In the next step, the membrane is soaked in a low surface tension liquid (such as isopropyl alcohol) and again the gas flux will be determined at different applied pressures. It

will result in a non-linear dependency between the gas flux and the applied pressure. Then the pore size distribution can be determined using theoretical expressions.

4. **Liquid displacement techniques**

   The liquid displacement method, commonly used to determine pore sizes and pore size distributions of a membrane, is close to (ultra)filtration practice. By this method dead-end pores are not evaluated and the membrane is characterized in wet conditions. In addition, the pressure is kept as low as possible so that no alteration of the membrane occurs. It is based on the measurement of the flux of a displacing liquid through the membrane as a function of the pressure applied. Thus, this method is similar to the bubble point method but a liquid in the pore is displaced by another liquid instead of gas. From the flux-pressure curve the pore size distribution is calculated using the Hagen-Poiseuille equation. Following assumptions are used for the calculation of pore size distribution.

   (a) The pores are cylindrical.
   (b) Parallel to each other.
   (c) Not interconnected and thus are straight through the whole membrane layer.
   (d) All pores have length l,
   where l is usually taken to be the thickness of the membrane (or thickness of the membrane skin layer in the case of an asymmetric membrane).

   Whereas pore size is a measure of the diameter of the pore, pore size distribution is a measure of the range of pore sizes. There are some practical techniques for measuring these parameters which are described below.

5. **Gas permeation**

   Permeation, from an engineering aspect, is the penetration of permeate, such as liquid, gas, or even vapor, through a microporous membrane, and is related to polymer's intrinsic permeability. This method allows measurement of the mean pore size (μm). An inert gas (either dried air or nitrogen) is employed as the standard gas. In this method, the gas permeation flux for the dry membrane is measured at various pressures. One of the limitations of this technique is that the pore size distribution cannot be determined.

6. **Bubble point**

   This method is based on determination of the pressure necessary to blow nitrogen through a liquid filled membrane. However, this method is able to measure only the maximum pore size present in the membrane.

7. **Wet/dry flow method**

   The bubble point together with the gas permeation test, which is known as the wet/dry flow technique, can be employed for measuring the maximum pore size, the mean pore size and the pore size distribution of membranes. In this method, the gas permeation is determined through a dry membrane sample, and a straight line is observed between the gas flux and the applied pressure. In the next step, the membrane is soaked in a low surface tension liquid (such as isopropyl alcohol) and again the gas flux will be determined at different applied pressures. It will result in a non-linear dependency between the gas flux and the applied pressure. Then the pore size distribution can be determined using theoretical expressions.

8. **Liquid displacement techniques**

   The liquid displacement method, commonly used to determine pore sizes and pore size distributions of a membrane, is close to (ultra)filtration practice. By this method dead-end pores are not evaluated and the membrane is characterized in wet conditions. In addition, the pressure is kept as low as possible so that no alteration of the membrane occurs. It is based on the measurement of the flux of a displacing liquid through the membrane as a function of the pressure applied. Thus, this method is similar to the bubble point method but a liquid in the pore is displaced by another liquid instead of gas. From the flux-pressure curve the pore size distribution is calculated using the Hagen-Poiseuille equation. Following assumptions are used for the calculation of pore size distribution.

   (e) The pores are cylindrical.
   (f) Parallel to each other.
   (g) Not interconnected and thus are straight through the whole membrane layer.
   (h) All pores have length l,
   where l is usually taken to be the thickness of the membrane (or thickness of the membrane skin layer in the case of an asymmetric membrane).

   With assumption (a) and (b), pore density function N(rp) can be calculated from the increase in the measured flux (dφs) upon the increase in transmembrane pressure (dΔP) using the following equation.

$$N\left(r_{\mathrm{p}}\right)=\frac{8\eta l}{\pi r_{\mathrm{p}}^{4}}\frac{d\varphi_{\mathrm{s}}}{d\Delta P} \tag{3.1}$$

where η is the viscosity of the displacing liquid. If l is not known, a relative pore size distribution can be calculated. The results obtained by this method become incorrect if the pores are connected to each other or if there is a resistance against flow in membrane sub-layer or in the measurement apparatus.

9. **Adsorption/desorption isotherms**

   Gas adsorption/desorption is one of the most widely used techniques in characterization of porous membranes for the determination of pore size, specific surface area and pore size distribution of membranes with spherical, cylindrical or slit shaped pores.

   In this method the pore size distribution is determined by the adsorption/desorption isotherms of a gas (usually nitrogen) subjected to adsorption and capillary condensation in the pores. The nitrogen adsorption BET (Brunauer-Emmett-Teller) analysis is very useful for determining surface area and pore size distribution of ceramic or polymeric membranes usually in the micro- and meso-size pore range. For conventional dense polymer membranes (considered as "nonporous") the BET analysis is rarely used. BET analysis provides precise specific surface area evaluation of materials by nitrogen multilayer adsorption measured as a function of relative pressure using a fully automated analyzer. The technique encompasses external area and pore area evaluations to determine the total specific surface area in m^2/g yielding important information in studying the effects of surface porosity and particle size in many applications. Amorphous materials are usually characterized using nitrogen adsorption isotherms at 77 K taken at pressures up to 1 bar to obtain pore size distributions.

There are many models available for the adsorption of gases onto solids where the volume adsorbed is a function of pressure with constant temperature. The fundamental equation to find the pore size distribution from capillary condensation isotherms is as follow:

$$V_s - V = \pi \int_R^{\infty} (R - t)^2 L(R) dR \tag{3.2}$$

where V_S is the volume of adsorbate at saturation vapor pressure (equal to the total pore volume), V the volume of adsorbate at intermediate vapor pressure P'', $L(R)dR$ the total length of pores whose total length fall between R and $R + dR$, R pore radius, and (t) the multilayer thickness that is built up at pressure P''. This equation states the fact that the volume of adsorbed at pressure P'' is equal to the volume of pores that has not yet been filled.

10. **Mercury porosimetry**

Mercury porosimetry characterizes a material's porosity by applying various levels of pressure to a sample immersed in mercury. The pressure required to intrude mercury into the sample's pores is inversely proportional to the size of the pores, so at the same times it finds pore size distribution.

The ratio between the volume of the pores and the total volume of the membrane is the membrane porosity, which can be measured by the use of the following expression:

$$P\% = (1 - \rho_m / \rho_b) \times 100 \tag{3.3}$$

where ρ_m and ρ_b are the density of the membrane and the density of the bulk polymer, respectively. Higher porosity of electrospun membranes significantly increase the permeation flux, and subsequently the overall process efficiency.

3.2.2 Membrane Morphology

Surface membrane morphology studies provide atomic or nano-scale structure information about pore shape, pore size distribution, roughness, electrical properties, surface adhesion/membrane fouling behavior, and correlation between membrane characteristics and process behavior. Analytical Imaging Techniques used for surface morphology and chemistry of membranes study include [1, 9].

1. Field Emission Scanning Electron Microscopy (FE-SEM)
2. High Resolution Optical Microscopy
3. Scanning Transmission Electron Microscopy (STEM)
4. Transmission Electron Microscopy (TEM)
5. Ultra High Resolution-SEM (UHR-SEM)
6. Focused Ion Beam–Scanning Electron Microscopy (FIB-SEM)
7. Atomic Force Microscopy (AFM)
8. Laser Confocal Scanning Microscopy (LCSM)
9. Rutherford Backscattering Spectroscopy (RBS)
10. Neutron Scattering (NS)
11. Electron Paramagnetic Resonance Spectroscopy (EPR)
12. Wide Angle X-ray Scattering (WAXS) and Small Angle X-ray
13. Scattering (SAXS)

3.2.2.1 Scanning Electron Microscopy (SEM)

Scanning electron microscopy is a commonly used tool for the determination of morphology and topography of membrane surface. In SEM, narrow beam of electrons scans across the membrane surface and deep inside. Image in SEM is produced due to combination of elastically scattered secondary electrons and elastically backscattered electrons. Deep penetration of electron beam (backscattered electrons) gives valuable information about composition of specimen whereas secondary electrons, being sensitive to topographic areas, give information about membrane surface. To get information about top layer and cross-sectional parts, analysis of membrane is done through secondary and back scattered electrons. SEM can also be used to estimate the porosity and pore size distribution [10]. Scanning electron microscope clearly shows the microstructure of a membrane material. Scanning electron microscopy (SEM) measurement is done by exposing the surface of the membrane to a beam of electrons in vacuum at a certain accelerating voltage. This technique requires minimum sample preparation that includes drying and coating of samples with conductive material, e.g., gold, carbon, etc. The resolution of SEM is in the range of 10 and 50 nm depending on the type of equipment available. Higher resolution can be obtained with transmission electron microscopy (TEM). The micro-marker on the SEM micrographs is used to estimate the pore size (diameter). SEM applications can focus on membrane structure characterization, hollow fiber membrane fabrication, and the study of the fouling process [11]. Chen et al. [12] studied nanoporous carbon composite membranes via SEM and Raman spectroscopy. It was revealed that every carbon fibre grown on a ceramic substrate exhibits a multiwall carbon nanotube structure.

3.2.2.2 Transmission Electron Microscopy (TEM)

Transmission electron microscopy (TEM) is a microscopic technique in which a beam of electrons is transmitted through an ultra-thin specimen, interacting with the specimen as it passes through it. An image is formed from the interaction of the electrons transmitted through the specimen; the image is magnified and focused onto an imaging device, such as a fluorescent screen, on a layer of photographic film, or detected by a sensor such as a CCD (charge-coupled device) camera.

Carbon molecular sieve (CMS) membranes are novel materials derived from the pyrolysis of the polymeric precursors and have a well-developed ultra-microporous structure that can separate small gas pairs with minor difference in diameter, and thus exhibit higher gas permeability and selectivity than polymeric membranes. It was found that preparation of hybrid CMS membranes by doping the metal (Ag, Pt, Pd, etc.), metal salts or the inorganic particles into precursors is effective to improve the gas permeation property of CMS membranes due to the effects of the particles on the different gases and the interfacial gaps between particles and their surrounding carbon matrix [13]. Ferrocene, a kind of organic transition metal compound with good solubility with DMAc, can form a homogeneous system with PAA solution, which helps improve the dispersion of the α-Fe obtained by the pyrolysis of ferrocene in the CMS membrane. The HRTEM (high-resolution transmission electron microscopy) image of the ferrocene/PAA based hybrid CMS membrane is shown as Fig. 3.1. The Fe nanoparticles identified by the EDX (energy dispersive X-ray) patterns with diameter of almost 5 nm are dispersed homogeneously in the disordered carbon matrix. The crystal structure of Fe particles with interplanar spacing of 0.206 nm are shown in the insert image. However, the Fe element content in the hybrid CMS membrane is low because of the sublimation of ferrocene [13].

Inukai et al. [14] synthesized high performance composite thin RO membrane using multi-walled carbon nanotubes (MWCNT) and aromatic polyamide (PA), by the interfacial polymerization. The microstructure of the MWCNT-PA nanocomposite membrane was studied by using high-resolution transmission electron microscopy (HRTEM). Figure 3.2 shows the TEM images of the MWCNT·PA nanocomposite RO membranes. Figure 3.2a exhibits the typical morphology of the pristine MWCNT, showing the characteristic and overall clean surface walls with a small amount of carbonaceous material deposited on the surface. Figure 3.2b shows the edge of the nanocomposite membrane with several MWCNT protruding from the matrix. A detail of these nanotubes (Fig. 3.2c) shows traces of PA attached to the surface, suggesting good interaction between the monomers and the MWCNT walls, forming an ordered region several nanometers thick, shown in Fig. 3.2d, which is in agreement with the observation of thicker diameter by SEM. On

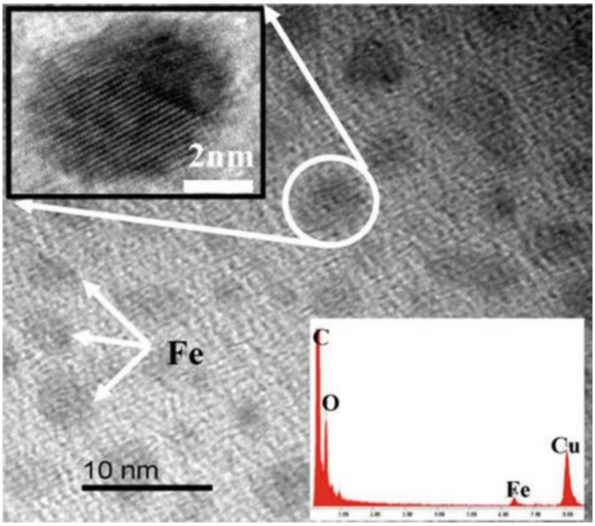

Fig. 3.1 HRTEM image of ferrocene/polyamic acid (PAA)-based hybrid CMS membrane [13]

conducting FFT(Fast Fourier Transform) of TEM images on several regions within the nanocomposite membrane (Fig. 3.2e), resulted in a pattern that suggested order of the polymer network along the nanotubes surfaces and might represent a unique aromatic PA structure when compared to the bulk PA. The structured model is graphically represented in Fig. 3.2f. Such a characteristic ordered region has a thickness roughly similar to the nanotube diameter. The FFT pattern on the nanotube showed the typical sharp peaks caused by the concentric graphitic layers, while the FFT pattern of the matrix exhibited only a diffuse halo characteristic of disordered.

3.2.2.3 Atomic Force Microscopy (AFM)

Membrane surface roughness can be analyzed by Atomic Force Microscopy (AFM). AFM is an important tool for the determination of the surface topology. The most common implementation of this technique uses a cantilever with a sharp tip to scan over sample surface to produce an image at atomic level. By using AFM technique, surface charges and van der walls forces between the tip and membrane surface can be estimated. In AFM, three types of modes can be used, i.e. contact mode, non-contact mode and tapping mode. Contact mode causes damage to membrane surface that is the reason why usually tapping mode is used for the characterization of membrane surface. Through AFM technique roughness, pore size, pore-size distribution and phases on the surface of membranes can be determined. AFM characterization can also give information about the fouling and antifouling behavior of membrane as these properties depend on the surface smoothness.

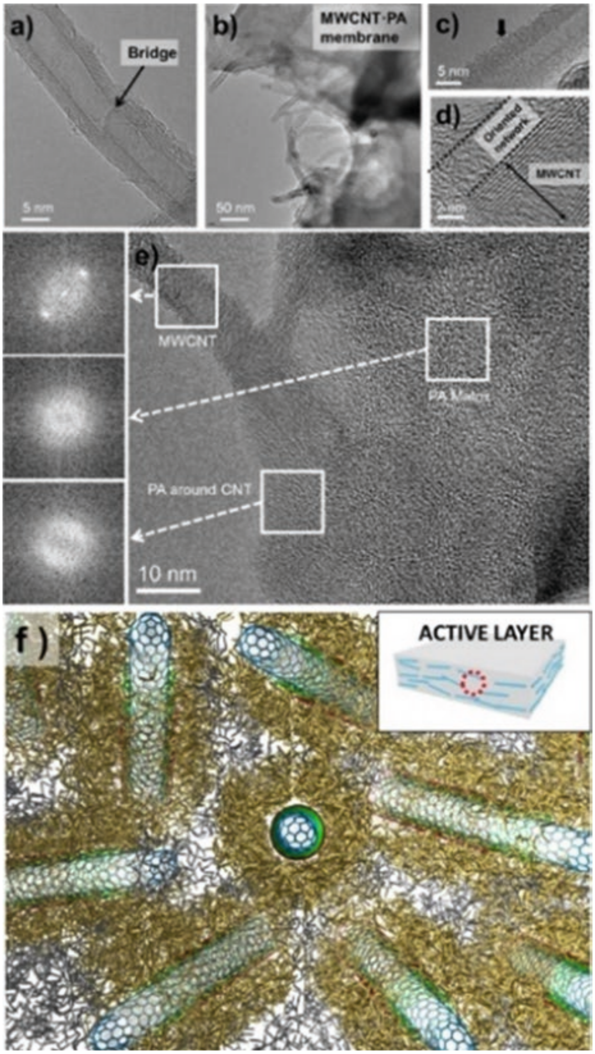

Fig. 3.2 TEM images of the MWCNT·PA nanocomposite RO membranes: (**a**) shows a pristine MWCNT. (**b**) shows the border of a cleaved MWCNT·PA nanocomposite RO membrane. MWCNTs can be seen protruding from the surface. (**c**) shows a magnification of one of these nanotubes that has been pulled out from the PA matrix. (**d**) shows the carbon nanotube embedded within the PA matrix. In (**e**) several FFT patterns of the nanocomposite RO membranes are shown, top; corresponding to MWCNT, middle; PA zone, bottom; PA zone around MWCNT. (**f**) Model of the MWCNT·PA nanocomposite microstructure, showing the proposed ordered PA regions in yellow around MWCNT fillers [14]

Table 3.2 NPs percentage and mass ratio **polymer, solvent and NPs**

Membrane	NPs percentage (wt.%)	Mass ratio of PSF:NMP:NPs
a. P0		1:5:0
b. Z2	ZnO 2%	1:5:0.02
c. ZG3	ZnO-GO 0.6%	1:5:0.006

Thus, one of the most practical surface features which can be directly measured using AFM is the surface roughness. AFM analysis can provide different roughness parameters which can be used for topographical studies as well as surface energy measurements. Zinc oxide nanoparticles are well-known for the enhanced antifouling and antibacterial properties which could be beneficial for membrane processes in desalination. Chung et al. [15] fabricated polysulfone nanohybrid membranes via wet phase inversion technique and embedded various percentage of ZnO (1, 2, 3 wt.%) and ZnO-GO (0.1, 0.3, 0.6 wt.%) nanoparticles. All the membranes with nanoparticles incorporation exhibited improved membrane properties in comparison with the pristine PSF membrane. The surface morphology investigation of the three fabricated membranes (Table 3.2) was performed by AFM analysis.

Figure 3.3 shows 3D images of the three synthesized membranes with the surface roughness values. It is known that more peaks or valleys represent rougher membrane surface. As shown in Fig. 3.3, the AFM image coincided well with mean RMS values which marked the higher surface roughness of P0 membrane in comparison with Z2 and ZG3 membranes. The addition of ZnO and ZnO-GO NPs altered the membrane structure and turned the larger peaks or valleys of the membranes into smaller ones. Eventually, the embedment of GO nanoplates would assist in creating smoother membrane surface due to the low electrostatic interaction and high compatibility of GO NPs with the PSF membrane matrix. Higher surface roughness would normally result in a higher fouling tendency and hydrophobicity. This phenomenon could be further explained by Wenzel's model, in which the degree of roughness is correlated proportionally to the surface hydrophilicity or hydrophobicity. Hence, the incorporation of functionalized ZnO nanomaterials would definitely enhance the membrane properties by providing smoother membrane structure. Characterization of membrane surface by AFM has become a routine nowadays.

3.2.2.4 Laser Confocal Scanning Microscopy (LCSM)

Confocal microscopy is a powerful instrument that creates sharp images of fixed or living cells and tissues and can greatly increase optical resolution and contrast over that of a conventional microscope. Recently LCSM is being used more and more for the surface characterization of [2] membranes. Hoves et al. [16] showed several examples that exploit the laser scanning confocal microscope's capabilities, such as pseudo-infinite depth of field imaging, topographic imaging, photo-stimulated luminescence imaging and Raman spectroscopic imaging. Confocal microscopy,

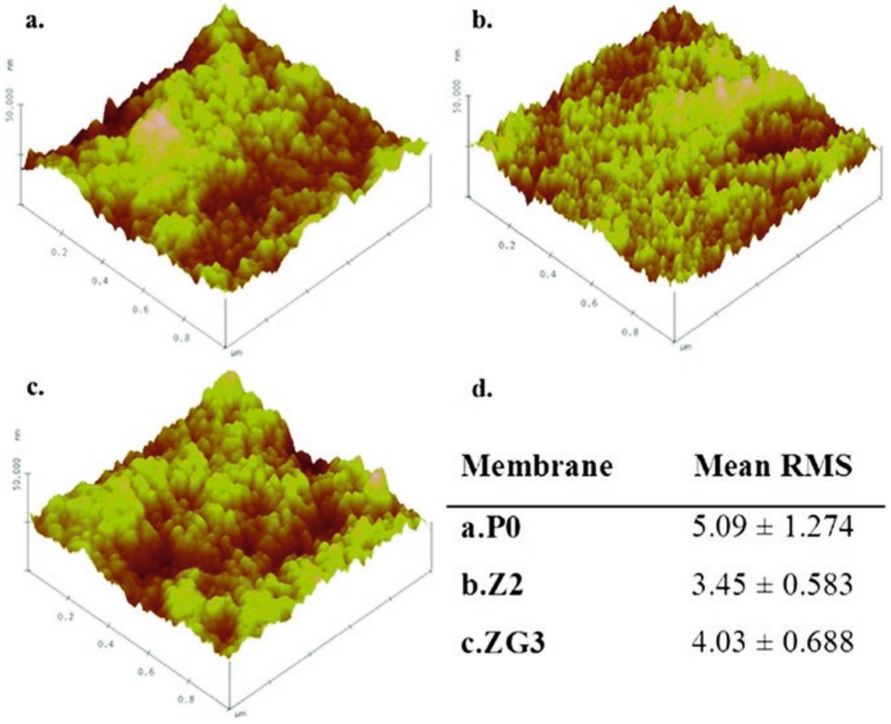

Membrane	Mean RMS
a.P0	5.09 ± 1.274
b.Z2	3.45 ± 0.583
c.ZG3	4.03 ± 0.688

Fig. 3.3 AFM images and surface roughness of membranes: (**a**) P0; (**b**) Z2; (**c**) ZG3; (**d**) Mean RMS value [15]

frequently called confocal laser scanning microscopy (LCSM) or laser confocal scanning microscopy (LCSM), is an optical imaging technique for increasing optical resolution and contrast of a micrograph by means of using a spatial pinhole to block out-of-focus light in image formation [17]. The principle of confocal imaging was patented in 1957 by Marvin Minsky [18] aimed at overcoming some limitations of traditional wide-field fluorescence microscopes [19].

A laser confocal scanning microscope (LCSM) can work in fluorescence mode or reflecting mode. Certain kinds of materials emit fluorescence when exposed to external light. The wavelength of fluorescence is usually longer than that of the exciting light. The difference between the wavelength of the emitted light and the exciting light is named as Stokes shift and this is summarized as Stokes law. The time delay between the exciting and the emitting behaviors is one millionth of a second or smaller. Light emitted beyond this time delay belongs to phosphorescence. Since LCSM images mainly contain the information of the focal plane, a three dimensional structure can be reconstructed from a series of images at different heights. Due to this phenomenon LCSM provides a three dimensional surface topography, the pore structure and structure of fouling on the membrane surface.

Recently LCSM is being used more and more for the surface characterization of membranes [2]. Figure 3.4 shows the schematic drawing of the LCSM [20].

Imaging of large areas of the sample is achieved by rastering the beam across the sample using mirrors controlled by piezoelectric actuators (Fig. 3.5).

Figure 3.6a shows LCSM image of dry MF membrane. The optical image of the dry MF membrane surface was in agreement between the LCSM image and the SEM image. The optical section of the membrane, located at inside the membrane, was significantly more reflective and degraded (Fig. 3.6b).

Lin et al. [21] reported for the first time three dimensional (3D) visualization of oil droplets on electrospun nanofiber microfiltration membranes after a period of membrane based separation of oil-in-water emulsions via a dual-channel LCSM technique in which both the fibers and the oil (dodecane) were fluorescently labeled (Fig. 3.7). To investigate the evolution of membrane fouling with time, PA6(3)T nanofiber membranes operated for 3, 10, and 30 min in the dead-end configuration

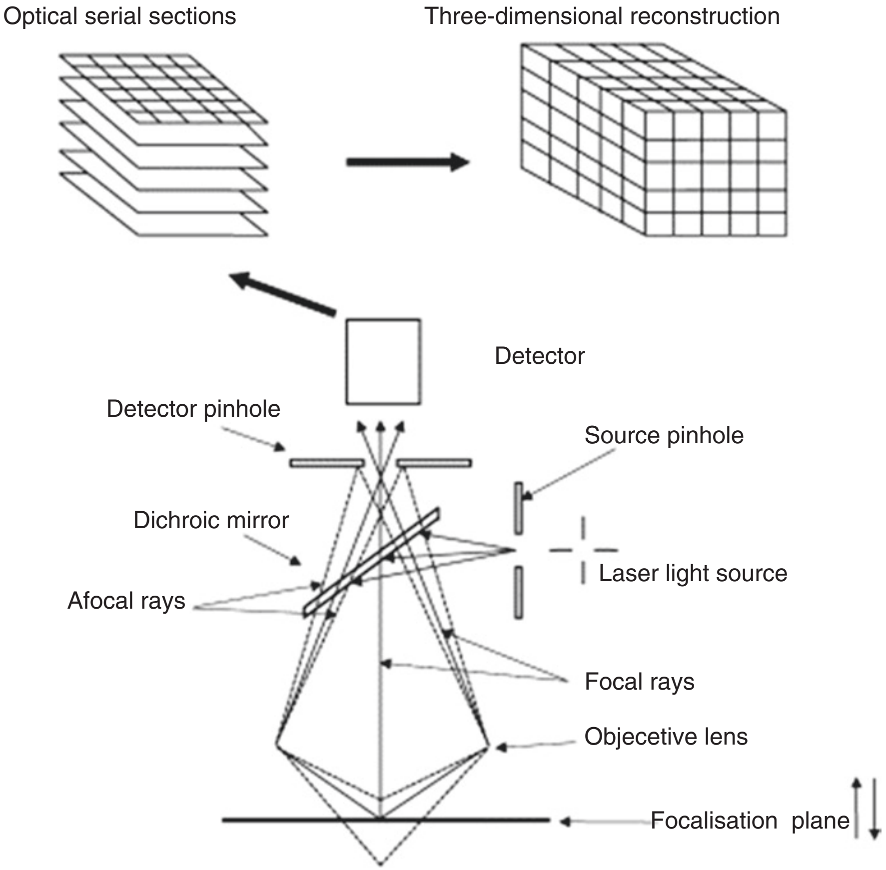

Fig. 3.4 Schematic drawing of the LCSM [20]

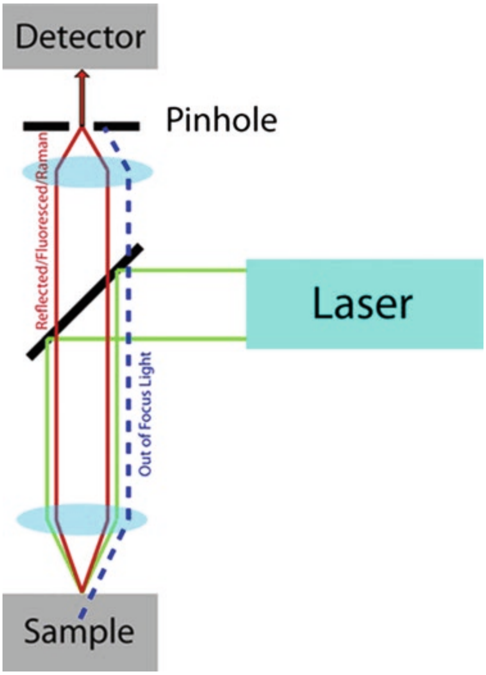

Fig. 3.5 The optical path of a confocal microscope. The use of point focus and a pinhole aperture located at a crossover focal point (i.e. the confocal point), before the detector provides superior rejection of out-of-focus light. The sample can be imaged by either rastering the sample or using mirrors to deflect the beam (not shown). The detector section can be one or more PMTs and/or a spectrometer [16]

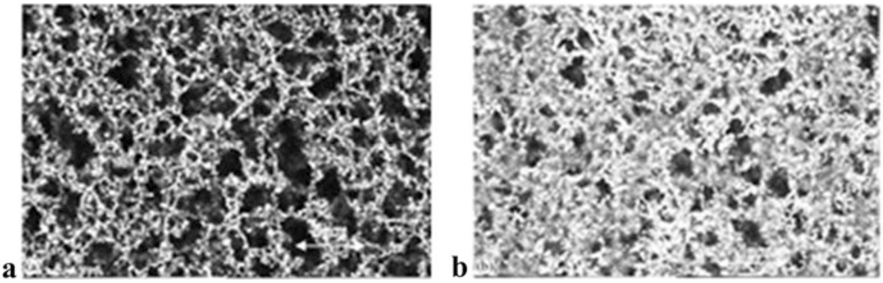

Fig. 3.6 LCSM image of the dry MF membrane. (**a**) (membrane surface) z = 0 µm, (**b**) z = 2 0 µm (×50 objective, numerical aperture 0.8) [20]

were imaged using LCSM. In order to observe the interaction between the rejected oil droplets and the nanofibers, PA6(3)T membranes fouled for 45 s were imaged using LCSM. The 3D images reconstructed using image J are presented in Fig. 3.5, where the PA6(3)T nanofibers are red and the rejected dodecane drops are bright green.

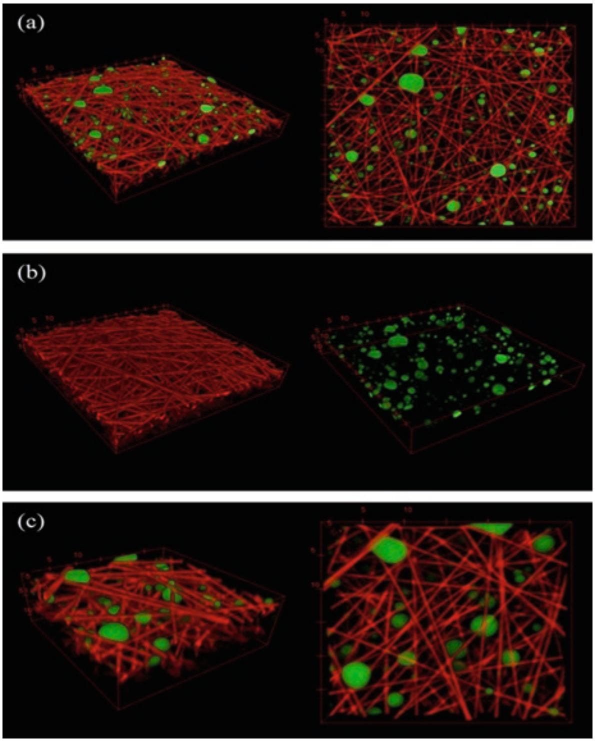

Fig. 3.7 3D image of the PA6(3) T fiber membrane fouled for 45 s reconstructed using Image J (**a**) Image size of 68 × 68 × 14 μm^3; (**b**) fibers and oil drops characterized in separate channels; and (**c**) magnified image of size of 30 × 30 × 14 μm^3 [21]

3.2.2.5 Rutherford Backscattering Spectroscopy (RBS)

Rutherford backscattering spectroscopy (RBS) uses the elastic scattering of a beam of ions (typically, 2 MeV He ions from an accelerator) to probe the composition and structure of materials [22]. RBS is a quantitative analytical technique and does not require the use of standards. Data analysis of layered structure (e.g., a composite membrane) can be performed using modeling software, which yields the number of atoms per unit area. Knowledge of the atomic density is needed to convert this real density to thickness. RBS has been successfully applied to determine characteristics of the top layer of several types of commercial reverse osmosis (RO) and nanofiltration (NF) membranes [23]. Coronell and coworkers used labeling by $Ba^{++}$and I^{-} ions to quantify the density and ionization behavior of positive and negative functional groups in RO and NF membranes [24] as well as ion partitioning using RBS [25].

3.2.2.6 Positron Annihilation Lifetime Spectroscopy (PALS)

Positron annihilation lifetime spectroscopy (PALS) is a technique to determine free volume in polymer membranes. It is based on the lifetime of the ortho-positronium (o-Ps), which is trapped inside free volume elements until it annihilates with an electron from the surroundings. In other words, it measures positronium (Ps) annihilation lifetimes and intensities, which can be related to the size and amount of defect structures, such as voids or pores in the range of several angstroms to tens of nanometers. Positron annihilation spectroscopy (PAS) or sometimes specifically referred to as 'Positron annihilation lifetime spectroscopy' (PALS) is a non-destructive spectroscopy technique to study voids and defects in solids. It uses positrons to probe material defects/voids/free volume at the sub-nm scale. The general working principle is based on correlating the lifetime (dwelling time) of the injected positrons against the sample void size (longer lifetimes correspond to large void sizes). The generation and subsequent behavior of Ps in porous films, through the use of a beam of positrons, are depicted in Fig. 3.8. When a positron (50 eV to 15 keV) is implanted into thin films, the positron will scatter off atoms and electrons in the solid to atomic-scale energy (several eV) within picoseconds.

In positron annihilation spectroscopy with positrons from radioactive source, positron is introduced in investigated sample and outgoing gamma rays which follow positron annihilation with electron in the sample are detected and analyzed. In the positron annihilation lifetime spectroscopy, when used with radioactive sources, ^{22}Na is usually used as positron source [27].

The typical setup of a PALS spectrometer includes a radioactive positron source (often ^{22}Na) and two or more scintillator detectors (Fig. 3.9). One of the detectors generates the start 'signal' for a TCSPC module using the gamma rays emitted simultaneously with the positron from the positron source. The other detectors are

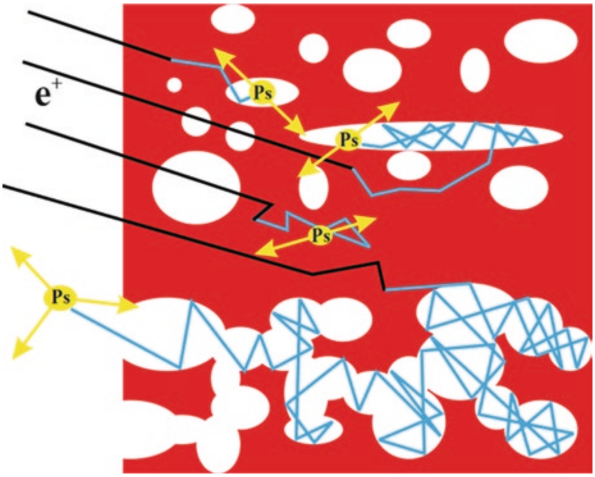

Fig. 3.8 Positronium formation in porous material [26]

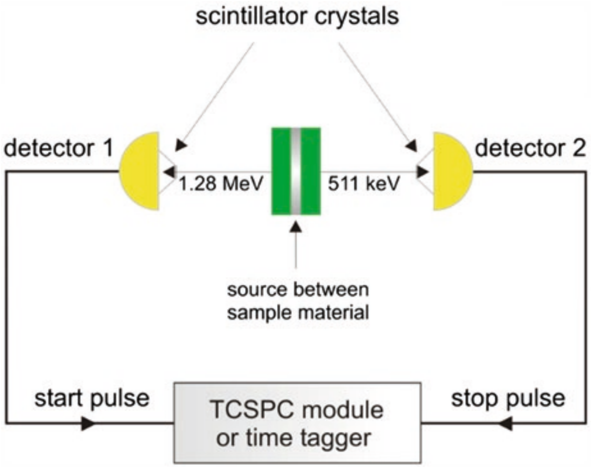

Fig. 3.9 PALS setup

arranged to detect the gamma rays emitted by the annihilation process at the sample. The resulting histogram can then be analysed to extract the average positron or positronium lifetimes.

Fong et al. [28] discussed how PALS can provide unique insight into the macroscopic transport properties of several porous biomembrane-like nanostructures and suggest how this insight may provide information on the release of drugs from these matrices to aid in developing therapeutic interventions.

PALS is capable of determining the free-volume and holes' properties directly at the atomic and nano- scale. This capability arises from the fact that positronium (bound state of positron and electron; Ps) is preferentially localized in regions of low electron density sites, such as free volumes, holes, interfaces, and pores. PALS technique can provide an unprecedented level of insight to our understanding of the internal structure of the active skin layer of membranes. It is capable of determining the free volume (FV) and hole properties directly at the atomic and nanoscale.

Kim et al. [29] showed that the thin films of cross-linked aromatic polyamide RO membranes are composed of two types of pores; i.e. pores with radii of about 2.1–2.4 Å were detected from the τ_3 lifetime component and those with 3.5–4.5 Å from τ_4 component by using PALS technique. They have identified the former pores as the network pore and the latter aggregate pore. Moreover, this study was applied to explain the flux-enhancement mechanism in thin-film-composite membranes. Tung et al. [30] characterized composite (TFC) polyamide nanofiltration (NF) membranes prepared by the interfacial polymerization method using positron annihilation spectroscopy technique. It was reported that the membranes have a composite structure containing three layers: a selective polyamide layer, a transition layer, and a porous support. A number of researchers are correlated free volume properties measured by Positron annihilation lifetime spectroscopy (PALS). PALS has been used to study subnanometer-sized holes, to determine their size distribution and free-volume fractions, and to probe molecular-sized vacancies in glassy polymers [31–34]. The polymer nanocomposite membranes with the MOF ZIF-8 as a filler and either polyimides (Matrimid, Ultem) or PIM-1 (polymer of intrinsic microporosity) as polymer matrix were tested for pure gas permeation. When Matrimid was used, PALS indicated that an increase in gas permeability is due to the free diffusion of the gas molecules through the ZIF-8 pores and a reduction in packing efficiency of the polymer. In the case of ZIF-8/PIM-1 PALS indicated that the introduction of ZIF-8 nanoparticles into the PIM-1 matrix resulted in an increase in free volume which was assumed to arise from a combination of the filler cavities and of more loosely packed polymer chains at the boundary between ZIF-8 particles and the PIM-1 matrix [35].

Jeazet et al. [36] reported the gas separation properties of a MOF-MMM made of MIL-101 and polysulfone and analyzed the free volume contributions with PALS. Pure gas (O_2, N_2, CO_2 and CH_4) permeation tests showed a significant increase of gas permeabilities of the mixed-matrix membranes without any loss in selectivity. PALS indicated that the increased gas permeability is due to the free volume in the PSF polymer and the added large free volume inside the MIL-101 particles. The trend of the gas transport properties of the composite membranes could be reproduced by a Maxwell model.

Thür et al. [37] studied the performance of bipyridine-based UiO-67 as novel filler in mixed-matrix membranes for CO_2-selective gas separation. At an optimal bipyridine concentration of 33%, the MOF increased both membrane selectivity (100%) and permeability (63%), compared to the unfilled polyimide membrane. The PALS results suggested that the UiO-67-33 MMM has larger and more free-volume elements than the MMM with UiO-67-100 and the reference Matrimid sample. When comparing UiO-67-100 with Matrimid, the intensity of o-Ps lifetimes for UiO-67-100 is twice as high, which might imply that the latter has a higher concentration of free-volume elements of 0.6 nm diameter. PALS hence suggests that UiO-66-33 has the least dense structure, followed by UiO-66–100, and further followed by pure Matrimid.

Shen et al. [38] developed fluorinated MOF-based mixed matrix membrane by incorporating the SIFSIX-3-Zn (or $Zn(pyrz)_2(SiF_6)$) nanoparticles into the polymer of intrinsic microporosity (PIM-1) matrix and studied its performance for C_3H_6/C_3H_8 separation. PALS results showed that the free volume of hybrid membranes increased dramatically. It was concluded that SIFSIX-3-Zn nanoparticles alter the molecular packing of PIM-1-based membranes providing a channel for gas molecules to diffuse freely through the PIM-1 matrix phase and through the pores of the SIFSIX-3-Zn cages.

3.2.2.7 Neutron Scattering (NS)

Neutron diffraction or elastic neutron scattering (NS) is the application of NS for the determination of the atomic and/or magnetic structure of a material. A sample to be examined is placed in a beam of thermal or cold neutrons to obtain a diffraction pattern that provides information of the structure of the material. It is an ideal technique for the analysis of biological membranes, since it permits the elucidation of structural details not attainable by X-ray scattering. Neutron scattering, the scattering of free neutrons by matter, can refer to either the physical process or the experimental technique which uses this process for the investigation of materials. In other words, neutron scattering is the technique of choice for condensed matter investigations in general because thermal/cold neutrons are a non-invasive probe; they do not change the investigated sample since they do not deposit energy into it. Since neutrons are electrically neutral, they penetrate matter more deeply than electrically charged particles of comparable kinetic energy. Therefore, they are valuable probes of bulk properties. Small-angle neutron scattering (SANS) is an experimental technique that uses elastic neutron scattering at small scattering angles to investigate the structure of various substances at a mesoscopic scale of about 1–100 nm. It is a powerful technique to understand the polymer chain nanostructure as well as the pore structure characteristics of the membrane in order to improve the membrane performance. Singh and Aswal [39] studied the typical polyamide RO PA membrane prepared by the interfacial reaction between an aqueous solution of m-phenylenediamine or piperazine and n-hexane solution of trimesoyl chloride using SANS. It was observed that membrane was comprised of nanoscale building blocks. In another work, Dahdal et al. [40] used small-angle neutron (SANS) technique to understand the fouling mechanism of RO membranes, mainly biofouling and scaling by calcium phosphate. Constituents of biological membranes show much larger differences in their scattering factors for neutrons than for X-rays [41].

3.2.2.8 Electron Paramagnetic Resonance Spectroscopy (EPR)

Electron Paramagnetic Resonance (EPR), also known as Electron Spin Resonance (ESR), is a technique for studying chemical species that have one or more unpaired electrons such as free radicals, odd electron molecules, transition metal complexes, lanthanide ions, and triplet state molecules. Free electrons are often short-lived, but still play crucial roles in many processes such as photosynthesis, oxidation, catalysis, and polymerization reactions.

Every electron has a magnetic moment (magnetic strength and orientation of a magnet or other object that produces a magnetic field) and spin quantum number S = (1/2) (the sets of numerical values which give acceptable solutions to the Schrödinger wave equation for the hydrogen atom) with magnetic components $m_s = -(1/2)$ and $m_S = +(1/2)$. In the presence of an external magnetic field with strength B_o, the electron's magnetic moment aligns itself either parallel ($m_s = -(1/2)$) or antiparallel ($m_s = +(1/2)$) to the field, each alignment having a specific energy due to the Zeeman effect:

$$E = m_s g_e \mu_B B_0 \tag{3.4}$$

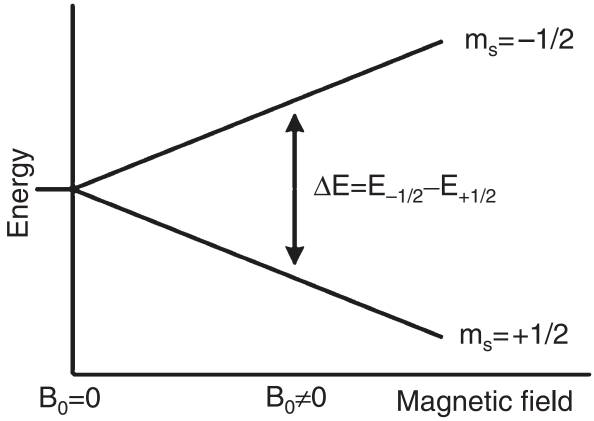

Fig. 3.10 An unpaired electron can move between the two energy levels by either absorbing or emitting a photon of energy hv such that the resonance condition, hv, is obeyed. This leads to the fundamental equation of EPR spectroscopy: $hv = g_e\mu_B B_0$

where, g_e is g-factor ($g_e = 2.0023$ for the free electron) [42] and μ_B is the Bohr magneton. Therefore, the separation between the lower and the upper state is $\Delta E = g_e\mu_B B_0$ for unpaired free electrons. This equation implies (since both g_e and μ_B are constant) that the splitting of the energy levels is directly proportional to the magnetic field's strength, as shown in the diagram below (Fig. 3.10).

EPR spectroscopy plays an important role in the understanding of organic and inorganic radicals, transition metal complexes, and some biomolecules including studying the structure and function of biological membranes. EPR was also applied to study synthetic membranes. Any substance that has unpaired electrons will give EPR. Polymers themselves may contain paramagnetic free radicals. A stable radical such a nitroxide radical can also be introduced into polymeric material. The radical, so introduced, is often called a spin label or a spin probe. It is invariably a nitroxide radical, which exhibits a three-line hyperfine structure. The peak shape and splitting depend on the radical's environments. Khulbe et al. [43] studied the structure of the skin layer of asymmetric cellulose acetate RO membranes with TEMPO probe (2,2,6,6-Tetramethylpiperidin-1-oxyl) and reported the following conclusions:

1. The space in the polymer network (the origin of the network pore) in the dense film is smaller when no swelling agent is added to the casting solution. The pore sizes of the asymmetric membranes are larger when they were shrunk at lower temperatures.
2. The space in the polymer network in the dense film is smaller when the membrane is dry.

In another publication, Khulbe et al. [44] reported the EPR study on the structure and transport of asymmetric aromatic polyamide membranes for RO. It was concluded that aromatic polyamide membranes contain water channels in the polymer matrix like cellulose acetate membranes. A comparison was then made with CA RO membrane. It was suggested that the EPR technique can be used to study the structure of RO membranes. The presence of water channels in the polymer matrix seems indispensable for the RO membrane.

Borbat et al. [45] discussed the electron spin resonance (ESR) techniques for studying basic molecular mechanisms in membranes and proteins by using nitroxide spin labels. Sahu and Lorigan [46] discussed some recent applications of nitroxide based SDSL (Site-directed spin labeling) EPR spectroscopic techniques to study membrane protein systems. It can provide important information on complicated biological systems which is very challenging or nearly impossible by using other biophysical techniques. EPR spectroscopy has the potential to become a powerful tool in membrane fouling analysis [47]. EPR can be applied to samples in gaseous, liquid or sold states over a wide range of temperatures.

Furthermore, EPR spectroscopy can be used to:

1. Detect, identify, and quantify free radicals,
2. Study molecular structures, geometry, and dynamics,
3. Observe labeled species in situ in biological systems,
4. Understand redox processes, reaction kinetics, catalysis and more.

3.2.2.9 Wide Angle X-Ray Scattering (WAXS) and Small Angle X-Ray Scattering (SAXS)

Wide-angle X-ray scattering is similar to small-angle X-ray scattering (SAXS) except the distance from sample to the detector is shorter and thus diffraction maxima at larger angles are observed. Small-angle X-ray scattering (SAXS) is a small-angle scattering (SAS) technique where the elastic scattering of X-rays (wavelength 0.1–0.2 nm) by a sample which has homogeneities in the nm-range, is recorded at very low angles (typically 0.1–10°). Wide-angle X-ray scattering (WAXS) or wide angle X-ray diffraction (WAXD) is an X-ray-diffraction technique that is often used to determine the crystalline structure of polymers. Depending on the measurement instrument used, it is possible to do WAXS and SAXS in a single run (small- and wide-angle scattering, SWAXS). Tamlin [48], and Akbari et al. [49] successfully used Grazing incidence small- and wide-angle X-ray scattering (GISAXS and GIWAXS) to study polyamide on polysulfone reverse osmosis membrane's morphology (interfaces). Cruz-Silva et al. [50] made a comprehensive study of the chemical and physical effects of carbon nanotubes on the fully cross-linked polyamide network. The microstructure of the nanocomposite membrane was studied by small and wide angle X-ray scattering, high resolution transmission electron microscopy, and molecular dynamics.

3.2.3 Membrane Chemistry

A wide variety of synthetic membranes are known. They can be produced from organic materials such as polymers and liquids, as well as inorganic materials. The most of commercially utilized synthetic membranes in separation industry are made of polymeric structures. They can be classified based on their surface chemistry, bulk structure, morphology, and production method. To know the membrane chemistry is therefore important for the development of membrane.

3.2.3.1 Attenuated Total Reflection Fourier Transform Infrared Spectroscopy (ATR-FTIR)

The use of Fourier Transform Infrared (FTIR) spectroscopy has been considered to be one of the most effective techniques to study and understand the chemical and surface chemistry in various types of membrane. Attenuated total reflectance (ATR) is a sampling technique used in conjunction with infrared spectroscopy which enables samples to be examined directly in the solid or liquid state without further preparation [51]. ATR is today the most widely used FTIR sampling tool. Figure 3.11 shows the schematic representation of an ATR-FTIR system.

The attenuated total reflection Fourier transform infrared spectroscopy (ATR-FTIR) technique was used to investigate chemical surface structure of the membrane and chemical changes induced by fouling.

Attenuated total reflectance is a sampling technique used in conjunction with the Fourier transform infrared spectroscopy in order to enable surfaces to be examined directly for infrared analysis. The infrared analysis spectrum can be used to determine the vibrational frequencies and the transition intensities of most molecules together with the characteristic of the functional group frequencies. Infrared spectroscopy is a technique used for chemical processes and structure identification. The use of infrared spectroscopy with the theories of reflection has made advances in surface analysis possible. When using ATR-FTIR, a beam of infrared light is passed

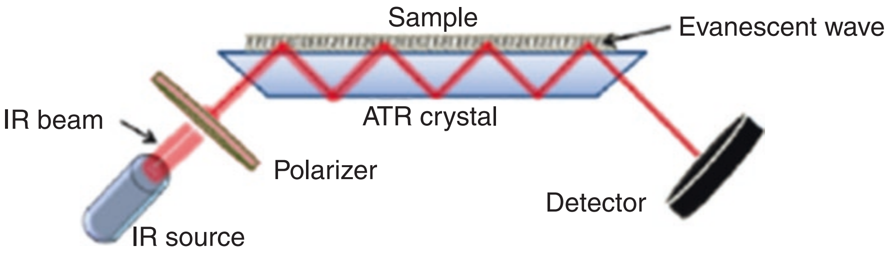

Fig. 3.11 Schematic representation of an ATR-FTIR system. The infrared beam passes through the ATR crystal covered on the top by the sample. The evanescent wave penetrates into the sample and is absorbed by the sample. The polarizer generates parallel and perpendicular polarized incident beam [52]

through the attenuated total reflection crystal in order to reflect at least once off the internal surface in contact with the membrane sample. The evanescent wave coupling extending into the sample is from this reflection. The number of reflections is varied by varying the angle of incidence, and the beam is collected by a detector while exiting the crystal. The importance of ATR-FTIR has recently led to substantial use by scientists.

Composite polysulfone membranes were synthesized and characterized for desalination in nanofiltration technique [49]. They used attenuated total reflectance Fourier transform infrared spectroscopy to study the evolution of chemical structures of the nanofiltration membranes after irradiation. Abdullah et al. [53] investigated the effects of ferrihydrite (Fh) nanoparticle loading on the physicochemical properties of polysulfone (PSf) membranes fabricated via the phase inversion method. On characterization of Fh/PSf membrane via Fourier transmission infra-red (FTIR), it was concluded that a new O-H band was formed when Fh was added into the membrane matrix.

3.2.3.2 Auger Electron Spectroscopy (AES)

Auger electron spectroscopy (AES) identifies elemental compositions of surfaces by measuring the energies of Auger electrons. Auger electron emission is stimulated by bombarding the sample with an electron beam. The Auger electron energies are characteristic of the elements from which the electrons come. Auger electron spectroscopy is a widespread method for analysis of surfaces, thin films, and interfaces. Auger Electron Spectroscopy (AES) provides quantitative elemental and chemical state information from surfaces of solid materials. The average depth of analysis for an AES measurement is approximately 5 nm. Physical Electronics Auger instruments provide the ability to obtain spectra with a lateral spatial resolution as small as 8 nm. Atoms that are excited by the electron beam can emit "Auger" electrons. AES measures the kinetic energies of the emitted electrons. The energy of the emitted electrons is characteristic of elements present at the surface and near the surface of a sample. A typical AES setup is shown schematically in Fig. 3.12. In this configuration, focused electrons are incident on a sample and emitted electrons are deflected into a cylindrical mirror analyzer (CMA). In the detection unit, Auger electrons are multiplied and the signal sent to data processing electronics. Collected Auger electrons are plotted as a function of energy against the broad secondary electron background spectrum.

Xu et al. [54] measure the thickness of graphene layers (different number of graphene layers on ~300 nm dry thermal SiO_2) by Auger electron spectroscopy (AES). The AES spectroscopy shows distinct spectrum shape, intensity, and energy characteristics with an increasing number of graphene layers. Similar work has been reported by Sutter and Sutter [55] [measuring few-layer of hexagonal boron nitride (h-BN) on Ru(0001)/Al_2O_3(0001) thin films by AES]. Hydrophobicity and hydrophilicity are controlled by the thin surface layer. Surface hydrogen and oxygen functionalities contribute to hydrophobic and hydrophilic properties, respectively. A

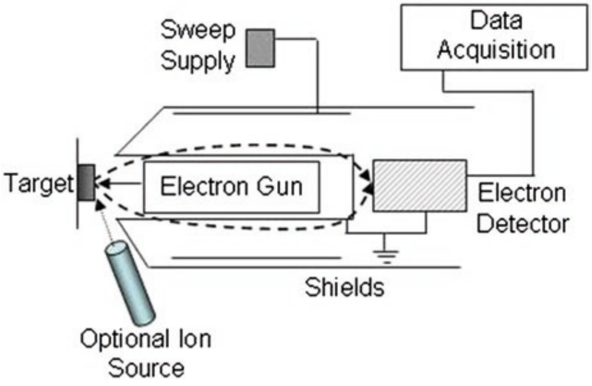

Fig. 3.12 AES experimental setup using a cylindrical mirror analyzer (CMA). (An electron beam is focused onto a specimen and emitted electrons are deflected around the electron gun and pass through an aperture towards the back of the CMA. These electrons are then directed into an electron multiplier for analysis. Varying voltage at the sweep supply allows derivative mode plotting of the Auger data. An optional ion gun can be integrated for depth profiling experiments

wettability characteristics of RO membranes was studied by AES, which details can be found elsewhere [56, 57].

3.2.3.3 X-ray Photoelectron Spectroscopy (XPS)

X-Ray Photoelectron Spectroscopy (XPS), also known as Electron Spectroscopy for Chemical Analysis (ESCA), is an analysis technique used to obtain chemical information about the surfaces of solid materials. Both composition and the chemical state of surface constituents can be determined by XPS. In other words, X-ray photoelectron spectroscopy (XPS) is a surface-sensitive quantitative spectroscopic technique that measures the elemental composition at the parts per thousand ranges. Sometimes called ESCA, it is used to study elemental compositions of composite RO membranes near the surface. This technique supplied verification of the polymer chemical structures expected from the interfacial polymerization reactions that formed the membranes. The average depth of analysis for an XPS measurement is approximately 5 nm. The information XPS provides about surface layers or thin film structures is important for many industrial and research applications where surface or thin film composition plays a critical role in performance including: nanomaterials, photovoltaics, catalysis, corrosion, adhesion, electronic devices, packaging, magnetic media, display technology, surface treatments, and thin film coatings used for numerous applications. From characterisation of nuclear waste materials to thin-film electronics and bio-active surfaces, XPS is the standard tool for surface material characterisation.

Yuso et al. [58] studied the surface changes in a Nafion membrane as a result of IL-cation doping with 1-butyl-3-methylimidazolium tetrafluoroborate ($BMIM^+BF_4^-$)

and phenyltrimethylammonium chloride ($TMPA^{+}Cl^{-}$) by XPS. Results revealed that the surface coverage of Nafion112 as a result of the doping gives rise to thermal stable membranes when compared with the original Nafion112 membrane, due to reduction of hydrophobic character.

Wagner et al. [59] studied by XPS the modified polyamide reverse osmosis (XLE, polyamide thin film composite membranes manufactured by Dow Water & Process Solutions (Edina, MN) extra low energy) membrane grafted by poly(ethylene glycol) (PEG) diglycidyl ether (PEGDE) to their top surfaces from aqueous solution to improve fouling resistance. XPS results indicated the qualitative evidence of the presence of PEGDE on the membrane surface and the thickness of PEGDE layer. Further, XPS results were qualitatively consistent with the ATR-FTIR results.

3.2.3.4 Electron Dispersive X-ray Spectroscopy

Energy-dispersive X-ray spectroscopy (EDS, EDX, or XEDS), sometimes called energy dispersive X-ray analysis (EDXA) or energy dispersive X-ray microanalysis (EDXMA), is an analytical technique used for the elemental analysis or chemical characterization of a sample. EDS analysis can be used to determine the elemental composition of individual points or to map out the lateral distribution of elements from the imaged area. It can also be used to obtain compositional information on quasi-bulk specimens (low SEM magnification, high accelerating voltage) or on specific particles, morphologies, or isolated areas on filters or within deposits. Energy dispersive X-ray spectroscopy (EDS) has an analytical capability that can be coupled with several applications including scanning electron microscopy (SEM), transmission electron microscopy (TEM) and scanning transmission electron microscopy (STEM). For instance, Beverly et al. [60] demonstrated that EDS, combined with XPS, FTIR and SEM, is a valuable diagnostic tool for failure analysis of polymeric RO membranes and provides valuable information to aid the manufacturers in designing better membranes for reverse osmosis.

3.2.3.5 Raman Spectroscopy (RS)

Raman Scattering: When a monochromatic electromagnetic radiation of energy, $h\nu_o$, is incident upon a sample, it may be reflected, absorbed, or scattered in all directions. The portion of scattered radiation is inelastic (approximately 1×10^{-7} of the scattered light) and has a frequency ($h\nu_o + h\nu$ or $h\nu_o - h\nu$) different from the frequency of the incident radiation ($h\nu$ is the energy difference between vibrational states). The scattered radiation having lower frequency ($h\nu_o - h\nu$) is called Stokes lines and that having higher frequency ($h\nu_o + h\nu$) is called anti-Stokes lines, as shown in Fig. 3.13. This change in wavelength of the scattered photons due to changes in the polarizability of the molecules provides the structural information of the sample.

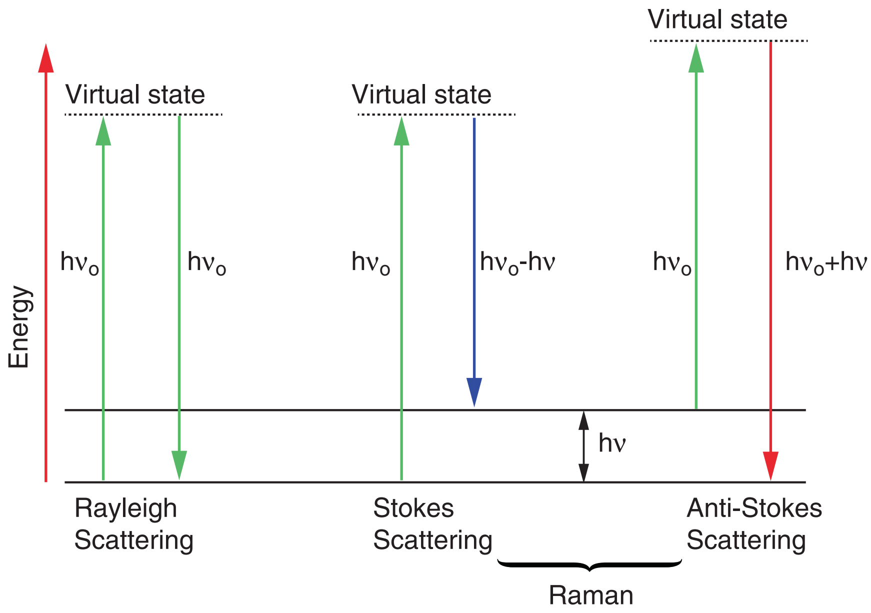

Fig. 3.13 Rayleigh and Raman scattering

Thus, Raman spectroscopy provides highly chemical-specific information about samples based on the fundamental vibrational modes of the molecules. It is a valuable tool for qualitative and quantitative polymeric membrane characterization. The interactions among the functional groups, chain orientation, structural changes upon treatment/modification, and interfacial properties of the polymeric composite are some of the interesting information that can be revealed from the Raman spectra [61].

Raman-based optical imaging is a promising analytical tool for non-invasive, label-free chemical imaging of lipid bilayers and cellular membranes [62]. RS is also developing its utility to characterise diverse cell membranes. Fogarty et al. [63] applied surface-enhanced Raman spectroscopy (SERS) to cationic gold-labeled endothelial cells to derive SERS-enhanced spectra of the bimolecular makeup of the plasma membrane, and suggested that SERS has great potential for the study and characterization of cell surfaces. High-vacuum tip-enhanced Raman spectroscopy (HV-TERS) is a powerful characterization tool in nanoscience and nanotechnology. HV-TERS is applied to analyzing multipolar Raman measurements, the nature of plasmon-driven chemical reactions, and surface molecular catalysis reactions [64]. John and George [65] discussed the advances in Raman spectroscopy, such as surface-enhanced Raman spectroscopy, resonance Raman spectroscopy, stimulated Raman spectroscopy, coherent anti-Stokes Raman spectroscopy, tip-enhanced Raman spectroscopy, and confocal Raman imaging, specifically highlighting its basic principle, experimental setups, and recent research progress in the field of nanomaterials.

3.2.3.6 Energy-Dispersive X-Ray Spectroscopy (EDX)

Energy-dispersive X-ray spectroscopy (EDS, EDX, EDXS or XEDS), sometimes called energy dispersive X-ray analysis (EDXA) or energy dispersive X-ray microanalysis (EDXMA), is an analytical technique used for the elemental analysis or chemical characterization of a sample. It is based on an interaction of some source of X-ray excitation and a sample. Its characterization capabilities are due in large part to the fundamental principle that each element has a unique atomic structure allowing a unique set of peaks on its electromagnetic emission spectrum [66]. It is an analytical method in physics and chemistry. EDX systems are attachments to Electron Microscopy (SEM or TEM) instruments where the imaging capability of the microscope identifies the specimen of interest. The technique can be qualitative, semi-quantitative, quantitative and also provide spatial distribution of elements through mapping. The EDX technique is non-destructive and specimens of interest can be examined in situ with little or no sample preparation. In membrane characterization it can be applied to study as;

1. Product deformulation and competitor analysis.
2. Adhesion, bonding, delamination investigations.
3. Product imperfections and defect analysis.
4. Contamination detection, isolations and identification.
5. Quality control, raw material and end product.
6. Filler, pigment, fibre, additive distribution, orientation.

3.2.3.7 Ellipsometry

Ellipsometry is an optical technique for investigating the dielectric properties (complex refractive index or dielectric function) of thin films. Ellipsometry measures the change of polarization upon reflection or transmission and compares it to a model. Ellipsometry has been shown to be capable of deriving the optical properties, as well as measuring the thickness of membranes that are just tens of nanometers. The measured signal is the change in polarization as the incident radiation (in a known state) interacts with the material structure of interest (reflected, absorbed, scattered, or transmitted). The polarization change is quantified by the amplitude ratio, and the phase difference. Because the signal depends on the thickness as well as the material properties, ellipsometry can be a universal tool for contact free determination of thickness and optical constants of films of all kinds [67]. Figure 3.14 shows the schematic setup of an ellipsometry experiment.

Variable-angle spectroscopic ellipsometry can be used to obtain meaningful information on the in situ swelling behavior of thin dense supported membrane [68]. Jaiswal et al. [69] fabricated plasmonic gold/alumina nanocomposite (Au/Al_2O_3 NC) thin films on a glass substrate at room temperature by RF (radio frequen-

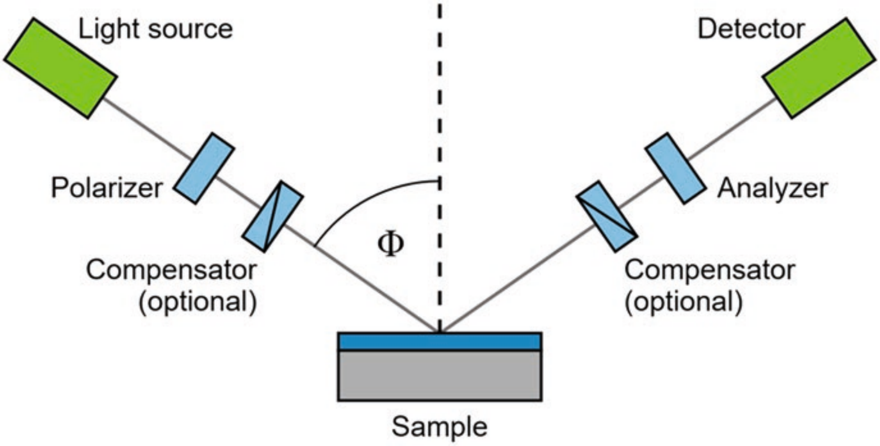

Fig. 3.14 Schematic setup of an ellipsometry experiment

cies) magnetron co-sputtering. The influence of the film thickness (~10 to 40 nm) on the optical and other physical properties of the samples was investigated using spectroscopic ellipsometry (SE) and correlated with the structural and compositional properties. It was revealed that the film thickness and surface roughness obtained from SE data are well corroborated with SEM and AFM measurements. Spectroscopic ellipsometry is a convenient technique for in situ studies of thin films, because of its non-invasive character and very high precision.

3.2.3.8 Fluorescence Microscopy

Fluorescence microscopy is usually used for biological membranes. Fluorescence microscopy is a technique whereby certain molecules can be excited with one wavelength of light and will emit another longer wavelength of light. Because each fluorescent molecule has a unique spectrum of absorption and emission, the location of particular types of molecules can be determined. This technique was used for determining the spatial extension and geometrical characteristics of multicomponent structures composed of diverse molecular constituents, such as proteins, lipids, carbohydrates, nucleic acids, and even cells with viruses [70]. Bagatolli [71] discussed how membrane model systems can be utilized to gain information about particular membrane-related process like protein(peptide)/membrane interactions from Fluorescence Microscopy. Tamime et al. [72] used white light interferometry (WLI) to characterize flat-sheet polyethersulfone (PES) membranes and hollow PVDF fibers. Figure 3.15 shows the schematic of a fluorescence microscope.

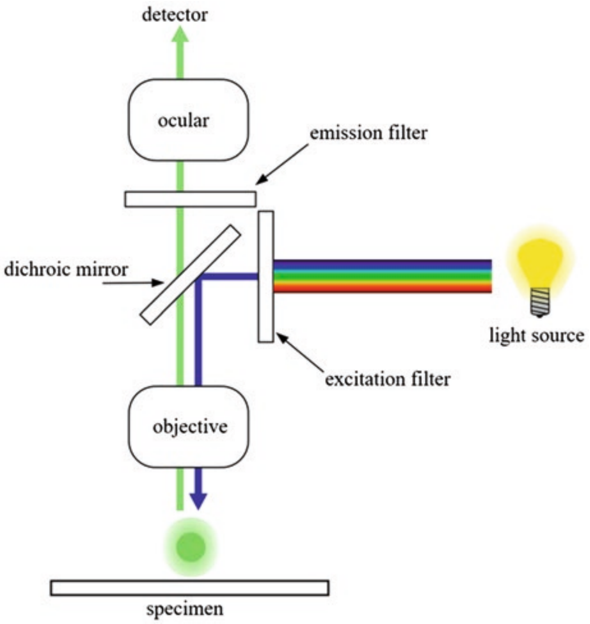

Fig. 3.15 Schematic of a fluorescence microscope

3.2.3.9 Nuclear Magnetic Resonance (NMR)

Nuclear magnetic resonance spectroscopy, most commonly known as NMR spectroscopy or magnetic resonance spectroscopy (MRS), is a spectroscopic technique to observe local magnetic fields around atomic nuclei. The sample is placed in a magnetic field and the NMR signal is produced by excitation of the nuclei sample with radio waves into nuclear magnetic resonance, which is detected with sensitive radio receivers. In other words, NMR is a physical observation in which nuclei in a strong constant magnetic field are perturbed by a weak oscillating magnetic field (in the near field and therefore not involving electromagnetic waves) [73] and respond by producing an electromagnetic signal with a frequency characteristic of the magnetic field at the nucleus. NMR spectra are unique, well-resolved, analytically tractable and often highly predictable for small molecules. Different functional groups are obviously distinguishable, and identical functional groups with differing neighboring substituents still give distinguishable signals.

Kong [74] explored the nanometer-scale structure of Nafion, the widely used fuel cell membrane, and its composites via NMR technology, and characterized chemical structure and composition, domain size and morphology, internuclear distances, molecular dynamics, etc., of Nafion. Glaves and Smith [75] discussed that nuclear magnetic resonance (NMR) may also be suitable for determining membrane pore structures. In another work, Schmid et al. [76] used NMR microscopy, for the first time, to study biofouling of industrial spiral wound RO modules [77]. NMR microscopy can provide a non-invasive quantitative measurement of RO membrane biofouling and its impact on hydrodynamics and mass transport in RO systems. Schulenburg et al. [78] demonstrated the application of NMR to a spiral wound RO membrane module to understand the key design and operational parameters influencing the biofilm fouling in the membrane module. Fridjonsson et al. [79] demonstrated that the use of Earth's field (EF) NMR can provide early non-destructive detection of active biofouling of a commercial spiral wound RO membrane module.

3.2.3.10 Photoacoustic Spectroscopy

Photoacoustic spectroscopy is the measurement of the effect of absorbed electromagnetic energy (particularly of light) on matter by means of acoustic detection. The absorbed energy from the light causes local heating and through thermal expansion a pressure wave or sound. A photoacoustic spectrum of a sample can be recorded by measuring the sound at different wavelengths of the light. This spectrum can be used to identify the absorbing components of the sample. The photoacoustic effect can be used to study solids, liquids and gases [80]. The major advantage of photoacoustic spectroscopy is that it is suitable for highly absorbing samples. For instance, Flemming [81] suggested that photoacoustic spectroscopy can be used for monitoring the biofilm formation on the membrane during RO process. Schmid et al. [76] used photoacoustic spectroscopy (PAS) as a new biofilm monitoring technique. PAS combines features of optical spectroscopy and ultrasonic tomography and allows a depth-resolved analysis of optically and acoustically inhomogeneous media.

3.3 Other Techniques

3.3.1 Zeta Potential Measurement

Zeta potential (ζ) is a scientific term for electrokinetic potential [82]. ζ is positive if the potential increases from the bulk of the liquid phase towards the interface. In calculating the electrokinetic potential from electrokinetic phenomena it is often assumed that the liquid adhering to the solid wall and the mobile liquid are separated by a sharp shear plane. Zeta potential analysis opens up new possibilities in the characterization of membranes used for complex industrial or scientific applications. It provides insights into the membrane surface chemistry and elucidates the membrane's interaction with charged species in the feed solution. The zeta potential of membrane surfaces and the resulting electrostatic interactions are determining factors of membrane fouling.

Zeta potential is an important tool to measure the electrical charge of the membrane surface. The zeta potential of particles in the suspension is calculated based on the electrophoretic mobility. On the other hand, zeta potential of the membrane surface is evaluated by measuring the streaming potential. The zeta potential of the membrane often changes from positive to negative as the pH of the solution is increased, affecting the deposition of charged particles (fouling) on the membrane surface. Membrane surface charge is not directly experimentally accessible. Instead, zeta potential is used as an approximation for both the magnitude and sign (+ or −) of membrane surface charge. Zeta potential (ζ) is the potential difference between the bulk of solution and the sheer (slipping) plane of the interfacial double layer. Zeta potential is a function of surface and solution chemistry (pH, ionic composition, and ionic strength) at the solid-liquid interface and is an important membrane characteristic for assessing membrane fouling potential and developing chemical cleaning protocols. Membrane zeta potential is typically determined from streaming potential measurements. A streaming potential is generated when an electrolyte solution flows through a thin channel or porous media (e.g., a sand column) and is related to zeta potential by the Helmholtz-Smoluchowski equation:

$$E / p = \left(\varepsilon\varepsilon_o\zeta\right) / \left(\lambda\eta\right) \tag{3.5}$$

where E is the streaming potential due to electrolyte flow through a capillary channel, p is the applied pressure driving the flow, ζ is the zeta potential, λ is the electrolyte conductivity, η is the viscosity of the electrolyte solution, ε is the relative permittivity of the solution (dimensionless), and ε_0 is the vacuum permittivity (fundamental constant). Values of E, p, and λ are measured by the streaming potential analyzer; while ε and η are calculated based on temperature measurement (empirical fit functions for pure water data are used).

Thin-film composite polymer membranes typically show a high negative zeta potential. The zeta potential helps to monitor fouling during filtration and to optimize the efficiency of membrane cleaning. Li et al. [83] observed that as the CNF (functionalized cellulose nanofibers) content in the polymer (CA, cellulose acetate) matrix increased, the membrane possessed more negative surface charges. For example, at a fixed pH value of 7.1, the zeta potential value for the CA, $CA - CNF$ 0.1 (0.1 wt.%), $CA - CNF$0.3 (0.3 wt.%), and $CA - CNF$0.6 (0.6 wt.%) were −8.2 mV, −13.6 mV, −15.2 mV, and −22.0 mV, respectively. The more negative zeta potential values of the nanocomposite membranes with increasing CNF content were related to the increasing carboxylate content on the membrane surface. More negative zeta potential values of membranes are desirable in water filtration, as it may assist to decrease the fouling tendency of the membranes as a result of the electrostatic repulsion between the membrane surface and the foulants in water. Also, a highly negative zeta potential may enhance contaminant rejection by an electrostatic repulsion mechanism. Wagner et al. [84] measured the zeta potential of a RO commercial membrane grafted with PEGDE by using an Anton Paar Sur PASS Electrokinetic Analyzer and associated software (Anton Paar USA, Ashland, VA). Two membrane samples separated by a spacer were loaded into the clamping cell, creating a channel for electrolyte flow. A 10 mM NaCl solution was used as the background electrolyte. Streaming potential was measured as a function of feed pH, and the Fairbrother–Mastin approximation was used in the calculation of zeta potential from streaming potential.

3.3.2 Contact Angle Measurement

Surface wetting properties of the membrane material plays an important role on membrane properties and performances during the separation process such as permeate flux, rejection, and fouling characteristics. The material composition of the membrane and its corresponding surface chemistry govern the interaction with water molecules, thus influencing its wettability. The analysis of surface energy and affinity of the liquid toward the solid substrate can provide an easy and effective approach to obtain the surface properties.

Contact angle is the angle between a tangential to the liquid surface at the line of meeting three phases and the plane of the solid surface (either real or apparent) on which liquid resides or moves. Contact angle is the most commonly used parameter to indicate membrane's hydrophilicity or hydrophobicity. Lower contact angle value signifies the hydrophilic nature of the material, i.e., high affinity of water molecules toward the substrate. The higher contact angle indicates the hydrophobic nature of the surface. Figure 3.16 shows the schematic representation of interaction of water molecules with different substrate.

There are four methods for measuring the contact angle:

1. Sessile Drop Technique.
2. Captive Bubble Method.
3. Wilhelmy Plate Method.
4. Capillary Rise at a Vertical Plate.

Sessile Drop Technique and Captive Bubble Method are most common. All techniques are well illustrated in literature [85]. The wettability characteristic of nonideal surfaces depends on the several physicochemical properties of the substrate. Contact angle measurement is significantly influenced by the physical properties of the materials;

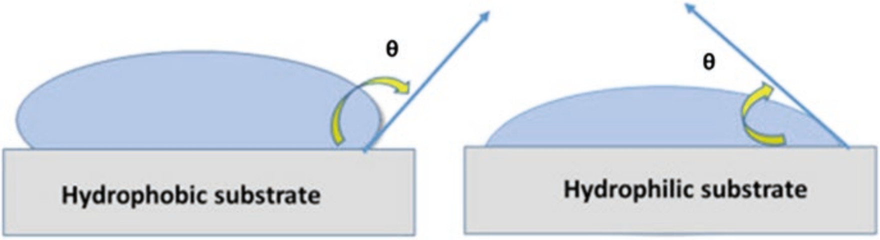

Fig. 3.16 Schematic representation of interaction of water molecules with different substrate [85]

1. heterogeneity,
2. surface roughness,
3. particle size, and
4. particle shape.

It is conducted to determine surface hydrophilicity of RO membrane with the intention of predicting membrane performance or fouling potential. It is necessary to consider effective factors for contact angle measurement such as measurement time, drop volume and membrane sample preparation. Due to this reason different contact angles were reported in literature for the same RO membrane [86].

3.3.3 Thin Film Characterization through Grazing Angle FT-IR Microscope

Grazing Angle Mcroscope was patented by Simon [87]. The GAM-FTIR technique permits high-sensitivity analyses of small areas of thin films deposited on reflective surfaces. The infrared spectra acquired can provide detailed information about the bonding of organic molecules on metals. Gaillard et al. [88] showed the potentiality of the GAM-FTIR technique for the characterization of very thin films (a few nanometres in thickness) deposited on a flat metallic substrate.

Grazing-angle sampling technology, improved the sensitivity of infrared reflectance measurements to be maximized for thin layers of organic materials on metallic surfaces. Grazing-angle reflectance theory can be explained by referring to Fig. 3.17.

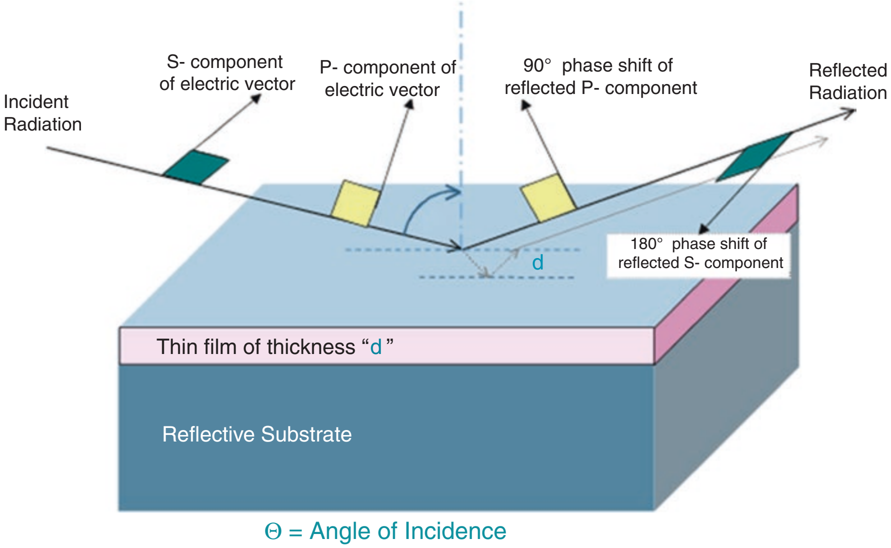

Fig. 3.17 Infrared energy striking a contaminated reflective substrate at a grazing angle of incidence

In reflection spectroscopy, a portion of the incident radiation beam (in this case infrared) reflects off the surface of a thin film, while the remaining portion travels (is refracted) through the film and reflects off a reflective substrate back through the film. This is known as “double-pass” reflection-absorption [89, 90].

Specular reflectance at high “grazing” angles (around 80 degrees from normal to the surface) has been recognized as one of the best spectroscopic techniques to monitor monomolecular layers on reflective surfaces due to the enhancement of the infrared signal [91]. Film SurveyIR™, Grazing Angle FT-IR Microscope is an indispensable tool for thin film (<1 μm thickness) characterization and identification. It can be used for materials characterization or defect analysis. Film Survey IR is a Fourier transform infrared (FT-IR) micro spectroscopy accessory that provides a chemical fingerprint of thin films on glass, metal, silicon and other surfaces [92]. Measurements of boundary lubrication thin film of less than 20 angstroms have been achieved using a grazing-angle-microscope/FTIR technique [93]. Automation of the grazing angle microscope expands its capability further to study micro spatial chemical mapping of polymer, organic, and even inorganic thin films on reflective surfaces. The results yield the thickness map of the thin film in a microscopic scale that could not possibly or easily be achieved [94]. Dunphy et al. [95] studied the nanostructure of silica and hybrid thin film mesophases template by phospholipids via an evaporation-induced self-assembly (EISA) process by grazing-incidence small-angle X-ray scattering (GISAXS) and reported that the nanostructure of silica- and hybrid-thin films synthesized using EISA with phospholipid templates that a variety of phases (1D, 2D, and 3D) can be formed by proper selection of the lipid structure.

3.3.4 Ultrasonic

The application of ultrasonic enhanced membrane separation process is mainly focused on ultrafiltration and microfiltration, and it is widely used in both dead-end (static) filtration and cross-flow filtration [96]. Ultrasonic (UR) is a versatile non-destructive, non-invasive, real-time, and low-cost methodology that can provide important information about a wide range of membrane-based separations. Ultrasonic measurements are based upon the propagation of mechanical waves; their velocity is dictated by the medium through which they travel. Ultrasonic velocity characterizes the speed at which the compression and subsequent rarefaction of medium molecules occur. Ultrasound has been widely used for characterization of materials including microporous membranes using low frequency ultrasonic guided waves.

The ultrasound signal is generated by exciting a piezoelectric crystal of a transducer by means of a difference in the applied potential. In general, a transducer is a device which converts one kind of energy into another. Ultrasonic transducers convert electric energy into mechanic energy and vice-versa. Since the emitted ultrasound signal crosses the membrane, the received signal brings with it information about the membrane's influence on the pattern of the ultrasonic wave. Thus, by analyzing the characteristics of the received ultrasound wave, it is possible to obtain information about the material which is under investigation. The basic measures performed in the ultrasound signals are: signal amplitude and signal's elapsed time. In general, the speed of the sound in an environment depends on the frequency of the ultrasonic pulse [97].

The characterization and monitoring of membranes through the use of ultrasonic measurements is based on extensive literature in the field of acoustics and a related literature in elasto-dynamics or waves in solids as well. To date the literature on membrane characterization has made use of frequencies which are above the audible range for humans, approximately 20 kHz [98]. The manner in which the membrane responds to the ultrasonic wave is dependent on the mechanisms of the separation processes and the associated membrane structure. In particular, while the theoretical framework for waves in porous materials [99] is applicable to microporous membranes in which the fluid permeates the pores, a reverse osmosis (RO) membrane would respond in a manner which is consistent with dense materials. UR (ultrasonic reflectometry) has been employed for characterization of membrane structure, formation, compaction, and inorganic and organic membrane fouling, the latter in both real-time and post-mortem modes.

Ultrasound can be applied in membrane technology, in the following way [100–102].

1. Membrane fouling and cleaning.
2. Membrane compaction.
3. Membrane swelling.
4. Membrane formation.
5. Membrane morphology.
6. Membrane quality control.
7. Membrane process control.

Ultrasonic time-domain reflectometry (UTDR) was employed as a visualization technique to provide real-time characterization of the fouling layer. Ramaswamy et al. [103] used an Ultrasonic Frequency Domain Reflectometry technique (UFDR) in which they observed that with the increase in the pore size, there is a significant increase in the attenuation of the frequency. The group also used a simple-model Artificial Neural Network in order to predict the size of PVDF and MCE membrane pores, which pores were in the range between 0.1 and 0.6 μm, based on the amplitude of the signal of the ultrasonic wave.

Lucas et al. [104] reported that 25 MHz immersion transducer can detect interactions of a microporous membrane in the pattern of the ultrasonic wave. Loest et al. [105] discussed the application of ultrasonic time-domain reflectometry (UTDR) for quantifying membrane compaction. Kujundzic et al. [103] [106] discussed the use of ultrasonic reflectometry (UR) for characterizing membranes and membrane processes. Bentama et al. [107] described that ultrasonic technique can be used as a powerful tool to detect default of porosity of a clay membrane after manufacturing. Álvarez-Arenas et al. [108] characterized ion-track membranes (ITM) by UR technique. Influence of membrane properties on ultrasound propagation in the pore space was analyzed.

3.3.5 Thermogravimetric Analysis

Thermogravimetric analysis or thermal gravimetric analysis (TGA) is a method in which the mass of a sample is measured over time as the temperature changes in a controlled atmosphere. This measurement provides information about physical phenomena such as mass changes, temperature stability, oxidation/reduction behaviour, decomposition, corrosion studies, compositional analysis and thermokinetics as well as chemical phenomena including chemisorptions, and solid-gas reactions (e.g., oxidation or reduction) [109].

TGA is conducted on an instrument known as a thermogravimetric analyzer. It continuously measures mass while the temperature of a sample is changed over time. Mass, temperature, and time are considered base measurements in thermogravimetric analysis while many additional measures may be derived from these three base measurements. A TGA can be used for materials characterization through analysis of characteristic decomposition patterns. Thermogravimetry analysis serves as a valuable tool to understand thermal events associated with nanomaterials and polymer composites when subjected to heating under predetermined heating rate and temperature conditions [110].

Macevele et al. [111] investigated the properties of composite membranes based on PVDF-HFP (Hexafluoropropylene) polymer modified with either silver nanoparticles and/or MWCNTs. From TGA analysis they reported that all membranes (PVDF-HFP, Ag/PVDF-HFP, MWCNTs/PVDF-HFP and Ag-MWCNTs/PVDF-HFP) remain stable up to 170 °C, with Ag doped PVDF-HFP membrane maintaining stability up to 300 °C, especially when compared to PVDF-HFP polymeric membrane. Both PVDF-HFP and MWCNTs doped PVDF-HFP showed a weight loss of 20% from 170 to 440 °C. The data indicated that MWCNTs do not improve the structural stability of the PVD-HFP membrane. The structure of the composites consisting of both Ag nanoparticles and MWCNTs on PVDF-HFP collapsed with a weight loss of 40% from 170 to 450 °C. However, all composites have shown stability within the limits of the daily temperature of water and can easily withstand purification of boiled water. Li et al. [83] investigated the thermal behavior of the pristine CA (cellulose acetate) membrane and the $CA - CNF0.6$ (functionalized cellulose nanofibers, 0.6 wt.%) nanocomposite membrane by thermogravimetric analysis (TGA) coupled with differential thermal analysis (DTA). The thermal behavior of the membranes followed a three-step degradation process. There was a mass loss of ~2% starting from room temperature up to 150 °C which is due to the elimination of moisture. Then, a sharp weight decline was observed in the pyrolytic temperature range of 231–390 °C. The main degradation, centered at 338 °C, was assigned to the pyrolytic degradation of the 1,4-β-glycosidic linkages followed by the degradation of C–C, C–O, and C–H bonds in the cyclic glucose units.

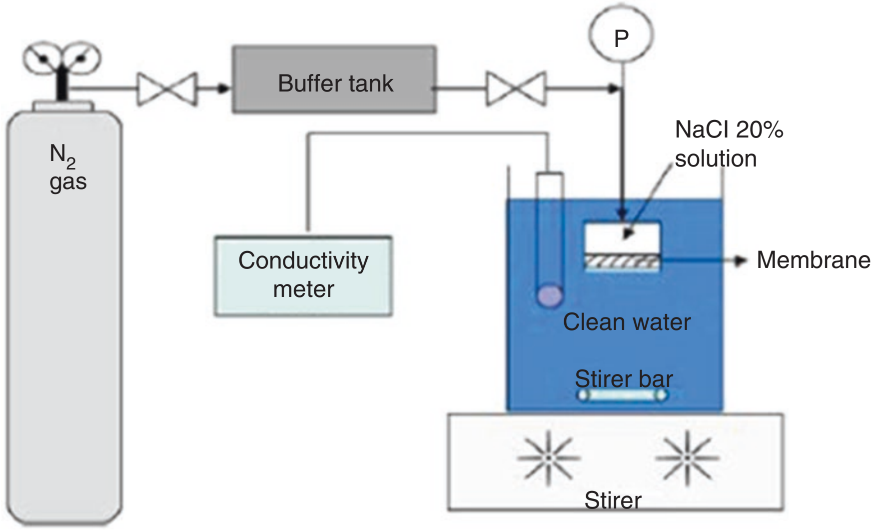

Fig. 3.18 General scheme of the LEP test apparatus

3.3.6 Liquid Entry Pressure

The liquid entry pressure (LEP) of a hydrophobic membrane is the pressure that must be applied to a dry membrane so that the liquid penetrates inside the membrane. Wetting of membrane pores by liquid streams (i.e. the loss of hydrophobic characteristics of membranes) is a crucial issue in MD treatment. The liquid entry pressure (LEP) of a liquid (mostly water), which is called wetting pressure and is sometimes faulty, is the pressure that must be applied onto deionized water before it penetrates into a dry microporous membrane. In other words, liquid entry pressure (LEP) is the minimum value of hydrostatic pressure difference at which the feed liquid penetrates into the largest pores of the membrane. LEP depends on many parameters, including the membrane maximum pore size, the surface tension of the liquid, the contact angle of the liquid on the membrane surface, and the geometrical structure of the membrane [112].

The experimental apparatus for this measurement is shown in following figure (Fig. 3.18).

3.3.7 Tensile Strength Measurement

Tensile strength is defined as the ability of a material to resist a force that tends to pull it apart. It is usually expressed as the measure of the largest force that can be applied in this way before the material breaks apart. It is an important property of an

RO membrane as it usually operates at high pressure. ASTM D882 is commonly used for testing the tensile strength of polymer films. Ginga and Sitaraman [113] discussed a new fracture testing technique that can be used to determine the tensile strength of low-strength thin films. This technique uses finite element analysis to extract the tensile strength from the experimental data.

3.3.8 *Graft Density*

RO membranes can be modified by grafting the active layer on the surface. For instance, Wagner et al. [60] measured the density of PEGDE on the membrane surface by using a Rubotherm Magnetic Suspension Balance (Rubotherm GmbH, Bochum, Germany). A diagram of the apparatus appears in Fig. 3.19.

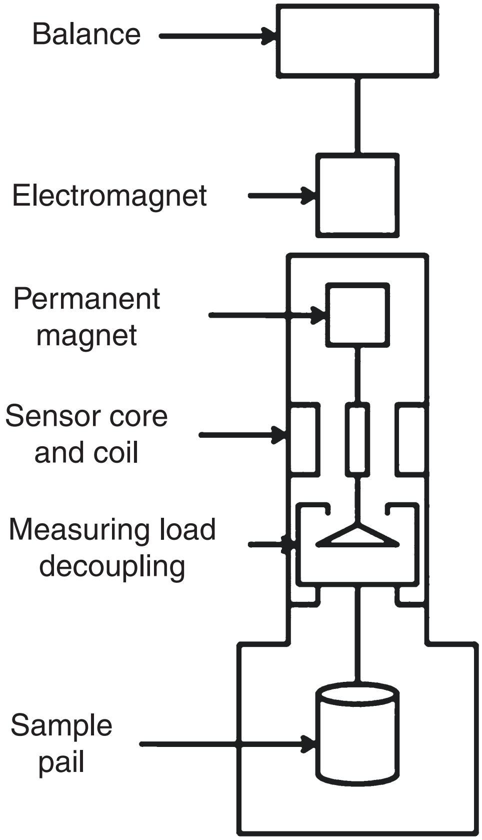

Fig. 3.19 Schematic of the magnetic suspension balance used to characterize PEGDE grafting density

3.4 Summary

In the present chapter, all methods which are used presently have been discussed. Membrane is the heart of the membrane separation processes. Characterization of membrane provides a crucial link between the preparation and performance of the membranes and their structure, chemistry, morphology, transport properties, and other characteristics, with the ultimate goal of how to make the best membrane and use it in the best way. It is an important part of membrane development. A variety of techniques and approaches are routinely used for characterizing the physical and chemical properties of membrane surfaces. For a proper characterization of membranes, the structure of the membrane should be known in relation to the performance or physical parameters that have to be described. In membrane, techniques for the characterization of membrane should be focused on the measurement of active parameters.

References

1. Khulbe KC, Feng CY, Matsuura T Membrane characterization, in desalination and water resources (DESWARE)—membrane process. In: UNESCO-EOLSS Joint Committee (ed) Encyclopedia of life support systems (EOLSS), developed under the auspices of the UNESCO, vol I. Eolss Publishers, Oxford
2. Xu H, Wan L (2009) Chapter 2. Techniques for membrane surface characterization. In: Surface engineering of polymeric membranes. Springer, pp 5–63
3. Lee E, Lee S, Hong S (2010) A new approach to the characterization of reverse osmosis membrane by dynamic hysteresis. Desalin Water Treat 18:257–263
4. Bernstein B, Kaufman Y, Freger V (2013) Membrane characterization. In: Membrane materials, characterization, and module design. Encyclopedia of membrane science and technology. Wiley, Hoboken
5. Tylkowski B, Tsibranska I (2015) Overview of main techniques used for membrane characterization. J Chem Technol Metallur 50(1):3–12
6. Ismail AF, Khulbe KC, Matsuura T (2015) Gas separation membranes: polymeric and inorganic. Springer, Basel
7. Electron Microscopy (2019) The latest electron microscopy news from across the AZoNetwork
8. Shirazi MMA, Kargari A, Ramakrishna S, Doyle J, Rajendrian M, Babu PR (2017) Electrospun membranes for desalination and water/wastewater treatment: a comprehensive review. JMSR 3:209–227
9. Giorno L (2015) Membrane morphology. In: Drioli E, Giorno L (eds) Encyclopedia of membranes. Springer, Berlin
10. Mulder M (1996) Basic principles of membrane technology. Kluwer, Dordrecht, pp 162–163
11. Agboola O, Maree J, Mbaya R (2014) Characterization and performance of nanofiltration membranes. Environ Chem Lett 12(2):241–255
12. Chen W, Chen S, Liang T, Zhang Q, Fan Z, Yin H, Huang KW, Zhang X, Lai Z, Sheng P (2018) High flux water desalination with interfacial salt sieving effect in nanoporous carbon composite membranes. Nat Nanotechnol 13:345–350
13. Li L, Xu R, Song C, Zhang B, Liu Q, Wang T (2018) A review on the progress in nanoparticle/c hybrid CMS membranes for gas separation. Membranes (Basel) 8:134

14. Inukai S, Cruz-Silva R, Ortiz-Medina J, Morelos-Gomez A, Takeuchi K, Hayashi T, Tanioka A, Araki T, Tejima S, Noguchi T, Terrones M, Endo M (2015) High-performance multi-functional reverse osmosis membranes obtained by carbon nanotube polyamide nanocomposite. Sci Rep 5:13562
15. Chung YT, Mahmoudi E, Mohammad AW, Benamor A, Johnson D, Hilal N (2017) Development of polysulfone-nanohybrid membranes using ZnO-GO composite for enhanced antifouling and antibacterial control. Desalin 402:123–132
16. Hoves DB, Heuer AH (2010) The use of laser scanning confocal microscopy (LSCM) in materials science. J Microsc 240(3):173–180
17. Pawley JB (2006) Handbook of biological confocal Microscopy, 3rd edn. Springer, Berlin. isbn:0-387-25921-X
18. Minsky M (1961) Microscopy apparatus. US3013467A
19. Minsky M (1988) Memoir on inventing the confocal scanning microscope. Scanning 10:128–138
20. Charcosset C, Cherfi A, Bernengo JC (2000) Characterization of microporous membrane morphology using confocal scanning laser microscopy. Chem Eng Sci 55(22):5351–5358
21. Lin YM, Song C, Rutledge G (2019) Direct three-dimensional visualization of membrane fouling by confocal laser scanning microscopy. ACS Appl Mater Interface Sci 11:17001–17008
22. Oura K, Lifshits V, Saranin A, Zotov A, Katayama M (2010) Surface science: an introduction. Springer, Berlin
23. Bartels CR (1989) A surface science investigation of composite membranes. J Membr Sci 45(3):225–245
24. Coronell O, González MI, Mariñas BJ, Cahill DG (2010) Ionization behavior, stoichiometry of association, and accessibility of functional groups in the active layers of reverse osmosis and nanofiltration membranes. Environ Sci Technol 44:6808–6814
25. Zhang X, Cahill DG, Coronell O, Mariñas BJ (2007) Partitioning of salt ions in FT30 reverse osmosis membranes. Appl Phys Lett 91:181904–181904
26. Gidley DW, Peng HG, Vallery RS (2006) Positron annihilation as a method to characterize porous materials. Annu Rev Mater Res 36:49–79
27. Rathore V (2016) Positron annihilation spectroscopy: a review of applications in nanomaterials thin films and semiconductors. Int J Theor Appl Sci 8(1):151–155
28. Fong C, Dong AW, Hill AJ, Boyd BJ, Drummond CJ (2015) Positron annihilation lifetime spectroscopy (PALS): a probe for molecular organisation in self-assembled biomimetic systems. Phys Chem Chem Phys 17:17527–17540
29. Kim SH, Kwak SY, Suzuki T (2005) Positron annihilation spectroscopic evidence to demonstrate the flux-enhancement mechanism in morphology-controlled thin film-composite (TFC) membrane. Environ Sci Technol 39(6):1764–1770
30. Tung KL, Jean YC, Nanda D, Lee KR, Hung WS, Lo CH, Lai JY (2009) Characterization of multilayer nanofiltration membranes using positron annihilation spectroscopy. J Membr Sci 343(1–2):147–156
31. Jiang X, Li S, Shao L (2017) Pushing CO_2-philic membrane performance to the limit by designing semi-interpenetrating networks (SIPN) for sustainable CO_2 separations. Energy Environ Sci 10:1339–1344
32. Song Q, Nataraj SK, Roussenova MV, Tan JC, Hughes DJ, Li W, Bourgoin P, Alam MA, Cheetham AK, Al-Muhtase SA, Sivaniah E (2012) Zeolitic imidazolate framework (ZIF-8) based polymer nanocomposite membranes for gas separation. Energy Environ Sci 5:8359–8369
33. Wolińska-Grabczyk A, Kubica P, Jankowski A, Wójtowicz M, Kansy J, Wojtyniak M (2017) Gas and water vapor transport properties of mixed matrix membranes containing 13X zeolite. J Membr Sci 526:334–347
34. Yin HH, Yin Z, Ma W, Zhu D (2005) A review of studies of polymeric membranes by positron annihilation lifetime spectroscopy. Plasma Sci Technol 7:3062–3064

35. Bushell AF, Attfield MP, Mason CR, Budd PM, Yampolskii Y, Starannikova L, Rebrov A, Bazzarelli F, Bernardo P, Jansen JC (2013) Gas permeation parameters of mixed matrix membranes based on the polymer of intrinsic microporosity PIM-1 and the zeolitic imidazolate framework ZIF-8. J Membr Sci 427:48–62
36. Jeazet HBT, Koschine T, Staudt C, Raetzke K, Janiak C (2013) Correlation of gas permeability in a metal-organic framework mil-101(cr)–polysulfone mixed-matrix membrane with free volume measurements by positron annihilation lifetime spectroscopy (pals). Membranes 3(4):331–353
37. Thür R, Velthoven NV, Slootmaekers S, Didden J, Verbeke R, Smolders S, Dickmann M, Egger W, Vos DD, Vankelecom IFJ (2019) Bipyridine-based UiO-67 as novel filler in mixed-matrix membranes for CO_2-selective gas separation. J Membr Sci 576:78–87
38. Shen Q, Cong S, He R, Wang ZJY, Li H, Cao X, Wang J, der Bruggen BV, Zhang Y (2019) SIFSIX-3-Zn/PIM-1 mixed matrix membranes with enhanced permeability for propylene/propane separation. J Membr Sci 588:117–201
39. Singh PS, Aswal VK (2013) SANS study on nanostructure of thin-film-composite membrane for desalination and water purification. Neutron Scattering Society of India 1:24–28
40. Dahdal YN, Pipich V, Rapaport H, Oren Y, Kasher R, Schwahn D (2014) Smallangle neutron scattering studies of mineralization on BSA coated citrate capped gold nanoparticles used as a model surface for membrane scaling in RO wastewater desalination. Langmuir 30(50):15072–15082
41. Schoenborn BP (1976) Neutron scattering for the analysis of membranes. Biochim Biophys Acta 457:41–55
42. Odom B, Hanneke D, D'Urso B, Gabrielse G (2006) New measurement of the electron magnetic moment using a one-electron quantum cyclotron. Phys Rev Lett 97(3):030801
43. Khulbe KC, Matsuura T, Lamarch G, Lamarch AM, Choi C, Noh SH (2001) Study of the structure of asymmetric cellulose acetate membranes for reverse osmosis using electron spin resonance (ESR) method. Polymer 42:6479–6484
44. Khulbe KC, Feng C, Matsuura T, Lamarche G, Lamarche AM (2003) Study of the structure of asymmetric polyamide membranes for reverse osmosis using the electron spins resonance (ESR) method. Desalin 154:1–8
45. Borbat PP, Costa-Filho AJ, Earle KA, Moscicki JK, Freed JH (2001) Electron spin resonance in studies of membranes and proteins. Science 291(5502):266–269
46. Sahu ID, Lorigan GA (2018) Site-directed spin labeling EPR for studying membrane proteins. Biomed Res Int 2018:3248289
47. Oppenheim SF, Buettnerb GR, Dardick JS, Rod VGJ (1994) Applying electron paramagnetic resonance spectroscopy to the study of fouling in protein ultrafiltration. J Membr Sci 95:289–297
48. Tamlin M (2010) Growth dynamics, charge density, and structure of polyamide thin-film composite membranes. Ph.D. Thesis, University of Illinois at Urbana-Champaign
49. Akbari A, Homayonfal M, Jabbari V (2010) Synthesis and characterization of composite polysulfone membranes for desalination in nanofiltration technique. Water Sci Technol 62:2655–2663
50. Cruz-Silva R, Inukai S, Takumi A, Morelos-Gomez A, Ortiz-Medina J, Takeuchi K, Hayashi T, Tanioka A, Tejima S, Noguchi T, Terrones M, Endo M (2016) High performance and chlorine resistant carbon nanotube/aromatic polyamide reverse osmosis nanocomposite membrane. MRS Adv 1(20):1469–1476
51. Harris DC (2006) Quantitative chemical analysis. W. H. Freeman and Co., New York
52. Ausilia A, Sánchez M, Gómez-Fernández JC (2015) Attenuated total reflectance infrared spectroscopy: a powerful method for the simultaneous study of structure and spatial orientation of lipids and membrane proteins. Biomed Spectrosc Imaging 4:159–170
53. Abdullah N, Yusof N, Gohari RJ, Ismail AF, Jafar J, Lau WJ, Misdan NH, Hairom NHH (2018) Characterizations of polysulfone/ferrihydrite mixed matrix membranes for water/wastewater treatment. Water Environ Res 90(1):64–73

54. Xu M, Fujita D, Gao J, Hanagata N (2010) Auger electron spectroscopy: a rational method for determining thickness of graphene films. ACS Nano 4(5):2937–2945
55. Sutter P, Sutter E (2014) Thickness determination of few-layer hexagonal boron nitride films by scanning electron microscopy and Auger electron spectroscopy. APL Mater 2:092502. https://doi.org/10.1063/1.4889815
56. Sharif A (2011) Material development and characterization for high salinity water after desalination by membrane distillation at high temperature and pressure. M.Sc. Thesis, University of Illinois at Urbana-Champaign
57. Pan Y, Li M, Hoek EMV (2011) Preparation and characterization of membranes formed by nonsolvent induced phase separation: a review. Ind Eng Chem Res 50(7):3798–3817
58. Yuso MDVM, Díaz AA, Bijani S, Romero V, Benavente J, Rodríguez-Castellón E (2014) Chemical surface, thermal and electrical characterization of nafion membranes doped with IL-cations. Appl Sci 4(2):195–206. https://doi.org/10.3390/app4020195
59. Wagner EMV, Sagle AC, Sharma MM, La YH, Freeman BD (2011) Surface modification of commercial polyamide desalination membranes using poly(ethylene glycol) diglycidyl ether to enhance membrane fouling resistance. J Membr Sci 367:273–287
60. Beverly S, Seal S, Hong S (2000) Identification of surface chemical functional groups correlated to failure of reverse osmosis polymeric membranes. J Vacuum Sci Technol A 18:1107. https://doi.org/10.1116/1.582308
61. Wolverson D (2013) Characterization of semiconductor heterostructures and nanostructures. 2nd edn.
62. Syed A, Smith EA (2017) Raman imaging in cell membranes, lipid-rich organelles, and lipid bilayers. Annu Rev Anal Chem (Palo Alto, Calif) 10(1):271–291
63. Fogarty SW, Patel LI, Martin FL, Fullwood NJ (2014) Surface-enhanced Raman spectroscopy of the endothelial cell membrane. PLoS One 9(9):e106283
64. Sun M (2017) Chapter 6. High-vacuum tip-enhanced Raman spectroscopy in spectroscopic methods for nanomaterials characterization (micro and nano technologies). Elsevier, pp 129–140
65. John N, George S (2017) Chapter 5. Raman spectroscopy. In: Spectroscopic (micro and nano technologies). Elsevier, pp 95–127
66. Goldstein J (2003) Scanning electron microscopy and X-ray microanalysis. 3rd edn. Springer. isbn: 978-0-306-47202-3
67. Tompkins H, Irene EA, Andrew W (2005) Ellipsometry science nanoscience. In: Norwich NY (eds) William Andrew Pub, Heidelberg. isbn: 978-0-8155-1747-4
68. Ogieglo W, Wormeester H, Wessling M, Benes NE (2012) Spectroscopic ellipsometry analysis of a thin film composite membrane consisting of polysulfone on a porous α-alumina support. ACS Appl Mater Interfaces 42:35–943
69. Jaiswal J, Mourya S, Malik G, Chandra R (2018) Tunable optical properties of plasmonic Au/Al_2O_3 nanocomposite thin films analyzed by spectroscopic ellipsometry accounting surface characteristics. J Optical Soc Am A 35(5):740–747
70. Clegg RM (1995) Fluorescence resonance energy transfer. Curr Opin Biotechnol 6:103–110
71. Bagatolli LA (2009) Membranes and fluorescence microscopy. In: Geddes CD (ed) Reviews in fluorescence. Springer Science+Business Media, LLC, Berlin, pp 33–51
72. Tamime R, Wyart Y, Siozade L, Baudin I, Deumie C, Glucina K, Moulin P (2011) Membrane characterization by microscopic and scattering methods: multiscale structure. Membranes (Basel) 1(2):91–97
73. Hoult DI, Bhakar B (1997) NMR signal reception: virtual photons and coherent spontaneous emission. Concepts Magn Reson 9:277–297
74. Kong X (2010) Characterization of proton exchange membrane materials for fuel cells by solid state nuclear magnetic resonance. Ph.D. Thesis, Iowa State University Ames, Iowa
75. Glaves C, Smith CD (1989) Membrane pore structure analysis via NMR spin-lattice relaxation experiments. J Membr Sci 46:167–184
76. Schmid T, Helmbrecht C, Panne U, Haisch C, Neissner R (2003) Process analysis of biofilms by photoacoustic spectroscopy. Anal Bioanal Chem 375:1124–1129

77. Duke MC, O'Brien-Abraham J, Milne N, Zhua B, Lin JYS, da Costa JCD (2009) Seawater desalination performance of MFI type membranes made by secondary growth. Sep Purif Technol 68:343–350
78. von der Schulenburg DAG, Vrouwenvelder JS, Creber SA, van Loosdrecht MCM, Johns ML (2008) Nuclear magnetic resonance microscopy studies of membrane biofouling. J Membr Sci 323:37–44
79. Fridjonsson EO, Vogt SJ, Vrouwenvelder JS, Johns ML (2015) Early non destructive biofouling detection in spiral wound RO membranes using a mobile earth's field NMR. J Membr Sci 489:227–236
80. Ball DW (2006) Photoacoustic spectroscopy. Spectroscopy 21(9):14–16
81. Flemming HC (2002) Biofouling in water systems, cases, causes and countermeasures. Appl Microbiol Biotechnol 59(6):629–640
82. IUPAC. (1997) Compendium of chemical terminology. In: McNaught AD, Wilkinson A (eds) Blackwell Scientific Publications, Oxford. isbn: 0-9678550-9-8. https://doi.org/10.1351/goldbook
83. Li N, Zheng J, Hadi P, Yang M, Huang X, Ma H, Walker HW, Hsiao BS (2019) Synthesis and characterization of a high flux nanocellulose–cellulose acetate nanocomposite membrane. Membranes 9(6):70
84. Van Wagner EM, Freeman BD, Sharma MM, Michael A, Hickner MA, Altman SJ (2010) Polyamide desalination membrane characterization and surface modification to enhance fouling resistance. Sandia Report SAND2010-5540, Printed August 2010
85. Hebbar RS, Isloor AM, Ismail AF (2017) Chapter 12—Contact angle measurements. In: Membrane characterization, pp 219–255
86. Baek Y, Kang J, Theato P, Yoon J (2012) Measuring hydrophilicity of RO membranes by contact angles via sessile drop and captive bubble method: a comparative study. Desalin 303:23–28
87. Simon A 1998 Grazing angle microscope. US6008936A
88. Gaillard F, Linossier I, Sweeney M, Reffner JA, Romand M (1999) Grazing-angle micro-FTIR spectroscopy(GAM-FTIR): applications to adhesion studies. Surf Interface Anal 27:865–870
89. Smith BC (1995) Fundamentals of fourier transform infrared spectroscopy. In: Ulman A (ed) Characterization of organic thin films, materials characterization series. Press LLC, Butterworth-Heinemann, Stoneham
90. Hoffard TA (2003) Grazing-angle fourier transform infrared spectroscopy for surface cleanliness, Technical ReportTR-2217-SHR, Naval facilities engineering service center Port Hueneme, California 93043-4370
91. Greenler RG (1966) Infrared study of adsorbed molecules on metal surfaces by reflection techniques. J Chem Phys 44(1):310
92. Thin film characterization through grazing angle ft-ir microscope. The latest thin film news from across the AZoNetwork March 1, 2019
93. Liang J (1995) Boundary lubrication thin film study by grazing-angle-microscope/ftir spectroscopy. http://hdl.handle.net/1811/29656, View open: 1995-RG-13.jpg (64.29Kb)
94. Eng F (1989) Proceedings volume 1145, 7th Intl Conf on Fourier transform spectroscopy, 1989, Fairfax, VA, United States; https://doi.org/10.1117/12.969474
95. Dunphy DR, Alam TM, Tate MP, Hillhouse HW, Smarsly B, Collord AD, Carnes E, Baca HK, Köhn R, Sprung M, Wang J, Brinker CJ (2009) Characterization of lipid-templated silica and hybrid thin film mesophases by grazing incidence small-angle X-ray scattering. Langmuir 25(16):9500–9509
96. Zhang R, Huang H, Sun C, Xiaozhen L, Bentian X, Wang Z (2019) Study on ultrasonic techniques for enhancing the separation process of membrane. Ultrason Sonochem 55:341–347
97. Massignan JPD, Nishida MY, Daciuk RJ, Neves Jr F, de Almeida F, de Carvalho RDM (2007) Medição da fração de vazios em escoamentos bifásicos. 4o PDPETRO, Campinas, SP 2.3.0065-1 - 1 21-24 de Outubro de 2007

98. Kujundzic E, Greenberg AR, Peterson M (2014) Review: ultrasonic characterization of membranes. Desalin Water Treat 52:1217–1249
99. Bourbie T, Coussy O, Zinszner B (1987) Acoustics in porous media. Technip, Paris
100. Safarpour M, Orooji Y, Vatanpour V (2019) A review on the applications of ultrasonic technology in membrane bioreactors. Ultrason Sonochem 58:10463
101. Krantz WB, Greenberg AR (2008) Membrane characterization by ultrasonic time-domain reflectometry. In: Li N, .Fane AG, Ho WS, Matsuura T (eds.) Advanced membrane technology and application, Wiley, Hoboken; ISBN: 978-0-471-73167-2
102. Kyllönen HM, Pirkonen P, Nyström M (2005) Membrane filtration enhanced by ultrasound: a review. Desalin 181(1–3):319–335
103. Ramaswamy S, Greenberg AR, Peterson ML (2004) Non-invasive measurement of membrane morphology via UFDR: pore-size characterization. J Membr Sci 239:143-154
104. Lucas CS, Baroni DB, Costa AMLM, Bittencourt MSQ (2009) Analysis of ultrasonic techniques for the characterization of microfiltration polymeric membranes. International Nuclear Atlantic Conference—INAC 2009 Rio de Janeiro, RJ, Brazil, September 27 to October 2, 2009 ASSOCIAÇÃO BRASILEIRA DE ENERGIA NUCLEAR—ABEN
105. Loest G, Brewster J, Greenberg AR, Bond L, Krantz WB (1994) Real-time noninvasive measurement of membrane compaction and fouling, 6th annual meeting of the North American membrane society, Breckenridge Colorado, May 1994
106. Kujundzic E, Greenberg AR, Peterson M (2014) A review ultrasonic characterization of membranes. Desalin Water Treat 52:1217–1249
107. Bentama J, El Ghzizal A, Ferrandis JY (2007) Ultrasonic waves for characterization of clay membranes. Desalin 206:1–8
108. Álvarez-Arenas TEG, Apel PY, Orelovich OL (2007) Characterization of ion-track membranes by non-contact ultrasonic magnitude and phase spectroscopy. J Membr Sci 301(1–2):210–220
109. Coats AW, Redfern JP (1963) Thermogravimetric analysis: a review. Analyst 88(1053):906–924
110. Loganathan S, Mishra RK, Babu VR, Pugazhenthi G, Thomas S (2017) Thermogravimetry analysis for characterization of nanomaterials. In: Thomas S, Thomas R, Zachariah A, Mishra R (eds), Thermal and rheological measurement techniques for nanomaterials characterization. Elsevier. https://doi.org/10.1016/B978-0-323-46139-9.12001-8
111. Macevele LE, Moganedi KLM, Magadzu T (2007) Investigation of antibacterial and fouling resistance of silver and multi-walled carbon nanotubes doped poly(vinylidene fluoride-co-hexafluoropropylene) composite membrane. Membranes 7(3):35
112. Rezaei M, Warsinger DV, Lienhard JH, Duke M, Matsuura T, Samhaber WM (2018) Wetting phenomenon in membrane distillation: mechanisms, reversal, and prevention. Water Res 139:329–352
113. Ginga NJ, Sitaram SK (2011) New method to measure tensile strength of low modulus thin films. Int J Fract 170:199–206

Chapter 4
Membrane Modification

4.1 Introduction

Membranes have become a fascinating domain of present day separation science technology and environmental care because of their inter disciplinary nature and a wide range of application areas. Membrane surface properties critically affect membrane performance as it is the membrane surface that contacts the feed. Surface modification of membranes has become a key issue in membrane science and technology. The aim of modification may have different aspects: e.g. narrow pore size distribution in the membrane top layer, increasing hydrophilicity, decreasing or increasing roughness, and fouling mitigation. Different types of surface modifying agents have been used to alter the membrane surface by covalent bonding that links the necessary chemical moieties by carboxylation, sulfonation, amination, and epoxidation. Khulbe et al. [1] wrote a review on surface modification of synthetic membrane, used in different fields (RO, UF, NF, GS, biomedical applications, etc.); especially the report covers the communications on this subject made after the year 2000. In the review Khulbe et al. [1] discussed the new techniques, particularly by plasma treatment (organic and inorganic), grafting of polymers on the membrane, blending different types of polymers, adding functional groups to the surface by exposing to UV or by other methods (irradiation), heat treatment, chemical treatment, ion implantation, dip coating etc. for the surface modification of synthetic polymeric membranes. The hydrophobicity or hydrophilicity of UF, NF, and MF membrane surfaces can be tailored by using surface-modifying macromolecules (SMMs). More attention has been given to SMMs, graft polymerization and different types of plasma treatment for surface modification of synthetic membranes. All kinds of modifications of membranes can help to improve surface polarity, reduce contact angle, and increase surface energy. Membranes containing surface-modification macromolecules generally showed improved flux when filtering river water or oil/water emulsions [2]. Thus, membrane modification is one of the most

K. C. Khulbe, T. Matsuura, *Nanotechnology in Membrane Processes*, Lecture Notes in Nanoscale Science and Technology 29,
https://doi.org/10.1007/978-3-030-64183-2_4

commonly used procedures for producing favourable properties in membranes. Modifications can be performed during membrane fabrication or after preparation (post modification).Various modification techniques are mentioned, including the use of additives, chemical treatments, grafting components, and coatings. Each of these methods has its merits and demerits [3].

The major aim of surface modification is improving the performance of the membranes with a view to altering a wide range of characteristics of the surface, such as roughness, surface energy, surface charge, hydrophilicity, biocompatibility, and functionality. Based on these characteristics, the modification methods can be divided into two groups.

1. physical modification (thermal treatment, solvent post-treatment, blending, coating and vapor deposition).
2. chemical modification (chemical procedures, plasma treatment, ultraviolet induced grafting, ozone treatment, high energy radiation, and enzymatic treatment).

From modified membranes, interesting results in the form of improved properties can be obtained. The modified membranes open a new avenue for the development of membrane technology. Properties of membrane surface and the feed critically affect membrane performance. The quest for developing membranes with excellent properties i.e. desirable results is on-going and many approaches have been attempted to synthesize robust membranes suitable for different applications. Some of the methods adopted to create enhanced properties include variation of functional groups, combination of polymers, adjustment of cross-link density, inclusion of additives and surface modification. In general, the main culprits are fouling or adsorption of undesirable species onto the membrane surface that affects membrane properties and leads to compromised performance. Many reviews on the surface modification are available in the literature [1–7].

4.2 Modification Methods

Modification refers to those processes which allow incorporation of different functionalities for altering the chemical structure and properties of the pristine mat. Different techniques were used to modify polymeric membranes, such as photo-irradiation, surface plasma irradiation, blending with suitable polymers, atomic layer deposition, chemical cross-linking, surfactants, nanoparticulates, additions to polymer casting, and so on. Nanocomposites are a composite in which at least one dimension of the dispersed phase (filler) is in the nanometer range. Nanoparticles, especially the hydrophilic types, are demonstrated to have great potential in improving the organic–inorganic nanocomposite membrane performance in terms of flux, rejection, antifouling characteristics, and thermal, mechanical, and chemical stability [8].

4.2.1 Modifications Pre Membrane Fabrication

4.2.1.1 Blending

Depending upon the mode of application, a wide variety of foreign materials has been incorporated into membranes preparation solution for improving its functional properties. These materials can be metal or metal oxide nanoparticles, enzymes, carbon nanotubes, biomolecules, super molecules, dendrimers, surfactants, functional alkyls and polymers. The blending of high polymer materials means that two or more kinds of high polymer materials blend to generate a new kind of material, which has a comprehensive characterization of original materials as well as new outstanding properties that can overcome their respective defects. Yu et al. [9] reported the performances of organic–inorganic polyvinylidene fluoride (PVDF)–titanium dioxide (TiO_2) composite hollow fiber ultrafiltration (UF) membranes, prepared by TiO_2 sol–gel method and blending method, respectively. It was reported that PVDF–TiO_2 composite UF membranes exhibited significant differences in surface properties and intrinsic properties because of the addition of inorganic particles. The TiO_2 particles improved the membrane strength and thermal stability of PVDF–TiO_2 composite UF membranes. In particular, hydrophilicity and permeability increased dramatically with the increase of TiO_2, whereas the retention property of UF membranes was nearly unchanged.

The addition of hydrophilic materials to the dope solution increases the water permeability of a membrane with similar pore size and pore distribution, owing to an increase in pore density as well as in the hydrophilicity of the membrane surface and inside the pores. Surface modification may be achieved by incorporating a surface-modifying additive (e.g. a hydrophilic component) into the membrane-casting solution before membrane formation. The hyrophobicity or hydrophilicity of the UF, NF, and MF membrane surfaces can be tailored by using SMMs. Blending of surface-modifying macromolecules (SMMs) into a base polymer solution is an attractive method. If such a polymer mixture is equilibrated in air, then the polymer with lower surface energy will migrate at the air interface, consequently reducing the interfacial tension without affecting the bulk properties of the base polymer. This phenomenon is termed as surface segregation [10]. Figure 4.1 represents the schematic diagram illustrating the surface segregation process.

Blending of additives in the polymer matrix is an important approach to reduce membrane hydrophobicity and improve the performance (flux, solute rejection, and reduction of fouling). Many factors need to be considered in the overall process of composite membrane preparation, such as precise control over the functional groups, uniformity, and reproducibility. The effectiveness of hydrophilicity will depend on the location of NPs (nanoparticles) in the membrane matrix because the location of NPs can change the diffusivity in the polymer matrix. The surface energy and concentration are other important factors that can affect NPs dispersion and location [11].

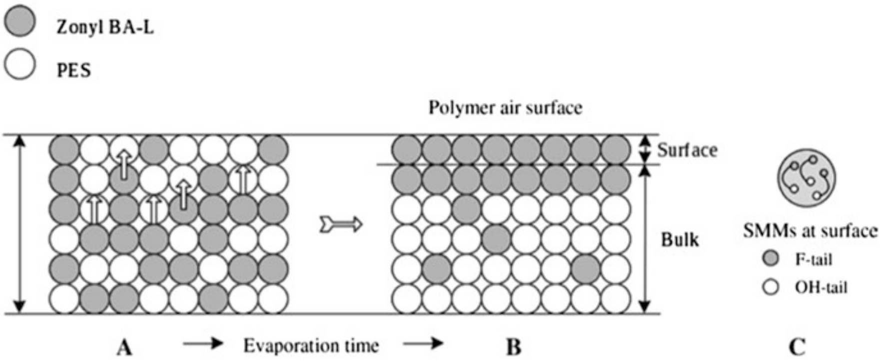

Fig. 4.1 Schematic diagram illustrating the surface segregation process (**a**) membrane before segregation, (**b**) membrane after segregation (**c**) surface modifying macromolecule [10]

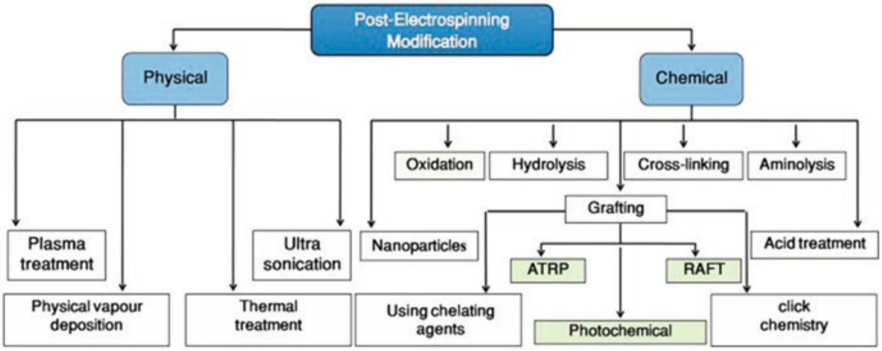

Fig. 4.2 Schematic categorization of post-modification techniques of electrospun membranes [12]

4.2.2 *Post-treatment*

The electrospinning to produce smooth and continuous nanofibers is an art. Modification of bulk and surface properties of electrospun membranes are considered as an effective strategy to design novel synthetic materials with improved properties. Electrospinning strategy with a single polymer matrix is unable to offer sufficient surface active sites for specific applications. Modification refers to those processes which allow incorporation of different functionalities for altering the chemical structure and properties of the pristine mat. Sagitha et al. [12] discussed the categories of possible modification strategies for improving the properties of electrospun membranes and its applications. Electrospun polymeric membranes can be functionalized either by pre or post electrospinning treatments. Various strategies under each category are schematically illustrated in Fig. 4.2.

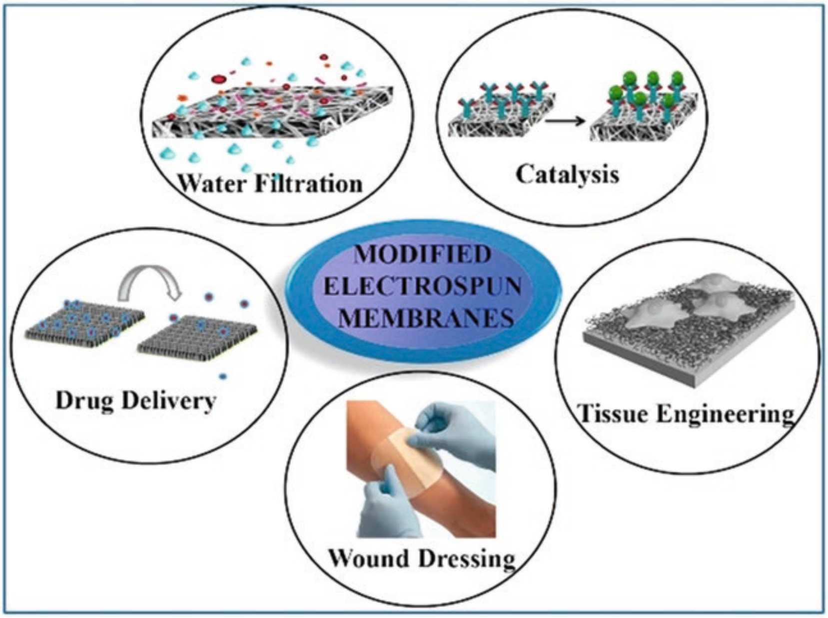

Fig. 4.3 Applications of modified electrospun membrane [12]

Figure 4.3 shows applications of modified electrospun membrane (Fig. 4.3) in environmental monitoring and health care. It has opened a new avenue for the researchers.

The combined benefits of modified hybrid inorganic-organic polymer nanofibers offer appreciable biocompatibility, wettability, nontoxicity, stability, biodegradability, cellular adhesion and mechanical strength [13]. In addition to this, the modified nanofibers explored their efficiency in many other fields such as catalysis, biosensors, solar cells and protective clothing materials [12, 13].

4.2.2.1 Physical Methods

Thermal Treatment

Heat treatment is usually carried out at temperature between the glass transition temperature (T_g) and melting temperature of the material. For electrospun fibers, these temperatures may be different from bulk material due to difference in the crystallinity and molecular orientation following the electrospinning process [8]. Heat treatment can be used to improve several properties of membrane including electrospun membranes. Some of the advantages of heat treatment are [14]:

1. Improve membrane compactness (eliminate ‘fluffiness’ or stray fibers).
2. Improve mechanical property.

3. Improve chemical stability.
4. Reduce intra-membrane layer delamination.

The heat treatment configuration may be varied as follows,

1. No force application on the membrane during treatment.
2. Membrane perimeters restrained during treatment.
3. Treatment under pressure (Hot pressing).

The first reported membrane modification method involved annealing of porous membranes by heat-treatment. Zsigmondy and Bachmann demonstrated that the pore size of a pre-formed nitrocellulose membrane could be decreased with a hot water or steam treatment [15]. Loeb and Sourirajan [16] used the same method to improve the salt rejection of integrally-skinned asymmetric cellulose acetate reverse osmosis membranes. The properties of gas separation membranes can also be improved by annealing with a heat-treatment, as shown by Kusuki et al. [17] and Hoehn [18]. Zhang et al. [19] studied the effects of heating time, temperature, and heating method during heat treatment on the morphology, mechanical properties, and chemical stability of PSf (polysulfone) electrospun membrane. After tension heating, dimensional stability, appearance, integrity, and mechanical properties improved; chemical stability in the alcohol solution increased greatly, but the membrane shrank quickly in the acetone solution.

Fujioka et al. [20] heated a polyamide reverse osmosis (RO) membrane ESPA2 by immersing the membrane samples in Milli-Q water at 70 °C for a specific duration. The heat treated membrane reduced the pure water permeability but improved the separation efficiency and fouling resistance. Further, the membrane surface characteristics (i.e. zeta potential, hydrophobicity, chemistry and roughness) were not significantly affected by heat treatment. Wang et al. [21] reported that the equivalent/apparent pore size, porosity and fiber diameter of electrospun PAN nanofibers were significant impacted, which was directly related to microfiltration performance. Further, the facile hot-pressing method has been proven to be very effective to reduce the porosity and to improve the rejection fraction of electrospun nanofiber membranes. Ma et al. [22] fabricated PSU membrane by electrospinning, and then the PSU fiber mesh was heated at 188 °C for 6 h to significantly improve the mechanical strength of the fiber mesh, and the adhesion between fibers was enhanced obviously without destroying in fiber structure, moreover, integrity and mechanical property of the treated membrane was improved greatly. Le et al. [23] synthesized a novel polyimide, copoly(1,5- naphthalene/3,5-benzoic acid-2,2′-bis(3,4-dicarboxyphenyl) hexafluoropropanedimide (6FDA-NDA/DABA), and modified it via thermal treatment. Thermal treatment at high temperature (425 °C) facilitated the decarboxylation-induced cross-linking, therefore restricting the membrane swelling, creating a higher *d*-space among polymer chains, and contributing to high permeation fluxes and comparable separation factors of the resultant membranes for ethanol dehydration.

Thermal annealing is known as an easy and economical post-treatment method for regulating polymer molecular chains to efficiently package denser morphology because thermoplastic polymer membranes can be softened by heating without irreversible changes in the material. Kusworo et al. [24] modified nano hybrid PES-nano ZnO membranes via thermal treatment to improve their performances and stability. The introduction of ZnO nanoparticles combined with surface modification significantly improved the structural and morphological properties as well as the perm-selectivity performance. Membrane selectivity reached 87% for COD rejection, however the average flux value decreased to 2.42 $L.m^{-2}.h^{-1}$ with the increasing of thermal annealing time. Li et al. [25] studied the effect of annealing treatment on electrospun poly (lactic acid) (PLA) membrane's structure, porosity, hydrophobicity and mechanical properties. The annealing time and temperature were varied from 30 to 120 min and from 90 to 105 °C, respectively. When either annealing time or temperature was increased, membrane shrinkage, fiber thickening and fusion were observed, which resulted in pore size reduction from 2.8 to 0.9 μm, along with a reduced porosity. On the other hand, annealing resulted in an increase in the membrane's mechanical strength and Young's modulus (2500 %), the contact angle of the membrane was also affected by the annealing process. Shintani et al. [26] investigated the performance of a heat treated reverse osmosis polyamide membrane with high resistance to chlorine. The polyamide barrier layer on the top surface was prepared from N,N′-dimethyl-m-phenylene-diamine (N,N′-DMMPD). and a mixture of isophthaloyl dichloride (IPC) and 1,3,5-benzenetricarbonyl trichloride (TMC). The polyamide barrier layer on the top surface was prepared from N,N′-DMMPD and a mixture of TMC and IPC. The monomer structures and the polymerization scheme are shown in Fig. 4.4.

The newly prepared polyamide membrane showed better chlorine resistance, compared with a commercial polyamide RO membrane and also cellulose acetate RO membrane. It was revealed for the membrane that the heat treatment over 80 °C

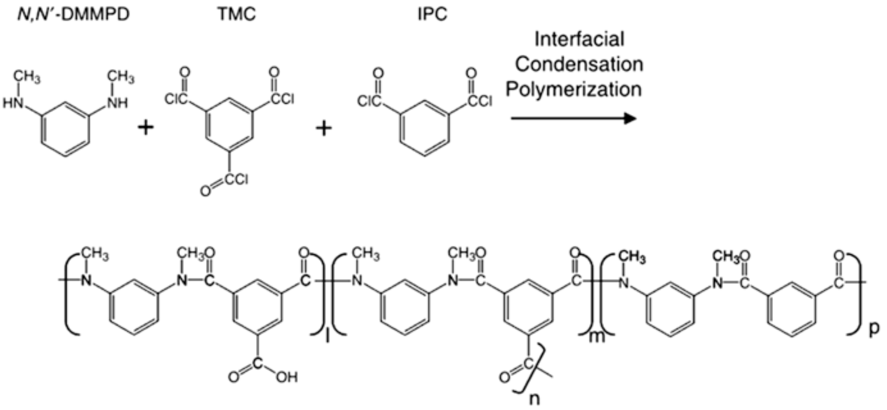

Fig. 4.4 Polymerization scheme [26]

decreased permeate flux of the RO membranes but increased their salt rejections. It was concluded by Shintani et al. [26] that a denser active skin layer was developed with the heat treatment, resulting in less solute passage and less water permeability. But they did not investigate the fouling behaviour of the membrane after heat treatment.

Vapor Deposition

The method of vapor deposition is discussed in Chap. 3. Physical vapour deposition is the general term used to represent surface coating. It represents coating of thin inorganic films over membrane surface. Vapour deposition process includes multiple steps such as heating, evaporation, sputtering of vaporized materials and deposition. Initiated chemical vapor deposition (iCVD) is a solvent-free method in which thin-film deposition of various polymers occurs on virtually any substrate. Monomers volatilization, their combination to form long chain polymers, and film deposition happen concurrently at modest vacuum and low temperature. Distinctive features of the iCVD technique include long-term stability, conformity, full functional retention, scalability, and ability to control thickness at the nanometer level [27]. Modification of electrospun membranes using tin-doped indium oxide (ITO), titanium, silver, Fe_2O_3 sputter coating techniques are also reported [12].

Polymerization

The most common technique to modify the membrane surface is IP (interfacial polymerization) reaction. Interfacial polymerization, a method to form a polyamide dense layer on the membrane surface, is typically based on 1,3,5-benzenetricarbonyl trichloride (TMC) and 1,3-phenylenediamine (MPD) reaction. Figure 4.5 shows the IP between TMC and MPD. Polymerization occurs at an interface between an aqueous solution containing one monomer and an organic solution containing a second monomer. The interfacial polymerization is a self growth polymerization.

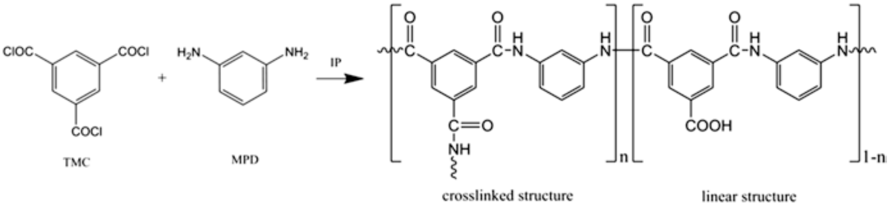

Fig. 4.5 IP between TMC and MPD

Plasma Treatment

Plasma treatment is a non-specific post-modification technique typically used for tailoring surface properties of membranes. Chemically reactive functional groups can be introduced on the membrane surface after plasma treatment. Plasma treatment mainly induces surface chemistry modifications, such as the introduction of oxygen and release of fluorine atoms that significantly changes polymer membrane wettability by a reduction of the contact angle of the polymer fibers and an over all decrease of the surface tension of the membrane [27]. Plasma treatment based surface modification is the fastest and meets environmental standards for clean technology [28, 29]. Plasma atmosphere of nitrogen, ammonia, oxygen, hydrogen, argon, helium and carbon dioxide are commonly used for surface treatments.

Zander et al. [30] fabricated PCL electrospun membrane through air plasma treatment to generate carboxyl groups for incorporating protein molecule.

Though plasma modification is clean, effective, and pollution-free, this kind of modification needs vacuum equipment which is unsuited for large-scale operation.

Ultrasonication

Sonication is the act of applying sound energy to agitate particles in a sample, for various purposes such as the extraction of multiple compounds from plants, microalgae and seaweeds. Ultrasonic frequencies (>20 kHz) are usually used, leading to the process also being known as ultrasonication or ultra-sonication. So far little work has been reported on producing individual, short micrometre-length fibres directly from electrospun membrane. Short fibres may be desirable for a number of applications, such as additives for incorporation into polymers and films to enhance properties such as modulus and toughness, whilst maintaining the transparency of the nanocomposite due to the similarity of the refractive index of the nanofibers and the matrix, including biomedical application. Sawawi et al. [31] demonstrated that, ultrasonication is the best method to scission electrospun membrane into short fibers under appropriate processing conditions. It was found that the chemical and physical properties of the short nanofibers were unaltered by the sonication process. Liposomes (liposome-lipid based vesicles) are microscopic vesicles, which can be artificially prepared as globular carriers into which active molecules can be encapsulated. These vesicles with diameters between 25 and 5000 nm are often used as drug carriers for topical purposes in the pharmaceutical and cosmetic industry, such as drug delivery, gene therapy, and immunization. Ultrasound (Ultrasonication) is a proven method of liposome preparation and the encapsulation of active agents into these vesicles [32].

4.2.2.2 Chemical Methods

Even though physical modifications are common, it is always associated with several disadvantages. Plasma treatment produces a mixture of functional groups on the membrane surface and limits its specificity. Physical vapour deposition is limited to inorganic coating over the nonwoven mat. In such cases, the attachment of active group will not be durable. Thermal treatment can cause damage to the fiber morphology at prolonged treatment. Ultrasonication has only meant to scission the fiber [12]. Chemical treatments can overcome this problem.

Chemical modification is an attractive method to impart desirable surface properties while retaining the desired bulk polymer properties such as mechanical and chemical resistance and membrane morphology. Chemical surface modification methods of gas separation membranes include treatment with fluorine, chlorine, bromine, or ozone. Typically, these treatments result in an increase in membrane selectivity coupled with a decrease in flux. Cross-linking of polymers is often applied to improve the chemical stability and selectivity of membranes for reverse osmosis, pervaporation, and gas separation applications [33]. Using recent advanced techniques (Fig. 4.6), surfaces of the membranes can be modified to obtain the desirable results.

Different types of surface modifying agents have been used which alter the membrane surface by covalent bonding that links the necessary chemical moieties by carboxylation, sulfonation, amination, and epoxidation [35]. Chemical modifications of PES membrane including blending, surface and bulk modifications are critical techniques used to diminish its biofouling effects. Surface modification to introduce hydrophilic functional groups is considered one of the most used option to enhance the hydrophilicity of PES without affecting the mechanical and thermal properties of PES backbone [7].

Grafting

‘Grafting’ is a method wherein monomers are covalently bonded (modified) onto the polymer chain, whereas in curing, the polymerization of an oligomer mixture forms a coating which adheres to the substrate by physical forces [36]. In other words, grafting is a popular technique for modifying the surface of many organic and inorganic substrates. Grafting reactions require the “activation” of polymer molecules, which can be achieved by chemical or physical methods. The chemical grafting process may create free radicals and ionic species and initiate polymerization which acts as the driving force for the attachment of the surface modifying agents. As one of the promising methods for the modification of polymeric membranes, grafting has received much attention recently. Plasma treatment and graft polymerization are the most popular techniques for surface hydrophilization.

Radiation grafting modification provides a highly advantageous means of grafting. A large concentration of free radicals is produced in the irradiated material without the use of chemical initiators. These radicals undergo reaction with a

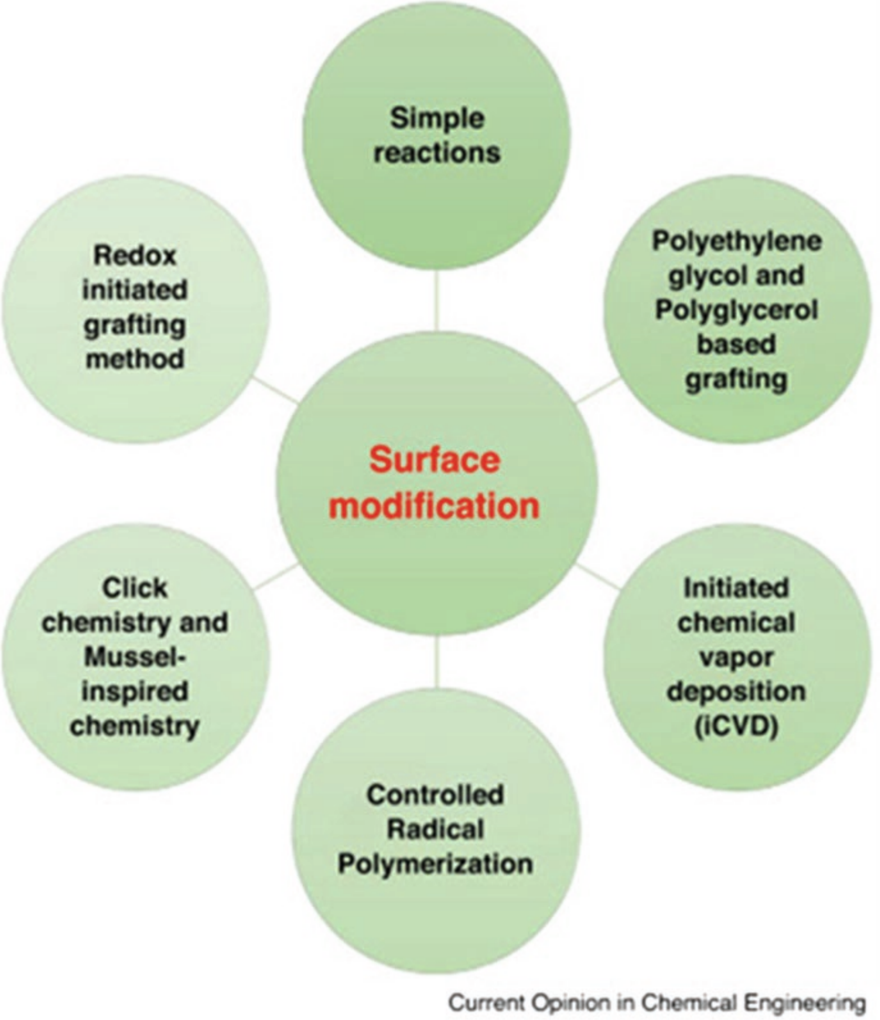

Fig. 4.6 Various strategies for chemical modification of membrane surfaces [34]

monomer of choice to produce macromolecular chains that are covalently bound to the irradiated specimen. Radiation induced grafting is based on irradiation of a base polymer by e-beam or gamma rays to create active reaction centers (mostly radicals). Then irradiated polymer is treated with vinyl monomer to produce a graft copolymer which can be sulfonated or doped to introduce proton conductivity. The high-energy radiation has strength on its high use ratio of energy and its security. However, it is too powerful to control the reaction on the surface, which easily affects its original property.

Various base polymers (in the film form) and monomer combinations have been employed for the development of membranes by radiation grafting. Nystrçmand co-workers studied the modification of PSf UF membranes by UV irradiation.

The plasma grafting modification consists of pulsed plasma, consecutive plasma, and microwave plasma, and so on. During the modification, a membrane surface will be exposed to plasma to make free radicals and graft hydrophilic monomers, thus successfully modifying the membrane. The plasma modification is clean, effective, and pollution-free, but this kind of modification needs vacuum equipment. As such, it is unsuited for large-scale operation.

Graft co-polymerization can be done by chemical treatment, photo-irradiation, high-energy radiation technique, etc. Plasma-induced graft copolymerization is an efficient, common and versatile way of introducing a selective polymeric layer on the surface of a hydrophobic membrane and is limited only to the surface. On plasma grafting on the surface, the symmetrical structure of the membrane converts to an asymmetrical structure. Due to this, selectivity of the membrane increases without increasing hydrodynamic resistance significantly [13], including separation properties. It is established that the exposure to plasma leads to changes in the chemical composition of the surface and increases the number of polar (carbonyl and carboxyl) functional groups in a thin near-surface layer of a TM (track membranes). The surface energy is also shown to grow owing to its polar component and surface reconstruction. The reconstruction consists in the growth of surface roughness owing to oxidation-reduction reactions, followed by the appearance of destructive areas. These changes promote a lyophilic behavior of the track-membrane surface [37].

Kaur et al. [38] used PVDF membrane as the base membrane for the preparation of graft polymerization for the surface modification. The membrane was placed in a glass tube containing aqueous solution of 10% (v/v) MAA monomer and tube was heated at 80 °C for 1 h to initiate the graft copolymerization. To terminate the copolymerization, the solution was exposed to air. After washing the PMAA-grafted membrane with deionized water, it was stored in 0.1 NaOH solution to remove adsorbed homopolymer or unreacted monomers. Figure 4.7 shows the summarized schematic of the plasma induced graft copolymerization method.

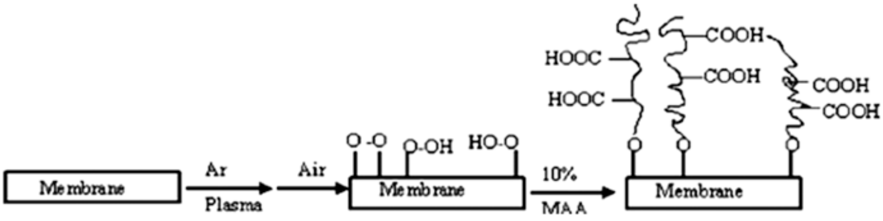

Fig. 4.7 Proposed mechanism of plasma induced graft polymerization on the surface of a membrane [38]

After grafting, the electro-spun nanofiber membrane (ENM) was transformed into a microfiltration membrane, similar in pore-size distribution with a commercial 0.45 μm hydrophilic phase inversed membrane HVLP (commercial hydrophobic PVDF membrane, Millipore, USA) but with significantly better flux. Cho et al. [39] modified electrospun PVDF nanofiber membrane by argon (Ar) plasma treatment to improve the surface hydrophilic and detection sensitivity for protein.

Various base polymers (in the film form) and monomer combinations have been employed for the development of membranes by radiation grafting. Radiation provides a highly advantageous means of grafting. A large concentration of free radicals is produced in the irradiated material without the use of chemical initiators. These radicals undergo reaction with a monomer of choice to produce macromolecular chains that are covalently bound to the irradiated specimen.

Oxidations/Ozone Treatment

Oxidation is another useful strategy to develop hydrophilic functional reactive groups on the membrane surface. The oxidation pre-treatment could improve filtration flux, lower the concentration of organic pollutants, reduce the possibility of biological contamination, while it might form the by-products (such as halide acetate and trihalomethanes), and oxidize the membrane. Ozone is a powerful oxidant that preferentially oxidizes electron rich moieties containing double carbon bonds and aromatic alcohols. It had obvious effect on modifying molecular weight distributions of organic matter. Through ozone oxidation, macromolecular organics could be oxidized into small molecules and small molecules could be oxidized into inorganic matters, which could further decrease the concentration of fouling pollutants and radically reduce membrane fouling. You et al. found that pollutants adhered to the membrane surface could be removed by ozone oxidation, so as to alleviate membrane fouling [3].

Ma et al. [40] synthesized protein functionalized electrospun cellulose acetate (CA) nanofiber affinity membrane for binding of immunoglobulin. Anari et al. [41] reported that a simple surface oxidation of Ethylenechlorotrifluoroethylene (ECTFE) membrane was found to be suitable for the processing of water production by membrane distillation. The commercial ECTFE membrane was treated with $KMnO_4$-HNO_3 mixture. Zhu et al. [42] used TiO_2-PVDF membrane modified by ozone aeration for treatment of municipal wastewater (raw water). Results suggested that the removal rate of organic matters with this new method (TiO_2-PVDF + O_3) was 66.4%, which is 13.3% higher than original membrane treated with O_3 (PVDF + O_3) under the same condition.

The combination of membrane technology and pre-treatment technologies are immature and only occur in several applications [3].

Atom Transfer Radical Polymerization (ATRP)

ATRP opens a new field for research connected to membrane's surface modification. It is a controlled/living radical polymerization (CRP) process and a new technique to modify the membrane surfaces with desirable tailored functionalities on polymer chains. However, it is in very early stage. Atom transfer radical polymerization (ATRP) is an example of a reversible-deactivation radical polymerization. Like its counterpart, ATRA, or atom transfer radical addition, ATRP is a means of forming a carbon-carbon bond with a transition metal catalyst. The polymerization from this method is called atom transfer radical addition polymerization (ATRAP). As the name implies, the atom transfer step is crucial in the reaction responsible for uniform polymer chain growth. ATRP (or transition metal-mediated living radical polymerization) was independently discovered by Kato et al. and by Matyjaszewski et al. [43, 44]. ATRP is among the most effective and most widely used methods of controlled radical polymerization (CRP). This allows easily to form polymers by putting together component parts, called monomers, in a controlled, piece-by-piece fashion. Assembling polymers in such a manner has allowed to create a wide range of polymers with site specific tailored functionalities targeting specific properties for high value applications. For example, polymers created using ATRP have been used for coatings and adhesives, and are currently under investigation for use in the medical, membrane and environmental fields. Polymers prepared by ATRP with degradable and biodegradable moieties were used for tissue engineering and drug delivery [45].

One of the advantages of ATRP is that the chain growth is controllable by stopping the polymerization after a specific time. ATRP can be carried out in bulk and in water under homogeneous and heterogeneous conditions. If high chain end functionality is required, polymerization could be stopped at partial monomer conversion and monomer is recovered. Under specific conditions, high conversion can be also attained. The range of monomers polymerizable by ATRP is constantly expanding [46].

Guo et al. [47] prepared functionally controlled nanoporous polymer samples via surface-initiated atom transfer radical polymerization (ATRP) and click chemistry. PHEMA (poly-(2-hydroxyethyl methacrylate)), PPEGMA (poly(ethyleneglycol) methacrylate) or MPEG (methoxy poly-(ethylene glycol)) in the increasing order of content of ethylene oxide units was grafted onto the surface of nanoporous PB (1,2-Polybutadiene). Guo et al. worked to broaden the spectrum of tools to create functionalized nanoporous polymers with well-defined morphologies. Werne and Patten [48] modified the surfaces of silica (SiO_2) nanoparticles with depositing a monolayer of polymerization initiators (vinyl monomers) via ATRP technique as vinyl monomers. Used these initiator-modified nanoparticles as macroinitiators, grafting was done densely on polystyrene or poly(methyl methacrylate) (MMA) layer. Thus, well-defined polymer chains were grown from the nanoparticle surfaces to yield individual particles composed of a silica core and a well-defined, densely grafted outer polystyrene or poly(methyl methacrylate) (MMA) layer. Polymerizations of styrene from smaller (75-nm-diameter) silica nanoparticles exhibited good molecular weight control, while polymerizations of MMA from the same nanoparticles exhibited good molecular weight control only when a small amount of free initiator was added to the polymerization solution. These findings provide guidance for future efforts in using ATRP for the controlled grafting of polymers from high surface area substrates (i.e., small-diameter cylinders and spheres, highly porous materials) and low surface area substrates (i.e., flat surfaces, large-diameter cylinders and spheres, low-porosity materials). Wang et al. [49] developed a novel ATRP surface modified polyacrylonitrile (PAN) electrospun membrane for removal of boric acid from aqueous solutions.

Reversible Addition-Fragmentation Chain-Transfer Polymerization (RAFT)

Reversible addition-fragmentation chain-transfer polymerization (RAFT) is another reversible-deactivation radical polymerization technique, similar to ATRP, but with more control over the polymerization. Due to it's ability to allow synthetic tailoring with block, comb, star and graft like complex structures, RAFT polymerization can be used for surface modification of electrospun membrane. Demirci et al. [50] manufactured cationic poly(VBTAC) (poly(ar-vinylbenzyl) trimethylammonium chloride)-g-CA nanofibers via combination of electrospinning and RAFT polymerization techniques with the goal of the adsorption of DNA. The DNA adsorption capacity was determined as 23.51 μg mg^{-1} from the Langmuir isotherm for poly(VBTAC)-g-CA nanofibrous web. It was concluded that poly(VBTAC)-g-CA nanofibers are useful for DNA immobilization and could open new opportunities for fabricating surface functionalized electrospun nanofibers/nanowebs and their applications in biotechnological uses. Dong et al. [51] developed molecularly imprinted membranes(MIMs) as an efficient adsorbent for the selective removal of *p*-hydroxybenzoic acid(*p*-HB) from acetylsalicylic acid (ASA, aspirin). The MIMs were grafted successfully from poly(vinylidene fluoride) microfiltration membranes *via* RAFT polymerization. Wu et al. [52] grafted polyacrylamide to the polypropylene macroporous membrane via RAFT. The protein filtration experiments showed that, in comparison with the unmodified membrane, the modified membrane can effectively reject proteins due to the densely grafted polymer chains.

Photochemical Grafting

When a chromophore on a macromolecule absorbs light, it goes to an excited state, which may dissociate into reactive free-radicals, whence the grafting process is initiated. If the absorption of light does not lead to the formation of free-radical sites through bond rupture, this process can be promoted by the addition of photosensitizers. Thus, the grafting process by a photochemical technique can proceed in two ways: with or without a sensitizer [36]. Herrera et al. [53] successfully achieved the photochemical grafting of methyl groups onto an n-type Si(1 1 1) substrate using a Grignard reagent. It was reported that the grafted surface was hydrophobic and electron affinity was lower than the bulk Si. Zhang et al. [54] studied N,;N-dimethyl-N-methacryloxyethyl-N-(3-sulfopropyl) ammonium (DMMSA) onto chitosan using cericammonium nitrate as an initiator under nitrogen atmosphere in 2% wt. acetic acid sol. The maximum percentage of grafting about 50% was obtained under optimum condition.

HSPCs are Human umbilical cord blood (UCB) hematopoietic cells that are capable of self-renew and differentiate into all mature blood cells in vivo. The possibilities of direct HSPCs transplantation treatments are limited due to their insufficient number and availability. Chua et al. [55] studied on the ability of amine functionalized electrospun polyethersulphone (PES) membranes to mediate HSPC (hematopoietic stem/progenitor cells) adhesion and proliferation. Electrospun PES membrane immersed in the aqueous solution containing acrylic acid (AA) and $NaIO_4$ were exposed to ultraviolet light to initiate photografting. Polyacrylic acid (PAAc) grafted PES membrane was further treated with 1,6-hexanediamine, 1,4-butane diamine and 1,2-ethane diamine by carbodiimide cross-linking to ensure amination. The ability of modified fibers on multypotency maintenance and ex-vivo expansion of HSPC's was evaluated. The results confirmed that it could expand HSPCs significantly compared to the unmodified mat.

Aminolysis

Aminolysis is reaction of any chemical compound with a molecule of ammonia or an amine and causes a molecule to split into two parts, containing the addition of an amino group —NH—. The subset of aminolysis reactions involving ammonia is known as ammonolysis and it is another widely applied technique for surface functionalization of polyesters with amino groups, which allow the grafting of biomolecules. Amine functionalized electrospun nanofibers are considered as the ideal candidates for biomedical applications because of their ability to form covalent linkages with biological molecules. Such modified electrospun scaffolds can provide high cell adhesion. In addition to their applications in the biomedical field, they can also be used for heavy metal ions and phenolic component removal from aqueous solutions [12].

Biodegradable electrospun PLLA/chitosan membrane has been successfully prepared by aminolysis method. The modification of chitosan promotes the hydrophilicity, enhances the bioactivity, and accelerates the degradation rate of PLLA electrospun membrane. In vitro cell culture shows that the modified membrane has a better biocompatibility and promotes cell proliferation compared with pure PLLA. Besides, it can also prevent fibroblasts invasion [56]. Chen et al. [57] fabricated an electrospun hyaluronic acid-grafted poly(caprolactone) (PCL-g-HA) nanofibrous membrane (NFM) and proposed as an alternative to current anti adhesion barrier films. HA is covalently grafted to surface-aminolyzed PCL nanofibers, using carbodiimide as the coupling agent. In vivo studies using a rabbit FDP tendon model demonstrated the advantage of the PCL-g-HA NFM in preventing paratendinous adhesion over the PCL NFM and a commonly used commercial anti adhesion barrier (Seprafilm), based on biomechanical, histological, and functional analyses.

Acid Treatment

Modification of electrospun nanofibers can also be performed by acid treatment. Lu et al. [58] fabricated nanofibers from a polymer solution polyether sulfone (PES)/perfluorosulfonic acid (PFSA) containing $CaCO_3$ as a nanomaterial to increase the surface roughness of nanofiber mat. These inorganic nanoparticles were mainly existing on the surface of nanofiber membrane and were then completely removed by acid treatment. The introduction and removal of $CaCO_3$ nanoparticles improve the specific surface area of the electrospun membrane by 70% than the pristine PES/PFSA nanofiber mat.

Benavent et al. [21] discussed the changes in electrical and transport parameters for aged composite polyamide/polysulfone membrane samples (PAC) and their porous support layers (PSU) as a result of chemical treatment (immersion in 1 M HNO_3 solution). Results showed the strong effect of aging on membrane parameters, particularly the decrease in salt permeability and the increase in membrane electrical resistance, while ion transport number was hardly affected by aging, chemical treatment, or treatment time.

Hydrolysis

Partial surface hydrolysis of electrospun membrane serves as simple, efficient and convenient method for creating new chemical functional moieties on nanofiber surface [59]. Several works are reported on modification of surface properties of PCL nanofibers by alkaline hydrolysis. Mei et al. [60] proposed to improve the hydrophilicity and permeation of poly (vinyl chloride)/polyacrylonitrile/SiO_2 (PVC/PAN/SiO_2) composite hollow fiber membranes (HFMs) by the interfacial hydrolysis of PAN between PVC and SiO_2. The alkaline hydrolysis occurred in the composite HFMs, resulted both water permeation and the anti-fouling performance improved while mechanical strength was still kept at a high level.

Nanoparticles on the Membrane Surface

Depending upon the mode of application, a wide variety of foreign materials has been incorporated on the surfaces of electrospun membranes for improving its functional properties.

Razzaz et al. [61] functionalized the surface of the chitosan nanofibers by TiO_2 nanoparticles using coating technique and used for the removal of Pb (II) and Cu (II) ions in a batch system. Nejad et al. [62] synthesized electrospun nanofibers functionalized with silver nanoparticles to evaluate the biocompatibility as well as antibacterial activity in vitro and further wound healing capacity in vivo. It performed by electrospinning of poly(dopamine meth acrylamide-co-methyl methacrylate) (MADO) followed by modification with dopamine and silver nanoparticles via dipping technique. Ma et al. [63] designed and fabricated a polyimide nanofibrous membrane (SNP/DA-TiO_2/PI) with pH-and ammonia-vapor-responsive surface wettability by electrospinning and solution dip-coating. Amarjargal et al. [64] presented an efficient method for the fabrication of a free standing SERS substrate material by in-situ growth of plasmonic silver nanoparticles on electrospun PU nanofibrous membranes. The electrospun polyurethane was surface modified with silver nanoparticles by polyol immersion method. The nonwoven PU mat was further immersed in precursor solution for the in-situ generation of plasmonic silver nanoparticles in the mat. Son et al. [65] functionalized the surface of polyvinyl alcohol (PVA) nanofibers using Au nanoparticles by immersing electrospun mat in Au nanoparticles aqueous solution. The gold nanoparticles decorated PVA provided high efficiency to serve as biosensor substrate material. Zhou et al. [66] demonstrated that the electrospun poly(vinylidene fluoride-co-hexafluoropropylene) (P(VDF-HFP)) nanofibrous mat functionalized with (3-aminopropyl) triethoxysilane is a versatile platform for the fabrication of hybrid nanofibrous mats by covalently attaching various types of inorganic oxide nanoparticles on the nanofiber surface via a sol-gel process. Zhang et al. [67] modified the surface of PVDF membrane with silver-decorated silica nanopollens (SNPs) via immersing the membrane into a coagulation bath containing 200 mg L^{-1} SNPs. The modified membrane demonstrated compelling antibiofouling performance. Moghimifar et al. [68] modified the surface of PES ultrafiltration membranes by corona air plasma and coating TiO_2 nanoparticles in order to improve the separation and antifouling properties.

Cell membrane-coated nanoparticles (CM-NPs) are drawing increasing attention because their surfaces preserve the natural structures of cell membranes, making them a unique class of biomimetic materials that combine both natural and synthetic component. Poly(ethylene glycol) (PEG)-coated AuNPs have been used as a representative carrier in which drugs are encapsulated in either a covalent or a noncovalent manner [69, 70]. Cancer cell membranes are the ideal candidate to wrap around NPs for oncological applications [71]. Zwitterionic polymer membrane-coated Fe_3O_4 shows enhanced photothermal therapy (PTT) efficacy on A549 tumors compared with the corresponding zwitterionic polymer brush or RBC membrane-coated Fe_3O_4 [72].

4.3 Other Technique's

4.3.1 Surface Coating

Coatings are applied on the surface of substrates to improve the functional properties and durability. Conventional coatings need extensive surface preparation for adhesion and need to build up thickness for performance. Surface coating is a simple and inexpensive method for surface modification of the membrane. In this way, the membrane surface is covered by a coated layer. Coating technology improved filtration results, including higher water flux, excellent resistance to damaging media, and even rejection of salt in desalinization treatment. Membrane process technology can also provide insights into other coating techniques and systems [73]. The coated layer can be controlled by adjusting the operating parameters. Membranes with a coated layer have a good stability in the long term without being wet. Typical coating methods can be used such as dip, spray, roll, flow coat, etc.

The dip-coating process can be separated into five stages.

1. Immersion: The substrate is immersed in the solution of the coating material at a constant speed (preferably jitter-free).
2. Start-up: The substrate is kept inside the solution for a while and then pulled up.
3. Deposition: The thin layer deposits itself on the substrate while it is pulled up. The withdrawing is carried out at a constant speed to avoid any jitters. The speed determines the thickness of the coating (faster withdrawal gives thicker coating material).
4. Drainage: Excess liquid drains from the surface.
5. Evaporation: The solvent evaporates from the liquid, forming the thin layer. For volatile solvents, such as alcohols, evaporation may start even during the deposition and drainage steps.

In the continuous process, the above steps are followed one after another, which allows the coating of a thin layer as low as <0.2 μm. The critical factors in dip coating is the viscosity of the solution and the coating speed or time. To form an inorganic multilayer, the first substrate layer is calcined, which is then followed by the repeated cycles of dipping, drying and calcination.

The surface coating is applied for the surface modification of both *hydrophilic* and hydrophobic surfaces. Especially, coating hydrophilic substances on the membrane surface can further strengthen the modification effect and improve the membrane flux. Despite this advantage, the coating layer is easily sloughed off. As a result, the flux of pure water will firstly increase greatly and then decline gradually.

4.3.2 Filler Modification

To control the surface chemistry of multi-walled (MWCNTs) and single-walled (SWCNTs) carbon nanotubes (CNTs) with different lengths, Morales-Torres et al. [74] used a specific methodology based on nitric acid hydrothermal oxidation. The methodology was adapted to the use of sulphuric acid containing ammonium persulfate as an oxidizing agent. For the textural properties, the oxidations performed with HNO_3 have a more relevant effect than those carried out with H_2SO_4, a decrease of the total pore volume and average pore diameter of CNT bundles was observed. Concerning the surface chemical properties, the amounts of CO, CO_2 and SO_2 as well as the O_2 content (determined by temperature programmed desorption (TPD) analysis and directly related with the amount of surface functional groups) can be correlated to the oxidizing agent concentration by using mathematical functions.

Besides all these surface modification techniques many other fruitful strategies are also known. Functionalization of electrospun membrane using nanotechnology-based techniques such as molecular imprinting, Layer by layer deposition, Sol-gel technique and atomic deposition are also well established.

4.4 Modification of Different Membranes

4.4.1 Flat Sheet Membrane

Surface modification of a flat sheet membrane can be done by using various methods such as coating, grafting, and surface treatment. Polymeric membranes often suffer from poor functionality which restricts their application in many industries. Their intrinsic hydrophobic nature also causes them to be easily fouled in protein filtration and purification processes. Surface functionalization is an efficient method to introduce polar groups on the surface of polymeric membranes [75]. Freeman and coworkers [76] used aqueous top surface treatment method to graft poly(ethylene glycol) diglycidyl ether (PEGDE) to the surfaces of commercial reverse osmosis (XLE) and nanofiltration (NF90) membranes. It was reported that due to surface modification, water flux decreased and NaCl rejection increased.

Ouyang et al. [77] synthesized PES ultrafiltration membranes blended with cobalt oxide/graphene oxide (Co_3O_4–GO) nanocomposites by the phase inversion method. The experimental results indicated that the pure water flux of the hybrid membrane was improved from 101.1 to 347.9 L m^{-2} h^{-1} compared to that of the pristine membrane. Furthermore, the remarkable improvement in the antibacterial performance (89.8%, against *Escherichia coli*) was also observed.

Xie et al. [78] demonstrated that PVDF-TiO_2 membrane assisted with ultrasonication enhanced the dispersion uniformity of nano-TiO_2 in PVDF-TiO_2 membrane structure, which positively affected membrane hydrophilicity, permeability, and anti-protein fouling ability, as compared with only mechanical stirring.

Layer-by-layer (LbL) technique has been used as an effective surface modification method for membranes used in desalination of brackish and seawater, reclamation of wastewater, and membrane bioreactors (MBR). Gao et al. [79] used LbL method to consecutively deposit TiO_2 nanoparticles and GO nanosheets on a commercial porous ultrafiltration polysulfone membrane, followed by partial reduction of GO via ethanol-UV treatment.

Ju et al. [80] fabricated a superhydrophilic and underwater superoleophobic PVDF-g-PEGDA membrane by phase inversion method and low-pressure plasma-induced surface copolymerization. The as-prepared membranes can effectively separate oil-in-water emulsions with high separation efficiency under ultralow pressure and much higher fluxes. Wu et al. [81] also reported grafting of crosslinked collagen on porous PVDF membrane with the aid of low-temperature plasma treatment.

Wet chemical functionalization is an easy and efficient method, which connects the polar functional groups to the surface of polymeric membranes. Surface functionalization of microporous polypropylene (PP) membranes (fabricated via thermally induced phase separation (TIPS) method) was done by Fonouni et al. [75] by using various oxidizing agents ($KClO_3$, $K_2Cr_2O_7$ and $KMnO_4$ solution in sulfuric acid). The results indicated that incorporation of hydrophilic functional groups on the surface of PP membranes improves the fouling resistance behavior. Kundu et al. [10] modified the surface of polymeric membranes by mixing 2-(perfluoroalkyl) ethanol with polyether sulfone to improve the hydrophobicity of the membrane. Shumskaya et al. [82] modified polyethylene terephthalate ion-track membranes with polyvinyl alcohol functionalizing layer for the separation of biological objects. The modified membrane was used for the separation of living cell (human lung cancer). Kim et al. [83] modified polyvinylidene fluoride membrane with low-temperature plasma to make PA-PVDF flat TFC membranes and to improve membrane hydrophilicity. The results showed that after being modified by plasma, the contact angle of polyvinylidene fluoride membrane decreased largely; the generated hydrophilic surface could be a supporting layer of TFC membrane, which exhibited a larger pure water flux. Gonzales et al. [84] fabricated a high-performance electrospun polyvinylidenefluoride (PVDF) nanofiber-supported thin film composite (TFC) membrane after molecular layer-by-layer polyelectrolyte deposition. Negatively-charged electrospun polyacrylic acid (PAA) nanofibers were deposited on electrospun PVDF nanofibers to form a support layer consisting of PVDF and PAA nanofibers. The PVDF-PAA nanofiber support then underwent a layer-by-layer deposition of polyethylenimine (PEI) and PAA to form a polyelectrolyte layer on the nanofiber surface prior to interfacial polymerization, which formed the selective polyamide layer of the TFC membrane. The resultant PVDF-LbL TFC membrane exhibited enhanced hydrophilicity and porosity, without sacrificing mechanical strength. It was reported that the layer-by-layer deposition of polyelectrolyte is a feasible modification method for improvement of hydrophilic property, as well as formation of polyamide active layer, of a nanofiber-supported TFC membrane. Ngo et al. [85] modified a commercial TFC-PA membrane (Filmtec BW30) by coating TiO_2 nanoparticles. The separation properties of these membranes were clearly improved with a much better flux and a great retention for the removal of reactive dye in an aqueous feed solution. The UV irradiated TiO_2-coated TFC-PA membranes also demonstrated the significant enhancement of the antifouling property with higher flux ratios and lower irreversible fouling factors compared to the uncoated TFC-PA membrane.

Khan et al. [86] fabricated composite ultrafiltration polysulfone membrane incorporated with oxidized nanocarbon black in matrix via phase inversion. The modified membrane showed excellent antifouling properties and mechanical strength, making it potential candidate as antifouling membrane for water purification. Kusworo et al. [87, 88] modified cellulose acetate flat membrane and PES flat membrane via thermal annealing and observed that modifying in both cases increases in flux and rejection when used them for water treatment.

Tomer et al. [89] demonstrated that room temperature, surface-initiated ATRP can be used to graft Poly(N-isopropylacrylamide) (PNIPAAm) and poly(N-isopropylacrylamide-block-ethylene glycol methacrylate) (PNIPAAm-block-PPEGMA) nano-layers on the surface of polyamide thin-film composite nanofiltration membranes. Modified membranes showed improved permeate water quality relative to unmodified membranes. These membranes maintained constant flux during filtration of coal bed methane produced water. Li et al. [90] demonstrated a method for preparing PSf membranes with surface dormant groups for further surface functionalization via ATRP. Protein adsorption experiments revealed substantial antifouling properties of the grafted PSf membranes in comparison with the those of the pristine PSF surface. Anuraj et al. [91] fabricated modified hydroxylated nylon membrane via adsorption of a macroinitiator followed by ATRP of 2-(methacryloyloxy)ethyl succinate from the immobilized initiator to form poly(acid) brushes. The hydraulic permeability of the poly(acid) membranes was four-fold higher than that of similar membranes prepared by growing brushes from immobilized silane initiators. Li et al. [92] reported the preparation, characterization and properties of a polyether sulfone membrane modified by surface-initiated electrochemically ATRP. Three kinds of copolymer brushes of the homopolymer, block copolymer, and random variety were covalently grafted onto the surface of the polyether sulfone membrane. Hydrophilicity of modified membranes was largely enhanced due to the hydrophilic polymer brush; and filtration experiments fed with water and BSA showed that both the permeation and anti-fouling properties of fabricated membranes were improved significantly. Wang et al. [93] synthesized polyvinylidene fluoride grafted with poly(ethylene glycol) methyl ether methacrylate (PVDF-g-PEGMA) via ATRP at different reaction times and studied the effect of the copolymer mixture additives with different synthesis times on cast membrane performance. The pure water fluxes of the blended membranes significantly improved. The membrane with PVDF-g-PEGMA at 19 h reaction time exhibited the best foulant rejection and cleaning recovery due to its narrow pore size distribution and high surface oxygen content. El-Arnaouty et al. [94] synthesised polyamide thin films incorporated with *N*-Isopropyl acrylamide (NIPAM) and ZnO nanoparticles via direct radiation technique. ZnO NPs were uniformly dispersed along the membrane surface which exhibited decrease in pore density and pore size. FTIR analysis showed the formation of coordinative bonding between NIPAM and ZnO NPs on the surface of thin film. The properties of ZnO NPs P(NIPAM)-g-PA(TFC) membranes were much better than those of the virgin PA(TFC) in sense of both the anti-biofouling and the chlorine resistance in comparison of a commercially available aromatic polyamide RO membrane.

The proton exchange membranes are utilized as both the electrolytes and separators for PEM (polymer electrolyte membranes) fuel cells. The development of cost effective proton exchange membranes to replace the state-of-the-art high cost perfluorinated membranes (e.g., Nafion® and derivatives) is an important challenge. The radiation induced grafting is a versatile technique allowing the functionalization of the base material for the introduction of a desired property. Ke et al. [95] fabricated polymer electrolyte membranes (PEM) by radiation-induced graft copolymerization. For this purpose, surface of commercial poly(ethylene-alt-tetrafluoroethylene) (ETFE) membranes was modified by electron beam treatment and subsequently grafted with the monomers glycidylmethacrylate (GMA), hydroxyethylmethacrylate (HEMA) and N,N′-methylenebis (acrylamide) (MBAA) as cross linker.

4.4.2 Hollow Fiber Membrane

Hollow fiber membranes (HFMs) are a class of artificial membranes containing a semi-permeable barrier in the form of a hollow fiber. Most commercial hollow fiber membranes are packed into cartridges which can be used for a variety of liquid and gaseous separations.

Membrane wetting is influenced mainly by membrane properties, absorption liquid properties and the mutual interaction between the absorption liquid and the membrane material. However, the corresponding causes of membrane wetting have always been disputed. Generally, increasing the membrane hydrophobicity is a useful way to prevent liquid from penetrating the microporous membrane [96]. Li et al. [97] modified PTFE hollow fiber membrane's surface to super hydrophobic surface via spraying hydrophobic fumed silica nanoparticle. The modified membrane was able to reach a water contact angle of 158.4° and sliding angle of 1.3°.

Polyglycerol (PG) based modification of PES hollow fiber UF membranes by Chung's school [98, 99] showed the specific chemical modification of hollow fiber membranes compared to traditional flat sheet membranes. The thio terminal group of PG was linked with polydopamine (PDA) coated hollow fibers through Schiff base reaction. This coated layer was then used to synthesize TFC polyamide membranes through interfacial polymerization. The membranes showed excellent resistance to fouling and bacterial adhesion during pressure retarded osmosis process with good shelf life. Wang et al. [100] modified polyvinylidene fluoride hollow fiber ultrafiltration membranes with low-temperature plasma, and grafted acrylic acid and acrylamide monomer to alleviate membrane fouling. The low-temperature plasma modification method could graft acrylic acid and acrylamide monomer to the membrane surface effectively. After the modification, polar groups were introduced to the membrane surface. The modified membrane had a higher zeta potential than the original membrane.

A novel functionalized multi-walled carbon nanotube (MWCNT) immobilized by polyethyleneimine–poly(amide–imide) (PEI–PAI) hollow fiber membrane was designed by Goh et al. [101] which was fabricated using an easily scalable method. PAI hollow fiber was spun via phase inversion, followed by functionalized MWCNTs immobilization via vacuum filtration before a chemical post-treatment using PEI was applied to obtain a positively charged selective layer. The resulting membranes were evaluated in the forward osmosis (FO) process. It was suggested that the enhancement in the water permeability can be attributed to additional nanocorridors between the MWCNTs and the PEI polymer matrix. Several key fabrication factors were also identified and optimized for developing a scalable protocol for mass production of this membrane. It was also suggested that the potential of using commercially available MWNCTs to enhance water flux for use in the FO process. Li et al. [97] reported that the silica NPTs incorporated PTFE modified membrane outperformed the original membrane (without silica) at elevated absorption pressures, and the highest CO_2 removal efficiency and absorption flux reached 97.1% and 1.85×10^{-3} mol m^{-2} s^{-1}, respectively.

Song et al. [102] modified hydrophobic PTFE (polytetrafluoroethylene hollow fiber) membranes via step-by-step coating or co-deposition of PDA (polymerized dopamine) and poly(ethyleneimine) (PEI). All the modified membrane showed improved hydrophilicity compared with original PTFE. The PTFE membranes co-deposited with PDA and PEI showed higher water permeate fluxes, long-term stability and durability in aqueous solution with wide pH range (pH 1–13). This work provides a one-step method to improve the hydrophilicity and chemical stability of the PTFE hollow fiber membranes for water treatment.

Zheng et al. [103] made low-temperature plasma treatment to improve the hemocompatibility of pristine PSF membrane for use in extracorporeal membrane oxygenators. Protein adsorption and platelet adhesion experiments showed that the hemocompatibility of surface-modified PSF membranes was significantly improved. Additionally, O_2 and CO_2 gas permeation experiments indicated that the excellent gas transmission properties of PSF membrane had been preserved.

Wan et al. [104] modified PSF HFMs with zwitterionic or charged polymers via, atom transfer radical polymerization (ATRP). It was reported that the membrane modified with neutrally charged CBMA (carboxybetaine methacrylate) showed the best antifouling property when compared to those modified by charged polymers and the pristine PSF HMF. The membrane modified with zwitterionic CBMA has the highest resistance to protein fouling for the ultrafiltration applications.

4.4.3 Nanofibrous Membranes

In a short period, elecrospun nanofiber membranes (ENMs) have gained popularity due to the facile fabrication, interconnectivity and large area/volume ratio. Electrospinning is a simple and versatile technique that relies on the electrostatic repulsion between surface charges to continuously draw nanofibers from a viscoelastic fluid. Electrospinning can generate nanofibers with a number of secondary structures . Pre-electrospinning technique or in situ modification is considered as the simplest method of membrane modification. In pre-treatment, the additives are added directly to the spinning solution. Establishing functionalizing agents into the spinning solution presents new formulations with specific properties. It is considered as the simplest method of modifying membrane performance. Surface and/or interior of nanofibers can be functionalized with molecular species or nanoparticles during or after an electrospinning process to obtain desirable results. Recently Khulbe and Matsuura [5] discussed the advancement in electrospun nanofibrous membranes modification to enhance their performance in various membrane separation processes.

Ifuku et al. [105] reported a method for surface phthaloylation of chitin nano fiber in aqueous media for the purpose of modifying its properties. The phthaloyl group quantitatively introduced into the amino group of surface-deacetylated chitin NF in aqueous media provides hydrophobic properties on the NF surface (Fig. 4.8).

Figure 4.8 shows that the degree of substitution (DS) of NH_2 (0.20) was reduced to 0.19 after phthaloyl group was introduced. This result indicates that the reactions primarily took place on the surface of the chitin NF. From the performances obtained from this modified chitin nanofiber, it was concluded that modified chitin nanofiber with a hydrophobic group can function a variety of applications, including as reinforcement filler and coating material to improve mechanical strength with UV-protectant property. Almasian et al. [106] modified the surfaces of the webs fabricated from electrospun polyacrylonitrile (PAN) nanofibers by three different sources of amine-containing compounds, including diethylamine, diethylenetriamine, and triethylenetetramine. From the different characterization techniques, it was revealed that amide groups were formed on the fiber surface by a chemical reaction between the nitrile groups of PAN and the amine groups of amine-containing compounds. It was reported that the functionalized PAN nanofibers could be used for anionic dye adsorption from colored wastewater with high dye adsorption capacity. Bao et al. [107] modified the electrospun nanofibers of poly(methyl methacrylate) (PMMA) for facilitating the growth of silver nanoparticles (Ag NPs), via oxygen plasma etching. The oxygen plasma etching is effective in increasing the hydrophilicity of the PMMA nanofibers and thus in facilitating the growth of the Ag NPs. The modified membrane can be used for broad applications. Liao et al. [108] modified the surfaces of electrospun PVDF nanofiber membrane to get two types of superhydrophobic membranes i.e. integrally-modified and surface-modified for MD process. Two types of modification which are integral and surface modifications were carried out as shown in Fig. 4.9.

Yalcinkaya et al. [109] produced various PAN, PVDF, and PVDF/PAN nanofiber layers, and their mechanical properties were improved via a lamination process. For the surface modification, low vacuum plasma treatment was applied. Argon was

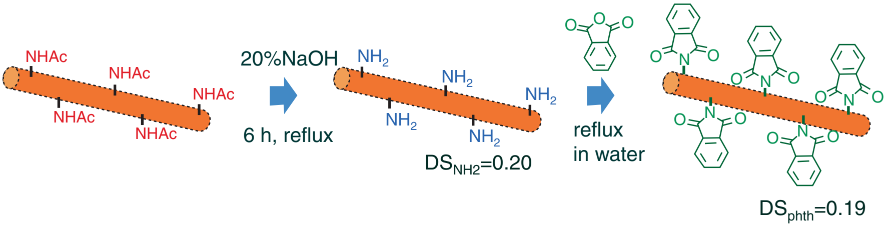

Fig. 4.8 Preparation scheme for the surface phthaloylated chitin nanofiber [105]

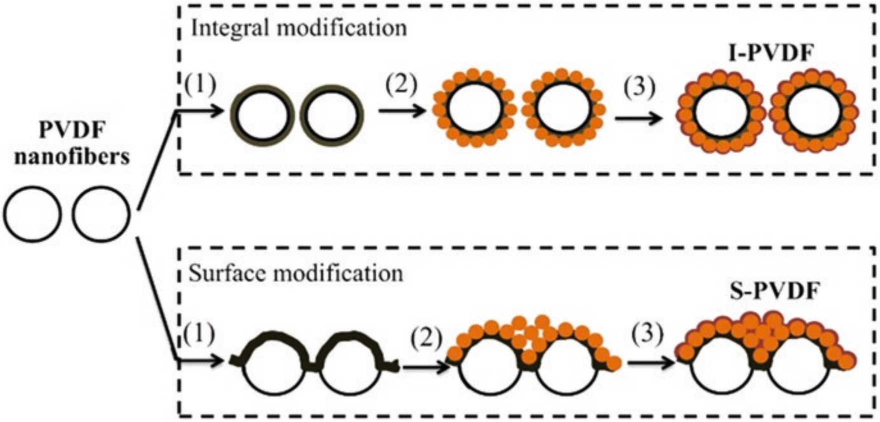

Fig. 4.9 Schematic diagram of preparing superhydrophobic PVDF nanofiber membranes by silver nanoparticle and 1-dodecanethiol hydrophobic modification [108]

used as the carrier gas, H_2, O_2 and N_2 were used for hydrophilic samples, and sulphur hexafluoride (SF_6) was used for hydrophobic samples as the reactive gasses. It was reported that the hydrophilic base membrane PAN showed better performance under plasma treatment. In another publication, Yalcinkaya et al. [110] described a method for producing nanofibrous composite membranes for the separation of a vegetable oil–water mixture. Neat polyvinylidenefluoride (PVDF), polyacrylonitrile (PAN) nanofibers and PVDF/PAN mixtures were used to prepare the membranes. Argon plasma treatment, followed by a chemical surface modification, was applied to alter the hydrophilicity and oleophobicity of the membranes. Zhang et al. [111] prepared electrospun nanofiber membranes consisting of polyvinylidene fluoride-co-hexafluoropropylene blended with nanosilica nanocomposites. Blended with 5 wt.% modified nanosilica, the water contact angle of membrane could reach up to a maximum value (136°). Membrane morphological analysis presented that the resultant membrane had the thinnest diameter and roughness surface, which confirmed the enhancement of hydrophobicity of the membrane. Lee et al. [112] loaded polymethylmethacrylate (PMMA) with Rhodanine (Rhd) through blending and tested its performance for the removal of Ag (I) and Pb (II) ions through dead-end filtration. Electrospun membranes exhibited good Ag (I) and Pb (II) ion uptake capabilities. Yang et al. [113] proposed to fabricate robust, breathable and waterproof polymer nanofiber membranes. In a typical process, polyamide-6 (PA-6) electrospun membranes were immersed into polyurethane (PU)/DMF solutions for 24 h, and then taken out and dried. Xu et al. [114] fabricated superhydrophobic electrospun polyacrylonitrile (PAN)/polyurethane (PU)/titanium dioxide (TiO_2) nanofibrous membranes. Membranes exhibited multifunction of UV resistance, waterproofness and breathability by coating modification with 2-hydroxy-4-n-octoxybenzophenone (UV531) and fluorinated acrylic copolymer (FAC). Schaub et al. [115] chemically modified the surface chemistry and hydrophilicity of poly-L-lactic acid (PLLA) fibers. Razzaz et al. [61] prepared chitosan/TiO_2 nanofibrous adsorbents by two methods:

1. TiO_2 nanoparticles coated chitosan ENFs (coating method).
2. Electrospinning of chitosan/TiO_2 solutions (entrapped method).

These adsorbents were investigated for the removal of Pb (II) and Cu (II) ions in a batch system. The maximum adsorption capacities of Cu (II) and Pb (II) ions using entrapped and coating methods were found to be 710.3, 579.1 and 526.5, 475.5 mg/g at equilibrium time of 30 min and 45 °C, respectively. The selectivity of metal sorption, using chitosan/TiO_2 nanofibrous adsorbent was in order of Cu (II)>Pb (II).

Uzal et al. [116] fabricated novel PSf/PEI-Al_2O_3 nanofiber membrane by electrospinning the PSf solution blended with different ratios of PEI and Al_2O_3 nanoparticles without any support for using in water based membrane filtration application. On addition of PEI and Al_2O_3 particles in PSf solution, the overall properties of the nanofiber membranes in terms of porosity, tensile strength and hydrophilicity improved. Shen et al. [117] attempted to make grafted hydrophobic PVDF membrane with hydrophilic hydroxyethyl acrylate (HEA) monomer via radiation grafting method. This grafted membrane showed an enhanced hydrophilicity (10° decrease of water contact angle), water content ratio, settling ability and wettability compared to the control membrane. Filtration tests showed an improved dependence of water flux of the grafted membrane. Phan et al. [118] modified cross-linked PVA nanofiber (with glutaraldehyde nanofibers) via the esterification of hydroxyl group on PVA with the carboxyl group of 3-mercaptopropionic acid under hydrochloric acid in aqueous environment. Membrane was tested for the adsorption of silver ions from the aqueous solution and they reported that the membrane showed the affinity towards silver ions. The maximum adsorption volume was found to be 26.2 mg g^{-1}.

Electrospinning combined with thermal treatment and plasma induced surface modification was utilized to develop an electrospun PPSU (polyphenylsulfone) ENM as nanofiber support layers in biomimetic TFNC (thin film composite membrane) FO membranes by Wang et al. [119]. Thermal treatment effectively converted the fluffy, highly porous and mechanically weak nanofiber membrane into a more compact and tougher membrane with interfused 3-dimensional nanofiber network. The TFNC FO membrane showed significant enhancement in osmotic water flux and much lower reserve salt flux, owing to its highly interconnected pore structure and hydrophilic surface when compared the performances with commercial membranes.

Liao et al. [120] reported the fabrication of robust superhydrophobic dual-layer membranes with high porosity and excellent mechanical properties via electrospinning in two ways.

1. Electrospinning an ultrathin 3D superhydrophobic selective skin, comprising PVDF and silica nanoparticles, on a porous PVDF nano fibrous support.
2. Electrospinning thicker 3D superhydrophobic PVDF—silica composite layers onto a commercial nonwoven support, which not only assists the PVDF—silica

> composite particles in shaping into a flat sheet but also provides outstanding mechanical properties to the composite membranes.

These membranes were superhydrophobic not only toward distilled water, but also towards salty water, oil-in-water emulsion, and beverages, which enables them to be used not only for desalination but also for other processes.

Pereao et al. [121] discussed the emerging and increasing use of electrospun nanofibers for metal ion adsorption especially for hazardous metals. For the better performance of functionalized nanofiber for the pollutant removal, greater exposure of the functional group on the surface of the nanofibers is necessary. Where the base material does not contain appropriate functional group, functionalization method such as blending and chemical treatment are useful. Xiao et al. [122] fabricated water-stable polyelectrolyte polyacrylic acid (PAA) nanofibrous by electrospinning and subsequent thermal crosslinking (using PVA). It was found that PAA/PVA nanofibrous mats can act as an effective sorbent or separation medium for removing Ca(II) ions from water may be used.

4.5 Functionalization of CNTs

Since carbon nanotubes (CNTs) were discovered by Iijima in 1991 [123], they have become the subject of many studies because of their unique electrical, optical, thermal, and mechanical properties. CNT is one of carbon allotropes such as diamond, graphite, graphene, fullerene and amorphous carbon. But, its one-dimensional carbon form which can have an aspect ratio greater than 1000 makes it interesting. The properties of nanotubes depend on atomic arrangement (on how the sheets of graphite are ‘rolled’), the diameter and length of the tubes, and morphology, or nano structure.

Prepared CNTs possess a variety of diameters, length distribution, and structures within the same sample. It is also well-known that the methods of production of CNTs generate impurities such as by-product carbonaceous species and residues from the transition metal catalysts used in preparing CNTs. Moreover, CNTs are insoluble in all solvents due to strong van der Waals interactions that tightly hold them together, forming bundles. All of the above decrease the overall yield of usable material and interfere with most of the desired properties of the CNTs [124].

Raw CNTs, persisting metallic nature, are highly hydrophobic. CNTs have exhibited diverse physical, chemical and mechanical properties suitable for a variety of applications. In last decade, medical applications of CNTs have undergone rapid progress. Their unique properties such as ultrahigh surface area, high aspect ratio and distinct optical properties have been applied to develop innovative, multi-functional CNT-based nano devices for broad applications [125]. In recent years, CNT based devices have been successfully utilized in membrane technology, tissue engineering and stem cell based therapeutic applications, including myocardial therapy, bone formation, muscle and neuronal regeneration. The properties of nanotubes depend on atomic arrangement (on how the sheets of graphite are 'rolled'), the diameter and length of the tubes, and morphology, or nano structure.

CNTs can be functionalized to attain desired properties that can be used in a wide variety of applications. Surface modification of CNTs makes them ideal for use in many applications such as in modifying the MMMs, medical use etc. To develop the CNTs containing MMMs, modification of CNT is interesting and necessary. The CNTs modification methods involved either non-covalent or covalent strategies. The non-covalent modification utilizes the hydrophobic nature of CNTs, especially, π-π interactions for coating of amphiphilic molecules. The covalent modification generates chemical bonds on carbon atoms on CNTs surface via chemical reactions followed by further conjugation of hydrophilic organic molecules or polymers rendering CNTs better solubility. These modifications not only offer CNTs water solubility, but also produce functional moieties that enable linking of therapeutic agents, such as genes, drugs, and recognition molecules for medical applications [125]. Functionalization of CNTs is sometimes performed in order to ensure uniform dispersion in the membrane matrix and improved adhesion of CNTs to the polymer. Moreover, depending on the functional group, functionalization could ensure additional ion exchange sites in the nanocomposite membrane to boost ion exchange. Figure 4.10 shows overview scheme of the functionalization of carbon nanotubes [124].

The PES-modified carbon nanotubes membranes had increased the permeability of methane gas and the CO_2/CH_4 selectivity. The carbon nanotubes have been potentially useful as in organic filler for mixed matrix membrane for the future biogas purification membrane [126].

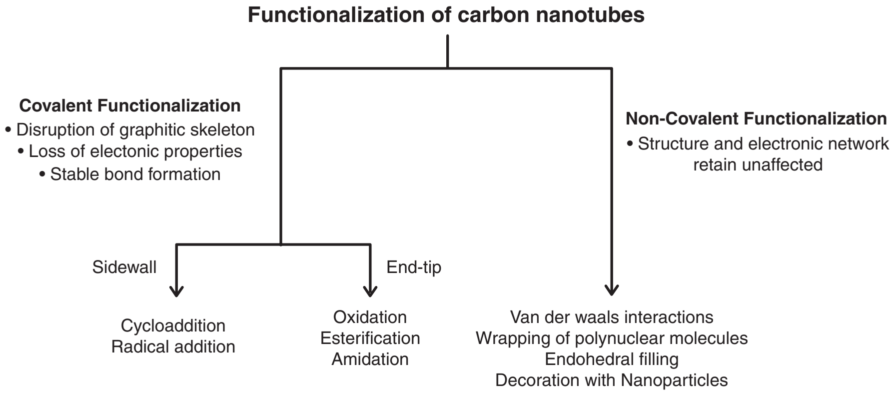

Fig. 4.10 Overview scheme of the functionalization of carbon nanotubes

4.6 Summary

All kinds of modifications methods for membranes can help to improve surface polarity, reduce contact angle, and increase surface energy. Various modification techniques have been developed, including the use of additives, chemical treatments, grafting components, and coatings. Each of these methods has its merits and demerits. Modified membranes have been widely used in various applications, such as in separation processes for liquid and gaseous mixtures (gas separation, reverse osmosis, pervaporation, nanofiltration, ultrafiltration, microfiltration), biomaterials, catalysis (including fuel cell systems). To date no one claimed that modified membranes are able to prevent fouling in experimental condition or real-time situations completely [33]. Uniformity, reproducibility, stability, process control, and reasonable cost, together with precise control over functional groups are the main factors that should be considered for the overall process of membrane modification.

Atom transfer radical polymerization (ATRP), a controlled/living radical polymerization (CRP) process, has emerged as a new technique to modify the membrane surfaces with desirable tailored functionalities of polymer chains. Various surface functionalities may be inserted via ATRP. The most common method to improve membrane anti-fouling properties is membrane surface modification. The surface modifications of the ENMs enhance the nanofibers matrix properties such as availability of functional groups on the surface of nanofibers. A wide range of functional molecules has been incorporated into electrospun nanofibers for pollutant adsorption. More kinds of modification methods will be invented when new materials for membrane are developed. Surface modification of CNTs makes them ideal for use in many applications such as in modifying the MMMs, medical use etc.

References

1. Khulbe KC, Feng C, Matsuura T (2010) The art of surface modification of synthetic polymeric membranes. J Appl Polym Sci 115(2):55–895
2. Miller DJ, Dreyer DR, Bielawski CW, Paul DR, Freeman BD (2017) Surface modification of water purification membranes. Agnew Chem Int Ed 56:4662–4711
3. Sun W, Liu J, Chu H, Dong B (2013) Pretreatment and membrane hydrophilic modification to reduce membrane fouling. Membranes (Basel) 3(3):226–241
4. Fang Y, Xu ZK, Wu J (2013) Surface modification of membranes (membrane materials, characterization, and module design). In: Encyclopedia of membrane science and technology. Wiley, Hoboken. https://doi.org/10.1002/9781118522318.emst061
5. Khulbe KC, Matsuura T (2020) The advances of electrospun nanofibers in membrane technology. JMSR 6:251–208
6. Rana D, Matsuura T (2010) Surface modifications for antifouling membranes. Chem Rev 110(4):2448–2471
7. Alenazi NA, Hussein MA, Alamry KL, Asiri AM (2017) Modified polyether-sulfone membrane: a mini review. Design Monomers Polymers 20(1):532–546
8. Dorraji MS, Vatanpour V, (2016) Organic–inorganic composite membrane preparation and characterization for biorefining. In: Figoli A, Cassano A, Basile A (eds) Membrane technologies for biorefining, Woodhead Publishing, Sawston. pp 85–102

9. Yu LY, Shen HM, Xu ZL (2009) PVDF-TiO_2 composite hollow fiber ultrafiltration membranes prepared by sol–gel method and blending method. J Appl Polym Sci 113:1763–1772
10. Kundu N, Lee HK, Deshwal BR (2019) Surface modification of polymeric flat sheet membranes by adding oligomeric fluoroalcohol. J Polym Eng 39(2):70–177
11. Otitoju TA, Ahmad AL, Ooi BS (2018) Recent advances in hydrophilic modification and performance of polyethersulfone (PES) membrane via additive blending. RSC Adv 8:22710–22728
12. Sagitha P, Reshmi CR, Sundaran SP, Sujith A (2018) Recent advances in post-modification strategies of polymeric electrospun membranes. Eur Polym J 105:227–249
13. Viswanathan P, Themistou E, Ngamkham K, Reilly GC, Armes SP, Battaglia G (2015) Controlling surface topology and functionality of electrospun fibers on the nanoscale using amphiphilic block copolymers to direct mesenchymal progenitor cell adhesion. Biomacromolecules 16:66–75
14. Teo WE (2019) Heat treatment of electrospun membrane. Electrospin Tech. http://electrospintech.com/heatmembrane.html#.XVQXNnspB2E. Accessed 14 Aug 2019
15. Zsigmondy R, Bachmann W (1922) Filter and method of producing same. US 1,421,341
16. Loeb S, Sourirajan S (1962) Seawater demineralisation by means of an osmotic membrane. Adv Chem Ser 38:117
17. Kusuki Y, Yoshinaga T, Shimazaki H (1992) Aromatic polyimide double layered hollow filamentary membrane and process for producing same. US 5,141,642
18. Hoehn H (1974) Treatment of membranes of selected polyimides. US 3,822,202
19. Zhang L, Liu L, Pan F, Wang D, Pan Z (2012) Effects of heat treatment on the morphology and performance of PSU electrospun nanofibrous membrane. J Eng Fibers Fabrics 7(3):7–16
20. Fujioka T, Nghiem LD (2013) Modification of a polyamide reverse osmosis membrane by heat treatment for enhanced fouling resistance. Water Sci Technol Water Supply 13(6):1553–1559
21. Wang Z, Crandall C, Sahadevan R, Menkhaus TJ, Fong H (2017) Microfiltration performance of electrospun nanofiber membranes with varied fiber diameters and different membrane porosities and thicknesses. Polymer 114:64–72
22. Ma Z, Kotaki M, Ramakrishna S (2006) Electrospun cellulose nanofiber as affinity membrane. J Membr Sci 271:179–187
23. Le NL, Wang Y, Chung TS (2012) Synthesis, cross-linking modifications of 6FDA-NDA/DABA polyimidemembranes for ethanol dehydration via pervaporation. J Membr Sci 415–416:109–121
24. Kusworo T, Aryanti N, Nurmalasari E, Utomo DP (2019) Surface modification and performance enhancement of polyethersulfone (pes) membrane using combination of ultra violet irradiation and thermal annealing for produced water treatment. Proceedings of 2nd international conference on chemical process and product engineering (ICCPPE) 2019 AIP Conf. Proc. 2197, 050012-1–050012-10. https://doi.org/10.1063/1.5140924
25. Li L, Hashaikeh R, Arafat HA (2013) Development of eco-efficient micro-porous membranes via electrospinning and annealing of poly (lactic acid). J Membr Sci 436:57–67
26. Shintani T, Matsuyama H, Kurata N (2009) Effect of heat treatment on performance of chlorine-resistant polyamide reverse osmosis membranes. Desalin 247(1–3):370–377
27. Zaidi SJ, Mauritz KA, Hassan MK (2018) Functional polymers (part of the polymers and polymeric composites: a reference series book series (POPOC)), pp 1–26
28. Correia DM, Ribeiro C, Sencadas V, Botelho G, Carabineiro SAC, Ribelles JLG, Mendez SL (2015) Influence of oxygen plasma treatment parameters on poly(vinylidene fluoride) electrospun fiber mats wettability. Prog Org Coat 85:151–158
29. Yao C, Li X, Neoh KG, Shi Z, Kang ET (2008) Surface modification and antibacterial activity of electrospun polyurethane fibrous membranes with quaternary ammonium moieties. J Membr Sci 320:259–267
30. Zander NE, Orlicki JA, Rawlett AM, Beebe TP (2012) Quantification of protein incorporated into electrospun polycaprolactone tissue engineering surface. ACS Appl Mater Interfaces 4:2074–2081

31. Sawawi M, Wang TY, Nisbet DR, Simon GP (2013) Scission of electrospun polymer fibres by ultrasonication. Polymer 54:4237–4252
32. Hielscher Ultrasound Technology, ultrasonic liposome preparation: ultrasonic liposome preparation for pharmaceuticals and cosmetics. https://www.hielscher.com/ultrasonic-liposome-preparation.htm
33. Pinnau I, Freeman BD (1999) Chapter 1. Formation and modification of polymeric membranes: overview. American Chemical Society, Washington
34. Upadhyaya L, Qian X, Wickramasinghe SR (2018) Chemical modification of membrane surface—overview. Curr Opin Chem Eng 20:13–18
35. Ayyavoo J, Nguyen TPN, Jun BM, Kim IC, Kwon YN (2016) Protection of polymeric membranes with antifouling surfacing via surface modifications. Colloids Surf A Physicochem Eng Asp 506:190–201
36. Bhattacharya A, Misra BN (2004) Grafting: a versatile means to modify polymers techniques, factors and applications. Prog Polym Sci 29:767–814
37. Filippova O, Karpov DA, Gradoboev AV, Sokhoreva VV, Pichugin VF (2016) Influence of low-temperature plasma and γ radiationon on the surface properties of PET track membranes. Inor Metals Appl Res 7(5):664–672
38. Kaur S, Ma Z, Gopal R, Singh G, Ramakrishna S, Matsuura T (2007) Plasma-induced graft copolymerization of poly(methacrylic acid) on electrospun poly(vinylidenefluoride) nanofiber membrane. Langmuir 23(26):13085–13092
39. Cho E, Kim C, Park JY, Hwang CH, Kim JH, Kim YA, Endo M, Chang DR, Kook JK (2013) Surface modification of electrospun polyvinylidene fluoride nanofiber membrane by plasma treatment for protein detection. J Nanosci Nanotechnol 13(1):674–677
40. Ma Z, Ramakrishna S (2008) Electrospun regenerated cellulose nanofiber affinity membrane functionalized with protein A/G for IgG purification. J Membr Sci 319:23–28
41. Anari Z, Sengupta A, Wickramasinghe SR (2018) Surface oxidation of ethylenechlorotrifluoroethylene (ECTFE) membrane for the treatment of real produced water by membrane distillation. Int J Environ Res Public Health 15(8):1561. https://doi.org/10.3390/ijerph15081561
42. Zhu Y, Zhang H, Zhang X (2013) Study on catalytic ozone oxidation with nano-tio2 modified membrane for treatment of municipal wastewater. Biomim Biomater Tissue Eng 18:113. https://doi.org/10.4172/1662-100X.1000113
43. Kato M, Kamigaito M, Sawamoto M, Higashimura T (1995) Polymerization of methyl methacrylate with the carbon tetrachloride/dichlorotris- (triphenylphosphine)ruthenium(ii)/methylaluminum bis(2,6-di-tert-butylphenoxide) initiating system: possibility of living radical polymerization. Macromolecules 28(5):1721–1723
44. Wang JS, Matyjaszewski K (1995) Controlled/"living" radical polymerization. Atom transfer radical polymerization in the presence of transition-metal complexes. J Am Chem Soc 117(20):5614–5615
45. Tsarevsky NV, Matyjaszewski K (2007) "Green" atom transfer radical polymerization: from process design to preparation of well-defined environmentally friendly polymeric materials. Chem Rev 107(6):2270–2299
46. Matyjaszewski K (2012) Atom transfer radical polymerization (atrp): current status and future perspectives. Macromolecules 45(10):4015–4039
47. Guo F, Jankova K, Schulte L, Vigild ME, Ndoni S (2010) Surface modification of nanoporous by atom transfer radical polymerization or click chemistry. Langmuir 26(3):2008–2013
48. Werne T, Patten TE (2001) Atom transfer radical polymerization from nanoparticles: a tool for the preparation of well-defined hybrid nanostructures and for understanding the chemistry of controlled/"living" radical polymerizations from surfaces. J Am Chem Soc 123(31):7497–7505
49. Wang J, Wang T, Li L, Wu P, Pan K, Cao B (2014) Functionalization of polyacrylonitrile nanofiber using ATRP method for boric acid removal from aqueous solution. Water Process Eng 3:98–104
50. Demirci S, Celebioglu A, Uyar T (2014) Surface modification of electrospun cellulose acetate nanofibers via RAFT polymerization for DNA adsorption. Carbohydr Polym 113:200–220

51. Dong Y, Yu P, Sun Q, Lu Y, Tan Z, Yu Z (2018) Grafting of MIPs from PVDF membranes via reversible addition-fragmentation chain transfer polymerization for selective removal of p-hydroxybenzoic acid. Chem Res Chin Univ 34:1051–1057
52. Wu XM, Wang LL, Wang Y, Gu JS, Yu HY (2012) Surface modification of polypropylene macroporous membrane by marrying RAFT polymerization with click chemistry. J Membr Sci 421–422:60–68
53. Herrera MU, Ichii T, Murase K, Sugimura H (2013) Photochemical grafting of methyl groups on a Si(111) surface using a grignard reagent. J Colloid Interf Sci 411:145–151
54. Zhang J, Yuan Y, Shen J, Lin S (2003) Synthesis and caracterization of chitosan grafted poly(N, N-dimethyl-N-methacryloxyethyl-N-(3-sulfopropyl) ammonium) initiated by ceric (IV) ion. Eur Polym J 39:847–850
55. Chua KN, Chai C, Lee PC, Ramakrishna S, Leong KW, Mao HK (2007) Functional nanofiber scaffolds with different spacers modulate adhesion and expansion of cryopreserved umbilical cord blood hematopoietic stem/progenitor cells. Exp Hematol 35(5):771–781
56. Chen S, Hao Y, Cui W, Chang J, Zhou Y (2013) Biodegradable electrospun PLLA/chitosan membrane as guided tissue regen-eration membrane for treating periodontitis. J Mater Sci 48:6567–6577
57. Chen SH, Chen CH, Shalumon KT, Chen JP (2014) Preparation and characterization of anti-adhesion barrier film from hyaluronic acid-grafted electrospun poly(caprolactone) nanofibrous membranes for prevention of flexor tendon postoperative peritendinous adhesion. Int J Nanomed 9(1):4079–4092
58. Lu PP, Xu ZL, Yang H, Wei YM (2012) Processing–structure–property correlations of polyethersulfone/perfluorosulfonic acid nanofibers fabricated via electrospinning from polymer–nanoparticle suspensions. ACS Appl Mater Interfaces 4:1716–1172
59. Jin SY, Kim MH, Jeong YG, Yoon I, Park WH (2017) Effect of alkaline hydrolysis on cyclization reaction of PAN nanofibers. Mater Des 124:69–77
60. Mei S, Xiao C, Hu X, Shu W (2011) Hydrolysis modification of PVC/PAN/SiO_2 composite hollow fiber membrane. Desalin 280(1–3):378–383
61. Razzaz A, Ghorban S, Hosayni L, Irani M, Alibadi M (2016) Chitosan nanofibers functionalized by TiO_2 nanoparticles for the removal of heavy metal ions. J Taiwan Inst Chem Eng 58:333–343
62. Nejad AG, Unnithan AR, Sasikala ARK, Samarikhalaj M, Thomas RG, Jeong YY, Nasseri S, Murugesan P, Wu D, Park CH, Kim CS (2015) Mussel-inspired electrospun nanofibers functionalized with size-controlled silver nanoparticles for wound dressing application. ACS Appl Mater Interfaces 7:12176–12183
63. Ma W, Samal SK, Liu Z, Xiong R, Smedt SC, Bhushan B, Zhang Q, Huang C (2017) Dual pH- and ammonia-vapor-responsive electrospun nanofibrous membranes for oil-water separations. J Membr Sci 537:128–139
64. Amarjargal A, Tijing LD, Shon HK, Park CH, Kim CS (2014) Facile in situ growth of highly monodispersed Ag nanoparticles on electrospun PU nanofiber membranes: flexible and high efficiency substrates for surface enhanced Raman scattering. Appl Surf Sci 308:396–401
65. Son HY, Ryu JH, Lee H, Nam YS (2013) Bioinspired templating synthesis of metal-polymer hybrid nanostructures within 3D electrospun nanofibers. ACS Appl Mater Interfaces 5:6381–6390
66. Zhou R, Liu W, Yao X, Leong YW, Lu X (2015) Poly(vinylidene fluoride) nanofibrous mats with covalently attached SiO_2 nanoparticles as an ionic liquid host: enhanced ion transport for electrochromic devices and lithium-ion batteries. J Mater Chem A 3:16040–16049
67. Zhang X, Ping M, Wu Z, Tang CY, Wang Z (2020) Microfiltration membranes modified by silver-decorated biomimetic silica nanopollens for mitigating biofouling: synergetic effects of nanopollens and silver nanoparticles. J Membr Sci 597:117773
68. Moghimifar V, Raisi A, Aroujalian A (2014) Surface modification of polyethersulfone ultrafiltration membranes by corona plasma-assisted coating TiO_2 nanoparticles. J Membr Sci 461:69–80

69. Prabaharan M, Grailer JJ, Pilla S, Steeber DA, Gong S (2009) Gold nanoparticles with a monolayer of doxorubicin-conjugated amphiphilic block copolymer for tumor-targeted drug delivery. Biomaterials 30:6065–6075
70. Cheng Y, Meyers JD, Broome AM, Kenney ME, Basilion JP, Burda C (2011) Deep penetration of a PDT drug into tumors by noncovalent drug-gold nanoparticle conjugates. J Am Chem Soc 133:2583–2591
71. Vijayan V, Uthaman S, Park IK (2018) Cell membrane-camouflaged nanoparticles: a promising biomimetic strategy for cancer the ragnostics. Polymers (Basel) 10:983
72. Peng S, Ouyang B, Men Y, Du Y, Cao Y, Xie R, Pang Z, Shen S, Yang W (2020) Biodegradable zwitterionic polymer membrane coating endowing nanoparticles with ultra-long circulation and enhanced tumor photothermal therapy. Biomaterials 231:119680
73. Miller M (2015) Coating matters|membrane process technology. http://www.pffc-online.com/coat-lam/12782. Accessed 7 Nov 2018
74. Morales-Torres S, Silva TLS, Pastrana-Martínez LM, Brandão ATSC, Figueiredo JL, Silva AMT (2014) Modification of the surface chemistry of single- and multi-walled carbon nanotubes by HNO_3 and H_2SO_4 hydrothermal oxidation for application in direct contact membrane distillation. Phys Chem Chem Phys 16:12237–12250
75. Fonouni M, Yegani R, Tavakkoli A, Mollazadeh S (2016) Investigating the effect of various oxidizing agents on the surface functionalization of microporous polypropylene membranes. J Text Polym 4(2):92–100
76. van Wagner EM, Sagle AC, Sharma MM, La YH, Freeman BD (2011) Surface modification of commercial polyamide desalination membranes using poly(ethylene glycol) diglycidyl ether to enhance membrane fouling resistance. J Membr Sci 367(1–2):273–287
77. Ouyang G, Hussain A, Li J, Li D (2015) Remarkable permeability enhancement of polyethersulfone (PES) ultrafiltration membrane by blending cobalt oxide/graphene oxide nanocomposites. RSC Adv 5:70448–70460
78. Xie W, Li J, Sun F, Dong W (2020) Ultrasonication favors TiO2 nano-particles dispersion in PVDF ultrafiltration membrane to effectively enhance membrane hydrophilicity and antifouling capability. Environ Sci Pollut Res Int 27(9):9503–9519
79. Gao Y, Hu M, Mi B (2014) Membrane surface modification with TiO_2-graphene oxide for enhanced photocatalytic performance. J Membr Sci 455:349–356
80. Ju J, Wang T, Wang Q (2015) Superhydrophilic and underwater superoleophobic PVDF membranes via plasma-induced surface PEGDA for effective separation of oil-in-water emulsions. Colloids Surf A Physicochem Eng Asp 481:151–157
81. Wu L, Sun J, Tong F (2014) Surface modification of a PVDF membrane by crosslinked collagen. RSC Adv 4(109):63989–63996
82. Shumskaya A, Kaniukov E, Yakimchuk D, Plisko T, Burts K, Bildyukevich A, Nikolaevich L, Kozlovskiy A, Zdorovets M (2019) Modified ion-track membranes for separation of biological objects. Mater Res Express 6(8):0850h3
83. Kim YJ, Yu QS, Deng BL (2009) Preparation and characterization of polyamide thin-film composite (TFC) membranes on plasma-modified polyvinylidene fluoride (PVDF). J Membr Sci 344:71–81
84. Gonzales RR, Park MJ, Tijing L, Han DS, Phuntsho S, Shon HK (2018) Modification of nanofiber support layer for thin film composite forward osmosis membranes via layer-by-layer polyelectrolyte deposition. Membranes (Basel) 8(3):70
85. Ngo THA, Nguyen DT, Do KD, Nguyen TTM, Mori S, Tran DT (2016) Surface modification of polyamide thin film composite membrane by coating of titanium dioxide nanoparticles. J Sci Adv Mater Devices 1(4):468–475
86. Khan A, Sherazi TA, Khan Y, Li SH, Naqvi SAR, Cui ZL (2018) Fabrication and characterization of polysulfone/modified nanocarbon black composite antifouling ultrafiltration membranes. J Membr Sci 554:71–82
87. Kusworo TD, Aryanti N, Firdaus MMM, Sukmawati H (2015) Surface modification of cellulose acetate membrane using thermal annealing to enhance produced water treatment. AIP Conf Proc 1699:040014

88. Kusworo TD, Arthatyanti N, Anggita RA, Setyorini TAD, Utomo DP (2017) Surface modification and performance enhancement of polyethersulfone (PES) membrane using combination of ultra violet irradiation and thermal annealing for produced water treatment. J Environ Sci Techno 10:35
89. Tomer N, Mondal S, Wandera D, Wickramasinghe SR, Husson SM (2009) Modification of nanofiltration membranes by surface-initiated atom transfer radical polymerization for produced water filtration. Sep Sci Technol 44(14):3346–3368
90. Li L, Yan G, Wu J (2009) Modification of polysulfone membranes via surface-initiated atom transfer radical polymerization and their antifouling properties. J Appl Polym Sci 111:1942–1946
91. Anuraj N, Bhattacharjee S, Geiger JH, Baker GL, Bruening ML (2012) An all-aqueous route to polymer brush-modified membranes with remarkable permeabilites and protein capture rates. J Memb Sci 389:117–125
92. Li D, Wu J, Yang S, Zhang W, Ran F (2017) Hydrophilicity and anti-fouling modification of polyethersulfone membrane by grafting copolymer chains via surface initiated electrochemically mediated atom transfer radical polymerization. New J Chem 41(18):9918–9930
93. Wang S, Li T, Chen C, Liu B, Crittenden JC (2018) PVDF ultrafiltration membranes of controlled performance via blending PVDF-g-PEGMA copolymer synthesized under different reaction times. Front Environ Sci Eng 12:3. https://doi.org/10.1007/s11783-017-0980-0
94. El-Arnaouty MB, Abdel Ghaffar AM, Eid M, Maysara E, Aboulfotouh ME, Taher NH, Soliman ES (2018) Nano-modification of polyamide thin film composite reverse osmosis membranes by radiation grafting. J Radiat Res Appl Sci 11(3):204–216
95. Ke X, Drache M, Gohs U, Kunz U, Beuermann S (2018) Preparation of polymer electrolyte membranes via radiation-induced graft copolymerization on poly(ethylene-alt-tetrafluoroethylene) (ETFE) using the crosslinker n,n-methylenebis (acrylamide). Membranes 8:102
96. Lv Y, Yu X, Tu ST, Yan J, Dahlquis E (2010) Wetting of polypropylene hollow fiber membrane contactors. J Membr Sci 362(1–2):444–452
97. Li Y, Wang L, Hu X, Jin P, Song X (2018) Surface modification to produce superhydrophobic hollow fiber membrane contactor to avoid membrane wetting for biogas purification under pressurized conditions. Sep Purif Technol 194:222–230
98. Li X, Cai T, Gl A, Chung TS (2017) Cleaning strategies and membrane flux recovery on anti-fouling membranes for pressure retarded osmosis. J Memb Sci 522:116–123
99. Li X, Cai T, Chen C, Chung TS (2016) Negatively charged hyperbranched polyglycerol grafted membranes for osmotic power generation from municipal wastewater. Water Res 89:50–58
100. Wang JH, Qing Y, Qing C (2009) Surface electrokinetic behavior of PVDF hollow fiber ultrafiltration membrane modified by low-temperature plasma method. Environ Sci Manag 34:54–57
101. Goh K, Setiawan L, Wei L, Jiang W, Wang R, Chen Y (2013) Fabrication of novel functionalized multi-walled carbon nanotube immobilized hollow fiber membranes for enhanced performance in forward osmosis process. J Membr Sci 446:244–254
102. Song H, Yu H, Zhu L, Xue L, Wu D, Chen H (2017) Durable hydrophilic surface modification for PTFE hollow fiber membranes. React Funct Polym 114:110–117
103. Zheng Z, Wang W, Huang X, Fan W, Li L (2018) Surface modification of polysulfone hollow fiber membrane for extracorporeal membrane oxygenator using low-temperature plasma treatment. Plasma Process Polym 15(1):1700122
104. Wan P, Bernards M, Deng B (2017) Modification of polysulfone (PSF) hollow fiber membrane (HFM) with Zwitterionic or charged polymers. Ind Eng Chem Res 56(26):7576–7584
105. Ifuku S, Suzuki N, Izawa H, Morimoto M, Saimoto H (2014) Surface phthaloylation of chitin nano fiber in a queous media to improve dispersibility in aromatic solvents and give thermo-responsive and ultraviolet protection properties. RSC Adv 4(37):19246–19250

106. Almasian A, Fard GC, Gashti MP, Mirjalili M, Shourijeh Z (2016) Surface modification of electrospun PAN nanofibers by amine compounds for adorption of anionic dyes. Desalin Water Treat 57(22):10333–10348
107. Bao Y, Lai Z, Zhu H, Fong C, Jiang C (2013) SERS-active silver nanoparticles on electrospun nanofibers facilitated via oxygen plasma etching. RSC Adv 3:8998–9004
108. Liao Y, Wang R, Fane AG (2013) Engineering superhydrophobic surface on poly(vinylidene fluoride) nanofiber membranes for direct contact membrane distillation. J Membr Sci 440:77–87
109. Yalcinkaya F, Yalcinkaya B, Pazourek A, Mullerova J, Stuchlik M, Maryska J (2016) Surface modification of electrospun pvdf/pan nanofibrous layers by low vacuum plasma treatment. Int J Polym Sci 2016:4671658
110. Yalcinkaya F, Siekierka A, Bryjak M (2017) Surface modification of electrospun nanofibrous membranes for oily wastewater separation. RSC Adv 89:56704
111. Zhang L, Shi X, Peng X, Chen BY, Kuang T (2014) Enhanced hydrophobicity of electrospun polyvinylidene fluoride-co-hexafluoropropylene membranes by introducing modified nanosilica, SPE ANTEC ® Anaheim 2017/586. ACS Appl Mater Interfaces 6(18):16035–16048
112. Lee CH, Chiang CL, Liu SJ (2013) Electrospun nanofibrous rhodanine/polymethylmethacrylate membranes for the removal of heavy metal ions. Sep Purif Technol 118:737–743
113. Yang W, Li R, Fang C, Hao W (2019) Surface modification of polyamide nanofiber membranes by polyurethane to simultaneously improve their mechanical strength and hydrophobicity for breathable and waterproof applications. Prog Org Coat 131:67–72
114. Xu Y, Sheng J, Yin X, Yu Z, Ding B (2017) Functional modification of breathable polyacrylonitrile/polyurethane/TiO_2 nanofibrous membranes with robust ultraviolet resistant and waterproof performance. J Colloid Interfaces Sci 508:508–516
115. Schaub NJ, Le Beux C, Miao J, Linhardt RJ, Alauzun JG, Laurencin D, Gilbert RJ (2014) The effect of surface modification of aligned poly-l-lactic acid electrospun fibers on fiber degradation and neurite extension. PLoS One 10(9):e0136780
116. Uzal N, Ates N, Saki S, Bulbul E, Chen YS (2017) Enhanced hydrophilicity and mechanical robustness of polysulfone nanofiber membranes by addition of polyethyleneimine and Al_2O_3 nanoparticles. Sep Purif Technol 187:118–126
117. Shen L, Feng S, Li J, Chen J, Li F, Lin H, Yu J (2017) Surface modification of polyvinylidene fluoride (PVDF) membrane via radiation grafting: novel mechanisms underlying the interesting enhanced membrane performance. Sci Rep 7:2721
118. Phan DN, Hasegawa Y, Song KH, Lee H, Kim IS (2018) Adsorption of silver ions from aqueous solution onto thiol modified polyvinyl alcohol nanofibers trends. Textile Eng Fashion Technol 1(5):4 pages
119. Wang Y, Górecki RP, Stamate E, Norrman K, Aili D, Zuo M, Guo W, Hélix-Nielsen C, Zhang W (2019) Preparation of super-hydrophilic polyphenylsulfone nanofiber membranes for water treatment. RSC Adv 9:278–286
120. Liao Y, Loh CH, Wang R, Fane AG (2014) Electrospun superhydrophobic membranes with unique structures for membrane distillation. ACS Appl Mater Interfaces 6(18):16035–16048
121. Pereao OK, Bode-Aluko C, Ndayambaje G, Fatoba O, Petrik LF (2017) Electrospinning: polymer nanofibre adsorbent applications for metal ion removal. J Polym Environ 25:1175–1189
122. Xiao S, Luo X, Peng Q, Deb H (2016) Effective removal of calcium ions from simulated hard water using electrospun polyelectrolyte nanofibrous mats. Fibers Polymers 17(9):1428–1437
123. Iijima S (1991) Helical microtubules of graphitic carbon. Nature 354(6348):56–58
124. Karousis N, Tagmatarchis N, Tasis D (2010) Current progress on the chemical modification of carbon nanotubes. Chem Rev 110(9):5366–5397
125. Sadegh H, Shahryari-ghoshekandi R (2015) Functionalization of carbon nanotubes and its application in nanomedicine: a review. Nanomed J 2(4):231–248
126. Mustafa A, Kusworo TD, Busairi A, Ismail AF, Budiyono (2012) Increasing the performance of PES-CNTs mixed matrix membrane using carbon nanotubes (CNTs) functionalization. Int J Waste Res 2(1):22–24

Chapter 5
Mechanism

5.1 Introduction

Gas separation through membranes can take place by different mechanisms. Three main diffusion mechanisms have been well-accepted to describe gas transport through membranes.

1. Knudsen diffusion (pore size is less than the free path of gas molecules).
2. Molecular sieving (molecular diffusion).
3. Solution-diffusion (sorption-diffusion).

In general, the diffusion mechanism is assumed to change from solution-diffusion to Knudsen diffusion with increase of the pore size in the membrane material. MMMs combine transport principles of both polymer and inorganic membranes, diffusion through them is understood via the solution-diffusion mechanism. This mechanism assumes that permeant molecules dissolve (adsorb) on one side of the membrane, diffuse across the membrane and then are released (desorbed) at the other side, as depicted in Fig. 5.1 for the CO_2/CH_4 separation [1]

Mixed matrix membranes (MMMs) are heterogeneous membranes consisting of inorganic fillers dispersed in a polymer matrix. In other words, they are organic–inorganic hybrids, so-called 'mixed matrix', materials comprising highly selective rigid phases, such as zeolites, dispersed in a continuous polymeric matrix. Currently MMMs are leading candidates for challenging membrane applications. This concept combines the advantages of each phase: high selectivity of the dispersed fillers, desirable mechanical properties, and economical process ability of polymers.

Consider the asymmetric MMMs depicted in Fig. 5.2, in which a flat configuration is shown in Fig. 5.2a while a hollow fiber configuration is shown in Fig. 5.2b. In both configurations, permeation occurs along the coordinate.

Theoretical predictions of the gas performance from the pure species permeation properties in MMMs become more and more important. Commonly, MMMs are

K. C. Khulbe, T. Matsuura, *Nanotechnology in Membrane Processes*, Lecture
Notes in Nanoscale Science and Technology 29,
https://doi.org/10.1007/978-3-030-64183-2_5

Fig. 5.1 Schematic representation of gas permeation through the solution-diffusion mechanism [1]

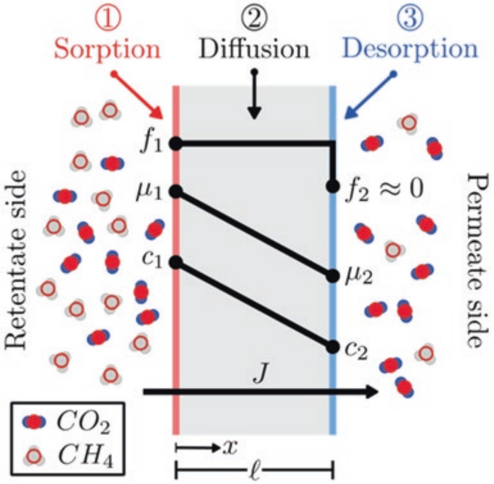

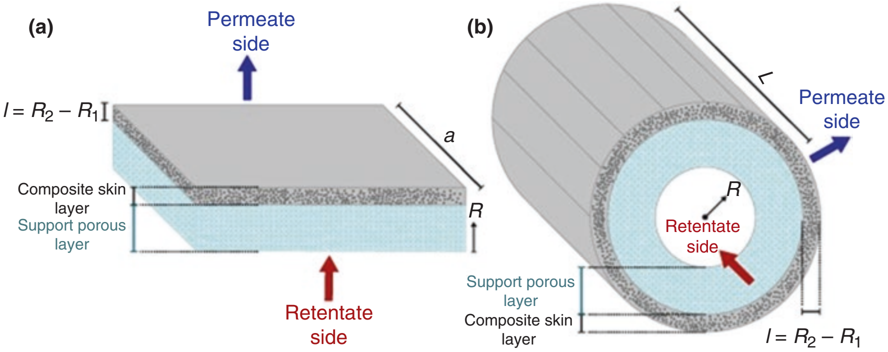

Fig. 5.2 Schematic representation of an asymmetric mixed-matrix membrane: (**a**) flat configuration, (**b**) hollow fiber configuration [44]

prepared either with (1) symmetric or (2) asymmetric structure. The symmetric MMMs consist of a uniform dense composite film (self-supported flat films), which is expected to provide both good mechanical properties, and, permeability and selectivity. On the other hand, asymmetric MMMs comprise a selective (composite) dense skin layer coated on a highly porous non-selective core layer. The non-selective support layer is expected to provide mechanical integrity, and the dense composite layer to offer the desired selectivity and permeability. Gas transport through a mixed-matrix membrane is a complicated problem. Different modeling attempts have been developed for the prediction of the performance of MMMs by various theoretical expressions depending on the MMM's morphology, and chemistry including ideal and nonideal MMMs [2].

5.2 Theory for MMMs for Gas Separation

Fabrication of ideal (defect free) MMMs in the laboratory is difficult due to the actual compatibility difference between the polymeric and the inorganic phases and higher tendency of the fillers for the formation of agglomerates, which results from weak polymer-particle adhesion. Hence, the presence of these interfacial defects severely affects the overall membrane performance properties. Mostly, interface defects can be categorized into three major cases namely; interfacial voids (sieves-in-a-cage), polymer rigidified chain layer near the molecular sieving particles, and partial pore blockage. Figure 5.3 shows the schematic diagram of various interface structure of MMMs.

From Fig. 5.3

Case 1 represents an ideal MMMs morphology where no defects are present at all.

Case 2 displays the poor adhesion of polymer chains from the molecular sieve surface, which causes the interface voids or sieves-in-a-cage.

Case 3 indicates the polymer chain rigidification in the vicinity of the molecular sieves.

Case 4 shows a condition in which the pore of molecular sieve has been partially blocked within the surface section of the molecular sieves.

5.2.1 *Interfacial Defects on Mixed Matrix Membranes (MMMs) for Gas Separation [3]*

The formation of an interfacial layer surrounding a filler particle during the fabrication of MMMs, however, often occurs. Poor adhesion, less mobility of polymer chains, and pore blockage by polymer matrix are some critical phenomena that are

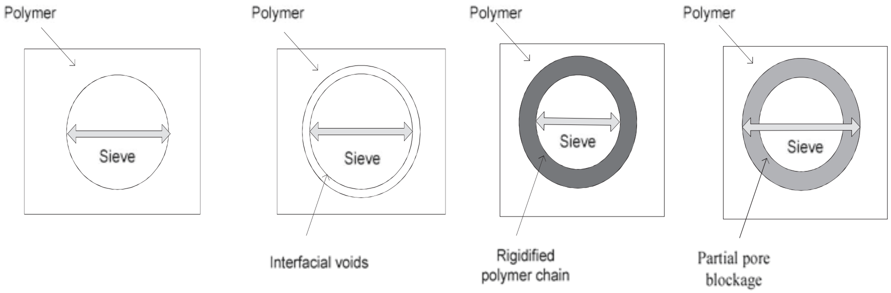

Case 1 Case 2 Case 3 Case 4

Fig. 5.3 Schematic representation of the interfacial structure of MMMs [3] often observed when dispersing filler particles into a polymer phase. The trend in the past decade has then shifted toward modeling these interfacial defects.

Poor adhesion at the polymer-molecular sieve interface, disruption of polymer packing near the inorganic phase, intermolecular repulsive force between the polymer matrix and the molecular sieve, difference in the thermal expansion coefficients between the polymer and the molecular sieve and the effects of stress are the most common causes for the formation of interfacial voids (Case 2) and rigidified polymer chain layer formation (Case 3). The formation of the two interface defects (Case 2 and 3) are most common when porous and nonporous molecular sieve are used as dispersed phases in MMMs. However, particle pore blockage (Case 4) is exceptional to porous fillers. In such cases, the molecular sieve pores are mostly blocked by solvents or some minor component of the feed gas or polymer. Depending on the extent of blockage of the molecular sieves or inorganic fillers, the process is mostly categorized as total and partial pore blockage.

The successful development of the MMMs depends on the judicious selection of polymer matrix and inorganic filler. The major challenge is to improve the poor contact or eliminate the interfacial defect between the two phases. This is still a very wide open area, as numerous pairs of polymers/inorganic fillers have been investigated [4]. Separation performance of MMMs depends on the physical structure and characteristic physical/chemical properties of the thin solid membrane. The strong or weak interaction between the penetrant and the membrane molecules, especially in the case of nonporous polymeric membranes, can decisively affect separation efficiency. The driving force of penetrant transport is chemical potential, which can generally be affected by concentration and pressure at a given temperature. Transport might be a complex process, especially in the case when there are strong interactions between the partner molecules, which even affects the structure properties of the membrane matrix; thus to establish the desired operating conditions transport also needs careful attention [5].

According to Suen [6] MMM can typically be divided into two categories:

1. With a dense structure. Mostly developed for the applications in gas separation, pervaporation, fuel cell, and so on. The fillers employed for improving the MMM performance in this category are usually inorganic nanomaterials (zeolite, carbon nanotube, metal organic framework, etc.) with specific features (shape, pore size, surface interaction, etc.).
2. With a porous structure. Specially designed for adsorption purpose. Micro-to-nano-size particles with functionality are regularly adopted as the fillers, to provide the adsorptivity with target solutes. The polymer matrix serves principally as the support of particles. On the other hand, membrane pores provide the pathways for solutes to pass through and then easily reach the adsorption sites on the filler particles. Their size is generally in the macropore range to avoid unwanted clogging and fouling.

Gas transport through a mixed matrix membrane is considered as complex phenomena. Due to its heterogeneity, a number of theoretical permeation models have been used to predict the permeation properties of mixed matrix (heterogeneous)

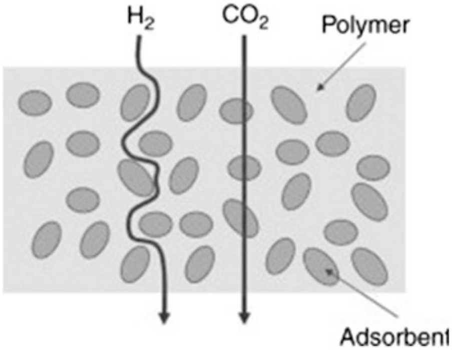

Fig. 5.4 Simplified representation for mixed-matrix membrane to have high CO_2/H_2 selectivity [4]

membranes as a function of the permeabilities of the continuous and dispersed phases [7]. MMMs, where inorganic fillers are dispersed at nanometer level in a polymer matrix, contain both promising selectivity benefits of the inorganic particles and economical processing capabilities of polymers. The presence of the solid particles modifies the polymer membranes through the following different effects:

1. increasing the sorption of gases (CO_2 etc.),
2. creating a barrier to reduce the permeability, especially for H_2,
3. disrupting the polymer structure, and hence its free volume and chain mobility,
4. improving the overall thermal and mechanical strength.

Figure 5.4 is a simplified diagram showing how MMMs can improve the selectivity of CO_2/H_2.

As discussed above, gas transport through a mixed-matrix membrane is a complicated problem. Different modeling attempts have been developed for the prediction of the performance of MMMs by various theoretical expressions depending on the MMM's morphology, and chemistry including ideal and nonideal MMMs [2]. For the purpose of prediction of gas permeance in MMMs, various permeation models have been used depending on the characteristic properties of continuous polymeric regime and the dispersed phase regime.

5.2.2 *Ideal Mixed Matrix Membrane*

Ideal MMM morphology is a two-phase system, which consists of inorganic fillers and polymer matrix with no defects and no distortion at the filler-polymer interface. A defect-free polymer−particle contact during the introduction of dispersed fillers in a polymer matrix is, however, difficult to achieve. The incorporation of filler particles can modify the properties of the neighbouring polymer phase, which affects the hybrid membrane separation performance [8]. The first mathematical studies of gas transport description through the MMMs concerned the ideal structure of these hybrid membranes, both their polymer matrix and the dispersed phase.

This theoretical two-phase morphology typically corresponds to the ideal Maxwell model. Maxwell model was mainly derived to represent thermal or electrical conductivity in composite media.

There are two main mechanisms of gas separation by membrane; the first is the separation by a membrane riddled with micropores (porous membrane), while the second mechanism occurs with a membrane that has no pores (nonporous membrane) [9]. They are well explained by the pore flow model and the solution–diffusion model, respectively. The solution–diffusion model explains that physical properties of a membrane, such as its rigidity, degree of cross linkage, and attractive forces between molecules of the constituent polymers, affect its gas permeability such that these properties are the primary factors that determine the rate at which a given gas molecule permeates the membrane. Permeation prediction models for MMMs have been developed to predict the effective permeability of a gaseous penetrant through these MMMs as a function of continuous phase (polymer matrix) and dispersed phase (porous or nonporous particles) permeabilities, as well as volume fraction of the dispersed phase. For a given penetrant (A), the permeability ($\mathrm{P_A}$) can be estimated as the product of diffusivity ($\mathrm{D_A}$) and solubility ($\mathrm{S_A}$).

$$\mathrm{P_A = D_A S_A} \tag{5.1}$$

The permselectivity, $\alpha_{\mathrm{A/B}}$, is the ideal ratio of permeabilities of the two components A and B:

$$\alpha_{\mathrm{A/B}} = \mathrm{P_A / P_B = D_A S_A / D_B S_B} \tag{5.2}$$

$\mathrm{P_{eff}}$ describes the effective steady-state permeability of a gaseous penetrant through a MMM. A minimum value of $\mathrm{P_{eff}}$ is calculated when a series two-layer model (series model) is applied:

$$P_{\mathrm{eff}} = \frac{P_{\mathrm{c}} P_{\mathrm{d}}}{\phi_{\mathrm{c}} P_{\mathrm{d}} + \phi_{\mathrm{d}} P_{\mathrm{c}}} \tag{5.3}$$

where ϕ_c and ϕ_d are the volume fraction of continuous and dispersed phase respectively.

A maximum value of P_{eff} is reached when both phases are assumed to diffuse through a parallel two-layer membrane (parallel model)

$$P_{eff} = P_c \phi_c + P_d \phi_d \tag{5.4}$$

where, $\phi_c = (1 - \phi_d)$.

Applying the Maxwell–Wagner–Sillar model, the P_{eff} of a MMM with a dilute dispersion of ellipsoids is given by the following expression;

$$P_{\mathrm{eff}} = P_{\mathrm{c}} \frac{nP_{\mathrm{d}} + (1-n)P_{\mathrm{c}} - (1-n)\phi_{\mathrm{d}}(P_{\mathrm{c}} - P_{\mathrm{d}})}{nP_{\mathrm{d}} + (1-n)P_{\mathrm{c}} + n\phi_{\mathrm{d}}(P_{\mathrm{c}} - P_{\mathrm{d}})} \tag{5.5}$$

Here, n is the particle shape factor. For prolate ellipsoids, where the longest axis of the ellipsoid is directed along the applied partial pressure gradient, 0 < n < 1/3. For oblate ellipsoids, that means the shortest axis of the ellipsoid is directed along the applied partial pressure gradient, 1/3 < n < 1. The limit of n = 0 leads to a parallel two-layer model and can be expressed as an arithmetic mean of the dispersed and continuous phase permeabilities (Eq. 5.4). At the limit of $n = 1/3$, Eq. (5.5) reduces to the following equation known as the original Maxwell equation with different expressions:

$$\begin{aligned} P_{\mathrm{eff}} &= P_{\mathrm{c}} \frac{P_{\mathrm{d}} + 2P_{\mathrm{c}} - 2\phi_{\mathrm{d}}(P_{\mathrm{c}} - P_{\mathrm{d}})}{P_{\mathrm{d}} + 2P_{\mathrm{c}} + \phi_{\mathrm{d}}(P_{\mathrm{c}} - P_{\mathrm{d}})} = \\ P_{\mathrm{c}} & \frac{2(1-\phi_{\mathrm{d}}) + \alpha(1+2\phi_{\mathrm{d}})}{(2+\phi_{\mathrm{d}}) + \alpha(1-\phi_{\mathrm{d}})} = P_{\mathrm{c}} \frac{1 + 2\phi_{\mathrm{d}}(\alpha-1)/(\alpha+2)}{1 - \phi_{\mathrm{d}}(\alpha-1)/(\alpha+2)} \end{aligned} \tag{5.6}$$

where $\alpha = P_d/P_c$.

The Bruggeman model was originally developed for the electric constant of particulate composites. It can be also adapted to estimate the permeability of MMMs as shown in following equation [10–12].

$$(P_{\mathrm{r}})^{1/3} \left(\frac{\alpha - 1}{\alpha - P_{\mathrm{r}}} \right) = (1-\phi_{\mathrm{d}})^{-1} \tag{5.7}$$

where, $P_{\mathrm{r}} = P_{\mathrm{eff}}/P_{\mathrm{c}}$.

This equation considers the effect of adding additional particles to a dilute suspension for a random dispersion of spherical particles. The Bruggeman model is an improvement over the basic Maxwell model for a larger range of ϕ_d; however, limitations similar to those of the basic Maxwell model are still obstacles in application. In addition, this model contains an implicit function that needs to be solved numerically.

The Böttcher formula and Higuchi models, originally applied to a random dispersion of spherical particles, are, respectively, expressed as follows [13, 14].

$$\left(1 - \frac{P_{\mathrm{c}}}{P_{\mathrm{eff}}}\right)\left(\alpha + 2\frac{P_{\mathrm{eff}}}{P_{\mathrm{c}}}\right) = 3\phi_{\mathrm{d}}(\alpha - 1) \tag{5.8}$$

$$P_{\mathrm{r}} = \frac{P_{\mathrm{eff}}}{P_{\mathrm{c}}} = 1 + \frac{3\phi_{\mathrm{d}}\beta}{1 - \phi_{\mathrm{d}}\beta - K_{\mathrm{H}}(1-\phi_{\mathrm{d}})\beta^2} \tag{5.9}$$

where, K_H is treated as an empirical constant and assigned a value of 0.78. β is useful to define the "reduced permeation polarizability" or a convenient measure of penetrant permeability difference between dispersed spheres and polymer matrix and given by,

$$\beta = \frac{\alpha - 1}{\alpha + 2} = \frac{P_d - P_c}{P_d + 2P_c} \tag{5.10}$$

This parameter is bounded by $-0.5 \le \beta \le 1$. The lower and upper limits correspond to totally nonpermeable and to perfectly permeable filler particles, respectively. Note that Eq. (5.8) is a second-order algebraic expression on P_{eff}. Therefore, like the Bruggeman model, a trial and error procedure is needed to estimate P_{eff} as a function of α and ϕ_d for the Böttcher formula.

For an elastic modulus of particulate composites, Lewis-Nielsen proposed the following formulae for predicting the effective permeability of MMMs [15, 16].

$$P_r = \frac{P_{\mathrm{eff}}}{P_c} = \frac{1 + 2\phi_d\left(\alpha - 1\right)/\left(\alpha + 2\right)}{1 - \psi\phi_d\left(\alpha - 1\right)/\left(\alpha + 2\right)} \tag{5.11}$$

where

$$\psi = 1 + \left(\frac{1 - \phi_m}{\phi_m^2}\right)\phi_d \tag{5.12}$$

and ϕ_m is the maximum filler volume fraction.

By considering the effect of particle morphology on permeability, this model might be representing a correct behavior of permeability over the range of $0 < \phi_d < m_e$. The relative permeability P_{eff} at $\phi_d = \phi_m$ is found to be, however, diverging when the permeability ratio $\alpha \to \infty$. Note that when $\phi_m \to 1$, the Lewis–Nielsen model reduces to the Maxwell equation.

A model proposed by Cussler is a form similar to the original Maxwell model applied to a dilute suspension of flake spheres [17], but considering a staggered array of high aspect ratio particles. The effective permeability of an ideal MMM is then expressed as follows.

$$P_{eff} = P_c \frac{1}{1 - \varnothing_d + 1/\left(\dfrac{P_d}{\varnothing_d P_c} + 4\dfrac{1 - \varnothing_d}{\propto_a^2 \varnothing_d^2}\right)} \tag{5.13}$$

where $\propto_a^2$ is the flake aspect ratio and ϕ_d is the volume fraction of flakes.

A generalized Maxwell model proposed by Petropoulous [18]. and extended by Toy and coauthors [19] to estimate the permeation properties of a binary structured composite, wherein the additive filler is randomly dispersed with sharp interfaces in a continuous polymer matrix, can be expressed as follows:

$$P_{\mathrm{eff}} = P_{\mathrm{c}}\left[1+\frac{(1+G)\phi_{\mathrm{d}}}{\left(\frac{P_{\mathrm{d}}/P_{\mathrm{c}}+G}{P_{\mathrm{d}}/P_{\mathrm{c}}-1}\right)-\phi_{\mathrm{d}}}\right] \tag{5.14}$$

where, G is a geometric factor accounting for the effect of dispersion shape. G equals to 1 for long and cylindrical (elongated) particles disposed transverse to the gas flow direction. G is 2 for spherical particles or isometric aggregates. In the case of planar (laminate) particles, G tends to become infinity if the dispersed particles are oriented in lamellae parallel to the gas flow direction, minimizing resistance to flow. On the other side, G tends to become zero if the dispersed particles are oriented in lamellae perpendicular to the gas flow direction, maximizing impedance of flow.

The Pal model, originally applied for thermal conductivity of particulate composites, was also adapted for prediction of permeability [20].

$$(K_r)^{1/3}\left(\frac{\lambda-1}{\lambda-K_r}\right)=\left(1-\frac{\phi}{\phi_m}\right)^{-\phi_m} \tag{5.15}$$

where K_r is relative thermal conductivity defined as K/K_c and λ is the thermal conductivity ratio defined as K_d/K_c (K, K_c and K_d are thermal conductivities of composite, continuous-phase(matrix), and dispersed-phase (filler), respectively.

Using the differential effective medium approach considering the packing difficulty of filler particles, this model also considers the effect of morphology as a function of the maximum packing volume fraction, ϕ_m, like the Lewis–Nielsen model. The Pal model, however, like the Bruggeman equation, should be solved numerically. Moreover, when $\phi_m \rightarrow 1$, the Pal model reduces to the Bruggeman model. Applied to an ideal morphology including a two-phase system (i.e., compatibility between fillers and polymer matrix with no defects and no distortion), the Pal model covers a wide range of ϕ ($0 < \phi < \phi_m$).

Gonzo et al. [21] presented an improved form of Maxwell's equation (the extended Maxwell equation) based on the hard-sphere model fluid proposed by Chiew and Glandt [22]. The model (GPG) proposed by Gonzo et al. based on the percolation theory, can describe the relation between composite permeability and filler concentration, as follows.

$$P_{\mathrm{r}} = \frac{P_{\mathrm{eff}}}{P_{\mathrm{c}}} = 1+3\beta\phi_{\mathrm{d}}+K\phi_{\mathrm{d}}^{2}+O(\phi_{\mathrm{d}})^{3} \tag{5.16}$$

where, K and O are the needed corrections of Maxwell expression. The coefficient K is a function not only of β (Eq. (5.9)) but also of ϕ (volume fraction of the dispersed phase).

$$K = a + b\phi^{3/2} \tag{5.17}$$

where 'a' and 'b' are functions of β.

In these equations, β is a convenient measure of penetrant permeability difference between the two phases. Like the Böttcher and Higuchi models, this parameter is bounded by $-0.5 \leq \beta \leq 1$. The second term represents the interaction between particles and polymer matrix, and the third term implies the interaction between these filler particles. At low values of particle loading ($\phi_d \ll 1$), GPG equations give the same results as the original Maxwell model. Compared with the original Maxwell model, the particle−polymer interfacial interaction is an additional issue, which is further considered in the GPG model.

Rybak et al. [8] proposed a modern computer application MOT (membrane optimization tool) for modeling of gas transport processes through mixed-matrix membranes (MMMs) based on the simplest Maxwell model. It can be successfully used to model the gas transport through the simplest types of hybrid membranes without any defects, consisting of two phases, organic and inorganic.

5.2.2.1 Non-ideal MMM

MMM should be considered as a three-phase system consisting of the polymer matrix, filler, and interfacial defects. For a nonideal MMM, interfacial defects affect the membrane performance and should be considered in prediction models. Interfacial defects can be classified into the following three major categories: (1) interfacial voids or sieves-in-a-cage, (2) rigidified polymer layer around the inorganic fillers, and (3) particle pore blockage. These defects are generally formed at the interfacial region between inorganic fillers and polymer matrix, namely, as an interphase.

Although existing theoretical models define the effective permeability well for binary MMMs with ideal contact between the two phases, they fail to predict the effective permeability of MMMs with nonideal morphologies [2, 23].

Funk and Lloyd reported a prediction model for microporous zeolite-filled MMMs, namely, ZeoTIPS membranes [24]. ZeoTIPS membranes, which are formed using the thermally induced phase separation (TIPS) process, consist of zeolite particles supported in a microporous polymer matrix. The model presented by Funk and Lloyd depends on the zeolite loading and the ratio of void volume to polymer volume in the membrane. Formation of a ZeoTIPS membrane begins with the suspension of zeolite particles in a homogeneous polymer–diluent solution at an elevated temperature. Upon cooling, diluent-rich liquid droplets form between the particles within a polymer-rich liquid phase. As the droplets continue to grow during the cooling of the liquid–liquid solution, they come in contact with the zeolite

Fig. 5.5 ZeoTIPS separation schematic for permeation of two species from the top to the bottom of the membrane is shown. The dashed lines represent the path of the larger component. The solid lines represent the path of the smaller component [24]

particles. Following solidification of the polymer-rich phase, extraction of the diluent, and evaporation of the volatile extractant, one is left with a structure in which the zeolite particles are held in place by the polymer and connected to the voids (represented schematically in Fig. 5.5). In Fig. 5.5 the clear circles represent the void spaces, the light grey squares represent zeolite particles, and the darker grey areas represent the polymer matrix. Figure 5.5 also shows the permeation paths of two species of different size, where permeation occurs from the top to the bottom of this schematic representation. The smaller component (represented by the solid line) can traverse the membrane through the void space and the zeolite particles, but the larger component (represented by the dashed line) is rejected near the upper surface of the ZeoTIPS membrane.

Funk–Lloyd model takes into account the zeolite loading as well as the ratio of void volume to polymer volume. In a non ideal ZeoTIPS membrane, a polymer layer of uniform thickness often coats the dispersed zeolites at the interfacial surface. The interfacial interaction between zeolite particles and polymer layer is assumed to be a good defect-free contact. In their report, different from a typical ideal MMM morphology including polymer and dispersed phases, an ideal ZeoTIPS structure is represented in terms of a mixture of three phase components in a parallel–series arrangement: polymer matrix, voids, and zeolite particles. As shown in Fig. 5.6a, the permeation molecules can pass through zones I and II in parallel pathways. In zone II, the gases cross through the void–zeolite–void sequence in series channel. However, as often reported in literature, the zeolite particles are often coated with a layer of polymer. Depending on the polymer–zeolite interaction, this interphase section has different effects on the permeation performance of MMMs. As shown in Fig. 5.6b, a more realistic nonideal ZeoTIPS MMM is depicted including the same two zones as in ideal ZeoTIPS morphology, except in zone II, the zeolite particles are coated with a polymer layer of uniform thickness. These polymer interphases are arranged in parallel and series pathways with the void–zeolite–void sequence.

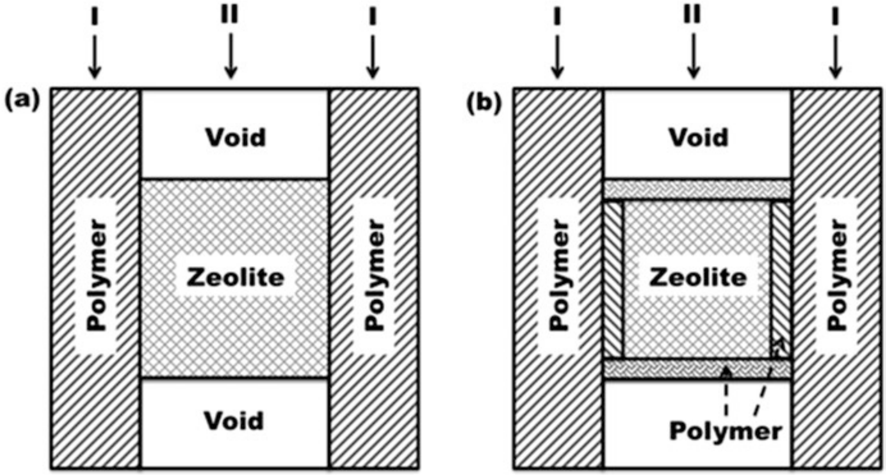

Fig. 5.6 (**a**) Ideal and (**b**) nonideal ZeoTIPS membrane [2]

As for the mathematical model for the nonideal MMM, the Felske [25] model, originally developed for thermal conductivity of composites of core–shell particles (core particle covered with an interfacial layer) was applied for permeability calculation.

$$P_{\mathrm{r}} = \frac{P_{\mathrm{eff}}}{P_{\mathrm{c}}} = \frac{2\left(1-\phi_{\mathrm{d}}\right)+\left(1+2\phi_{\mathrm{d}}\right)\beta/\gamma}{\left(2+\phi\right)+\left(1-\phi_{\mathrm{d}}\right)\beta/\gamma} \tag{5.18}$$

$$\beta = \left(2+\delta^{3}\right)\lambda_{d} - 2\left(1-\delta^{3}\right)\lambda_{i} \tag{5.19}$$

$$\Upsilon = 1+2\delta^{3} - \left(1-\delta^{3}\right)\lambda_{di} \tag{5.20}$$

where, δ is the ratio of outer radius of interfacial shell to a core radius. In this model, ϕ_d is the volume fraction of core−shell particles. For consideration of a single core−shell particle surrounded by a matrix material in the same volumetric proportion as in the whole composite, the ϕ_d is equal to the combined volume fractions of core−shell particle divided by its surrounded matrix material. P_d, P_i, and P_m are the permeabilities of filler core particle, interfacial shell, and polymer matrix, respectively. λ_{dm}, λ_{im}, and λ_{di} are the permeability ratios P_d/P_m, P_i/P_m, and P_d/P_i, respectively.

The Pal model [20], originally developed for thermal conductivity of particulate composites using the differential effective medium approach taking into consideration the packing difficulty of filler particles, can be adapted to permeability as:

$$\left(P_{r}\right)^{1/3}\left(\frac{\lambda_{d}-1}{\lambda_{d}-P_{r}}\right) = \left(1-\frac{\phi}{\phi_{M}}\right)^{-\phi_{M}} \tag{5.21}$$

where ϕ_M is the maximum packing volume fraction of filler particles, and λ_d is the ratio of dispersed filler permeability to the permeability of continuous polymer matrix.

Note that when $\phi_M \rightarrow 1$, the Pal model reduces to the Bruggeman model.

A modified Felske model was introduced by Pal [20, 25] as:

$$P_r = \frac{1+2\phi\left(\beta-\gamma\right)/\left(\beta+2\gamma\right)}{1-\psi\phi\left(\beta-\gamma\right)/\left(\beta+2\gamma\right)} \tag{5.22}$$

where P_r is the ratio of effective permeabilities of two competing gas penetrants, and 'ψ' denotes the parameter described as function of packing volume fraction of filler particle, The Felske model has the same limitations as that of the modified Maxwell model. It is valid only when the volume fraction of dispersed filler particles ϕ is small. The modified Felske model reduces to the Maxwell model when $\delta = 1$, that is, when the interfacial layer is absent. The Felske model has the same limitations as that of the modified Maxwell model. It is valid only when the volume fraction of dispersed filler particles ϕ is small.

Mahajan and Koros [26] developed the following equations for MMMs which contain filler phase, polymer phase and interface layer by using a two step method. In the first step, the Maxwell equation can be used to obtain the permeability of the combined interface rigidified layer and the filler in which the rigidified layer is the continuous phase and the filler is the dispersed phase. Thus, the permeability of the combined interface layer and filler phase is obtained as follows:

$$P_{eff} = P_I\left[\frac{P_d + 2P_I - 2\phi_s\left(P_I - P_d\right)}{P_d + 2P_I + \phi_s\left(P_I - P_d\right)}\right] \tag{5.23}$$

where P_{elf} is the permeability of the combined filler and interface layer phases, P_d is the permeability of the disperse phase, P_I is the permeability of the interface layer and φ_s is the volume fraction of the disperse phase in the combined filler and interface layer phase. φ_s can be calculated by using the following equation:

$$\phi_s = \frac{\phi_d}{\phi_d + \phi_I} \tag{5.24}$$

where ϕ_d and φ_i are the overall volume fractions in the membrane of the insert and the interphase, respectively.

At the second step, this calculated p_{eff} can be used with the continuous polymer phase permeability P_c to obtain a predicted permeability of P_{MMM}, using the following equation:

$$P_{MMM} = P_M\left[\frac{\left(P_{eff} + 2P_c - 2\left(\varphi_d + \varphi_I\right)\left(P_c - P_{eff}\right)\right)}{\left(P_{eff} + 2P_c + \left(\varphi_d + \varphi_I\right)\left(P_c - P_{eff}\right)\right)}\right] \tag{5.25}$$

One can model the three-phase (continuous, dispersed and interphase) MMM as a pseudo two-phase MMM with the continuous being one phase and the combined dispersed and interphase being the other phase (called combined phase hereafter) [27]. Models for these more complicated systems are based on 'nested applications' of the Maxwell or Lewis–Nielsen models.

The Hashemifard−Ismail−Matsuura (HIM) model is capable of predicting both permeability and selectivity through a nonideal MMM over a wide range of filler loadings. Hashemifard et al. [7] compared the accuracy of the model prediction for the MMM gas permeabilities. The models considered were: Maxwell model, modified Maxwell model, Lewis–Nielsen model, modified Lewis–Nielsen model and Felske model. The average relative errors, *% AARE*, between the experimental and predicted values were in the decreasing order of Lewis–Nielsen model > Maxwell model > modified Lewis–Nielsen model > modified Maxwell model > Felske model. This indicates that the most reliable model for predicting gas permeability in MMM is the Felske model. In another publication Hashemifard et al. [28] developed a new theoretical model based on resistance modeling approach to predict mixed matrix membrane (MMM) performance. The element of MMM is considered as a unit cell of body centered cubic (BCC). The network of permeation resistances is developed based on this unit cell. The unit cell of a BCC structure is a cube or a cuboid, containing eight particles in the corners and one particle in the centre (Fig. 5.7). As it is clear, seven other cubes from the neighboring unit cells share the particle in every corner. Therefore, every BCC unit cell has a net total of two particles per unit cell (8 × 1/8 + 1).

The newly developed model is based on the flow patterns of the permeant gas through the MMM element shown in Fig. 5.8 (series of parallel flow) and Fig. 5.9 (parallel of series flow).

In Fig. 5.8, the gas permeates progressively through zone III, consisting of continuous phase only, then through zone II, consisting of continuous and interphase as a parallel channel, and finally through zone I, consisting of continuous, interphase and dispersed phase as a parallel channel. After zone I, the flow through zones II and III is repeated before the gas leaves the MMM element. In Fig. 5.9, the gas permeates through zone III, consisting of continuous phase only, and through zone II, consisting of continuous and interphase as a series channel, as well through zone III, consisting of continuous, interphase and dispersed phase as a series channel. The flow through each zone is parallel to each other. The flows through different zones are finally combined before leaving the MMM element.

The main parameters involved in the model prediction are dispersed filler loading, polymer matrix permeability, dispersed filler permeability, interphase permeability and interphase thickness, as follows [7].

$$P_{\mathrm{r}} = \left[1 + \phi_{\mathrm{II}} \left(\frac{1}{\phi_{\mathrm{iII}} \left(\lambda_{\mathrm{i}}^{u} - 1 \right) + 1} - 1 \right) + \phi_{\mathrm{I}} \left(\frac{1}{\phi_{\mathrm{dI}} \left(\lambda_{\mathrm{d}}^{u} - 1 \right) + \phi_{\mathrm{iI}} \left(\lambda_{\mathrm{i}}^{u} - 1 \right) + 1} - 1 \right) \right]^{-u} \tag{5.26}$$

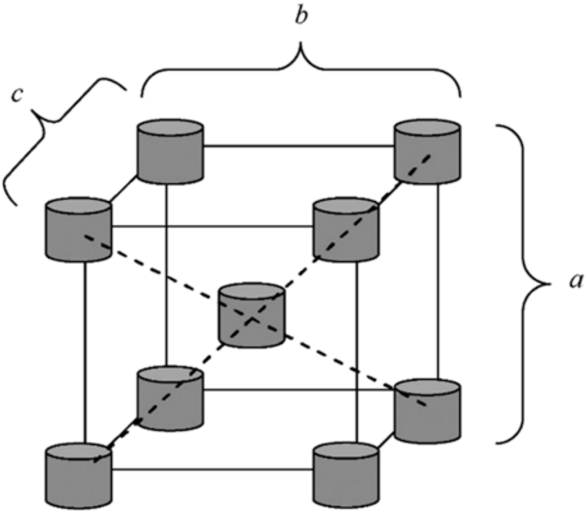

Fig. 5.7 Unit cell of BCC structure considered for particle distribution in MMM [7]

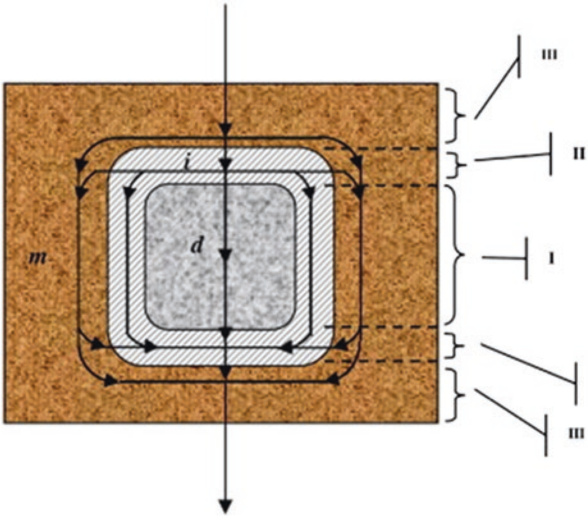

Fig. 5.8 Penetrant gas flow path through MMM element for void in MMM morphology [7]

where λ_i and λ_d are, respectively, P_i/P_m and P_d/P_m, which are the ratios of interphase permeance and dispersed phase permeance to the permeance of the continuous phase. ϕ_{I}, ϕ_{II} and ϕ_{III} represents the volume fractions of zones I, II and III in the entire MMM element.

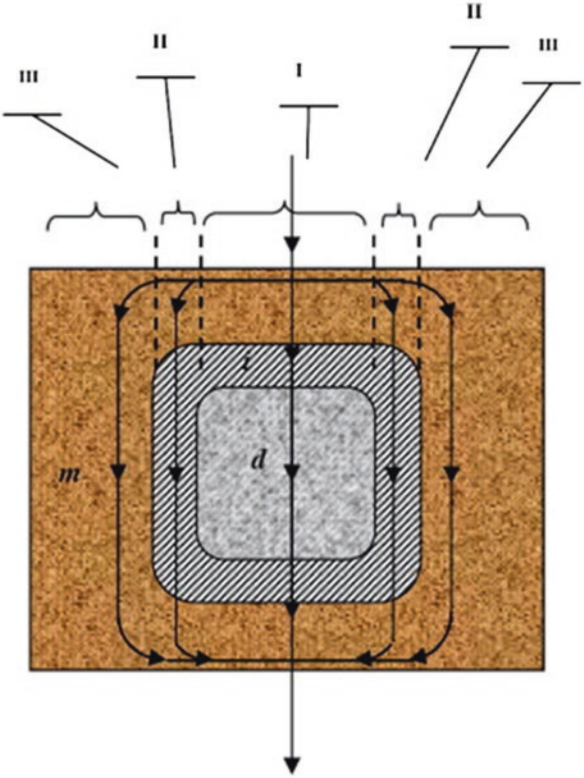

Fig. 5.9 Penetrant gas flow path through MMM element for rigidified MMM morphology [7]

The results generated from the proposed model have been verified using seven cases through the published experimental data.

Monsalve-Bravo and Bhatia [29] proposed a theory for estimation of the effective permeability of pure gases in flat mixed-matrix membranes (MMMs), in which effective medium theory (EMT) is extended to systems with finite filler size and membrane thickness. The new theory for the permeation of pure gases in flat mixed-matrix membranes, considering nonuniformity of the filler fraction in finite sized membranes. The mixed-matrix membrane flux, estimated through EMT, satisfies the transport equation for the composite, while using a position-dependent local permeability (diffusivity); this leads the MMM permeability to be dependent on the filler particle size and the membrane thickness. The effective MMM permeability (P_m) may be estimated from the steady state flux in the membrane,

$$P_m = \frac{\ell\left[-\mathcal{D}_m(x)\frac{dC_b^m}{dz}\right]}{RT\left(C_{b_1}-C_{b_2}\right)} = \frac{J_x\ell}{RT\left(-\Delta C_b\right)} \tag{5.27}$$

Where, C^b_m pseudo-bulk concentration, D_m local diffusivity of the mixed-matrix membrane, l flat mixed matrix membrane of finite thickness, J_x flux through the MMM

5.2.3 MMMs Containing Nanotubes

Chehrazi et al. [30] proposed gas permeation behavior of nanotube-containing mixed matrix membranes (nanotube–MMMs). Two new parameters, "interfacial thickness" (a_{int}) and "interfacial permeation resistance" (R_{int}), are introduced to account for the role of nanotube/matrix interfacial interactions in the proposed model. The obtained values of a_{int}, independent of the nature of the permeate gas, increased by increasing both the nanotubes aspect ratio and polymer–nanotube interfacial strength. Chehrazi et al. proposed the following equation for the effective gas permeation through a nonideal nanotube–MMM.

$$\frac{P_{\text{eff}}}{p_{\text{m}}} = \frac{3+\varphi\left(\frac{2\left(d/a_{int}-1\right)}{d/a_{int}+1}+\frac{P_{NT}/P_{\text{m}}}{1+\frac{2a_{int}}{1}\frac{P_{NT}}{P_{\text{m}}}}+\frac{L}{a_{int}}-1\right)}{3-\varphi\frac{2\left(d/a_{int}-1\right)}{d/a_{int}+1}} \tag{5.28}$$

where P_{eff}, P_{m}, and P_{NT} are the gas permeability coefficients of the MMM, matrix, and nanotube, respectively. Also, φ represents the volume fraction of nanotubes. The parameter a_{int} is introduced as the "interfacial thickness", in analogy with the Kapitza radius in thermal conductivity:

$$\alpha_{\text{int}} = R_{\text{int}}P_m \tag{5.29}$$

In fact, the value of a_{int} is the thickness of the interfacial region that connects chemically or mechanically the nanotubes and the matrix phases and plays a crucial role in the entire properties of composites.

Hamilton and Crosser [31] developed a model for the prediction of effective thermal conductivity of a tubular filler-containing composite, which can also be used for prediction of gas permeation of a NT-MMMs on the basis of analogy between heat and mass transfer phenomena.

$$\frac{P_{\mathrm{eff}}}{P_{\mathrm{m}}}=\frac{P_{\mathrm{f}}+5P_{\mathrm{m}}-5\varphi\left(P_{\mathrm{m}}-P_{\mathrm{f}}\right)}{P_{\mathrm{f}}+5P_{\mathrm{m}}+\varphi\left(P_{\mathrm{m}}-P_{\mathrm{f}}\right)} \tag{5.30}$$

where P_{eff} is the effective gas permeability of the MMM, P_{m} and P_{f} are gas permeabilities of the polymer matrix and nanotubes, respectively, and φ is the volume fraction of nanotubes.

Kang et al. [32] proposed an equation, known as the KJN model, based on the parallel-series resistance model to predict the gas permeability of MMMs with tubular fillers.

$$\frac{P_{\mathrm{eff}}}{P_{\mathrm{m}}}=\left[\left(1-\frac{\cos\theta}{\cos\theta+\frac{1}{\alpha}\sin\theta}\varphi\right)+\frac{P_{\mathrm{m}}}{P_{\mathrm{f}}}\left(\frac{1}{\cos\theta+\frac{1}{\alpha}\sin\theta}\right)\varphi\right]^{-1} \tag{5.31}$$

where α and θ are the aspect ratio and the orientation angle of tubular fillers. P_{eff} is the effective gas permeability of the MMM, P_{m} and P_{f} are gas permeabilities of the polymer matrix and fillers, respectively, and φ is the volume fraction of nanotubes in the polymer matrix (the ratio of the outside volume of the nanotubes to the overall volume of the polymer matrix).

The above mentioned models predict the gas permeability of NT-MMMs as a function of gas permeability of matrix, gas permeability of nanotube and volume fraction of fillers. These models have been derived based on the assumption of an ideal NT/matrix interface (ideal MMM), ignoring the effects of interfacial characteristics.

Chehrazi et al. [33] developed a new theoretical model to predict the gas permeation behavior of mixed matrix membranes containing nanotubes (NT-MMMs). The proposed model explored the role of nanotube/matrix interface, by introducing the interfacial layer thickness parameter. The procedure for developing the new mHC model is described as follows: First, a mixed matrix membrane containing nanotubes is considered as a two-phase system (Fig. 5.10).

One phase is the pseudo-dispersed phase that consists of nanotubes surrounded by interface voids dispersed in the second phase i.e., the polymer matrix. Then, the Hamilton-Crosser (HC) model is used to calculate the gas permeability of the pseudo-dispersed phase, assuming the nanotube as the dispersed phase and the interface layer as the continuous phase. Finally, the overall gas permeability of the NT-MMMs is calculated by the developed modified Hamilton-Crosser (mHC) model as follows:

$$\frac{P_{\mathrm{eff}}}{P_{\mathrm{m}}}=\frac{P_{\mathrm{ps}}+5P_{\mathrm{m}}-5\left(\varphi_{\mathrm{NT}}+\varphi_{\mathrm{int}}\right)\left(P_{\mathrm{m}}-P_{\mathrm{ps}}\right)}{P_{\mathrm{ps}}+5P_{\mathrm{m}}+\left(\varphi_{\mathrm{NT}}+\varphi_{\mathrm{int}}\right)\left(P_{\mathrm{m}}-P_{\mathrm{ps}}\right)} \tag{5.32}$$

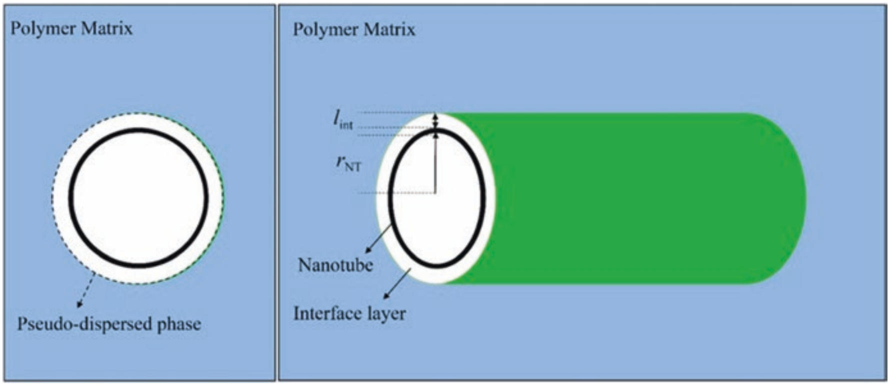

Fig. 5.10 Schematic of a nanotube with radius r_{NT} surrounded by a thin interface layer with thickness l_{int} embedded in a polymer matrix [33]

where P_{eff} and P_m are the effective gas permeability of the MMM and gas permeability of the matrix, respectively. P_{ps}, P_{NT} and P_{int} are the gas permeability of the pseudo-dispersed phase, gas permeability of nanotubes and gas permeability of interface layer, respectively. φ_{NT} and φ_{int} are the volume fractions of nanotubes and interface layer around nanotubes, respectively.

KJN and HC models were developed to explore the gas permeation behavior through MMMs by accounting two-phase systems i.e. continuous phase (polymer matrix) and the dispersed phase (MWCNTs fillers particles) and ignored the influence of the interfacial layer. Saqib et al. [34] developed a new model based on the KJN model to predict the gas permeability behavior through MMMs more precisely by incorporating the influence of their most significant phase which is known as the pseudo-dispersed phase.

$$P_{eff} = \frac{\varphi_{NT}}{\varphi_{NT} + \varphi_v + \varphi_p} P_{eff,d} + \frac{\varphi_v}{\varphi_{NT} + \varphi_v + \varphi_p} P_{eff,v} + \frac{\varphi_p}{\varphi_{NT} + \varphi_v + \varphi_p} P_{eff,p} \quad (5.33)$$

where $P_{eff,d}$ denotes the effective permeability of a gas through an ideal composed MMMs based on MWCNTs filler and polymer matrix. $P_{eff,v}$ denotes the effective permeability of the interfacial voids in MMMs based on voids and polymer matrix. $P_{eff,p}$ denotes the effective permeability of a gas through a pinhole MMMs based on MWCNTs filler and polymer matrix. The φ_{NT}, φ_v, and φ_p denote the volume fractions of the MWCNTs fillers, interfacial void, and pinholes, respectively. The new proposed theoretical model is able to estimate the gas permeability behavior with significantly reduced average absolute relative error (%AARE) of 1.26% compared to 52.43% and 42.71% for unmodified KJN and HC models, respectively.

It is normal to ignore the interfacial characteristics of the tubular filler particles i.e. multi-walled structured carbon nanotubes (MWCNTs) and a matrix composed of polymeric material, especially, in the Kang-Jones-Nair (KJN) model and Hamilton-Crosser model (HC).

5.3 Modeling of Reverse Osmosis

Water flux through the membrane is a function of the water permeability coefficient, the hydrodynamic pressure difference and osmotic pressure across the membrane. The solute flux through the membrane is a function of the solute permeability constant and the solute concentration gradient across the membrane. Reverse osmosis uses a large pressure difference across the membrane to separate water from salt solutions. In RO, the important driving forces are pressure and concentration gradients for the permeation flux of solvent and solute, respectively. The solute and solvent transport equations in a reverse osmosis membrane are described by the irreversible thermodynamics. Concentration polarization and fouling of the membrane are the two serious problems that would prevent the use of RO into many of the processes. Concentration polarization may be defined as the presence of a higher concentration of rejected species, at the surface of a membrane than in the bulk solution, due to the convective transport of both solute and solvent. The fouling in the membrane is the condition, in which membrane undergoes plugging or coating by some element in the stream being treated, in such a way that its output or its flux is reduced. Prediction of the performance of any membrane system involves prediction of the process throughput, which is related to the permeate flux (J) and the permeate quality (represented by the concentration in the permeate or the observed retention).

In membrane science and technology, concentration polarization refers to the emergence of concentration gradients at a membrane/solution interface resulted from selective transfer of some species through the membrane under the effect of transmembrane driving forces [35]. Generally, the cause of concentration polarization is the ability of a membrane to transport some species more readily than the other(s) (which is the membrane permselectivity): the retained species are concentrated at the upstream membrane surface while the concentration of transported species decreases. Thus, concentration polarization phenomenon is inherent to all types of membrane separation processes. In the cases of gas separations, pervaporation, membrane distillation, reverse osmosis, nanofiltration, ultrafiltration, and microfiltration separations, the concentration profile has a higher level of solute nearest to the upstream membrane surface compared with the more or less well mixed bulk fluid far from the membrane surface.

The solute and solvent transport equations in a reverse osmosis membrane are described by the irreversible thermodynamics. One of the concepts of IT (Irreversible thermodynamics) is that the system may be partaged into a small subsystem in which local equilibrium may occur and consequently thermodynamic quantities may be formulated for these subsystems. For systems that are not too distant from equilibrium, IT proposes logical formulas between forces and fluxes [36]. Various

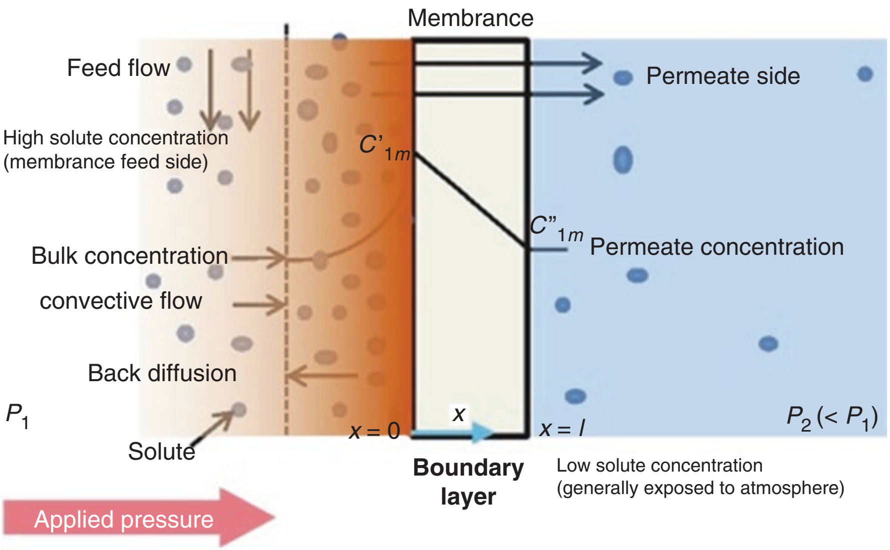

Fig. 5.11 Thermodynamic principle of reverse osmosis [37]

models and mechanism for the solvent and solute transport through reverse osmosis membrane have been developed and proposed by a number of investigator [37]. There are several models used to calculate the permeate flux using the osmotic pressure model [38].

The solute and solvent transport equations in a reverse osmosis membrane are described by the irreversible thermodynamics. A general description of the reverse osmosis process is shown in Fig. 5.11.

5.3.1 Solution-Diffusion (SD) Model

The solution-diffusion model assumes that the pressure within a membrane is uniform and that the chemical potential gradient across the membrane is expressed only as a concentration gradient.

SD model is based on the assumption that the solute and solvent primarily dissolve in the dense skin film of a membrane and after that diffuse across the membrane; consequently, the solubility's and diffusivities of the solution component are of great significance.

Onsager proposed that the fluxes and forces may be formulated by the following linear equations [39, 40].

$$J_i = L_{ii}F_i + \sum_{i \neq j} L_{ij}F_j; \qquad i = 1, n \tag{5.34}$$

where the fluxes, J_i, are linked to the forces, F_j, by the phenomenological coefficients, *Lij*. For membrane systems, the driving forces may be linked to the pressure and concentration differences through the membranes, and the fluxes are solvent and solute permeate fluxes. Equation (5.34) may be made easier to understand by supposing that cross coefficients are the same [39].

$$L_{ij} = L_{ji} \qquad for\, i \neq j \tag{5.35}$$

The above Onsager reciprocal relationship (ORR), Eq. (5.34), is acceptable if the system is near equilibrium, the linear laws (i.e., Eq. (5.34)) are acceptable, and the exact selection of fluxes and forces has been performed. For systems that are distant from equilibrium, as is frequently the situation in RO, Eq. (5.34) may not be exact.

Sherwood et al. enlarged the SD model by supposing some imperfections, or holes, on the membrane surface film which participate to the pore flow of solute and solvent, which is famous as the Solution-Diffusion-Imperfection model [36, 41]. Within the scope of this model the membrane is considered as a parallel connection of a perfect matrix having the solution- diffusion mechanism of solute transport and of imperfections where solutes are convectively transported without change of concentration. The corresponding transport equations usually are written as

$$J_\mathrm{v} = L_\mathrm{m}\left(\Delta p - \Delta \pi\right) + L_\mathrm{i}\Delta p \tag{5.36}$$

$$J_\mathrm{s} = P_\mathrm{m}\left(c_o - c_p\right) + L_i c_o \Delta p \tag{5.36}$$

where c_o and c_p are the solute concentrations in the feed and permeate; L_m and L_i are the partial mechanical permeabilities of the matrix and imperfections; J_v, and J_s are the volume and solute fluxes; P_m is the partial diffusional permeability of the matrix.

5.3.1.1 Spielger–Kedem (Kedem–Katchalsky) Model

This model describes water flux and solute flux as follows [42].

$$J_v = -A\left(\frac{dP}{dx} - \sigma \frac{d\pi}{dx}\right) \tag{5.38}$$

$$J_s = -B\frac{dC}{dx} + \left(1-\sigma\right)J_w \bar{C} = J_v C_p \tag{5.40}$$

The permeate flux (J_v) is dictated by both the hydraulic pressure (P) and osmotic pressure (π) gradient. The effect of the osmotic pressure difference is corrected by a theoretical reflection coefficient (Staverman reflection coefficient) that represents the correction for non-ideality in a semi-permeable membrane. For an ideal semi-permeable membrane, which passes water but has 100% rejection of solutes $\sigma = 1$; while for a completely non-selective porous membrane, $\sigma < 1$. The solute flux (J_s)

combines the contribution of a diffusion term (embedded in the solute permeance, *B*) as well as the convection of bulk solution.

Chen et al. [43] developed a mathematical modeling of glucose–water separation through a reverse osmosis (RO) membrane. The model was developed by coupling the concentration–polarization (CP) model, which uses one-dimensional flow assumption, with the irreversible thermodynamic Spiegler–Kedem model, and was exactly the same as Sherwood's model

$$J_v = L_p\left[\Delta p - \sigma RT\left(C_f - C_p\right)\left\{\left(R_r\left(1-R_o\right)\right)/R_o\left(1-R_r\right)\right\}\right] \tag{5.41}$$

where J_w solvent (pure water) flux, Δp Trans membrane pressure différences, σ reflection coefficient, C_p permeate solution concentration, C_f feed solution concentration, *R* universal gas constant, R_o membrane rejection fraction/real rejection fraction, R_r real rejection fraction, *T* absolute température.

Jamal et al. [36] developed a simulation model and verified for a small-scale reverse osmosis system. The proposed model combines material balances on the feed tank, membrane module and product tank with membrane mass transfer models. The model developed by Jamal et al. [36] depicts the ideal mass transfer, but does not include the concentration polarization and fouling of the membrane, which causes the significant decline in the solvent flux.

The equation of the model suggested by Jamal et al. [36] is as follows:

$$\partial C_{ty}/\partial t = \theta - \left\{U_b\left(C_b - C_p\right)/\delta\right\}\tau\exp\left[\tau\left(y/\delta\right)\right] \tag{5.42}$$

C_{ty} Concentration as a function of time and space, kg m^{-3}, t Time, h, U_b BuIk feed velocity, m h^{-1}, C_b Solute concentration in bulk flow, kg m^{-3}, C_p Solute concentration in permeate, kg m^{-3}, δ Thickness of the boundary layer, m, y Space coordinate, m

All of the above RO models were developed for a single phase membrane. The development of mathematical models for MMMs is called for.

5.4 Glossary of Model Designation

Table 5.1 shows the glossary of model designation [2]

5.5 Summary

Future of the mixed-matrix membrane is dependent on the development of new classes of inorganic particles and polymer materials. As for the inorganic particles, their shapes have a considerable effect in the MMM performance. This aspect has

Table 5.1 Glossary of model designation

Series	Two-layer MMM model with series combination
Parallel	Two-layer MMM model with parallel combination
Maxwell−Wagner−Sillar	Developed for a MMM with dilute dispersion of ellipsoids
Maxwell	Developed by Maxwell for a MMM with dilute suspension of spherical particles at low loadings
Bruggeman	Developed by Bruggeman for the electric constant of particulate composites
Bőttcheř	Developed by Bőttcher for a random dispersion of spherical particles
Higuchi	Developed by Higuchi for a random dispersion of spherical particles
Lewis−Nielsen	Developed by Lewis and Nielsen for an elastic modulus of particulate composites
Cussler	Proposed by Cussler with a form similar to the original Maxwell model applied to a dilute suspension of flake spheres
Generalized Maxwell	A generalization of the original Maxwell model proposed by Petropoulous and extended by Toy and coauthors for binary structured composites
Pal	Developed by Pal for thermal conductivity of particulate composites
Gonzo−Parentis−Gottifredi	An extension of the original Maxwell model in terms of φ_d proposed by Gonzo, Parentis, and Gottifredi
Funk−Lloyd	Developed by Funk and Lloyd for microporous zeolite-filled Zeo TIPS membranes
Kang−Jones−Nair	Developed by Kang, Jones, and Nair for an ideal composite membrane with tubular fillers
Modified Maxwell	A modification of the original Maxwell model proposed by Mahajan and Koros and extended by Li and coauthors in order to take into account interfacial defects
Felske	Developed by Felske for thermal conductivity of composites of core−shell particles
Modified Felske	A modification of the Felske model proposed by Pal for a composite morphology with packing density of particles
Hashemifard−Ismail−Matsuura	Developed by Hashemifard, Ismail, and Matsuura for MMMs based on the flow pathways of penetrant gas in both series and parallel channels
Modified Pal	A modification of the Pal model by Shimekit and co-authors in order to take into account interfacial rigidified polymer chain defect
Monsalve-Bravo-Bhatia	Extended effective medium theory (EMT) by Monsalve-Bravo-Bhatia to composite hollow fiber mixed matrix membranes
Rybak-Rybak-Sysel	Proposed a modern computer application MOT (membrane optimization tool) by Modeling of Gas Permeation for modeling of gas transport processes through mixed-matrix membranes (MMMs) which was based on the simplest Maxwell model
Chehrazi- Raef-Noroozi-Panahi-Sarmad	A theoretical model for the gas permeation prediction of nanotube-mixed matrix membranes: Unveiling the effect of interfacial layer

not yet been thoroughly investigated. As for the inorganic particles dispersed in the continuous polymer phase, two groups of theoretical models have been written, depending on the interaction between the continuous and dispersed phases. In the so-called ideal interface morphology, the interfacial layer contains no defects and no distortion and its thickness is considered zero. Numerous research groups have performed many examples of using the original Maxwell and Bruggeman models to predict the permeation behavior of several kinds of MMMs. The formation of an interfacial layer surrounding a filler particle during the fabrication of MMMs, however, often occurs. Poor adhesion, less mobility of polymer chains, and pore blockage by polymer matrix are some critical phenomena that are often observed when dispersing filler particles into a polymer phase. The trend in the past decade has then shifted toward modeling these interfacial defects.

Regarding reverse osmosis, only few works have been done especially for the prediction of MMM performance. This is considered as one of the challenging fields of the future.

References

1. Monsalve-Bravo GM, Bhatia SK (2018) Modeling permeation through mixed-matrix membranes: a review. Processes 6:172. https://doi.org/10.3390/pr6090172
2. Vinh-Thang H, Kaliaguine S (2013) Predictive models for mixed-matrix membrane performance: a review. ACS Chem Rev 313:4980–5028
3. Shimekit B, Shariff A, Mukhtar H, Bustam A, Elkhalifah AEI, Ullah S, Riaz N (2014) Interfacial defects on mixed matrix membranes and mitigation techniques for gas separation: a review. Appl Mechan Mater 625:653–656
4. Doong SJ (2012) Separation in functional materials for sustainable energy applications. In: Functional materials for sustainable energy applications, Woodhead Publishing Series in Energy, pp 179–216
5. Nagy E (2019) Chapter 18. Basic equations of mass transport through a membrane layer, 2nd edn. In: Membrane gas separation, Elsevier, pp 457–481
6. Suen SY (2015) Mixed matrix membranes for adsorption application. J Chem Eng Process Technol 6:1. https://doi.org/10.4172/2157-7048.1000e119
7. Hashemifard SA, Ismail A, Matsuura T (2010) Prediction of gas permeability in mixed matrix membranes using theoretical models. J Membr Sci 347(1–2):53–61
8. Rybak A, Rybak A, Sysel P (2018) Modeling of gas permeation through mixed-matrix membranes using novel computer application MOT. Appl Sci 8:1166. https://doi.org/10.3390/app8071166
9. Jeon YW, Lee DS (2015) Gas membranes for CO_2/CH_4 (biogas) separation: a review. Environ Eng Sci 32(2):71–85
10. Bruggeman DAG (1935) Berechnung verschiedener physikalischer konstanten von heterogenen substanzen. i. dielektrizitatskonstanten und leitfahigkeiten der mischkorper aus isotropen substanzen. Ann Phys 24:636–679
11. van Beek LKH (1967) Dielectric behaviour of heterogeneous mixtures. Prog Dielectr 7:69–114
12. Bánhegyi G (1986) Comparison of electrical mixture rules for composites. Colloid Polymer Sci 264:1030–1050
13. Bottcher CJF (1945) The dielectric constant of crystalline powders. Recueil des Travaux Chimiques des Pays-Bas 64:47–51

14. Higuchi WI, Higuchi T (1960) Theoretical analysis of diffusional movement through heterogeneous barriers. J Am Pharm Assoc Sci Ed 49:598
15. Lewis L, Nielsen LE (1970) Dynamic mechanical properties of particulate-filled composites. J Appl Polym Sci 14:449–1471
16. Nielsen LE (1973) Thermal conductivity of particulate-filled polymers. J Appl Polym Sci 17:3819–3820
17. Cussler E (1990) Membranes containing selective flakes. J Membr Sci 52:275–288
18. Petropoulos JHJ (1985) A comparative study of approaches applied to the permeability of binary composite polymeric materials. Polym Sci Polym Phys Ed 23:1309–1324
19. Toy LG, Freeman BD, Spontak RJ (1997) Gas permeability and phase morphology of poly (1-(trimethylsilyl)-1-propyne)/poly (1-phenyl-1-propyne)) blends. Macromolecules 30(16):4766–4769
20. Pal R (2007) New models for thermal conductivity of particulate composites. J Reinf Plast Compos 26:643–651
21. Gonzo EE, Parentis ML, Gottifredi JC (2006) Estimating models for predicting effective permeability of mixed matrix membranes. J Membr Sci 277(1-2):46–54
22. Chiew YC, Glandt ED (1983) The effect of structure on the conductivity of a dispersion. J Colloid Interface Sci 94:90–104
23. Nasir R, Mukhtar H, Man Z (2016) Prediction of gas transport across amine mixed matrix membranes with ideal morphologies based on the Maxwell model. RSC Adv 6:30130–30138
24. Funk CV, Lloyd DR (2008) Zeolite-filled microporous mixed matrix (ZeoTIPS) membranes: prediction of gas separation performance. J Membr Sci 313:224–231
25. Felske JD (2004) Effective thermal conductivity of composite spheres in a continuous medium with contact resistance. Int Heat Mass Transfer 47:3453–3461
26. Mahajan R, Koros HJ (2002) Mixed matrix membrane materials with glassy polymers Part 1. Polym Eng Sci 42(7):1420–1431
27. Moore TT, Mahajan R, Vu DQ, Koros WJ (2004) Hybrid membrane materials comprising organic polymers with rigid dispersed phases. AIChE J 50:311–321
28. Hashemifard SA, Ismail AF, Matsuura T (2010) A new theoretical gas permeability model using resistance modeling for mixed matrix membrane systems. J Membr Sci 350:259–268
29. Monsalve-Bravo GM, Bhatia SK (2017) Extending effective medium theory to finite size systems: theory and simulation for permeation in mixed-matrix membranes. J Membr Sci 531:148–159
30. Chehrazi E, Sharif A, Omidkhah M, Karimi M (2017) Modeling the effects of interfacial characteristics on gas permeation behavior of nanotube–mixed matrix membranes. ACS Appl Mater Interfaces 9(42):37321–37331
31. Hamilton R, Crosser O (1962) Thermal conductivity of heterogeneous two-component systems. Ind Eng Chem Fundam 1:187–191
32. Kang DY, Jones CW, Nair S (2011) Modeling molecular transport in composite membranes with tubular fillers. J Membr Sci 381:50–63
33. Chehrazi E, Raef M, Noroozi M, Panahi-Sarmad M (2019) A theoretical model for the gas permeation prediction of nanotube-mixed matrix membranes: unveiling the effect of interfacial layer. J Membr Sci 570–571:168–175
34. Saqib S, Rafiq S, Muhammad N, Khan AL, Mukhtar A, Mellon NB, Man Z, Ullah S, Al-Sehemi AG, Jamil F (2020) Influence of interfacial layer parameters on gas transport properties through modeling approach in MWCNTs based mixed matrix composite membranes. Cheml Eng Sci 218:115543
35. Hoek EMV, Guiver M, Nikonenko V, Tarabara VV, Zydney AL (2013) Membrane terminology. In: Hoek EMV, Tarabara VV (eds) Encyclopedia of membrane science and technology, vol 3. Wiley, Hoboken, pp 2219–2222
36. Jamal K, Khan MA, Kamil M (2004) Mathematical modeling of reverse osmosis systems. Desalin 160:29–42

37. Mondal S, De S (2020) Chapter 8. Reverse osmosis modeling, simulation, and optimization in current trends and future developments on (bio-) membranes (reverse and forward osmosis: principles, applications). Advances, Elsevier, pp 186–206
38. Onsager L (1931) Reciprocal relations in irreversible processes. Phys Rev 37:405–425
39. Ghernaout D (2017) Communication reverse osmosis process membranes modeling–a historical overview. J Civil Constr Environ Eng 2(4):112–122
40. Sherwood TK, Brian PLT, Fisher RE (1967) Desalination by reverse osmosis, I&EC Fund 6:2–12 and 37
41. Kezia K, Lee J, Hill AJ, Kentish SE (2013) Convective transport of boron through a brackish water reverse osmosis membrane. J Membr Sci 445:160–169
42. Niewersch C, Rieth C, Hailemariam L, Gilabert G, Justyna O (2020) Reverse osmosis membrane element integrity evaluation using imperfection model. Desalin 476:114175
43. Chen C, Qin H (2019) A Mathematical modeling of the reverse osmosis concentration process of a glucose solution. Processes 7:271. https://doi.org/10.3390/pr7050271
44. Monsalve-Bravo GM, Bhatia SK (2018) Comparison of hollow fibers and flat mixed-matrix membranes: theory and simulation. Chem Eng Sci 187:174-178

Chapter 6
Membrane Applications

6.1 Separation of Gases

The key characteristics of membrane to be used in gas separation process are its permeability and selectivity. Gas mixtures can be effectively separated by synthetic membranes made from polymers such as polyamide or cellulose acetate, or even from ceramic materials. While polymeric membranes are economical and technologically useful, they are bounded by their performance, known as the Robeson limit (permeability must be sacrificed for selectivity and vice versa) [1]. The upper bound correlation follows the relationship.

$$P_i = k\alpha_{jn}^{n} \tag{6.1}$$

where P_i is the permeability of the fast gas, α_{ij} (P_i/P_j) is the separation factor, k is referred to as the "front factor" and n is the slope of the log–log plot of the noted relationship. Below this line on a plot of log α_{ij} versus log P_i, virtually all the experimental data points exist. Figure 6.1 shows the typical polymer upper limits for O_2/N_2 and CO_2/CH_4 separations.

Membrane-based separation processes are very common and being the subject of numerous worldwide academic studies. Due to low cost, high process ability, good mechanical stability, and excellent transport properties polymeric membranes are the first and most common commercial membranes for gas separations. Both rubbery and glassy polymers, including poly(dimethyl siloxane), silicone rubber, nitrilbutadiene, ethylene-propylene and polychloroprene rubbers, cellulose acetate, polysulfone, polyethersulfone, polyamides, polyimides, polyetherimides, polypropylene, poly(vinyl chloride), poly(vinyl fluoride), and sulfonated poly(ether ketone), have been recognized as promising polymers for the preparation of membranes. However, poor resistance to contaminants, low chemical and thermal stability, and a limit in the trade-off between permeability and selectivity (polymer upper bound limit) are among some of their disadvantages. On the other hand, inorganic

K. C. Khulbe, T. Matsuura, *Nanotechnology in Membrane Processes*, Lecture Notes in Nanoscale Science and Technology 29,
https://doi.org/10.1007/978-3-030-64183-2_6

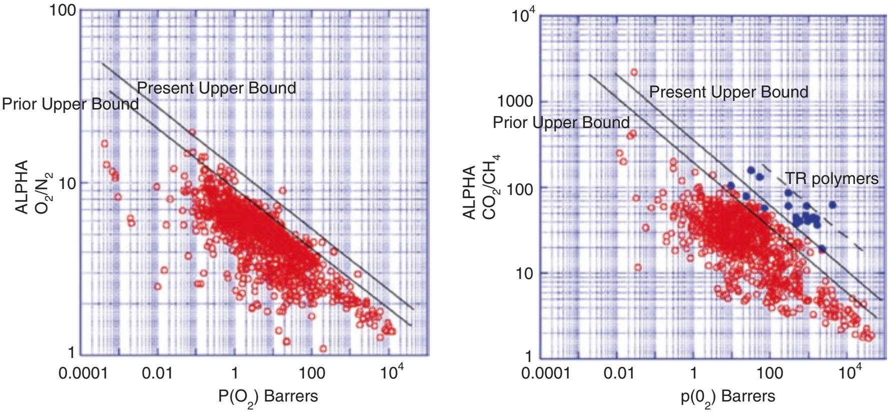

Fig. 6.1 Upper bound correlation for O_2/N_2 (left) and CO_2/CH_4 (right) separations [2]

membranes such as zeolite and carbon molecular sieve (CMS) membranes are overcoming some of the drawbacks of polymer membranes [3].

Due to low energy requirements, potentially low fabrication cost, and steady-state operation, membrane-based separations are frequently used in chemical industrial processes. Polymeric hollow-fiber membrane modules that typically have attractive, large surface area/volume ratios (>1000 m^2 m^{-3}) are especially suitable for membrane gas separation processes [1, 4]. Metal–organic frameworks (MOFs), as porous fillers possessing molecular sieving properties, have been combined with polymers to give mixed-matrix membranes (MMMs) with enhanced separation performance. This field of research has produced a large number of different membranes, and many MOF/polymer combinations have been tested and reported to show potential application to industrial gas separation [5]. MOF-polymer MMMs were investigated for the permeability of the single gases H_2, N_2, O_2, CH_4, CO_2 and of the gas mixtures O_2/N_2, H_2/CH_4, CO_2/CH_4, H_2/CO_2, CH_4/N_2 and CO_2/N_2 (preferentially permeating gas named first). Permeability increases can be traced to the MOF porosity. Since the porosity of MOFs can be tuned very precisely, which is not possible with polymeric material, MMMs offer the opportunity of significantly increasing the selectivity compared to the pure polymeric matrix [6]. Li et al. [7] reported that the preparation of hybrid CMS (carbon molecular sieve) membranes provides a simple and convenient route to efficiently improve the trade-off relationship between permeability and selectivity, and to enable the construction of carbon-based composite materials with novel functionalities in membrane science.

Ghazali et al. [8] suggested the agricultural waste as potential filler in MMM used for gas separation application. In addition, the gas permeation mechanisms through polymeric and MMM as well as the chemical and physical properties of the agricultural waste fillers were also reviewed. From the literature, the agricultural waste fillers have significant effects on the MMM performance. But the number of research that can be found in the literature on the production and application of agricultural waste filler particles incorporated into MMM for purification and separation of gases is still minimal compared to that of pure polymeric membranes [8].

6.1.1 CO_2/N_2 and CO_2/CH_4

The consequent emission of huge amounts of CO_2 into the atmosphere after burning fossil fuels has been recognized as the main contributor to global warming and climate change. The Transnational Paris Agreement signed in 2016 set the goal for governments to limit the further emission of CO_2 into the atmosphere in order to reduce interference with Earth's climate system, which is essential for sustainable food production and economic development [9]. Selyanchyn and Fujikawa [10] attempted to summarize the recent developments in supported nanomembranes used for CO_2/N_2 separation as well as the potential of freestanding nanomembranes. It was reported that on reaching the ultimate thickness, membrane materials change their properties toward gas separation. At reaching submicron range, gas permeance starts to improve. Most materials exhibit a decrease in permeability. This phenomenon in glassy polymers has been attributed to physical aging. However, despite the fact that aging is not characteristic for rubbery polymers, they also show decreased permeability with a decreasing membrane thickness, for which, so far, there is no clear explanation. On using the most common tri-layer membrane assembly (porous support/gutter layer/selective layer), the influence of the support also becomes significant once the selective layer becomes ultrathin. Due to this, the change of the chemistry of membrane is needed in order to improve gas separation performance, especially the gas flux. Freestanding nanomembranes are one of the alternative approaches, although they are not yet well developed. Gas adsorption and desorption are mainly governed by the surface properties, which can be more flexibly modified by post treatment or during preparation. Nanomembranes might potentially help meet Europe's CO_2 reduction targets. NANOGLOWA's (Nano Membranes against Global Warming) nano-structured membranes are built to separate CO_2 from flue gases of coal-fire power plants, which make up for one third of Europe's power plant emissions, at a cost-effective price [11].

Boroglu and Yumru [12] synthesized ZIF-11 loaded 6FDA-DAM mixed matrix membranes. The measured permeability's for H_2, CO_2 and CH_4 gases were found to be 272, 257 and 8.3 Barrers for 20 wt.% ZIF-11 containing MMMs measured at 30 °C and 4 bar. The ideal selectivity of MMMs did not show significant change but the selectivity of 6FDA-DAM-ZIF-11 at 20 wt.% loading approached the 2008 Robeson upper bound. Guerrero et al. [13] studied two different types of polyhedral oligomeric silsesquioxanes (POSS®) functionalized nanoparticles as additives into a PVA layer for the fabrication of nanocomposite membranes for CO_2 separation, one with amidine functionalization (Amidino POSS®) and the second with amine and lactamide groups functionalization (Lactamide POSS®). FTIR characterization showed a good compatibility between the nanoparticles and the polymer. It was concluded that the interaction of the POSS® nanoparticles increased the crystallinity of the composite membranes, thereby playing an important role in the gas separation performance. Moreover, these nanocomposite membranes did not show separation according to a facilitated transport mechanism as expected, based on their functionalized amino-groups, thus, solution-diffusion was the main mechanism responsible for the transport phenomena. In another work, Guerrero et al. [14] incorporated amine-POSS® nanoparticles in PVA-based gas separation membranes in an effort to improve the CO_2/N_2 separation properties. Amine-POSS® nanoparticles were obtained via sol-gel process through the hydrolysis of 3-aminopropyltriethoxysilane with a mean particles size of 3 nm. PVA based films functionalized with nanoparticles were deposited by dip-coating on PSf supports. The CO_2 permeance of the obtained membranes is strongly influenced by the degree of feed gas humidity. Selectivity increases when amine-POSS® is introduced in the system, but after this first increment, the value appears to be rather stable or decreasing. On the other hand, the permeance does not appear to be significantly influenced by the content of the amine-POSS® nanoparticles at lower humidity, with values oscillating between 0.04 and 0.06 (m^3 (STP) m^{-2} h^{-1} bar). However, the performance of the membranes at high humidity is more promising: starting from a value for pure PVA of 0.22, the permeance increases up to 0.4 (m^3 (STP) m^{-2} h^{-1} bar^{-1}). Introduction of SO_2 results in a decrease of the permeance for all gases, which, as a combined effect, results in a minor decrease in CO_2/N_2 selectivity. However, this decrease in permeance is explained by the decrease in humidity of the feed gas mixture occurring during the SO_2 exposure. After removal of SO_2 from the feed stream, the membrane showed a gradual recovery in CO_2 permeance, showing that the SO_2 does not have a negative effect on the membrane performance.

Mixed-matrix membranes (MMMs) with metal-organic frameworks (MOFs) as additives (fillers) exhibit enhanced gas permeabilities and possibly also selectivities when compared to the pure polymer. Crystalline particles of MOFs are known for their large surface area and high adsorption and storage capacity for CO_2 gas. Zaman et al. [15] used polyacrylonitrile (PAN) fibers incorporated with nanoparticles of Cu-based MOF known as HKUST-1 for the CO_2 capturing. To make natural gas and biogas suitable for use, the methane has to be separated from the CO_2. Natural gas always contains quite a bit of carbon dioxide (the greenhouse gas CO_2), sometimes up to 50%. This involves the use of membranes: filters that stop the methane and let the CO_2 pass through. Researchers at KU Leuven (University of Leuven), Belgium, have developed a new membrane that makes the separation process much more effective [16]. The best available membranes consist of a polymeric matrix with a filler in it. Kertik et al. [17] fabricated a novel type of amorphous mixed matrix membrane (MMM) able to separate CO_2/CH_4 mixtures with the highest selectivities ever reported for MOF (*i.e.* ZIF-8) based MMMs.

Metal–organic frameworks (MOFs) are a relatively new class of porous materials which show promise as membranes for gas separation applications. Venna et al. [18] developed a technique to modify and optimize the surface of UiO-66-NH_2 (zirconium(iv) dicarboxylate porous material) based MOF particles to improve its interaction with Matrimid® polymer. The MMMs showed significantly enhanced gas separation properties; CO_2 permeability was increased by ~200% and CO_2/N_2

ideal selectivity was increased by ~25%. Jeazet et al. [6] investigated MOFs for MMMs which include [Cu(SiF(6))(4,4′-BIPY)(2)], [Cu(3)(BTC)(2)(H(2)O)(3)] (HKUST-1, Cu-BTC), [Cu(BDC)(DMF)], [Zn(4)O(BDC)(3)] (MOF-5), [Zn(2-methylimidazolate)(2)] (ZIF-8), [Zn(purinate)(2)] (ZIF-20), [Zn(2-carboxyaldehyde imidazolate)(2)] (ZIF-90), [Mn(HCOO)(2)], [Al(BDC)(μ-OH)] (MIL-53(Al)), [Al(NH(2)-BDC)(μ-OH)] (NH(2)-MIL-53(Al)) and [Cr(3)O(BDC)(3)(F,OH)(H(2)O)(2)] (MIL-101) (4,4′-BIPY = 4,4′-bipyridine, BTC = benzene-1,3,5-tricarboxylate, BDC = benzene-1,4-dicarboxylate, terephthalate). Perez et al. [19] fabricated MOF-5/Matrimid® MMMs and reported that gas mixtures (CO_2/CH_4, N_2/CH_4) showed a marked increase in selectivity for CH_4 due to the larger solubility of CO_2 and N_2 in the polymer matrix. Bano et al. [20] synthesized thermally stable metal organic framework (MOF) of yttrium and 1,3,5-benzenetricarboxylate, and incorporated it with Matrimid V R 5218 to make MMMs. It was reported that on characterizations and gas permeation results of the prepared MMMs, better adhesion and distribution of filler particles in the polymer was confirmed. Permeability of CO_2 increased from 7.24 to 27.29 Barrer by increasing the particle content from 0 to 30% in pure gas experiments. With 30 wt% concentration of synthesized MOF in MMM at 50:50 feed compositions, the selectivity increased for CO_2/CH_4 and CO_2/N_2 was 67% and 68%, respectively.

Ozen and Ozturk [21] manufactured MMMs by introducing metal organic frameworks (MOFs) within polyimide (PI) in order to investigate their separation performances for H_2, CO_2 and CH_4 gases. MOF-5, Cu, Co and Ni doped MOF-5 and CuCo, CuNi and NiCo doped MOF-5 particles have been produced and used as fillers for the manufacturing MMMs. MOF-5 is one of the most outstanding framework due to its excellent properties. The structure of MOF-5 built up from $[Zn_4O]^{6+}$ cluster linked with terephthalate acid ligands, to obtain three dimensional porous cubic frameworks, resulted in high surface area, high porosity and tuneable structure [22]. Figure 6.2 compares the effectiveness of MMMs over the pure PI for permeability of gases. It can be seen from the figure that the MMMs produced using Cu doped MOF-5 have higher permeability for all gases used.

An overall comparison of the gas separation performances of MMMs manufactured for H_2/CO_2, H_2/CH_4 and CO_2/CH_4 mixtures is shown in Fig. 6.3 and compared to the Robeson’s upper bond trade-off line revised in 2008.

As it can be seen from the figure, H_2/CO_2 selectivity is above the trade-off line which means that MMMs including MOFs can be used for the separation of H_2 from reforming gas mixture produced by steam reforming of CH_4 for H_2 production. MOF/PI-MMMs can be used for the enrichment of CH_4 from natural or biogas streams.

Ge et al. [23] fabricated MMMs consisting of metal-organic frameworks (MOFs) of amine-modified Cu-BTC (NH_2-Cu-BTC; BTC = 1,3,5benzenetricarboxylic acid) and submicrometer-sized amine-modified Cu-BTC (sub-NH_2-Cu-BTC) incorporated into a Pebax Polyether-block-amide (Pebax-1657) polymer for the gas separation. Gas adsorption analysis indicated that NH_2-Cu-BTC and sub-NH_2-Cu-BTC had a higher gas adsorption capacity for CO_2 compared to the unmodified

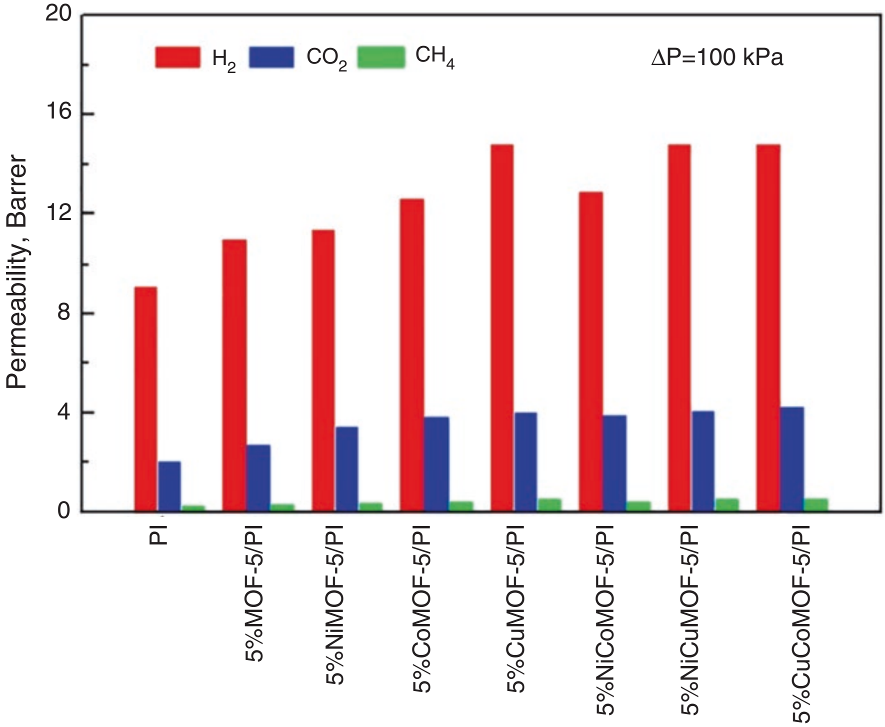

Fig. 6.2 Effect of membrane type on gas permeability [21]

Cu-BTC. The gas separation performance indicated that the Pebax/sub-NH_2-Cu-BTC MMMs evidently improved the CO_2/N_2 and CO_2/CH_4 selectivity at the expense of a slight CO_2 permeability. The results reveal that modified MOF-filled MMMs possess great potential for applications in the CO_2 separation field. Hu et al. [24] prepared MMMs by incorporating the amorphous amino-modified silica nanoparticles (AAMSN) with the polyimide (PI) 4,4′-oxydiphthalic anhydride-2,2′-bis(trifluoromethyl) benzidine (ODPA-TFMB) for gas separation. The CO_2 permeation properties and CO_2/N_2 selectivity of the MMM with 20 wt.% AAMSN were 210.1 barrer and 30.8, respectively, while those of the control membrane were 66.7 barrer and 27.8, respectively. Mixed gas permeation results also showed that the gas permeability of the MMMs improves and their gas selectivity is maintained compared with those of the control PI membrane (pure PI membrane). The unique structure of the AAMSN/PI membrane makes it an attractive candidate for CO_2 capture and O_2 enrichment applications.

Zahri et al. [25] fabricated PSf-GO hollow fiber MMM and reported that the incorporation of GO nanosheets into PSf polymer showed significant improvement of CO_2/CH_4 separation properties even at low loading (0.25 wt.%). The special properties present in GO that consists of polar groups and π-π conjugate bond help to improve CO_2 permeance. Golzar et al. [26] utilized simulation techniques to

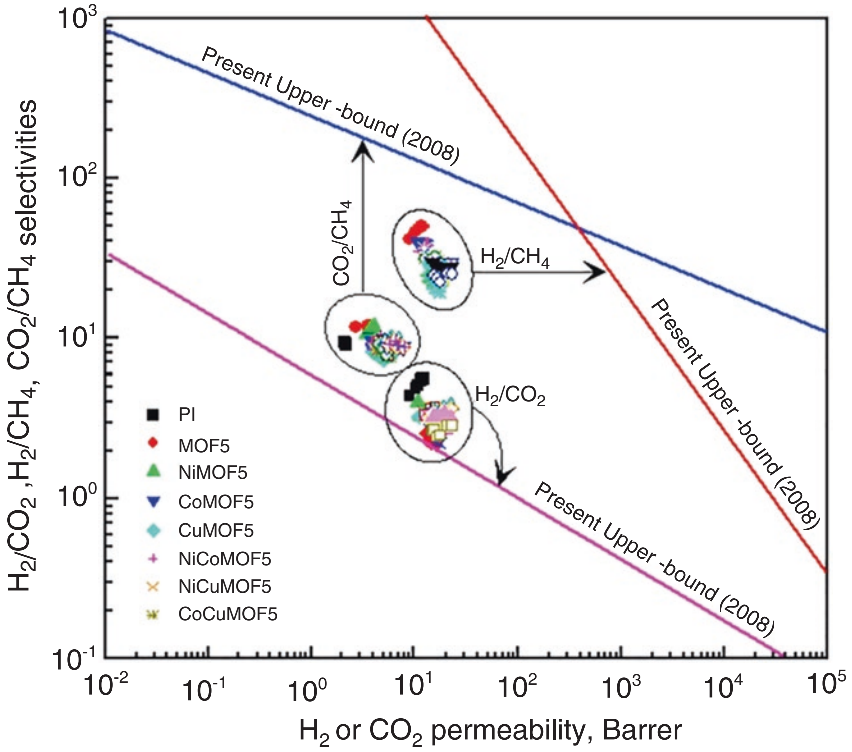

Fig. 6.3 H_2/CO_2, H_2/CH_4 and CO_2/CH_4 separation performances of MMMs [21]

investigate the structural, physical and separation properties of penetrant gases including oxygen, nitrogen, carbon dioxide and methane through pure and nano-sized silica particles filled PSf membranes. The parameters such as fractional free volume, average cavity size and cavity size distributions of pure and silica-filled PSF were calculated using an energetic based cavity-sizing algorithm. These parameters for the silica-filled membrane were higher than those of pure PSF and increased with the amount of the filler content and as a result, the diffusion coefficient, solubility and permeability of penetrant gases in silica-filled PSf membranes were greater than pure PSF membrane. The simulated results were in agreement with the available experimental data. Kiadehi et al. [27] studied MMMs (CNFs/PSf) fabricated from carbon nanofibers (CNFs) and PSf for single gas permeation (N_2, O_2, CO_2, and CH_4) at ambient temperature. The morphological studies showed that the incorporation of CNFs appreciably changed the surface properties of membranes. The permeation test showed that the mixed matrix membrane exhibited high permeability. With increasing CN concentration, CNFs/PSf membrane permeability was raised from 2.134 to 12.04 Barrer for CO_2. It was found that this unique membrane had increased permeability and enhanced selectivity. Also it has a great potential to be used practically in gas separation.

Ahn et al. [28] improved the gas separation performance by incorporation of silica nanoparticles in PSf. The interface between the polymer and silica agglomerates was studied in relation with the gas transport properties. The gas permeabilities of hydrogen, helium, oxygen, nitrogen, methane, and carbon dioxide were measured as a function of silica volume fraction and diffusion and solubility coefficients were determined by the time-lag method. The effect of silica nanoparticles in PSf membranes on gas permeability was in contrast with predictions based on the Maxwell model. The O_2 permeability is approximately four times higher and CH_4 permeability was over five times greater than in a pure PSf membrane. However, the performance comprising permeability versus selectivity of PSf/silica MMMs for O_2/N_2 and CO_2/CH_4 follows a similar slope to that of the trade-off upper bound with increasing silica content.

Duval et al. [29] reported that zeolites (silicalite-1, 13X and KY) improve, to a large extent, the separation performances of poorly selective rubbery polymers for a CO_2/CH_4 mixture. Jang et al. [1] demonstrated the fabrication of continuous mesoporous silica membranes on polymeric hollow fibers via a facile, low-temperature process. The membranes were defect-free and showed high gas flux. It is an example of modification of the mesopores for enhancing the gas separation selectivity of the membrane. Lin et al. [30] fabricated a novel CNT/metal-organic framework (MOF) composite membrane via the growth of NH_2-MIL-101(Al) on the surface of CNTs and applied to fabricate polyimide-based MMMs. Extra amino groups and active sites were introduced to external surface of CNTs after MOF decoration. The good adhesion between the synthesized CNT-MIL fillers and polymer phase was observed, even at some high filler loadings up to 15%. Consequently, MMMs containing the synthesized MOF/CNT composite exhibited not only a large CO_2 permeability but also a high CO_2/CH_4 selectivity; the combined performance of permeability and selectivity is even above the Robeson upper bound. Etxeberria-Benavidesa et al. [31] presented the development of high performance mixed matrix membranes (MMMs) composed of ZIF-94 filler and 6FDA-DAM polymer matrix. The CO_2/N_2 separation performance was evaluated by mixed gas tests ($15CO_2$:$85N_2$) at 25 °C and 1–4 bar transmembrane pressure difference. The CO_2 permeability was increased by the addition of the ZIF-94 particles, maintaining a constant CO_2/N_2 selectivity of ~22. Chakrabarty et al. [32] studied the separation of CO_2 over CH_4 by using ZIF-7 nanoparticles-PAN composite MMMs. These hybrid membranes with various loadings (20, 30 and 40 wt.%) were tested for the separation of CO_2 over CH_4. Best performance was seen at 40% ZIF-7 loaded membrane with an ideal selectivity of 39 for CO_2 over CH_4. The obtained selectivity was 105% higher than the selectivity of the pristine polymer with a slight decrease in permeance. Morphological characterization of such developed membranes showed an excellent compatibility between the polymer and the particle. Sarfraz and Shammak [33] fabricated hydrothermally stable high performance MMMs by incorporating multi-walled CNTs and ZIF-301 nanofillers to selectively capture CO_2 from post combustion flue gas. The hybrid membrane demonstrated more than five-fold increment in CO_2 permeability as compared to that of a bare PSf membrane, while the CO_2/N_2 ideal selectivity was enhanced by more than three-fold. The separation performance of the composite membranes produced in this work was above the Robeson 1991 upper bound and the CO_2/N_2 ideal selectivity is considered to be high enough to meet industrial application.

Khan et al. [34] studied on the gas transport behavior of MMMs which were prepared from multi-walled carbon nanotubes (MWCNTs) dispersed within polymers of intrinsic microporosity (PIM-1) matrix. The MWCNTs were chemically functionalized with poly(ethylene glycol) (PEG) for a better dispersion in the polymer matrix. The f-MWCNTs (functionalized multiwalled carbon nanotubes) MMM showed better performance in terms of permeance and selectivity in comparison to pristine MWCNTs. It was shown that the improvement in homogeneous dispersion of MWCNTs in the MMM is due to covalent functionalization of MWCNTs with poly(ethylene glycol). With good interfacial adhesion and the absence of voids between f-MWCNTs and polymer matrix, the MMMs show higher permeabilities which are coupled with increased CO_2/N_2 and O_2/N_2 selectivities.

Casado-Coterillo et al. [35] investigated the performance of new robust mixed matrix composite hollow fiber (MMCHF) membranes with a different selective layer composition in the absence and presence of water vapor in CO_2/N_2 and CO_2/CH_4 separation. The selective layer of these membranes was made of highly permeable hydrophobic poly(trimethyl-1-silylpropine) (PTMSP) and hydrophilic chitosan-ionic liquid (IL-CS) hybrid matrices, respectively, filled with hydrophilic zeolite 4A particles in the first case and HKUST-1 nanoparticles in the second, and coated over compatible supports. The effect of water vapor in the feed or using a commercial hydrophobic PDMSXA-10 HF membrane has also been studied for comparison. The N_2 and CH_4 permeance were less influenced by water vapor presence than they were for the hydrophobic PTMSP/P84 CHF and PDMSXA-10 HF membranes, and so the CO_2/N_2 and CO_2/CH_4 selectivity increased around 34% and 46%, respectively**,** from dry to humid conditions. Khan et al. [36] fabricated zeolitic imidazole framework-8 (ZIF-8) blended polysulfone (PSf) hollow fiber membranes for natural gas purification. MMMs were tested using pure gases with a significant improvement of 36% in CO_2 permeability and 28% in CO_2/CH_4 selectivity compared to the neat membrane (without zeolite). However, the high ZIF-8 loading reduced the separation performances. Burmann et al. [37] embedded different types of fillers of inorganic (titanosilicate ETS-10 and mesoporous silica type MCM-41) and organic-inorganic nature (ZIF-8 and NH_2-MIL-53), with different pore size (micro- and mesoporosity) and structure, diverse particle shape, and particle sizes in the 85–400 nm range in a polysulfone matrix via spin coating, and tested for H_2/CH_4 and O_2/N_2 mixed-gas separations. It was reported that the homogeneous MMMs containing 8 wt.% of the various fillers showed significant improvements for H_2/CH_4 and O_2/N_2 mixed-gas separations when compared with neat polymer membrane achieving over the neat polymer. NH_2-MIL-53 MMMs revealed the highest separation performance (a rise in selectivity higher than 60% compared to the pure polymer for H_2/CH_4 and O_2/N_2 separations).

Single-walled carbon nanotubes (SWNTs) were incorporated into triptycene-based polyimide (6FDA-TP polyimide) to fabricate MMMs for gas separation by Zhang et al. [38]. For their study Zhang et al. used three types of SWNTs:

1. as-purchased SWNTs (AP-SWNTs)
2. purified SWNTs (P-SWNTs) (AP-SWNTs were purified by refluxing in 3 M HNO_3 for 12 h)
3. acid-treated SWNT (A-SWNTs) (Purified SWNTs (P-SWNTs) were cut into shorter length by a treatment using a HNO_3 and H_2SO_4 mixture (3:1) with sonication for 6 h at room temperature)

MMMs with 2 wt.% of different type of fillers (AP-SWNT, P-SWNT and A-SWNT) were prepared and the pure gas permeabilities were tested following the same procedure. The permeation data and ideal selectivity are summarized in Table 6.1. Regardless of different physical properties of carbon nanotubes, all composite membranes showed significantly higher permeabilities than the pure 6FDA-TP membrane for all gases, indicating that SWNTs effectively introduce barrier-free gas transport pathways in the MMMs.

Rouzitalab et al. [39] reported the fabrication of walnut shell-derived nanoporous carbon with chemical adsorption sites for CO_2 adsorption at mediate (1 bar) and high pressures (10 bar) under room temperature by varying the preparation parameters. It was suggested by authors that N-doped nanoporous carbon from walnut shell has great potential to separate CO_2 from CO_2/CH_4 and CO_2/N_2 binary mixtures.

6.1.2 Oxygen Enrichment

Oxygen enrichment is an established technology for increasing the efficiency of combustion, and has been adopted in various forms by a number of industries using high-temperature combustion processes. The oxygen-enriched air is highly demanded for various industrial applications such as medical, chemical and enhanced combustion processes. The conventional oxygen/nitrogen production is

Table 6.1 Pure gas permeation data and ideal selectivity's of 6FDA-TP membrane and the MMMs with 2 wt.% of AP-SWNT, P-SWNT and A-SWNT for comparison [38]

Permeabilities						
	H_2	**CH_4**	**N_2**	**O_2**	**CO_2**	
6FDA-TPa	59	0.5	1.0	5.6	20	
2% AP-SWNT	144 ± 2	2.2 ± 0.1	3.6 ± 0.1	18 ± 0.2	81 ± 1	
2% P-SWNT	140 ± 3	1.9 ± 0.1	3.2 ± 0.1	18 ± 0.4	74 ± 2	
2% A-SWNT	122 ± 3	1.4 ± 0.1	2.7 ± 0.1	17 ± 0.4	63 ± 1	
Ideal selectivity						
	H_2/CH_4	**H_2/N_2**	**H_2/CO_2**	**CO_2/N_2**	**CO_2/CH_4**	**O_2/N_2**
6FDA-TP[a]	113	60	3.0	20	37	5.6
2% AP-SWNT	75 ± 3	44 ± 1	1.9 ± 0.1	23 ± 0.8	39 ± 1	5.7 ± 0.2
2% P-SWNT	88 ± 3	45 ± 2	1.9 ± 0.1	23 ± 0.7	46 ± 2	6.1 ± 0.2
2% A-SWNT	88 ± 3	45 ± 2	1.9 ± 0.1	23 ± 0.7	46 ± 2	6.1 ± 0.2

[a] Pure 6FDA-TP permeability and selectivity

either cryogenic distillation or pressure swing adsorption (PSA). Both of these techniques possess the production capability of 20–300 tonnes of oxygen per day and oxygen purity of more than 95%. However, these techniques are energy intensive. The advancement of the membrane materials indicates the potential of the membrane technology to be commercially feasible in the O_2/N_2 separation process. However, there is still large improvement required to compete with the currently available O_2/N_2 separation techniques. Membrane technology is regarded as an emerging gas separation technique in the industry due to the lower cost in both initial capital and energy consumption, compared to cryogenic distillation and pressure swing adsorption. To date, membrane technology has been reported to produce 10–25 tonnes of oxygen per day with the purity of 25–40% [40]. Nanotechnology research is improving the production or enrichment of O_2. Composite membranes are widely searched for this purpose. Ma et al. [41] fabricated the polyimide hollow fiber membrane having defect free skin layer thickness about 0.1μm for O_2/N_2 separation and recorded a promising performance with an oxygen permeability of 63 ± 7 GPU and selectivity of 4.6 ± 0.1.

Chong et al. [42] modified the surface properties of the PSF hollow fiber membranes by subjecting the membranes to dip-coating process using either PDMS (polydimethylsiloxane) or PEBAX (poly(ether block amide)) at different concentrations. Results showed that the membranes coated with PDMS exhibited better permeance and selectivity in oxygen/nitrogen separation process in comparison to the membranes coated with PEBAX.

Kusworoa et al. [43] reported that the PES-activated carbon MMMs had increased the permeability and selectivity of oxygen and nitrogen gas and the O_2/N_2 selectivity. The activated carbon has a potential as inorganic filler for MMM for the future oxygen enrichment membrane. Fernández-Barquín et al. [44] fabricated MMMs composed of small-pore zeolites with various topologies (CHA (Si/Al = 5), LTA (Si/Al = 1 and 5), and Rho (Si/Al = 5)) as dispersed phase and poly(1-trimethylsilyl-1-propyne) (PTMSP) as continuous phase via solution casting. The O_2/N_2 gas separation performance of the MMMs has been analyzed in terms of permeability, diffusivity, and solubility in the temperature range of 298–333 K. The O_2/N_2 permselectivity of the MMMs increases with temperature, the O_2/N_2 selectivities being considerably higher than those of the pure PTMSP. In consequence, most of the MMMs prepared in this work exceeded Robeson's upper bound for the O_2/N_2 gas pair in the temperature range under study, with not much decrease in the O_2 permeabilities, reaching O_2/N_2 selectivities of up to 8.43 and O_2 permeabilities up to 4800 Barrer at 333 K.

Rybak et al. [45] studied the N_2, O_2 and air permeabilities on inorganic-organic hybrid membranes, prepared from ethyl cellulose (EC) or linear polyimide (LPI) and magnetic neodymium powder particles MQP-14-12. The results showed that the membrane permeation properties were improved by the addition of magnetic neodymium particles to the polymer matrix. The magnetic ethylcellulose and polyimide membranes exhibited higher gas permeability and diffusivity, while their permeability selectivity and solubility were either unchanged or slightly increased.

Weng et al. [46] fabricated multilayer composite membranes using large-pore mesoporous silica molecular sieve SBA-15, PPO polymer, and CMS/Al_2O_3 as substrate. The SBA-15 was used at different aging temperatures to transform into different crystal sizes. The selectivity for O_2/N_2 separation increased remarkably from 6.2 to 8.8, which corresponded to the increase in aging temperature of SBA-15 used for the PPO/SBA-15/CMS/Al_2O_3 composite membrane from 90 to 110 °C, respectively. This phenomenon confirms that blockage and reduced mobility of polymer chains as a result of mixing the SBA-15 aged at 110 °C with a PPO matrix may significantly improve the gas separation. Ridzuan and Musa [47] investigated the performance of MMMs using treated zeolite and untreated zeolite incorporated with PES to see the effect of the coupling agent towards the separation of O_2 and N_2. Treated zeolite was prepared by using aminopropyl-trimethoxysilane (APTMOS), a silane coupling agent. The prepared membranes were coated with silicone and n-hexane in order to decrease the surface defect of the membrane. The best performance was found for membranes using treated zeolite where the selectivity was 3.3 for 15% zeolite concentration at 3 bar operating pressure. It was concluded that surface modification of zeolite plays an important role to the incompatibility of zeolite and polymer to the formation of large free voids and it affected the overall selectivity and permeability.

Zeolites were incorporated in highly flexible rubbers such as polydimethylsiloxane and ethylene−propylene diene rubber (EPDM), and in glassy flexible polymers, such as cellulose acetate and polyvinyl acetate (PVAc) [48]. Ren et al. [49] reported that higher O_2 permeabilities (from 571 to 655 Barrer) and O_2/N_2 selectivities (from 2.14 to 2.92) could be achieved by silicalite-1 filled silicone rubber (PDMS) membranes than unfilled membrane, when MMMs are composed of small-pore zeolites with various topologies (CHA (Si/Al = 5), LTA (Si/Al = 1 and 5), and Rho (Si/Al = 5)).

Zhang et al. [38] used three types of SWNTs for the separation of O_2 from O_2/N_2 mixture as discussed in previous section. The overall separation performance of O_2 from O_2/N_2 mixtures for MMMs is compared with the Robeson's upper bounds in Fig. 6.4. In general, using the acid-treated, shortened A-SWNTs as filler produced composite membrane with the best overall performance.

6.1.3 SO_2 and H_2S

Hydrogen sulfide is a corrosive toxic gas that can be oxidized rapidly to sulfur dioxide, which is a contributor to acid rain. Many efforts have been made in the last couple of years to develop an effective method for the separation and subsequent removal of impurities from natural gas. To capture CO_2 from the combustion of fossil fuel plants, CO_2 capture and separation (CCS) technologies, which are often based on the chemical absorption process, are used. The SO_2 in the emission gas affects the sorbents in the CCS process. Flue gas from coal-power plants contains 6–196 ppm of SO_2 after the CCS process. To remove the remaining SO_2, another

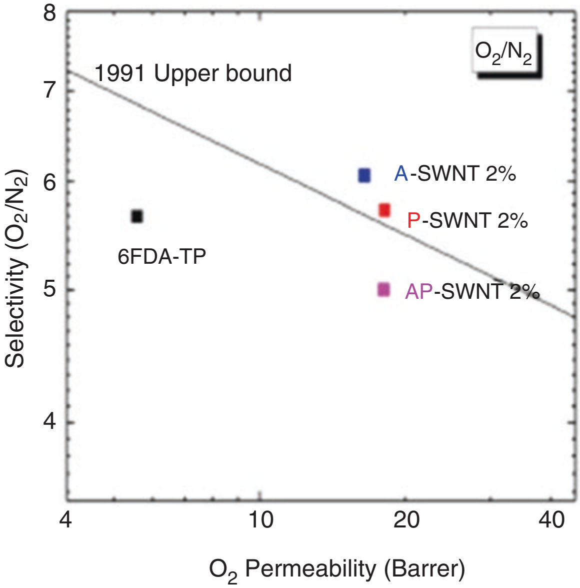

Fig. 6.4 Permeability/selectivity trade-off plots for O_2/N_2 gas pairs comparing the separation performance of pure 6FDA-TP membrane and MMMs containing 2 wt.% AP-SWNT, P-SWNT and A-SWNT/6FDA-TP as labeled [38]

CCS process is necessary. Some studies have been made to apply polymeric membranes for flue gas applications [50]. Kim et al. [51] prepared a hollow fiber composite membrane by coating PEI HF with a poly(vinyl chloride)-graft-poly(oxyethylenemethacrylate (PVC-g-POEM)). The inner and outer diameters of the HFM was 261 and 429μm, respectively, and the selective coating layer on the outer surface was around 0.1μm. The membrane was tested for the permeance of pure gases (SO_2, CO_2, and N_2) at different operating conditions. It was reported that the permeance of SO_2 was 105–2705 GPU and the selectivity of SO_2/CO_2 was 3.9–175.6. From the mixed gas separation experiment, the maximum SO_2 removal efficiency reached 84.5%.

Zhang et al. [52] fabricated poly(vinylidene fluoride) (PVDF)-based mixed matrix membrane contactor (MMMC) that contained a core-shell hierarchical Cu@4A composite filler (Cu@4A). The Cu@4A plays double role. First, it regulated the physical structure of MMMC, which enhanced gas permeation and thus resulted in the increment of physical SO_2 absorption flux. In other way it changed the chemical environment of MMMC by remarkably increased SO_2 facilitated transport sites, which elevated SO_2 concentration around Cu@4A by the enhancement of adsorption and oxidation of SO_2, resulting in the increase of chemical SO_2 absorption flux. Moreover, the copper nanosheets on 4A helped to construct facilitated transport pathways along the Cu@4A fillers at polymer-filler interface. It was observed that Cu@4A loaded MMMC exhibited increased SO_2 removal efficiency and SO_2 absorption flux compared with PVDF control membrane. Specifically, the M1040 MMMC loaded with 40 wt.% Cu@4A and PVDF concentration 10 wt.% exhibited the highest SO_2 removal efficiency and SO_2 absorption flux, which was up to 73.6% and 9.1×10^{-4} mol m^{-2} s^{-1} at the liquid flow rate of 30 Lh^{-1}.

6.2 Water/Wastewater Treatment

Major sources of water pollution include industrial wastes, municipal wastewater, and agricultural activities. Pesticides, toxic heavy metals, organic acids, fertilizers, dyes, phenolic, halogenated compounds, and microorganisms are present in the wastewater. Among different types of above mentioned pollutants, the heavy metals are the most noxious due to their toxicity and non-biodegradability [53]. Clean water is the base for economic development of any society. Water treatment includes sedimentation, filtration, aeration, solar treatment, chlorination, and sterilization by boiling. A wide range of treatment processes have evolved to suit the different local conditions. Water treatment must produce ‘clean water’, which is having all contaminants safely below the maximum permissible limits (MPL). With often revised MPL, new materials are explored to address the presence of contaminants such as microbes, heavy metal ions, oils, pesticides, disinfection by product precursors, and innumerable chemicals.

The basic goal of water treatment is to remove undesired constituents from water. Membrane technology is widely used for water treatment. The research in membrane technology has gained a considerable attention in both industry and academia. There are different types of membrane technologies such as microfiltration, ultrafiltration, nanofiltration, reverse osmosis, forward osmosis, pressure retarded osmosis, gas separation, pervaporation, membrane distillation, membrane bioreactor, and separation by liquid membranes depending upon separation strategies and properties of membrane. Many treatment methods are currently available for removing organic pollutants from water, such as reverse osmosis, distillation, adsorption, chemical precipitation, coagulation, electroplating, oxidation–reduction, and ion exchange. Table 6.2 summarizes major limitations associated with conventional methods

Das et al. [55] draw the attention some major threats to common water purification systems, as summarized in Fig. 6.5. It clearly reflects that a single method is insufficient to remove all pollutants from water. The pathogen removal processes of conventional water treatment plants may affect effluent water quality (turbidity, pH, temperature) and decrease pathogen sensing ability. Certain bacteria in treated water may release toxins, which may seriously affect the overall quality of water during the treatment process.

Nanotechnology provides less expensive and highly efficient methods for the treatment of surface water, groundwater, wastewater, and other environmental materials contaminated by toxic metal ions, organic and inorganic solutes, and microorganism. Due to the unique activity toward recalcitrant contaminants, nano photo catalyst has great potential for use in the treatment of water and contaminated sites. The present market of nano photo catalyst-based technologies applied in water treatment is applicable to not only wastewater treatment but also drinking water production.

With the fast depletion of fresh water resources, it is expected that engineered nanomaterials will play an important role in more efficient seawater desalination,

Table 6.2 Major limitations associated with conventional methods [54]

Conventional methods	Limitation
Distillation	Most contaminants remain behind and require high amounts of energy and water. Pollutants with boiling point >100 °C are difficult to remove
Chemical transformation	Excess reagents are required. Product may be a low-quality mixture and cannot be released into environment. Inactive in harsh conditions. This is not highly selective method
Coagulation and flocculation	This is a complex and less-efficient method and requires alkaline additives to achieve optimum pH
Biological treatment	Microorganisms are sensitive to environmental factors and difficult to control. Intermediates damage the microbial cells. This is not cost effective. Time consuming
Ultraviolet treatment	Expensive method and inactivated by water cloudiness and turbidity. Ineffective for heavy metals and other nonliving contaminants removal
Reverse osmosis	This method removes minerals from water which is unhealthy, and the treated water will be acidic. This method cannot remove volatile organics, chemicals, chlorine, chloramines and pharmaceuticals. Requires high energy
Nanofilteration	This technique requires high energy, and pre-treatment. Limited retention for salts and univalent ions. Membrane fouling will occur with limited lifetime and expensive
Ultrafiltration	This method will not remove dissolved inorganics. Requires high energy. Susceptible to particulate plugging and difficult to clean
Microfiltration	Cannot remove nitrates, fluoride, metals, sodium, volatile organics, color, and so on. Requires regular cleaning. Membrane fouling will occur. Less sensitive to microbes, especially virus
Carbon filter	Cannot remove nitrates, fluoride, metals, sodium, and so on. Clogging occurs with undissolved solids. Susceptible to mold. Requires frequent changing of filters

water recycling, and water remediation. Nanotechnology has brought a great revolution for treatment of wastewater and it could help to meet the need for affordable, clean drinking water through rapid, low-cost detection and treatment of impurities in water. Engineers have developed a thin film membrane with nanopores for energy-efficient desalination. For example, molybdenum disulphide (MoS_2) membrane filtered two to five times more water than current conventional filters [56]. Materials developed on the basis of nanotechnology and having unique physical, chemical and mechanical properties can become a promising alternative to traditional adsorbents, both independently and as a part of hybrid materials for more efficient removal of heavy metal pollutants from wastewater effluents [57]. Kima and Bruggen [58] discussed the role of engineered nanomaterials in (pressure driven) membrane technology for water treatment, to be applied in drinking water production and wastewater recycling.

Nanomaterials are fabricated with features, such as high aspect ratio, reactivity, and tunable pore volume, electrostatic, hydrophilic, and hydrophobic interactions, which are useful in adsorption, catalysis, sensoring, and optoelectronics.

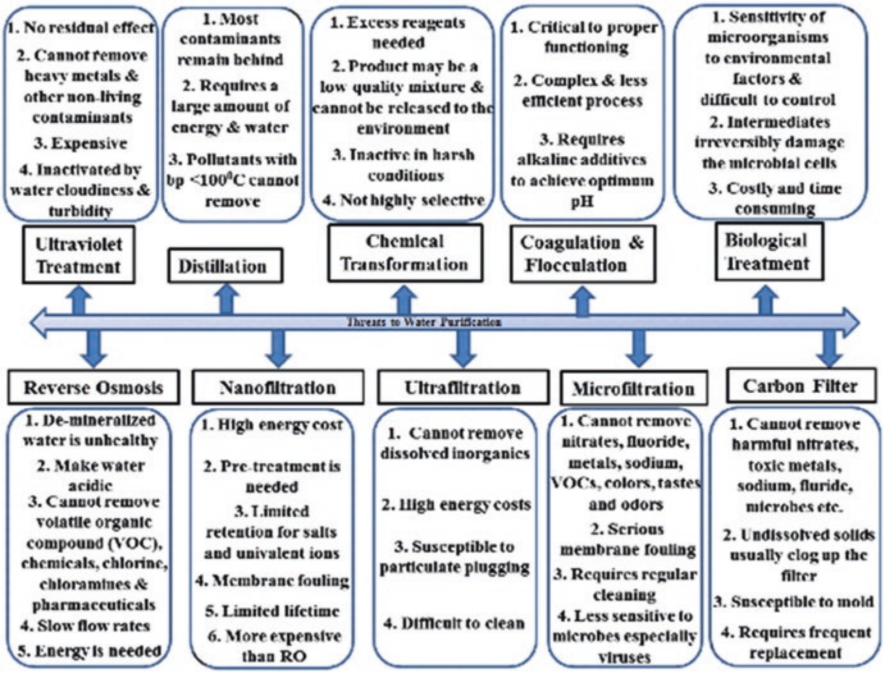

Fig. 6.5 Some major threats to conventional water purification systems [56]

Nanomaterials for purifying drinking water must be environment-friendly and non-toxic. Nanomaterials are typically less than 100 nm in dimension and contain materials with novel and significantly changed physical, chemical, and biological properties. Metal oxides nanoparticles are of potential interest for pressure-driven membranes in view of flux increase and reduced fouling resistance. Arsuaga et al. [59] used polyethersulfone (PES) flat-sheet membranes fabricated via phase inversion method, for wastewater treatment application. Membranes were modified by dispersing nanoparticles of TiO_2, Al_2O_3 and ZrO_2 in a PES solution. Membrane fouling was studied with BSA and humic acids as model organic foulants. Entrapped metal oxides changed the membrane morphology to more open and porous structure and the antifouling property and long term flux stability of metal oxide modified membranes were significantly enhanced. The rejection potential of new membranes was hardly affected by the metal-oxide doping, being similar to the control membrane. The fouling of modified membranes was significantly reduced, showing that the particle distribution is a key parameter for the membrane fouling reduction. But no significant change was observed in the rejection potential of membranes.

Membrane performance improves in the order:

$$Al_2O_3 > TiO_2 > ZrO_2 \tag{6.2}$$

Nasrollahi et al. [60] fabricated PES UF membranes blended with different amine-functionalized CuO (FCN) and ZnO (FZN) nanoparticles. All membranes showed a significant increase in porosity and hydrophilicity, leading to considerable improvement in the pure water flux, as compared with the bare PES membrane. Pang et al. [61] reported the performance and antifouling properties of polyethersulfone (PES) membrane incorporated with dual nanofiller, zinc oxide (ZnO) and multi-walled carbon nanotube (MWCNT). The filtration performance of the membranes was tested using 50 mg L^{-1} humic acid (HA) solution as model solution. The incorporation of both MWCNT and ZnO into the PES membrane improved porosity significantly up to 46.02%. Lower water contact angle of PES membrane incorporated with equal ratio of MWCNT and ZnO revealed that it has neat PES membrane properties and more hydrophilic membrane surface than single filler.

Table 6.3 presents overview of different nanomaterials in water and wastewater treatment [54].

Worldwide, water supply struggles to keep up with the fast growing demand, which is exacerbated by population growth, global climate change, and water quality deterioration. Nanotechnology holds great potential in advancing water and wastewater treatment to improve treatment efficiency as well as to augment water supply through safe use of unconventional water sources.

Table 6.4 present and potential applications of membrane nanotechnology in water and wastewater treatment [62].

Nanoporous membrane for water purification can generally be divided into three types based on their material composition: inorganic, organic, and inorganic-organic hybrid membranes. Inorganic membranes are mainly made of ceramics (Al_2O_3,

Table 6.3 Overview of different nanomaterials in water and wastewater treatment [54]

Nanomaterial	Properties/Applications	Limitations
Nanoadsorbents	Have high specific surface and very good adsorption capacity Used to remove organic and inorganic contaminants, and bacteria	High production costs
Nanometals and nanometal oxides	Contain high specific surface area and short intraparticle diffusion distance, compressible without change in the surface area, abrasion resistant, magnetic, and photo catalytic in nature Used to remove heavy metals and radionuclides Used in media filters, slurry reactors, powders, and pellets	Less reusable
Membranes and membrane process	Highly reliable and mostly automated process Applied in all fields of water and waste treatments	Requires high-energy source
Photocatalysis	Photocatalytic activity in UV and possibly visible light range, low human toxicity, high stability, and low cost	Reaction selectivity
Disinfection and microbial control	Strong and wide-spectrum antimicrobial activity, low toxicity to humans, ease of use	Lack of disinfection residue

Table 6.4 Current and potential applications of membrane nanotechnology in water and wastewater treatment [62]

Applications	Representative nanomaterials	Desirable nanomaterial properties	Enabled technologies
Adsorption	Carbon nanotubes	High specific surface area, highly assessable adsorption sites, diverse contaminant-CNT interactions, tunable surface chemistry, easy reuse	Contaminant preconcentration/ detection, adsorption of recalcitrant contaminants
	Nanoscale metal oxide	High specific surface area, short intraparticle diffusion distance, more adsorption sites, compressible without significant surface area reduction, easy reuse, some are superparamagnetic	Adsorptive media filters, slurry reactors
	Nanofibers with core shell structure	Tailored shell surface chemistry for selective adsorption, reactive core for degradation, short internal diffusion distance	Reactive nano-adsorbents
Membranes and membrane processes	Nano-zeolites	Molecular sieve, hydrophilicity	High permeability thin film nanocomposite membranes
	Nano-Ag	Strong and wide-spectrum antimicrobial activity, low toxicity to humans	Anti-biofouling membranes
	Carbon nanotubes	Antimicrobial activity (unaligned carbon nanotubes). Small diameter, atomic smoothness of inner surface, tunable opening chemistry, high mechanical and chemical stability	Anti-biofouling membranes Aligned carbon nanotube membranes
	Aquaporin	High permeability and selectivity	Aquaporin membranes
	Nano-TiO_2	Photocatalytic activity, hydrophilicity, high chemical stability	Reactive membranes, high performance thin film nanocomposite membranes
	Nano-magnetite	Tunable surface chemistry, superparamagnetic	Forward osmosis
	Nano-TiO_2	Photocatalysis Photocatalytic activity in UV and possibly visible light range, low human toxicity, high stability, low cost	Photocatalytic reactors, solar disinfection systems
	Fullerene derivatives	Photocatalytic activity in solar spectrum, high selectivity	Photocatalytic reactors, solar disinfection systems
Disinfection and microbial control	Nano-Ag	Strong and wide-spectrum antimicrobial activity, low toxicity to humans, ease of use	POU water disinfection, anti-biofouling surface

(continued)

Table 6.4 (continued)

Applications	Representative nanomaterials	Desirable nanomaterial properties	Enabled technologies
	Carbon nanotubes	Antimicrobial activity, fiber shape, conductivity	POU[a] water disinfection, anti-biofouling surface
	Nano-TiO_2	Photocatalytic ROS generation, high chemical stability, low human toxicity and cost	POU* to full scale disinfection and decontamination
Sensing and monitoring	Quantum dots	Broad absorption spectrum, narrow, bright and stable emission which scales with the particle size and chemical component	Optical detection
	Noble metal nanoparticles	Enhanced localized surface plasmon resonances, high conductivity	Optical and electrochemical detection
	Dye-doped silica nanoparticles	High sensitivity and stability, rich silica chemistry for easy conjugation	Optical detection
	Carbon nanotubes	Large surface area, high mechanical strength and chemical stability, excellent electronic properties	Electrochemical detection, sample preconcentration
	Magnetic nanoparticles and purification	Tunable surface chemistry, super paramagnetism	Sample preconcentration

[a]Point-of-use

TiO_2, ZrO_2, SiO_2, TiO_2-SiO_2, TiO_2-ZrO_2, Al_2O_3-SiC), graphene, and carbon nanotubes (CNTs). Organic membranes are mainly made of polymeric materials such as PVA, PI, PP, PES, CA, cellulose nitrates, PSf, PVDF, PAN, PTFE, and biomacromolecules. Inorganic-organic hybrid membranes are usually made by introducing inorganic materials (metals, metal oxide, or carbon-based materials) into a polymeric matrix system [63]. Addition of limited amount of inorganic fillers (nanoparticles) into conventional polymeric membranes for water treatments, enhanced the performance of the membrane. Thus, nanocomposite membranes opened a new avenue for scientists working on water treatment applications such as wastewater treatment, water purification, removal of microorganisms, chemical compounds, heavy metals, etc. The incorporation of different nanofillers, such as carbon nanotubes, zinc oxide, graphene oxide, silver and copper nanoparticles, titanium dioxide, 2D materials, and some other novel nano-scale materials into polymeric membranes has provided great advances, e.g., enhancing hydrophilicity, suppressing the accumulation of pollutants and foulants, enhancing rejection efficiencies and improving mechanical properties and thermal stabilities [64].

Yang et al. [65] developed a nanoporous membrane for virus's filtration with good dimensional stability at higher filtration pressures, while maintaining high selectivity for the filtration of viruses. The membrane consisted a double layer: The upper layer was a nanoporous film with pore size of ∼17 nm and a thickness of ∼160 nm, which was prepared by polystyrene-*block*-poly(methyl methacrylate) copolymer (PS-*b*-PMMA) where PMMA block was removed by ultraviolet irradiation followed by rinsing with acetic acid. The nanoporous block copolymer film was combined with a conventional micro-filtration membrane to enhance mechanical strength. The membrane did not show any damage or crack even at a pressure of 2 bar, while high selectivity was maintained for the filtration of human rhinovirus type 14 (major pathogen of the common cold in humans) which has a diameter of ∼30 nm. Furthermore, due to cross-linked PS matrix during the UV irradiation, the nanoporous membrane showed excellent resistance to all organic solvents. This could be used under harsh filtration conditions such as high temperature and strong acidic (or basic) solution.

Rieger et al. [66] fabricated Ag^+ ion containing zeolites and immobilized on electrospun cellulose nanofiber mats. The prepared Ag^+ ion exchanged zeolites (Ag-LTA-Large, Ag-LTA-Small, and Ag-LTA-Meso) immobilized on the nanofiber mats achieved a high inactivation rate, 92% loss of *E. coli* K12 viability after a 60 min incubation period. The Ag-LTA-Small and Ag-LTA-Meso zeolites immobilized on the nanofiber mats exhibited the same antibacterial activity. Table 6.5 presents some application examples of nanoporous membranes for water purification.

6.2.1 Nanomaterials/Nanoparticles in Water Purification

Details of nano particles were discussed in Chap. 1. Nanomaterials have unique size-dependent properties related to their high specific surface area (fast dissolution, high reactivity, strong sorption) and discontinuous properties (such as superparamagnetism, localized surface plasmon resonance, and quantum confinement effect). These specific nanobased characteristics allow the development of novel high-tech materials for more efficient water and wastewater treatment processes, namely membranes, adsorption materials, nanocatalysts, functionalized surfaces, coatings, and reagents. Table 6.6 summarizes the most important properties, applications, and innovative approaches involving nanometals and nanometal oxides. Whether in the midterm nanometals and nanometal oxides will be widely established in the water and wastewater sector strongly depends on the efficiency (nano-TiO_2) and stability of the metals (magnetic nanoparticles, nano zero-valent iron, nanosilver) [67].

Table 6.7 shows the application of different nanoparticles into polymeric membranes for water treatment.

Magnetic nanoparticle (Fe_3O_4) is also used for removing water pollutants in groundwater, especially the removal of arsenic [68]. “Pump-and-treat” is the conventional method for groundwater treatment. In this method, the groundwater was pumped up onto the surface for remediation by activated carbon which was the time-consuming and expensive method. Magnetic nanoparticles are injected into the contaminated groundwater to remove loaded particles by a magnetic field [69].

Table 6.5 Application examples of nanoporous membranes for water purification [63]

Membrane	Synthesis method	Target and efficiency	Water flux
PVDF	Electrospinning	NaCl (<280 ppm)	5–28 kg m^{-2} h^{-1}
Aquaporin reconstituted	Vacuum suction and amine-catechol adduct formation	NaCl (66.2%), $MgCl_2$ (88.1%)	
Zr-MOF	Solvothermal synthesis	Al^{3+} (99.3%), Mg^{2+} (98.0%), Ca^{2+} (86.3%)	0.28 L m^{-2} h^{-1} bar^{-1}
CNT-PcH	Electrospinning	NaCl (>99.99%)	24–29 L m^{-2} h^{-1}
MCM41-PA-TFN	Interfacial polymerization	NaCl (97.9 ± 0.3%), Na_2SO_4 (98.5 ± 0.2%)	46.6 ± 1.1 L m^{-2} h^{-1}
GO-PA-TFN	Interfacial polymerization	NaCl (93.8 ± 0.6%), Na_2SO_4 (97.3 ± 0.3%)	59.4 ± 0.4 L m^{-2} h^{-1}
K^+-controlled GO	Drop-casting	Mg^{2+}, Ca^{2+}, Na^+ (~100%)	0.36 L m^{-2} h^{-1}
Single-layer graphene	Oxygen plasma etching	K^+, Na^+, Li^+, Cl^- (~100%)	10^6 g m^{-2} s^{-1}
$Ti_3C_2T_x$ Mxene	Electrospinning	Metal cations and dye cations (diameter ≥ 6 Å)	37.4 L m^{-2} h^{-1} bar^{-1}
GO	Impregnation	Salt cations (6–46%), Methylene blue (46–66%), Raodamine-WT (93–95%)	27.6 L m^{-2} h^{-1} bar^{-1}
GO@PAN	Vacuum suction	Na_2SO_4 (56.7%), Congo red	8.2 L m^{-2} h^{-1} bar^{-1}
rGO	Hydriodic acid vapor, water-assisted delamination	Cu^{2+}, Na^+, orange 7 (~100%)	12.0 L m^{-2} h^{-1} bar^{-1}
GO-based	Shear-induced	Alignment organic probe molecules (>90%), salt cations (30–40%)	71 ± 5 L m^{-2} h^{-1} bar^{-1}
Bicontinuous cubic	Self-assembly	Br^- (83%), Cl^- (59%), SO_4^{2-} (33%), NO_3^- (81%)	2.8–5.7 L m^{-2} h^{-1} bar^{-1}
NPN	Track-etching	Au nanoparticles (>80%)	
Cellulose	Freeze-extraction technique	Nanoparticles with diameter > 10 nm	1.14 × 104 L m^{-2} h^{-1} bar^{-1}
CNT	Chemical vapor deposition	CdS (80%), Au (100%), TiO_2 (100%) nanoparticle	
CNCs	Freeze-drying process	Victoria Blue 2B (98%), Methyl Violet 2B (84%), Rhodamine 6G (70%)	6.4 L m^{-2} h^{-1} bar^{-1}
VAMWNTs	Chemical vapor deposition	Lubricating oil	1580 L m^{-2} h^{-1}
Ag-APAN	Electroless plating, surface modification	1,2-dibromoethane	
CNs-SA	Thermal oxidation etching	Ethanol	2469 g m^{-2} h^{-1}
PAA-g-PVDF	Phase inversion	Hexadecane, toluene, diesel (>99.99%)	15,500–23,200 L m^{-2} h^{-1} bar^{-1}

(continued)

Table 6.5 (continued)

Membrane	Synthesis method	Target and efficiency	Water flux
PSF nanofibers	Electrospinning, interfacial polymerization	Soybean oil (~100%)	5.5 $m^3 m^{-2} day^{-1}$
uGNM	Filtration-assisted assembly	99.8% of methyl blue and 99.9% of direct red 81	21.8 $L m^{-2} h^{-1} bar^{-1}$
GO	Vacuum suction	Dimethyl carbonate (95.2%)	1702 $g m^{-2} h^{-1}$
GO	Pressurized ultrafiltration	Ethanol (~100%)	
GO-TiO_2	Self-assembly	Rhodamine B, acid orange 7, humic acid (>90%)	60 $L m^{-2} h^{-1}$
MoS_2	Vacuum filtration	Evans blue (89%)	245 $L m^{-2} h^{-1} bar^{-1}$
WS_2	Vacuum filtration	Evans blue (>90%)	730 $L m^{-2} h^{-1} bar^{-1}$
TiO_2 nanowire	Hydrothermal synthesis, hot-press process	Polyethylene glycol, polyethylene oxide, HA, E. coli	
rGO-CNT	Vacuum-assisted filtration	Nanoparticles, dyes, BSA, sugars, and humic acid (>99%)	20–30 $L m^{-2} h^{-1} bar^{-1}$
PMMA	Ultraviolet irradiation, acid rinsing	Human rhinovirus type 14 (~100%)	
MCCNs-PEI	Electrospinning	MS_2 bacteriophage virus (99.99%), E. coli (99.9999%)	85 $L m^{-2} h^{-1} bar^{-1}$

PVDF polyvinylidene fluoride, *Zr-MOF* zirconium(IV)-based metal-organic framework membrane, *CNT-PcH* carbon nanotube incorporated polyvinylidene fluoride-co-hexafluoropropylene nanofiber membrane, *MCM41-PA-TFN* MCM-41 silica nanoparticles enhanced polyamide thin-film nanocomposite membrane, *GO* graphene oxide, *GO-PA-TFN* graphene oxide enhanced polyamide thin-film nanocomposite membrane, *PAN* polyacrylonitrile, *rGO* reduced graphene oxide, *NPN* nanoporous silicon nitride, *CNT* carbon nanotube, *CNCs* cellulose nanocrystals, *VAMWNTs* vertically-aligned multi-walled carbon nanotubes, *APAN* polyacrylonitrile, *CNs-SA* g-C_3N_4 nanosheets incorporated into sodium alginate matrix, *PAA-g-PVDF* poly(acrylic acid)-grafted PVDF, *PSF* polysulfone, *uGNM* ultrathin graphene nanofiltration membrane, *PMMA* polystyrene-block-poly(methyl methacrylate), *MCCNs* microcrystalline cellulose nanofibers, *PEI* polyethylenimine

Another advantage of magnetic nanoparticles is that they can be recovered by a magnetic field.

Carbon has been in use for water treatments with evidence found dating back to the Harappan civilization. The latest technologies involve ultrafiltration (UF), reverse osmosis (RO), and desalination methods. Carbon is also an essential component in all water treatments available today in the form of graphene. Graphene nanomaterials offer novel solutions for water purification and facilitate the development of advanced water purification membranes, especially for water desalination. Owing to its atomic thickness, assuring high fluid permeability and thus energy/cost

Table 6.6 Overview of types of nanomaterials applied for water and wastewater technologies [67]

Nanomaterial	Properties	Applications
Nanoadsorbents	+ high specific surface, higher adsorption rates, small footprint	Point-of-use, removal of organics, heavy metals, bacteria
	− high production costs	
Nanometals and nanometal oxides	+ short intraparticle diffusion distance compressible, abrasion-resistant, magnetic	Removal of heavy metals (arsenic) and radionuclides, media filters, slurry reactors, powders, pellets
	+ photocatalytic (WO_3, TiO_2)	
	− less reusable	
Membranes and membrane processes	+ reliable, largely automated process	All fields of water and wastewater treatment processes
	− relative high energy demand	

efficiency, extraordinary mechanical stability and potential for size-selective transport, graphene is an ideal candidate for future membranes. Graphene-based membranes possess several fascinating advantages over conventional membranes [70]. The fabrication procedure of graphene membranes based on GO nanosheets, is quite simple and scalable and enables the technical readiness for scaling up membrane production. This kind of membrane can be further improved by engineering the spacing between the GO layers through the inclusion of different-sized cross-linkers. In addition, the membrane charge and thus the charge-based selectivity can be modified by functionalizing GO with various functional groups. There are some challenges to develop graphene membranes for water treatment. For example, the selectivity of graphene multilayer membranes is mainly limited to large organic molecules and hydrated ions. Thus, the membranes can perform solely as ultrafiltration or NF.

Abdullah et al. [71] investigated the effects of ferrihydrite (Fh) nanoparticle loading on the physicochemical properties of polysulfone (PSf) membranes fabricated via the phase inversion method. On characterization of Fh/PSf membrane via FTIR, it was concluded that a new O-H band was formed when Fh was added into the membrane matrix. Increasing the loading of Fh significantly enhanced membrane pure water flux from 230.2 L m^{-2} h^{-1} (M-Fh 0%) to 726.6 L m^{-2} h^{-1} (M-Fh 15.3%), attributed to the improved membranes structures, membranes wettability, surface roughness, and overall porosity. The findings suggest incorporation of Fh into PSf membranes improves physicochemical properties of the membranes which are applicable for water/wastewater treatment.

6.2.2 *Polymer Nanocomposite Membranes*

The polymer nanocomposite membranes (PNCMs) are the most favorable choice in the membrane technology for water treatment. The PNCMs are obtained by addition of nano-entities (fibrous, platelets, spherical) into the polymer matrix. Nasir

Table 6.7 Application of different nanoparticles into polymeric membranes for water treatment [64]

Nanoparticle	Membrane process	Application	Polymer	Filler concentration
ZnO	MF	Treatment of synthetic wastewater	PVDF	6.7–26.7 wt.%
		Removal of copper ions		1–5 wt.%
		Removal of COD from wastewater		0–1 wt.%
		Removal of HA	PES	3.6 wt.%
	UF	Removal of HA	PSf	0.1 wt.%
		Removal of salt	PA	0.003–0.009 g
		Evaluation of antifouling properties in composite membranes for water treatment. Mixture model: BSA	PVDF	1 g
		Evaluation of antifouling properties in composite membranes for water treatment. Mixture model: BSA	PES	0.5–2 wt.%
		Removal of micelle from aqueous solutions		0–10 wt.%
		Removal of pollutants, Sodium alginate, BSA and humic acid (HA)		0.25–0.75 wt.%
		Evaluation of antifouling properties in composite membranes for water treatment. Mixture model: BSA		0.4 g
		Evaluation of antifouling properties in composite membranes for water treatment. Mixture model: BSA	PES-PVA	0.04–1.3 g
		Treatment of wastewaters	PSf	0.1–1 wt.%
		Bacterial removal from aqueous solutions		0.7 mg
		Evaluation of antifouling properties in composite membranes for water treatment. Mixture model: BSA	PVC	3 wt.%

(continued)

Table 6.7 (continued)

Nanoparticle	Membrane process	Application	Polymer	Filler concentration
	NF	Removal of HA	PES	0.035–4 wt.%
		Water purification (removal of HA)	PVP	100 mg
		Removal of salt and metal ions (Zn^{2+}, Cd^{2+}, Pb^{2+}, Mn^{2+}, Ni^{2+}, Fe^{2+}, Al^{3+}, Sb^{3+}, Sr^{3+})	CA	0.02–0.05 g
		Separation of Rhodamine B	CTA	0.6 g
		Removal of HA	PSf	2 wt.%
		Removal of inorganic salts and HA	PVDF	0–0.2 wt.%
		Removal of HA		1 wt.%
		Removal of salts (model $MgSO_4$)	Poly(piperazine amide)	1.5 wt.%
	FO	Desalination and water treatment	PVDF	0–8 wt.%
	RO	Removal of salt, bivalent ions (Ca^{2+}, SO_4^{2-} and Mg^{2+}), monovalent ions (Cl^- and Na^+), and bacterial retention	PA	0.005–0.4 wt.%
GO	MF	Treatment of effluents with high dyes content	PSf	0.75–2.5 wt.%
		Filtration of wastewaters	PVDF	3 wt.%
	UF	Evaluation of antifouling properties in composite membranes for water treatment. Mixture model: BSA	PSf	0.025–0.15 wt.%
		Evaluation of antifouling properties in composite membranes for water treatment. Mixture model: BSA	PVP-PVDF	0–0.50 wt.%
		Evaluation of antifouling properties in composite membranes for water treatment. Mixture model: BSA	PVDF	2.5 g mL^{-1}
		Natural organic matter removal		0.1–1 wt.%

(continued)

Table 6.7 (continued)

Nanoparticle	Membrane process	Application	Polymer	Filler concentration
		Evaluation of antifouling properties in composite membranes for water treatment. Mixture model: BSA		0–2 wt.%
		Natural organic matter removal	PA	0.004–0.012 wt.%
		Wastewater treatment	PSf	0.02–0.39 wt.%
		Degradation of organic pollutants in salty water	Cellulose ester	2 g L^{-1}
		Treatment of distillery effluent	PES	0.5–1 wt.%
	NF	Na_2SO_4 rejection from water streams	PSf	2000 ppm
		Water softening production	PAI-PEI	5 mg mL^{-1}
		Treatment of effluents with high dyes content	PMIA	0.05–0.5 wt.%
		Treatment of solutions with high dyes content	PAN	0.25–1 g L^{-1}
		Evaluation of dye removal capacity for water treatment	PES	0.1–1 wt.%
		Water purification	PPA	100–400 mg L^{-1}
	RO	Desalination: Salt removal (NaCl)	PA	5–76 ppm
		Desalination: Salt removal (NaCl, $CaCl_2$ and Na_2SO_4)	PSf	0.005–0.3 wt.%
		Desalination: Salt removal (NaCl)		100–300 ppm
	FO	Possible prospect for desalination of sea water	PA	1.5 wt.%
Graphene	UF	Wastewater treatment	PSf	0.1–2 wt.%
	NF	Water purification	PVDF	0.864 μg mL^{-1}
$AgNO_3$	UF	Reduction of the microbial load of raw milk during the concentration process by the UF process	PES	2–4–6 wt.%
		Evaluation of antifouling properties in composite membranes for water treatment. Mixture model: BSA	PSf	0.5 wt.%

(continued)

Table 6.7 (continued)

Nanoparticle	Membrane process	Application	Polymer	Filler concentration
AgNPs	MF/UF	Evaluation of antifouling properties in composite membranes for water treatment. Mixture model: BSA		0–0.05–0.1–2.5–5–10 wt.%
	UF	Water purification	PES	0–0.32–0.64 wt.%
		Evaluation of antifouling and antibacterial properties in composite membranes for water treatment. Model bacteria: E. coli	PES, PSf, CA	0.03–0.06–0.09 wt.%
		Evaluation of antifouling and antibacterial properties in composite membranes for water treatment. Model bacteria: E. coli. Mixture model: BSA and dextran solution	PSf	0.25–0.5–1.0 wt.%
		Evaluation of antifouling and antibacterial properties in composite membranes for water treatment. Model bacteria: P. putida. Mixture model: BSA		3.6 g
		Evaluation of antifouling properties in composite membranes for water treatment. Mixture model: polyethylene glycol (PEG) and Dextran solutions	CA	0–0.1–0.4 wt.%
	NF	Evaluation of antibacterial properties in composite membranes for water treatment. Model bacteria: E. coli, S. aureus		0.5–1–2 wt.%

(continued)

Table 6.7 (continued)

Nanoparticle	Membrane process	Application	Polymer	Filler concentration
Ag-NO_3		Evaluation of antibacterial properties and removal of salt (Na_2SO_4). Model bacteria: E. coli	PA-PVA	10 mL
	RO	Evaluation of antibacterial properties and removal of salt (NaCl). Model bacteria: E. coli, P. aeruginosa, S. aureus	PA	10 mL
		Evaluation of antibacterial properties and removal of salt (NaCl). Model bacteria: E. coli, Bacillus subtilis	PA/PSf/PET	4 g L^{-1}
		Evaluation of antibacterial properties. Model bacteria: E. coli, Bacillus subtilis	CA	–
	DCMD	Deposition of silver nanoparticles layers to optimize surface roughness and enhance membrane hydrophobicity. Desalination of seawater. Model water: NaCl 3.5 wt.%	PVDF	1 wt.%
	PRO/RO	Evaluation of antifouling and antibacterial properties in composite membranes for water treatment. Model bacteria: E. coli. Mixture model: BSA	PES	40 g L^{-1}
Ag-NPs	PRO	Evaluation of antifouling and antibacterial properties in composite membranes for water treatment. Model bacteria: E. coli, Bacillus subtilis. Mixture model: C. testosteroni	PAN	0.01–0.02–0.05–0.10 wt.%

(continued)

Table 6.7 (continued)

Nanoparticle	Membrane process	Application	Polymer	Filler concentration
Bio-Ag$_0$	UF	Evaluation of antifouling and antibacterial properties in composite membranes for water treatment. Model bacteria: E. coli, P. aeruginosa	PES	0.1–0.3–0.5–1 wt.%
	NF	Evaluation of antibacterial properties and removal of salt (Na_2SO_4). Model bacteria: E. coli, P. aeruginosa	PA	0.1 mM 40 mL
		Evaluation of antibacterial properties and removal of salt (Na_2SO_4). Model bacteria: P. aeruginosa	PSF	0.005–0.025–0.05 wt.%
Cu-NPs	UF	Evaluation of antifouling and antibacterial properties in composite membranes for water treatment. Model bacteria: P. putida. Mixture model: BSA		3.6 g
CuAc2		Evaluation of antifouling and antibacterial properties in composite membranes for water treatment. Model bacteria: E. coli. Mixture model: HA	PAN/PEI	1000 mg L^{-1}
Cu-NPs		Treatment of wastewaters (sludge filtration) and evaluation of antifouling properties in composite membranes for water treatment. Mixture model: BSA	PES	0.002–0.01–0.03–0.05 wt.%

(continued)

Table 6.7 (continued)

Nanoparticle	Membrane process	Application	Polymer	Filler concentration
Ag-NPs Cu-NPs		Evaluation of antifouling and antibacterial properties in composite membranes for water treatment. Model bacteria: E. coli. Mixture model: PEO	PSF	3.2 g
$CuSO_4$	NF	Seawater softening, removal of salt (SO_4^{2+}, Mg^{2+}, Na^+, Cl^-). Evaluation of antibacterial properties in composite membranes for water treatment. Model bacteria: E. coli	PAN/PEI	0–0.4 g
		Evaluation of antibacterial properties and removal of salt (NaCl). Model bacteria: E. coli		50 mM
$CuCl_2$	RO	Evaluation of antifouling and antibacterial properties in composite membranes for water treatment. Model bacteria: E. coli. Mixture model: BSA	PA	30 mL
Cu-NPs		Evaluation of antibacterial properties in composite membranes for water treatment and removal of salt (NaCl). Model bacteria: E. coli, P. aeruginosa, S. aureus		50 mL

(continued)

Table 6.7 (continued)

Nanoparticle	Membrane process	Application	Polymer	Filler concentration
TiO_2-NPs	MF	Evaluation of antifouling properties using whey solution	PVDF	0.05 wt.%
	UF	Evaluation of antifouling properties in composite membranes for water treatment. Mixture model: HA		0.1 g L^{-1}
		Evaluation of antifouling properties in composite membranes for water treatment. Mixture model: BSA, PEG and $MgSO_4$		0.5–1 wt.%
		Treatment of wastewaters		0–0.15–0.3–0.45–1.5–3–6 wt.%
		Evaluation of UV-cleaning properties		0–1.5 wt.%
		Evaluation of UV-cleaning and antifouling properties. Mixture model: BSA		0–7 wt.%
		Evaluation of antifouling properties. Mixture model: BSA and Lys	PP	–
		Evaluation of antifouling properties and removal of salt (NaCl). Mixture model: BSA and pepsin	PSF	0.1, 0.25 and 0.5 wt.%.
		Water treatment	CA	0–25 wt.%
		Evaluation of UV-cleaning properties and antifouling properties. Mixture model: red dye and BSA	PA	10–80 ppm
Titanium tetraisopropoxide (TIP)		Evaluation of antifouling properties. Mixture model: BSA		29.58 mL

(continued)

Table 6.7 (continued)

Nanoparticle	Membrane process	Application	Polymer	Filler concentration
TiO_2-NPs	FO	Evaluation of removal of salt (NaCl)	PSF	0.01, 0.05, and 0.1 wt./v%
		Evaluation of removal of salt (NaCl)		0–0.5–0.75–0.99 wt.%
	MF/MBR	Evaluation of antifouling properties. Mixture model: BSA, PEG and $MgSO_4$	PVDF	–
nanoTiO_2	MBR	Algal membrane bioreactor evaluation		5 wt.%
TiO_2-NPs	NF	Wastewater treatment application	PES	0.125 g
CNTs	NF	Evaluation of antifouling and removal of salts (NaCl, Na_2SO_4)	PSF	5 wt.%
	NF	Drinking-water purification	Nitrocellulose	3 wt.%
	UF	Water treatment and biofouling control application	PES	0–4 wt.%
	NF	Wastewater treatment application	PES	0.1 wt.%
	NF	Water treatment	PA	5 wt.%
	NF	Metal removal (Cr^{6+}), (Cd^{+2})	PSF	0.1–1 wt.%
	NF	Water treatment for salt removal (NaCl, Na_2SO_4)	PMMA	0.67 wt.%
	NF	Evaluation of antifouling properties in composite membranes for water treatment	Polyimide 84	0.1–1 wt.%
	UF	Water treatment for UF applications	PSf	0.1–0.5 wt.%
	UF	Wastewater treatment by membrane bioreactor	PSf	0.1–1 wt.%
	MF	Bleach effluent treatment by membrane bioreactor	PSf	0.04 wt.%

(continued)

et al. [53] discussed the progress of polymeric nanocomposite membranes for wastewater treatment. An overview of the advantages and disadvantages of polymers used in nanocomposite membranes is given in Table 6.8.

6.2.3 *Nanofibers in Water Treatment*

Electrospun nanofiber scaffolds with a membrane structure could be used as effective membrane materials for water treatment due to its high porosity, interconnected pore structure, ease of incorporation of special functionality, and versatility to be used safely. Electrospinning is a simple, inexpensive, and efficient technique to fabricate nanofibers. The physical and chemical parameters of electrospun nanofibers can be easily manipulated for different applications. Functional nanofiber membranes or nanofiber-based composite membranes can be used for several water purification systems, including adsorption, filtration.

Details regarding to nanofiber in water treatment is given in Sect. 6.6.7.

Table 6.9 shows few examples for the removal of heavy metals/pollutants from water/wastewater by nanofiber/membranes.

Table 6.8 Comparison of most commonly used polymers in nanocomposite membranes [53]

Polymer	Advantages	Disadvantages	References
Cellulose acetate	Low cost, hydrophilicity, fabrication flexibility	Poor chlorine resistance, poor thermal resistance (<30 °C), poor chemical resistance	[72]
Polystyrene polyethersulfone	Superior thermal resistance (up to 75 °C), wide PH range (1–13), superior chlorine resistance, fabrication flexibility, high mechanical properties	Hydrophobicity, less operating pressure limit	[73]
Polyvinylidine fluoride	Good mechanical strength	Hydrophobicity	[72]
Polyvinyl alcohol	Good mechanical properties, low thermal properties and strength for few applications, fabrication flexibility, low cost, film forming ability, chemical resistance, limited biological performance	Dissolve in aqueous solutions	[74, 75] [76]
Chitosan	Fabrication flexibility, chelating properties, insoluble in water, chemical stability, film forming ability	Failure in acidic pH range	[77–79]
Polyamide	High mechanical properties	Poor chlorine resistance	[80, 81]

Table 6.9 Few examples for the removal of heavy metals/pollutants from water/wastewater by nanofiber/membranes

Membrane	Type	Results	Reference
Thiol-modified cellulose nanofibrous composite membranes	Adsorption	Adsorption capacities for both Cr(VI) (87.5 mg/g) and Pb(II) (137.7 mg/g)	[82]
Piezoelectric electrospun nanofiber/PVDF	MF	(5573 LMH bar^{-1}) and rejection 99.87% for particulates	[83]
PES/PET	Microfiltration	Enhanced the mechanical properties thereby the selectivity of the membranes 60,000 L m^{-2} h^{-1} psi^{-1}	[84]
Silkfibroin-cellulose acetate	Adsorption	Cu^{2+} adsorbed reached 22.8 mg/g adsorption promising material for removing heavy metals ion in water	[85]
Polysulfone -cellulose	UF	950 improved the performance of UF membranes Flux 950 L m^{-2} h^{-1} psi^{-1} (cellulose and polysulfone at 1.5 TMP*)	[86]
PAN-PVA (TFNC) thin film nanofibrous composite	UF performance in BSA filtration	Flux 173.0 Lm^{-2} h^{-1} and rejection above 98.0%	[87]
Electrospun PAN-GO composite nanofibers	Water purification	PAN-based composite nanofibers exhibited improved overall properties as water purification membranes when the amount of filler GO was incorporated 0.2 and 0.3 wt.%	[88]
Carbon nanofiber (CNF) mats	NP filtration	Efficiently reject nanoparticles of different types (Au, Ag, and TiO_2) and size (from 10 to 100 nm in diameter) flux 47,620 L m^{-2} h^{-1} bar^{-1}	[89]
Functionalized by ZnO-polyacrylonitrile–chitosan bi-layer membranes	Anti-bacterial and water filtration	Bacteria filtration has a log reduction value 2 orders of magnitude higher than PAN membranes	[90]
Carbon nanofibers/TiO_2-PAN	Metal ions (such as Pb^{2+}, Cu^{2+}, Cd^{2+}) and cationic dye (such as methylene blue (MB)) from wastewater	Maximum rejection around 87%, 73%, 66%, for Pb^{2+}, Cu^{2+}, Cd^{2+} metal ions and 84% for methylene blue dye	[91]
Modified Polyvinylidene fluoride (PVDF)	Oil/water separation	20,664 L m^{-2} h^{-1} under gravity	[92]

(continued)

Table 6.9 (continued)

Membrane	Type	Results	Reference
PAN/TiO_2	Pb(II) and Cd(II)	Adsorption capacities for Pb^{2+} and Cd^{2+} are remarkably increased by approximately 114 and 47%, respectively, compared to those of pure PAN electrospun nanofibers	[93]
CS-DTPA/PEO NFs***	Cu^{2+}, Pb^{2+} and Ni^{2+} ion removal from wastewater	Adsorb metal ions in the following order: $Cu^{2+} > Pb^{2+} > Ni^{2+}$	[94]
Plasma treated PPSU (TFC-based forward osmosis membrane)	Water treatment	Significant enhancement in osmotic water flux and much lower reserve salt flux	[95]
Carbon–Silica Nanofibrous membrane	Gravity-driven process (UF)	Excellent oil–water separation efficiency High-flux	[96]
FPU (fluorinated polyurethane /(PAN/PU)	Filtration	Superhydrophobic CA 154° with water and superoleophobic oil CA 151°. Different oil aerosol particles in a single-unit operation, with >99.9% filtration efficiency	[97]
PSf/TiO_2	FO	Higher water flux than commercial membranes and electrospun membranes without nano-TiO_2	[98]
PU	Filtration	Flux 1000 $Lm^{-2} h^{-1} psi^{-1}$	[99, 100]

TMP transmembrane pressure, *TEA* Triethylamine, *PFDT* 1H, 1H, 2H, 2H-perfluorodecanethiol, *PDA* p-phenylenediamine, *CS-DTPA/PEO NFs* Diethylenetriaminepentaacetic acid-modified chitosan/polyethylene oxide nanofibers

6.2.4 Aquaporin-Based Membranes in Water Treatment

In recent years, biomimetic membranes, such as the aquaporin membrane, have emerged as strong candidates for membrane-based water purification technology. Biomimetic approaches have the potential to overcome the problems associated with existing membranes including limited permeability, low selectivity, and excessive energy consumption. Fuwad et al. [101] discussed the state-of-the-art of membrane-based water purification technologies, summarizing the role and limitations of conventional membrane materials while evaluating the latest progress in the field of biomimetic membrane fabrication.

Aquaporins are pore-forming proteins and ubiquitous in living cells. Under certain conditions, they form highly selective water channels that are able to reject most ionic molecules. The combination of high water permeability and selective rejection make them an ideal material for creating novel high flux biomimetic membranes. To stabilize the aquaporins, they are incorporated in vesicles. Since stand-alone membranes based on these vesicles are too mechanically weak for their intended technical applications, like osmosis, they are embedded in a polymeric matrix or deposited onto polymeric substrates such as nanofiltration membranes. The first demonstration of functional AQP incorporation was presented by Kumar in 2007 who incorporated bacterial AqpZ from *E.coli* in PMOXA-PDMS-PMOXA polymersomes [102]. Aquaporin Inside™ (Aquaporin A/S, Copenhagen, Denmark) is the first commercially available biomimetic membrane with aquaporins embedded. This kind of membrane is able to withstand pressures up to 10 bar and allow a water flux >100 L m^{-2} h^{-1} for example required for brackish water desalination [54, 67].

Xie et al. [103] reconstituted aquaporins into self-assembled polymer vesicles and used in situ "surface imprinting" polymerization to generate a dense hydrophobic polymer layer. This novel membrane possesses a well-controlled nanostructured selective layer and as high mechanical strength as necessary to withstand pressure-driven water filtration processes.

Aquaporin based biomimetic membranes have been shown to provide a potential benefit for water purification and desalination [104]. Li et al. [104] tested a novel aquaporin based biomimetic membrane in simulated membrane cleaning processes. The effects of cleaning agents on water flux and salt rejection were evaluated. The membrane showed a good resistance to the chemical agents. Camilleri-Rumbau et al. [105] investigated the applicability of aquaporin-based forward osmosis membranes while separation of biogas digestate liquid fractions was investigated. The results showed that Total Ammonia-Nitrogen rejection was higher than 95.5% in all experiments, independently of the type of draw solution (NaCl and hide preservation effluents), experimental period and the use of feed acidification. The results showed the potential of this technology to achieve enhanced ammonia-nitrogen rejections and low-fouling propensity. He et al. [106] demonstrated a new functional aquaporin stabilizing agent FBP1, and immobilized AqpZ (AquaporinZ) – FBP1 (propargyl functionalized β-sheet peptide complex) onto a polymeric surface by circulating click reaction to fabricate a novel biomimetic membrane. However, the salt rejection of PSU–AqpZ membrane only improved moderately compared to the control sample (from 5 to 12.5%). Future work on minimizing defects and optimizing the click reaction to further increase salt rejection can be performed to fabricate qualified desalination membranes.

6.3 Removal of Dyes

The presence of dyes in wastewater is a major concern for environmental conservation and human health. Factories across the world are dumping thousands of tonnes of untreated dyes into rivers and waterways every year. The majority of these dyes are toxic to the environment and may lead to mutations and cancers in animals. Particularly in textile industries where considerable amounts of water and chemicals are used during the dyeing process the wastewater contains about 20% of dye as well as organic matter, salts and other substances. For example, azo dyes, a commonly used dye to color fabrics can cause cancer if released into the environment with wastewater. The release of untreated wastewater has strong color, high chemical oxygen demand, low biodegradability and high variability, it poses a threat to the animal and human health, environment and the most serious problems are ground water and surface water pollution. Further, the discharge of colored effluents into water bodies affects the sunlight penetration which in turn decreases both the photosynthetic activity and dissolved oxygen levels. The removal of dyes from wastewater is one of the major problem. Removal of dyes from water/wastewater has gained a huge attention in recent years. So far, biological, chemical and physical methods are the traditional techniques, of which adsorption is found to be a more effective and cheap method for removing dyes. The advancement of nanotechnology has attracted tremendous interest from many researchers in the field of removal of dyes from wastewater. Nanosized metal or metal oxide-based materials as inorganic nanomaterials are used broadly for the removal of dyes. Nanosized metals or metal oxides, including nano zerovalent iron, nano zerovalent zinc, magnetic Fe_3O_4, magnesium oxide (MgO), titanium dioxide (TiO_2), zinc oxide (ZnO), provide high surface area and specific affinity [107].

Activated CNTs are a promising adsorbent nanomaterial for organic pollutants from aqueous solutions. Jun et al. [108] investigated the removal of acid red B (ARB) by using single-walled CNTs (SWCNTs) and multi-walled CNTs (MWCNTs) and reported that the adsorption capacities of SWCNTs and MWCNTs were 585 and 85 mg g^{-1} respectively. Kinetic study showed that the equilibrium time for adsorption of ARB to CNTs is 60 min, and the adsorption kinetic can be well described by the pseudo-second-order model. The adsorption increases with the increase in solution pH, and coexisting NaCl and $CaCl_2$ enhance the removal. Ma et al. [109] studied the removal of anionic and cationic dyes in aqueous solutions by using activated carbon nanotubes (CNTs-A) with a high specific surface area (SSA), and a large number of mesopores. Experimental results indicated that CNTs-A have excellent adsorption capacity for methyl orange (149 mg g^{-1}) and methylene blue (399 mg g^{-1}). Hao et al. [110] investigated the adsorption of Rhodamine B (RhB) onto hausmannite/λ-MnO_2 composite and the results unveiled that both decolorization and degradation rate could reach up to 97% and 90% respectively in 1 h reaction time at pH 3.0. Zhang et al. [111] reported that sodium dodecyl sulfonate (SDSn) surface-modified mesoporous $ZnFe_2O_4$ nanoparticles (10–50 nm) have a remarkably high maximum adsorptive capacity (~699.30 mg g^{-1}) for aqueous Methylene Blue (MB) removal at 288 K and pH of 12.

The nanofibrous membranes (NFM) exhibited quite high adsorption capacity and fast removal rate for cationic dyes [112]. Zhang et al. [113] used chitosan coated nylon for the membranes for papain adsorption. These membranes had excellent chemical and thermal resistance as well as high wettability. The dye Cibacron Blue F3GA (CB) as a ligand was covalently immobilized on the CS-coated membranes. The maximum adsorption capacity for papain was up to 133.2 mg g^{-1}. The chemically-modified CS-nylon nanofiber membrane with the CB as ligand could become the low-cost but high efficiency affinity membranes for papain separation.

Rashidi et al. [114] evaluated polyamide nano-membrane for the removal of five different fiber reactive dyes from wastewater, namely reactive blue 15, reactive red 194, reactive yellow 145, reactive black 5, and reactive orange 16. The flux for all the samples ranged between 7.8 and 9.2 mL cm^{-2} s^{-1}. The rejection rate in nano-membranes was in the range of 90–97%, and was based on structures, sizes, and the electrical charge of dye molecules in each sample. GO based membranes have attracted tremendous research interests as a promising substrate for the preparation of various graphene-based nanocomposites for the removal of dyes from waste water. Wang et al. [115] fabricated polyacrylonitrile nanofibrous mat (GO@PAN) which is a graphene oxide (GO) based PAN nanofiltration membrane (highly porous) for water treatment application. Water flux under an extremely low external pressure (1.0 bar) significantly increased and showed high rejection performance (nearly 100% rejection) of Congo red, and 56.7% for Na_2SO_4. Manoukian et al. [116] synthesised highly uniform carbon spheres (CSs) membranes with high surface area of 1791.5 m^2 g^{-1} and activated it by using CO_2 to produce highly uniform activated CSs (HUACSs) with negative charges as demonstrated by zeta potential measurements. Polysulfone-HUACS mixed-matrix membranes (PSf-HUACS MMMs) with different HUACS contents, i.e. 0.5, 1, 3, 5 and 7% with respect to the PSf weight were prepared. It was demonstrated that, all MMMs exhibit enhanced water flux compared to the PSf pristine membrane by at least 80%. On using PSf-HUACS MMMs with HUACS content as low as 0.5%, methylene blue rejection efficiency of 99.9% was achieved. This high dye rejection efficiency can be explained based on the synergistic contribution of size exclusion and adsorption mechanisms involved in nanofiltration applications.

Chaúque et al. [117] modified the surface of electrospun polyacrylonitrile (PAN) nanofibers with ethylenediaminetetraacetic acid (EDTA) and ethylenediamine (EDA) as cross linker. The modified PAN nanofibers showed efficient sorption of methyl orange (MO) and reactive red (RR) from aqueous synthetic samples. The maximum adsorption capacities for MO and RR was (at 25 °C) was 99.15 and 110.0 mg g^{-1}, respectively. The fabricated nanofibers showed appreciable removal efficiency of the target dye sorptives from wastewater.

Li et al. [118] incorporated ZIF-67 on PP membrane surface and pore walls with the assistance of PDA as biomimetic adhesive layer. The hydrophilicity and permeability of PDA/ZIF-67@PP membrane enhanced by 47.3% and 150.0% respectively. Li et al. designed the visible-light PDA/ZIF-67@PP/PMS system to remediate dye wastewater by concurrent filtration, photocatalysis and peroxymonosulfate (PMS) activation. It was reported the removal of MB and MO with high efficiency above 92.0%. Wang and Wei [119] evaluated the adsorption properties of two kinds of anionic dyes, orange IV (OIV) and glenn black R (GR) and two kinds of cationic dyes, acridine orange (AO) and crystal violet (CV) on magnetic graphene oxide modified with 1-amine-3-methyl imidazole chloride ionic liquid (LI-MGO). The maximum adsorption capacities for GR, OIV, AO and CV were 588.24, 57.37, 132.80 and 69.44 mg g^{-1} at 298 K, respectively. LI-MGO has better selective adsorption for anionic dyes than magnetic graphene oxide (MGO) due to electrostatic interactions. Moreover, the LI-MGO adsorbent can be magnetically separated and is easy to prepare. It was demonstrated that LI-MGO would have great potential as an efficient environmentally friendly adsorbent for the removal of anionic dyes in water treatment. Aluigi et al. [120] studied keratin nanofibrous membranes (mean diameter of about 220 nm), prepared by electrospinning, tested as adsorbents for Methylene Blue through batch adsorption tests. The adsorption capacity increased with increasing the initial dye concentration and pH, while it decreased with increasing the adsorbent dosage and temperature, indicating an exothermic process.

Fard et al. [121] decorated α-Fe_2O_3 nanofiber surface with cellulose nanoparticles and reported that the incorporation of Cell NP onto the surface of inorganic nanofiber drastically increased the dye adsorption property. Also, the result showed that the maximum of dye removal occurred at alkaline pHs due to presence of high amounts of hydroxyl group on the nanofiber surface.

Lou et al. [122] reported that 80% of RhB was degraded within 6 h at the wavelength of 546 nm, which clearly falls within the visible spectra on PVDF/TiO_2 nanofiber webs (with TiO_2 concentration of 20%). Chen et al. [123] demonstrated a free-standing sandwich-structured polyamide 6 (PA 6) @GO@PA 6 nanofiltration membrane incorporated with TiO_2 nanoparticles with high water flux via electrospraying combined with electrospinning method. The membrane showed a pure water flux up to 13.77 L m^{-2} h^{-1} bar^{-1} even under an extremely low external pressure (1.0 bar), which increased by 80.7% from that of PA 6@GO (120) @PA 6 nanofiltration membrane (7.62 L m^{-2} h^{-1} bar^{-1}) without nanoparticles intercalated, while maintaining high organic dye rejection capabilities (>85% for BF, >92% for MB, >99% for MO, and 99.85% for EB).

Large surface area of electrospun nanofibers allows more dye to be removed from the wastewater through surface adsorption. Yu et al. [124] has shown that electrospun nylon-6 (PA-6) membrane was able to remove indigo dye solution without any additional modifications to its chemistry. Akduman et al. [125] investigated dye (Reactive Red 141) sorption capacity of electrospun TPU (thermoplastic polyurethane) and PVA nanofiber membranes from textile wastewater. Due to hydrophobic structure, TPU membranes showed quite low adsorptions (14.48 mg g^{-1}). BTCA (butanetetracarboxylic acid) cross-linked PVA nanofiber membranes showed good performance in sorption of Reactive red 141 dye. The maximum sorption capacity reached 88.31 mg g^{-1}. Lv et al. [126] fabricated a reusable positively-charged PES NFMs by introducing QAS (Quaternary ammonium salt) polymer (PMETAC) in PES for the removal of bacteria and dyes from wastewater. SEM images revealed that the PMETAC-decorated NFMs were composed of randomly arranged and interwoven nanofibers, which possessed large surface area and high porosity, providing abundant sites for adsorption. The adsorption capacity towards Congo Red (CR) was up to 208 mg g^{-1}, which was much higher than those of other reported adsorbents, such as the PAN-based 2D nanofibrous mats (77.5 mg g^{-1}) [127]. Fendi et al. [128] demonstrated that in electrospun phenol-cresol formaldehyde/polystyrene membranes when zinc oxide nanoparticles were added to it for removal of methylene blue. With the addition of ZnO nanoparticles, the rate of methylene blue adsorption is faster and there was also an increase in the adsorption capacity with both reaching saturation point less than 15 minutes. Adsorption capacity of ZnO loaded electrospun phenol-cresol formaldehyde/polystyrene membranes continues to perform better than membrane without ZnO in the presence of NaCl and KCl in the dye solution and at elevated temperature.

Xiong et al. [129] used ZnO-deposited PTFE membranes as adsorbents for the removal of ***positively*** charged RhB and negatively charged AO7. It was observed that in both cases the removal efficiencies were higher than 98%. Foroozmehr et al. [130] prepared polyacrylonitrile (PAN) nanofibers functionalized with β– cyclodextrin (βCD) during an electrospinning process and used to treat a reactive dye wastewater stream by dynamic method. It was found that the dye removal efficiency was increased from 15.5% for PAN to 24% for PAN/βCD nanofiber mats. Table 6.10 shows few examples of adsorbents for dye removal.

Table 6.11 presents some recent mixed polymeric membranes for dye separations.

Aizat and Aziz [150] discussed the chitosan nanocomposites' application in waste water treatment. The antimicrobial activity of chitosan nanocomposites was also included in the review. Significant work has been reported on chitosan nanocomposites for the removal of dyes from wastewater. Table 6.12 presents some recent works on chitosan based nanocomposites for dye removal.

Photocatalysis is a degradative process where attack by reactive oxygen species results in the overall oxidation of an organic pollutant via intermediate products. Though many processes and materials including catalysts are used to remove pollutants from water or wastewater, they are not always efficient and cost-effective. To overcome this challenge, the technology owners have developed an environmentally-benign and recoverable nano-photocatalytic system that acts by mineralizing the pollutants in waste water before it is discharged into the environment. The photocatalyst is activated upon exposure to natural visible light and is regenerated by using diluted peroxide.

Photocatalysis is one of the efficient and environmentally friendly techniques to purify waste water. The principle of photocatalysis is very simple: A catalyst harnesses the (UV) radiation from sunlight and uses the energy to break down different substances. Photocatalysis can be used to break down a wide variety of organic materials, organic acids, estrogens, pesticides, dyes, crude oil, microbes (including viruses and chlorine resistant organisms), inorganic molecules such as nitrous oxides (NOx) and, in combination with precipitation or filtration, can also remove metals (such as mercury) [158, 159].

Due to this universal applicability, photocatalysis with nanoparticles as catalysts is used to reduce air pollution, in building materials for self-cleaning surfaces, in addition to water purification. Functional photocatalytic nanofiber webs [160, 161] are promising environmentally friendly candidates for the photodegradation of organic pollutants, such as dyes and pigments.

The catalyst is developed by growing photocatalytic metal compounds (such as iron oxide nanoparticles) in situ within aluminosilicate mineral materials, such as clays or zeolites. The developed catalyst can be considered advantageous when compared to commercially available technologies. Some of the key points are highlighted below:

Table 6.10 Few examples of adsorbents for dye removal

Adsorbents	Preparation and modification	Adsorbate	Efficiency	Reference
Fe_3O_4 nanomaterials	NPs were synthesized by chemical method using CTAB	Acridine orange	0.050 mol g^{-1}	[131]
		Coomassie brilliant blue R-250	0.082	
		Congo red	0.078	
HA-Fe_3O_4	Fe_3O_4 NPs modified by humic acid	Rhodamine B	Adsorption qmax-161.8 mg g^{-1} (98.5%)	[132]
Fe_3O_4 nanomaterials	Ionic liquids were used to modify Fe_3O_4 NPs	Reactive red 120	166.67 mg g^{-1}	[133]
Fe_3O_4 nanomaterials	Polyacrylic acid bound Fe_3O_4 nanoparticles, which act as core and PAA as ionic exchange	Rhodamine 6G	55.8 mg g^{-1}	[134]
Fe_3O_4 nanomaterials	Silica based cyclodextrin immobilized on magnetic nanoparticles	Direct blue 15	98%	[135]
MgO nanoparticles	Co-precipitation method	Reactive black 5	500 mg g^{-1}	[136]
MgO nanoparticles		Reactive orange	333.34 mg g^{-1}	
MgO nanorods	Artinite and MgO nanorods prepared by precipitation method	Malachite green and Congo red	95.1% and 86.28%	[137]
Mgo nanostructures	Hierarchical hydromagnesite and MgO nanostructures prepared by reflux method	Malachite green and Congo red	99.94% and 9.98%	
MgO nanoflakes	Hydromagnesite and MgO nanoparticles prepared by hydrothermal method	Malachite green and Congo red	97.42% and 92.68%	
Mgo nanoparticles	Activated carbon immobilized on MgO nanoparticles	Rhodamine B	16.2%	[138]
Rice straw charcoal/MgO nanocomposite	Rice straw charcoal immobilized on MgO	Reactive blue 221	27.78%	[139]

(continued)

Table 6.10 (continued)

Adsorbents	Preparation and modification	Adsorbate	Efficiency	Reference
GO	–	Methylene blue	714 mg g^{-1}	[140]
Magnetite/reduced graphine oxide	Solvothermal strategy using non-toxic and cost-effective precursors	Rhodamine B	91%	[141]
	–	Malachite green	94%	
nZVI/rGO	Liquid-phase reduction method in a nitrogen atmosphere	Rhodamine B	87.72%	[142]
PI based CNFs	Electrospining polyamic acid solutions followed by thermal imidization and carbonization	MB	272.48 mg g^{-1}	[143]
Pb@$ZnFe_2O_4$	Synthesized by co-precipitation method	Congo Red	96.49%	[144]
Fe_3O_4-loaded activated carbon (AC)	Coprecipitation method	Malachite green (MG) and Rhodamine B (RB)	96.11% for MG and 98.54% for RB	[145]
GO-based PES core-shell particles	Facile method	Methylene blue	352.11 mg g^{-1}	[143]

1. The catalyst production involves the use of raw materials that are available abundantly and cost-effective in nature, thereby potentially minimizing the final cost of the product.
2. The manufacturing and usage of the catalytic system is simple and easy to deploy.
3. The photocatalyst is fully recyclable in nature.
4. The developed catalyst can be considered robust and durable and has the ability to destroy the targeted pollutants instead of just adsorbing them.

It was reported that photocatalysis was more effective than ultraviolet irradiation (UVA photolysis) photolysis in destroying the oestrogenic effect of 17-B-oestradiol, esterone and estriol [162, 163]. Research efforts in photocatalysis have dramatically expanded since the discovery of the photocatalytic properties of TiO_2 and the demonstration of its effectiveness to generate hydroxyl radicals in the presence of UV. TiO_2 photocatalysis is of particular interest because of its environmentally friendly features. The process can completely oxidize virtually all organic contaminants (nonselective) without addition of any other chemicals for the reaction and thus produce no harmful end products in most cases. Especially, TiO_2 photocatalysis forms no disinfection by-products unlike other chemical oxidation processes when

Table 6.11 Some recent mixed polymeric membranes for dye separations

Membrane	Dyes	Result	Reference
PES/PEI NFMs	Anionic dyes	1000.00 mg g^{-1}, 344.83 mg g^{-1}, 454.44 mg g^{-1}, 94.34 mg g^{-1}, 161.29 mg g^{-1} and 357.14 mg g^{-1} for Sunset Yellow FCF, Fast Green FCF, Amaranth, Pb^{2+}, Cu^{2+} and Cd^{2+}	[146]
Negatively-charged PES NFMs	Separation of MB/ Amaranth mixture	Separation 98.29%	[147]
PEN/GO-PDA nanofibrous composite	Anionic dyes separation	Permeate flux of 99.7 L m^{-2} h^{-1} (0.1 MPa, pH = 3.0) and a high rejection (99.8%) for Direct Blue 14	[148]
PMETAC/PES	Congo Red	208 mg g^{-1}	[126]
PAN NF 2D mats	Congo red	77.5 mg g^{-1}	[127]
Copolymer of acrylic acid and methyl methacrylate-PES	Methylene blue (MB)	2257.88 mg g^{-1}	[140]
ZnO-PTFE	Positively charged RhB and negatively charged AO7	Removeable efficiencies higher than 98%	[129]
MoO_3 nanowire-based membrane	MB and RhB	Adsorbability up to 521 and 321 mg g^{-1} for MB and RhB, respectively	[149]
PAN/βCD nanofiber mats	Reactive dyes	Dye removal efficiency increased from 15.5% for PAN to 24% for PAN/βCD nanofiber mats	[130]

Table 6.12 Recent studies regarding the adsorption capacities of synthesized chitosan nanocomposites for dyes removal in wastewater

Chitosan nanoparticles/Nanocomposite	Dyes studied	Adsorption capacity (mg g^{-1})	pH	References
Chitosan/KSF montmorillonite beads	Remazol blue	310.00	3.0	[151]
Chitosan grafted sodium acrylate-co-acrylamide/nanoclay superabsorbent	Crystal violet	256.41	4.0	[152]
	Sunset yellow	208.33	4.0	
	Naphtol green	221.72	4.0	
Chitosan/SiO_2/CNTs	Direct blue 71	61.35	6.8	[153]
	Reactive blue 19	97.08	2.0	
Magnetic chitosan–graphene oxide (MCGO)	Methyl orange	398.08	4.0	[154]
Graphene oxide-doped porous chitosan aerogels	Methyl orange	686.89	4.6	[155]
	Amido black	573.47	4.0	
Chitosan/bio-silica	Acid red 88	25.84	3.0	[156]
Magnetic β-cyclodextrin–chitosan/ graphene oxide	Methylene blue	84.32	11.0	[157]

sufficient time is allowed for organic mineralization. In general, the photocatalytic process has features of a green engineering process. Although various materials (oxides: TiO_2, ZnO, ZrO_2, CeO_2, SnO_2, Fe_2O_3, $SbrO_4$; sulfides: CdS, ZnS) have been used for photocatalysis, generally TiO_2 is the most promising photocatalyst, considering its energy efficiency, durability, photo stability, water insolubility and nontoxicity [164–169].

In photocatalytic membranes, nanoscale inorganic photocatalysts are embedded in a membrane matrix to enhance the properties of the resultant polymer. Several methods have recently been developed and optimised for the fabrication of TiO_2-based photocatalytic membranes. Among them are dip-coating or spin-coating of porous supports using TiO_2 precursor sols, filtration of TiO_2 nanofibers through glass filters followed by hot pressing or liquid phase pressurisation, hydrothermal growth of free-standing TiO_2 nanowire membranes, anodization of titanium films sputtered on to stainless steel substrates, embedding TiO_2 nanoparticles into the polymeric membranes matrix, electrospinning TiO_2 fibres or flat membranes by recasting, development of TiO_2 layers with rapid atmospheric plasma spray coating and the fabrication of free-standing and flow-through TiO_2 nanotube membranes among others [170].

Photocatalytic membranes can be broadly classified into four categories, based on the location of the nanoparticles on the membrane (Fig. 6.6) [171]. Conventional nanocomposites

1. Thin-film nanocomposites (TFC)
2. Thin film nanocomposite with nanocomposite substrate
3. Surface-located nanocomposites

A number of polymers have successfully been used as supports for photocatalysts, and these include polymers such as polyamide, polyvinylidene fluoride (PVDF), polysulfone (PSf), polyethersulfone (PES), sulfonated polyethersulfone (SPES), polyurethane (PU), polyethylene terephthalate (PET), polyester, polyacrylonitrile (PAN) and polytetrafluoroethylene (PTFE) [172, 173].

Heterogeneous photocatalysis using titanium dioxide (TiO_2) has been shown to be a promising advanced oxidation technique for treatment of air and water pollution because it can oxidize a variety of environmental pollutants with high decomposition efficiency instead of accumulating them. Prahsarn et al. [174] prepared webs of electrospun PAN/TiO_2 nanofiber for water treatment. Different amounts of TiO_2 (1–3 wt.%) were added into PAN/DMF/(H_2O) solutions and then electrospun into nanofiber webs. Photodecomposition of MB (methylene blue) solution under UV irradiation showed that PAN webs containing 2 and 3 wt.% TiO_2 showed good photocatalytic activity.

Photocatalytic activity (photooxidative decomposition of methylene blue) of neat and silicon-doped titanium (IV) oxide or titania fibers obtained by combined sol–gel and electrospinning techniques was studied by Watthanaarun et al. [175]. Titania NFs were fabricated by electrospinning a solution of PVP and titanium tetraisopropoxide (TTIP) in ethanol followed by calcination. To study the effect of secondary metal (Si), tetraethylorthosilcate (TEOS) was added in the dopant. It was

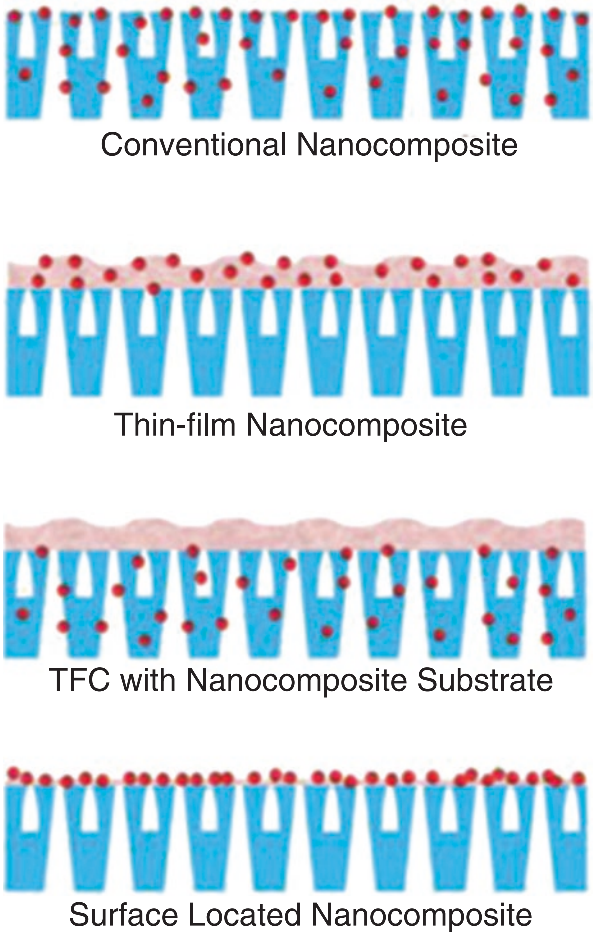

Fig. 6.6 Typical type of nanocomposite membranes (The red spheres represent photocatalyst nanoparticles) [171]

revealed by Watthanaarun et al. that both the neat and the silicon-doped titania fibers showed much better activity for the decomposition of methylene blue than the reference titania powder. The presence of silica enhanced the photocatalytic activity of the obtained titania fibers considerably. It was suggested that TiO_2 of nanofibers and nanoparticles be suitable for the degradation of organic pollutants. Geltmeyer et al. [176] used TiO_2 functionalized PA 6 (polyamide) nanofibrous membranes for isoproturon removal from water. The highest removal rate was obtained using the 35 wt.% inline functionalized PA (polyamide) 6 samples, being the PA 6 sample with the highest TiO_2 load. The decoloring of methylene blue (MB) was used as a probe to demonstrate the activity of a photocatalyst in the membrane. High photocatalytic activity was shown by methylene blue and isoproturon removal.

Rajak et al. [177] used TiO_2/styrofoam composite EFMs for water purification applications. Composite fiber membrane was fabricated from precursor solution prepared by dissolving styrofoam in the mixture of tetrahydrofuran (THF), citronella oil and cajuput oil. It was reported that a significant degradation (69%) of textile dye solutions was observed within 30 hours under the bulb light.

Among hybrid structures containing a ferromagnet with semiconducting properties of ZnO and adsorption properties of Fe_3O_4, Fe–ZnO nanostructures emerged as a promising composite material and generally it is referred to as diluted magnetic semiconductors (DMS). Fe–ZnO nanostructures and nanocomposites have attracted attention due to the vast possibility of their use in various applications. The Fe–ZnO nanocomposite material exhibited dual properties of adsorption and the photocatalysis [178].

6.4 Oil/Water Separation

Membrane separation is the most promising technology to treat oily wastewater, and ultrafiltration and nanofiltration membranes have been used in many industrial oil–water separation processes. Conventional ultrafiltration and nanofiltration membranes have fairly high separation efficiency for oil/water emulsions, but suffer from low flux, which is attributed to their limited permeability and serious surface fouling. To overcome these problems two aspects should be considered: constructing a hydrophilic surface to avoid oil fouling of the membranes, and increasing the porosity and decreasing the thickness of the separation layer. Researchers have developed a nanofabric "paper towel" woven from tiny wires of potassium manganese oxide that can absorb 20 times its weight in oil for cleanup applications [179].

Researchers have also placed magnetic water-repellent nanoparticles in oil spills and used magnets to mechanically remove the oil from the water [180]. On viewing the oil-repellent abilities of creatures in nature (such as fish scales), a superhydrophilic and underwater superoleophobic surface could be constructed by combining a hydrophilic chemical surface and appropriate roughness [181]. Gore et al. [182] have discussed the various nano-functionalized superwetting materials like Janus fabrics, membranes, nanofibers, sponges/foams, and meshes for the treatment of oil/solvent-water emulsions, as they render high separation efficiency, recyclability, mechanical durability, and high performance against harsh environments. These superwetting nano-engineered materials are promising potential candidates for treating oil/solvent-water emulsions in large quantities, as compared to traditional separation techniques in the near future.

Arora and Balasubramanian [183] introduced an extensively porous sorbent material coalesced with nano silicon carbide, PVDF/nano-SiC, which has extraordinary absorption capacity including remarkable durability and easy conduct during the course of absorption. The absorption capacity of the foam was determined by varying the weight percentage of nano-SiC in PVDF. Optimised absorption was achieved with a 5% w/w inclusion of nano-SiC. The absorbent allows oil to selectively permeate through it, while being completely water repellent, and absorbs up to 21.5 times and 20.5 times its weight equivalent of engine oil and paraffin oil, respectively. Cao et al. [184] developed a copper mesh with a superhydrophobic coating by spray deposition of modified polyurethane and hydrophobic silica nanoparticles. It was reported that SiO_2/SiWPU-coated mesh can efficiently separate oils (such as toluene, kerosene, petroleum ether, hexane, and tetrachloromethane) from water with high separation efficiency of up to 99.3% for the kerosene/water mixture. Wang and Guo [185] electroplated the Cu nanoparticles on copper mesh and reported that the resulted mesh showed good superhydrophobic and superoleophilic properties so that it can be applied to separate oil from water effectively and rapidly. Xu et al. [186] successfully fabricated super hydrophobic nano-Al films on stainless steel meshes via EPD (electrophoretic deposition) and observed that it exhibited stable performance on the oil-water separation, and oil-water separation efficiency was up to 95.8 ± 0.9%. Liu et al. [187] fabricated modified CS-based mesh with superhydrophilicity and underwater superoleophobicity and reported that water can pass through the mesh by gravity force while oils can block up underwater. The modified CS-based mesh can separate various oil/water mixtures with >99% separation efficiency. Preparation of durable underwater superoleophobic mesh via layer-by-layer (LBL) assembly of poly(diallyldimethylammonium chloride) (PDDA) and halloysite nanotubes (HNTs) on a stainless steel mesh was described by Hou et al. [188]. The resultant mesh showed an outstanding oil–water separation performance with a separation efficiency of over 97% for various oil/water mixtures, which allowed water to pass through while repelled oil completely. Yuan et al. [189] reported the preparation of multilayer TiO_2 films deposited on the CuO NNA (nanoneedle arrays) mesh via layer-by-layer self assembly. It was reported that Yuan et al. displayed superhydrophlicity and underwater superoleophobic properties. The fabricated mesh demonstrated a high separation efficiency and excellent water flux.

Al-Husain et al. [190] separated synthetic crude oil-in-water emulsion by using novel PES ENMs (electrospun nanofibrous membranes) incorporating HMO (hydrous manganese dioxide nanoparticles) via ultrafiltration. The HMO-incorporated ENMs exhibited an excellent oil rejection (97.98% and 94.04%) and a promising water flux recovery (89.29% and 71.10%) when used to treat a synthetic oily solution containing 5000 or 10,000 ppm oil, respectively. Ao et al. [191] fabricated superhydrophilic graphene oxide (GO)@electrospun cellulose nanofiber (CNF) membrane by immersing the electrospun cellulose nanofiber in a 0.01 wt% GO aqueous suspension to load the GO nanosheets. The membrane exhibited a high separation efficiency, excellent antifouling properties including high flux for the gravity-driven oil/water separation.

Islam et al. [192] coated PVAc layer onto the electrospun nylon 6/Silica (N6/SiO_2) nanofiber membrane (composite micro filtration (MF) membrane), through casting and then phase inversion techniques. The fabricated membrane was highly hydrophilic (water contact angle 21°) with both high porosity and mechanical strength. The fabricated membrane also showed a high water flux of 4814 LMH bar^{-1} and almost 99% oil rejection at oil concentrations of 250 mg L^{-1}, 500 mg L^{-1} and 1000 mg L^{-1} in the feed mixture.

Alayande et al. [193] added zeolite to modify the surface of the non-beaded electrospun expanded polystyrene (EPS) fibrous films. Films were characterized using SEM, BET, FTIR and optical contact angle. The fibers exhibited superhydrophobic and superoleophillic wetting properties with water (>15°) and crude oil (0°). Addition of zeolite in the composite fiber increased the pore size, and thus it enhanced penetration of oil into the composite fiber. This opens a new route of enhancing oil adsorption properties of polymeric material and re-use of abundant polymer wastes.

Makaremi et al. [194] reinforced PAN ENM with halloysite nanotubes (HNTs) in order to improve their mechanical properties, thermal stability and water filtration performance for the possible application as water filtration membranes**.** The presence of HNTs enhanced the mechanical properties of the membranes (tensile strength and elongation at break) including significant improvement of their thermal properties. Moreover, PAN/HNTs membranes showed excellent oil/water separation performance and also increase in water flux rate. Rejection ratio of 99.5% was obtained for oil/water separation test while heavy metal ion adsorption of the membranes remarkably increased up to 760% when compared with the results obtained for neat PAN ENM. Lin et al. [195] reported that nanoporous polystyrene (PS) fibers prepared via a one-step electrospinning process can be used as oil sorbents for oil spill cleanup. The oleophilic–hydrophobic PS oil sorbent with highly porous structures showed a motor oil sorption capacity of 113.87 g g^{-1}, approximately 3–4 times that of natural sorbents and nonwoven polypropylene fibrous mats.

Obaid et al. [196] incorporated SiO_2 NPs and GO nanoflakes in the PSf electrospun nanofiber membranes. The nanofibers were prepared by electrospinning of a colloid composed of PSF/DMF solution and either SiO_2 NPs and GO nanoflakes. It was reported by Obaid et al. that PSf–SiO_2 NPs electrospun nanofiber membrane possesses high flux in petroleum fraction/water separation process. But, incorporation of GO has relatively small improvement in the PSF electrospun membrane separation performance.

Kahraman et al. [197] studied the PAN/n-OMMT(Organo-montmorillonite) nano clay nanofibers as an oil and solvent absorbent material due to their super hydrophobicity and super oleophilic properties. The generated composite nanofibers were found to have a very high oil and solvent absorption capacity in the case of 3% n-OMMT clay loading. It showed excellent absorption capacity up to 160 times its own weight for motor oil.

Table 6.13 summarised the few examples of nanotechnology used for oil/water separation.

Table 6.13 Nanotechnology used for oil/water separation

Membrane	Separation of oil/ water	Result	Reference
Nano-SiC/PVDF	Engine oil, paraffin oil + water	Water repellent. Absorbs 21.5 times and 20.5 times its weight equivalent of engine oil and paraffin oil respectively	[183]
Electroplated the Cu nanoparticles on copper mesh	Oil from water	Good superhydrophobic and superoleophilic properties	[185]
Nano-aluminum films on stainless steel meshes	Oil-water	Separation efficiency up to 95.8 ± 0.9%	[186]
CS-based mesh	Oil-water	>99% separation	[187]
Silicone elastomer films/ Cu mesh	Organic solvents (hexane, petroleum ether and toluene) from water	Exceptionally efficient	[198]
TiO_2/CuO NNA	Oil-water	Superhydrophlicity and underwater superoleophobicity. High separation efficiency and excellent water flux	[189]
LBL- assembly of PDDA and HNTs/steel mesh	Various oil/water mixtures	Outstanding oil–water separation. Efficiency over 97%	[188]
SiO_2/SiWPUcoated mesh	Toluene, kerosene, petroleum ether, hexane water mixture	Efficiently separate oils. Separation efficiency of up to 99.3% for the kerosene/water mixture	[184]
PES ENMs/HMO	Synthetic crude oil-in-water emulsion, (UF)	Excellent oil rejection, up to 97.98% and a promising water flux recovery (89.29%)	[190]
PVAc/ nylon 6/Silica (N6/SiO_2) nanofiber	Oil-water emulsion, (MF)	Highly hydrophilic. High water flux of 4814 LMH bar^{-1} and almost 99% oil rejection at oil	[192]
GO@electrospun cellulose nanofiber	Oil/water	High separation efficiency, excellent antifouling properties and capable of a high flux for the gravity-driven oil/water separation. Superhydrophilic	[191]
Electrospun polystrene and polysytrene-zeolite fiber	Crude oil-water separation	Zeolite increased the pore size, enhanced penetration of oil into the composite fiber, superoleophillic property	[193]
PAN/HNTs	Oil/water filtration	Rejection ratio of 99.5%	[194]

(continued)

Table 6.13 (continued)

Membrane	Separation of oil/water	Result	Reference
Nanoporous PS ENFs	Oil spill cleaning	Motor oil sorption capacity 113.87 g g^{-1} approximately 3–4 times that of natural sorbents and nonwoven polypropylene fibrous mats	[195]
SiO_2 NPs and GO nanoflakes in the PSf ENFs	Petroleum/water	High flux in petroleum fraction/water	[196]
Polysulfone -SiO_2 NPs	Fast oil separation (absorption)	Excellent absorption capacity up to 160 times its own weight for motor oil	[197]

6.5 Desalination

Desalination is the process of removing salts or other minerals and contaminants from seawater, brackish water, and wastewater effluent and it is an increasingly common solution to obtain fresh water for human consumption and for domestic/industrial utilization. Desalination of seawater and brackish groundwater is universally recognized as an attractive option to produce fresh water for drinking purposes, especially where there is no alternative water supply or where other alternatives to augment conventional water supplies have grown more expensive than the cost of desalination. To provide solutions of problems in waste treatment and environmental remediation in the areas of desalination, a remarkable progress has been made. However, there are still many problems such as cost and fouling of membranes. Application of engineered nanomaterials in the membrane fabrication has enabled the exploration of a new generation of nano-enabled desalination membranes. Many advances have been made in the areas of material science for the development of desalination membranes based on nanoparticles and nanocomposites. Goh et al. [199] predicted that nano-enabled membrane technology will serve as a key element to render feasible solutions for sustainable development in membrane desalination technology. Main desalination methods are RO, FO and PRO. But, pervaporative desalination of the seawater is considered to be the potential alternative methods for solving the water scarcity owing to several advantages, like high energy conservation at the expense of low cost, high efficiency (~100% of salt rejection) and better handling ability of water with high salinity. Compared with the membrane distillation, pervaporative desalination using hydrophilic materials can effectively reduce membrane fouling and maintain membrane separation performance [200].

There are both challenges and advantages to use nanotechnology in desalination (Fig. 6.7).

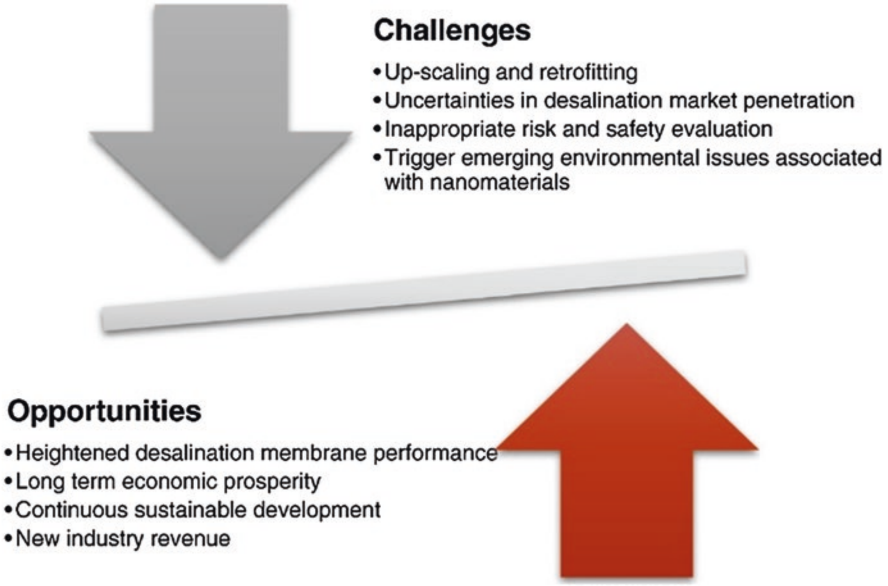

Fig. 6.7 Challenges and opportunities in nano-enabled membrane desalination. Transformation of challenges to opportunities is the crucial strategy to ensure the commercial success and industry engagement of the technology [199]

6.5.1 Reverse Osmosis

RO is a process which applies transmembrane pressure to cause selective movement of solvent against the osmotic pressure difference. Desalination by reverse osmosis (RO) has become the most cost-effective process to convert seawater into freshwater for potable use at large scale. RO membrane is non-porous and water is the only component that can diffuse across it. Reverse osmosis (RO) and nanofiltration (NF) membranes have been widely used for water reclamation, desalination, and other separation processes.

Ghanbari et al. [201] studied a new type of thin film nanocomposite (TFN) RO membranes, prepared by incorporating different amounts of halloysite nanotubes (HNTs) into the PA selective layer *via in situ* interfacial polymerization. Upon addition of HNTs, the hydrophilicity, surface roughness and water flux of TFN membranes have all increased. The water flux enhancement can be ascribed to higher hydrophilicity and additional water pathways through porous HNTs in TFN membranes.

Researchers at Hiroshima University developed an ultra-thin layered membrane that improves the removal of salt from seawater. The partly silicon membrane, can resist heat and cleansing agents like chlorine, enabling an improved industrial process. The ultra-thin layered membrane acts as a sieve and separates salt from seawater to produce fresh water [202]. The polymeric support is a porous sulfonated polyethersulfone nanofiltration membrane and the layered-hybrid membrane was prepared via sol–gel spin-coating and heat-treatment. The membranes showed a high degree of water permeability and modest salt rejection. These layered-hybrid membranes displayed good stability and reproducibility in the RO process, and showed a stable and high degree of water permeability (approximately 1.2×10^{-12} m^3 m^{-2} s^{-1} Pa^{-1}) with salt rejection that was competitive (96%) with conventional processing.

The TFC FO membrane using Zn_2GeO_4-nanowire-modified PES membrane as the substrate showed improved performance in PRO and FO mode. In PRO mode, the water permeability of the membrane was increased by ~45% while retaining the salt rejection. In FO mode, the incorporation of Zn_2GeO_4 nanowires to the membrane produced higher J_w/J_s ratio which may be due to the improved interfacial polymerization of polyamide. The membrane may also be used as nanofiltration (NF) or RO membrane since they are less affected by ICP (internal concentration polarization) effects [203].

Mahdi et al. [204] modified PES membranes with different concentrations of discrete TiO_2 nanotubes (NTs) via non-solvent-induced phase separation (NIPS) and used for water treatment (steam assisted gravity drainage (SAGD) wastewater obtained from the Athabasca oil sands of Alberta). Zeta potential and contact angle measurements showed enhanced hydrophilicity and surface negative charge in TiO_2 NTs/PES nanocomposite membranes compared to unmodified PES membranes. All discrete TiO_2 NTs incorporated PES membranes showed better organic matter rejection and water flux when compared with the pristine PES membrane. The flux recovery ratio (FRR) experiments have confirmed notable improvement in the antifouling property of discrete TiO_2 NTs incorporated PES membrane.

Research and development efforts are still needed for RO membranes;

1. To provide a feed water with a fouling potential as low as possible.
2. To lower the energy requirements of desalination plants by seawater and environmental impacts.

6.5.2 Nanofiltration (NF)

The main reasons for adoption of membrane filtration technology are their benefits in terms of quality water treatment, effective disinfection and low space requirement for plant. Beside this, it is highly economical and simple in design compared to other treatment techniques. NF membranes have been widely used for water reclamation, desalination, and other separation processes.

Nano- membrane separation technology can be efficiently applied for removal of dyes and heavy metals. In terms of environmental concerns, the nano-membranes have large ecological footprint during their manufacturing process [205]. It is a separation process in which particles and dissolved macromolecules smaller than 2 nm are rejected. Nanofiltration is a technique that has prospered over the past few years. Today, nanofiltration is mainly applied in drinking water purification process steps, such as water softening, decolouring and micro pollutant removal. During industrial processes nanofiltration is applied for the removal of specific components, such as colouring agents. Nanofiltration is a pressure related process, during which separation takes place, based on molecular size. The technique is mainly applied for the removal of organic substances, such as micro pollutants and multivalent ions. Nanofiltration membranes have a moderate retention for univalent salts. The applications of nanofiltration are mainly:

1. The removal of pesticides from groundwater
2. The removal of heavy metals from wastewater
3. Wastewater recycling in laundries
4. Water softening
5. Nitrates removal

Kiani et al. [206] used heat treated polyphenylsulfone (PPSU) nanofibrous membranes for determination of pure water flux and filtration of canned beans production wastewater. Pure water flux of 7323 L m^{-2} h^{-1} was observed for the heat-treated membrane. Heat treated membrane showed high porosity and improvement in mechanical stability. In another publication, Kiani et al. [207] fabricated novel thin film nanofibrous composite (TFNC) polyphenylsulfone (PPSU) membrane by casting a thin PPSU barrier layer on the surface of the electrospun nanofibrous PPSU support. The PWF (Pure water flux (L m^{-2} h^{-1})) of the TFNC PPSU membranes was 5.2, 4.5, and 16.4 fold higher by using 20, 22, and 24 wt.% PPSU in the casting solutions, respectively, as compared to the unsupported by nanofibrous PPSU membranes.

Wang et al. [208] fabricated a triple-layered composite NF membranes by the interfacial polymerization of diamine and acyl chloride on a cellulose nanocrystal interlayer supported by a microporous substrate. The cellulose nano-crystal interlayer plays a crucial role in the polyamide skin layer formation and the following nanofiltration process. It can store aqueous diamine monomers and slow down the interfacial polymerization for a relatively low cross-linking degree of the skin layer. This hydrophilic interlayer also facilitates water permeation through a "dragging effect". The constructed membranes exhibit an ultra-high permeation flux up to 204 L m^{-2} h^{-1} under 0.6 MPa with a Na_2SO_4 rejection above 97%.

Soyekwo et al. [209] presented a facile technique to produce highly-permeable polymer nanofiltration membranes by employing ultrathin nanoporous nanomaterial on macroporous support. Ultrathin crosslinked-PEI selective layer was formed by interfacial polymerization on ultrafine cellulose nanofiber as the intermediary layer. It was reported that the membrane was hydrophilic and highly-permeable nanofiltration membrane. It exhibited a high pure water flux of up to 32.68 L m^{-2} h^{-1} bar^{-1} that is an order of magnitude higher than those of previously reported similar nanofiltration membranes. The rejections of the salt solutions were in the order of $MgCl_2 > MgSO_4 > Na_2SO_4 > NaCl$ at operating pH of 6.5, $Na_2SO_4 > MgSO_4 > MgCl_2 > NaCl$ at operating pH of 7.5, and

$MgCl_2$ > $MgSO_4$ > NaCl > Na_2SO_4 at operating pH of 3. The membranes have a great potential for application in fast water purification.

Hosseini et al. [210] demonstrated the performance of a new mixed matrix PES-co-Magnesium oxide nanoparticles (MGO) nanocomposite nanofiltration membrane which was prepared through phase inversion method. Results showed that membrane permeation flux was improved 32% by utilizing of MgO nanoparticles into the membrane matrix including improvement in the salt rejection (49%).

Zhao et al. [211] fabricated GO-TFN membranes that exhibited an improved water flux and chlorine-resistance without compromising the salt rejection under low pressure (4 bars) through a facilitated interfacial polymerization (IP) reaction between low concentrations of piperazine (PIP) and organic trimesoyl chloride (TMC) in the presence of graphene oxide (GO) nanosheets. At the optimized GO dosage of 0.01 wt%, the synthesized GO-TFN membrane achieved a water permeance of 15.63 Lm^{-2} h^{-1} bar with the Na_2SO_4 rejection of 96.56% and $MgSO_4$ rejection of 90.5%.

Yin and co-workers prepared nanocomposite membranes by using MCM-41 silica nanoparticles and GO-enhanced PA thin films via the interfacial polymerization method, and both nanoporous membranes exhibited high performances for water purification [212, 213]. By increasing concentration of MCM-41 NPs, hydrophilicity, roughness and zeta potential of TFN membranes all increased. Notably, the permeate water flux increased from 28.5 ± 1.0 to 46.6 ± 1.1 L m^{-2} h^{-1} with the incorporation of MCM-41 NPs, while maintaining high rejections of NaCl and Na_2SO_4 (97.9 ± 0.3% and 98.5 ± 0.2%, respectively). TFN membrane containing graphene oxide (GO) nanosheets was prepared by the in-situ interfacial polymerization process. Aqueous *m*-phenylenediamine (MPD) and organic trimesoyl chloride (TMC)–GO mixture solutions were used in this process. With an increasing concentration of GO from 0 to 0.015 wt.% in the TMC-hexane phase during the fabrication, the permeate flux under 300 psi increased from 39.0 ± 1.6 to 59.4 ± 0.4 L m^{-2} h^{-1}, while rejections of NaCl and Na_2SO_4 slightly decreased from 95.7 ± 0.6% to 93.8 ± 0.6% and 98.1 ± 0.4% to 97.3 ± 0.3%, respectively. Interlayer spacing of GO nanosheets may have served as water channels and hence contributed to the water permeability enhancement.

6.5.3 Forward Osmosis (FO)

Forward osmosis (FO) is a membrane-separation process that uses osmotic pressure difference between a concentrated draw solution and a feed stream to drive water across a semipermeable membrane. The PRO (pressure restarted osmosis) process is not only considered for desalination and water purification, but has a big potential also within energy production, biomedical applications and food processing.

FO as a method to desalinate water has been investigated for almost four decades, stimulating great advances in FO membrane preparation and theory. With the right draw solution, the technology can desalinate water without supplying extra energy.

Batchelder patented in 1965 a method of FO-desalination suggesting a draw solution with sulfur dioxide [214]. Forward osmosis is being widely studied for desalination. However, it was concluded that the conventional RO membrane was not suitable for FO because of higher internal concentration polarization caused by a higher concentration of draw solution. Forward osmosis (FO) utilizes the osmotic gradient to draw water from a low osmotic pressure solution to a high osmotic pressure one (i.e., the draw solution). The diluted draw solution is then treated by reverse osmosis or thermal processes to generate pure water. FO has two major advantages over the pressure-driven reverse osmosis: it does not require high pressure, and the membrane is less prone to fouling.

Principle

1. Naturally driven
2. Process without hydraulic pressure
3. Run by chemical potential difference (i.e., concentration difference)

Advantages

1. Inherently low fouling
2. Low energy requirements
3. Low chemical consumption
4. High Availability
5. Reduced product boron levels

Limitations

1. Lack of suitable membrane for FO
2. Lack of appropriate draw solution

The performance of the FO unit can be further improved by improving the membrane to withstand higher internal concentration polarization. The schematic representation of the FO system is shown in Fig. 6.8 [215].

The key to FO is to have a draw solute with high osmolality and easily separable from water. Chemicals currently employed for draw solutions include NaCl and ammonia bicarbonate. Therefore, RO or thermal treatment, both energy intensive, is required to recover water from the draw solution. Magnetic nanoparticles were recently explored as a new type of draw solute for its easy separation and reuse. Hydrophilic coating was employed to aid dissolution and increase osmotic pressure. An FO permeate flux higher than 10 L m^{-2} h^{-1} was achieved using 0.065 M poly(ethylene glycol) diacid-coated magnetic nanoparticles when deionized water was used as the feed solution [216]. Magnetic nanoparticles were also applied to recover draw solutes. In a recent study, magnetic nanoparticles ($Fe_3O_4@SiO_2$) were used to recover $Al_2(SO_4)_3$ (the draw solute) through flocculation [217]. From the published data on FO, it was revealed that organic–inorganic hybrid nanocomposite membranes have significantly higher water flux, mechanical strength, selectivity, stability and hydrophilicity compared with conventional polymeric FO membranes [218]. Arzhandi et al. [219] fabricated TFN membranes by incorporating highly hydrophilic halloysite nanotubes (HNTs) and self-synthesized graphitic carbon

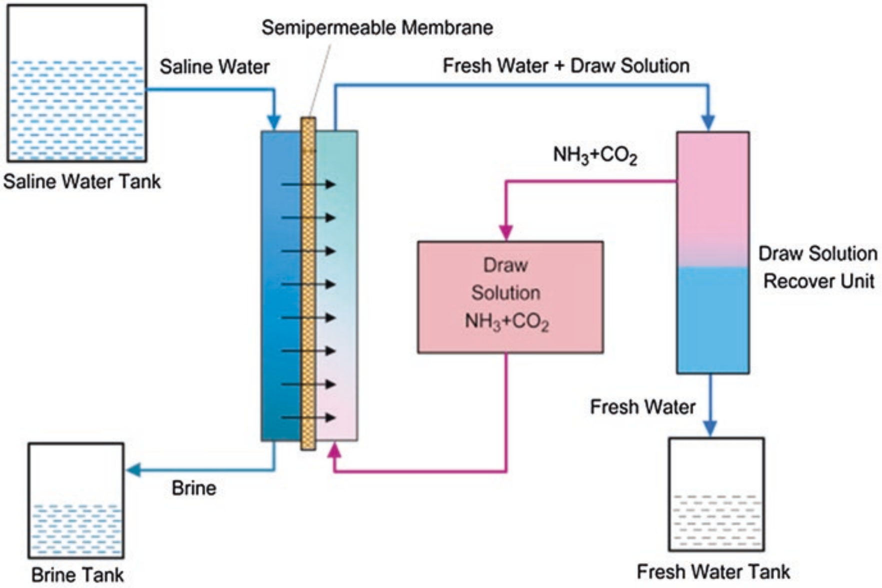

Fig. 6.8 Forward osmosis unit using NH_3-CO_2 as draw solution [215]

nitride (g-C_3N_4) nanoparticles into polysulfone-based substrate and interfacially polymerized polyamide top layer, respectively. The TFN membranes were evaluated for their performance in FO applications. It was reported that the newly fabricated TFN FO membrane surpassed the desalination results obtained from TFC and commercial membranes and also the anti-fouling property was greatly enhanced.

Ma et al. [220] incorporated zeolite into the polysulfone support layer of an FO membrane to obtain a lower ICP (internal concentration polarization). The resulting membrane had a decreased structure parameter from 0.96 to 0.34 mm and increased water flux. This result was attributed to the higher porosity, enhanced hydrophilicity and additional water channels supplied by the addition of porous zeolite. This was the first study to exhibit the feasibility of employing an organic–inorganic hybrid nanocomposite FO membrane to limit ICP (internal concentration polarization) in the FO process. Ling et al. [221] applied highly water-soluble functionalized magnetic nanoparticles as novel draw solutes in forward osmosis (FO) and reported that magnetic nanoparticles capped with polyacrylic acid can yield the highest driving force and subsequently highest water flux among others. It was also observed that surface hydrophilicity and magnetic nanoparticle size is crucial in the application of nanoparticles as draw solutes in FO. CNTs have gained increasing attention due to their inner hollow cavities, which are similar to aquaporins. Song et al. [222] suggested a novel method to fabricate high performance FO membranes. They designed double-skinned membranes, which showed excellent solute rejection, and incorporated polydopamine with CNTs as the active layer by interfacial polymerization. They found that the CNTs had significant effects on the characteristics of the fabricated membranes. Therefore, it can be concluded that hybrid nano-composite membranes incorporated with CNTs have higher FO water flux and remarkable antifouling capacity compared to conventional membranes.

6.5.4 Pressure Retarded Osmosis (PRO)

PRO was invented by Prof. Sidney Loeb in 1973 at the Ben-Gurion University of the Negev, Beersheba, Israel, with his first publication released in 1975 [223]. It is the process through which osmotic energy can be harnessed and power generated. In PRO, a water flow is diverted at low pressure into a module wherein a semipermeable membrane keeps it separated from a pressurized and saltier water flow. The saltier water flow draws the less concentrated water through the semipermeable membrane due to its higher osmotic pressure, increasing the volume of the flow. A turbine is coupled to the pipe containing the increased pressure flow to generate power. Power generated via PRO is referred to as 'osmotic power'. In other words, 'The pressure exerted by the flow of water through a semipermeable membrane separating two solutions with different concentrations of solute'. Membrane performance in PRO is usually measured in terms of power output per unit area of membrane—referred to as membrane power density. A schematic diagram showing the configuration of a PRO plant with pressure exchangers is shown in Fig. 6.9.

The first PRO prototype facility was constructed by the Norwegian electric company. Statkraft, in order to implement the PRO technology for electricity production [225], a process where seawater was used as the draw solution, and river water was selected as the feed solution (Fig. 6.10).

Li et al. [226] modified the TFC membrane by polydopamine cross-linking, to reinforce polyamide-imide substrate casted on the polyester fabrics, and a post-treatment with chloride and ethanol. Compared with the untreated TFC membrane, the modified TFC membrane showed a three-fold increase in water flux, and a 16-fold increase in power density.

Yip et al. [227] fabricated a TFC membranes for high performance in PRO and also made a theoretical model to predict the water flux, from which we can predict the power density that can be achieved by a membrane. The fabricated membranes consisted of a selective polyamide layer formed by interfacial polymerization on top of a polysulfone support layer (highly porous) made by phase separation. It was reported that a hand-cast membrane that balances permeability and selectivity ($A = 5.81$ L m^{-2} h^{-1} bar^{-1}, $B = 0.88$ L m^{-2} h^{-1}) is projected to achieve the highest potential peak power density of 10.0 Wm^{-2} for a river water feed solution and seawater draw solution.

Han et al. [228] developed a TFC PRO membrane with a polyamide thin film layer, post-treated by hypochlorite and methanol, and a robust fully sponge-like Matrimid® support layer. The membrane achieved a power density of 9 Wm^{-2} with synthetic seawater (0.59 M NaCl) as the draw solution, and deionized water as feed

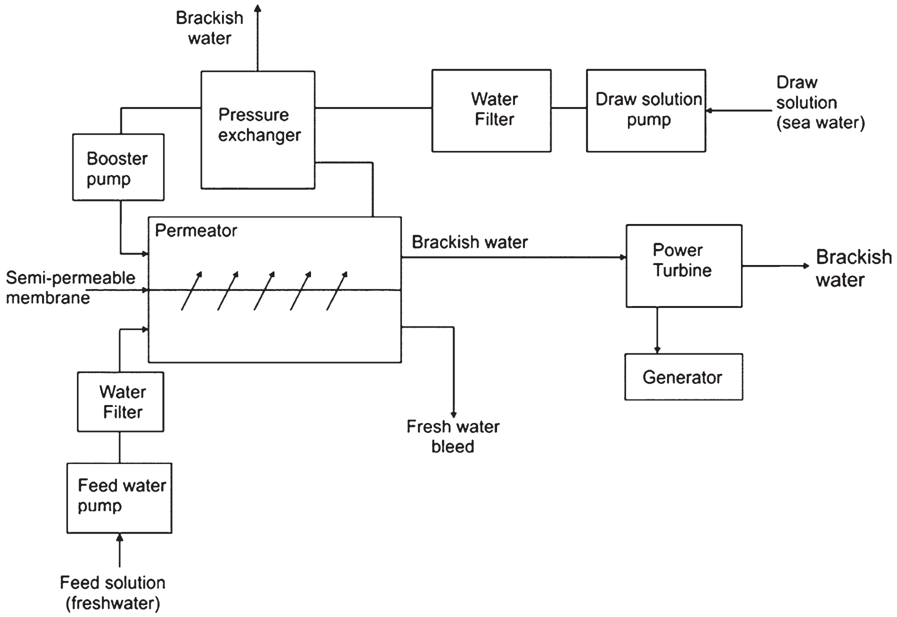

Fig. 6.9 Power production from a PRO scheme powered by pressure exchangers [224]

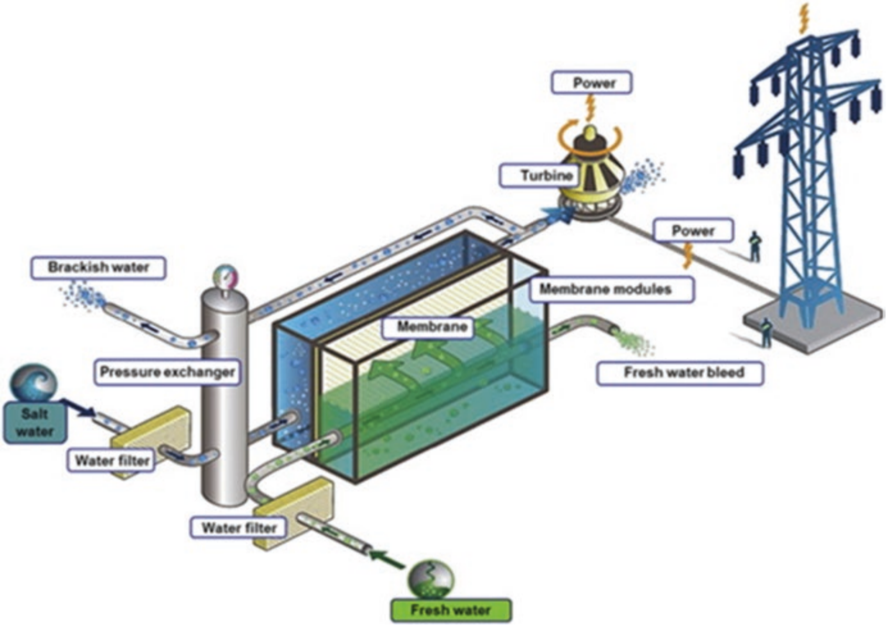

Fig. 6.10 Seawater–river water PRO process for electricity production, adopted by Statkraft [225]

at 13 bar, and 12 Wm^{-2} with synthetic RO brine (1 M NaCl) as the draw solution, and deionized water as feed at 15 bar.

Bui and McCutcheon [229] fabricated a novel electrospun nanofiber-supported thin-film composite PRO membrane. The support was tiered with layers of nanofibers of different diameters to better withstand hydraulic pressure. Tetraethylorthosilicate was used as a source of SiO_2 to reinforce the electrospun PAN nanofibrous support. Also, a cross-linked PVA was coated on the electrospun nanofiber mat before PA layer formation. The membranes successfully withstood an applied hydraulic pressure of 11.5 bar and exhibited performance that would produce an equivalent peak power density near 8.0 Wm^{-2} under real conditions (using 0.5 M NaCl and deionized water as the draw and feed solutions, respectively). This result shows the immense promise of nanofiber supported thin-film composite membranes for use in PRO. Song et al. [230] fabricated electospun nanofibers from polyacrylonitrile (PAN) solution in N,N-dimethyl formamide with tetraethylorthosilicate. Tetraethylorthosilicate was used to improve the mechanical strength of the fiber. The fibers were coated with PVA and used as a support material. PA layer was deposited on the top surface via IP using m-phenylenediamine aqueous solution with triethylamine camphor sulfonic acid. The PA layer (selective layer) was modified by chlorine by using sodium hypochlorite (NaClO) solution. This highly efficient membrane achieved a power density of 15.2 Wm^{-2} and maximum energy recovery of 0.86 kW h m^{-3}, using synthetic brackish water (80 mM NaCl,

$\pi = 3.92$ bar) and seawater brine (1.06 M NaCl, $\pi = 51.8$ bar) as feed and draw solution, respectively in PRO process.

Electro-spun nanofiber was used to fabricate a porous support layer for a PRO membrane. The ultrafine electro-spun nanofiber, bonded onto a nonwoven backing, could become a highly porous, interconnected, and low tortuosity support layer with an acceptable mechanical stability. The novel electro-spun nanofiber supported the TFC membrane, and a reached power density of 11.4 Wm^{-2}, using synthetic brackish water (80 mM NaCl) as feed, and seawater brine (1.06 M NaCl) as the draw solution [231].

6.5.5 Pervaporation

Advanced nanotechnology aided commercially viable products/solutions that enhance/replace existing desalination/purification. Desalination via pervaporation has the potential to be an efficient way of getting fresh water from non-potable saline sources with the advantages of a high rejection of salt and the capability of coping with high-salinity solutions. In desalination applications, pervaporation has the advantage of near 100% of salt rejection. The pervaporation of an aqueous salt solution can be regarded as separation of a pseudo-liquid mixture containing free water molecules and bulkier hydrated ions formed in solution upon dissociation of the salt in water.

Pervaporation (PV) has been well known in application to separate liquid mixtures, such as dehydration of organic solvents, evaporation of volatile organic compounds from aqueous solutions, and separation of mixed anhydrous organic mixtures. PV involves a hydrophilic dense polymeric membrane or molecularly porous inorganic membrane that is in contact with the feed salt solution on one side, while the target compound-water preferentially permeates and is removed as vapor from the opposite side. As shown in Fig. 6.11, desalination by PV is a combination of diffusion of water through a membrane and its evaporation into the vapor phase on the other side of the membrane to produce fresh water.

Rostovtseva et al. [233] separated ethylene glycol (EG) from EG/water mixtures by using hybrid membranes based on poly (2,6-dimethyl-1,4-phenylene oxide) (DMPO) modified with heteroarm stars (HAS) via pervaporation. The HAS consist of a small branching center fullerene C 60 and 12 arms of different nature, six arms of nonpolar polystyrene and six arms of polar poly-tert-butyl methacrylate (PTBMA). It was reported that DMPO/HAS (5%) membrane exhibited strongly selective properties in the EG dehydration as compared with reported data. The high-water selectivity of the modified membranes was due to the change of the internal structure of the walls in the transport channels by EG sorption. Moreover, water diffusion is facilitated due to the hydrogen bonding with the hydroxyl groups of EG.

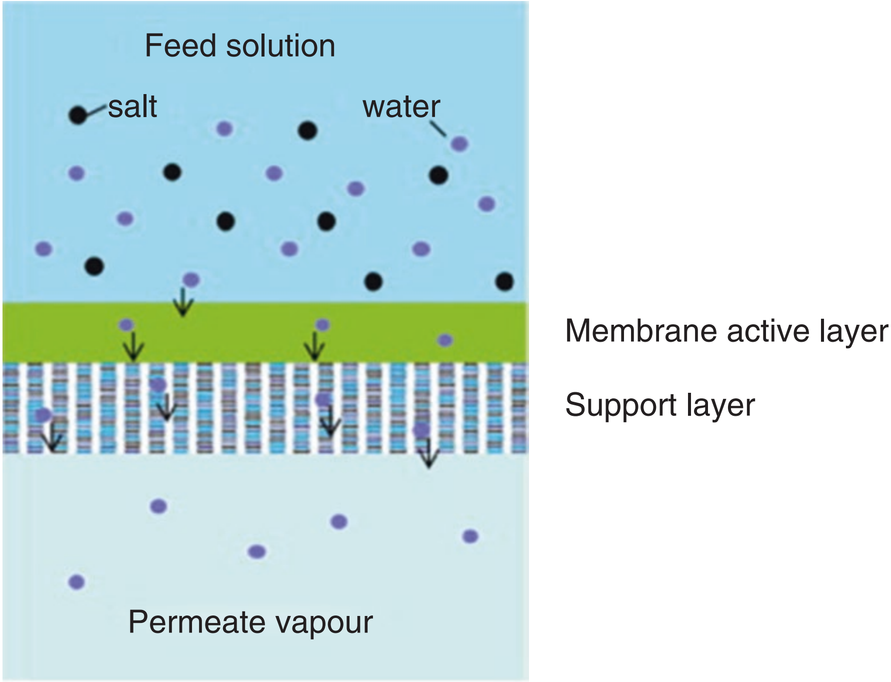

Fig. 6.11 Desalination by pervaporation process where water passes through a dense pervaporation membrane [232]

Liang et al. [234] prepared three-layer thin film nanofibrous pervaporation composite (TFNPVC) membrane by sequential deposition using electrospraying/electrospinning. The TFNPVC membranes showed excellent desalination performance (high water flux and salt rejection >99.5%) for different salt concentrations with virtually no change in performance after 50 h of operation. The flux with a 5 g L^{-1} NaCl feed solution was 8.53 kg m^{-2} h^{-1} at room temperature. Chaudhri et al. [235] prepared a composite membrane with a highly stable hydrophilic thin PVA layer of 0.1–1µm thickness coated over a polysulfone hollow fiber support by an automatic dip coating method. The highest water flux of 7.4 kg m^{-2} h^{-1} was obtained at a NaCl concentration of 30 g L^{-1} at 70 °C for the composite membrane with a thinnest skin layer due to the reduced resistance to the mass transport. All membranes exhibited 99.9% salt rejection with the feed concentration of 30–50 g/L NaCl. The GO/PAN composite membrane exhibited a high water flux of up to 65.1 kg m^{-2} h^{-1} as well as high rejection of about 99.8% for desalination by PV at 90 °C [236]. Xie et al. [237] introduced highly dispersed homogeneous hybrid polymer–inorganic membranes based on PVA, maleic acid (MA) and inorganic silica, synthesized via a sol–gel method. A high flux of 6.93 kg m^{-2} h^{-1} and salt rejection above 99.5% could be achieved at a 6 Torr vacuum and 22 °C. Marian et al. [238] used PEBA/PAN/PE, PEBA/PSF/PE and PEBA+NaX/PSF/PE composite membranes for desalination of

Kashan city's water via pervaporation process. For all experiments under 45 °C, salt rejection was very high and equaled to 99.9%. However, it decreased above 45 °C. Yang et al. [239] studied desalination via PV by using three types of MMMs comprised of PVA and different MWCNTs; i.e. PVA/MWCNT, PVA/C-MWCNT and PVA/C-MWCNT/MA. The improvement of the PVA/CNT membranes was observed by increases in water flux between 38.8 and 154.1% compared with the control PVA/MA membrane while maintaining a relatively high salt rejection of greater than 99% for PVA/C-MWCNT/MA with 0.5–1 wt.% C-MWCNT loading.

6.5.6 Membrane Distillation

The alternative of RO to desalinate hypersaline water is membrane distillation which is a water separation process. The membrane distillation (MD) is a relatively new and promising technology for brackish and seawater desalination. It is one of the emerging desalination technologies for the production of fresh water. Compared to other membrane systems, MD has several advantages, such as higher salt rejection, lower operating temperature than conventional distillation processes, low energy consumption, (when the alternative energy source is used), lower operating pressure etc. The principle of separation in membrane distillation is based on the difference in volatility of each substance, and vapor pressure difference between feed and permeate side is the driving force of the process. The movement of water across the membrane is the result of an imbalance in the vapor pressure between the different sides of the membrane due to a corresponding temperature difference. Water evaporates at an entrance to the membrane pore, enters into a region of high water vapor concentration in the air within the membrane, and diffuses down by a concentration gradient. The water vapor moves through the membrane until it reaches the region of low water vapor concentration at the exit of the pore. Here it is condensing, and can be collected as pure water. The MD process is illustrated in Fig. 6.12.

MD technology is applicable for many application areas such as wastewater remediation, sea water distillation, and separation of volatile liquids. Due to low flux and permeability of the membranes, possible pore wetting and water loss,

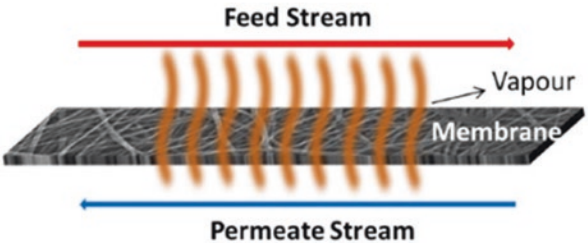

Fig. 6.12 Illustration of membrane distillation process [240]

energy consumption, and machinery cost, MD technology could not find place in the industrial stage. Though, the rejection of MD membranes is 100%. Khayet and Matsuura [241] and Wang and Chung [242] reported several configurations of MD unit such as direct contact membrane distillation (DCMD), air gap membrane distillation, sweeping gas membrane distillation (SGMD), and vacuum membrane-distillation (VMD). The membrane is the most important part of the MD process (Fig. 6.13).

Sweeping gas membrane distillation (SGMD): In SGMD, instead of a cold permeate solution, a cold inert gas sweeps in the permeate side of the membrane. The vapor is passing through the membrane pores toward cold gas side and condensation takes place out of MD module.

Vacuum membrane distillation (VMD): Using a vacuum pump, a lower vacuum pressure is applied to permeate side, generating driving force for the vapor transport. As in the SGMD, the condensation takes place out of MD module.

In DCMD, a membrane is placed between a cold permeate and a hotter feed solution. It has to have a temperature gradient between feed and permeate. The membrane is in contact with both feed and permeate. A magnetic stirrer or circulating

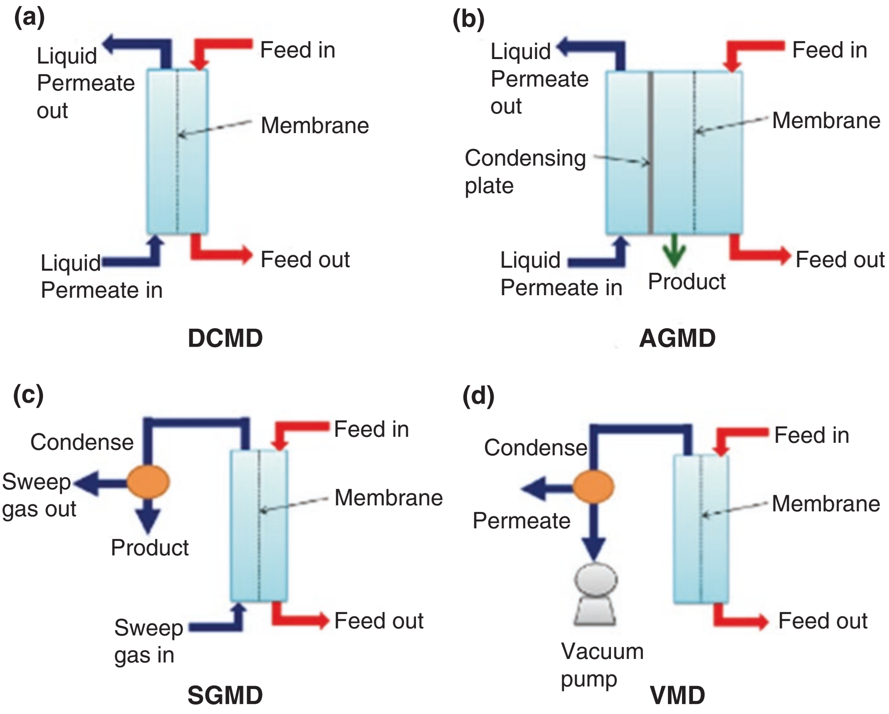

Fig. 6.13 Some of MD process configurations. (**a**) DCMD, (**b**) AGMD, (**c**) SGMD, and (**d**) VMD (originate from 110). *MD* membrane distillation, *DCMD* direct contact membrane distillation, *AGMD* air gap membrane distillation, *SGMD* sweeping gas membrane distillation, *VMD* vacuum membrane distillation [241]

pumps are used to circulate feed and permeate solution to the membrane surfaces. As a result of heat difference on both sides of the membrane, vapor pressure gradient is generated. The vapor of feed solution is passing through the membrane pores via diffusion or convection.

In air gap membrane distillation (AGMD), there is a gap between permeate and condensation plate. The membrane is in direct contact with feed solution. The vapor of feed solution is passing through the membranes to air gap and condenses on the condensing plate. The filtrated liquid is collected between feed and permeate solution.

The operation of membrane distillation systems faces several major barriers that may impair operation, or prevent it from being a viable option. The principal challenge is membrane wetting, where saline feed leaks through the membrane, contaminating the permeate [243]. For membranes to be used in MD, they must be hydrophobic, be porous, have high liquid entry pressure (LEP), and have good chemical/mechanical/thermal stability. In MD process, the polymeric membranes should demonstrate high permeability and hydrophobicity without wetting, narrow pores; as well as pore size distribution, thermal stability over a wide range of temperatures and a chemical stability, and possess strong mechanical strength. To make membranes for MD with these properties including low cost is a major challenge for the commercialization of MD technology.

Li et al. [244] repared SiO_2 porous ceramic membrane through phase inversion tape casting and pressureless sintering method. Flower-like Si_2N_2O nanowires was in-situ formed on the surface of the SiO_2 membrane, in NH_3 atmosphere, through vapor–solid (VS) process. The prepared membrane had a very good performance in membrane distillation (MD) experiments, with water flux as 11.11 L m^{-2} h^{-1} and >99.9% salt rejection for 4 wt.% NaCl aqueous solution at 90 °C.

Larbot et al. [245] demonstrated that grafted ceramic membranes can be used in membrane distillation process. These membranes are hydrophobic, and transport of water through the membrane is only by transport of vapour. The salt rejection in this process is close to 100%. Values of water flux through the membrane in the membrane distillation process depend strongly on temperature differences. Values of water flux do not depend on the salt concentration when it is lower than or equal to 0.1 M. Cerneaux et al. [246] investigated the desalination performance of zirconia and titania ceramic membranes which were chemically modified from their hydrophilic feature into hydrophobic via grafting the $C_8F_{17}(CH_2)_2Si(OC_2H_5)_3$ perfluoroalkylsilane molecule. Desalination of NaCl solutions of 0.5 and 1 M was performed using three MD configurations, AGMD, DCMD and VMD, with the aim to compare their efficiency. It was concluded that the easiest technique to be used would be the AGMD system, particularly if heating of the feed solution might be ensured using natural energy sources such as solar or geothermal ones. To conclude, the choice of the appropriate method is directly related to the source of salt solutions and reliant on the conditions of desalination. Subramanian et al. [247] evaluated the potentiality of superhydrophobic nanoporous alumina membranes for DCMD and reported that the ceramic membranes containing anodized aluminum oxide (AAO) were superhydrophobic and were able to separate counter-flowing streams (around 0.2 m s^{-1}) of hot salty water (343 K, 0.7 M NaCl) and cold deionized water (292 K).

Fan et al. [248] investigated the performance of fluorinated TiO_2 (titania) nanofibers membranes for membrane distillation (MD). During direct contact membrane distillation process, the prepared membrane displayed an excellent desalination performance with flux of 12 LMH and salt rejection of 99.92%. Moreover, the prepared membrane possesses a good stability for long-term MD operation in pure water and even desalinating high saline water. It was suggested by the authors that the superhydrophobic titania nanofibrous ceramic membrane modified by fluorination holds promise for practical applications due to its excellent performance for water desalination. Krajewski et al. [249] prepared fluorosilanes grafted ceramic membranes and studied its performance in the air-gap membrane distillation (AGMD) process. The hydrophobic active layer was created by grafting 1H,1H,2H,2H-perfluorodecyltriethoxysilane (C8 compound) on the commercial ceramic membrane (zirconia layer on the microporous alumina support). Results showed that the rejection of NaCl was close to 100%, indicating good hydrophobic behaviour of the FAS grafted ceramic membranes. The permeate fluxes were dependent on the NaCl concentration, pore diameter of the zirconia layer and the temperature difference between feed and permeate side of the membrane.

Feng et al. [250] were the first for using PVDF nanofiber membrane in MD to produce drinking water from saline water. Extensive research involving the modification of MD membranes with NPTs has been conducted to overcome the challenges associated with membrane flux, fouling, wetting, and porosity. NPTs are particulate materials with at least one dimension smaller than100 nm but larger than atoms and molecules. NPTs include particulate metals such as silver (Ag), silica (SiO_2), and titania (TiO_2) [251]. To reduce the fouling (formation of biofilms on the surface or inside the pores of the membrane), addition of Ag NPTs in the membrane system is very effective. Disadvantage of using high concentration of Ag NPTs is that it will block the pores of the membrane and reduce the water flux. The performance of TiO_2 NPTs toward water molecule depends on its different sizes and degree of crystallinity. It was reported that the rutile nanoparticles are more hydrophilic than anatase nanoparticles of the same size, both at room temperature ($T = 300$ K, $P = 1$ bar) and under hydrothermal conditions ($T = 523$ K, $P = 50$ bar). Small sized TiO_2 NPs exhibited high hydrophilic properties [252]. Thus, this material can be used to make hydrophobic surfaces hydrophilic for decreasing the surface adsorption of hydrophobic organic foulants. Membranes have to be configured into membrane modules which can be in the type of hollow fiber, spiral wound, and plate modules for practical applications. For an efficient membrane module, the key factors are a membrane with high packing density, good control of concentration polarization and membrane fouling, low operating and maintenance costs, and also cost-efficient production. Considering the properties of efficient membranes, nanofibers seem a good candidate for MD process. Generally, PVDF is preferred due to its solubility and spinnability.

In seawater distillation and wastewater treatment, there are two main obstacles.

1. Membrane wetting.
2. Formation of fouling and scaling on the membrane surface.

Due to these two obstacles, process efficiency declines, against the widespread use of the membrane technology.

Su et al. [253] developed a facile method to construct composite membranes with high MD performance via one-step electrospinning of PVDF solutions blended with hydrophobic silica NPs. It was revealed that incorporation of silica NPs altered the membrane surface morphology and endowed the composite membrane with hierarchical structure on both surface and bulk layers (three-dimensional (3D) superhydrophobic membrane). The hydrophobicity of the membranes depends on the concentration of Si NPs. Water contact angle (WCA) of the membranes can be optimized to be 157 ± 1°, which was close to that of the lotus leaf (160°). Furthermore, the incorporation of silica NPs has promoted the mechanical strength, salt rejection, and water permeation flux of the membranes. The composite membrane containing 7.47 wt% silica NPs (designated as SIL40) can achieve a high MD performance with a water flux of 25.73 kg m^{-2} h^{-1} and a permeate conductivity below 5.0μS cm^{-1} during a 100 h test-period. Sameh et al. [254] evaluated pure PES, pure PVDF, PES/GNPs, PVDF/GNPs, PES/PVDF blend and PES/PVDF/GNPs (graphene nanoplates) composite membranes for desalination by using DCMD process. The addition of only 2 wt.% GNPs into the PES/PVDF (3:1 w/w) blend increased its water contact angle up to 132.3 ± 0.8°. This composite membrane achieved a flux of about 19.35 kg m^{-2} h^{-1} at feed inlet temperature of 65 °C, flow rate of 30 L h^{-1}, and salt concentration of 10,000 ppm. The experimental results obtained from PES/PVDF/GNPs composite membrane showed a comparable performance to pure PVDF and PVDF/GNPs composite membranes.

Zahirifar et al. [255] fabricated a novel dual-layer membrane by coating a very smooth layer of octadecylamine functionalized graphene oxide (GO-ODA) on the surface of PVDF membrane. Modified membranes in comparison with unmodified membrane showed a superior performance in terms of surface roughness, hydrophobicity, water flux and NaCl rejection. In air gap membrane AGMD experiments using a 3.5 wt% NaCl solution as feed at 80 °C, unmodified, M1 (low GO-ODA loading), and M2 (high GO-ODA loading) modified membranes showed water fluxes of 18.2, 13.8, and 16.7 kg m^{-2} h^{-1} and salt rejections of 88.5%, 96.3%, and 98.3%, respectively.

Zhang et al. [256] fabricated nanostructure superhydrophobic membranes for MD via spraying a mixture of PDMS and hydrophobic SiO_2 nanoparticles on PVDF flat sheet membranes. On variation of the content of the particles in the spraying dispersion from 0 to 1.5 wt.%, the water contact angle (WCA) and the liquid entry pressure (LEP) of the membrane varied from 107° and 210 kPa to 156° and 275 kPa, respectively. The DCMD experiment with 25 wt.% sodium chloride solution had been run for 180 h. The results indicated that the permeate flux of the modified membrane slightly decreased with the NaCl rejection rate above 99.99%. Liao et al. [257] fabricated dual-layered superhydrophobic membranes composed of PVDF polymers with silica nanoparticles for improved desalination by the MD process. These fabricated membranes have shown significantly high water flux and salt rejection. The researchers concluded that to use these membranes in water industries, modification, as well as optimization, is required for controlling the pore size of the membrane and enhancing the long-term performance of the membranes by optimizing the SiO_2 composition. Yan et al. [258] fabricated CNTs coated PVDF superhydrophobic electrospun nanofiber membranes via spraying method. The presence of CNTs significantly enhanced the hydrophobicity and liquid entry pressure of membranes. The VMD results indicated that the CNTs coated membranes had superior performance both in anti-wetting and water flux in desalination process. The properties of CNTs coated membranes exhibited no significant change after VMD tests. Chen et al. [259] reported that nanoporous carbon composite membranes, which comprise a layer of porous carbon fibre structures grown on a porous ceramic substrate, can exhibit 100% desalination and a freshwater flux that is 3–20 times higher than existing polymeric membranes. The membrane was also successfully applied to RO, MD and FO membrane desalination. Using a combination of VMD, FO and energy accounting experiments, water was found to transport through the gaps of the carbon fibres. Thermal accounting experiments demonstrated that the carbon composite membrane saved over 80% of the latent heat consumption. Theoretical calculations combined with molecular dynamics simulations revealed the unique microscopic process occurring in the membrane.

Jiříček et al. [100] prepared four flat sheet nanofiber PUR membranes of different thickness by continuous needleless electrospinning process and used in MD for waste water treatment. It was reported that the highest flux was achieved with the synthesized PVDF- titanium tetraisopropoxide (PVDF-TTIP) hybrid membrane via electrospinning. The membrane was successfully employed in vacuum enhanced membrane distillation process for total removal of trace heavy metal contaminants and production of ultra-pure water in one step. Introduction of the Ti-O-Ti condensed structure into the PVDF electrospun membrane dramatically increased the membrane performance in terms of durability, enrichment enhancement etc., but did not improve the permeate flux of the membrane.

Table 6.14 presents the summary of few nanoparticle-embedded membranes prepared using different methods and their potential impact on membrane distillation (MD).

Table 6.14 Summary of nanoparticle-embedded membranes prepared using different methods and their potential impact on membrane distillation (MD)

Method	Polymer	Nanoparticles	Impact	References
Coating	PVDF	TiO_2 NPs	High fouling resistance	[260]
Spraying	PVDF	PDMS/SiO_2 NPs	High salt rejection (99.99%)	[256]
Phase inversion	PVDF	SiO_2 NPs	High salt rejection (99.98%)	[261]
Flat sheet coated	PVDF	SiO_2 NPs chitosan hydrogel and fluoro-polymer	High oil-fouling resistance	[262]
Hollow fiber	PVDF/PAN	Clay	High flux (55 L m^{-2} h^{-1}) and fouling resistance	[263]
Coating	PVDF	Octadecylamine functionalized graphene oxide (GO-ODA)	Superior performance in terms of surface roughness, hydrophobicity, waterflux and NaCl rejection.	[255]

6.6 Electrospun Nanofibers/Membrane for Water/ Wastewater Treatment

Energy and the environment are the most important factors that influence the shape of society in the twenty-first century. Nanosized fibers have great advantages due to their high surface area to volume ratio, electrospun nanofibers have potential applications in the field of clean energy (solar cells, fuel cells and batteries), electronics, health (biomedical scaffolds, artificial organs), and environment (filter membranes)" [264].

Water pollution is the contamination of water bodies (e.g., lakes, rivers, oceans, aquifers, and groundwater), and it occurs when pollutants are discharged directly or indirectly into water bodies without adequate treatment to remove harmful compounds. Direct sources include effluent outfalls from factories, refineries, waste treatment plants, etc., that emit fluids of varying quality directly into urban water supplies. Indirect sources include contaminants that enter the water supply from soils/groundwater systems and from the atmosphere via rainwater. Soils and groundwaters contain the residue of human agricultural practices (fertilizers, pesticides, etc.) and industrial wastes that are improperly disposed of. Atmospheric contaminants are also derived from human practices (such as gaseous emissions from automobiles, factories, and even bakeries). In addition to organic chemical pollutants, using nuclear energy has generated huge amounts of radioactive substances, the disposal of which might be the most difficult task. Inexpensive and scalable methods to clean freshwater and wastewater are in high demand [265].

Several types of membranes and filtration systems are employed in water treatment processes based on their pore sizes and particle filtration as shown in Fig. 6.14 [240].

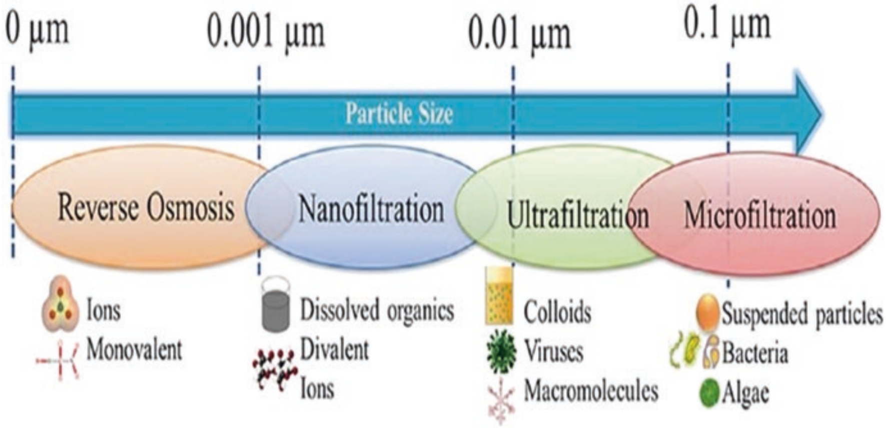

Fig. 6.14 Particle size removal range by filtration [240]

Nanofibers can be considered for advanced systems for separation processes due to its following properties;

1. high porosity,
2. small interfibrous pore sizes (ranging from tens of nanometers to several micrometers)
3. interconnected open pore structures
4. high permeability
5. large surface per unit volume
6. flexibility in surface functionalities

Thus, ENFs represent a valuable alternative to conventional water purification and wastewater treatment plants offering at the same time both filtration and adsorption capabilities. Beside this, electrospun nanofiber membranes have been found to exhibit better transmembrane fluxes than currently used hydrophobic microfiltration membranes. Wastewater contains pathogens, such as bacteria, viruses, protozoa, molds, fungus, and helminthes and many chemical constituents. Electrospun nanofiber membranes can swiftly and sensitively eliminate TDS, pathogens, monovalent and multivalent anions and cations, salts, mineral and extra suspended nanomaterials from the water [266].

6.6.1 Nanofiltration

Nanofiltration technology, which is a category of membrane technology placed between RO and UF, has been attracting a great deal of interesting characteristics of membrane technology.

Safarik et al. [267] fabricated, multifunctional nano/ultra filtration, magnetically modified electrospun nanocomposite fibers based on a naturally derived biocompatible and biodegradable polysaccharide chitosan (CS) and the hydrophilic and biocompatible poly(vinylpyrrolidone) (PVP). Magnetic nanoparticles (MNPs) were anchored on the surface of CS-PVP via chemical coprecipitation, by immersing the produced fibrous mats in an aqueous solution containing Fe(II) and Fe(III) salts followed by the addition of a weak base to yield MNPs. It was reported that magnetically modified, chitosan-based electrospun nanofibers were also very good supports for enzyme and yeast cell immobilization due to their biocompatibility.

Wang et al. [268] reported that the interfacial polymerization of poly amide around the ultrafine cellulose nanofibers layer in TFNC showed a good rejection of $MgCl_2$ and $MgSO_4$, depending on the adapted interfacial polymerization. Zeytuncu et al. [269] fabricated a polyvinyl alcohol (PVA) organic-inorganic hybrid nanofiber (PVA/SiO_2) membranes by electrospinning with UV irradiation. The membranes produced are suitable for use in various applications, including filtration.

6.6.1.1 Membrane Distillation

Membranes for MD process should have following characteristics;

1. High permeability and high hydrophobicity without wetting,
2. Narrow pores; as well as pore size distribution.
3. Thermal stability over a wide range of temperatures.
4. Chemical stability.

For an efficient membrane module, the key factors are a membrane with high packing density, good control of concentration polarization and membrane fouling, low operating and maintenance costs, and also cost-efficient production. Considering the properties of efficient membranes, nanofibers seem a good candidate for MD process [240].

To make above mentioned properties with low cost MD membrane manufacturing technique is a major challenge for the commercialization of MD technology. Beside this, MD membranes still suffer from low permeate water flux and frequent pore wetting due to low hydrophobicity. While novel membrane designs can overcome these limitations, such membranes must be fabricated using a scalable, environmentally benign, and low-cost technique. Shaulsky et al. [243] suggested for tunable membrane structural parameters and performance without compromising surface hydrophobicity, two process are necessary i.e., (1) controlling the penetration depth of the dope solution, and, (2) consequently, the thickness of the polymeric coating layer on the electrospun substrate. The important factors for MD membranes are, (1) proper choice for a solvent which does not damage the polymeric fibers and (2) control over the polymer loading. The electrospun fiber substrates coated with a controlled polymeric layer thickness exhibited stable desalination performance in MD due to the enhanced surface wetting resistance.

Ren et al. [270] generated superhydrophobic membrane by first coating TiO_2 nanoparticles on PVDF electrospun membranes surface followed by fluorosilanizing with low surface energy material of FTCS (1H,1H,2H,2H-per-fluorododecyl trichlorosilane). The TiO_2-FTCS modified PVDF ENM exhibited stable hydrophobicity and wetting resistance under severe thermal, mechanical and operated conditions. A mean permeate flux of 73.4 LMH was obtained during the DCMD process for 3.5 wt% NaCl solution with a salt rejection of 99.99%. All these indicated that TiO_2-FTCS modified PVDF ENM could be a suitable candidate for seawater desalination using MD.

Tijing et al. [271] fabricated a very high flux and stable DCMD performance electrospun CNT/PcH (polyvinylidene fluoride-co-hexafluoropropylene) membrane. The electrospun membrane has been designed to have two cohesive layers, a thin CNT/PcH top layer and a thick neat PcH bottom layer. Loading of CNTs improved the mechanical properties of the electrospun membrane. The resulting flux of the 5 wt% CNT-incorporated nanofiber membrane (24–29.5 L m^{-2} h^{-1}) was consistently higher than the commercial PVDF membrane (18–18.5 L m^{-2} h^{-1}), with an average increase of 33–59% depending on the feed water type (35 or 70 g L^{-1} NaCl solution) without compromising the salt rejection (>99.99%). Ya et al. [272] prepared carbon nanotubes (CNTs) coated on superhydrophobic electrospun nanofiber membranes (PVDF) via spraying the CNTs/ethanol dispersion on membrane's surface. The CNTs network significantly enhanced the hydrophobicity and liquid entry pressure of membranes. It was observed that the CNTs coated membranes had superior performance both in anti-wetting and water flux in desalination when used in vacuum membrane distillation (VMD). It was suggested that such approach to fabricate superhydrophobic membranes has the potential applications towards other hydrophobic membranes fabrication. An et al. [273] studied the performance of functionalized carbon nanotubes (CNTs), anchored to nanofibres of electrospun poly (vinylidene fluoride-hexafluoropropylene) (PVDF-HFP) membranes via MD. It was observed that on functionalization of the membranes, the surface roughness, water contact angles and hydrophobicity of the membranes were increased significantly.

Jiřıček et al. [100] fabricated four PUR membranes with varying thickness by needle-free industrial electro-spinning system and tested to find the optimum structural parameters and operational conditions for the best MD performance in waste water treatment. It was reported that the highest flux was achieved with the thinner membranes and the best energy efficiency was achieved with the thicker membranes. An et al. [274] fabricated amphiphobic polyvinylidene fluoride-co-hexafluoropropylene (PVDF-HFP) electrospun nanofibrous membranes with anti-wetting property. Their approach was to fluorinate PVDF-HFP fibers by using1H,1H,2H,2H-perfluorodecyltriethoxysilane (FAS) followed by crosslinking to form a network upon dealcoholization under thermal treatment. These FAS coated membranes showed less reduction in permeability and increase in salt rejection in the long term operation.

Liao et al. [275] fabricated specially designed PVDF nanofiber membranes for DCMD application. In fabricating the fibers, the structures and properties of resultant membranes were optimized by controlling a series of factors including polymer dope compositions and spinning parameters. Membranes exhibited a rough surface with high hydrophobicity (>135° water contact angle). Heat-press post-treatment effect on the MD performance of membranes has also been examined. Heat-press post treatment enhanced the membrane performance in DCMD. The post-treated PVDF nanofiber membranes were able to present a steady water permeation flux of about 21 kg m^{-2} h^{-1} throughout the entire testing period of 15 h, using a 3.5 wt % NaCl solution as the feed under the feed and permeate inlet temperatures of 323 K and 293 K, respectively.

Khayet et al. [276] prepared dual-layered electrospun nanofibrous membranes (DL-ENMs) using hydrophobic polyvinylidene fluoride (PVDF) and hydrophilic polysulfone (PSF) and its performance was studied by using it in direct contact membrane distillation (DCMD) for desalination (with different sodium chloride feed aqueous solutions). The thickness of each layer was varied via changing the electrospinning time of each polymer solution. The DCMD permeate flux of the DL-ENMs was found to be higher than that of the single layer PVDF ENMs (SL-ENMs). It has also increased with the decrease of the PVDF layer. It was observed that polysulfone (PSF) layer exhibited more open structure than polyvinylidene fluoride (PVDF) layer.

Shaulsky et al. [243] demonstrated a novel solution-based approach for the fabrication of membrane distillation (MD) membranes with adjustable pore size and performance through non-solvent induced phase separation of a polymeric solution over an electrospun fiber mat. Highly porous electrospun fiber mat with an average pore diameter of ~1.2μm was obtained by poly(vinylidene fluoride-hexafluoropropylene) (PVDF-HFP) in a mixture of acetone and dimethylacetamide. PVDF was coated on the surface via phase separation to control the membrane pore size by filling the empty domains between the fibers. By controlling the depth of the PVDF coating layer within the substrate, robust membranes were obtained. These membranes were tested in DCMD for desalination. The results showed near complete salt rejection (>99.9%) and a water flux of 30 L m^{-2} h^{-1} with 40 °C temperature difference between the feed and permeate solutions.

Woo et al. [277] modified the surface of an omniphobic PVDF membrane, prepared by electrospinning, with CF_4 plasma treatment without significantly altering the morphology and its physical properties. The membrane performance was evaluated using real reverse osmosis (RO) brine produced from coal seam gas (CSG) water as feed solution via AGMD. Plasma treatment lowered its surface energy and gave omniphobic property to the membrane. AGMD performance showed stable normalized flux. The highest water vapor flux observed for P/CF-15 (15-min plasma treatment) ENM membrane was 15.3 ± 0.8 L m^{-2} h^{-1} (neat nanofiber membrane 8.5 L m^{-2} h^{-1}) and salt rejection was 100%. Authors claimed that the omniphobic membrane has good potential for producing clean water from challenging waters containing high salinity and organic contaminants.

Dong et al. [278] prepared superhydrophobic FAS-PVDF-SiO_2 nanofiber membranes with high water contact angles via electrospinning of PVDF-SiO_2 blend solutions followed by a fluorosilanization process with FAS (fluoroalkylsilane). It was reported that superhydrophobic modified nanofiber membranes maintained a stable flux of about 31.5 kg m^{-2} h^{-1} with a permeate conductivity approximately 10μs/cm over the entire test. On the other hand, the flux and conductivity of the unmododified membrane showed a significant decrease and increase, respectively.

Figoli et al. [279] fabricated Keratin ENMs coated on Nylon woven fabric and characterized in terms of morphology, pore size contact angle, and performance of water and air permeability. Roughness and hydrophobicity of produced nanofibers increased by increasing electrospinning time, while the pore size and water permeability decreased. It was also observed that, electrospun NFMs exhibited better transmembrane fluxes than currently used hydrophobic microfiltration membranes. Keratin NF membranes (NFMs) also demonstrated good adsorption properties for heavy metals ions. Membranes were initially stabilized for 30 min at a transmembrane pressure (TMP) of 0.65 bar. At the highest electrospinning time (2 h), the produced NFMs showed a PWP of about 45.7 m^3 m^{-2} h^{-1} bar^{-1} and air permeability of about 40 L m^{-2} s^{-1}. Li et al. [280] fabricated the Fe_3O_4/PAN magnetic nanofibers (MNFs) firstly, followed by the HRP (horseradish peroxidase) immobilizationon on the MNFs surface with the help of dopamine and glutaraldehyde solution. The HRP immobilized MNFs (H-MNFs) was applied to catalyze phenol removal. For 40% H-MNFs for the remediation of phenol wastewater, the removal efficiency of phenol was 85% in the first round use, and remained 52% of efficiency after 5 recycles using. It was expected that the H-MNFs could have a potential application in wastewater treatment such as phenol removal.

Table 6.15 shows the summary of few nanoparticle-embedded membranes prepared using different methods and their potential impact on membrane distillation (MD).

Table 6.15 Summary of few nanoparticle-embedded membranes prepared using different methods and their potential impact on membrane distillation (MD)

Method	Polymer	Nanoparticle	Impact	Reference
Electrospinning	PVDF	CNTs	Improved flux ($24–29\ L\ m^{-2}\ h^{-1}$) and salt rejection (99.9%)	[271]
Electrospinning	PVA	SiO_2 NPs	Improved amphiphilic properties leading to high fluxes ($45\ L\ m^{-2}\ h^{-1}$) in the presence of surfactants in solution	[281]
Electrospinning	PVDF	TiO_2 NPs	Stabilized high water flux ($40\ L\ m^{-2}\ h^{-1}$)	[282]
Electrospinning	PVDF	SiO_2 NPs	High water flux in oil–water separations ($24\ L\ m^{-2}\ h^{-1}$)	[257]
Electrospinning	PVDF	Al_2O_3 NPs	High metal rejection (95%)	[283]
Electrospinning	PVDF	SiO_2 NPs	High stable flux ($31\ L\ m^{-2}\ h^{-1}$)	[278]
Electrospinning	PVDF	SiO_2 NPs	High stable flux ($48\ L\ m^{-2}\ h^{-1}$)	[284]
Electrospinning	PVDF	TiO_2 NPs	High flux ($38\ L\ m^{-2}\ h^{-1}$)	[285]
Electrospinning	PVDF	CNTs	Flux enhancement ($45\ L\ m^{-2}\ h^{-1}$)	[273]
Electrospinning	PVDF	Clay	Wetting resistance	[286]
Electrospinning	CTAB[a] / PVDF-HFP[b]	Fuorinated SiNPs	Antiwetting omniphobic and antifouling	[287]
Electrospinning and coating	PVDF	SiO_2 NPs	Fouling and wetting resistance	[255]
Electrospinning	PVDF-HFP	Graphene	Stable flux ($23\ L\ m^{-2}\ h^{-1}$)	[288]
Electrospinning	PVDF-HFP	Fluorosilane-coated TiO_2 NPs	Stable wetting resistance	[289]

(continued)

Table 6.15 (continued)

Method	Polymer	Nanoparticle	Impact	Reference
Hollowfiber	PVDF/PAN	Clay	Highflux (55 L m^{-2} h^{-1}) and fouling resistance	[262]
Electrospinning	PAN	Ag	Water disinfection	[290]
Electrospinning andhydrothermal technique	(PVDF-HFP)	TiO_2 nanorods	High and stable salt rejection of >99.9%,	[291]
Electrospinning	PVDF	PPO on PVDF	High water recovery ratio of 80 and 60% toward seawater and shale gas wastewater desalination	[292]

[a]Cetyltrimethylammonium bromide
[b]Hexafluoropropylene

The application of nanotechnology for water/wastewater treatment is gaining tremendous interest among scientists for water treatment. Electrospun nanofibrous membranes have shown promising results in the laboratory testing stage; however, their readiness for large-scale commercialization still faces some technical challenges, such as compatibility with the existing infrastructures, environmental and health risks, potential degradation of polymer with time and cost [293].

6.7 Separation of Organic Mixtures Via Pervaporation

The word ‘pervaporation’ was first coined by Kober [294] who used collodion (cellulose acetate) bag to allow fast evaporation of water from the aqueous solution. In 1935, Farber [295] used this technique for the concentration of the protein solution. Since the report of Binning et al. in 1961 [296] PV has gained much wider popularity, especially for dehydrating alcohols, leading to both product recovery and wastewater treatment. Pervaporation combines both evaporation and membrane permeation and is unique among membrane separations in that it involves a liquid-vapour phase change. Pervaporation (PV) has been considered as one of the most active and promising areas in membrane technologies in separating close boiling or azeotropic liquid mixtures, heat sensitive biomaterials, water or organics from its mixtures that are indispensable constituents for various important chemical and bioseparations [200, 290]. Many reviews have been published on pervaporation [297, 298].

In PV, a liquid feed is contacted with one side of the membrane and vapour is withdrawn from the other (Fig. 6.15).

In other words, PV is a membrane process involving separation of liquid mixture through a dense selective layer of an asymmetric membrane. PV is being tried extensively on systems which are difficult to separate by the existing separation

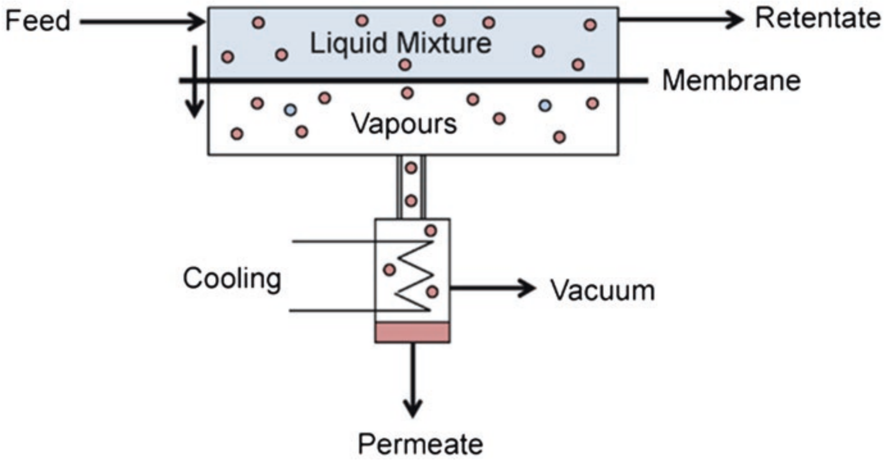

Fig. 6.15 Schematic of a typical pervaporation process

processes, like distillation, adsorption and extraction. In fact, PV is an effective candidate for separating azeotropic and close boiling liquids, heat sensitive materials, organic mixtures along with removal of dilute volatile organic compounds (VOCs) from wastewater and recovery of volatile aroma compounds from fruit juices [299]. It is very difficult to find a suitable membrane for potential organic-organic separation. PV permits the separation of azeotropic mixtures without using a third component that may steer towards undesired side effects, like hydrolysis. In the PV process, the membrane plays the most pivotal role and is of paramount importance in governing the overall efficiency.

Among membrane processes, pervaporation systems are developed in many applications such as alcohols and ethylene glycols dehydration etc.

6.7.1 Separation of Organic Solvents

Separation of organic-organic compounds is one of main areas in which pervaporation (PV) is employed together with solvent dehydration and removal of volatile organic compounds (VOCs) from aqueous solutions. Pervaporative organic-organic separation is the least developed field of application of pervaporation, and it is still very challenging principally due to the lack of membranes able to resist to the harsh conditions of solvents and the high temperatures required by the process [298]. Niemistö et al. [300] studied the performance of a PDMS membrane with a support layer of PAN for the removal of acetone, butanol and ethanol from dilute aqueous model solutions. It was reported that the partial fluxes and permeate concentrations were found to be in the order of acetone≈butanol>ethanol, while the permeance order was butanol > ethanol ≈ acetone at feed temperature of 42 °C. Separation factors from water were in the range of 21–26, 22–29 and 5–7 for acetone, butanol and ethanol, respectively.

Kopec et al. [301] prepared homogenous, composite and mixed matrix membranes (MMMs) based on polyamide-6. The filler materials for composite membrane were metal oxides (Al_2O_3, TiO_2 and ZrO_2). Prepared membranes via dry phase inversion method, were used to separate methanol from MeOH/MTBE and MeOH/DMC mixtures by pervaporation. It was found that membranes were selective to methanol and their separation factors were much higher in contact with MeOH/MTBE mixture than with MeOH/DMC one. The pervaporation separation index (PSI) for methanol removal was the highest for PA-6 membranes filled with 10 wt.% ZrO_2.

CNT-incorporated membranes are extensively studied in PV for organic-organic separations. The PV separation of benzene-cyclohexane mixtures has been studied by Peng et al. using PVA membranes modified with CS-wrapped MWCNTs [302]. It was reported that, for benzene/cyclohexane (50/50, w/w) mixtures at 323 K, permeation flux and separation factor of pure PVA membrane were only 20.3 g m^{-2} h^{-1}) and 9.6, respectively, while the corresponding values of PVA–CNT(CS) (CNT content: 1%) nanocomposite membrane were 65.9 g m^{-2} h^{-1} and 53.4, respectively. Shen et al. [303] investigated separation of benzene/cyclohexane mixtures by pervaporation using chitosan membrane incorporated with functionalized multiwalled carbon nanotubes (MWCNTs). Pervaporation results showed that the separation performance of MWCNTs–Ag^+/chitosan hybrid membrane was better than MWCNTs/chitosan hybrid membrane and pristine chitosan membrane. The modified membrane was observed to absorb more benzene with an increase in the content of the MWNTs-Ag^+ in the membrane and the benzene content in the feed mixtures. The poly(phenylene isophtalamide) (PA) membrane fabricated with 2 wt.% CNTs showed high selectivity and permeability for pervaporative separation of MeOH/MTBE (methyl tert-butyl ether) mixtures [304]. It was shown that the selectivity with respect to methanol and permeability were the highest for membranes containing 2 wt.% CNT as compared to membranes of pure PA and PA containing 5 wt.% CNT.

Liu et al. [305] coated poly(ether-block-amide) (PEBAX 2533) on top of the PVDF substrate to fabricate composite membranes for the removal of thiophene from *n*-heptane. When feed thiophene concentration was 1000μg g^{-1} and feed temperature was 40 °C, total flux and separation factor were 3.8 kg m^{-2} h^{-1} and 4.0, respectvely.

Sabzevari et al. [306] studied PA/nano silica mixed matrix membranes for dehydration of ethylene glycol via pervaporation technique. It was reported that nano silica with 0.5 wt.% loading showed the best PV performance. Azimi et al. [307] investigated PV separation of organic compounds from acetone-butanol-ethanol (ABE) fermentation model solutions, using activated carbon (AC) nanoparticle-poly(dimethylsiloxane) (PDMS) MMM. Based on the results obtained from this study, the presence of the activated carbon nanoparticles in the matrix of the PDMS membrane was shown to be beneficial for the pervaporation separation performance of the butanol from ABE model solutions. Manipulation of the PDMS membranes' structure and properties using AC nanoparticles in this work resulted in a higher flux (at 8 wt.%) and higher separation factor for butanol (at 10 wt.%) compared to the commercial PDMS membrane.

Following Table 6.16 shows MMMs for organic–organic separation via PV [297].

6.7.2 Alcohol Dehydration

Jose et al. [308] investigated the influence of functionalized MWCNT (a-MWCNT) on the pervaporation and dielectric properties of PVA nanocomposites. The PVA/MWCNT nanocomposite membranes were used for the separation of azeotropic composition of water-ethanol mixture. Initially at lower concentration, the separation factor values increased from 36 to 160 (344% increase) as compared to pure cross-linked PVA membranes, and decreased when the a-MWCNT content increased 0.5–2 wt.%.

Liu et al. [309] used PA/ceramic thin-film composite membrane for IPA dehydration. The membrane was fabricated by constructing interfacially polymerized PA selective layer on the surface of TiO_2 modified ceramic hollow fiber (CHF). The prepared composite membranes exhibited the superior separation performance with the permeate flux of 6.44 kg m^2 h^{-1} and separation factor over 12,000 for PV dehydration of 90 wt% aqueous IPA solution at 60 °C.

Various polymeric materials such as PVA, chitosan, PA, PI, PAN, PTFE, PES, PSF have been used for preparation of the different types of pervaporation membranes for dehydration purposes. Several inorganic compounds have also been used as filler in the synthesis of the mixed matrix membranes for solvent dehydration by the pervaporation process [310]. Panahian et al. [310] prepared a multilayer MMMs containing CNTs, PVA, PES and polyester as filler and selective top, intermediate and support layer, respectively. The PVA–CNT selective top layer was synthesized on the PES/polyester support by solution casting and the solvent evaporation technique. The membrane was used for dehydration of ethanol/water mixtures by the PV process. All mixed matrix membranes had lower total flux than the neat membranes due to an increase of the membrane top layer resistance by incorporating the MWCNT filler. Finally, it was observed that the modification of CNTs led to better dispersion of MWCNTs into the polymeric matrix and improved the separation performance of the multilayer MMMs. Kazemimoghadam and Rigi [311] studied the separation performances of nano-pore hydroxysodalite (HS) zeolite membrane for water-ethanol mixtures using PV technique. The membranes showed good selectivity towards water in the water-ethanol mixtures. Water permeates faster because of its preferential adsorption into the nano-pores of the hydrophilic zeolite membrane. Zuo et al. [312] fabricated organic–inorganic thin film composite (TFC) membranes with an introduction of an inorganic component 3-glycidyloxypropyltri methoxy-silane (GOTMS) in the in situ synthesized polyamide layer. These membranes were used for the dehydration of isopropanol. It was observed that

Table 6.16 Mixed matrix membranes (MMMs) for organic–organic separation

Feed mixture (A/B)	Membrane	Particle/hybrid component loading (wt.%)	Configuration	Temperature (°C)	Flux (g m^{-2} h^{-1})	Separation factor (B/A)
Cyclohexane/benzene (60/40 wt.%)	Polyvinylchloride/H-β-zeolite	10	Flat-sheet	30	11.5	19.3
Cyclohexane/benzene (60/40 wt.%)	Polyvinylchloride/ Rh/H-β-zeolite	10	Flat-sheet	30	18.5	17
EtOH/toluene (90/10 wt.%)	CS/silicalite	5	Flat-sheet	30	1810	217
MeOH/toluene (90/10 wt.%)	CS/silicalite	5	Flat-sheet	30	1700	200
t-BuOH/*n*-BuOH (50/50 wt.%)	Polyamide-imide/β--cyclodextrin	15	Flat-sheet	60	4.4	1.53
Butanediol/BuOH (52.6/47.4 wt.%)	PDMS/ZSM-5	80	Flat-sheet	N.A	16	18.4
MeOH/DMC (70/30 wt.%)	PDMS/silica	15	Flat-sheet	40	702	4
o-Xylene/*p*-xylene (85/15 wt.%)	Poly(acrylic acid) sodium/ silane-modified silicalite	6	Flat-sheet	30	38	1.8
m-Xylene/*p*-xylene (85/15 wt.%)	Poly(acrylic acid) sodium/ silane-modified silicalite	6	Flat-sheet	30	36	2.2
Benzene/MeOH (80/20 wt.%)	PVA/H-ZSM-5	5	Flat-sheet	30	71	47

BuOH butanol, *DMC* dimethylcarbonate, *EtOH* ethanol, *MeOH* methanol pervaporation separation performance surpassed most of previous polymeric membranes and inorganic ceramic membranes for isopropanol dehydration. The TFC membrane prepared exhibited an optimized flux of 3.5 kg m^{-2} h^{-1} with a separation factor of 278 for a feed composition of 85/15 wt.% isopropanol (IPA)/water at 50 °C.

Wang et al. [313] demonstrated that highly water-selective hybrid membranes could be prepared by blending g-C_3N_4, O-g-C_3N_4 and PDA@O-g-C_3N_4 into PVA matrix. The membrane performances were tested in the PV process for the dehydration of 90 wt.% ethanol/water mixtures at 75 °C and it was reported that the total flux decreased from 4634 to 2328 g m^{-2} h^{-1} and the separation factor increased from 32.4 to 57.9. Liu et al. [314] fabricated two kinds of zeolitic imidazolate frameworks (two-dimensional ZIF-L nanosheets and zero-dimensional ZIF-8 nanoparticles) with the same building blocks. Both ZIF-L and ZIF-8 materials were incorporated into sodium alginate (SA) matrix to fabricate hybrid membranes for pervaporation dehydration of ethanol. At the filler content of 4 wt%, the ZIF-L-filled membrane displayed permeation flux of 1218 g m^{-2} h^{-1} and separation factor of 1840, while the ZIF-8-filled membrane displayed permeation flux of 879 g m^{-2} h^{-1} and separation factor of 678. In another publication Liu et al. [315] demonstrated that the ZIF-71/PEBA (polyether-block-amide) MMMs could be potential candidates for practical biobutanol production via PV process. Zeolite 4A was incorporated into Na-Alg matrix and tested for IPA dehydration by Sudhakar et al. [316]. Both permeability and selectivity were increased by the zeolite loading. Subhas et al. [317] fabricated MMMs of PVA loaded with zeolite particles having different silica alumina ratio and investigated their performance for dehydration of ethanol and isopropanol (IPA) from their aqueous mixtures via PV. Both membrane selectivity to water and flux were increased as the alumina content in the zeolite increased. Separation factors of zeolite with lower alumina incorporated membranes were, respectively, 236 and 334 for the feed mixture compositions of 4 wt.% water in ethanol and 10 wt% water in IPAg m^{-2} h^{-1} at 30 °C. On the other hand, membranes containing zeolites with higher alumina content showed slightly higher separation factors of 349 and 568, respectively, for the same feed mixtures at 30 °C.

Sun et al. [318] used H-ZSM-5 filled chitosan (CS) membranes for pervaporation dehydration of aqueous ethanol solution. Compared with chitosan control membrane (permeation flux 54.18 g m^{-2} h^{-1} and separation factor 158.02 for 90 wt.% aqueous ethanol solution at 80 °C), the H-ZSM-5(50)-CS-08 membranes (mass ratio of H-ZSM-5(50) to chitosan is 8 wt.%) exhibited the remarkably improved pervaporation performance with permeation flux 230.96 g m^{-2} h^{-1} and separation factor 152.82 under the identical experimental conditions.

Cheng et al. [319] fabricated novel PA thin film nanofibrous composite (TFNC) membrane via interfacial polymerization (IP) with a modified GO (eGO) interlayer on highly porous electrospun PAN nanofibrous substrate for isopropanol dehydration by PV. The PA/eGO/PAN TFNC membranes exhibited an excellent separation performance for dehydrating 90 wt.% aqueous isopropanol solution with remarkably enhanced separation factor (1866) and high permeate flux (4150 g m^{-2} h^{-1}) at 70 °C. Subhas et al. [320] incorporated H_2O_2 treated graphene into CS/PVP blend matrix and tested for PV dehydration of ethanol as a function of GO loading, feed composition and feed temperature. The H_2O_2 treatment proved to be effective to enhance PV performance of the nanocomposite membranes.

Zhao et al. [321] fabricated polyelectrolyte complexes (PECs) nanohybrid membranes via traditional methods. Five types of PEC/SiO_2 nanohybrids, with incorporation of SiO_2 nanoparticles into PEC matrices, were prepared. All the five PEC/SiO_2 nanohybrid membranes showed very high performance in isopropanol dehydration as compared with other polymeric nanohybrid membranes. The high selectivity of nanohybrid membranes was maintained with increasing feed temperature up to 75 °C. For example, a performance of $J = 2.3$ kg m^{-2} h^{-1}, $\alpha = 1721$ was reported for CMCNa (sodium carboxymethyl cellulose) –PDDA (diallyldimethylammonium chloride) PEC nanohybrid membrane (SiO_2-PEC) containing 5 wt.% SiO_2 in dehydrating 10 wt.% water–isopropanol at 75 °C.

Bakhtiari et al. [322] introduced three types of particles (zeolite 4A, silica and CMS) into two polyimide matrices (Matrimid® and P84) for IPA dehydration. It was reported that the water selectivity is in the order of zeolite 4A > CMS > aerosil silica. Among these fillers, only zeolite 4A enhanced the flux of the MMMs while two others did not alter the flux significantly. Veerapur et al. [323] used mixed matrix membranes of NaAlg (sodium alginate) filled with sub-micron size magnesium aluminum silicate (MAS) particles for pervaporation separation of water–isopropanol mixtures. It was found that NaAlg membrane filled with 15 wt.% MAS gave the highest selectivity of 17,991 when tested for 10 wt.% of water containing feed mixture. Comparatively, a lower selectivity of 653 was observed for plain crosslinked NaAlg membrane for 10 wt.% water containing feed mixture. Flux values of NaAlg filled with 15 wt.% of MAS increased from 0.056 to 0.174 kg m^{-2} h^{-1}, suggesting no significant improvement.

Jyothi et al. [324] discussed the various types of membranes used in pervaporation for dehydration of alcohols. Many interesting works have been published on PV dehydration of alcohols. Jyothi et al. [324] recommend that the future researchers to work on enhancing the surface area and density of polar functional groups on fillers before mixing with the polymer. This approach would enhance interfacial compatibility between filler and polymer, thereby enhancing the membrane performance. Table 6.17 shows the few examples of membrane nanotechnology working on the dehydration/separation from water- alcohol mixture via pervaporation.

6.8 Removal of Heavy Metals Via Adsorption

Membranes for membrane adsorption (MA) have the dual function of membrane filtration and adsorption to be very effective to remove trace amounts of pollutants such as cationic heavy metals, anionic phosphates and nitrates. Adsorption is a surface phenomenon whereby molecules of a substance (adsorbate) adsorb on some solid surface (adsorbent). Various factors affecting adsorption are temperature, the nature of the adsorbate and adsorbent, the presence of other impurities, particle size, contact time and chemical environment. Heavy metals, when in abundance, can be

Table 6.17 Few examples of membrane nanotechnology working on the dehydration/separation from water-alcohol via pervaporation

Membrane	Dehydration/separation from water	Result	Reference
TiO_2/PA/ceramic	IPA	Permeate flux of 6.44 kg m^{-2} h^{-1}, separation factor over 12,000	[309]
PA/eGO/PAN TFNC ethylenediamine modified graphene oxide (eGO)	IPA	Separation factor 1866 permeate flux 4150 g m^{-2} h^{-1} at 70 °C	[319]
Na^+MMT^a-5^1/PVA	Isopropanol	Separation factor to water 1116, flux 0.051 kg m^{-2} h^{-1} lower than pristine PVA	[325]
Na^+MMT-10^1/PVA,	Isopropanol	Separation factor to water 2241, flux and 0.075 kg m^{-2} h^{-1} lower than pristine PVA	[325]
Na^+MMT-5/PVA and	1,4-dioxane	Separation factor to water 216, flux 0.076 kg m^{-2} h^{-1}	[325]
Na^+MMT-10/PVA	1,4-dioxane	Separation factor to water 369, flux 0.093 kg m^{-2} h^{-1}	[325]
Graphene/sodium alginate (NaAlg) nanocomposite me	Isopropanol	Permeance value of 3122 GPU, selectivity 4623 for a 10 wt.% water containing feed mixture at 30 °C	[326]
H_2O_2 treated GO/CS/PVP	Ethanol	Enhance PV performance of the nanocomposite membranes	[320]
H-ZSM5/PVA	Ethanol and isopropanol	Selectivity to water and flux were increased as the alumina content in the zeolite increased. Separation factors of zeolite with lower alumina incorporated membranes were, respectively, 236 and 334 for the feed mixture compositions of 4 wt.% water in ethanol and 10 wt.% water in IPA at 30 °C	[327]
H-ZSM-5/chitosan	Dehydration of aqueous ethanol	Flux 230.96 g m^{-2} h^{-1} and separation factor 152.82	[321]
Modified clay particle/NaAlg matrix	Isopropanol	Selectivity of 5781, permeance 3423 GPU for 10 wt% water containing isopropanol feed mixtureat 30 °C	[328]

(continued)

Table 6.17 (continued)

Membrane	Dehydration/separation from water	Result	Reference
CNTs, PES and polyester	Ethanol water mixture	Improved the separation performance	[310]
g-C_3N_4, O-g-C_3N_4 and PDA@O-g-C_3N_4/PVA m	Ethanol water mixture	Flux decreased from 4634 to 2328 g m^{-2} h^{-1} separation factor increased from 32.4 to 57.9	[313]
ZIF-8/SA	Ethanol water mixture	Permeation flux of 879 g m^{-2} h^{-1} and separation factor of 678	[314]
ZIF-L/SA	Ethanol	Permeation flux of 1218 g m^{-2} h^{-1} and separation factor of 1840	[314]
Hydrophobic-ZIF-71 filled PEBA	Recovery of biobutanol	Potential candidates for practical biobutanol production	[318]
4A zeolite/SA	IPA-water mixtures	Permeability and selectivity increased	[316]
SiO_2/PEC	IPA-water mixtures	Flux of 2.3 kg m^{-2} h^{-1}, separation factor 1721	[321]
Zeolite 4A, silica and CMS into two polyimide matrices	IPA dehydration	Best results for hydrophile zeolite 4A filler	[325]
15% MAS[b]/NaAlg	IPA-water mixtures	Flux 0.174 kg m^{-2} h^{-1}, selectivity 17,991	[323]
$AlPO_4$-5 (20 wt.%)/ NaAlg	IPA-water mixtures	Flux 0.386 kg m^{-2} h^{-1}, selectivity 69,358	[329]
PDMS/PE/Brass	Butanol-water mixture	Total flux 132 g/h/m^2, separation factor of 32	[330]

[a] Sodium montmorillonite
[b] Magnesium aluminum silicate

very toxic to the medium in which it is dissolved. Adsorption has been used as a suitable water treatment process to remove heavy metals.

Nanomaterials have proved to be excellent adsorbent materials due to their exotic properties that include small size, catalytic potential, high reactivity, larger surface area and a large number of active sites for interaction with various impurities. These properties contribute toward their exceptional adsorption capacities. Adsorption is commonly employed as a polishing step to remove organic and inorganic contaminants in water and wastewater treatment. Liu et al. [331] discussed the basic principles of adsorption and membranes.

Electrospun nanofibers have a great potential to be functionalized via incorporation of functional materials into the fibers, or via surface chemistry and coating techniques. The surface modifications of the ENMs enhance the nanofibers matrix properties such as availability of functional groups on the surface of nanofibers. A wide range of functional molecules can be incorporated into electrospun nanofibers for pollutant adsorption. Electrospun nanofibres for metal ion adsorption especially for hazardous metals are emerging and their use is increasing. As the base material does not contain appropriate functional groups, functionalization methods such as blending and chemical treatment are necessary [332]. A wide range of functional molecules can be incorporated into electrospun nanofibers for pollutant adsorption. The functionalized nanofibers may be able to collect small molecules or metal ions from a solution. For examples, electrospun cellulose nanofibers were surface functionalized with a dye Cibacron Blue F3GA (CB), and the functionalized nanofiber membrane showed strong affinity to bovine serum albumin (BSA) and bilirubin, with a capture ability of 13 mg and 4 mg per gram nanofibers, respectively [333].

Lee et al. [334] loaded PMMA with Rhodanine (Rhd) through blending and tested its performance for the removal of Ag (I) and Pb (II) ions through dead-end filtration. Electrospun membranes exhibited good Ag (I) and Pb (II) ion uptake capabilities. Huang et al. [335] reported that the Pd NPTs -immobilized electrospun polyethyleneimine (PEI)/PVA nanofibers reduced hexavalent chromium (Cr(VI)) to trivalent chromium (Cr(III)). Ki et al. [336] confirmed that the SF (Silk fibroin) and WK (oxidized wool protein commonly called wool keratose)/SF nanofibrous membranes exhibited an excellent performance as a heavy metal ions adsorbent. Wool protein is composed of various amino acids, especially containing many hydrophilic amino acids which have high affinity for ionic species such as metal ions. By blending the WK with SF, the electrospinnability and structural stability of WK/SF blend membrane was markedly improved and the WK/SF nanofibrous membrane exhibited higher Cu^{2+} adsorption capacity (2.88μg mg^{-1}) than SF nanofibrous membrane (1.65μg mg^{-1}).

Affinity membranes will play a critical role in wastewater treatment to remove (or recycle) heavy metals ions in the future. Polymer nanofibers functionalized with a ceramic nanomaterial, such as hydrated alumina/alumina hydroxide and iron oxides, could be suitable materials for fabrication of affinity membranes for water industry applications. The polymer nanofiber membrane acts as a carrier of the reactive nanomaterial that can attract toxic heavy metal ions, such as As, Cr and Pb by adsorption/chemisorption and electrostatic attraction mechanisms [337]. Gore et al. [338] developed the core–shell structured RF (resorcinol–formaldehyde) /PVA nanofibers and used for the adsorption of As^{3+} ions from the mimicked liquid effluents. The developed nanofibers demonstrated an adsorption capacity of 11.09 mg g^{-1} at a pH of 7, and an adsorption efficiency of 97.46% on protracted exposure, which is even adaptable at high temperatures with 93.1% reclamation.

Chaúque et al. [339] modified the surface of electrospun aminated EDA (ethylenediamine)- PAN nanofibers, by coating EDTA (polyethylenediaminetetraacetic acid) in presence of tetrahydro-furan. EDA was used as a cross-linker. The modified nanofibers (EDTA-EDA-PAN) were used in the wastewater treatment for the removal of Cd(II) and Cr(VI). It was revealed that the EDTA-EDA-PAN nanofibers showed effective sorption affinity for both Cd(II) (max. capacity 32.68 mg g^{-1} at 298 K) and Cr(VI) (max. capacity 66.24 mg g^{-1} at 298 K), and, nanofibers were regenerated by simple washing with 2 M HCl solution.

Neghlani et al. [340] modified polyacrylonitrile nanofibers (PAN-nFs) by grafting amine groups on nanofiber and microfiber surfaces. Diethylenetriamine was used to produce aminated polyacrylonitrile (APAN) nanofibers. The adsorption capacity for Cu^{+2} was 116.522 mg g^{-1} which was five times more than the reported value for APAN microfibers [341].

Gohari et al. [342] fabricated a novel UF MMMs composed of organic polyethersulfone (PES) and inorganic Fe–Mn binary oxide (FMBO) particles via phase inversion process for adsorptive elimination of As(III) from the contaminated water. It was reported that the best performing membranes prepared from the FMBO/PES ratio of 1.5:1 demonstrated the pure water flux as high as 94.6 L m^{-2} h^{-1} at operating pressure of 1 bar and maximum As(III) uptake capacity of around 73.5 mg g^{-1}. Phan et al. [343] modified crosslinked PVA nanofiber (with glutaraldehyde) via the esterification of hydroxyl group on PVA with the carboxyl group of 3-mercaptopropionic acid under hydrochloric acid in aqueous environment. Membrane was tested for the adsorption of silver ions from the aqueous solution and the membrane showed the affinity towards silver ions. The maximum adsorption volume was found to be 26.2 mg g^{-1}.

Cai et al. [344] modified the surfaces of electrospun poly(5-cyanoindole) nanofibers by treating with hydroxylamine. The prepared membrane, named as surface amidoxime-modified polyindole (SAMPI) nanofiber membrane, was used for the removal of Cr(VI) from aqueous solution via adsorption. The maximum adsorption capacities (Q_m) calculated from Langmuir model were 340.14, 380.23 and 404.86 mg g^{-1} at 25, 35 and 45 °C, respectively. These results indicated that the SAMPI nanofiber membrane might have potential applications in wastewater treatment for removal of Cr(VI). Yang et al. [82] grafted oxidized cellulose nanofibers (thiol-modified cellulose nanofibers, m-CNF) embedded in an electrospun polyacrylonitrile (PAN) nanofibrous scaffold with cysteine to increase the adsorption capability for chromium (VI) and lead (II). From the adsorption studies, it was revealed that these membranes have high adsorption capacities for both Cr(VI) (87.5 mg g^{-1}) and Pb(II) (137.7 mg g^{-1}) due to the large surface area and high concentration of thiol groups (0.9 mmol of –SH g^{-1} m-CNF). It was also reported that these membranes were stable in morphology and property and could be used and regenerated multiple times with high recovery efficiency.

Xiao et al. [345] fabricated water-stable polyelectrolyte polyacrylic acid (PAA) nanofibers by electrospinning and subsequent thermal crosslinking (using PVA). It was found that PAA/PVA nanofibrous mats can act as an effective sorbent or separation medium for removing Ca(II) ions from water. Chitpong [346] investigated cadmium removal by using poly(acrylic acid) and poly(itaconic acid) modified electrospun cellulose nanofiber membranes. Carboxyl functional groups were grafted on membrane fiber surfaces with polymeric ligands. It was reported that cadmium removal productivities of PAA-and PIA-modified membranes were found to be 6–15 times higher than commercial ion-exchange resins, and the membranes could be reused at least five times without decline in performance.

TiO_2/SiO_2-functionalized CNTs are among the most promising heterogeneous photocatalytic candidates for the degradation of a range of organic compounds, heavy metals reduction, and selective oxidative reactions [347]. The potential applications of TiO_2/SiO_2 functionalized CNTs are the remediation of a variety of environmentally-related pollutants of high concern, including synthetic dyes or dye-based hazardous waste effluents, polycyclic aromatic hydrocarbons (PAHs), pharmaceutically active compounds, pesticides, toxic heavy metal elements, metal-contaminated soil, and miscellaneous organic contaminants. Oxidized CNTs have high adsorption capacity for metal ions with fast kinetics. The surface functional groups (e.g., carboxyl, hydroxyl, and phenolic) of CNTs are the major adsorption sites for metal ions, mainly through electrostatic attraction and chemical bonding. It is commonly believed that the chemical interaction between the metal ions and the surface functional groups of CNTs is the major sorption mechanism. Protons in the carboxylic and phenolic groups of CNTs exchange with the metal ions in the aqueous phase [348]. Azamat et al. [349] made molecular dynamics simulations for the separation of zinc ions from water using boron nitride (BN) nanotubes embedded in a silicon–nitride membrane. It was revealed that that the (7,7) and (8,8) BN nanotubes were exclusively selective for ions. The (7,7) BN nanotube selectively conducted Zn^{2+} ions, while the (8,8) BN nanotube selectively conducted Cl^- ions. It was also reported that the passage of ions through nanotubes was related to the diameter of the BN nanotubes.

Razzaz et al. [350] prepared chitosan/TiO_2 nanofibrous adsorbents by two methods:

1. TiO_2 nanoparticles coated chitosan ENFs (coating method).
2. Electrospinning of chitosan/TiO_2 solutions (entrapped method).

These adsorbents were investigated for the removal of Pb(II) and Cu(II) ions in a batch system. The maximum adsorption capacities of Cu(II) and Pb(II) ions using entrapped and coating methods were found to be 710.3, 579.1 and 526.5, 475.5 mg g^{-1} at equilibrium time of 30 min and 45 °C, respectively. The selectivity of metal sorption, using chitosan/TiO_2 nanofibrous adsorbent was in order of Cu(II) > Pb(II).

The nano-adsorbents are novel materials which contain different functional groups on the external surface, and are enhancer to the adsorption process. Anitha et al. [351] studied the adsorption behavior of divalent metal cations (Cd^{2+}, Cu^{2+}, Pb^{2+}, and Hg^{2+}) with functional groups –COO–, –OH, and $–CONH_2$ via molecular dynamics (MD) simulations. The results show that adsorption capacity was improved significantly using surface modification of SWCNT with carboxyl, hydroxyl, and amide functional groups. In addition, the adsorption capacity is found to increase with increasing metal-ion concentration. Following order of adsorption of the metal ions on functionalized CNT was observed: $Pb^{2+} > Cu^{2+} > Cd^{2+} > Hg^{2+}$.

Moradi et al. [352] used atomic absorption spectroscopy technique to study interaction/adsorption of heavy metal ions (Pb(II), Cd(II) and Cu(II)) from aqueous solution by surfaces of single walled carbon nanotube (SWCNTs) and carboxylate group functionalized single walled carbon nanotube (SWCNT-COOH). Maximum adsorption capacities (q_m) for Pb^{2+}, $Cu^{2+}$and Cd^{2+} ions on to SWCNT-COOH were obtained as 96.02, 77.00 and 55.89 mg g^{-1}, respectively, and by SWCNTs, as 33.55, 24.29 and 24.07 mg g^{-1}, respectively. Draouil et al. [353] studied the sorption of cesium ions (Cs$^+$) from liquid outflows by using single-walled carbon nanotubes (SWCNTs), functionalized with copper hexacyanoferrate (CuHCF) nanoparticles. It was reported that the total sorption capacity of the material was 230 mg g^{-1}, and that about one third of the sorbed Cs (80 mg g^{-1}) was selectively complexed in the CuHCF nanoparticles grafted on SWCNT. Naghizadeh and Eivazi [354] reported that, compared with non- functionalized nanotubes, functionalized nanotubes have higher adsorption capacity of Pb from water. Zhang et al. [355] investigated the adsorption of Hg^{2+} and methylmercury (MeHg) to multi-walled carbon nanotubes (MWCNTs) modified with hydroxyl, amine and carboxyl groups. It was found that amine-modified MWCNTs showed a strong adsorption capacity to Hg^{2+} and MeHg, and the removal efficiency could reach up to 92% (0.5 g L^{-1} MWCNTs, and 100μg L^{-1} Hg^{2+} and MeHg) which was independent of pH. Bankole̱ et al. [356] investigated the removal of heavy metals (As, Pb, Cr, Cd, Ni, Cu, Fe, and Zn) via batch adsorption process from industrial electroplating wastewater using two different nano-adsorbents; purified carbon nanotubes (P-CNTs) and polyhydroxyl butyrate functionalized carbon nanotubes (PHB-CNTs). Both adsorbents were produced through catalytic chemical vapour deposition (CCVD) method. The heavy metals removal efficiencies by the nano-adsorbents followed the order of PHB-CNTs > P-CNTs based on ion exchange and electrostatic forces mechanism. Table 6.18 shows the mean concentration of heavy metals in electroplating wastewater (before and after adsorption process) [356]. Cellulose-based nanocrystals and nanofibers were developed by Corsi et al. [357] and used as adsorbents to capture heavy metals. Tests performed at room temperature and neutral pH on 150 ppm metal solutions revealed adsorption efficiencies of 84, 77, 101 and 160 mg g^{-1} in the case of Cu^{2+}, Cd^{2+}, Zn^{2+} and Pb^{2+}.

In some cases, the functionalized nanofiber membrane was even able to directly convert metal ions collected into elemental metal (electroless recovery). When a nanofiber membrane was surface coated with a thin layer of conducting polymer,

Table 6.18 Mean concentration of heavy metals in electroplating wastewater (before and after adsorption process) [356]

Physico-chemical parameters	Raw value	Batch adsorption by P-CNTs	Batch adsorption by PHB-CNTs	WHO/EPA[a] permissible limits
pH	0.83	5.63	5.65	5.5–8.5
Iron (mg L^{-1})	127.5	18.01	23.115	0.3/0.2
Nickel (mg L^{-1})	106.1	8.2325	10.1105	0.07/0.02
Cadmium (mg L^{-1})	3.02	0.04	0.02	0.005
Lead (mg L^{-1})	4.94	0.0160	0.0395	0.01/0.05
Copper (mg L^{-1})	97.57	5.8575	6.4735	2/0.05
Zinc (mg L^{-1})	167.6	10.09	8.215	5
Chromium (mg L^{-1})	72.34	0.1360	0.9005	0.05
Arsenic (mg L^{-1})	58.03	0	0	0.01/0.05

[a]*WHO* World Health Organization, *EPO* Environmental Protection Agency

polypyrrole, the nanofiber membrane was able to collect gold ions from aqueous solution and simultaneously convert the gold ions into elemental gold particles [358]. Badruddoza et al. [359] synthesized carboxymethyl-β-cyclodextrin (CM-β-CD) polymer incorporated with Fe_3O_4 nanoparticles (CDpoly-MNPs) for selective removal of Pb^{2+}, Cd^{2+}, Ni^{2+} ions from water. It was reported that CDpoly-MNPs preferentially adsorb Pb^{2+} ions with an affinity in an order of $Pb^{2+} >> Cd^{2+} > Ni^{2+}$.

Huang et al. [360] reported that the palladium (Pd) nanoparticle-immobilized electrospun polyethyleneimine (PEI)/polyvinyl alcohol (PVA) nanofibers reduced hexavalent chromium (Cr(VI)) to trivalent chromium (Cr(III)). Ma et al. [361] demonstrated that functional nanofibrous membranes fabricated by the electrospinning technology can be used to remove heavy metal ions through adsorption from contaminated water. These membranes exhibit higher permeation flux and lower pressure drop than conventional microfiltration membranes. However, these membranes also possess a high surface-to-volume ratio and functionalizable surface that can remove toxic metal ions with a capability comparable to typical absorbents. Yang et al. [362] prepared thiol modified natural polysaccharide chitin nanofibers and used as an absorbent material for arsenic (As(III)) removal. The arsenic adsorption performance of thiol-modified chitin nanofibers was evaluated under different pH conditions and at different metal ion concentrations, where the maximum adsorption capacity was found to be 149 mg/g at pH 7.0 using the Langmuir model.

Wang et al. [363] fabricated silver NPs decorated electrospun CA nanofibrous membranes. From the test results, it was revealed that $_{Ag}$ decorated highly porous CA ENFs membrane had effective antibacterial property including dye adsorption. These membranes could be very promising in water treatment. Wang et al. developed a microfiltration membrane, based on a two-layered nanoscale polyacrylonitrile (PAN)/microscale polyethylene terephthalate (PET) fibrous scaffold containing infused ultra-fine functional cellulose nanofibers (diameter about 5 nm). It was demonstrated by Wang et al. that these membranes can simultaneously remove bacteria, viruses and/or toxic heavy metal ions. Muthulakshmi and Anuradha [364] surveyed on the adsorption capacity of chitosan derivatives prepared by five different methods (thiocarbonyl, PVA blend, xanthate, Nano based and grafting) and concluded that chitosan grafted with γ-cyclodextrin possesses better chelating ability in isolating Cd^{2+} ions from waste water. He et al. [365] designed a Zr-based nanoparticle embedded PSF hollow fiber membrane for removal of arsenate ion (AsO_4^{3-}) from water. It was observed that the mg g^{-1} maximum adsorption capacity of arsenate on the membrane was as high as 131.78 mg g^{-1} under experimental conditions.

Khulbe et al. [366] discussed the recent progresses in the development of MA (membrane adsorption) membranes. In addition, recent progresses in the development of advanced adsorbents such as nanoparticles are summarized, since they are potentially useful as fillers in the host membrane to enhance its performance. Table 6.19 presents few recent examples of the removal of heavy metal pollutants from water/wastewater via nanotechnology.

The nano-adsorbents are novel materials which contain different functional groups on the external surface, and act as enhancer to the adsorption process. Cai

Table 6.19 Few examples of the removal of heavy metals pollutant from water/wastewater via adsorption/nanotechnology

Membrane	Removal of	From	References
CM-β-CD/Fe_3O_4	Pb^{2+}	Industrial wastewater	[359]
PES/Fe–Mn binary oxide UF MMMs	As^{3+}	Contaminated water solution	[342]
MWCNTs modified with hydroxyl, amine and carboxyl groups	Hg^{2+} and MeHg	Water solution	[355]
SWCNTs/Cu HCF nanoparticles	Cs^{+}	Water	[353]
SWCNT-COOH	Pb^{2+}, Cd^{2+}, Cu^{2+}	Aqueous solution	[351]
PHB-CNTs[a]	Heavy metals (As, Pb^{+2}, Cr^{6+}, Cd^{+2}, Ni^{2+}, Cu^{2+}, Fe^{3+}, and Zn^{2+})	Heavy metals (As, Pb, Cr, Cd, Ni, Cu, Fe, and Zn)	[356]
Silica- and cellulose-based MF	Pb^{2+}, $Cu^{2+,}$ and Cd^{+2}	Drinking and industrial water	[367]
Functionalized single-walled CNTs	Cd^{2+}, Cu^{2+}, Pb^{2+}, and Hg^{2+}	Aqueous solution	[351]
PAN/PET MF	Cr^{6+}, Pb^{2+}, *Escherichia coli* (by size extrusion)	Aqueous solution	[368]
Chitosan/γ- cyclodextrin	Cd^{2+}, Pb^{2+}, Ni^{2+}	Wastewater	[364]
CH/nylon-based chitosan	Cu^{2+}	Water	[369]
CAP-active alumina MMMs	F ion	Water	[370]
Thiol functionalizaed cellulose nanofiber	Cu^{2+}, Cd^{+}, Pb^{2+}	Water	[371]
Cellulose-*g*-oxolane-2,5-dione nanofibers	Cu^{2+}, Cd^{2+}, Pb^{2+},Fe^{3+}, Zn^{2+}	Gasoline	[372]
CA-PVP	Fe^{3+}, Cu^{+2}	Liquid phase	[373]
PVA/SA	Cr^{3+}	Aqueous solution	[374]
Hybrid membrane			
Cellulose/thiol dendrimer	Cd^{2+}, Hg^{2+}, Pb^{2+}	Heavy metal solutions	[375]
Polystyrene and polyHIPE/iron hydroxides	As	Water	[376]
Poly(vinyl alcohol)/poly(ethyleneimine)	Pb^{2+}, Cd^{2+}, Cu^{2+}	Aqueous solutions	[377]
PAZ/UF membrane (Ca-activated zeolites)	Phosphate recovery	Aqueous solutions	[378]
$ZnA1_2O_4$–TiO_2-clay	Cd^{2+}, Cr^{3+}, Pb^{2+} methylene blue and orange acid	Water	[379]
AC/PSF-PEI-Ag	Cd^{2+}, Cr^{+3}, Ag^{+1}, Pb^{2+}	Synthetic wastewater	[380]
Zr-PSF	As	Contaminated water	[365]
Cellulose/alginic acid ion-exchange membrane	Cd^{2+}, Sr^{2+}	Aqueous solutions	[381]

(continued)

Table 6.19 (continued)

Membrane	Removal of	From	References
Electrospun CeO_2 nanofiber functionalized with mercapto groups	Pb^{2+}, Cu^{2+}	Aqueous solution	[382]

[a] Polyhydroxylbutyrate functionalized carbon nanotubes

Table 6.20 Few examples of the removal of heavy metals pollutant from water/wastewater by nanomaterials

Nanomaterial	Adsorption result	Reference
Pt NPS-Zeolite-4A	Co^{2+}, Ba^{2+}, La^{3+} and Ni^{2+} from aqueous solutions	[384]
Nano Al_2O_3	Excellent adsorption capacity for heavy metal ions, such as Zn^{2+}, Ni^{2+}, Cr^{6+}, Cd^{2+} and Pb^{2+}	[386]
Single-walled CNTs	Single-walled CNTs (SWCNTs) show higher affinity for Cr^{6+} than multiwalled CNTs (MWCNTs)	[387]
Oxidized CNTs	Au^{3+} from aqueous solutions. The maximum adsorption capacity obtained by O-MWCNTs for Au^{3+} was 62.3 mg g^{-1}	[388]
Molecules modified on the CNTs' surface	Removal of lead from water by amino modified multi-walled carbon nanotubes	[389]
Amino groups on the surface of the CNTs	Removal of Cu^{2+} from aqueous solution	[390]
Amine functionalized carbon nanotubes	Removal of Cu^{2+} from aqueous solution	[391]
Modified MWCNTs	Removal of zinc in biological and water samples. The detection limit for Zn^{2+} was 0.07 pg mL^{-1}	[392]
Silver nanoparticles/multiwalled carbon nanotubes	Removal of Cu^{+2} and Cd^{2+} from water	[393]
MnO_2/CNTs	Hg ions removal from aqueous solution	[394]
Magnetic multi-walled carbon nanotube	Simultaneous adsorption of atrazine and Cu^{2+} from wastewater by magnetic multi-walled. Maximum adsorption for Cu^{2+} was 38.91 mg g^{-1}	[395]
Graphene oxides with different oxidation degrees	Reemove Co^{2+} ions and other heavy metal ions from wastewater	[396]
Graphene oxide nanosheets	Super adsorbents to remove Co^{2+} and Cd^{2+}	[397]
Graphene oxide nanosheets (GONS)	Maximum adsorption capacity of Eu^{3+} (Europium) on GONS was175.44 mg·g^{-1}	[398]
β-cyclodextrin/ graphene oxide	Removal of cobalt from aqueous solution. The maximum sorption capacity of Co^{2+} on β-CD–GO (72.4 mg g^{-1})	[399]
Herbs (EH, TH)	Cu, Ni, Co from aqueous solution	[385]

et al. [383] reported that highly active MgO nanoparticles synthesized via sol–gel and calcination processes can be used for the simultaneous bacterial disinfection and heavy metal ions removal from aqueous solution. Mehdizadeh et al. [384] reported that the removal of heavy metals from aqueous solution in a batch adsorption mode can be done by using platinum nanoparticles/Zeolite-4A as adsorbent. The platinum nanoparticles/Zeolite-4A exhibited effectiveness in the removal of Co (II), Ba (II), La (III) and Ni (II) ions from aqueous solutions. Plants are one type of alternative material that can be used to adsorb heavy metals from water systems and soil. Al-Senani and Al-Fawzan [385] used nanoparticles of wild herbs (Equisetum, *EH* and Teucrium, *TH*) as adsorbent for the removal of heavy metal (Cu, Ni, Co) from their aqueous solution.

Table 6.20 shows few examples of the removal of heavy metals pollutant from water/wastewater by nanomaterials.

6.9 Ion Exchange Membranes

An ion-exchange membrane is a semi-permeable membrane that transports certain dissolved ions, while blocking other ions or neutral molecules. Ion-exchange membranes are therefore electrically conductive. They are often used in desalination and chemical recovery applications, moving ions from one solution to another with little passage of water. Ion exchange is widely used in the food and beverage industry, hydrometallurgy, metals finishing, chemical, petrochemical, pharmaceutical technology, sugar and sweetener production, ground- and potable-water treatment, softening, industrial water treatment, nuclear, semiconductor, power, and many other industries. Electromembrane desalination processes, such as electrodialysis and membrane capacitive deionization, belong to a category of desalination technologies, which involve the removal of ions from ionic solutions with the use of electrically charged membranes termed ion exchange membranes. Alabi et al. [400] discussed the advances in nanomaterials incorporated ion exchange membranes applicable to desalination. The nanomaterials employed in ion exchange membranes fabrication include carbon nanotubes, graphene-based nanomaterials, silica, titanium (IV) oxide, aluminum oxide, zeolite, iron (II, III) oxide, zinc oxide, and silver.

Hosseini et al. [401] prepared PVC/PANI (polyaniline)–MWCNT nanoparticle anion exchange membranes. It was observed that the membrane potential, transport number and selectivity were improved in NaCl and Na_2SO_4 ionic solutions by the increase of PANI/MWCNT nanoparticles. Modified membranes showed superior performance. In another article, Hosseini et al. [402] incorporated iron–nickel oxide (Fe_2NiO_4) nanoparticles in polyvinylchloride/styrene–butadiene-rubber (SBR) blend heterogeneous cation exchange membranes. Membrane permeability, flux and conductivity were enhanced initially in monovalent ionic solution by increase in additive concentration to 0.5 wt.% and then began to decrease by more additive loading. Permeability was improved for bivalent ions with increase in additive concentration. Modified membranes showed higher permeability for bivalent ions compared to monovalent type.

Kowsari et al. [403] prepared a series of sulfonated polyimide (SPI) composite proton exchange membranes with different contents of an ionic liquid-functionalized graphene oxide (FGO) in order to study the effects of FGO fillers on the membranes properties. The proton conductivity values were improved in SPI/FGO composite membranes. The pure SPI showed its maximum proton conductivities of 0.0282 and 0.0864 S cm^{-1} at ambient and 80% RH, respectively, while SPI/FGO 5% showed the maximum proton conductivity values of 0.0772 S cm^{-1} (at 160 °C and ambient humidity) and 0.1243 S cm^{-1} (at 120 °C and 80% RH) among all of the samples. Gahlot et al. [404] studied the GO/SPES (sulfonated polyethersulfone) nanocomposite ion-exchange membranes (IEMs) for desalination. 10% GO nanocomposite membrane showed 3.51 mol m^{-2} h^{-1} ionic flux, 4.3 kW h kg^{-1} power consumption and 97.4% current efficiency for salt removal.

Zendehnam et al. [405] studied the effects of Ag-nanolayer film thickness on membrane physicochemical and antibacterial characteristics of nanocomposite PVC-blend-SBR/Iron-oxide nanoparticles. It was reported that the electrical conductivity of prepared membranes was enhanced sharply by the increase in nanolayer thickness. Ionic permeability and flux increased initially by silver nanolayer coatng up to 5 nm in prepared membranes. The ionic permeability and flux decreased again with more increase in deposited nano layer thickness from 5 to 10 nm. Ionic flux also showed increasing trend. Membranes showed good ability in E-Coli removal. 20 nm Ag-nanolayer coated membrane showed better performance compared to others.

6.10 Liquid Membranes

Liquid membrane technology makes it possible to attain high selectivity as well as efficient use of energy and material relative to many other separation systems. Liquid membrane technology has found applications in the fields of chemical and pharmaceutical technology, biotechnology, food processing and environmental engineering. On the other hand, its use in other fields, such as hydrogen separation, the recovery of aroma compounds from fruits, the application of ionic liquids in the membrane formulation, etc., is increasing rapidly [406] Membranes are barriers that separate two fluid phases and allow the selective permeation of solutes from one side of the barrier to the other. Solids are not the only materials that have been used as membranes and it is possible to use a liquid as a membrane. Liquid membranes are present in various forms in daily life; an oil layer on a water surface is a typical organic liquid membrane of an immiscible liquid phase. Beer froth, foam on soap, detergent or surfactant solutions, oil films coated on a metal surface—popularly used in rust protection and lubrication are familiar liquid films separating two phases.

The potential for industrial applications of supported liquid membrane (SLM) was first reported by Ward and Robb in 1967. They showed that an aqueous bicarbonate–carbonate solution membrane supported in porous cellulose acetate film was more permeable for CO_2 than O_2 [407]. The SLM technology resolved the problems of ELM stability. The immobilization of the organic liquid containing an active complexing agent (carrier) in suitable diluent within a porous structure or solid membrane (polymeric or inorganic membranes) promises physical stability for practical use. In this technology the membrane is clamped between two compartments which are filled with an aqueous source and receiving phase (Fig. 6.16).

Sharma and Kulshrestha [408] synthesised polymer electrolyte membranes i.e. silica 6 sulfonated GO-sulfonated chitosan based PVA. Membranes with various MGO concentrations (1%, 2% and 5%) with sulfonated chitosan were prepared by adding MGO to the casting solution i.e. homogeneous mixture of poly(vinyl alcohol) and sulfonated chitosan in deionized water. Solution was casted and dried on a glass plate at 80 °C. Then, the resultant dried film was further subjected to cross-linking with formaldehyde to convert it into a water insoluble material. From the performances of the membranes, it was reported that the hybrid membranes had electrochemical properties with higher stability and may be good candidates for PEMs. The MGO–SCH-5 (containing 5% MGO) membrane showed the stability at temperatures as high as 300 °C with better electrochemical performance. The proton conductivity of the MGO–SCH-5 membrane was calculated to be 6.77×10^{-2} S cm^{-1}, which increases to 11.2×10^{-2} S cm^{-1} at 90 °C. The maximum ionic conductivity has been found in the MGO–SCH-5 hybrid membrane with higher methanol crossover resistance and selectivity.

Klaysom et al. [409] introduced a new class of organic–inorganic nanocomposite ion-exchange membranes containing a sulfonated functionalized polymer (sulfonated polyethersulfone) and sulfonated mesoporous silica (SS). The effect of SS filler size (20 and 100 nm) on membrane structures and properties has been investigated. The results revealed the significant impact of filler sizes on macroscopic properties, such as morphologies, physico-electrochemical performance, and mechanical and thermal stabilities of the resultant composite membrane. The performance of the composite membranes in the desalination of a NaCl solution was evaluated by a lab-scale electrodialysis cell in comparison with a commercial membrane, FKE. The results revealed that the optimized composite with 0.5 wt.% inorganic SS additive with a smaller particle size (20 nm diameter) exhibited an overall desalination performance comparable to that of the pristine polymer membrane.

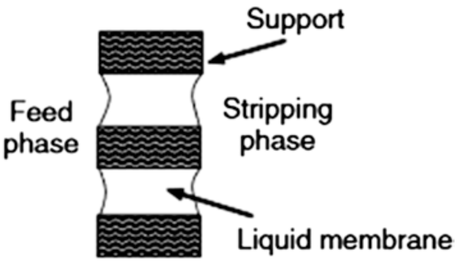

Fig. 6.16 Supported liquid membrane (SLM)

6.11 Medical and Pharmaceutical

In the past few years, the application of nanotechnology in medical and pharmaceutical field is growing very fast. To write all the advancement of nanotechnology in these fields is beyond the present book.

Nanotechnology holds enormous potential for healthcare, from delivering drugs more effectively, diagnosing diseases more rapidly and sensitively, and delivering vaccines via aerosols and patches. It plays an important role in advanced biology and medical research particularly in the development of potential site specific delivery systems with lower drug toxicities and greater efficiencies. The era of nanotechnology has allowed novel research strategies to flourish in the field of drug delivery. Nanotechnology designed drug delivery systems have been seen to be suitable for treating chronic intracellular infections [410]. Recent years have seen an explosion in the number of studies showing the variety of medical applications of nanotechnology and nanomaterials. Nanotechnology in medicine involves applications of nanoparticles currently under development, as well as longer range research that involves the use of manufactured nano-robots to make repairs at the cellular level (sometimes referred to as *nanomedicine*). To date, much progress has been made through the use of nanomedicine in wound healing due to the ability of such materials to mimic the natural dimensions of tissue. Their unique size-dependent properties make these materials superior and indispensable in many areas of human activity. This is being achieved by developing nanoscale particles or molecules to improve the pharmacokinetic and pharmacodynamic properties of a drug. The introduction of nanotechnology in medicine is the pharmaceutical approach to formulating drugs as nanoparticles for diagnostic and curing diseases in a targeted drug delivery system.

Patel et al. [411] discussed the rise of nanoparticle DDS platforms for cancer and explored concepts of gene/drug delivery and cytotoxicity in pre-clinical and clinical contexts. Table 6.21 shows examples of different nanomaterial platforms available for use in drug delivery systems (DDS).

Nanoporous materials are crucial to many biomedical applications such as immunoisolation devices, dialysis, smart as well as targeted drug delivery systems, bioanalytical devices and biosensors. Nanoporous membranes are also suitable for a wide variety of biomolecular analysis applications. In implantable devices the membrane would function as a semipermeable compartment that holds the implant or drug while allowing passage of desired molecules in a controlled way. Adiga et al. [412] discussed an overview of nanoporous membranes for biomedical applications. While the applications are classified based on the functionality of the membrane, there is clearly some overlap between them. These applications are summarized with a schematic diagram in Fig. 6.17.

A synthetic membrane around an artificial pancreas would allow the passage of glucose, oxygen and other small molecules, but exclude the passage of proteins and other large molecules. Perhaps the likelihood of success in designing biocompatible membranes with desired functionality will increase if an effort is made to mimic the

Table 6.21 Examples of different nanomaterial platforms available for use in drug delivery systems (DDS) [411]

Platform	Characteristics
Liposomes	Drug encapsulation, hydrophilic interior, individual lipids can be changed to accommodate particular functionality (surface charge, *etc*)
Dendrimers	Large number of peripheral functional groups allows for the multiple drug, label, ligand functionalization
Polymers	Most widely used drug delivery vehicles, some are self- assembling, can be coated with solubilizing agents, non-immunogenic and highly versatile
Metallic particles	Generally used as diagnostic agents, drug delivery, thermal-ablation via laser excitation, multifunctional
Carbon nanotubes	High functionality, limited solubility, functionalized CNT acts as an inert bioconjugate *in vivo*, drug delivery "missiles"
Lipoproteins	Biocompatible protein-lipid based molecules which can carry hydrophobic drugs to tumor targets with minimal toxicity

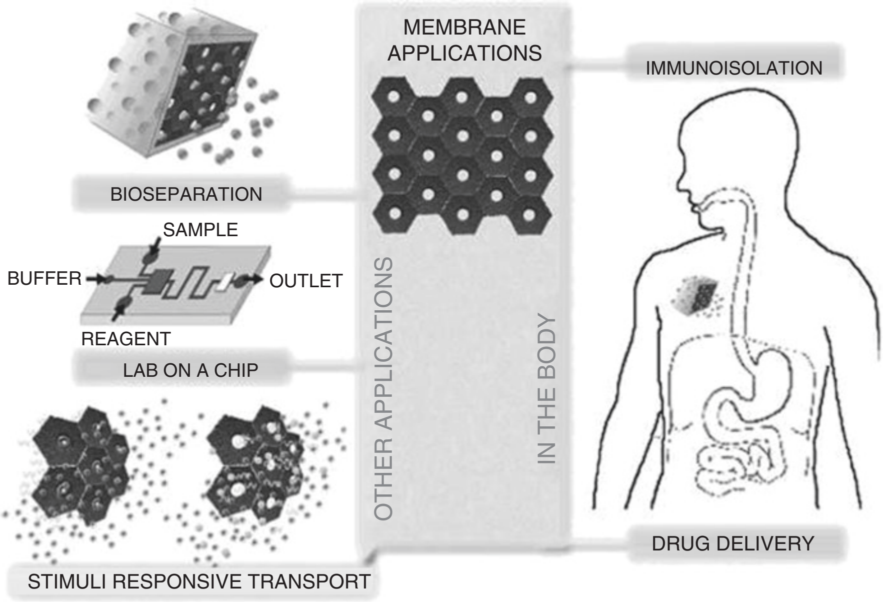

Fig. 6.17 Biological applications of nanoporous materials [412]

function of biological membranes as closely as possible. As we move into the era of nanomedicine, the development of such smart nanoporous membranes becomes critical for a variety of implantable medical devices, including controlled as well as signal-responsive drug delivery, immunoisolation devices, and microdialysis systems. Despite the extensive research carried out in fabrication, characterization, and modeling of nanoporous materials, there are still several challenges that must be overcome in order to create synthetic nanoporous systems that behave similarly to their biological counterparts [413]. Irfan et al. [414] studied the performance of polyethersulfone (PES) hemodialysis (HD) membrane using carboxylic functionalized multiwall carbon nanotubes (c-MWCNT) and lower molecular weight grade of polyvinylpyrrolidone (PVP-k30). The results showed that PVP-k30/NCs (nanocomposites) improved the surface properties of the membrane and the urea and creatinine removal increased to 72% and 75% from the pure PES membranes. Nuxoll et al. [415] developed a block polymer film with a thin (100 micron) silicon substrate and evaluated its mechanical integrity, and demonstrated its transport properties for model solutes of large and small molecular weight. It was suggested that this composite membrane is an attractive candidate for interfacing implantable sensing and drug-delivery devices with biological hosts.

Nanoporous anodic aluminium oxide (AAO) has become increasingly important in biomedical applications over the past years due to its biocompatibility, increased surface area, and the possibility to tailor this nanomaterial with a wide range of surface modifications. AAO membrane is beneficial for various applications such as in biotechnology and medicine ranging from biofiltration membranes, lipid bilayer support structures, biosensing devices, and implant coatings to drug delivery systems with AAO capsules and scaffolds for tissue engineering [413]. Further, nanoporous alumina is in use as implant modifications, co-culture substrates or immunoisolation devices [416, 417].

Due to very large surface area to volume ratio, distribution of nano to microsized porosity, lightweight, and flexibility in surface functionalities are some of the characteristics that make the nanofibers appropriate candidates for wide range applications in medical and pharmceuticl field such as scaffolds in tissue engineering, wound dressing, drug delivery etc.

One of the key priorities of nanomedicine research is using nanotechnology in delivery of drugs. This is being achieved by developing nanoscale particles or molecules to improve the pharmacokinetic and pharmacodynamic properties of a drug. The drugs are encapsulated in biodegradable polymers (which acts as membrane) such as liposomes and microspheres, which ensure sustained delivery of the medicine. Nanofiber technology has recently shown compelling advancement in drug loading and releases. Polymeric nanofibers are useful for a variety of biomedical applications, such as filtration devices, medical prostheses, scaffolds for tissue engineering, wound dressing, controlled drug delivery systems, cosmetic skin masks, protective clothing etc. These could be fabricated from a variety of polymers including nondegradable polymers such as PAN, nylon, PU, PEO, polycarbonate, and biodegradable polymers such as PCL (poly(ε-caprolactone)), PU, polyhydroxyacids, polyanhydrides as well as from blends and copolymers [418]. Surgical meshes fabricated from lead nanofibers are used to repair the protective membrane that covers the brain and spinal cord. According to MacEwan and Xie of Washington University the lead nanofiber mesh is thinner, more flexible and more likely to integrate with the body's own tissues. Every thread of the nanofiber mesh is thousands of times smaller than the diameter of a single cell. The idea is to use the nanofiber material not only to make operations easier for surgeons to carry out, but also to rduce post-op complications for patients [419, 420]. Electrospun polymeric nanofibers possess various advantages as skin substitutes because they can prevent fluid and proteins loss from the wound area, help in the removal of exudates, inhibit microbial infection, exhibit excellent anti–adhesion properties and guide endogenous cells to proliferate and remodel [421]. Membrane-coated nanomedicines (MCNs) are highly biocompatible, and can realize prolonged circulation and/or tumor-targeting depending on the nature of their shell-membrane [422]. Chen et al. [423] discussed the potentiality of electrospun nanofibers in many biomedical applications including biosensing, regenerative medicine, tissue engineering, drug delivery and wound healing. Hassiba et al. [424] discussed the recent studies on the physiology of wound healing and various wound dressing materials made of nanofibers fabricated using the electrospinning technique. Argonide company fabricates nanoporous ceramic materials for endotoxin filtration and DNA and protein separation [425]. Surgical meshes fabricated from lead nanofibers are used to repair the protective membrane that covers the brain and spinal cord. Also used in bio- and nanosensors for bacteria, viruses, and other pathogens and hormones, biomarkers and cancer detection, and health scanning and monitoring [426, 427]. Aligned micro-fibers are of specific attention to nerve-tissue engineering based on the size and diameters of axons and myelinated nerve fibers [428]. Katti et al. [429] demonstrated that PLAGA (poly(lactide-*co*-glycolide)) nanofibers can be tailored to desired diameters through modifications in processing parameters, and that antibiotics such as cefazolin can be incorporated into these nanofibers. Therefore, PLAGA nanofibers show potential as antibiotic delivery systems for the treatment of wounds. Chitosan is known as a biodegradable and non-toxic natural polymer that enhances wound healing and bone formation. Yunshin et al. [430] evaluated the biocompatibility of chitosan nanofiber membranes and examined their effect on bone regeneration. Their findings suggested that chitosan nanofiber membrane may be useful as a tool for guided bone regeneration. Liu et al. [431] prepared multilayer polylactide nanofiber mats doped with oxaliplatin and reported that the recurrence of liver cancer was significantly retarded after the membrane was used for drug delivery. Ni et al. [432] prepared polypropylene carbonate nanofibers loaded with paclitaxel and TMZ (temozolomide). The authors showed that the co-delivery of paclitaxel and TMZ on site was highly efficient to inhibit *in vitro* growth of glioma cells, indicating great possibility of the nanofibers as drug delivery devices for glioma therapy. Nano fibers which have pore size between 500 and 100μm are suitable for protecting the wounds from bacteria. Duan et al. [433] fabricated antibacterial electrospinning nanofibers of poly(ε-caprolactone) (PCL) with little nanoparticles of silver-loaded zirconium phosphate (nano AgZr) for potential use in wound dressing usage. Ignatova et al. [434] discussed on nanofibers prepared by electrospinning of poly-vinyl-pyrrolidone iodine complex and poly-ethyleneoxide/poly-vinyl-pyrrolidone iodine complex as prospective route to antimicrobial wound dressing materials. Different kinds of artificial and natural polymers have been successfully electro-spun into small and fine fibers. Many kinds of drugs such as antibiotics, anticancer, ribonucleic acid (RNA) and deoxyribonucleic acid (DNA) have been used by electrospun fibers [435, 436]. Li et al. [437] explored the possible usage of electro-spun protein fibers as scaffolds for tissue engineering. The authors developed human tropoelastin for electrospinning. It was reported that tropoelastin nanofibers seeded with human embryonic palatal mesenchymal cells supported cell adhesion and proliferation and showed satisfactory results when compared with nanofibers of collagen or elastin. In another study, Woerdeman et al. [438] have explored the possibility of using wheat gluten, a plant protein, as a new material for electro-spinning nanofibers that can be used for tissue engineering applications.

Boland et al. [439] developed electrospun micro and nanofibrous scaffolds from natural polymers such as collagen and elastin for vascular tissue engineering. Their results demonstrated that electrospun collagen and elastin nanofibers were able to mimic the complex architecture required of vascular constructs and were able to provide good mechanical properties that are desired in the environment of the blood stream. Electrospun mesh/materials have been used as scaffolds for tissue engineering for a number of years, but there is surprisingly few reports in the literature on the interactions of fibers with bacteria and co-cultures of cells and bacteria [440].

Xue et al. [441] demonstrated the unique capabilities of electrospun nanofibers as porous supports for heterogeneous catalysis and as functional scaffolds for tissue regeneration by giving some examples. Electrospun nanofibers have been developed with huge porosity, excellent humidity absorption, a better oxygen exchange rate, and some antibacterial activities. Nanofibers loaded with chemical, biochemical active pharmaceutical ingredient (API) or even stem cells can be wonderful dosage forms for the treatment of DFU (diabetic foot ulcer) [442].

Nanofibers used in various type of tissue engineering [426].

1. musculoskeletal tissue engineering.
2. cartilage tissue engineering.
3. bone tissue engineering.
4. ligament tissue engineering.
5. skeletal muscle tissue engineering.
6. skin tissue engineering
7. blood vessel tissue engineering

Table 6.22 shows application of some nanofibers in medical/pharmaceutical field [418].

Table 6.23 summarizes few different electrospun polymers developed for wound dressing and the corresponding therapeutic agent loaded on the mat /membrane.

Table 6.24 summarizes the few different electrospun polymers developed for cancer treatment.

Table 6.22 Application of some nanofibers in medical/pharmaceutical field [418]

Nanofibers	Application
Poly (L-lactide-co-(PLLA) nanofibers	3D scaffold for blood vessel tissue engineering [443–446]
Collagen	For culturing smooth muscle cell [443]
Polyester/urethane	Skeletal muscle tissue engineering [444]
Polyurethane	Wound dressing material to effectively exude fluid from the wound [445]
PVP-iodine	Antibacterial, antimycotic and antiviral applications [434, 436]
Gelatin/PVA	Controlled release of drug [446]
PCL/gelatin	Scaffold for wound healing and layered dermal reconstitution [447]

Table 6.23 Few different electrospun polymers developed for wound dressing and the corresponding therapeutic agent loaded on the mat membrane [419]

Electrospun polymers fibers	Therapeutic agent
Silk fibroin/vitamin C 2-phosphate	Vitamin C 2-phosphate
Polycaprolactone/polyethylene glycol	Basic fibroblast growth factor/ epidermal growth factor
Poly(vinyl alcohol)/poly(vinyl acetate)	Ciprofloxacin
Silk fibroin/poly(lactide-co-glycolic acid)	Silk fibroin
Silk fibroin/polyethylenimine	Silk fibroin
Gelatin/poly(vinyl alcohol)	Raspberry ketone
Poly(vinyl alcohol)/poly(vinyl pyrrolidone)/chitosan	Chitosan
Poly(vinyl alcohol)/poly(vinyl pyrrolidone)-iodine	Poly(vinyl pyrrolidone)-iodine
Poly(ε-caprolactone)–poly(ethyleneglycol)–poly(ε-caprolactone)	Curcumin
Chitosan/poly(ethylene oxide)	Ciprofloxacin moxifloxacin
Poly(ε-caprolactone urethane urea)	Tigecycline

Table 6.24 Few different electrospun polymers developed for cancer treatment

Nanofiber	Cancer cells	Reference
PCL	Colorectal human (HT-29) cell line	[448]
PLLA poly(L-lactic acid) (PLLA)	HeLa cells	[449]
PLA	Lung cancer cell line spca-1	[450]
Poly(3-hydroxybutyrate-co-3-hydroxyvalerate)	MKN28 gastric cancer cell	[451]
Chitosan/PEO	Prostate cancercell lineDU14	[452]
Chitosan/coPLA (poly(L-lactide-co-D,L-lactide)	MCF-7 breast cancer cells	[453]
PLGA-gelatin (ferulic acid predominantly resides in the core of PLGA/PEO)	HepG2	[454]
PLGA-gelatin	HepG2 cell lines	[455].

Membrane-coated nanomedicines (CNs) are highly biocompatible, and can realize prolonged circulation and/or tumor-targeting depending on the nature of their cell-membrane [422]. Milane et al. [456] discussed the drugs carried by polymer-coated nanoparticles to treat multidrug-resistant breast and ovarian cancer with the chemotherapies paclitaxel, which inhibits cell division, and lonidamine, which suppresses energy metabolism in cancer cells. The nanoparticles are designed to target an epidermal growth factor receptor, which is overexpressed in tumour cells. Huang et al. [457] investigated a biodegradable multi-layer PCL (polycaprolactone) membrane device loaded with TMZ (temozolomide) and NGF (neuron growth factor) for its medical use. The investigation results suggested that these membranes could have high potential to be used as surgical residual cavity tampon to improve the local bioavailability of TMZ and NGF, exerting strengthened on site effects on prevention of glioma recurrence and metastasi. Molday and MacKenzie [458] fabricated ferromagnetic iron dextran particles, prepared by reacting a mixture of ferrous chloride and ferric chloride with dextran polymers under alkaline conditions. Cells labeled with these immune specific ferromagnetic particles were quantitatively retained by a simple permanent magnet and could be separated from unlabeled

Table 6.25 Therapeutic agents incorporated into nanofibers to improve wound healing

Therapeutic agents	Nanofibers	Purpose
Lysozyme	Chitosan/PVA	Antibacterial
Silver	Gelatin/polyurethane; gelatin; polyurethane; poly(ethylene-co-vinyl alcohol)	Antibacterial
ZnO	PCL; alginate/PVA	Antibacterial
Cefoxitin sodium	PLGA	Antibacterial
Gentamicin	Chitosan	Antibacterial
Ciprofloxacin HCl	Polyurethane/dextran; PVA/poly(vinyl acetate)	Antibacterial
Polyhexamethylene biguanide	Cellulose acetate/polyester urethane	Antibacterial
Lidocaine, mupirocin	PLLA	Pain management and antibacterial
Fibrinogen	PLLA	Hemostasis
Curcumin	PCL	Antioxidant
VEGF	Chitosan/PEO; HA/collagen	Angiogenesis
PDGF-BB	Polyurethane; HA/collagen	Angiogenesis, granulation tissue formation
EGF	PCL–PEG/PCL; poly(l-lactic acid)-co-poly-(ε-caprolactone); HA/collagen; PCL/PEG	Keratinocytes migration and maturation, angiogenesis
Basic-FGF Cell	PELA; HA/collagen	Cell adhesion, proliferation, ECM secretion, re-epithelialization and skin appendages regeneration, angiogenesis

cells. Applications of these novel reagents in the separation of cells, cell membranes and receptors in drug targeting are suggested.

Table 6.25 shows the therapeutic agents incorporated into nanofibers to improve wound healing [459].

Cell membrane-coated nanoparticles inherently mimic the properties of the source cells from which their membrane is derived, bestowing a wide range of functions such as long circulation and disease-relevant targeting [460]. Figure 6.18 shows the cell membrane-coated nanoparticles.

A variety of cell types have been used as sources of membranes to coat over nanoparticles as summarized in Table 6.26. Each cell membrane type can utilize unique properties to provide functionalities to nanoparticulate cores, the material of which can be varied depending on the desired application. Cell membranes are composed of a mixture of lipids, proteins, and carbohydrates. Many types of membranes have been used to construct biomimetic core-shell nanoparticles for cancer therapy [422].

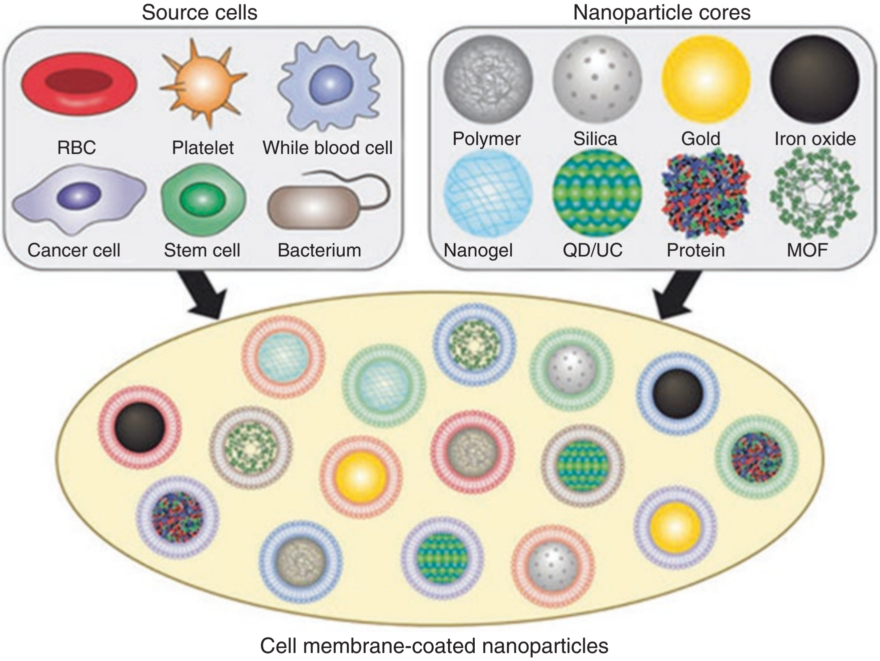

Fig. 6.18 Cell membrane-coated nanoparticles. A variety of cell types have been used as sources of membranes to coat over nanoparticles. Each cell membrane type can utilize unique properties to provide functionalities to nanoparticulate cores, the material of which can be varied depending on the desired application [460]

Table 6.26 Currently explored source cells for membrane coated nanoparticles [422]

Source cells	Key features
RBCs	Suppressing immune attack by the abundant "self-markers" on their surface Prolonged blood circulation time (about 120 days) Biocompatible and biodegradable
Platelets	Selective adherence to the vasculatures of the disease sites Specific aggregation surrounding circulating tumor cells through P-selection and CD44 receptors Good immune-compatibility
Bacteria	Immunogenicity Tumor tropism Secret outer membrane vesicles
Immune cells	Homing to the diseased sites Ability to penetrate the vasculature Targeting metastatic cancer cells through VCAM-1-α4 integrins interaction Ability of avoiding the immune clearance
Cancer cells	Achieve vaccine applications by promoting a tumor-specific immune response Allow a unique tumor sites targeting by an inherent homotypic binding
Stem cells	Natural active target effect to solid tumors at diverse developmental stages

6.12 Fuel Cells

Fuel cells contain membranes that allow hydrogen ions to pass through the cell but do not allow other atoms or ions, such as oxygen, to pass through. Companies are using nanotechnology to create more efficient membranes; this will allow them to build lighter weight and longer lasting fuel cells. Fuel cell is a device which converts a fuel directly into electricity in an electrochemical reaction. This is in contrast to most methods of generating electricity, which use the heat from burning fuel to generate electricity mechanically. There are many limitations preventing fuel cells from reaching widespread commercial use, however. Expensive materials such as platinum are needed for the electrode catalysts. Fuels other than hydrogen can cause fouling of the electrodes, and hydrogen is costly to produce and difficult to store. The most efficient types of fuel cell operate at very high temperatures, which reduces their lifespan due to corrosion of the fuel cell components. Nanotechnology may be able to ease many of these problems. Recent nanotechnology research has produced a number of promising nanomaterials which could make fuel cells cheaper, lighter and more efficient.

In a fuel cell there are two electrodes, an anode and a cathode, with an electrolyte between them. The catalytic electrodes in fuel cells are most often made from platinum which is very costly. One potential improvement to the current technology is to support the platinum nanoparticles on a porous surface, such as an activated carbon, or nanostructures like carbon nanotubes or nanowalls. This further increases the accessibility of the platinum surfaces, decreasing the amount of the expensive metal which is needed to make an effective catalytic electrode. Modified carbon nanotubes are able to replace platinum in fuel cells. Fabrication technology for carbon nanotubes is advancing rapidly, and the cheap and abundant raw material means that catalysts based on carbon nanotubes can be produced for a fraction of the cost of platinum catalysts. Beside this, adoption of these catalysts will remove major barrier to many applications of fuel cells. By doping carbon nanotubes with nitrogen, or coating them in an electron-withdrawing polymer (polydiallyldimethylammonium chloride, or PDDA), the electronic properties of the nanotubes can be altered so as to make them effective as a catalyst. The nanotube electrodes are also more robust. Their catalytic activity is not damaged by carbon monoxide or the crossover effect when using methanol as the fuel, unlike platinum, which improves the lifetime of the cell.

The critical component of a proton exchange membrane fuel cell (PEMFC) system is the proton exchange membrane (PEM). Proton exchange membrane fuel cells (PEMFCs) are a type of fuel cell used for a variety of power generation applications. PEM is an electrolyte polymer. This specially treated material, which looks something like ordinary kitchen plastic wrap, only conducts positively charged ions. Nafion® is the most widely used electrolyte membrane for PEMFCs due to its high proton conductivity, thermal stability, mechanical strength, chemical stability and durability in the hydrated state. To obtain a desirable conductivity (10^{-1} S cm^{-1} or higher), Nafion-based PEMFCs must therefore operate at low temperatures, i.e., ≤100 °C, otherwise the membrane is quickly dehydrated and the ionic domains in the membrane structure collapse, leading to a significant reduction in conductivity [461]. Nafion is currently used for PEMFCs in industry, despite suffering from reduced proton conductivity due to dehydration at higher temperatures. The membrane blocks electrons. For a PEMFC, the membrane must be hydrated in order to function and remain stable. The challenge in the PEM development is to allow hydrogen ions to pass through PEM as much as possible while preventing other atoms or ions from passing through it. So, for this purpose membranes with better characteristics are needed. Research scientists who are involved in fuel cell are concentrated on the membrane material and on preparation methods to achieve high proton conductivity, thermal, mechanical and chemical stability, low fuel cross-over and lower cost at high temperatures.

Choi et al. [462] fabricated ionic conductive Nafion/graphene oxide (GO) composite membranes for application in direct methanol fuel cells. This composite membrane-based DMFC, compared to the Nafion 112-based DMFC, remarkably enhanced cell performance, especially in severe operating conditions.

Incorporation of nanomaterials (NMs) into IEMs has been investigated as a means of improving their properties [463, 464]. Cao et al. [465] presented a poly (ethylene oxide)/graphene oxide (PEO/GO) composite membrane aimed for the low temperature polymer electrolyte membrane fuel cells without any chemical modification. The ionic conductivity of this PEO/GO membrane increases from 0.086 to 0.134 S cm^{-1} when the operation temperature increases from 25 to 60 °C with 100% relative humidity.

The perovskite-type oxides are known as high temperature proton conductors, which are promising materials for fuel cells. $BaZrO_3$ with considerable levels of protonic conductivity has an enormous potential for use in fuel cells [466]. Hooshyari et al. [466] fabricated $BaZrO_3$/PBI (polybenzimidazole) -based nanocomposite membrane and reported that the proton conductivity of PBI improved (125 mS cm^{-1} at 180 °C). Incorporation of Fe_2TiO_5 nanoparticles in Nafion matrix improved the thermal stability of Nafion membranes which is important for HT-PEM (high temperature proton exchange membrane) fuel cells. In another publication, Hooshyari et al. [467] reported that Fe_2TiO_5 nanocomposite membranes showed a higher water uptake, proton conductivity and thermal stability compared with the pure commercial Nafion membranes. The highest proton conductivity (226 mS cm^{-1}) was observed for the membranes containing 2 wt.% of Fe_2TiO_5 nanoparticles and prepared in de-ionized water (DI) as solvent.

Sigwadi et al. [468] reported that incorporation of zirconium phosphates (ZrP) into Nafion® 117 membrane by impregnating method, reduced methanol permeation and improved proton conductivity for fuel cell application. Incorporation of ZrP in the membranes also enhanced the water uptake. The Nafion®/2.5% ZrP (209.71 mW cm^{-2}) and Nafion®/5% ZrP (206.79 mW cm^{-2}) nanocomposite membranes obtained a higher power density than those of commercial Nafion® 117 membranes (126.04 mW cm^{-2}).

TiO_2 nanoparticles are the good inorganic material candidate for using as hydrophilic filler in nanocomposite membranes. They increase the mechanical and thermal stability as well as the proton conductivity of the PEMs by increasing the transport proton pathway [469]. Salarizadeh et al. [470] studied sulfonated poly(ether ether ketone) (SPEEK)/amine functionalized titanium dioxide nanoparticle (AFT) composite membrane for proton exchange membrane fuel cells (PEMFC). The nanocomposite membrane with the optimal amount of AFT nanoparticles, 7.5 wt%, showed a proton conductivity of 0.135 S cm^{-1} at 80 °C which was 159.6% higher than that of the nanocomposite membrane with 7.5% TiO_2. Further, it showed a 40.8% decrease in swelling, a 132.7% increase in conductivity and an 86.7% increment in maximum power density (PD_{max}) (230 mW cm^{-2}) compared with the pristine SPEEK membrane, which indicated its potential application in PEMFCs.

Shabanikia et al. [471] studied the PBI (polybenzimidazole)/Fe_2TiO_5 membranes (PFT) and reported that highest acid uptake (156%) and proton conductivity (78 mS/cm at 180 °C) were observed for the PBI nanocomposite membranes containing 4 wt.% of Fe_2TiO_5 nanoparticles (PFT_4). Namazi and Ahmadi [472] prepared polymer-grafted SiO_2 and TiO_2 nanoparticles as a functional additive to prepare PPBI (poly{2,2′-(m-pyrazolidene)-5,5′-(bibenzimidazole)})/polymer-grafted SiO_2 and TiO_2 nanocomposite membranes. Imidazole and sulfonated vinyl benzene groups on the surface of modified nanoparticles formed linkages with PPBI chains, improved the compatibility between PPBI and nanoparticles, and enhanced the mechanical strength of the prepared nanocomposite membranes. The prepared nanocomposite membranes showed higher water uptake and acid doping levels compared to PPBI. It was suggested by authors that PPBI/modified SiO_2 and TiO_2 nanocomposite membranes could be utilized as proton exchange membranes for medium temperature fuel cells. Vinodh et al. [473] fabricated a composite anion exchange membrane, zirconia incorporated quaternized polysulfone (QPSU/ZrO_2) and studied its performances in alkaline membrane fuel cell (AMFC). Results showed that the maximum power density was 250 mW cm^{-2} for QPSU/10% ZrO_2 at 60 °C. The QPSU/ZrO_2 composite membrane constitutes a good candidate for alkaline membrane fuel cell applications.

Chan et al. [474] fabricated a novel PEM (polymer electrolyte membrane) fuel cell, with cathode catalyst layer structure, from randomly oriented (RNL) and orthogonally aligned (OAN) electrospun carbon nanofibers (CNF) decorated with Pt nanowires, and coated with ionomer. The PEM was successfully integrated into MEAs (Membrane Electrode Assemblies) for performance evaluation. Wei et al. [475] fabricated graphene doped PAN/PVDF (GPP) electrospun nanofiber electrode with high electrical conductivity and porosity. It was reported that the novel electrospun electrode with 2 wt.% GO (HP) possesses the high ECSA (electrochemical active surface area) up to 84.3 m^2 g^{-1} which was larger than that of the conventional electrode. Chuang et al. [476] studied polybenzimidazole (PBI)/silica nanocomposite membranes, prepared via sol–gel process from an organosoluble, fluorine-containing PBI copolymer with a silica precursor, tetraethoxysilane (TEOS), and a bonding agent. The modulus of the PBI/10 wt.% silica nanocomposite membranes showed a 37% increase compared to the pure PBI films, and the methanol permeability decreased by 58% with respect to the pure PBI membranes.

Jang and Goddard [477] introduced the concept of a dendrimer-grafted polymer using precisely defined water-soluble dendritic architecture (sulfonic poly aryl ether dendrimer) in a copolymer with a linear polymer backbone for applications such as PEMFCs (polymer electrolyte membrane fuel cells). On studying three different types of linear polymers: poly (epichlorohydrin) (PECH), poly (styrene) (PS) and poly (tetrafluoroethylene) (PTFE), combined with the second-generation sulfonic poly aryl ether dendrimer to form PECH-D2, PS-D2, and PTFE-D2, via simulations, they reported that the extent of nanophase-segregation in the membrane increases in order of PECH-D2 (~20 Å) < PS-D2 (~35 Å) < PTFE-D2 (~40 Å) at the same water content, which can be compared to 30 ~ 50 Å for Nafion and ~30 Å for Dendrion at the same water content. Based on the predicted proton and water transport rates, it was expected that the PTFE-D2 may have a performance comparable with Nafion and Dendrion. Tsuchiya et al. [478] reported that the combination of specially designed nanoscale yttria-stabilized zirconia membranes with a nanostructured dense oxide cathode can achieve a power density of 155 mW cm^{-2} at 510 °C. With a single fuel-cell chip, total power output of more than 20 mW could be achieved.

6.13 Sensor

In the broadest definition, a sensor is a device, module, machine, or subsystem whose purpose is to detect events or changes in its environment and send the information to other electronics, frequently a computer processor. A sensor's sensitivity indicates how much the sensor's output changes when the input quantity being measured changes. There are several classifications of sensors made by different authors and experts. Some are very simple and some are very complex.

Nanotechnology-enabled sensors provide new solutions in physical, chemical, and biological sensing, enabling increased detection sensitivity, specificity, multiplexing capability, and portability for a wide variety of health, safety, and environmental assessments. It can also enable sensors to detect very small amounts of chemical vapors. Various types of detecting elements, such as carbon nanotubes, zinc oxide nanowires or palladium nanoparticles can be used in nanotechnology-based sensors. These detecting elements change their electrical characteristics, such as resistance or capacitance, when they absorb a gas molecule.

The following is a list of different types of sensors that are commonly used in various applications. All these sensors are used for measuring one of the physical properties like Temperature, Resistance, Capacitance, Conduction, Heat Transfer etc.

1. Temperature Sensor
2. Proximity Sensor
3. Accelerometer
4. IR Sensor (Infrared Sensor)
5. Pressure Sensor
6. Light Sensor
7. Ultrasonic Sensor
8. Smoke, Gas and Alcohol Sensor
9. Touch Sensor
10. Color Sensor
11. Humidity Sensor
12. Tilt Sensor
13. Flow and Level Sensor

As sizes of nanotubes, nanowires, or nanoparticles are very small, a few gas molecules are sufficient to change the electrical properties of the sensing elements. This allows the detection of a very low concentration of chemical vapors.

Zhang et al. [479] presented a comprehensive survey on strategies that have been utilized to fabricate functional fibrous nanostructures for the amplification of the detection signals of nanostructure-based biosensors. Electrospinning is one of the most convenient and useful techniques to fabricate PMNF-NBB ((poymer nanofiber-nanoscale building block) polymer nanofibers based biosensors). Recent advances in the electrospinning fabrication of hybrid polymer nanofibers decorated with functionalized NBBs have been discussed by Zhang et al. Table 6.27 demonstrates the advantages and disadvantages for the fabrication and biosensing application of the electrospun porous, hollow, and core-shell nanostructures.

Although there are certain technical and mechanistic difficulties that still need to be solved or improved, electrospinning has become one of the most effective routes to fabricate functional PMNFs (polymer nanofibers) with desired compositions and structures. The binding and assembling of NBBs with PMNFs via the electrospinning technique have been proved to be a powerful strategy to prepare biosensors.

Table 6.27 Comparisons of the advantages and disadvantages of several electrospun nanostructures

Morphology	Advantages	Shortcomings
Porous	Simple versatile equipment-independent	Complex pre-treatment inevitable for loading of NBB is uncontrollable
Hollow	Specific equipment complex operation	Specific equipment complex operation
Core-shell	Large surface area unique properties selectable core and shell materials	Complex operation harsh post-treatments

However, to obtain a high-performance biosensor, some challenges, such as how to improve NBB contents without aggregation, and how to increase immobilization sites for tested biomolecules, should be overcome [479].

Recent trends in the development of molecularly imprinted polymer based sensor technology for rapid assessment of the medical applications, as well as future research directions were comprehensively discussed by Saylan et al. [480].

Quantum dots (QDs) are tiny semiconductor particles a few nanometres in size, having optical and electronic properties that differ from larger particles due to quantum mechanics. These particles play an important role in the development of sensors, medical field etc. Quantum dots (QDs) and molecular imprinting are two extensively explored techniques which have been applied in diversified chemo or biosensors. Recently many articles about quantum dots have been reported to develop optical sensors with their unique physical and optical properties, which can be used to detect analytes by means of the fluorescence quenching due to the electron transfers between the QDs and the target molecule. The QDs in biosensors are also a promising method for the detection of target protein. Zhang et al. [481] fabricated a fluorescent molecularly imprinted membrane (MIM) by embedding QDs into molecularly imprinted polymer matrix for direct and selective detection of lysozyme. As biosensor, this fluorescent molecularly imprinted membrane can directly generate readable optical signals to report molecule recognition events without any pre-treatment and complex instrument systems. Molecular imprinting method is based on the polymerization of a functional monomer and a cross-linker around a template molecule. At first, a pre-complex is formed between a template molecule and a functional monomer and then the polymerization is carried out around the pre-complex with initiator and cross-linker addition [482, 483]. Finally, the template molecule is removed to generate three-dimensional cavities for specific recognition in several times. Imprinted nanostructured materials are characterized by their small sizes, large reactive surface area and, most importantly, with rapid and specific analysis of analytes due to the formation of template driven recognition cavities within the matrix. Irshad et al. [484] suggested that the Imp-NPs (imprinted nanomaterials) could be used for developing an imprinted membrane sensor. Nanomaterials with a two-dimensional (2D) structure, typically such as nanosheets, nanoplates, and nanomembranes, have attracted significant attention for diverse applications ranging from optoelectronics, electro catalyst, energy storage, nano fluidics, and photodetectors to sensor devices.

Tancharoen et al. [485] developed an electrochemical sensor based on graphene oxide and polymers imprinted for Zika virus detection. Zika virus is a member of the Flaviviridae virus family and infects individuals typically by developing a mild fever, red eyes, a skin rash, conjunctivitis, muscle and joint pain, malaise, headache and then serious problems.

Gas sensors play an important role in scientific research because of their attractive applications in toxic gas detection, environmental monitoring, health care, and medicine diagnosis. Nanotechnology-enabled sensors and solutions are now able to detect and identify chemical or biological agents in the air and soil with much higher sensitivity than ever before. Researchers are investigating particles such as self-assembled monolayers on mesoporous supports (SAMMS™), dendrimers, and carbon nanotubes to determine how to apply their unique chemical and physical properties for various kinds of toxic site remediation. Another sensor has been developed by NASA as a smartphone extension that firefighters can use to monitor air quality around fires [486]. Carbon nanotubes (CNT) based sensors are, highly sensitive and able to detect gas concentrations down to 10–7 moles per litre. Sensors based on arrays of multi-walled CNTs are also being used to detect DNA and other biomolecules [487]. Yavari et al. [488] synthesized macro graphene foam-like three-dimensional network and demonstrated parts-per-million level detection of NH_3 and NO_2 in air at room-temperature.

Iyengar et al. [489] demonstrated that the PANi coated PVDF/rGO nanofibers have provided a robust response to humidity and can be calibrated to measure %RH (relative humidity) levels from desiccated to saturated conditions (10–95%RH). Sensor characteristics reveal high sensitivity, especially under near-saturated conditions of 70–95% RH, confirming its viability for breath sensing. Khalid et al. [490] fabricated a composite of Polylactic-co-glycolic acid (PLGA) and Polycaprolactone (PCL) for biodegradable piezo-capacitive pressure sensor which can be used at low pressure measurement in tactile ranges of ($0 < P < 5$ kPa). An electrospun PLGA-PCL composite membrane has been used as elastomeric dielectric sandwiched between two biodegradable iron-zinc (Fe-Zn) bilayer electrodes, deposited on degradable polyvinyl alcohol (PVA) substrate using electron beam deposition, and encapsulated in PLGA thin films for device fabrication. The sensitivity of the sensor was found to be $0.863 \pm 0.025\ \text{kPa}^{-1}$ in the low pressure region ($0 < P \leq 1.86$ kPa) which is quite high as compared to previous literature on biodegradable sensors so far while it adapted to a value of $0.062 \pm 0.005\ \text{kPa}^{-1}$ for high pressure region ($1.86\ \text{kPa} < P \leq 4.6$ kPa).

Asmatulu et al. [491] demonstrated a highly sensitive and reliable electrospun polyaniline nanofiber-based biosensors for COX-2 enzymes detection. The nano textured sensing platforms were able to detect the COX-2 biomarker at concentrations as low as 0.01 pg/mL in PBS and human serum solutions, respectively. This study may open new possibilities to enhance the selectivity and detection levels of many diseases. Song et al. [492] demonstrated that the mechanical properties, thermal stability and electrochemical properties of electrospun PU separators were remarkably enhanced by addition of GO nanosheets.

Perkins et al. [493] fabricated a sensor using a single monolayer of molybdenum disulfide (MoS_2) on a silicon dioxide wafer and reported that the MoS_2 sensor exhibited a much higher selectivity than carbon nanotube-based sensors. The MoS_2 sensor is sensitive to triethylamine (TEA), a chemical associated with the V-series nerve gas agents.

Liu et al. [494] fabricated Ln^{3+}-doped (Yb^{3+}, Tm^{3+} or Yb^{3+}, Er^{3+} co-doped) $NaYF_4$ nanoparticle/polystyrene hybrid fibrous membrane (HFM) via electrospinning technique. The membrane showed an upconversion luminescence (UCL), flexibility, superhydrophobicity and processability and could be used as a fluorescence sensor to detect bioinformation from a single water droplet (~10μL). Based on the fluorescence resonance energy transfer, the detection limits of this sensor can reach 1 and 10 ppb for the biomolecule, avidin, and the dye molecule, Rhodamine B, respectively, which are superior to most of the fluorescence sensors reported previously.

Metal oxide semiconductor (MOS) nanomembranes hold a great potential for electronic devices. Liu et al. [495] for the first time fabricated Rolled-up SnO_2 nanomembranes gas sensor. The sensor displayed high and fast response for selective detection of acetone. Grimm et al. [496] fabricated inorganic rolled-up nanomembranes for field effect transistors and fluidic sensing applications.

Synthetic biomimetic membranes provide biological environments to membrane proteins. By exploiting the central roles of biological membranes, it is possible to devise biosensors, drug delivery systems, and nanocontainers using a biomimetic membrane system integrated with functional proteins. Kim et al. [497] discussed recent technologies used to create synthetic biomimetic membranes and their engineered sensors applications.

The implementation of nanotechnology in the form of small sensors and monitoring devices will create a positive impact on the future use of precision farming methodologies [498].

6.14 Air Purification

Nanotechnology is playing a significant role in pollution prevention technologies by minimizing quantities and exposure of hazardous wastes to the air and also by providing maintenance and enhancement. Most popular applications of nanotechnology is the use of nano compounds, devices and tools for air remediation. Activated carbon and fiberglass are widely used in air filtration industry. Nanotechnology field is booming in an exceptionally impressive manner. Nanofibers are one of the unique materials which have one order of magnitude smaller than conventional fibers. The high surface-to-volume ratio, low resistance and enhanced filtration performance make nanofibers an attractive material for many applications such as healthcare, energy and air filtration.

Many airplane cabin and other types of air filters are nanotechnology-based filters that allow “mechanical filtration,” in which the fiber material creates nanoscale pores that trap particles larger than the size of the pores. The filters also may contain charcoal layers that remove odors.

Volatile organic compounds (VOCs) are released from various sources and are unsafe for human health. VOCs are not only present in air but are also the product of volatilization of building materials, detergents, pesticides, and cosmetics. Prolonged exposure to VOCs can potentially affect human health. Porous materials are promising candidates for the adsorption of VOCs owing to their increased ratio of surface area to volume.

Patil et al. [499] developed an activated carbon (AC) impregnated cellulose acetate electrospun nanofiber mat for the adsorption of VOCs (volatile organic compounds) from the air mixture. The adsorption capacities were measured for acetone, benzene, and dichloromethane, and it was reported that adsorption capacity increased with the increase in AC. Dichloromethane resulted in a faster adsorption process than acetone and benzene owing to its smaller molecular size. VOCs were desorbed with the N_2 gas purging, while VOCs were adsorbed at higher temperatures owing to the increased vapor pressures.

Balamurugan et al. [500] discussed the modern concepts and current research progress on various nanofibrous membranes, such as water and air filtration media. They believed that the potential application of nanofibers is enormous and one of the breakthrough domains in future will be to use them as filter media in clean air applications in hospitals. Ahn et al. [501] have studied the filtration efficiency of nylon-6 nanofibrous membranes, which is better than the commercialized high-efficiency particulate air filter (HEPA). One of the drawbacks is that they observed high pressure drop across the membrane.

Activated carbon and fiberglass are widely used in air filtration industry. Nanotechnology field is booming in an exceptionally impressive manner. Electrospun nanofibers have been explored for the adsorption of volatile organic compounds (VOC) present in the air by various authors. Scholten et al. [502] reported that adsorption and desorption of VOC by electrospun nanofibrous membranes were faster than conventional activated carbon.

In the conventional (HEP) filters, according to filtration theory, non-slip flow is the dominant mechanism. However, when the nanofibrous layer is coated on the conventional filter (Fig. 6.19), the slip flow mechanism becomes dominant due to the smaller fiber size ability to disturb the air flow. As can be seen from Fig. 6.20a, depth filtration is taking place on the conventional filter media (dust loading), where as surface loading of dust particles (Fig. 6.20b) is taking place on the nanofiber coated on conventional filter [503].

For air treatment applications, an immobilization material is necessary to prevent fine TiO_2 powders from blowing away with treated air. A range of substrates have been used as catalyst supports for the photocatalytic degradation of air pollutants. Jo and Kang [504] prepared PAN-TiO_2 fibers with different PAN to TiO_2 ratios, using PAN as a carbon source, *N*,*N*-dimethyl formamide as a solvent, and TiO_2 as a photocatalyst. The mixture was heated at at 110 °C for 1 h and then fibers were made by electrospinning. These fibers were used for the photocatalytic decomposition of airborne aromatic compounds (BTEX). Kim et al. [505] modified the surfaces of

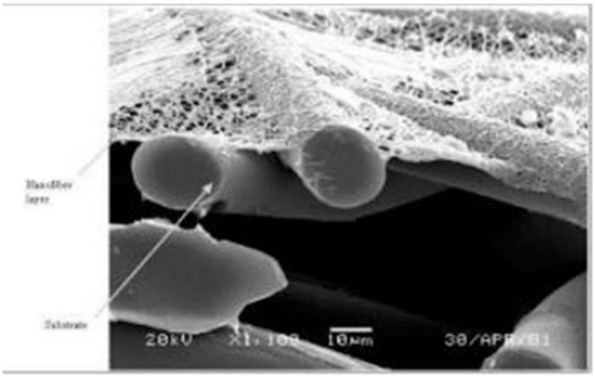

Fig. 6.19 Electrospun nanofibers on a polyester substrate. (Reproduced with permission from [503])

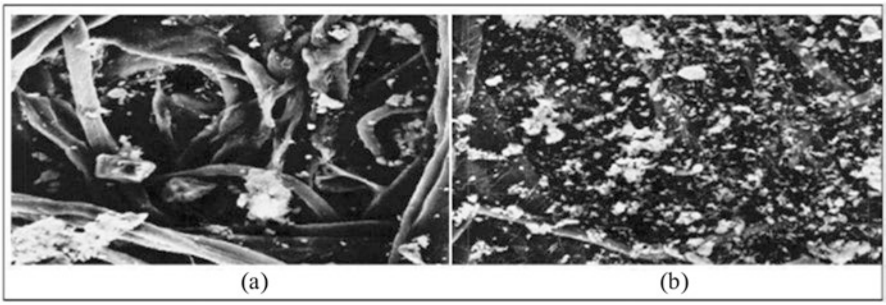

Fig. 6.20 ISO Fine dust loading on (**a**) cellulose and (**b**) cellulose/nanofiber composite. (Reproduced with permission from [503])

electrospun polyacrylonitrile nanofibers (EPNFs) by oxygen plasma treatment and thus generated functional groups such as –$CONH_2$, –COOH and –COOR on the surface. The membranes were used as air-filter. It was reported that the modified membrane was very effective air filtration (particulate matter ≤ 2.5µm) with removal 94.02% and pressure drop of 18 Pa. Zhang et al. [506] developed high-efficiency (>99.5%) polyimide-nanofiber air filters for the high temperature $PM_{2.5}$ removals. $PM_{2.5}$ refers to atmospheric particulate matters (PM) that have a diameter of less than 2.5µm, which is about 3% the diameter of a human hair. It is an air pollutant that is a concern for people's health when levels in air are high.

The polyimide nanofibers exhibited high thermal stability, and the $PM_{2.5}$ removal efficiency was kept unchanged when temperature ranged from 25–370 °C. Zou et al. [507] fabricated a graphene oxide (GO) membrane with a large specific surface area and a continuous pore structure via a coating method, and adsorption properties of the GO membrane were investigated. It was reported that the GO membrane's removal efficiency was more significant when the import concentration was higher and the wind velocity was lower, with a lower pressure drop observed while maintaining high removal efficiency. Through fully simulating air pollution and testing, the GO membrane showed a high $PM_{2.5}$ (sandalwood-burning to simulate $PM_{2.5}$ in the air) removal rate of up to 99.46%, low pressure drop of 7 Pa, and a high QF (quality factor) of 0.75 Pa^{-1} under a wind velocity of 0.1 ms^{-1}. The GO membrane is highly efficient and its preparation is green and pollution-free, which provides technical support for research and application in the field of air purification.

6.15 Military

The US Army is conducting extensive R&D designed to lead to the development of nanomaterials systems for military applications incorporating unique properties such as self-repair, selective removal, corrosion resistance, sensing, ability to modify coatings' physical properties, colorizing, and alerting logistics staff when tanks or weaponry require more extensive repair. Also is developing NanoSyntTex, Inc. durable nonwoven fabrics that integrate blends of various fibrous webs that impart water absorbency or repellency, fire and thermal resistance, antimicrobial treatment, etc. These reinforced multilayer nonwoven composite fabrics have been engineered to be lighter in weight, significantly more breathable, and superior in tear and breaking strength [508].

During war, there is often the threat of chemical agents used in the battlefield. Protective jumpsuit using activated charcoal is usually heavy and bulky. Functionalized fabrics using electrospun nanofibers or electrospun nanofibers as one of the components may give rise to a new class of protective clothing that is lightweight, waterproof and breathable while offering the same or better protection against chemical agents. Thus it will help to maximize the survivability, sustainability, and combat effectiveness of the individual soldier system against extreme weather conditions, ballistics, and NBC (nuclear, biological, and chemical) warfare. Figure 6.21 shows fabric used in military with electrospun membrane layer.

High surface area of electrospun nanofiber and its ease of functionalizing have made it an ideal material for use in defence technology especially in the area of decontamination and protection against chemical and biological agents. Almost any equipment or apparels that give protection to the soldier will benefit from the use of nanofibers. The most common form of personal protective equipment (PPE) is the protective jumpsuit and the facemask. Currently, activated charcoal in the form of cloth or pellets is often used for the removal of chemical toxicants. For facemask, a separate filtering layer is needed for removing particulate matters. Facini et al. [510] explored nylon nanofibers as the potential candidate for the filtration of nanoparticles in protective clothing applications. A thin coating of nanofibers over textiles provided 80% retention of 20 nm nanoparticles and over 50% retention of 200 nm size nanoparticles, which was further improved to 99% efficiency by increasing the

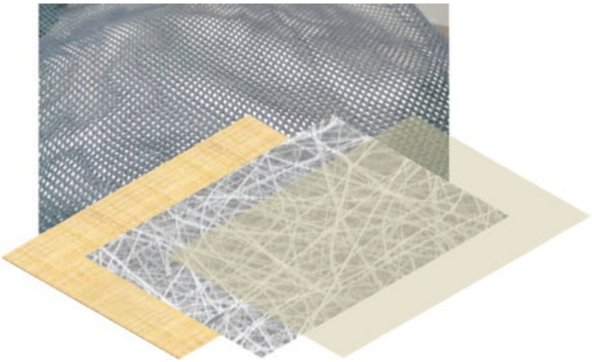

Fig. 6.21 Fabric with electrospun membrane layer [509]

thickness of the nanofibers. Electrospun nylon 6 nanofibers deposited over nylon/cotton woven fabric was evaluated for 300 nm NaCl particles filtration efficiency in PC applications by Vitchuli et al. [511]. Vitchuli et al. achieved an efficiency of greater than 99.5% without sacrificing air permeability and pressure drop. Electrospinning technique in combination with electrospraying has been utilized in water-soluble nanofilters to be used in the collection of biological micro- and nano-aerosols by Morozov et al. [512].

Electrospun membrane offers several advantages over conventional activated charcoal based PPE. Electrospun membrane is already used commercially as an air filter media. When functionalized with detoxification property, this membrane is able to perform two functions simultaneously. This potentially cuts down on the weight of the facemask by eliminating the need for two separate materials. High porosity and small interfiber pore size also makes electrospun membrane a possible candidate for making breathable fabric. Electrospinning has already been used for making clothing and apparels from a US startup company called Electroloom in 2015 [513].

The fabricated membrane based on MgO was found to be about two times more reactive than currently used charcoal [514]. Ramaseshan [515] used electrospinning to produce $ZnTiO_3$ nanofibers from its precursor. The annealed fibers have diameters mainly in the range of 50–300 nm. $ZnTiO_3$ containing α-Zn_2TiO_4 demonstrates the best efficiency with Paraoxon, simulant for the organophosphorus compounds, with decomposition of 91% in the first 50 min and CEES (2-chloroethyl ethyl sulfide), simulant for mustard gas, with decomposition of 69% in the first 10 min. Instead of using pure inorganic fibers which can be brittle, another method is to incorporate active agents into polymeric fibers.

There are a few ways of fabricating a fabric or filter media using electrospun nanofibers that offers protection against both chemical and biological agents. Since electrospun nanofibers can be easily functionalized by blending, having both additives in the same nanofiber, it will be the most direct way to imbue the fiber with both properties. Alternatively, nanofibers with specific functionality may be electrospun to form a layer by layer composite structure [509, 516]. This way, there will not be any interference in the reaction of both additives. Chen [516] developed electrospun fiber-based chemical and/or biological detoxifying protective fabrics containing a-nucleophilic oxime moieties that are capable of hydrolytically decomposing toxic organophosphate (OP) chemical nerve agents and pesticides, and/or biocides acting against bacterial contaminants. The layer-by-layer (LbL) electrostatic assembly technique was applied in combination with electrospinning technique to fabricate novel, breathable electrospun fiber-based protective fabrics and filters for both chemical and biological protection. Reactive polyanion, polyhydroxamic acid, which can decompose OP nerve agents, and antimicrobial polycation, poly (N-vinylguanidine), were synthesized and LbL-assembled onto electrospun fibers to achieve multifunctional coatings.

Electrospun membrane has been functionalized with anti-bacterial and anti-viral properties for various applications including healthcare and in military use. Different types of active compounds have been added to electrospun nanofibers and were shown to be effective against bacteria. Inorganic additives such as silver nanoparticles, MgO and CuO are known for their antibacterial property. Electrospun nanofiber membrane containing silver nanoparticles [517], MgO [518] and CuO [519] have been shown to be effective in inhibiting bacteria growth. Incorporation of these additives is usually achieved through direct blending into the electrospinning solution.

A drawback of using blending to incorporate functional additives into nanofibers is that the covering of additives by the polymer matrix may reduce its effectiveness.

Organic compounds with anti-bacterial properties have also been used for loading into electrospun fibers. Kim et al. [520] selected quaternary ammonium salt (benzyl triethylammonium chloride, BTEAC) to be blended with polycarbonate solution for electrospinning. The resultant fiber diameter was reduced significantly from more than 8μm to about 1μm with improved fiber uniformity. The electrospun membrane exhibited antibacterial property with good filtration performance.

Electrospun fibers containing drugs such as chlorhexidine have also shown good anti-bacterial functionality. For drugs loaded into the fibers by blending, a zone of inhibition is seen on the bacteria culture plates where the drugs have leached out and killed the bacteria [516]. It is important to note that once the drug level in the fiber has fallen below a certain level, its anti-bacterial property will also diminish. Therefore, it may be advisable to chemically bind the anti-bacterial agent to the fiber polymer matrix.

Beside clothing, the military would be able to create sensor systems that could detect biological agents and water purification via using membrane process.

6.16 Food Industry

Membrane technology has been used in specialized applications in the food industry for more than 50 years. The technology can be applied to several production methods, including milk-solids separations in the dairy industry, juice clarification and concentration, concentration of whey protein, sugar and water purification, beer production and waste management etc. Nanotechnology has been also used in various areas of food engineering and technology. Nabetani et al. [521] discussed the present and future prospect of membrane technology in food industry. Heavy metallic ions in water are difficult to biodegrade, and they can enter the human body through the food chain, causing a series of irreversible physiological disease. Nanocomposites offer added stability, which is important for sustaining antimicrobial activity and reducing the likelihood of migration of metal ions into stored foods. Polymers are largely engineered to form nanocomposites with metal/metal oxide nanomaterials for food application.

He and Hwang [522] wrote a review on nanotechnology in food science and addressed the safety concerns and regulatory policies on its manufacturing, processing, packaging, and consumption. At the end of this article, the perspectives of nanotechnology in active and intelligent packaging applications are highlighted. However, United States Environmental Protection Agency, National Institute for Occupational Safety and Health, the Food and Drug Administration (FDA), the Health and Consumer Protection Directorate of the European Commission, International organizations such as the International Organization for Standardization and the Organization for Economic Cooperation and Development, as well as many regulatory bodies have issued multiple guidance documents with respect to the potential risks posed by nanomaterials.

1. On August 5, 2015, U.S. FDA issued one final guidance document related to the use of nanotechnology in food for animals.
2. On April 6, 2015, U.S. Environmental Protection Agency proposed one-time reporting and record keeping requirements under the Toxic Substances Control Act Section 8(a).
3. On June 24, 2014, U.S. FDA issued three final guidance documents related to the use of nanotechnology in regulated products, including cosmetics and food substances.

In November 2007, The Working Party on Manufactured Nanomaterials of the Organization for Economic Cooperation and Development launched the Sponsorship Program for the Testing of Manufactured Nanomaterials (Testing Programme) [523].

Most researches emphasize the regulation of nanotechnology in food packaging and processing [522]. Unfortunately, there is no comprehensive review on the potential risks associated with the functionality and applicability of food nanotechnology yet. The applications of nano-based technology in food industry may include nanoparticulate delivery systems (e.g. micelles, liposomes, nanoemulsion, biopolymeric nano-particles, and cubosomes), food safety and biosecurity (e.g. nanosensors), and nanotoxicity.

The application of nanotechnology in food processing and preservation has benefits including reducing waste, extending shelf life of products and improving taste. Food nanotechnology can affect the bioavailability and nutritional value of food on the basis of its functions [522]. It is recognized that the biological properties (including toxicological effects) of nanomaterials are largely dependent on their physicochemical parameters. Figure 6.22 shows the major links between nanotechnology and the food industry, enhancing food security, extending storage life, improving flavor and nutrient delivery, allowing pathogen/toxin/pesticide detection, and serving functional foods.

Nanotechnology will offer some energizing potential advantages for food safety assessment and to maintain the quality of our foods [524].

1. Contamination Sensor: Flash a light to uncover the nearness of E. coli microorganisms.
2. Antimicrobial Packaging: Eatable food films made with oregano oil or cinnamon, or nano particles of zinc, calcium different materials that eliminate microorganisms.
3. Enhanced Food Storage: Nano-improved boundary keeps oxygen-touchy foods fresher.
4. Improved Nutrient Delivery: Nano- encapsulating enhances solvency of vitamins, cancer prevention agents, solid omega oils and other ‘nutraceuticals’.
5. Green Packaging: Nano-fibers produced using shells of lobsters or natural corns are both biodegradable and antimicrobial.

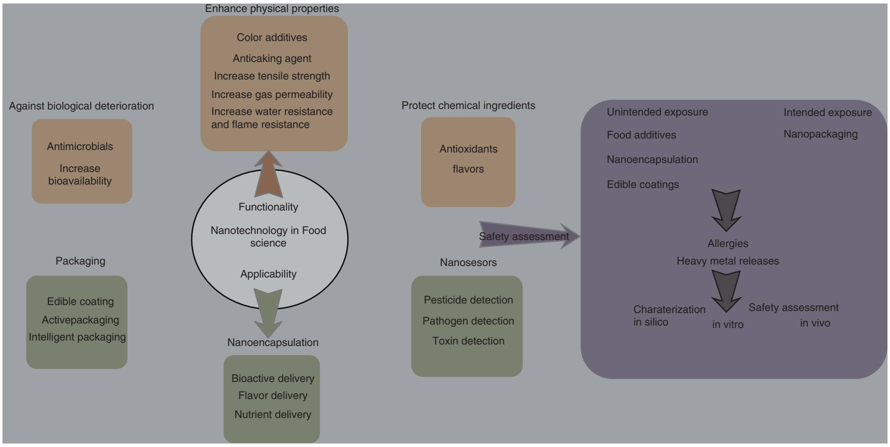

Fig. 6.22 Diagram showing the development of nanotechnology in food science/industry and its functionality, applicability, and safety assessments [522]

6. Pesticide Reduction: A cloth can be saturated with the nano fibers gradually discharges pesticides, disposing of requirement for extra splashing and decreasing concoction spillage into the water supply.
7. Following, tracing; Brand Protection: Nanobarcodes can be made to label singular items and follow flare-ups.
8. Texture: Food will have ability to spread and strength enhance with nano-sized gems and lipids for better low fat nourishments.
9. Flavour: Trap the tongue with extreme blockers or sweet and salty enhancers.
10. Microorganisms Identification and Elimination: Nano starch particles tie with microscopic organisms so they can be distinguished and killed.

The applications of various nanoparticles in food packaging are briefly shown in Table 6.28 [525].

Nanomaterials are used as ingredients and additives (e.g., vitamins, antimicrobials, antioxidants) in nutrients and health supplements for enhanced absorption and bioavailability [525]. Yu et al. [526] fabricated polyvinyl alcohol/chitosan polymer-based biodegradable films decorated with silica nano particles and reported that the films extended the preservation time of cherries by three-fold compared to normal packaging. This was due to significant reduction in the permeability of oxygen and moisture by 25.6% and 10.2%, respectively. Swaroop and Shukla [527] developed a food packaging material using a combination of nanostructures of magnesium oxide (MgO) and polylactic acid biopolymer, and found that the material effectively protected against bacterial biofilms. Foltynowicz et al. [528] synthesized zero-valent iron particles to act as oxygen scavengers in food packaging. Sarwar et al. [529] developed polyvinyl alcohol (PVA), nanocellulose and Ag nanocomposite films and applied them to antimicrobial food packaging. Films coated with various effective antimicrobial components can result in higher antimicrobial potential.

Ahmed et al. [530] reported that films loaded with Ag-Cu NPs and 50% CEO showed maximum antimicrobial activity against Listeria monocytogenes, *Salmonella* Typhimurium and *Campylobacter* jejuni. Chicken samples contaminated with *S.* Typhimurium and *C.* jejuni*,* packed in the composite films containing 4% (w/w) Ag-Cu and 50% CEO (w/w), and stored at refrigerated temperature for

Table 6.28 Nanoparticles for application in food packaging

Types of nanoparticles	Matrix	Application
Silver	Asparagus, Orange juice, Poultry meat, Fresh-cut melon, Beef meat exudates	Retards the growth of aerobic psychrotrophics, yeasts and molds; antimicrobial effect against *Escherichia coli* and *Staphylococcus aureus*
Zinc oxide	Orange juice, Liquid egg albumen	Effectively reduces *Lactobacillus plantarum*, *Salmonella,* yeast and mold counts without changes in quality parameters
Titanium oxide	Chinese jujube, Strawberry	Reduces browning, slow-down ripening, senescence and decay
Silver oxide	Apple slice	Retards microbial spoilage

21 days showed a complete inhibition. The nanoparticles TiO_2 and SiO_2 and amorphous silica are used as food additives. TiO_2 is used as a coloring in the powdered sugar coating on doughnuts [531, 532]. Silver nanoparticles are one of the most widely used nanomaterials, as antimicrobials, in the food industry. Silver nanoparticles likely serve as a source of Ag^+ ions, binding to membrane proteins, forming pits, causing other morphological changes, and catalyzing the generation of ROS (reactive oxygen species) in bacterial cells, subsequently leading to cell death through oxidative stress. Nevertheless, multiple of latest research studies suggested that silver nanocomposites are safe for food packaging, with no detectable or insignificant levels of silver nanoparticles that are released and migrated from impregnated containers into real food samples and food simulants [533, 534].

The food industry is beginning to use nanotechnology to develop nanoscale ingredients to improve color, texture and flavor of food. Several nano systems are still at the stage of being developed as efficient nanocomponents to find application in the food industry. Researchers are trying to develop better and more efficient nanocarriers with increased level of bioavailability without compromising the appearance and taste of the food (e.g. food packaging), but the entry of manufactured nanoparticles into food chain may result in an accumulation of the toxic contaminant in foods and adversely affect human health. Nutrition and food science research areas that might benefit from applying or understanding nanotechnology include research that aims to: (1) identify sites of action (molecular targets) for bioactive food components; (2) characterize biomarkers that reflect exposure, response, and susceptibility to foods and their components; (3) identify new target delivery systems for optimizing health; and (4) improve food composition [535].

6.17 Others

Recently, membrane technology plays an important role in purification and separation technologies for various applications. Faneer et al. [536] purified the xylitol during production of xylitol via biomass fermentation (common biomass fermentation from sugar cane bagasse, corncobs or rice husk in the presence of yeast) by using PES-nanoparticles of silicon dioxide (SiO_2) NF membrane. The membrane was prepared from polyethersulfone (PES) and nanoparticles (NP) of 5 wt.% via phase inversion technique. The hydrophilicity of the PES/SiO_2 membrane measured by contact angle improved from 79.7 ± 0.65° to 59.1 ± 0.15° for PES/SiO_2 and PES membranes, respectively. In terms of flux and contact angle, the synthesized membrane of PES/ SiO_2 was found to be more effective compared to pure PES membrane.

Nanotechnology is one of the most promising avenues for future innovation in the resistance (tyre lifetime) while maintaining wet grip (safety). A large number of different nanomaterials are currently being researched and are at different stages of development. Yet uncertainty over environmental health and safety (EHS) risks appears to be a main and continuous concern for the development of new nanomaterials in tyre production, even for those closest to market [537] tyre industry. The key advantage of nanotechnologies is that they may allow improvements in one or more tyre properties without sacrificing performance in other areas. New nanomaterials are in research or just entering the market, with the potential to significantly improve rolling resistance (fuel consumption) and wear.

NASA's Johnson Space Center awarded Argonide Corporation, a nanomaterials company, headquartered in Sanford, Florida, a Phase I Small Business Innovation Research (SBIR) contract in 2000 and a Phase II SBIR contract in 2002. Argonide had developed unique filtration media with the potential to revolutionize water purification and provide methods for sanitizing recycled water in space. The special ingredients of Argonide's nonwoven filtration media are nanoalumina fibers made up of the mineral boehmite [538].

6.18 Summary

The use of nanoparticles or in any nano form, in any process is called 'nanotechnology'. There are many processes to use nanotechnology in different membrane processes in different ways, but mixing nanoparticles in membrane formation material is the main. Nanotechnology in membrane process is helping to considerably improve, even revolutionize, many technology and industry sectors: gas separation, water/wastewater treatment, pharmaceutical and medical field, military, food industry, air purification, environmental science, space science, and many others. MMMs are playing an important role for the development of nanotechnology in membrane process. Nanofibers have gained much interest for use in various biomedical applications over the past few decades due to their unique functional properties. In the medical world, nanotechnology is also seen as a boon since these can help with creating what is called smart drugs. These help cure people faster and without the side effects that other traditional drugs have. Research of nanotechnology with cooperation with membrane technology in medicine is now focusing on areas like tissue regeneration, bone repair, immunity and even cures for such ailments like cancer, diabetes, and other life threatening diseases.

Nanotechnology opens up a whole universe of new possibilities for the food industry.

References

1. Jang KS, Kim HJ, Johnson JR, Kim W, Koros WJ, Jones CW, Nair S (2011) Modified mesoporous silica gas separation membranes on polymeric hollow fibers. Chem Mater 23(1–2):3025–3028
2. Robeson LM (2008) The upper bound revisited. J Membr Sci 320(1–2):390–400
3. Vinh-Thang H, Kaliaguin S (2013) Predictive models for mixed-matrix membrane performance: a review. Chem Rev 113:4980–5028
4. Baker RW (2004) Membrane technology and applications, 2nd edn. Wiley, Chichester

5. Dechnik J, Sumby CJ, Janiak C (2017) Enhancing mixed-matrix membrane performance with metalorganic framework additives. Cryst Growth Des 17(8):4467–4488
6. Jeazet HBT, Staudt C, Janiak C (2012) Metalorganic frameworks in mixed-matrix membranes for gas separation. Dalton Trans 41(46):14003–14327
7. Li L, Xu R, Song C, Zhang B, Liu Q, Wang T (2018) A review on the progress in nanoparticle/C hybrid CMS membranes for gas separation. Membranes (Basel) 8(4):134
8. Ghazali AA, Rahman SA, Samah RA (2020) Potential of adsorbents from agricultural wastes as alternative fillers in mixed matrix membrane for gas separation: a review. Green Process Synth 9:219–229
9. Rogelj J, den Elzen M, Höhne N, Fransen T, Fekete H, Winkler H, Schaeffer R, Sha F, Riahi K, Meinshausen M (2016) Paris agreement climate proposals need a boost to keep warming well below 2 °C. Nature 534:631–639
10. Selyanchyn R, Fujikawa S (2017) Membrane thinning for efficient CO_2 capture. Sci Technol Adv Mater 18(1):816–827
11. EUR 24524—Successful European Nanotechnology Research, Outstanding science and technology to match the needs of future society, Luxembourg: Publications Office of the European Union, 2011. isbn: 978-92-79-15623-6
12. Boroglu MS, Yumru AB (2017) Gas separation performance of 6FDA-DAM-ZIF-11 mixed-matrix membranes for H_2/CH_4 and CO_2/CH_4 separation. Sep Purif Technol 173:269–279
13. Guerrero G, Hägg MB, Simon C, Peters T, Rival N, Denonville C (2018) CO_2 separation in nanocomposite membranes by the addition of amidine and lactamide functionalized POSS® nanoparticles into a PVA layer. Membranes (Basel) 8(2):28
14. Guerrero G, Venturi D, Peters T, Rival N, Denonville C, Simon C, Henriksen PP, Hägg MB (2017) Influence of functionalized nanoparticles on the CO_2/N_2 separation properties of PVA-based gas separation membrane. Energy Procedia 114:627–635
15. Zaman W, Khan M, Absar S, Harp S, Edwards K, Takas N (2015) Fabrication of polyacrylonitrile nanofiber membranes functionalized with metal organic framework for CO_2 capturing, ASME 2015 International Mechanical Engineering Congress and Exposition, vol. 9: Mechanics of Solids, Structures and Fluids, Houston, Texas, USA, November 13–19, isbn: 978-0-7918-5752-6
16. Leuven KU (2017) More efficient separation of methane and CO2. https://phys.org/news/2017-10-efficient-methane-co2.html. Accessed 24 May 2020
17. Kertik A, Wee LH, Pfannmöller M, Bals S, Martens JA, Vankelecom IFJ (2017) Highly selective gas separation membrane using *in situ* amorphised metalorganic frameworks. Energy Environ Sci 10:2342–2351
18. Venna SR, Lartey M, Li T, Spore A, Kumar S, Nulwala HB, Luebke DR, Rosi NL, Albenze E (2015) Fabrication of MMMs with improved gas separation properties using externally-functionalized MOF particles. J Mater Chem A 3:5014–5022
19. Perez EV Jr, Balkus KJ, Ferraris JP, Musselman IH (2009) Mixed-matrix membranes containing MOF-5 for gas separations. J Membr Sci 328(1–2):165–173
20. Bano S, Tariq SR, Ilyas A, Aslam M, Bilad MR, Nizami AS, Khan A (2020) Synergistic solution of CO_2 capture by novellanthanide-based MOF-76yttrium nanocrystals in mixed-matrix membranes. Energy Environ 31(4):692–712
21. Ozen HA, Ozturk B (2019) Gas separation characteristic of mixed matrix membrane prepared by MOF-5 including different metals. Sep Purif Technol 211:514–521
22. Rosi NL, Eckert J, Eddaoudi M, Vodak DT, Kimm J, O'Keeffe M, Yaghi OM (2003) Hydrogen storage in microporous metal-organic frameworks. Science 300:1127–1129
23. Ge B, Xu Y, Zhao H, Sun H, Guo Y, Wang W (2018) High performance gas separation mixed matrix membrane fabricated by incorporation of functionalized submicrometer-sized metal-organic framework. Materials 11:1421. https://doi.org/10.3390/ma11081421
24. Hu CC, Cheng PH, Chou SC, Lai CL, Huang SH, Tsai HA, Hung WS (2020) Separation behavior of amorphous amino-modified silica nanoparticle/polyimide mixed matrix membranes for gas separation. J Membr Sci 595:117542

25. Zahri K, Goh PS, Ismail AF (2016) The incorporation of graphene oxide into polysulfone mixed matrix membrane for CO_2/CH_4 separation. IOP Conf Ser Earth Environ Sci 36:012007. https://doi.org/10.1088/1755-1315/36/1/012007
26. Golzar K, Amjad-Iranagh S, Amani M, Modarress H (2014) Molecular simulation study of penetrant gas transport properties into the pure and nanosized silica particles filled polysulfone membranes. J Membr Sci 451:117–134
27. Kiadehi AD, Rahimpour A, Jahanshahi M, Ghoreyshi AA (2015) Novel carbon nano-fibers (CNF)/polysulfone (PSf) mixed matrix membranes for gas separation. J Ind Eng Chem 22:199–207
28. Ahn J, Chung WJ, Pinnau I, Guiver MD (2008) Polysulfone/silica nanoparticle mixed-matrix membranes for gas separation. J Membr Sci 314(1):123–133
29. Duval JM, Folkers B, Mulder MHV (1993) Adsorbent-filled membranes for gas separation. Part 1. Improvement of the gas separation properties of polymeric membranes by incorporation of microporous adsorbents. J Membr Sci 80(1–2):189–198
30. Lin R, Ge L, Liu S, Rudolph V, Zhu Z (2015) Mixed-matrix membranes with metal-organic framework-decorated CNT fillers for efficient CO_2 separation. ACS Appl Mater Interfaces 7(27):14750–14757
31. Etxeberria-Benavidesa M, David O, Johnsonb T, Łozińskac MM, Orsic A, Wrightc PA, Masteld S, Hillenbrandd R, Kapteijnf F, Gasco J (2018) High performance mixed matrix membranes (MMMs) composed of ZIF-94 filler and 6FDA-DAM polymer. J Membr Sci 550:198–207
32. Chakrabarty T, Neelakanda P, Peinemann KV (2018) CO_2 selective, zeolitic imidazolate framework-7 based polymer composite mixed-matrix membranes. J Mate Sci Res 7(3). issn: 1927-0585, e-issn: 1927-0593
33. Sarfraz M, Shammakh MB (2018) Harmonious interaction of incorporating CNTs and zeolitic imidazole frameworks into polysulfone to prepare high performance MMMs for CO_2 separation from humidified post combustion gases. Brazilian J Chem Eng 35(1):217–228
34. Khan MM, Filiz V, Bengtson G, Shishatskiy S, Rahman M, Abetz V (2012) Functionalized carbon nanotubes mixed matrix membranes of polymers of intrinsic microporosity for gas separation. Nanoscale Res Lett 7(1):504. https://doi.org/10.1186/1556-276X-7-504
35. Casado-Coterillo C, Fernández-Barquín A, Irabien A (2020) Effect of humidity on CO_2/N_2 and CO_2/CH_4 separation using novel robust mixed matrix composite hollow fiber membranes: experimental and model evaluation. Membranes 10(1):6. https://doi.org/10.3390/membranes10010006
36. Khan IU, Hafiz M, Othman D, Jilani A, Ismail AF, Hashim H, Jaafar J, Zulhairun AK, Rahman MA, Rehman GU (2020) ZIF-8 based polysulfone hollow fiber membranes for natural gas purification. Polymer Testing 84:106415
37. Burmann P, Zornoza B, Téllez C, Coronas J (2014) Mixed matrix membranes comprising MOFs and porous silicate fillers prepared via coating for gas separation. Chem Eng Sci 107:66–75
38. Zhang Q, Li S, Wang C, Chang HC, Guo R (2020) Carbon nanotube-based mixed-matrix membranes with supramolecularly engineered interface for enhanced gas separation performance. J Membr Sci 598:117794
39. Rouzitalab Z, Maklavany DM, Rashidi A, Jafarinejad S (2018) Synthesis of N-doped nanoporous carbon from walnut shell for enhancing CO_2 adsorption capacity and separation. J Environ Chem Eng 6(5):6653–6663
40. Sanders DF, Smith ZP, Guo R, Robeson LM, McGrath JE, Paul DR, Freeman BD (2013) Energy-efficient polymeric gas separation membranes for a sustainable future: a review. Polymer 54:4729–4761
41. Ma C, Zhang C, Labreche Y, Fu S, Liu L, Koros WJ (2015) Thin-skinned intrinsically defect-free asymmetric mono-esterified hollow fiber precursors for crosslinkable polyimide gas separation membranes. J Membr Sci 493:252–262
42. Chong KC, Lai SO, Lau WJ, Thiam HS, Ismail AF, Roslan RA (2018) Preparation, characterization, and performance evaluation of polysulfone hollow fiber membrane with PEBAX or

PDMS coating for oxygen enhancement process. Polymers 10:126. https://doi.org/10.3390/polym10020126

43. Kusworoa TD, Ismail AF, Mustafa A, Budiyonoa (2010) Application of activated carbon mixed matrix membrane for oxygen purification. Int J Sci Eng 1(1):21–24
44. Fernández-Barquín A, Casado-Coterillo C, Valencia S, Irabien A (2016) Mixed matrix membranes for O_2/N_2 separation: the influence of temperature. Membranes (Basel) 6:28
45. Rybak A, Dudek G, Krasowska M, Strzelewicz A, Grzywna ZJ, Syse P (2014) Magnetic mixed matrix membranes in air separation. Chem Pap 68:1332–1340
46. Weng TH, Wey MY, Tseng HH (2010) Enhanced O_2/N_2 separation performance of poly(phenylene oxide)/SBA-15/carbon molecule sieve multilayer mixed matrix membrane using SBA-15 zeolite particles. Proceedings from the 2010 international conference on chemistry and chemical engineering, Kyoto, Japan, 1–3 August, 2010, pp 245–248
47. Ridzuan N, Musa MH (2012) Comparison between treated and untreated zeolite towards the performance of polyethersulfone mixed matrix membranes (MMMs) for O_2/N_2 gas separation. Adv Mater Res 550–55:728–735
48. Bernardo P, Drioli E, Golemme G (2009) Membrane gas separation: a review/state of the art. Ind Eng Chem Res 48(10):4638–4663
49. Ren H, Jin J, Hu J, Liu H (2012) Affinity between metal–organic frameworks and polyimides in asymmetric mixed matrix membranes for gas separations. Ind Eng Chem Res 51(30):10156–10164
50. Khulbe KC, Matsuura T (2018) Thin film composite and/or thin film nanocomposite hollow fiber membrane for water treatment, pervaporation, and gas/vapor separation. Polymer 10:1051. https://doi.org/10.3390/polym10101051
51. Kim K, Hong SU, Kim JH, Lee HK (2014) Preparation and performance evaluation of composite hollow fiber membrane for SO_2 separation. AIChE J 60(6):2298–2306
52. Zhang L, Xin Q, Lou L, Li X, Zhang L, Wang S, Li Y, Zhang Y, Wu H, Jiang Z (2019) Mixed matrix membrane contactor containing core-shell hierarchical Cu@4A filler for efficient SO_2 capture. J Hazard Mater 376:160–169
53. Nasir A, Masood F, Yasin T, Hameed A (2019) Review: progress in polymeric nanocomposite membranes for wastewater treatment: preparation, properties and applications. J Ind Eng Chem 79:29–40
54. Kunduru KR, Nazarkovsky M, Farah S, Pawar RP, Basu A, Domb AJ (2017) Chapter 2. Nanotechnology for water purification: applications of nanotechnology methods in wastewater treatment. In: Water purification. Academic, New York, pp 33–74
55. Das R, Ali ME, Hamid SBA, Ramakrishna S, Chowdhury ZZ (2014) Carbon nanotube membranes for water purification: a bright future in water desalination. Desalin 336:97–109
56. Nanotechnology: Concept and its application; Nano mission of India…. https://himachalpradesh.pscnotes.com/main-notes/ras-mains-paper-2/general-science-and-technoloy/nanotechnology-concept-and-its-application-nano-mission-of-india/. Accessed 20 Apr 2020
57. Burakov AE, Galunin EV, Burakova IV, Kucherova AE, Agarwal S, Tkachev AG, Gupta VK (2018) Adsorption of heavy metals on conventional and nanostructured materials for wastewater treatment purposes: a review. Ecotoxicol Environ Saf 148:702–712
58. Kima J, Van der Bruggen B (2010) The use of nanoparticles in polymeric and ceramic membrane structures: review of manufacturing procedures and performance improvement for water treatment. Environ Pollut 158(7):72335–72349
59. Arsuaga JM, Sotto A, del Rosario G, Martínez A, Molina S, Teli SB, de Abajo J (2013) Influence of the type, size, and distribution of metal oxide particles on the properties of nanocomposite ultrafiltration membranes. J Membr Sci 428:131–141
60. Nasrollahi N, Aber S, Vatanpour V, Mahmoodi NM (2018) The effect of amine functionalization of CuO and ZnO nanoparticles used as additives on the morphology and the permeation properties of polyethersulfone ultrafiltration nanocomposite membranes. Composit Part B Eng 154:388–409
61. Pang WY, Ahmad AL, Zaulkiflee ND (2019) Antifouling and antibacterial evaluation of ZnO/MWCNT dual nanofiller polyethersulfone mixed matrix membrane. J Environ Manag 249:109358. https://doi.org/10.1016/j.jenvman.2019.109358

62. Qu X, Alvarez PJJ, Li Q (2013) Applications of nanotechnology in water and wastewater treatment. Water Res 47:3931–3946
63. Wang Z, Wu A, Ciacchi LC, Wei G (2018) Recent advances in nanoporous membranes for water purification. Nanomaterials 8(2):65. https://doi.org/10.3390/nano8020065
64. Ursino C, Castro-Muñoz R, Drioli E, Gzara L, Albeirutty MH, Figoli A (2018) Progress of nanocomposite membranes for water treatment. Membranes 8(2):18. https://doi.org/10.3390/membranes8020018
65. Yang SY, Park J, Yoon J, Ree M, Jang SK, Kim JK (2008) Virus filtration membranes prepared from nanoporous block copolymers with good dimensional stability under high pressures and excellent solvent resistance. Adv Funct Mater 18(9):1371–1377
66. Rieger KA, Cho HJ, Yeung HF, Fan W, Schiffman JD (2016) Antimicrobial activity of silver ions released from zeolites immobilized on cellulose nanofiber mats. ACS Appl Mater Interfaces 8(5):3032–3040
67. Gehrke I, Geiser A, Somborn-Schulz A (2015) Innovations in nanotechnology for water treatment. Nanotechnol Sci Appl 8:1–17
68. Gupta AK, Deva D, Sharma A, Verma N (2010) Fe-grown carbon nanofibers for removal of arsenic (V) in wastewater. Ind Eng Chem Res 49:7074–7084
69. Jung JY, Chung YC, Shin HS, Son DH (2004) Enhanced ammonia nitrogen removal using consistent biological regeneration and ammoniumexchange of zeolite in modified SBR process. Water Res 38:347–354
70. Homaeigohar S, Elbahri M (2017) Graphene membranes for water desalination. NPG Asia Mater 9:e427. https://doi.org/10.1038/am.2017.135
71. Abdullah N, Yusof N, Gohari RJ, Ismail AF, Jafar J, Lau WJ, Misdan N, Hairom NHH (2018) Characterizations of polysulfone/ferrihydrite mixed matrix membranes for water/wastewater treatment. Water Environ Res 90(1):64–73
72. Lalia BS, Kochkodan V, Hashaikeh R, Hilal N (2013) A review on membrane fabrication: structure, properties and performance relationship. Desalin 326:77–95
73. Liu SX, Kim JT (2011) Characterization of surface modification of polyethersulfone membrane. J Adhes Sci Technol 25(1–3):193–212
74. Gaaz T, Sulong A, Akhtar M, Kadhum A, Mohamad A, Al-Amiery A (2015) Properties and applications of polyvinyl alcohol, halloysite nanotubes and their nanocomposites. Molecules 20:22833–22847
75. Liu L, Kentish SE (2018) Pervaporation performance of crosslinked PVA membranes in the vicinity of the glass transition temperature. J Membr Sci 553:63–69
76. Marin E, Rojas J, Ciro Y (2014) A review of polyvinyl alcohol derivatives: Promising materials for pharmaceutical and biomedical applications. Afr J Pharm Pharmacol 8:674–684
77. Nataraj D, Sakkara S, Meghwal M, Reddy N (2018) Crosslinked chitosan films with controllable properties for commercial applications. Int J Biol Macromol 120:1256–1264
78. Liu QH, Fang Z, Zhang X, Zhang B (2009) Magnetic chitosan nanocomposites: a useful recyclable tool for heavy metal ion removal. Langmuir 25(1):3–8
79. Elgadir MA, Uddin MS, Ferdosh S, Adam A, Chowdhury AJK, Sarker MZI (2015) Impact of chitosan composites and chitosan nanoparticle composites on various drug delivery systems: a review. J Food Drug Anal 23:619–629
80. More AS, Pasale SK, Wadgaonkar PP (2010) Synthesis and characterization of polyamides containing pendant pentadecyl chains. Eur Polym J 46(3):557–567
81. Buch P, Mohan DJ, Reddy A (2008) Preparation, characterization and chlorine stability of aromatic–cycloaliphatic polyamide thin film composite membranes. J Membr Sci 309:36–44
82. Yang R, Aubrecht KB, Ma H, Wang R, Grubbs RB, Hsiao BS, Chu B (2014) Thiol-modified cellulose nanofibrous composite membranes for chromium (VI) and lead (II) adsorption. Polymer 55:1167–1176
83. Bae J, Baek I, Choi H (2017) Efficacy of piezoelectric electrospun nanofiber membrane for water treatment. Chem Eng J 307:670–678

84. Homaeigohar S, Koll J, Lilleodden ET, Elbahri M (2012) The solvent induced interfiber adhesion and its influence on the mechanical and filtration properties of polyethersulfone electrospun nanofibrous microfiltration membranes. Sep Purif Technol 98:456–463
85. Zhou W, He J, Cui S, Gao W (2011) Preparation of electrospun silk fibroin/cellulose acetate blend nanofibers and their applications to heavy metal ions adsorption. Fibers Polym 12:431–437
86. Dobosz KM, Kuo-Leblanc CA, Martin TJ, Schiffman JD (2017) Ultrafiltration membranes enhanced with electrospun nanofibers exhibit improved flux and fouling resistance. Ind Eng Chem Res 56:5724–5733
87. Shen L, Yu X, Cheng C, Song C, Wang X, Zhu M, Hsiao BS (2016) High filtration performance thin film nanofibrous composite membrane prepared by electrospraying technique and hot-pressing treatment. J Membr Sci 499:470–479
88. Lee J, Yoon J, Kim JH, Lee T, Byun H (2018) Electrospun PAN–GO composite nanofibers as water purification membranes. J Appl Polym Sci 135:45858
89. Faccini M, Borja G, Boerrigter M, Martín DM, Crespiera SM, Vázquez-Campos S, Aubouy L, Amantia D (2015) Electrospun carbon nanofiber membranes for filtration of nanoparticles from water. J Nanomater 2015:247471. https://doi.org/10.1155/2015/247471
90. Makaremi M, Lim CX, Pasbakhsh P, Lee SM, Goh KL, Chang H, Chan ES (2016) Electrospun functionalized polyacrylonitrile–chitosan Bi-layer membranes for water filtration applications. RSC Adv 6:53882–53893
91. Kumar S, Venkatesh K, Gui EL, Jayaraman S, Singh G, Arthanareeswaran G (2018) Electrospun carbon nanofibers/TiO2-PAN hybrid membranes for effective removal of metal ions and cationic dye. Environ Nanotechnol Monit Manag 10:366–376
92. Obaid M, Mohamed HO, Yasin AS, Yassin MA, Fadali OA, Kim HY, Barakat NAM (2017) Under-oil superhydrophilic wetted PVDF electrospun modified membrane for continuous gravitational oil/water separation with outstanding flux. Water Res 123:52
93. Haddad MY, Alharbi HF, Karim MR, Aijaz MO, Alharthi NH (2018) Preparation of TiO_2 incorporated polyacrylonitrile electrospun nanofibers for adsorption of heavy metal ions. J Polym Res 25:218
94. Surgutskaia NS, DiMartino A, Zednik J, Ozaltin K, Lovecká L, Bergerová ED, Kimmer D, Svoboda J, Sedlarik V (2020) Efficient Cu^{2+}, Pb^{2+} and Ni^{2+} ion removal from wastewater using electrospun DTPA-modified chitosan/polyethylene oxide nanofibers. Sep Purif Technol 247:116914. https://doi.org/10.1016/j.seppur.2020.116914
95. Wang Y, Górecki RP, Stamate E, Norrman K, Aili D, Zuo M, Guo W, Nielsen CH, Zhang W (2019) Preparation of super-hydrophilic polyphenylsulfone nanofiber membranes for water treatment. RSC Adv 9:278–286
96. Tai MH, Gao P, Tan BAY, Sun DD, Leckie JO (2014) Highly efficient and flexible electrospun carbon–silica nanofibrous membrane for ultrafast gravity-driven oil–water separation. ACS Appl Mater Interfaces 6(12):9393–9940
97. Wang N, Zhu Z, Sheng J, Al-Deyab SS, Yu J, Ding B (2014) Superamphiphobic nanofibrous membranes for effective filtration of fine particles. J Colloid Interface Sci 428:41–48
98. Zhang C, Huang M, Meng L, Li B, Cai T (2017) Electrospun polysulfone (PSf)/titanium dioxide (TiO_2) nanocomposite fibers as substrates to prepare thin film forward osmosis membranes. J Chem Technol Biotechnol 92:2090–2097
99. Zhuo H, Hu J, Chen S, Yeung L (2008) Preparation of polyurethane nanofibers by electrospinning. J Appl Polym Sci 109:406–411
100. Jiříček T, Komárek M, Lederer T (2017) Polyurethane nanofiber membranes for waste water treatment by membrane distillation. J Nanotech 2017:7143035
101. Fuwad A, Ryu H, Malmstadt N, Kim SM, Jeon TJ (2019) Biomimetic membranes as potential tools for water purification: preceding and future avenues. Desalin 458:97–115
102. Kumar M, Grzelakowski M, Zilles J, Meier WP (2007) Highly permeable polymeric membranes based on the incorporation of the functional water channel protein aquaporin Z. Proc Natl Acad Sci U S A 104:20719–20724. https://doi.org/10.1073/pnas.0708762104

103. Xie W, He F, Wang B, Chung TS, Jeyaseelan K, Armugam A, Tong YW (2013) An aquaporin-based vesicle-embedded polymeric membrane for low energy water filtration. J Mater Chem A 1:7592–7600
104. Li Z, Linares RV, Bucs S, Fortunato L, Hélix-Nielsen C, Vrouwenvelder JS, Ghaffour N, Leiknes TO (2017) Aquaporin based biomimetic membrane in forward osmosis: chemical cleaning resistance and practical operation. Desalin 420:208–215
105. Camilleri-Rumbau MS, Soler-Cabezas JL, Christensen KV, Norddahl B, Mendoza-Roca JA, Vincent-Vela MC (2019) Application of aquaporin-based forward osmosis membranes for processing of digestate liquid fractions. Chem Eng J 371:583–592
106. He Y, Hoi H, Montemagno CD, Abraham S (2018) Functionalized polymeric membrane with aquaporin using click chemistry for water purification application: research article. J Appl Polym Sci 135:46678
107. Ruan W, Hu J, Qi J, Hou Y, Zhou C, Wei X (2019) Removal of dyes from wastewater by nanomaterials: a review. Adv Mater Lett 10(1):9–20
108. Jun JJ, Jia PX, Kun LZ, Bin F, Jun W, Wei ZC (2009) Removal of dyes from water by carbon nanotubes. Fresenius Environ Bulletin 18(5):615–618
109. Ma J, Yu F, Zhou L, Jin L, Yang M, Luan J, Tang Y, Fan H, Yuan Z, Chen J (2012) Enhanced adsorptive removal of methyl orange and methylene blue from aqueous solution by alkali-activated multiwalled carbon nanotubes. ACS Appl Mater Interfaces 4(11):5749–5760
110. Hao X, Zhao J, Zhao Y, Ma D, Lu Y, Guo J, Zeng Q (2013) Mild aqueous synthesis of urchin-like MnOx hollow nanostructures and their properties for RhB degradation. Chem Eng J 229:134–143
111. Zhang P, Lo I, O'Connor D, Pehkonen S, Cheng H, Hou D (2017) High efficiency removal of methylene blue using SDS surface-modified $ZnFe_2O_4$ nanoparticles. J Colloid Interface Science 508:39–48
112. Xu Y, Yuan D, Bao J, Xie Y, He M, Shi Z, Chen S, He C, Zhao W, Zhao C (2018) Nanofibrous membranes with surface migration of functional groups for ultrafast wastewater remediation. J Mater Chem A 6(27):13359–13372
113. Zhang HT, Han J, Xue Y, Nie HL, Zhu, LM, Branford-White C (2009) Surface modification of electrospun nylon nanofiber based dye affinity membrane and its application to papain adsorption, ICBBE 2009. 3rd International Conference on 11–13 June 2009, Beijing, China. https://doi.org/10.1109/ICBBE.2009.5163544
114. Rashidi HR, Sulaiman NMN, Hashim NA, Hassan CRC, Ramli MR (2014) Synthetic reactive dye wastewater treatment by using nano-membrane filtration. Desalin Water Treat 55(1):1–10
115. Wang J, Zhang P, Liang B, Liu Y, Xu T, Wang L, Cao B, Pan K (2016) Graphene oxide as effective barrier on a porous nanofibrous membrane for water treatment. ACS Appl Mater Interfaces 8(9):6211–6218
116. Manoukian M, Fashandi H, Tavakol H (2019) Polysulfone-highly uniform activated carbon sphere mixed-matrix membrane intended for efficient purification of dye wastewater. Mater Res Express 6(5):055313
117. Chaúque EFC, Dlamini LN, Adelodun AA, Greyling CJ, Ngila JC (2017) Electrospun polyacrylonitrile nanofibers functionalized with EDTA for adsorption of ionic dyes. Physics Chemistry of the Earth 100:201–211
118. Li N, Chen G, Zhao J, Yen B, Cheng Z, Meng L, Chen V (2019) Self-cleaning PDA/ZIF-67@PP membrane for dye wastewater remediation with peroxymonosulfate and visible light activation. J Membr Sci. 591:117341
119. Wang H, Wei Y (2017) Magnetic graphene oxide modified by chloride imidazole ionic liquid for the high-efficiency adsorption of anionic dyes. RSC Adv 7:9079–9089
120. Aluigi A, Rombaldoni F, Tonetti C, Jannoke L (2014) Study of methylene blue adsorption on keratin nanofibrous membranes. J Hazard Mater 268:156–165
121. Fard GC, Mirjalili M, Najafi F (2018) Preparation of nano-cellulose/A-Fe_2O_3 hybrid nanofiber for the cationic dyes removal: optimization characterization, kinetic, isotherm and error analysis. Bulgarian Chem Commun 50:251–261

122. Lou L, Wang J, Lee YJ, Ramkumar SS (2019) Visible light photocatalytic functional TiO_2/PVDF nanofibers for dye pollutant degradation. Part Part Syst Charact 36(9):1900091. (12 pages)
123. Chen L, Li N, Wen Z, Zhang L, Chen Q, Chen L, Si P, Feng J, Li YH, Lou J, Ci L (2018) Graphene oxide based membrane intercalated by nanoparticles for high performance nanofiltration application. Chem Eng J 347:12–18
124. Yu Y, Ma R, Yan S, Fang J (2018) Preparation of multi-layer nylon-6 nanofibrous membranes by electrospinning and hot pressing methods for dye filtration. RSC Adv 8:12173–12178
125. Akduman C, Kumbasar EPA, Morsunbul S (2017) Electrospun nanofiber membranes for adsorption of dye molecules from textile wastewater. IOP Conf Ser Mater Sci Eng 254:102001. https://doi.org/10.1088/1757-899X/254/10/102001
126. Lv C, Chen S, Xie Y, Wei Z, Chen L, Bao J, He C, Zhao W, Sun S, Zhao C (2019) Positively-charged polyethersulfone nanofibrous membranes for bacteria and anionic dyes removal. J Colloid Interface Sci 556:492–502
127. Sadasivam RK, Mohiyuddin S, Packirisamy G (2017) Electrospun polyacrylonitrile (PAN) templated 2D nanofibrous mats: a platform toward practical applications for dye removal and bacterial disinfection. ACS Omega 2(10):6556–6569
128. Fendi WJ, Naser JA (2018) Adsorption isotherms study of methylene blue dye on membranes from electrospun nanofibers. Orient J Chem 34(6):2884–2894
129. Xiong S, Kong L, Zhong Z, Wang Y (2016) Dye adsorption on zinc oxide nanoparticulates atomic-layer-deposited on polytetrafluoroethylene membranes. AIChE J 62:3982–3991
130. Foroozmehr F, Borhani S, Hosseini SA (2016) Removal of reactive dyes from wastewater using cyclodextrin functionalized polyacrylonitrile nanofibrous membranes. J Text Polym 4(1):45–52
131. Liang P, Qin PF, Lei M, Zeng QR, Song HJ, Yang J, Shao JH, Liao BH, Gu JD (2012) Modifying Fe_3O_4 nanoparticles with humic acid for removal of Rhodamine B in water. J Hazard Mater 209:193–198
132. Chaudhary GR, Saharan P, Kumar A, Mehta SK, Mor S, Umar A (2013) Gamma-Fe_2O_3 nanospindles for environmental remediation: a study on the adsorption and desorption characteristics of acridine orange and direct red dyes. J Nanosci Nanotechnol 13:3240–3245
133. Absalan G, Asadi M, Kamran S, Sheikhian L, Douglas MG (2011) Removal of reactive red-120 and 4-(2-pyridylazo) resorcinol from aqueous samples by Fe_3O_4 magnetic nanoparticles using ionic liquid as modifier. J Hazard Mater 192(2):476–484
134. Zhang X, Zhang PWZ, Zhang L, Zeng G, Zhou C (2013) Adsorption of methylene blue onto humic acid-coated Fe_3O_4 nanoparticles. Colloids Surf A 435:85–90
135. Arslan M, Sayin S, Yilmaz M (2013) Removal of carcinogenic azo dyes from water by new cyclodextrin-immobilized iron oxide magnetic nanoparticle. Water Air Soil Poll 224(1):1527
136. Jamil N, Mehmood M, Lateef A, Nazir R, Ahsan N (2015) MgO nanoparticles for the removal of reactive dyes from wastewater. Adv Mater Tech Connect Briefs:353–356
137. Dhal JP, Sethi M, Mishra BG, Hota G (2015) MgO nanomaterials with different morphologies and their sorption capacity for removal of toxic dyes. Mater Lett 141:267–271
138. Daniel S, Shoba US (2015) Synthesis, characterization and adsorption behaviour of MgO nano particles on Rhodamine B dye. J Chem Pharma Res 7:713–723
139. Moazzam A, Jamil N, Nadeem F, Qadir A, Ahsan N, Zameer M (2017) Reactive dye removal by a novel biochar/mgo nanocomposite. J Chem Soc Pak 39(1):26–34
140. Yang ST, Chen S, Chang YL, Cao A, Liu YF, Wang HF (2011) Removal of methylene blue from aqueous solution by graphene oxide. J Colloid Interface Sci 359:24–29
141. Sun HM, Cao LY, Lu LH (2011) Magnetite/reduced graphene oxide nanocomposites: one step solvothermal synthesis and use as a novel platform for removal of dye pollutants. Nano Res 4:550–562
142. Shi XD, Ruan WQ, Hu JW, Fan MY, Cao RS, Wei XH (2017) Optimizing the removal of rhodamine B in aqueous solutions by reduced graphene oxide-supported nanoscale zerovalent iron (nZVI/rGO) using artificial neural network-genetic algorithm (ANN-GA). Nanomaterials. Nanomaterials 7(6):134

143. Zhang Y, Ou H, Liu H, Ke Y, Zhang W, Liao G, Wang D (2018) Polyimide-based carbon nanofibers: a versatile adsorbent for highly efficient removals of chlorophenols, dyes and antibiotics. Colloids Surf A Physicochem Eng Asp 537:92–101
144. Jethave G, Fegade U, Attarde S, Ingle S, Ghaedi M, Sabzehmeidani MM (2019) Exploration of the adsorption capability by doping Pb@$ZnFe_2O_4$ nanocomposites (NCs) for decontamination of dye from textile wastewater. Heliyon 5(9):e02412. https://doi.org/10.1016/j.heliyon.2019.e024
145. Datta D, Kuyumcu ÖK, Bayazit ŞS, Salam MA (2017) Adsorptive removal of malachite green and rhodamine B dyes on Fe_3O_4-activated carbon composite. J Dispersion Sci Technol 38(11):1556–1562
146. Min M, Shen L, Hong G, Zhu M, Zhang Y, Wang X, Chen Y, Hsiao BS (2012) Micro-nano structure poly(ether sulfones)/poly(ethyleneimine) nanofibrous affinity membranes for adsorption of anionic dyes and heavy metal ions in aqueous solution. Chem Eng J 197:88–100
147. Chen S, Du Y, Zhang X, Xie Y, Shi Z, Ji H, Zhao C, Zhao W (2018) One-step electrospinning of negatively-charged polyethersulfone nanofibrous membranes for selective removal of cationic dyes. J Taiwan Inst Chem Eng 82:179–188
148. Zhan Y, Wan X, He S, Yang Q, He Y (2018) Design of durable and efficient poly(arylene ether nitrile)/bioinspired polydopamine coated graphene oxide nanofibrous composite membrane for anionic dyes separation. Chem Eng J 333:132–145
149. Zhang Y, Park SJ (2019) Fabrication of MoO_3 nanowire-based membrane devices for the selective adsorption of cationic dyes from aqueous solutions with high performance and reusability. Micromachines 10(9):586. https://doi.org/10.3390/mi10
150. Aizat MA, Aziz F (2019) Chapter 12. Chitosan nanocomposite application in wastewater treatments, in nanotechnology in water and wastewater treatment (theory and applications). Elsevier, pp 243–265
151. Pereira FAR, Sousa KS, Cavalcanti GGRS, França DB, Queiroga LNF, Santos IMG, Fonseca MG, Jaber M (2017) Green biosorbents based on chitosan-montmorillonite beads for anionic dye removal. Environ Chem Eng 5:3309–3318
152. Nagarpita MV, Roy P, Shruthi SB, Sailaja RRN (2017) Synthesis and swelling characteristics of chitosan and CMC grafted sodium acrylate-co-acrylamide using modified nanoclay and examining its efficacy for removal of dyes. Int J Biol Macromol 102:1226–1240
153. Abbasi M (2017) Synthesis and characterization of magnetic nanocomposite of chitosan/SiO2/carbon nanotubes and its application for dyes removal. J Clean Prod 145:105–113
154. Jiang Y, Gong JL, Zeng GM, Ou XM, Chang YN, Deng CH, Zhang J, Liu HY, Huang SY (2016) Magnetic chitosan–graphene oxide composite for anti-microbial and dye removal applications. Int J Biol Macromol 82:702–710
155. Wang Y, Xia G, Wu C, Sun J, Song R, Huang W (2015) Porous chitosan doped with graphene oxide as highly effective adsorbent for methyl orange and amido black 10B. Carbohydr Polym 115:686–693
156. Soltani RDC, Khataee AR, Safari M, Joo SW (2013) Preparation of bio-silica/chitosan nanocomposite for adsorption of a textile dye in aqueous solutions. Int Biodeterior Biodegrad 85:383–391
157. Fan L, Luo C, Sun M, Qiu H, Li X (2013) Synthesis of magnetic beta-cyclodextrin—chitosan/graphene oxide as nanoadsorbent and its application in dye adsorption and removal. Colloids Surf B 103:601–607
158. Rickerby D, Morrison M (2007) Report from the workshop on nanotechnologies for environmental remediation. JRC Ispra. http://www.nanowerk.com/nanotechnology/reports/reportpdf/report101.pdf
159. Kwon S, Fan M, Cooper A, Yang H (2008) Photocatalytic applications of micro- and nano-TiO_2 in environmental engineering. Crit Rev Environ Sci Technol 38(3):197–226. https://doi.org/10.1080/10643380701628933
160. Lee SS, Bai H, Liu Z, Sun DD (2013) Novel-structured electrospun TiO_2 /CuO composite nanofibers for high efficient photocatalytic cogeneration of clean water and energy from dye wastewater. Water Res 47:4059–4407

161. Liu Z, Sun DD, Guo P, Leckie JO (2007) An efficient bicomponent TiO_2/SnO_2 nanofiber photocatalyst fabricated by electrospinning with a side-by-side dual spinneret method. Nano Lett 7:1081–1085
162. Coleman HM, Eggins BR, Byrne JA, Palmer FL, King E (2000) Photocatalytic degradation of 17-ß-oestradiol. Appl Catal B Environ 24:L1–L5
163. Coleman HM, Routledge EJ, Sumpter JP, Eggins BR, Byrne JA (2004) Rapid loss of estrogenicity of steroid estrogens by UVA photolysis and photocatalysis over an immobilised titanium dioxide catalyst. Water Res 38:3233–3240
164. Jiang Y, Zhang P, Liu ZW, Xu F (2006) The preparation of porous nano- TiO_2 with high activity and the discussion of the cooperation photocatalysis mechanism. Mater Chem Phy 99:498–504
165. Liu BS, Wen LP, Zhao XJ (2008) The study of photocatalysis under ultraviolet + visible two-beam light irradiation using undoped nano-titanium dioxide. Mater Chem Phy 112:35–40
166. Cui LF, Huang F, Niu MT, Zeng LW, Xu J, Wang Y (2010) A visible light active photocatalyst: nano-composite with Fe-doped anatase TiO_2 nanoparticles coupling with TiO_2(B) nanobelts. J Mol Catal A Chem 326:1–7
167. Liu BS, Zhao XJ (2010) A kinetic model for evaluating the dependence of the quantum yield of nano-TiO_2 based photocatalysis on light intensity, grain size, carrier lifetime, and minority carrier diffusion coefficient: Indirect interfacial charge transfer. Electrochimica Acta 55:4062–4070
168. Sarasidis VC, Patsios SI, Karabelas AJ (2011) A hybrid photocatalysis—ultrafiltration continuous process: the case of polysaccharide degradation. Sep Purif Technol 80:73–80
169. Chen EZ, Su HJ, Zhang WY, Tan TW (2011) A novel shape-controlled synthesis of dispersed silver nanoparticles by combined bioaffinity adsorption and TiO_2 photocatalysis. Powder Tech 212:166–172
170. Romanos GE, Athanasekou CP, Likodimos V, Aloupogiannis P, Falaras P (2013) Hybrid ultrafiltration/photocatalytic membranes for efficient water treatment. Ind Eng Chem Res 52:13938–13947. https://doi.org/10.1021/ie303475b
171. Kuvarega AT, Mamba BB (2016) Chapter 19. Photocatalytic membranes for efficient water treatment. In: Semiconductor photocatalysis—materials, mechanisms and applications. Intech Open, London
172. Bet-Moushoul E, Mansourpanah Y, Farhadi KH, Tabatabaei M (2016) TiO_2 nanocomposite based polymeric membranes: a review on performance improvement for various applications in chemical engineering processe. Chem Eng J 283:29–46
173. Paz Y (2010) Application of TiO_2 photocatalysis for air treatment: patents' overview. Appl Catal B 99:448
174. Prahsarn C, Klinsukhon W, Roungpaisan N (2011) Electrospinning of PAN/DMF/H_2O containing TiO_2 and photocatalytic activity of their webs. Mater Lett 65:2498–2501
175. Watthanaarun J, Supaphol P, Pavarajarn V (2007) TiO_2 functionalized nanofibrous membranes for removal of organic (micro) pollutants from water. J Nanosci Nanotechnol 7(7):2443–2450
176. Geltmeyer J, Teixido H, Meire M, Acker TV, Deventer K, Vanhaecke F, Hulle SV, Buysser KD, Clerck KD (2017) TiO_2 functionalized nanofibrous membranes for removal of organic (micro) pollutants from water. Sep Purifi Technol 179:533–541
177. Rajak A, Munir MM, Mikrajuddin A, Khairurrijal K (2015) Photocatalytic activities of electrospun TiO_2/styrofoam composite nanofiber membrane in degradation of waste water. Mater Sci Forum 827:7–12
178. Khan SH, Pathak B, Fulekar MH (2018) Synthesis, characterization and photocatalytic degradation of chlorpyrifos by novel Fe:ZnO nanocomposite material. Nanotechnol Environ Eng 3:13. https://doi.org/10.1007/s41204-018-0041-3
179. Hassani P (2017) NanoTechnology—Part of our everyday life in many forms (part-1). https://blogs.systweak.com/nanotechnology-part-of-our-everyday-life-in-many-forms/
180. NNI. https://www.nano.gov/you/nanotechnology-benefits. Accessed 29 Apr 2019

181. Ge J, Fu Q, Yu J, Ding B (2019) Chapter 13. Electrospun nanofibers for oil–water separation. In: Electrospinning: nanofabrication and applications (micro and nano technologies), pp 391–417
182. Gore PM, Purushothaman A, Naebe M, Wang X, Kandasubramanian B (2019) Nanotechnology for oil-water separation. In: Prasad R, Karchiyappan T (eds) Advanced research in nanosciences for water technology. Nanotechnology in the life sciences. Springer, Cham
183. Arora R, Balasubramanian K (2014) Hierarchically porous PVDF/nano-SiC foam for distant oil-spill cleanups. RSC Adv 4:53761–53767
184. Cao M, Luo X, Ren H, Feng J (2018) Hot water-repellent and mechanically durable superhydrophobic mesh for oil/water separation. J Colloid Interface Sci 512:567–574
185. Wang B, Guo Z (2013) Superhydrophobic copper mesh films with rapid oil/water separation properties by electrochemical deposition inspired from butterfly wing. Appl Phys Lett 103:063704
186. Xu Z, Jiang D, Wei Z, Chen J, Jing J (2018) Fabrication of superhydrophobic nano-aluminum films on stainless steel meshes by electrophoretic deposition for oil-water separation. Appl Surf Sci 427:253–261
187. Liu J, Li P, Chen L, Feng Y, He W, Yan X, Lü X (2016) Superhydrophilic and underwater superoleophobic modified chitosan-coated mesh for oil/water separation. Surf Coat Technol 307:171–176
188. Hou K, Zeng Y, Zhou C, Chen J, Wen X, Xu S, Cheng J, Lin Y, Pi P (2017) Durable underwater superoleophobic PDDA/halloysite nanotubes decorated stainless steel mesh for efficient oil–water separation. Appl Surf Sci 416:344–352
189. Yuan S, Chen C, Raza A, Song R, Zhang T-J, Pehkonen SO, Liang B (2017) Nanostructured TiO_2 /CuO dual-coated copper meshes with superhydrophilic, underwater superoleophobic and self-cleaning properties for highly efficient oil/water separation. Chem Eng J 328:497–510
190. Al-Husaini IS, Yusoff ARM, Lau WJ, Ismail AF, Al-Abri MZ, Al-Ghafri BN, Wirzal MDH (2019) Fabrication of polyethersulfone electrospun nanofibrous membranes incorporated with hydrous manganese dioxide for enhanced ultrafiltration of oily solution. Sep Purifi Technol 212:205–214
191. Ao C, Yuan W, Zhao J, He X, Zhang X, Li Q, Xia T, Zhang W, Lu C (2017) Superhydrophilic graphene oxide@electrospun cellulose nanofiber hybrid membrane for high-efficiency oil/water separation. Carbohydr Polym 175:216–222
192. Islam MS, McCutcheon JR, Rahaman MS (2017) A high flux polyvinyl acetate-coated electrospun nylon 6/SiO_2 composite microfiltration membrane for the separation of oil-in-water emulsion with improved antifouling performance. J Membr Sci 537:297–309
193. Alayande SO, Dare EO, Msagati TAM, Akinlabi AK, Aiyedun PO (2016) Superhydrophobic and superoleophillic surface of porous beaded electrospun polystrene and polysytrene-zeolite fiber for crude oil-water separation. Phys Chem Earth 92:7–13
194. Makaremi M, De Silva RT, Pasbakhsh P (2015) Electrospun nanofibrous membranes of polyacrylonitrile/halloysite with superior water filtration ability. J Phys Chem C 119(14):7949–7958
195. Lin J, Shang Y, Ding B, Yang J, Yu J, Al-Deyab SS (2012) Nanoporous polystyrene fibers for oil spill cleanup. Marine Pollut Bull 64(2):347–352
196. Obaid M, Tolba GMK, Motlak M, Fadali OA, Khalil KA, Almajid AA, Kim B, Barak NAM (2015) Effective polysulfone-amorphous SiO_2 NPs electrospun nanofiber membrane for high flux oil/water separation. Chem Eng J 279:631–663
197. Kahraman HT, Avci A, Pehlivan E (2019) Effective polysulfone-amorphous SiO_2 NPs electrospun nanofiber membrane for high flux oil/water separation. Iranian Polym J 28:445–453
198. Crick CR, Gibbins JA, Parkin IP (2013) Superhydrophobic polymer-coated copper-mesh; membranes for highly efficient oil–water separation. J Mater Chem A 1:5943–5948
199. Goh PS, Ismail AF, Hilal N (2016) Nano-enabled membranes technology: sustainable and revolutionary solutions for membrane desalination? Desalin 380(5):100–104

200. Roy S, Singha NR (2017) Polymeric nanocomposite membranes for next generation pervaporation process: strategies. Challenges and future prospects. Membranes 7(3):53
201. Ghanbari M, Emadzadeh D, Lau WJ, Matsuura T, Ismail AF (2015) Synthesis and characterization of novel thin film nanocomposite reverse osmosis membranes with improved organic fouling properties for water desalination. RSC Adv 5:21268–21276
202. Gong G, Nagasawa H, Kanezashi M, Tsuru T (2015) Reverse osmosis performance of layered-hybrid membranes consisting of an organosilica separation layer on polymer supports. J Membr Sci 494:104–112
203. Low ZX, Liu Q, Shamsaei E, Zhang X, Wang H (2015) Preparation and characterization of thin-film composite membrane with nanowire-modified support for forward osmosis process. Membranes 5:136–149
204. Mahdi N, Kumar P, Goswami A, Perdicakis B, Shankar K, Sadrzadeh M (2019) Robust polymer nanocomposite membranes incorporating discrete TiO_2 nanotubes for water treatment. Nanomaterials 9(9):1186
205. Anjum M, Miandad R, Waqas M, Gehany F, Barakat MA (2019) Remediation of wastewater using various nano-material. Arabian J Chem 12(8):4897–4919
206. Kiani S, Mousavi SM, Shahtahmassebi N, Saljoughi E (2016) Preparation and characterization of polyphenylsulfone nanofibrous membranes for the potential use in liquid filtration. Desalin Water Treat 57:16250–16259
207. Kiani S, Mousavi SM, Saljoughi E, Shahtahmassebi N (2017) Novel high flux nanofibrous composite membrane based on polyphenylsulfone thin barrier layer on nanofibrous support. Fibers Polymers 18:1531–1544
208. Wang JJ, Yang HC, Wu MB, Zhang X, Xu ZK (2017) Nanofiltration membranes with cellulose nanocrystals as an interlayer for unprecedented performance. J Mater Chem A 5:16289–16295
209. Soyekwo F, Zhang Q, Gao R, Qu Y, Lin C, Huang X, Zhu A, Liu Q (2017) Cellulose nanofiber intermediary to fabricate highly-permeable ultrathin nano filtration membranes for fast water purification. J Membr Sci 524:174–185
210. Hosseini SM, Bagheripour E, Ansari M (2017) Adapting the performance and physicochemical properties of PES nanofiltration membrane by using of magnesium oxide nanoparticles. Korean J Chem Eng 34(3):1–7
211. Zhao W, Liu H, Meng N, Zhang X (2018) Graphene oxide incorporated thin film nanocomposite membrane at low concentration monomers. J Membr Sci 565:380–389
212. Yin J, Kim ES, Yang J, Deng BL (2012) Fabrication of a novel thin-film nanocomposite (TFN) membrane containing MCM-41 silica nanoparticles (NPs) for water purification. J Membr Sci 423:238–246
213. Yin J, Zhu GC, Deng BL (2016) Graphene oxide (GO) enhanced polyamide (PA) thin-film nanocomposite (TFN) membrane for water purification. Desalin 379:93–101
214. Batchelder GW (1965) Process for the demineralization of water. US 3,171,799
215. Zheng H (2017) Chapter 1. General problems in seawater desalination. In: Solar energy desalination technology. Elsevier, pp 1–46
216. Ge QC, Su JC, Chung TS, Amy G (2011) Hydrophilic superparamagnetic nanoparticles: synthesis, characterization, and performance in forward osmosis processes. Ind Eng Chem Res 50(1):382–388
217. Liu ZY, Bai W, Lee J, Sun DD (2011) A low-energy forward osmosis process to produce drinking water. Science 4(7):2582–2585
218. Sun W, Shi J, Chen C, Li N, Xu Z, Li J, Lv H, Qian X, Zhao L (2018) A review on organic–inorganic hybrid nanocomposite membranes: a versatile tool to overcome the barriers of forward osmosis. RSC Adv 8:10040–10056
219. Arzhandi MRD, Sarrafzadeh MH, Goh PS, Lau WJ, Ismail AF, Mohamed MA (2018) Development of novel thin film nanocomposite forward osmosis membranes containing halloysite/graphitic carbon nitride nanoparticles towards enhanced desalination performance. Desalin 447:18–28

220. Ma N, Wei J, Qi S, Zhao Y, Gao Y, Tang CY (2013) Nanocomposite substrates for controlling internal concentration polarization in forward osmosis membranes. J Membr Sci 441:54–62
221. Ling MM, Wang KY, Chung TS (2010) Highly water-soluble magnetic nanoparticles as novel draw solutes in forward osmosis for water reuse. Ind Eng Chem Res 49(12):5869–5876
222. Song X, Wang L, Tang CY, Wang Z, Gao C (2015) Fabrication of carbon nanotubes incorporated double-skinned thin film nanocomposite membranes for enhanced separation performance and antifouling capability in forward osmosis process. Desalin 369:1–9
223. Loeb S (1975) Osmotic power plants. Science 189:654–655
224. Helfer F, Lemckert C, Anissimov YG (2014) Osmotic power with pressure retarded osmosis: theory, performance and trends—A review. J Membr Sci 453:337–358
225. Bræin S, Sandvik ØS, Skilhagen SE (2010) Osmotic power from prototype to industry—what will it take? In: 3rd International Conference on Ocean Energy, European Commission Enterprise and Industry Brokerage Event ICOE-2010 Marine Energy Bilbao, 6–7 October 2010
226. Li X, Zhang S, Fu F, Chung TS (2013) Deformation and reinforcement of thin-film composite (TFC) polyamide-imide (PAI) membranes for osmotic power generation. J Membr Sci 434:204–217
227. Yip N, Tiraferri A, Phillip WA, Schiffman JD, Hoover LA, Kim YC, Elimelech M (2011) Thin-film composite pressure retarded osmosis membranes for sustainable power generation from salinity gradients. Environ Sci Techno 45(10):4360–4369
228. Han G, Zhang S, Li X, Chung TS (2013) High performance thin film composite pressure retarded osmosis (PRO) membranes for renewable salinity-gradient energy generation. J Membr Sci 440:108–121
229. Bui NN, McCutcheon JR (2014) Nanofiber supported thin-film composite membrane for pressure-retarded osmosis. Environ Sci Technol 48(7):4129–4136
230. Song X, Liu Z, Sun DD (2013) Energy recovery from concentrated seawater brine by thin-film nanofiber composite pressure retarded osmosis membranes with high power density. Energy Environ Sci 6(4):1199–1210
231. Sarp S, Li Z, Saththasivam J (2016) Pressure retarded osmosis (PRO): past experiences, current developments, and future prospects. Desalin 389:2–14
232. Wang Q, Li N, Bolto B, Hoang M, Xie Z (2016) Desalination by pervaporation: a review. Desalin 387:46–60
233. Rostovtseva V, Pulyalina A, Rudakova D, Vinogradova L, Polotskaya G (2020) Strongly selective polymer membranes modified with heteroarm stars for the ethylene glycol dehydration by pervaporation. Membranes 10(5):86
234. Liang B, Pan K, Li L, Giannelis EP, Cao B (2014) High performance hydrophilic pervaporation composite membranes for water desalination. Desalin 347:199–206
235. Chaudhri SG, Rajai BH, Singh PS (2015) Preparation of ultra-thin poly(vinyl alcohol) membranes supported on polysulfone hollow fiber and their application for production of pure water from seawater. Desalin 367:272–284
236. Liang B, Zhan W, Qi G, Lin S, Nan Q, Liu Y, Cao B, Pan K (2015) High performance graphene oxide/polyacrylonitrile composite pervaporation membranes for desalination applications. J Mater Chem A 3:5140–5147
237. Xie Z, Hoang M, Duong T, Ng D, Dao B, Gray S (2011) Sol–gel derived poly(vinyl alcohol)/maleic acid/silica hybrid membrane for desalination by pervaporation. J Membr Sci 383:96–103
238. Marian SA, Asghari M, Amini Z (2017) Desalination of Kashan city's water using peba-based nanocomposite membranes via pervaporation. J Water Environ Nanotechnol 2(2):96–102
239. Yang G, Xie Z, Cran M, Ng D, Gray S (2019) Enhanced desalination performance of poly (vinyl alcohol)/carbon nanotube composite pervaporation membranes via interfacial engineering. J Membr Sci 579:40–51
240. Yalcinkaya F (2019) A review on advanced nanofiber technology for membrane distillation. J Eng Fibers Fabrics 14:1–12

241. Khayet MS, Matsuura T (2011) Membrane distillation: principles and applications. Elsevier. https://books.google.cz/books
242. Wang P, Chung TS (2015) Recent advances in membrane distillation processes: membrane development, configuration design and application exploring. J Membr Sci 474:39–56
243. Shaulsky E, Nejati S, Boo C, Perreault F, Osuji CO, Elimelech M (2017) Post-fabrication modification of electrospun nanofiber mats with polymer coating for membrane distillation applications. J Membr Sci 530:158–165
244. Li L, Abadikhah H, Wang JW, Xu X, Agathopoulos S (2018) One-step synthesis of flower-like Si_2N_2O nanowires on the surface of porous SiO_2 ceramic membranes for membrane distillation. Mater Lett 232:74–77
245. Larbot A, Gazagnes L, Krajewski S, Bukowska M, Kujawski W (2004) Water desalination using ceramic membrane distillation. Desalin 168:367–372
246. Cerneaux S, Struzyńska I, Kujawski WM, Persin M, Larbot A (2009) Comparison of various membrane distillation methods for desalination using hydrophobic ceramic membranes. J Membr Sci 337:55–60
247. Subramanian N, Qamara A, Alsaadia A, Gallo A Jr, Ridwana MG, Lee JG, Pillai S, Arunachalama S, Anjum D, Sharipov F, Ghaffour N, Mishra H (2019) Evaluating the potential of superhydrophobic nanoporous alumina membranes for direct contact membrane distillation. J Colloid Interface Sci 533:723–732
248. Fan Y, Chen S, Zhao H, Liu Y (2017) Distillation membrane constructed by TiO_2 nanofiber followed by fluorination for excellent water desalination performance. Desalin 405:51–58
249. Krajewski SR, Kujawski W, Bukowska M, Picard C, Larbot A (2006) Application of fluoroalkylsilanes (FAS) grafted ceramic membranes in membrane distillation process of NaCl solutions. J Membr Sci 281(1–2):253–259
250. Feng YC, Khulbe KC, Matsuura T, Gopal R, Kaur S, Ramakrishna S, Khayet M (2008) Production of drinking water from saline water by air-gap membrane distillation using polyvinylidene fluoride nanofiber membrane. J Membr Sci 311(1–2):1–6
251. Nthunya LN, Gutierrez L, Derese S, Nxumalo EN, Verliefde AR, Mamba BB, Mhlanga SD (2019) A review of nanoparticle-enhanced membrane distillation membranes: membrane synthesis and applications in water treatment. J Chem Technol Biotechnol 94(9):2757–2771
252. Hao YQ, Wang YF, Weng YX (2008) Particle-size-dependent hydrophilic-ity of TiO_2 nanoparticles characterized by Marcus reorganiza-tion energy of interfacial charge recombination. J Phys Chem C 112:8995–9000
253. Su CL, Chang JJ, Tang KX, Gao F, Li YP, Cao HB (2017) Novel three-dimensional superhydrophobic and strength-enhanced electrospun membranes for long-term membrane distillation. Sep Purif Technol 178:279–287
254. Sameh M, Nady N, El-Shazly A, Elmarghany MR, Na. Sabry M (2019) PES/PVDF blend membrane and its composite with graphene nanoplates: preparation, characterization, and water desalination via membrane distillation. Desalin Water Treat 166:9–23
255. Zahirifar J, Karimi-Sabet J, Moosavian SMA, Hadi A, Parsi PK (2018) Fabrication of a novel octadecylamine functionalized graphene oxide/PVDF dual-layer flat sheet membrane for desalination via air gap membrane distillation. Desalin 428:227–239
256. Zhang J, Song Z, Li B, Wang Q, Wang S (2013) Fabrication and characterization of superhydrophobic poly (vinylidene fluoride) membrane for direct contact membrane distillation. Desalin 324:1–9
257. Liao Y, Loh CH, Wang R, Fane AG (2014) Electrospun superhydrophobic membranes with unique structures for membrane distillation. ACS Appl Mater Interface 6(18):16035–16048
258. Yan KK, Jiao L, Lin S, Ji X, Lu Y, Zhang L (2018) Superhydrophobic electrospun nanofiber membrane coated by carbonnanotubes network for membrane distillation. Desalin 437:26–36
259. Chen W, Chen S, Liang T, Zhang Q, Fan Z, Yin H, Huang KW, Zhang X, Lai Z, Sheng P (2018) High-flux water desalination with interfacial salt sieving effect in nanoporous carbon composite membranes. Nature Nanotechnol 13:345–350

260. Razmjou A, Arifin E, Dong G, Mansouri J, Chen V (2012) Superhy-drophobic modification of TiO_2 nanocomposite PVDF mem-branes for applications in membrane distillation. J Membr Sci 415–416:850–863
261. Ifome JE, Rana D, Matsuura T, Lan CQ (2016) Enhanced performance of PVDF nanocomposite membrane by nano fiber coating: a mem-brane for sustainable desalination through. Water Res 89:39–49
262. Wang Z, Hou D, Lin S (2016) Composite membrane with under water-oleophobic surface for anti- oil-fouling membrane distillation. Environ Sci Technol 50:3866–3874
263. Bonyadi S, Chung TS (2007) Flux enhancement in membrane distillation by fabrication of dual layer hydrophilic–hydrophobic hollow fiber membranes. J Membr Sci 306:134–146
264. Thavasi V, Singh G, Ramakrishna S (2008) Electrospun nanofibers in energy and environmental applications. Energy Environ Sci 1:205–221
265. Modesti M, Boaretti C, Roso M (2015) Electrospun nanofibers for water and wastewater treatment applications. In: Drioli E, Giorno L (eds) Encyclopedia of membranes. Springer, Berlin
266. Yoshikawa M, Yoshioka T, Fujime J, Murakami A (2001) Pervaporation separation of MeOH/MTBE with hydrophilic polymer/agarose blended membranes. J Membr Sci 26:259–264
267. Safarik K, Pospiskova E, Baldikova I, Savva L, Vekas O, Marinica E, Tanasa T, Krasia-Christoforou T (2018) Fabrication and bioapplications of magnetically modified chitosan-based electrospun nanofibers. Electrospinning 2:29–39
268. Wang X, Yeh TM, Wang Z, Yang R, Wang R, Ma H, Hsiao BS, Chu B (2014) Nanofiltration membranes prepared by interfacial polymerization on thin-film nano fibrous composite scaffold. Polymer 55:1358–1366
269. Zeytuncu B, Akman S, Yucel O, Kahraman MV (2014) Preparation and characterization of UV-cured hybrid polyvinyl alcohol nanofiber membranes by electrospinning. Mater Res 17(3):565–569
270. Ren LF, Xia F, Chen V (2017) TiO_2-FTCS modified super-hydrophobic PVDF electrospun nanofibrous membrane for desalination by direct contact membrane distillation. Desalin 423:1–11
271. Tijing LD, Woo YC, Shim WG, He T, Choi JS, Kim HS, Shon HK (2016) Superhydrophobic nanofiber membrane containing carbon nanotubes for high-performance direct contact membrane distillation. J Membr Sci 502(15):158–170
272. Ya KK, Jiao L, Lin S, Ji X, Lu Y, Zhang L (2018) Superhydrophobic electrospun nanofiber membrane coated by carbon nanotubes network for membrane distillation. Desalin 437:26–33
273. An AK, Lee EJ, Guo J, Jeong S, Lee JG, Ghaffour N (2017) Enhanced vapor transport in membrane distillation via functionalized carbon nanotubes anchored into electrospun nanofibers. Sci Rep 7:41562
274. An X, Liu Z, Hu Y (2018) Enhanced vapor transport in membrane distillation via functionalized carbon nanotubes anchored into electrospun nanofibers. Sci Rep 7:41562
275. Liao Y, Wang R, Tian M, Qiu C, Fane AG (2013) Fabrication of polyvinylidene fluoride (PVDF) nanofiber membranes by electro-spinning for direct contact membrane distillation. J Membr Sci 425–426:30–39
276. Khayet M, García-Payo MC, García-Fernández L, Contreras-Martínez J (2018) Dual-layered electrospun nanofibrous membranes for membrane distillation. Desalin 426:174–184
277. Woo YC, Chen Y, Tijing LD, Phuntsho S, He T, Choi JS, Kim SH, Shon K (2017) CF_4 plasma-modified omniphobic electrospun nanofiber membranefor produced water brine treatment by membrane distillation. J Membr Sci 529:234–242
278. Dong ZQ, Ma XH, Xu ZL, Gu ZY (2015) Superhydrophobic modification of PVDF–SiO_2 electrospun nanofiber membranes for vacuum membrane distillation. RSC Adv (83):67962–67970
279. Figoli A, Ursino C, Ramirez DOS, Carletto RAA, Tonetti C, Varesano A, De Santo MP, Cassano A, Vineis C (2019) Fabrication of electrospun keratin nanofiber membranes for air and water treatment. Polym Eng Sci 59(7):1472–1478

280. Li J, Chen X, Xu D, Pan K (2019) Immobilization of horseradish peroxidase on electrospun magnetic nanofibers for phenol removal. Ecotoxicol Environ Saf 170:716–721
281. Huang Y, Wang Z, Hou D, Lin S (2017) Coaxially electrospun superamphiphobic silica-based membrane for anti-surfactant-wetting membrane distillation. J Membr Sci 531:122–128
282. Lee E, Kyoungjin A, Hadi P, Lee S, Chul Y (2017) Advanced multi-nozzle electrospun functionalized titanium dioxide/composite membranes for direct contact membrane distillation. J Membr Sci 524:712–720
283. Attia H, Alexander S, Wright CJ, Hilal N (2017) Superhydrophobic electrospun membrane for heavy metals removal by air gap membrane distillation (AGMD). Desalination 420:318–329
284. Hou D, Lin D, Ding C, Wang D, Wang J (2017) Separation and purification technology fabrication and characterization of electrospun superhydrophobic PVDF-HFP/SiNPs hybrid membrane for membrane distillation. Sep Purif Technol 189:82–89
285. Mahdi S, Shahabadi S, Rabiee H, Mojtaba S, Mokhtare A, Brant JA (2017) Superhydrophobic dual layer functionalized titanium dioxide/polyvinylidene fluoride-co-hexafluoropropylene (TiO_2/PH) nano fibrous membrane for high flux membrane distillation. J Membr Sci 537:140–150
286. Prince JA, Singh G, Rana D, Matsuura T, Anbharasi V, Shanmugasundaram TS (2012) Preparation and characterization of highly hydrophobic poly (vinylidene fluoride)–Clay nanocomposite nanofiber membranes (PVDF-clay NNMs) for desalination using direct contact membrane distillation. J Membr Sci 397–398:80–86
287. Huang Y, Wang Z, Jin J, Lin S (2017) Superhydrophobic dual layer functionalized titanium dioxide/polyvinylidene fluoride-co-hexafluoropropylene (TiO_2/PH) nano fibrous membrane for high flux membrane distillation. Environ Sci Technol 51:13304–13310
288. Chul Y, Tijing LD, Shim W, Choi J, Kim S, He T, Drioli E, Shon HK (2016) Waterdesalination using graphene-enhanced electrospun nano fiber membrane via air gap membrane distillation. J Membr Sci 520:99–110
289. Lee E, Kyoungjin A, He T, Chul Y, Kyong H (2016) Electrospun nanofiber membranes incorporating fluorosilane-coated TiO_2 nanocomposite for direct contact membrane distillation. J Membr Sci 520:145–154
290. Shalaby T, Mahmoud O, Al-Oufy A (2015) Antibacterial silver embedded nanofibers for water disinfection. Int J Mater Sci Appl 4:293–298
291. Li X, Qing W, Wu Y, Shao S, Peng LE, Yang Y, Wang P, Liu F, Tang CY (2019) Omniphobic nanofibrous membrane with pine-needle-like hierarchical nanostructures: toward enhanced performance for embrane distillation. ACS Appl Mater Interfaces 11(51):47963–47971
292. Du Y, Wang D, Wang W, Fu J, Chen X, Wang L, Yang W, Zhang X (2019) Electrospun nanofibrous polyphenylene oxide membranes for high-salinity water desalination by direct contact membrane distillation. ACS Sustain Chem Eng 7(24):20060–20069
293. Tlili I, Alkanhal TA (2019) Nanotechnology for water purification: electrospun nanofibrous membrane in water and wastewater treatment. J Water Reuse Desalin 9(3):232–248
294. Kober PA (1995) Pervaporation, perstillation and percrystallization. J Membr Sci 100(1):61–64
295. Farber L (1935) Applications of pervaporation. Science 82:58–158
296. Binning R, Lee R, Jennings J, Martin E (1961) Separation of liquid mixtures by permeation. Ind Eng Chem 53:45–50
297. Ong YK, Shi GM, Le NL, Tang YP, Zuo J, Nunes CTS (2016) Recent membrane development for pervaporation processes. Pro Polym Sci 57:1–31
298. Figoli A (2013) Separation of organic from organic components (pervaporation application). In: Drioli E, Giorno L (eds) Encyclopedia of membranes. Springer, Berlin
299. Roy S, Singha NR (2017) Review polymeric nanocomposite membranes for next generation pervaporation process: strategies, challenges and future prospects. Membranes 7:53
300. Niemistö J, Kujawski W, Keiski RL (2013) Pervaporation performance of composite poly(dimethyl siloxane) membrane for butanol recovery from model solutions. J Membr Sci 434:55–64

301. Kopec R, Meller M, Kujawski W, Kujawa J (2013) Polyamide-6 based pervaporation membranes for organic–organic separation. Sep Purif Technol 110:63–73
302. Peng F, Pan F, Sun H, Lu L, Jiang Z (2007) Novel nanocomposite pervaporation membranes composed of poly(vinyl alcohol) and chitosan-wrapped carbon nanotube. J Membr Sci 300:13–19
303. Shen JN, Chu YX, Ruan HM, Wu LG, Gao CJ, Van der Bruggen B (2014) Pervaporation of benzene/cyclohexane mixtures through mixed matrix membranes of chitosan and Ag+/carbon nanotubes. J Membr Sci 462:160–169
304. Penkova AV, Polotskaya GA, Gavrilova VA, Toikka AM, Liu JC, Trchova M, Slouf M, Pientka Z (2010) Polyamide membranes modified by carbon nanotubes: application for pervaporation. Sep Sci Technol 45(1):35–41
305. Liu K, Fang CJ, Li ZQ, Young M (2014) Separation of thiophene/n-heptane mixtures using PEBAX/PVDF-composited membranes via pervaporation. J Membr Sci 451:24–31
306. Sabzevari O, Marjani A, Daripour A (2016) Polyamide/nano mixed matrix membranes for pervaporation dehydration ethylene glycols. Oriental J Chem 31(2):1091–1098
307. Azimi H, Ebneyamini A, Tezel FH, Thibault J (2018) Separation of organic compounds from ABE model solutions via pervaporation using activated carbon/PDMS mixed matrix membranes. Membranes 8:40
308. Jose T, George SC, Maya MG, Thomas S (2015) Functionalized MWCNT and PVA nanocomposite membranes for dielectric and pervaporation applications. J Chem Eng Process Technol 6:233
309. Liu X, Cao Y, Li YX, Xu ZL, Li Z, Wang M, Ma XH (2019) High-performance polyamide/ceramic hollow fiber TFC membranes with TiO_2 interlayer for pervaporation dehydration of isopropanol solution. J Membr Sci 576:26–35
310. Panahian S, Raisi A, Aroujalian A (2015) Multilayer mixed matrix membranes containing modified-MWCNTs for dehydration of alcohol by pervaporation process. Desalin 355:45–55
311. Kazemimoghadam M, Rigi ZA (2018) Evaluation and synthesis of nano-pore hydroxysodalite (hs) zeolite membranes: application to pervaporation of ethanol/water mixture. J Water Environ Nanotechnol 3(2):173–190
312. Zuo J, Wang Y, Chung TS (2013) Novel organic–inorganic thin film composite membranes with separation performance surpassing ceramic membranes for isopropanol dehydration. J Membr Sci 433:60–71
313. Wang J, Lia M, Zhoua S, Xuea A, Zhanga Y, Zhaoa Y, Zhong J (2018) Controllable construction of polymer/inorganic interface for poly(vinylalcohol)/graphitic carbon nitride hybrid pervaporation membranes. Chem Eng Sci 181:237–250
314. Liu G, Jiang Z, Cao K, Nair S, Cheng X, Zhao J, Gomaa H, Wu H, Pan F (2017) Pervaporation performance comparison of hybrid membranes filled with two-dimensional ZIF-L nanosheets and zero-dimensional ZIF-8 nanoparticles. J Membr Sci 523:185–196
315. Liu S, Liu G, Zhao X, Jin W (2013) Hydrophobic-ZIF-71 filled PEBA mixed matrix membranes for recovery of biobutanol via pervaporation. J Membr Sci 446:181–188
316. Sudhakar H, Prasad CV, Sunitha K, Rao KC, Subha M, Sridhar S (2011) Pervaporation separation of IPA-water mixtures through 4A zeolite-filled sodium alginate membranes. J Appl Polym Sci 121:2717–2725
317. Suhas DP, Aminabhavi TM, Raghu AV (2014) Mixed matrix membranes of H-ZSM5-loaded poly(vinyl alcohol) used in pervaporation dehydration of alcohols: influence of silica/alumina ratio. Polym Eng Sci 54:1774–1782
318. Sun H, Lu L, Chen X, Jiang Z (2008) Pervaporation dehydration of aqueous ethanol solution using H-ZSM-5 filled chitosan membranes. Sep Purif Technol 58:429–436
319. Cheng C, Li P, Shen K, Zhang T, Cao X, Wang B, Wang X, Hsiao BS (2018) Integrated polyamide thin-film nanofibrous composite membrane regulated by functionalized interlayer for efficient water/isopropanol separation. J Membr Sci 553:70–81
320. Suhas DP, Aminabhavi TM, Jeong HM, Raghu AV (2015) Hydrogen peroxide treated graphene as an effective nanosheet filler for separation application. RSC Adv 5:100984–100995

321. Zhao Q, Qian JW, Zhu CX, An QF, Xu TQ, Zheng Q, Song Y (2009) A novel method for fabricating polyelectrolyte complex/inorganic nanohybrid membranes with high isopropanol dehydration performance. J Membr Sci 345:233–241
322. Bakhtiari O, Mosleh S, Khosravi T, Mohammadi T (2012) Mixed matrix membranes for pervaporative separation of isopropanol/water mixtures. Desalin Water Treat 41:45–52
323. Veerapur RS, Gudasi KV, Aminabhavi TM (2008) Sodium alginate–magnesium aluminum silicate mixed matrix membranes for pervaporation separation of water–isopropanol mixtures. Sep Purif Technol 59(2):221–230
324. Jyothi MS, Reddy KR, Soontarapa K, Naveen S, Raghu AV, Kulkarni RV, Suhas DP, Shetti NP, Nadagouda MN, Aminabhavi TM (2019) Membranes for dehydration of alcohols via pervaporation. J Environ Manag 242:415–419
325. Adoor SG, Sairam M, Manjeshwar LS, Raju K, Aminabhavi TM (2006) Sodium montmorillonite clay loaded novel mixed matrix membranes of poly (vinyl alcohol) for pervaporation dehydration of aqueous mixtures of isopropanol and 1, 4-dioxane. J Membr Sci 285:182–195
326. Suhas DP, Raghu AV, Jeong HM, Aminabhavi TM (2013) Graphene loaded sodium alginate nanocomposite membranes with enhanced isopropanol dehydration performance via a pervaporation technique. RSC Adv 3:17120–17130
327. Suhas DP, Aminabhavi TM, Raghu AV (2014) Mixed matrix composite membranes of HZSM5 loaded poly(vinyl alcohol) used in pervaporation dehydration of alcohols: influence of silica/alumina ratio. Polym Eng Sci 54:1774–1782
328. Suhas DP, Aminabhavi TM, Raghu AV (2014) paraToluene sulfonic acid treated clay loaded sodium alginate membranes for enhanced pervaporative dehydration of IPA. Appl Clay Sci 101:419–429
329. Bhat SD, Mallikarjuna NN, Aminabhavi TN (2006) Microporous alumino-phosphate (AlPO4-5) molecular sieve-loaded novel sodium alginate composite membranes for pervaporation dehydration of aqueous–organic mixtures near their azeotropic compositions. J Membr Sci 282(1–2):473–483
330. Li SY, Srivastava R, Parnas RS (2010) Separation of 1-butanol by pervaporation using a novel tri-layer PDMS composite membrane. J Membr Sci 363:287–294
331. Liu L, Luo XB, Ding L, Luo SL (2019) Application of nanotechnology in the removal of heavy metal from water. Micro Nano Technol 4:83–147
332. Pereao OK, Bode-Aluko C, Ndayambaje G, Fatoba O, Petrik LF (2017) Application of nanotechnology in the removal of heavy metal from water. J Polym Environ 25:1175–1189
333. Fang J, Niu H, Lin T, Wang X (2008) Applications of electrospun nanofibers. Chinese Sci Bull 53(15):2265–2286
334. Lee CH, Chiang CL, Liu SJ (2013) Electrospun nanofibrous rhodanine/polymethylmethacrylate membranes for the removal of heavy metal ions. Sep Purif Technol 118:737
335. Huang Y, Ma H, Wang S, Shen M, Guo R, Cao X, Zhu M, Shi X (2012) Efficient catalytic reduction of hexavalent chromium using palladium nanoparticle-immobilized electrospun polymer nanofibers. ACS Appl Mater Interfaces 4(6):3054–3061
336. Ki CS, Gang EH, Um IC, Park YH (2007) Nanofibous membrane of wool keratose/silk fibroin blend for heavy metal ion adsorption. J Membr Sci 302:20–26
337. Ramakrishna S, Fujihara K, Teo WE, Yong T, Ma Z, Ramaseshan R (2006) Electrospun nanofibers: solving global issues. Mater Today 9(3):40–50
338. Gore P, Khraisheh M, Kandasubramanian B (2018) Nanofibers of resorcinol–formaldehyde for effective adsorption of As (III) ions from mimicked effluents. Environ Sci Pollut Res 25:11729–11745
339. Chaúque EFC, Dlamini LN, Adelodun AA, Greyling CJ, Ngila JC (2016) EDTA for the removal of Cd and Cr ions from water effluents. Appl Surf Sci 369:19–28
340. Neghlani PK, Rafizadeh M, Taromi FA (2011) Preparation of aminated-polyacrilonitril nano fiber membranes for the adsorption of metal ions: comparison with microfiber. J Hazard Mater 186:182–189

341. Deng S, Bai R, Chen JP (2003) Aminated polyacrylonitrile fibers for lead and copper removal. Langmuir 19(12):5058–5064
342. Gohari RJ, Lau WJ, Matsuura T, Ismail AF (2013) Fabrication and characterization of novel PES/Fe–Mn binary oxide UF mixed matrix membrane for adsorptive removal of As(III) from contaminated water solution. Sep Purif Technol 118:64–72
343. Phan DN, Hasegawa Y, Song KH, Lee H, Kim IS (2018) Adsorption of silver ions from aqueous solution onto thiol modified polyvinyl alcohol nanofibers. Trends Textile Eng Fashion Technol 1(5):120–122
344. Cai Z, Song X, Zhang Q, Liu Y (2017) Amidoxime surface modification of polyindole nanofiber membrane for effective removal of Cr(VI) from aqueous solution. J Mater Sci 52(9):5417–5434
345. Xiao S, Luo X, Peng Q, Deb H (2016) Effective removal of calcium ions from simulated hard water using electrospun polyelectrolyte nanofibrous mats. Fibers Polymers 17(9):1428–1437
346. Chitpong N (2016) Functionalized cellulose nanofiber membranes for heavy metals removal from impaired waters. Dissertations, Ph.D. Thesis, Clemson University. https://tigerprints.clemson.edu/all_dissertations/1851
347. Rasheed T, Adeel M, Nabeel F, Bilal M, Iqba H (2019) TiO_2/SiO_2 decorated carbon nanostructured materials as a multifunctional platform for emerging pollutants removal. Sci Total Environ 688:299–311
348. Rao GP, Lu C, Su F (2007) Sorption of divalent metal ions from aqueous solution by carbon nanotubes: a review. Sep Purif Technol 58(1):224–231
349. Azamat J, Khataee A, Joo SW (2014) Separation of a heavy metal from water through a membrane containing boron nitride nanotubes: molecular dynamics simulations. J Mol Model 20:2468
350. Razzaz A, Ghorban S, Hosayni L, Irani M, Alibadi M (2016) Chitosan nanofibers functionalized by TiO_2 nanoparticles for the removal of heavy metal ions. J Taiwan Inst Chem Eng 58:333–343
351. Anitha K, Namsani S, Singh JK (2015) Removal of heavy metal ions using a functionalized single-walled carbon nanotube: a molecular dynamics study. J Phys Chem A 119:8349–8358
352. Moradi O, Zare K, Yari M (2011) Interaction of some heavy metal ions with single walled carbon nanotube. Int J Nano Dim 1(3):203–220
353. Draouil H, Alvarez L, Causse J, Flaud V, Zaibi MA, Bantignies JL, Oueslati M, Cambedouzou J (2017) Copper hexacyano ferrate functionalized single-walled carbon nanotubes for selective cesium extraction. New J Chem 41:7705–7713
354. Naghizadeh A, Eivazi H (2015) Removal of lead and cobalt ions from aqueous solution by functionalized and non-functionalized carbon nanotubes. Journal of Behdasht dar Arseh (Journal of Health field) 3(1)
355. Zhang D, Yin Y, Liu L (2017) Removal of $Hg^{2+}$and methylmercury in waters by functionalized multi-walled carbon nanotubes: adsorption behavior and the impacts of some environmentally relevant factors. Chem Spec Bioavail 29(1):161–169
356. Bankole MT, Abdulkareem AS, Mohammed IA, Ochigbo SS, Tijani JO, Abubakre OK, Roos WD (2019) Heavy metals removal from electroplating wastewater by purified and polyhydroxylbutyrate functionalized carbon nanotubes adsorbents. Sci Rep 9:4475
357. Corsi I, Fiorati A, Grassi G, Bartolozzi I, Daddi T, Melone L, Punta C (2018) Environmentally sustainable and ecosafe polysaccharide-based materials for water nano-treatment: an eco-design study. Materials (Basel) 11(7):1228
358. Wang H, Ding J, Lee B, Wang X, Lin T (2007) Polypyrrole-coated electrospun nanofibre membranes for recovery of Au(III) from aqueous solution. J Membr Sci 303(1–2):119–125
359. Badruddoza AZM, Shawon ZBZ, Daniel TWJ, Hidajat K, Uddin MS (2013) Fe_3O_4/cyclodextrin polymer nanocomposites for selective heavy metals removal from industrial wastewater. Carbohydr Polym 91:322–332
360. Huang Y, Ma H, Wang S, Shen M, Guo R, Cao X, Zhu M, Shi X (2012) Efficient catalytic reduction of hexavalent chromium using palladium nanoparticle. ACS Appl Mater Interfaces 4(6):3054–3061

361. Ma H, Hsiao BS, Chu B (2013) Electrospun nanofibrous membrane for heavy metal ion adsorption. Curr Org Chem 17(13):1361–1370
362. Yang R, Su Y, Aubrecht KB, Wang X, Ma H, Grubbs RB, Hsiao BS, Chu B (2015) Thiol-functionalized chitin nanofibers for As(III) adsorption. Polymer 60:9–17
363. Wang K, Ma Q, Wang SD, Liu H, Zhang SZ, Bao W, Zhang KQ, Ling LZ (2016) Electrospinning of silver nanoparticles loaded highly porous cellulose acetate nanofibrous membrane for treatment of dye wastewater. Appl Phys A 122:40
364. Muthulakshmi AN, Anuradha J (2015) Removal of cadmium ions from water/waste water using chitosan—a review. Res Rev 9–14
365. He J, Matsuura T, Chen JP (2014) A novel Zr-based nanoparticle-embedded PSF blend hollow fiber membrane for treatment of arsenate contaminated water: material development, adsorption and filtration studies, and characterization. J Membr Sci 452:433–445
366. Khulbe KC, Matsuura T (2018) Removal of heavy metals and pollutants by membrane adsorption techniques. Appl Water Sci 8:19
367. Ritchie SMC, Bachas LG, Olin T, Sikdar SK, Bhattacharyya D (1999) Surface modification of silica- and cellulose-based microfiltration membranes with functional polyamino acids for heavy metal sorption. Langmuir 15(19):6346–6357
368. Wang R, Guan S, Sato A, Wang X, Wang Z, Yang R, Hsiao BS, Chu B (2013) Nanofibrous microfiltration membranes capable of removing bacteria, viruses and heavy metal ions. J Membr Sci 446:376–382
369. He ZY, Nie HL, Branford-White C, Zhu LM, Zhou YT, Zheng Y (2008) Removal of Cu^{2+} from aqueous solution by adsorption onto a novel activated nylon-based membrane. Bioresour Technol 99:7954–7958
370. Chatterjee S, De S (2014) Adsorptive removal of fluoride by activated alumina doped cellulose acetate phthalate (CAP) mixed matrix membrane. Sep Purif Technol 125:223–238
371. Choi HY, Bae JH, Hasegawa Y, An S, Kim IS, Lee H, Kim M (2020) Thiol-functionalized cellulose nanofiber membranes for the effective adsorption of heavy metal ions in water. Carbohydr Polym 234:11588
372. Nomngongo PN, Ngila AJC, Musyoka SM, Msagati TAM, Moodley B (2013) A solid phase extraction procedure based on electrospun cellulose-*g*-oxolane-2,5-dione nanofibers for trace determination of Cd, Cu, Fe, Pb and Zn in gasoline samples by ICP-OES. Anal Methods 5:3000–3008
373. Krason J, Pietrzak R (2016) Membranes obtained on the basis of cellulose acetate and their use in removal of metal ions from liquid phase. Polish J Chem Technol 18(2):104–110
374. Chen JH, Li GP, Liu L, Ni JC, Wu WB, Lin JM (2010) Cr(III) ionic imprinted polyvinyl alcohol/sodium alginate (PVA/SA) porous composite membranes for selective adsorption of Cr(III) ions. Chem Eng J 165(2):465–447
375. Algarra M, Vázquez MI, Alonso B, Casado CM, Casado J, Benavente J (2014) Characterization of an engineered cellulose based membrane by thiol dendrimer for heavy metals removal. Chem Eng J 253:472–477
376. Katsoyiannis IA, Zouboulis AI (2002) Removal of arsenic from contaminated water sources by sorption onto iron-oxide-coated. polymeric materials. Water Res 36(20):5141–5515
377. Bessbousse H, Rhlalou T, Verchere JF, Lebrun L (2008) Removal of heavy metal ions from aqueous solutions by filtration with a novel complexing membrane containing poly (ethyleneimine) in a poly (vinyl alcohol) matrix. J Membr Sci 307:249–259
378. Hermassi M, Valderrama C, Gibert O, Moreno N, Font O, Querol X, Batis NH, Cortina JL (2016) Integration of powdered Ca-activated zeolites in a hybrid sorption−membrane ultrafiltration process for phosphate recovery. Ind Eng Chem Res 55(21):6204–6212
379. Saffaj N, Loukili H, Younssi SA, Albizane A, Bouhria M, Persin M, Larbot A (2004) Filtration of solution containing heavy metals and dyes by means of ultrafiltration membranes deposited on support made of Moroccan clay. Desalin 168:301–306
380. Mohamad Said KA, George GG, Mohamed Alipah NA, Ismail NZ, Jama'in RL, Mili N, Salleh SF, Mohamed Amin MA, Muslimen R, Yakub I, Mohamed Sutan N (2017) Effect

of activated carbon in polysufone-polyethyleneimine-silver composite membrane towards adsorption of chromium (Cr), lead (Pb), silver (Ag) and cadmium (Cd) in synthetic wastewater. JMES 8(10):3740–3746

381. Zhang L, Zhou J, Zhou D, Tang Y (1999) Adsorption of cadmium and strontium on cellulose/alginic acid ion-exchange membrane. J Membr Sci 162:103–109
382. Yari S, Abbasizadeh S, Mousavi SE, Moghaddam MS, Moghaddam AZ (2015) Adsorption of Pb(II) and Cu(II) ions from aqueous solution by an electrospun CeO_2 nanofiber adsorbent functionalized with mercapto groups. Process Environ Protect 94:159–171
383. Cai Y, Li C, Wu D, Wang W, Tanwrap F, Wang X, Wong PK (2017) Highly active MgO nanoparticles for simultaneous bacterial inactivation and heavy metal removal from aqueous solution. Chem Eng J 312:158–166
384. Mehdizadeh S, Sadjadi S, Ahmadi SJ, Outokesh M (2014) Removal of heavy metals from aqueous solution using platinum nanopartcles/Zeolite-4A. J Environ Health Sci Eng 12:7
385. Al-Senani GM, Al-Fawzan FF (2018) Adsorption study of heavy metal ions from aqueous solution by nanoparticle of wild herbs. Egypt J Aquat Res 44(3):187–194
386. Rahmani A, Mousavi HZ, Fazli M (2010) Effect of nanostructure alumina on adsorption of heavy metals. Desalin 253:94–100
387. Dehghani MH, Taher MM, Bajpai AK, Heibati B, Tyagi I, Asif M, Agarwal S, Gupta VK (2015) Removal of noxious Cr (VI) ions using single-walled carbon nanotubes and multi-walled carbon nanotubes. Chem Eng J 279:344–352
388. Shaheen HA, Marwani HM, Soliman EM (2015) Selective adsorption of gold ions from complex system using oxidized multi-walled carbon nanotubes. J Mol Liq 21:480–486
389. Vuković GD, Marinković AD, Škapinc SD, Ristić MD, Aleksić R, Perić-Grujić AA, Uskoković PS (2011) Removal of lead from water by amino modified multi-walled carbon nanotubes. Chem Eng J 173(3):855–865
390. Xie Y, Huang Q, Liu MY, Wang K, Wan Q, Deng FJ, Lu L, Zhang XY, Wei Y (2015) Mussel inspired functionalization of carbon nanotubes for heavy metal ion removal. RSC Adv (84):68430–68438
391. Zhang XY, Huang Q, Liu MY, Tian JW, Zeng GJ, Li Z, Wang K, Zhang QS, Wan Q, Deng FJ, Wei Y (2015) Preparation of amine functionalized carbon nanotubes via a bioinspired strategy and their application in Cu^{2+} removal. Appl Surf Sci 343:19–27
392. Tajik S, Taher MA (2011) A new sorbent of modified MWCNTs for column preconcentration of ultratrace amounts of zinc in biological and water samples. Desalin 278:57–64
393. Ramana DKV, Yu JS, Seshaiah K (2013) A new sorbent of modified MWCNTs for column preconcentration of ultratrace amounts of zinc in biological and water samples. Surf Chem Eng J 223:806–815
394. Moghaddam HK, Pakizeh M (2015) Experimental study on mercury ions removal from aqueous solution by MnO_2/CNTs nanocomposite adsorbent. J Ind Eng Chem 21:221–229
395. Tang WW, Zeng GM, Gong JL, Liu Y, Wang XY, Liu YY, Liu ZF, Chen L, Zhang XR, Tu DZ (2012) Simultaneous adsorption of atrazine and Cu (II) from wastewater by magnetic multi-walled carbon nanotube. Chem Eng J 211–212:470–478
396. Liu X, Huang YS, Duan SX, Wang YN, Li JX, Chen YT, Hayat T, Wang XK (2016) Graphene oxides with different oxidation degrees for Co(II) ion pollution management. Chem Eng J 302:763–772
397. Zhao GX, Li JX, Ren XM, Chen CL, Wang XK (2011) Few-layered graphene oxide nanosheets as superior sorbents for heavy metal ion pollution management. Environ Sci Technol 45:10454–10462
398. Sun YB, Wang Q, Chen CL, Tan XL, Wang XK (2012) Interaction between Eu(III) and graphene oxide nanosheets investigated by batch and extended X-ray absorption fine structure spectroscopy and by modeling techniques. Environ Sci Technol 46:6020–6027
399. Song WC, Hu J, Zhao YG, Shao DD, Li JX (2013) Efficient removal of cobalt from aqueous solution using β-cyclodextrin modified graphene oxide. RSC Adv 3:9514–9521
400. Alabi A, Hajaj AA, Cseri L, Szekely G, Budd P, Zou L (2018) Review of nanomaterials-assisted ion exchange membranes for electromembrane desalination. npj Clean Water 1:10

401. Hosseini SM, Jeddi F, Nemati M, Madaeni SS, Moghadassi AR (2014) Electrodialysis heterogeneous anion exchange membrane modified by PANI/MWCNT composite nanoparticles: preparation, characterization and ionic transport property in desalination. Desalin 341:107–114
402. Hosseini SM, Madaeni SS, Heidari AR, Amirimehr A (2012) Preparation and characterization of ion-selective polyvinyl chloride based heterogeneous cation exchange membrane. Desalin 284:191–199
403. Kowsari E, Zare A, Ansari V (2015) Phosphoric acid-doped ionic liquid-functionalized graphene oxide/sulfonated polyimide composites as proton exchange membrane. Int J Hydrog Energy 40:13964–13978
404. Gahlot S, Sharma PP, Gupta H, Kulshrestha V, Jha PK (2014) Preparation of graphene oxide nano-composite ion-exchange membranes for desalination application. RSC Advances (47):24662–24670
405. Zendehnam A, Arabzadegan M, Hosseini SM, Robatmili N, Madaeni SS (2013) Fabrication and modification of polyvinyl chloride based heterogeneous cation exchange membranes by simultaneously using Fe-Ni oxide nanoparticles and Ag nanolayer: physico-chemical and antibacterial characteristics. Korean J Chem Eng 30:1265–1271
406. Roman MFS, Bringas E, Ibanez R, Ortiz I (2010) Liquid membrane technology: fundamentals and review of its applications. J Chem Techno Biotechnol 85:2–10
407. Araki T, Tsukube H (1990) Liquid membranes: chemical applications. CRC Press, Boca Raton
408. Sharma PP, Kulshrestha V (2015) Synthesis of highly stable and high water retentive functionalized biopolymer-graphene oxide modified cation exchange membranes. RSC Adv 5:56498–56506
409. Klaysom C, Moon SH, Ladewig BP, Lu GQ, Wang L (2011) Synthesis of highly stable and high water retentive functionalized biopolymer-graphene oxide modified cation exchange membranes. J Phys Chem C 115(31):15124–15132
410. Martis EA, Badve RR, Degwekar MD (2012) Nanotechnology based devices and applications in medicine: an overview. Chron Young Scientist 3(1):65–73
411. Patel S, Bhirde AA, Rusling JF, Chen X, Gutkind JS, Patel V (2011) Nano delivers big: designing molecular missiles for cancer nano delivers big: designing molecular missiles for cancer therapeutics. Pharmaceutics 3:34–52
412. Adiga SP, Jin C, Curtiss LA, Monteiro-Riviere NA, Narayan RJ (2009) Nanoporous membranes for medical and biological applications. Wiley Interdiscip Rev Nanomed Nanobiotechnol 1(5):568–581
413. Brüggemann D (2013) Nanoporous aluminium oxide membranes as cell interfaces. J Nanomaterials 2013:460870
414. Irfan M, Irfan M, Idris A, Baig N, Saleh TA, Nasiri R, Iqbal Y, Muhammad N, Rehman F, Khalid H (2019) Fabrication and performance evaluation of blood compatible hemodialysis membrane using carboxylic multiwall carbon nano-tubes and low molecular weight polyvinylpyrrolidone based nanocomposites. J Biomed Mater Res Part A 2019(107A):513–525
415. Nuxoll EE, Hillmyer MA, Wang R, Leighton C, Siegel RA (2009) Composite block polymer-microfabricated silicon nanoporous membrane. ACS Appl Mater Interfaces 1(4):888–893
416. Ingham CJ, Maat JT, de Vos WM (2012) Where bio meets nano: the many uses for nanoporous aluminum oxide in biotechnology. Biotechnol Advan 30(5):1089–1099
417. Gultepe E (2010) Nanoporous inorganic membranes or coatings for sustained drug delivery in implantable devices. Advan Drug Deliv Rev 62(3):305–315
418. Panda PK, Sahoo B (2013) Chapter 14. Synthesis and applications of electrospun nanofibers—a review. In: Navani NK, Sinha S, Govil JN (eds) Nanotechnology, fundamental and applications, vol. 1. Studiun Press LLC, pp 399–416
419. Arbanas C (2012) MD-PhD student starts nanotechnology company. Lead product is surgical mesh made of nanofibers. https://source.wustl.edu/2012/01/mdphd-student-starts--nanotechnology-company/. Accessed 30 Oct 2018
420. Paddock C (2012) Nanotechnology in medicine: huge potential, but what are the risks? Medical News Today

421. Sundaramurthi D, Krishnan UM, Sethuraman S (2014) Electrospun nanofibers as scaffolds for skin tissue engineering. Polym Rev 54(2):348–376
422. Zhai Y, Su J, Ran W, Zhang P, Yin Q, Zhang Z, Yu H, Li Y (2017) Preparation and application of cell membrane-camouflaged nanoparticles for cancer therapy. Theranostics 7(10):2575–2592
423. Chen S, Liu B, Carlson MA, Gambart AF, Reilly DA, Xie J (2017) Recent advances in electrospun nanofibers for wound healing. Nanomedicine (London) 12(11):1335–1352
424. Hassiba AJ, El Zowalaty ME, Nasrallah GK, Webster TJ, Luyt AS, Abdullah AM, Elzatahry AA (2016) Review of recent research on biomedical applications of electrospun polymer nanofibers for improved wound healing. Nanomedicine (Lond) 11(6):715–737
425. Salata V (2004) Applications of nanoparticles in biology and medicine. J Nanobiotechnology 2(1):3
426. Vasita R, Katti DS (2006) Nanofibers and their applications in tissue engineering. Int J Nanomedicine 1(1):15–30
427. Asmatulu R, Khan WS (2019) Chapter 11. Electrospun nanofibers for tissue engineering in synthesis and applications of electrospun nanofibers. In: Micro and nano technologies. Elsevier, pp 215–237
428. Mirjalili M, Zohoori S (2016) Review for application of electrospinning and electrospun nanofibers technology in textile industry. J Nanostruct Chem 6(3):207–213
429. Katti DS, Robinson KW, Ko FK, Laurenci CT (2004) Bioresorbable nanofiber based systems for wound healing and drug delivery: optimisation of fabrication parameters. J Biomed Mater Res 70:282–296
430. Yunshin S, Park HN, Kim KH (2005) Biologic evaluation of chitosan nanofiber membrane for guided bone regeneration. J Periodontol 76:1778–1784
431. Liu S, Wang X, Zhang Z, Zhang Y, Zhou G, Huang Y, Xie Z, Jing X (2015) Use of asymmetric multilayer polylactide nanofiber mats in controlled release of drugs and prevention of liver cancer recurrence after surgery in mice. Nanomed Nanotechnol Biol Med 11(5):1047–1056
432. Ni S, Fan X, Wang J, Qi H, Li X (2014) Biodegradable implants efficiently deliver combination of paclitaxel and temozolomide to glioma c6 cancer cells in vitro. Ann Biomed Eng 42(1):214–221
433. Duan YY, Jia J, Wang SH, Yan W, Jin L, Wang ZY (2007) Preparation of antimicrobial poly(ϵ-caprolactone) electrospun nanofibers containing silver-loaded zirconium phosphate nanoparticles. J Appl Polym Sci 106(2):1208–1214
434. Ignatova M, Manolova N, Rashkov I (2007) Electrospinning of poly(vinyl pyrrolidone)–iodine complex and poly(ethylene oxide)/poly(vinyl pyrrolidone)–iodine complex—a prospective route to antimicrobial wound dressing materials. Eur Polym J 43(5):1609–1623
435. Hu X, Liu S, Zhou G, Huang Y, Xie Z, Jing X (2014) Electrospinning of polymeric nanofibers for drug delivery applications. J Control Release 185:12–21
436. Sill TJ, von Recum HA (2008) Electrospinning: applications in drug delivery and tissue engineering. Biomaterials 29(13):1989–2006
437. Li M, Mondrinos MJ, Gandhi MR, Ko FK, Weiss AS, Lelkes PI (2005) Electrospun protein fibers as matrices for tissue engineering. Biomaterials 26(30):5999–6008
438. Woerdeman DL, Ye P, Shenoy S, Wnek GE, Trofimova O (2005) Electrospun fibers from wheat protein: investigation of the interplay between molecular structure and the fluid dynamics of the electrospinning process. Biomacromolecules 6:707–712
439. Boland ED, Matthews JA, Pawlowski KJ, Simpson DG, Wnek GE, Bowlin GL (2004) Electrospinning collagen and elastin: preliminary vascular tissue engineering. Front Biosci 1(9):1422–1432
440. Abrigo M, McArthur SL, Kingshott P (2014) Electrospun nanofibers as dressings for chronic wound care: advances, challenges, and future prospects. Macromol Biosci 14(6):772–729
441. Xue J, Xie J, Liu W, Xia Y (2017) Electrospun nanofibers: new concepts, materials, and applications. ACC Chem Res 50(8):1976–1987
442. Liu Y, Zhou S, Gao Y, Zhai Y (2019) Review: electrospun nanofibers as a wound dressing for treating diabetic foot ulcer. Asian J Pharm Sci 14(2):130–143

443. Huang ZM, Zhang YZ, Kotaki M, Ramakrishna S (2003) A review onpolymer nanofibers by electrospinning and their applications in nano composites. Composite Sci Technol 63:2223–2253
444. Subbiah T, Bhat GS, Tock RW, Parameswaran S, Ramkumar SS (2005) Electrospinning of nanofibers. J Appl Polym Sci 96:557–569
445. Liu X, Lin T, Gao Y, Xu Z, Huang C, Yao G, Jiang L, Tang Y, Wang X (2012) Antimicrobial electrospun nanofibers of cellulose acetate and polyester urethane composite for wound dressing. J Biomed Mater Res B Appl Biomater 100(6):1556–1565
446. Yang D, Li Y, Nie J (2007) Preparation of gelatin/PVA nanofibers and their potential application in controlled release of drugs. Carbohydr Polym 69(3):538–543
447. Chong EJ, Phan TT, Lim IJ (2007) Evaluation of electrospun PCL/gelatin nanofibrous scaffold for wound healing and layered dermal reconstitution. Acta Biomater 3(3):321–330
448. Yohe ST, Herrera VLM, Colson YL, Grinstaff MW (2012) 3D superhydrophobic electrospun meshes as reinforcement materials for sustained local drug delivery against colorectal cancer cells. J Control Release 162(1):92–101
449. Qiu K, He C, Feng W, Wang W, Zhou X, Yin Z, Chen L, Wang H, Mo X (2013) Doxorubicin-loaded electrospun poly(l-lactic acid)/mesoporous silicananoparticles composite nanofibers for potential postsurgical cancer treatment. J Mater Chem B 1(36):4601
450. Chen P, Wu Q, Ding Y, Chu M, Huang Z, Hu W (2010) A controlled release system of titanocene dichloride by electrospun fiber and its anti-tumor activity in vitro. Eur J Pharm Biopharm 76(3):413–420
451. Kim YJ, Bae HI, Kwon OK, Choi MS (2009) Three-dimensional gastric cancer cell culture using nanofiber scaffold for chemosensitivity test. Int J Biol Macromol 45(1):65–71
452. Ma G, Liu Y, Peng C, Fang D, He B, Nie J (2011) Paclitaxel loaded electrospun porous nanofibers as mat potential application for chemotherapy against prostate cancer. Carbohydr Polym 86(2):505–551
453. Ignatova M, Yossifova L, Gardeva E, Manolova N, Toshkova R, Rashkov I, Alexandrov M (2011) Antiproliferative activity of nanofibers containing quaternized chitosan and/or doxorubicin against MCF7 human breast carcinoma cell line by apoptosis. J Bioact Compat Polym 26(6):539–551
454. Vashisth P, Kumar N, Sharma M, Pruthi V (2015) Biomedical applications of ferulic acid encapsulated electrospun nanofibers. Biotechnol Rep 8:36–44
455. Wei J, Hu J, Li M, Chen Y, Chen Y (2014) Multiple drug-loaded electrospun PLGA/gelatin composite nanofibers encapsulated with mesoporous ZnO nanospheres for potential postsurgical cancer treatment. RSC Adv 4(53):28011–28019
456. Milane L, Duan Z, Amiji M (2011) Development of EGFR-targeted polymer blend nanocarriers for combination paclitaxel/lonidamine delivery to treat multi-drug resistance in human breast and ovarian tumor cells. Mol Pharm 8(1):185–203
457. Huang D, Lin C, Wen X, Gu S, Zhao P (2016) A potential nanofiber membrane device for filling surgical residual cavity to prevent glioma recurrence and improve local neural tissue reconstruction. PLoS One 11(8):e0161435
458. Molday RS, MacKenzie D (1982) Immunospecific ferromagnetic iron dextran reagents for the labeling and magnetic separation of cells. J Immunol Methods 52:353–367
459. Chen S, Liu B, Carlson MA, Gambart AF, Reilly DA, Xie J (2017) Recent advances in electrospun nanofibers for wound healing. Nanomedicine (Lond) 12(11):1335–1352
460. Fang RH, Kroll AV, Gao W, Zhang L (2018) Cell membrane coating nanotechnology. Adv Mater 30(23):e1706759
461. Esmaeili N, Gray EMA, Webb CJ (2019) Non-fluorinated polymer composite proton exchange membranes for fuel cell applications—a review. Chemphyschem 20(16):2016–2053
462. Choi BG, Huh YS, Park YC, Jung DH, Hong WH, Park HS (2012) Enhanced transport properties in polymer electrolyte composite membranes with graphene oxide sheets. Carbon 50(15):5395–5402
463. Mishra AK, Bose S, Kuila T, Kim NH, Lee JH (2012) Silicate-based polymer-nanocomposite membranes for polymer electrolyte membrane fuel cells. Prog Polym Sci 37:842–869

464. Kim DJ, Jo MJ, Nam SY (2015) A review of polymer–nanocomposite electrolyte membranes for fuel cell application. J Ind Eng Chem 21:36–52
465. Cao YC, Xu C, Wu X, Wang X, Xing L, Scott K (2011) A poly (ethylene oxide)/graphene oxide electrolyte membrane for low temperature polymer fuel cells. J Power Sources 196:8377–8382
466. Hooshyari K, Javanbakht M, Shabanikia A, Enhessari M (2015) Fabrication $BaZrO_3$/PBI-based nanocomposite as a new proton conducting membrane for high temperature proton exchange membrane fuel cells. J Power Sources 276:62–72
467. Hooshyari K, Javanbakht M, Naji L, Enhessari M (2014) Nanocomposite proton exchange membranes based on Nafioncontaining Fe2TiO5nanoparticles in water and alcohol environmentsfor PEMFC. J Membr Sci 454:74–81
468. Sigwadi R, Dhlamini MS, Mokrani T, Ṋemavhola F, Nonjola PF, Msomi PF (2019) The proton conductivity and mechanical properties of Nafion®/ZrP nanocomposite membrane. Heliyon 5(8):e02240
469. Luo M, Wen Q, Liu J, Liu H, Jia Z (2011) Fabrication of SPES/nano-TiO_2 composite ultrafiltration membrane and its anti-fouling mechanism. Chin J Chem Eng 19:45–51
470. Salarizadeh P, Javanbakht M, Pourmahdian S (2017) Enhancing the performance of SPEEK polymer electrolyte membranes using functionalized TiO_2 nanoparticles with proton hopping sites. RSC Adv 7:8303–8313
471. Shabanikia A, Javanbakht M, Amoli H, Hooshyari K, Enhessari M (2015) Novel nanocomposite membranes based on polybenzimidazole and Fe_2TiO_5 nanoparticles for proton exchange membrane fuel cells. Ionics 21:2227–2236
472. Namazi H, Ahmadi H (2011) Improving the proton conductivity and water uptake of polybenzimidazole-based proton exchange nanocomposite membranes with TiO2 and SiO2 nanoparticles chemically modified surfaces. J Power Sources 196(5):2573–2583
473. Vinodh R, Purushothaman M, Sangeetha D (2011) Novel quaternized polysulfone/ZrO2 composite membranes for solid alkaline fuel cell applications. Int J Hydrogen Energy 36(12):7291–7302
474. Chan S, Jankovic J, Susac D, Saha M, Tam M, Yang H, Ko F (2018) Electrospun carbon nanofiber catalyst layers for polymer electrolyte membrane fuel cells: structure and performance. J Power Sources 392:239–250
475. Wei M, Jiang M, Liu X, Wang M, Mu S (2016) Graphene-doped electrospun nanofiber membrane electrodes and proton exchange membrane fuel cell performance. J Power Sources 327:384–393
476. Chuang SW, Hsu SLC, Liu YH (2007) Synthesis and properties of fluorine-containing polybenzimidazole/silica nanocomposite membranes for proton exchange membrane fuel cells. J Membr Sci 305:353–363
477. Jang SS, Goddard WA (2019) Computational nanotechnology approach—JOUR. https://www.researchgate.net/publication/266607736
478. Tsuchiya M, Lai B, Ramanathan S (2011) Scalable nanostructured membranes for solid-oxide fuel cells. Nature Nanotech 6:282–286
479. Zhang M, Zhao X, Zhang G, Wei G, Su Z (2017) Electrospinning design of functional nanostructures for biosensor applications. J Mater Chem B 5:1699–1711
480. Saylan Y, Akgönüllü S, Yavuz H, Ünal S, Denizli A (2019) Molecularly imprinted polymer based sensors for medical applications. Sensors (Basel) 19(6):1279
481. Zhang X, Yang S, Jiang R, Sun L, Pang P, Luo A (2018) Fluorescent molecularly imprinted membranes as biosensor for the detection of target protein. Sens Actuat B Chem 524:1078–1086
482. Say R, Keçili R, Denizli A, Ersöz A (2016) Biomimetic imprinted polymers: theory, design methods, and catalytic applications. Molecularly imprinted catalysts (Principles, syntheses, and applications), pp 103–120
483. Li S, Cao S, Piletsky SA, Turner APF (2016) Molecularly imprinted catalysts Elsevier, pp 295

484. Irshad M, Iqbal N, Mujahid A, Afzal A, Hussain T, Sharif A, Ahmad E, Athar MM (2013) Molecularly imprinted nanomaterials for sensor applications. Nanomaterials (Basel) 3(4):615–637
485. Tancharoen C, Sukjee W, Thepparit C, Jaimipuk T, Auewarakul P, Thitithanyanont A, Sangma C (2019) An electrochemical biosensor based on surface imprinting for zika virus detection in serum. ACS Sens 4:69–75
486. Nano.Gov; NNI. https://www.nano.gov/you/nanotechnology-benefits. Accessed 29 Apr 2019
487. Bogue R (2004) Nanotechnology: what are the prospects for sensors? Sensor Rev 24(3):253–260
488. Yavari F, Chen Z, Thomas AV, Ren W, Cheng HM, Koratkar N (2011) High sensitivity gas detection using a macroscopic three-dimensional graphene. Sci Rep 1:166
489. Iyengar SA, Pillalamarri S, Jana SK, Islam MR, Ahuja T, Mohanty JS, Pradeep T (2019) Surface treated nanofibers for high current yielding breath humidity sensors for wearable electronics. ACS Appl Electron Mater. https://doi.org/10.1021/acsaelm.9b00123; http://pubs.acs.org. Accessed 11 Jun 2020
490. Khalid MAU, Ali M, Soomro AM, Kim SW, Kim HB, Choi KH (2019) A highly sensitive biodegradable pressure sensor based on nanofibrous dielectric. Sens Actuat A Phys 294:140–147
491. Asmatulu R, Veisi Z, Uddin MN, Mahapatro A (2019) Highly sensitive and reliable electrospun polyaniline nanofiber based biosensor as a robust platform for COX-2 enzyme detections. Fibers Polym 20(5):966–974
492. Song K, Zhang P, Huang Y, Xu F, Ding YI (2018) Electrospun PU/PVP/GO separator for Li-ion batteries. J Membr Sci 555:1–6
493. Perkins FK, Friedman AL, Cobas E, Campbell PM, Jernigan GG, Jonker BT (2013) Chemical vapor sensing with monolayer MoS2. Nano Lett 13(2):668–673
494. Liu K, Zhang Z, Shan CX, Feng ZQ, Li JS, Song CL, Bao YN, Qi XH, Dong B (2016) A flexible and super hydrophobic upconversion-luminescence membrane as an ultrasensitive fluorescence sensor for single droplet detection. Light Sci Appl 5:e16136
495. Liu X, Ma T, Xu Y, Sun L, Zheng L, Schmidt OG, Zhang J (2018) Rolled-up SnO2 nanomembranes: a new platform for efficient gas sensors. Sens Actuat B Chem 264:92–99
496. Grimm D, Bufon C, Deneke P, Atkinson DJ (2013) Rolled-up nanomembranes as compact 3D architectures for field effect transistors and fluidic sensing applications. Nano Lett 3(1):213–218
497. Kim YR, Jung S, Ryu H, Yoo YE, Kim SM, Jeon TJ (2012) Synthetic biomimetic membranes and their sensor applications. Sensors (Basel) 12(7):9530–9550
498. Soutter W (2019) Nanotechnology in agriculture. AZoNano. https://www.azonano.com/article.aspx?ArticleID=3141. Accessed 3 Nov 2019
499. Patil K, Jeong S, Lim H, Byun HS, Han S (2019) Removal of volatile organic compounds from air using activated carbon impregnated cellulose acetate electrospun mats. Environ Eng Res 24. https://doi.org/10.4491/eer.2018.336
500. Balamurugan R, Sundarrajan S, Ramakrishna S (2011) Recent trends in nanofibrous membranes and their suitability for air and water filtrations. Membranes (Basil) 1(3):232–248
501. Ahn YC, Park SK, Kim GT, Hwang YJ, Lee CG, Shin HS (2006) Development of high efficiency nanofilters made of nanofibers. Curr Appl Phys 6:1030–1035
502. Scholten E, Bromberg L, Rutledge GC, Hatton TA (2011) Electrospun polyurethane fibers for absorption of volatile organic compounds from air. ACS Appl Mater Interface 3:3902
503. Graham K, Ouyang M, Raether T, Grafe T, McDonald B, Knauf P (2002) Polymeric nanofibers in air filtration applications. Presented at the fifteenth annual technical conference & expo of the American Filtration & Separations Society, Galveston, Texas, April 9
504. Jo WK, Kang HJ (2013) Polyacrylonitrile-TiO2 fibers for control of gaseous aromatic compounds. Ind Eng Chem Res 52(12):4475–4483
505. Kim HK, Park SJ, Park CS, Le TH, Lee SH, Kim TH, KimJ LCS, Yoon H, Kwon OS (2018) Surface-modified polymer nanofiber membrane for high-efficiency microdust capturing. Chem Eng J 339:204–213

506. Zhang R, Liu C, Hsu PC, Zhang C, Liu N, Zhang J, Lee HR, Lu Y, Qiu Y, Chu S, Cui Y (2016) Nanofiber air filters with high-temperature stability for stability for efficient PM 2.5 removal from the pollution sources. Nano Lett 16(6):3642–3649
507. Zou W, Gu B, Sun S, Wang S, Li X, Zhao H, Yang P (2019) Preparation of a graphene oxide membrane for airpurification. Mater Res Express 6:105624
508. Edwards E, Brantley C, Ruffin PB (2017) Overview of nanotechnology in military and aerospace applications. In: Mensah TO, Wang B, Bothun G, Winter J, Davis V (eds) Nanotechnology commercialization: manufacturing processes and products. Wiley Connections. https://doi.org/10.1002/9781119371762.ch5
509. Introduction to electrospun fibers for defence technology. http://electrospintech.com/defenceintro
510. Faccini M, Vaquero C, Amantia D (2012) Development of protective clothing against nanoparticle based on electrospun nanofibers. J Nanomater 2012:892894
511. Vitchuli N, Shi Q, Nowak J, McCord M, Bourham M, Zhang X (2010) Electrospun ultrathin nylon fibers for protective applications. J Appl Polym Sci 116(4):2181–2187
512. Morozov VN, Mikheev AY (2012) Water-soluble polyvinylpyrrolidone nanofilters manufactured by electrospray-neutralization technique. J Membr Sci 403–404:10–120
513. White J, Foley M, Rowley A (2015) Novel approach to 3d-printed fabrics and garments. 3D Print Addit Manufac 2(3):145–149
514. Sundarrajan S, Ramakrishna S (2007) Fabrication of nanocomposite membranes from nanofibers and nanoparticles for protection against chemical warfare stimulant. J Mater Sci 42(20):8400–8407
515. Ramaseshan R (2011) Decontamination of chemical warfare simulants using electrospun media. PhD thesis, National University of Singapore
516. Chen L (2009) Next generation of electrospun textiles for chemical and biological protection and air filtration. PhD thesis, Massachusetts Institute of Technology
517. Yuan J, Geng J, Xing Z, Shen J, Kang IK, Byun H (2010) Electrospinning of antibacterial poly(vinylidene fluoride) nanofibers containing silver nanoparticles. J Appl Polym Sci 116(2):668–672
518. Dhineshbabu NR, Karunakaran G, Suriyaprabha R, Manivasakan P, Rajendran V (2014) Electrospun MgO/nylon 6 hybrid nanofibers for protective clothing. Nano Micro Lett 6:46–54
519. Haider A, Kwak S, Gupta KC, Kang IK (2015) Antibacterial activity and cytocompatibility of plga/cuo hybrid nanofiber scaffolds prepared by electrospinning. J Nanomater 2015:107
520. Kim SJ, Nam YS, Rhee DM, Park HS, Park WH (2007) Preparation and characterization of antimicrobial polycarbonate nanofibrous membrane. Eur Polym J 43(8):3146–3152
521. Nabetani H, Iwamoto S (2004) Present state and future potential of membrane technology in food industry. Foods Food Ingredients J Jpn 209(10)
522. He X, Hwang HM (2016) Nanotechnology in food science: functionality, applicability, and safety assessment. J Food Drug Analysis 24(4):671–681
523. Testing programme of manufactured nanomaterials. Organisation for Economic Co-operation and Development; 2007. http://www.oecd.org/chemicalsafety/nanosafety/testing--programme-manufactured-nanomaterials.htm. Accessed 18 July 2016
524. Peddinti S (2016) Nanotechnology applications in food industry—a review. Res Rev 4(2):2016, e-issn: 2347–7857
525. Bajpai VK, Kamle M, Shukla S, Mahato DK, Chandra P, Hwang SK, Kumar P, Huh YS, Han YK (2018) Prospects of using nanotechnology for food preservation, safety, and security. J Food Drug Analysis 26(4):1201–1214
526. Yu Z, Lib B, Chud J, Zhang P (2018) Silica in situ enhanced PVA/chitosan biodegradable films for food packages. Carbohydr Polym 184:214–220. https://doi.org/10.1016/j.carbpol.2017.12.043. Epub 2017 Dec 20
527. Swaroop C, Shukla M (2018) Nano-magnesium oxide reinforced polylactic acid biofilms for food packaging applications. Int J Biol Macromol 113:729–736
528. Foltynowicz Z, Bardenshtein A, Sängerlaub S, Antvorskov H, Kozak W (2010) Nanoscale, zero valent iron particles for application as oxygen scavenger. Food Packag Shelf Life 11:74–83

529. Sarwar MS, Niazi MBK, Jahan Z, Ahmad T, Hussain A (2018) Preparation and characterization of PVA/nanocellulose/Ag nanocomposite films for antimicrobial food packaging. Carbohydr Polym 184:453–464
530. Ahmed J, Mulla M, Arfat YA, Bher A, Jacob H, Auras R (2018) Compression molded LLDPE films loaded with bimetallic (Ag-Cu) nanoparticles and cinnamon essential oil for chicken meat packaging applications. LWT 91:329–333
531. Srinivas PR, Philbert M, Vu TQ, Huang Q, Kokini JL, Saos E, Chen H, Peterson CM, Friedl KE, McDade-Ngutter C, Hubbard V, Starke-Reed P, Miller N, Betz J, Dwyerj MJ, Ross SA (2010) Nanotechnology research: applications in nutritional sciences. J Nutr 140:119–124
532. Smolkova B, El Yamani N, Collins AR, Gutleb AC, Dusinska M (2015) Epigenetic changes induced by nanomaterials and possible impact on health. Food Chem Toxicol 77:64–73
533. Metak AM, Nabhani F, Connolly SN (2015) Migration of engineered nanoparticles from packaging into food products. LWT Food Sci Technol 64:781–787
534. Addo Ntim S, Thomas TA, Begley TH, Noonan GO (2015) Characterisation and potential migration of silver nanoparticles from commercially available polymeric food contact materials. Food Addit Contam Part A 32:1003–1011
535. Chau CF, Wu SH, Yen GC (2007) The development of regulations for food nanotechnology. Trends Food Sci Technol 18:269–280
536. Faneer KA, Rohani R, Mohammad AW (2016) Polyethersulfone nanofiltration membrane incorporated with silicon dioxide prepared by phase inversion method for xylitol purification. Polym Polym Composites 24(9):803–808
537. Nanotechnology and tyres, greening industry and transport. 2014. OECD Publishing, Paris. https://doi.org/10.1787
538. Nanofiber filters eliminate contaminants (2009) Environmental and agricultural resources. Spinoff 2009:92–93. https://www.nasa.gov/pdf/413408main_Nanofiber.pdf

Index

K. C. Khulbe, T. Matsuura, *Nanotechnology in Membrane Processes*, Lecture Notes in Nanoscale Science and Technology 29,
https://doi.org/10.1007/978-3-030-64183-2